NASA Conference Publication [illegible]

NASA Aircraft Controls Research 1983

(NASA-CP-2296) NASA AIRCRAFT CONTROLS RESEARCH, 1983 (NASA) 592 p HC A25/MF A01 CSCL 01C
N84-20567
THRU
N84-20600
Unclas
G3/08 18813

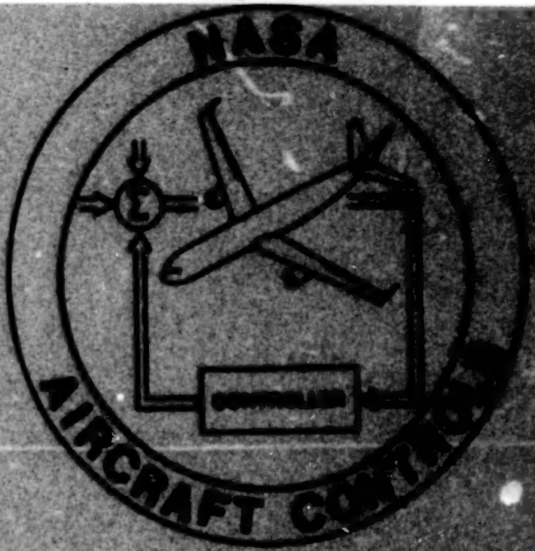
NASA
CONTROLLER
AIRCRAFT CONTROLS

Proceedings of a workshop held at
NASA Langley Research Center
Hampton, Virginia
October [illegible]

NASA

NASA Conference Publication 2296

NASA Aircraft Controls Research 1983

Gary P. Beasley, *Compiler*
Langley Research Center

Proceedings of a workshop held at
NASA Langley Research Center
Hampton, Virginia
October 25-27, 1983

National Aeronautics
and Space Administration

Scientific and Technical
Information Branch

1984

PREFACE

This publication contains the proceedings of the First Annual NASA Aircraft Controls Workshop, which was held October 25-27, 1983, at NASA Langley Research Center. This workshop highlighted ongoing aircraft controls research sponsored by NASA's Office of Aeronautics and Space Technology and provided a forum for critique of ongoing research as well as suggestions for needed research from controls experts or users of control technology. The workshop was initiated in response to a recommendation from the NASA Advisory Council's Informal Subcommittee on Aircraft Controls and Guidance.

About 200 aircraft controls experts from industry, government, and universities participated in the workshop. The workshop consisted of 24 technical presentations on various aspects of aircraft controls, ranging from the theoretical development of control laws to the evaluation of new controls technology in flight test vehicles. It also included a special report on the status of foreign aircraft technology and a panel session with seven representatives from organizations which use aircraft controls technology. This panel addressed the controls research needs and opportunities for the future as well as the role envisioned for NASA in that research. Input from the panel and response to the workshop presentations will be used by NASA in developing future programs.

This document contains copies of the visual material presented by each participant, together with descriptive material for each visual. A list of conference attendees is also included.

Use of trade names or names of manufacturers in this report does not constitute an official endorsement of such products or manufacturers, either expressed or implied, by the National Aeronautics and Space Administration.

Gary P. Beasley
Langley Research Center

PRECEDING PAGE BLANK NOT FILMED

CONTENTS

PREFACE iii

PARTICIPANTS ix

NASA CONTROL RESEARCH OVERVIEW 1
Duncan E. McIver

SESSION I: CONTROL SYSTEM DESIGN REQUIREMENTS

FLYING QUALITIES CRITERIA FOR SUPERAUGMENTED AIRCRAFT 25
Donald T. Berry

LARGE AIRCRAFT HANDLING QUALITIES 37
William D. Grantham

A SUMMARY OF ROTORCRAFT HANDLING QUALITIES RESEARCH AT NASA AMES RESEARCH CENTER 51
Robert T. N. Chen

FLEXIBLE AIRCRAFT FLYING AND RIDE QUALITIES 69
Irving L. Ashkenas, Raymond E. Magdaleno, and Duane T. McRuer

IMPLICATIONS OF CONTROL TECHNOLOGY ON AIRCRAFT DESIGN 93
Steven M. Sliwa and P. Douglas Arbuckle

RELIABILITY AND MAINTAINABILITY ASSESSMENT FACTORS FOR RELIABLE FAULT-TOLERANT SYSTEMS 115
Salvatore J. Bavuso

SESSION II: PARAMETER AND STATE ESTIMATION AND OPTIMAL GUIDANCE TECHNIQUES

PRACTICAL ASPECTS OF MODELING AIRCRAFT DYNAMICS FROM FLIGHT DATA 135
Kenneth W. Iliff and Richard E. Maine

APPLICATIONS OF MODEL STRUCTURE DETERMINATION TO FLIGHT TEST DATA 155
James G. Batterson and Vladislav Klein

MIXING 4D-EQUIPPED AND UNEQUIPPED AIRCRAFT IN THE TERMINAL AREA 171
L. Tobias, H. Erzberger, H. Q. Lee, and P. J. O'Brien

APPLICATION OF FUEL/TIME MINIMIZATION TECHNIQUES TO ROUTE PLANNING AND TRAJECTORY OPTIMIZATION 191
Charles E. Knox

FEEDBACK LAWS FOR FUEL MINIMIZATION FOR TRANSPORT AIRCRAFT 209
Douglas B. Price and Christopher Gracey

IDENTIFICATION OF MULTIVARIABLE HIGH-PERFORMANCE TURBOFAN ENGINE DYNAMICS FROM CLOSED-LOOP DATA 221
Walter C. Merrill

PRECEDING PAGE BLANK NOT FILMED

SESSION III: CONTROL SYSTEM DESIGN TECHNIQUES

EIGENSPACE DESIGN TECHNIQUES FOR ACTIVE FLUTTER SUPPRESSION 241
William L. Garrard and Bradley S. Liebst

TOOLS FOR ACTIVE CONTROL SYSTEM DESIGN 263
William M. Adams, Jr., Sherwood H. Tiffany, and Jerry R. Newsom

ALGORITHMS FOR OUTPUT FEEDBACK, MULTIPLE-MODEL, AND DECENTRALIZED CONTROL PROBLEMS 281
Nesim Halyo and John R. Broussard

PILOT MODELING, MODAL ANALYSIS, AND CONTROL OF LARGE FLEXIBLE AIRCRAFT 305
David K. Schmidt

NONLINEAR SYSTEMS APPROACH TO CONTROL SYSTEM DESIGN 329
George Meyer

ADAPTIVE CONTROL: MYTHS AND REALITIES 343
Michael Athans and Lena Valavani

SPECIAL REPORT

FOREIGN TECHNOLOGY SUMMARY OF FLIGHT CRUCIAL CONTROL SYSTEMS 365
H. A. Rediess

SESSION IV: RECENT EXPERIENCES IN IMPLEMENTATION
OF ADVANCED CONTROL SYSTEMS

FUNCTIONAL INTEGRATION OF VERTICAL FLIGHT PATH AND SPEED CONTROL USING ENERGY PRINCIPLES 389
A. A. Lambregts

FLIGHT TEST RESULTS FOR THE DIGITAL INTEGRATED AUTOMATIC LANDING SYSTEM (DIALS) - A MODERN CONTROL FULL-STATE FEEDBACK DESIGN 411
R. M. Hueschen

APPLICATION OF ADVANCED CONTROL TECHNIQUES TO AIRCRAFT PROPULSION SYSTEMS . . . 429
Bruce Lehtinen

L-1011 TESTING WITH RELAXED STATIC STABILITY 443
J. J. Rising and K. R. Henke

AFTI/F-16 DIGITAL FLIGHT CONTROL SYSTEM EXPERIENCE 469
Dale A. Mackall

EXPERIENCES WITH THE DESIGN AND IMPLEMENTATION OF FLUTTER SUPPRESSION SYSTEMS . 489
Jerry R. Newsom and Irving Abel

SESSION V: RESEARCH OPPORTUNITIES FOR THE FUTURE

RESEARCH OPPORTUNITIES FOR FUTURE COMMERCIAL TRANSPORTS 511
J. F. Longshore

A BRIEF REVIEW OF AIRCRAFT CONTROLS RESEARCH OPPORTUNITIES IN THE GENERAL AVIATION FIELD 519
Eric R. Kendall

RESEARCH OPPORTUNITIES FOR ROTORCRAFT 537
Bruce Blake

FIGHTER AIRCRAFT FLIGHT CONTROL TECHNOLOGY DESIGN REQUIREMENTS 549
W. E. Nelson, Jr.

MILITARY AIRCRAFT RESEARCH OPPORTUNITIES FOR THE FUTURE 559
Robert C. Schwanz

OPPORTUNITIES FOR AIRCRAFT CONTROLS RESEARCH 571
Thomas B. Cunningham

PROPULSION CONTROL TECHNOLOGY 585
Edward C. Beattie

PARTICIPANTS

Imran Abbasy
c/o Brig Abbasy
Cabinet Division
Rawalpindi
PAKISTAN

Irvin Abel
M/S 243
Langley Research Center
Hampton, VA 23665

Volkmar K. Adam
564 Logan Place,#7
Newport News, VA 23601

William M. Adams, Jr.
M/S 152A
Langley Research Center
Hampton, VA 23665

W. J. Alford
Dynamic Engineering, Inc.
703 Middle Ground Blvd.
Newport News, VA 23606

Carl Anderson
Lockheed-California Company
8509 Wyngate Street
Sunland, CA 91040

R. O. Anderson
Chief, Control Dynamics Branch
Flight Control Division
AFWAL/FIGC
Wright-Patterson AFB, OH 45433

Willard W. Anderson
M/S 152
Langley Research Center
Hampton, VA 23665

Robert A. Andes
US Air Force
ASD/BIEFT
Wright Patterson AFB, OH 45433

Ernie L. Anglin
M/S 267
Langley Research Center
Hampton, VA 23665

P. Douglas Arbuckle
M/S 152A
Langley Research Center
Hampton, VA 23665

Ernest S. Armstrong
M/S 161
Langley Research Center
Hampton, VA 23665

Irving L. Ashkenas
Systems Technology, Inc.
13766 S. Hawthorne Boulevard
Hawthorne, CA 90250

B. R. Ashworth
M/S 125B
Langley Research Center
Hampton, VA 23665

Michael Athans
M.I.T.
Room 35-406
Cambridge, MA 02139

Robert A. August
Grumman Aerospace Corp.
Mailstop T03-05
Bethpage, NY 11714

A. J. Bailey, Jr.
Honeywell
7338 Cornelia Drive
Minneapolis, MN 55435

Siva S. Banda
AFWAL/FIGC
WPAFB, OH 45433

Lex Barker
M/S 125B
Langley Research Center
Hampton, VA 23665

Roger Barron
General Research Corp.
7655 Old Springhouse Road
McLean, VA 22102

James G. Batterson
M/S 161
Langley Research Center
Hampton, VA 23665

Robert I. Baumgartner
Lockheed-California Co.
12129 E. El Dorado Avenue #15
Sylmar, CA 91342

PRECEDING PAGE BLANK NOT FILMED

Salvatore J. Bavuso
M/S 130
Langley Research Center
Hampton, VA 23665

Gary P. Beasley
M/S 152
Langley Research Center
Hampton, VA 23665

Edward C. Beattie
Pratt & Whitney
Mail Stop 121-05 400 Main Street
East Hartford, CT 06108

Henry L. Beaufrere
Grumman Aerospce Corporation
15 Noel Court
Huntington, NY 11743

Chris Belcastro
M/S 494
Langley Research Center
Hampton, VA 23665

Hugh P. Bergeron
M/S 152E
Langley Research Center
Hampton, VA 23665

Donald T. Berry
NASA Dryden Research Facility
43613 Lively Avenue
Lancaster, CA 93534

Paul W. Berry
The Analytic Sciences Corp. (TASC)
1 Jacob Way
Reading, MA 01867

Gaudy M. Bezos
M/S 247
Langley Research Center
Hampton, VA 23665

Bruce B. Blake
Boeing Vertol Company
P. O. Box 16858
Philadelphia, PA 19142

Neal Blake
Deputy Associate Administrator
for Development & Logistics for
Engineering
Code AED-2
Federal Aviation Administration
Washington, DC 20591

Michael P. Bland
McDonnell Douglas Corp.
66 Chartley Lane
Bridgeton, MO 63044

Philip D. Bridges
Mississippi State University
Department of Aerospace Engineering
Drawer A
Mississippi State, MS 39762

W. Thomas Bundick
M/S 494
Langley Research Center
Hampton, VA 23665

John A. Burns
Air Force Office of Scientific
Research
AFOSR/NM
Bolling AFB, DC 20332

Carey S. Buttrill
Technology Applications, Inc.
21 Argall Place
Newport News, VA 23602

Anthony J. Calise
Drexel University
Mechanical Engineering & Mechanics
Dept.
Philadelphia, PA 19104

Michael F. Card
M/S 244
Langley Research Center
Hampton, VA 23665

Preston I. Carraway
Old Dominion University
Department of Electrical Engineering
Norfolk, VA 23508

Mr. Edward S. Carter, Jr.
Director of Technology
Sikorsky Aircraft Division
United Technologies Corporation
Stratford, CT 06602

Charles R. Chalk
Calspan Corp.
P.O. Box 400
Buffalo, NY 14225

Phillip R. Chandler
AFWAL/FIGL
ASD/AFWAL/FIGL
WPAFB, OH 45433

Robert T. N. Chen
NASA Ames Research Center
Mailstop 211-2
Moffet Field, CA 94035

E. M. Cliff
VPI&SU
Randolph 215
Blacksburg, VA 24061

Roy B. Cotta
McDonnell Douglas Corp.
M/S 36-81
3855 Lakewood Boulevard
Long Beach, CA 90846

Leonard Credeur
M/S 152E
Langley Research Center
Hampton, VA 23665

Jeremiah F. Creedon
M/S 469
Langley Research Center
Hampton, VA 23665

Luci Crittenden
Sperry
M/S 125B
Langley Research Center
Hampton, VA 23665

Thomas B. Cunningham
Honeywell Inc.
Systems and Research Center
2600 Ridgway Parkway
P. O. Box 312, MN17-2370
Minneapolis, MN 55440

Ralph L. Davies
Calspan Corporation
Buffalo, NY

Dwain Deets
NASA Dryden Flight Research Facility
M/S D-OFD
P. O. Box 273
Edwards, CA 93523

Oded Degani
Lear Siegler, Inc.
Astronics Division
3400 Airport Avenue
Santa Monica, CA 90406

S. C. Dixon
M/S 398
Langley Research Center
Hampton, VA 23665

Rolf Duerr
Sperry Corp.
3217 North Armistead Avenue
Hampton, VA 23602

John Edwards
M/S 341
Langley Research Center
Hampton, VA 23665

Jarrell R. Elliott
M/S 152A
Langley Research Center
Hampton, VA 23665

Eric T. Falangas
Rockwell International
3101 S. Bristol #140
Santa Ana, CA 92704

Philip Felleman
C. S. Draper Laboratory
555 Technology Square
Cambridge, MA 02139

Robert E. Fennell
Clemson University
Dept. of Mathematical Sciences
Clemson, SC 29631

Dr. Eliezer Gai - MS 60
The Charles Stark Draper Laboratory
555 Technology Square
Cambridge, MA 02139

Dagfinn Gangsaas
Boeing Company
16047 NE 27 Street
Bellevue, WA 98008

H. D. Garner
M/S 494
Langley Research Center
Hampton, VA 23665

William L. Garrard
Dept. of Aerospace Engineering
University of Minnesota
107 Akerman Hall
Minneapolis, MN 55455

John F. Garren, Jr.
M/S 469
Langley Research Center
Hampton, VA 23665

Joseph Gera
NASA Ames Research Center
Box 273
Edwards, CA 93523

Dan Giesy
Kentron
Mail 161
Langley Research Center
Hampton, VA 23665

Michael G. Gilbert
M/S 243
Langley Research Center
Hampton, VA 23665

William D. Grantham
M/S 152A
Langley Research Center
Hampton, VA 23665

Robert Gregory
Bendix Aerospace Technology Center
9140 Old Annapolis Road/MD108
Columbia, MD 21045

Arlene D. Guenther
Sperry Systems Management
3217 N. Armistead Avenue
Hampton, VA 23666

Wiley A. Guinn
Lockheed California Company
P. O. Box 551
Burbank, CA 91520

Sol W. Gully
Alphatech Inc.
2 Burlington Executive Center
111 Middlesex Turnpike
Burlington, MA 01803

Dave Hahne
M/S 355
Langley Research Center
Hampton, VA 23665

Francis J. Hale
N. C. State University
Box 5246
Raleigh, NC 27650

Kenneth R. Hall
Mississippi State University
Dept. of Aerospace Engineering
Drawer A
Mississippi State, MS 39762

Nesim Halvo
Information and Control Systems
28 Research Drive
Hampton, VA 23665

M. J. Hamilton
Sperry Systems Management
3217 N. Armistead Avenue
Hampton, VA 23666

Margery E. Hannah
1048 Willow Green Dr.
Newport News, VA 23602

P. W. Hanson
M/S 398
Langley Research Center
Hampton, VA 23665

Herman J. Hassig
Lockheed-California Company
P.O. Box 551
Burbank, CA 91520

Earl C. Hastings, Jr.
M/S 286
Langley Research Center
Hampton, VA 23665

G. A. Haynes
M/S 256
Langley Research Center
Hampton, VA 23665

Michael P. Healy
Grumman Aerospace
140 6th Street
St. James, NY 11780

Kenneth R. Henke
Lockheed-California Company
P. O. Box 551
Burbank, CA 91520

Larry S. Henry
MPC Products Corporation
7426 North Linder Avenue
Skokie, IL 60077

Michael Herb
Analytical Mechanics Associate, Inc.
17 Research Drive
Hampton, VA 23185

Ray V. Hood
M/S 158
Langley Research Center
Hampton, VA 23665

Dan T. Horak
Bendix Aerospace Technology Center
9140 Old Annapolis Road
Columbia, MD 21045

W. E. Howell
M/S 494
Langley Research Center
Hampton, VA 23665

Bob Huber
General Electric Company
Binghamton, NY

Richard M. Hueschen
M/S 494
Langley Research Center
Hampton, VA 23665

George Hunt
Sperry Systems Management
3217 N. Armistead Avenue
Hampton, VA 23666

Kenneth W. Iliff
Code D-OF
Dryden Flight Research Facility
Edwards, CA 93523

Obi Iloputaife
Northrop Corporation
1 Northop Avenue
M/S 3833/85
Hawthorne, CA 90250

Pete Jacobs
M/S 294
Langley Research Center
Hampton, VA 23665

S. M. Joshi
M/S 161
Langley Research Center
Hampton, VA 23665

Jer-Nan Juang
M/S 230
Langley Research Center
Hampton, VA 23665

William Karger
Rockwell International
NAAO-GB15
Los Angeles, CA

Jerry R. Karwac, Jr.
Sperry Systems Management
3217 N. Armistead Avenue
Hampton, VA 23666

Howard Kaufman
Rensselaer Polytechnic Institute
ECSE Dept.
Troy, NY 12181

G. M. Kelly
Analytical Mechanics Association
17 Research Drive
Hampton, VA 23666

James R. Kelly
M/S 265
Langley Research Center
Hampton, VA 23665

Eric Kendall
Gates Learjet
1511 N. West Street, #9
Wichita, KS 67203

Ralph D. Kimberlin
University of Tennessee Space
Institute
103 Autumn Lane, Rt. 2
Tullahoma, TN 37388

Martin J. Klepl
Rockwell International
2178 Paseo Del Mar
San Pedro, CA 90732

Charles E. Knox
M/S 156A
Langley Research Center
Hampton, VA 23665esota

Fred Lallman
M/S 152A
Langley Research Center
Hampton, VA 23665esota

Antonius A. Lambregts
Boeing CAC
P. O. Box 3707
Seattle, WA 98124

Beth Lee
M/S 494
Langley Research Center
Hampton, VA 23665

Bruce Lehtinen
NASA Lewis Research Center
21000 Brookpark Road
MS 100-1
Cleveland, OH 44135

Brad Liebst
University of Minnesota
Dept. of Aerospace Eng.
107 Akerman Hall
110 Union Street, SE
Minneapolis, MN 56455

Wai K. Lim
Northrop Corporation
1 Northrop Avenue
M/S 3833/85
Hawthorne, CA 90250

James F. Longshore
Douglas Mail Code 36-49
3855 Lakewood Boulevard
Long Beach, CA 90846

John D. Louthan
Director, Vehicle Projects
Vought Corporation
P.O. Box 225907
Dallas, TX 75265

William Lynn
Kentron Technical Center
3221 Armistead Avenue
Hampton, VA 23666

Dale A. Mackall
NASA Dryden Flight Research Facility
Code E-EDC
Edwards, CA 93523

Michael A. Masi
AFWAL/FIG1
ASD/AFWAL/FIGL
WPAFB, OH 45433

William E. McCain
M/S 243
Langley Research Center
Hampton, VA 23665

D. J. McFerron
Old Dominion University
Dept. of Mechanical Engineering and Mechanics
Norfolk, VA 23508

Duncan E. McIver
NASA Headquarters
Code RTH-6
Washington, DC 20546

Dr. Griffith J. McRee
Old Dominion University
Department of Electrical Engineering
Norfolk, VA 23508

D. T. McRuer
Systems Technology, Inc.
13766 S. Hawthorne Boulevard
Hawthorne, CA 90250

Walter C. Merrill
NASA Lewis Research Center
21000 Brookpark Road
MS 100-1
Cleveland, OH 44135

George Meyer
M/S 210-3
NASA Ames Research Center
Moffett Field, CA 94035

R. T. Meyer
Lockheed Georgia Company
865 Cobb Drive
Marietta, GA 30065

David B. Middleton
M/S 158
Langley Research Center
Hampton, VA 23665

Dr. Roland R. Mielke
Old Dominion University
Department of Electrical Engineering
Norfolk, VA 23508

Ernest W. Millen
M/S 156A
Langley Research Center
Hampton, VA 23665

Raymond C. Montgomery
M/S 161
Langley Research Center
Hampton, VA 23665

Kurt Moses
Bendix Corp., Flight Systems Division
Mailstop 2/8
Teterboro, NJ 07608

Martin T. Moul
104 Yorkview Road
Yorktown, VA 23692

Patrick C. Murphy
M/S 152A
Langley Research Center
Hampton, VA 23665

Wallace Nelson
Northrop Corporation
Org. 3833-85
1 Northrop Avenue
Hawthorne, CA 90250

Jerry R. Newsom
M/S 243
Langley Research Center
Hampton, VA 23665

D. W. Nixon
General Dynamics/Ft. Worth Division
P. O. Box 748, Mail Zone 2834
Fort Worth, TX 76101

Warren J. North
NASA Johnson Space Center
Houston, TX 77058

Aaron J. Ostroff
M/S 494
Langley Research Center
Hampton, VA 23665

Joe Pahle
NASA Dryden Flight Research Facility
P. O. Box 273
Edwards, CA 93523

Robert Palmer
Naval Air Development Center
Warminster, PA 18974

Richard S. Pappa
M/S 230
Langley Research Center
Hampton, VA 23665

Boyd Perry
M/S 243
Langley Research Center
Hampton, VA 23665

Lee Person
M/S 255A
Langley Research Center
Hampton, VA 23665

Richard H. Petersen
M/S 103A
Langley Research Center
Hampton, VA 23665

W. H. Phillips
M/S 152A
Langley Research Center
Hampton, VA 23665

Kenneth S. Pollock
M/S 125B
Langley Research Center
Hampton, VA 23665

Joseph Post
Sikorsky Aircraft
N. Main Street
Stratford, CT

Anthony S. Pototsky
Kentron
3221 N. Armistead Avenue
Hampton, VA 23666

David W. Potts
AFWAL/FIGL
ASD/AFWAL/FIGL
WPAFB, OH 45433

Douglas B. Price
M/S 152A
Langley Research Center
Hampton, VA 23665

Shepherd G. Pryor III
Lockheed-Georgia Company
86 S. Cobb Drive
Marietta, GA 30063

J. K. Ramage
WPAFB, OH 45433

Perry N. Rea
5 Willowood Drive, #204
Hampton, VA 23666

W. H. Reed III
Dynamic Engineering Inc.
703 Middle Ground Blvd
Newport News, VA 23606

Dr. Herman A. Rediess
Vice President Systems Engr. Div.
HR Textron, Inc.
2485 McCabe Way
Irvine, CA 92714

Philip A. Roberts
U.S. Air Force
9301 Harness Horse Court
Springfield, VA 22153

John D. Rollins
M/S 125B
Langley Research Center
Hampton, VA 23665

Harold M. Rosenbaum
Northrop Corporation
8900 E. Washington Boulevard
E743/1S
Pico Rivera, CA 90660-3737

Dr. J. Roskam
The University of Kansas
Rt. 4 Box 274
Ottawa, KS 66067

Irving Ross
Hydraulic Units, Inc.
1700 Business Center Drive
Duarte, CA 91010

Edmund G. Rynaski
Flight Sciences Branch
Research Department
ARVIN/CALSPAN
P.O. Box 400
Buffalo, NY 14225

Peter Sadler
Lockheed-Georgia Company
Marietta, GA 30063

Himankush Saha
462 Lost Rock Drive
Webster, TX 77598

Philip W. Saunders
Northrop Corporation
824 E. Grand Avenue, #7
El Segundo, CA 90245

Sue Sawyer
Sperry Systems Management
3217 N. Armistead Avenue
Hampton, VA 23666

Frederick W. Schaefer
Grumman
729 Riviera
Mastic Beach, NY 11951

Mr. Richard Schoenman
The Boeing Company
Commercial Airplane Company
Box 3707 (M.S. 77-19)
Seattle, WA 98124

Purdue Univeristy
David K. Schmidt
Dept. of Aeronautics and
Astronautics
West Lafayette, IN 47907

Ted Schulman
Northrop
621 8th Street
Hermosa Beach, CA 90254

Robert C. Schwanz
Flight Mechanics Laboratory
Wright Patterson AFB
WPAFB, OH 45433

Albert A. Schy
M/S 161
Langley Research Center
Hampton, VA 23665

John D. Shaughnessy
M/S 152E
Langley Research Center
Hampton, VA 23665

Sahjendra N. Singh
M/S 161
Langley Research Center
Hampton, VA 23665

Charles A. Skira
USAF
AFWAL/POTC
WPAFB, OH 45433

Steven M. Sliwa
M/S 152A
Langley Research Center
Hampton, VA 23665

Capt. John D. Smith
6340 Americana Drive, Apt. 702
Clarendon Hills, IL 60514

Paul M. Smith
Kentron Technical Center
3221 N. Armistead Avenue
Hampton, VA 23666

Ronald H. Smith
M/S 247
Langley Research Center
Hampton, VA 23665

Richard K. Smyth
Milco International
15628 Graham Street
Huntington Beach, CA 92649

Cary R. Spitzer
M/S 472
Langley Research Center
Hampton, VA 23665

R. Srivatsan
University of Kansas at Langley
M/S 494
Langley Research Center
Hampton, VA 23665

George G. Steinmetz
M/S 156A
Langley Research Center
Hampton, VA 23665

James F. Stewart
NASA Dryden Flight Research Facility
P. O. Box 273
Edwards, CA 93523

William T. Suit
M/S 161
Langley Research Center
Hampton, VA 23665

N. Sundararajan
M/S 161
Langley Research Center
Hampton, VA 23665

David A. Tawfik
Director, Engineering
Flight System Division
Bendix Corporation
MC 2/10
Teterboro, NJ 07600

Lawrence W. Taylor, Jr.
M/S 161
Langley Research Center
Hampton, VA 23665

Glen J. Tauke
Lockheed-California Company
8509 Wyngate Street
Sunland, CA 91040

Sherwood H. Tiffany
M/S 152A
Langley Research Center
Hampton, VA 23665

Leonard Tobias
NASA Ames Research Center
Mailstop 210-9
Moffett Field, CA 94035

Ronald D. Toles
General Dynamics-Fort Worth Division
103 Valley Lane
Weatherford, TX 76086

Robert H. Tolson
M/S 103
Langley Research Center
Hampton, VA 23665

Charles N. Valade
M/S 125B
Langley Research Center
Hampton, VA 23665

Lena Valavani
L.I.D.S/M.I.T.
Rm. 35-437
Cambridge, MA 02139

Wallace E. Vander Velde
M.I.T.
77 Mass Avenue
Bldg. 33-109
Cambridge, MA 02139

V. Variakojis
Douglas Aircraft Company
Mail Code 36-49
3855 Lakewood Boulevard
Long Beach, CA 90846

Marlen Varnovitsky
Corporate R&D Center, General
Electric
Bldg. 5 Room 333C
Schenectady, NY 12301

Samuel L. Venneri
Langley Research Center
Hampton, VA 23665

Dan Vicroy
M/S 156A
Langley Research Center
Hampton, VA 23665

Robert von Husen
National Transportation Safety Board
1552 Coat Ridge Road
Herndon, VA 22070

Thomas A. Waldeck
Boeing Wichita
3517 E. Skinner
Wichita, KS 67218

Raymond M. Wallace
United Technologies Research Center
Silver Lane
E. Hartford, CT 06108

James F. Watson
Engineering Incorporated
41 Research Drive
Hampton, VA 23666

Joe Whiting
Sperry Systems Management
3217 N. Armistead Avenue
Hampton, VA 23666

Carol Wieseman
M/S 243
Langley Research Center
Hampton, VA 23665

Craig S. Willey
Lockheed California Company
P. O. Box 551
Burbank, CA 91520

James L. Williams
M/S 161
Langley Research Center
Hampton, VA 23665

Charles M. Wilson
U.S. Air Force
6510 TW/TEG
Mail Stop 256
Edwards AFB, CA 93523

Yuk K. Woo
U.S. Air Force
6510 TW/TEG
Mail Stop 236
Edwards AFB, CA 93523

John H. Wykes
North American Aircraft Operation
Rockwell International
P.O. Box
Los Angeles, CA 90009

N84
20568

UNCLAS

N84 20568

NASA CONTROL RESEARCH OVERVIEW

Duncan E. McIver
NASA Headquarters
Washington, DC

First Annual NASA Aircraft Controls Workshop
NASA Langley Research Center
Hampton, Virginia
October 25-27, 1983

INTRODUCTION

The intent of this presentation is to provide an overview of NASA research activities related to the control of aeronautical vehicles. A groundwork is laid by showing the organization at NASA Headquarters for supporting programs and providing funding. Then a synopsis of many of the ongoing activities is presented, some of which will be presented in greater detail elsewhere. A major goal of the workshop is to provide a showcase of ongoing NASA-sponsored research. Then, through the panel sessions and conversations with workshop participants, it is hoped to glean a focus for future directions in aircraft controls research.

OFFICE OF AERONAUTICS AND SPACE TECHNOLOGY'S GOAL

The Office of Aeronautics and Space Technology, which sponsors most of the controls-oriented research for aircraft, publishes a long-range plan. The overall goal is stated in figure 1. Notice that the purpose of NASA's program in space and aeronautics is to continue to be long-term contributors toward the continued preeminence of the U. S. in civil and military aerospace activities.

STRENGTHEN THE AGENCY'S AERONAUTICS AND ADVANCED SPACE R&T PROGRAMS AS EFFECTIVE, PRODUCTIVE, AND LONG-TERM CONTRIBUTORS TOWARD THE CONTINUED PREEMINENCE OF U.S. IN CIVIL AND MILITARY AEROSPACE

Figure 1

HIGH-PRIORITY TECHNICAL GOALS/THRUST

Figure 2 shows the high-priority technical goals of OAST. It includes all the major thrusts proposed by OAST for the next 5 to 10 years. Ones of specific interest to the controls discipline are item 4, realize the full potential of advancing technologies for aircraft controls, guidance, and flight systems; item 7, provide technology to enhance flight management and crew effectiveness in aircraft operations and air traffic control systems; and, item 8, provide the technology base for exploitation of the use of modern computers in aeronautics. Other areas relate in terms of systems integration in an interdisciplinary nature. However, those three have generic and specific applications for aeronautical controls.

- BRING EXTERNAL AND INTERNAL COMPUTATIONAL FLUID DYNAMICS TO STATE OF PRACTICAL APPLICATION TO AIRCRAFT AND ENGINE DESIGN
- SIGNIFICANTLY REDUCE AIRCRAFT VISCOUS DRAG OVER THE FULL SPEED RANGE AND IMPROVE THE UNDERSTANDING OF REYNOLDS NUMBER EFFECTS AT TRANSONIC SPEEDS
- REALIZE THE FULL POTENTIAL OF COMPOSITE MATERIALS FOR PRIMARY STRUCTURES IN CIVIL AND MILITARY AIRCRAFT
- REALIZE THE FULL POTENTIAL OF ADVANCING TECHNOLOGIES FOR AIRCRAFT CONTROLS, GUIDANCE, AND FLIGHT SYSTEMS
- PROVIDE TECHNOLOGY ADVANCES TO EXPLOIT THE FULL POTENTIAL OF ROTORCRAFT FOR MILITARY AND CIVIL APPLICATION

Figure 2

HIGH-PRIORITY TECHNICAL GOALS

- PROVIDE TECHNOLOGY FOR AND FULLY SUPPORT THE DEVELOPMENT OF ADVANCED MILITARY AIRCRAFT AND MISSILE SYSTEMS
- PROVIDE TECHNOLOGY TO ENHANCE FLIGHT MANAGEMENT AND CREW EFFECTIVENESS IN AIRCRAFT OPERATIONS AND AIR TRAFFIC CONTROL SYSTEMS
- PROVIDE THE TECHNOLOGY BASE FOR EXPLOITATION OF THE USE OF MODERN COMPUTERS IN AERONAUTICS
- EXPLOIT THE FULL POTENTIAL OF HIGHLY INTEGRATED PROPULSION AIRFRAME SYSTEMS
- ADVANCE THE TECHNOLOGY FOR SMALL TURBINE ENGINES TO A LEVEL COMPARABLE WITH THAT OF LARGE TURBINE ENGINES
- ESTABLISH THE TECHNICAL FEASIBILITY OF HIGH-SPEED TURBOPROP PROPULSION
- PROVIDE COMPONENT TECHNOLOGY ADVANCES FOR FUEL-EFFICIENT SUBSONIC TRANSPORT ENGINES
- PROVIDE SAFETY TECHNOLOGY FOR IMPROVED DESIGN AND OPERATION OF CURRENT, ADVANCED CIVIL AND MILITARY AIRCRAFT AND SYSTEMS

Figure 2 (Concluded)

NASA ORGANIZATION

The overall organization of NASA is shown in figure 3. Most of the aircraft controls research is performed through the Office for Aeronautics and Space Technology (OAST). The three field centers supported by OAST's program are Ames, Langley, and Lewis. Although diverse activities occur at all three centers, each center is usually charged with a number of lead roles for specific research thrusts.

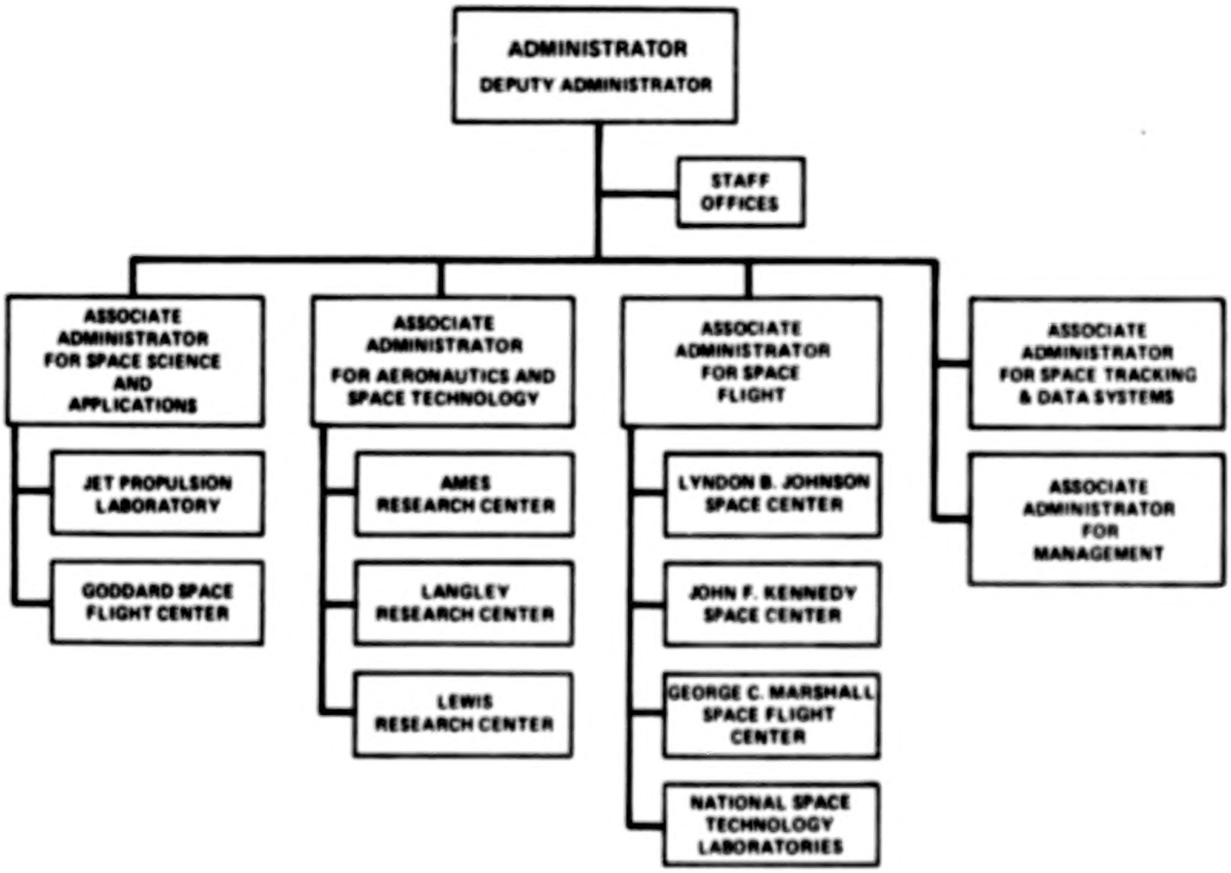
ADMINISTRATOR
DEPUTY ADMINISTRATOR
STAFF OFFICES
ASSOCIATE ADMINISTRATOR FOR SPACE SCIENCE AND APPLICATIONS
JET PROPULSION LABORATORY
GODDARD SPACE FLIGHT CENTER
ASSOCIATE ADMINISTRATOR FOR AERONAUTICS AND SPACE TECHNOLOGY
AMES RESEARCH CENTER
LANGLEY RESEARCH CENTER
LEWIS RESEARCH CENTER
ASSOCIATE ADMINISTRATOR FOR SPACE FLIGHT
LYNDON B. JOHNSON SPACE CENTER
JOHN F. KENNEDY SPACE CENTER
GEORGE C. MARSHALL SPACE FLIGHT CENTER
NATIONAL SPACE TECHNOLOGY LABORATORIES
ASSOCIATE ADMINISTRATOR FOR SPACE TRACKING & DATA SYSTEMS
ASSOCIATE ADMINISTRATOR FOR MANAGEMENT

Figure 3

OAST ORGANIZATION

The OAST organization at NASA Headquarters is depicted in figure 4. Aircraft controls are sponsored in both the Aerospace Research Division (Code RT) and in the Aeronautical Systems Division (Code RJ). In code RT the research is usually of a general nature and could be applied to several vehicles or categories of vehicles. The Controls and Human Factors Branch administers research programs for Applied Control Theory and Analysis, Flight Crucial/Fault-Tolerant Controls and Guidance, Spacecraft Controls and Guidance, Flight Management, Flight Simulation Technology, and Space Human Factors. Code RJ sponsors vehicle specific research in each of the indicated areas. Code RJ research often results in a wind tunnel or flight research test of a specific configuration. One way of viewing the organization is that as the generic research of code RT matures it is picked up by code RJ-type programs for validation and fine tuning for specific applications. If fundamental problems are encountered during the vehicle specific research of code RJ, it identifies an area for more effort for code RT.

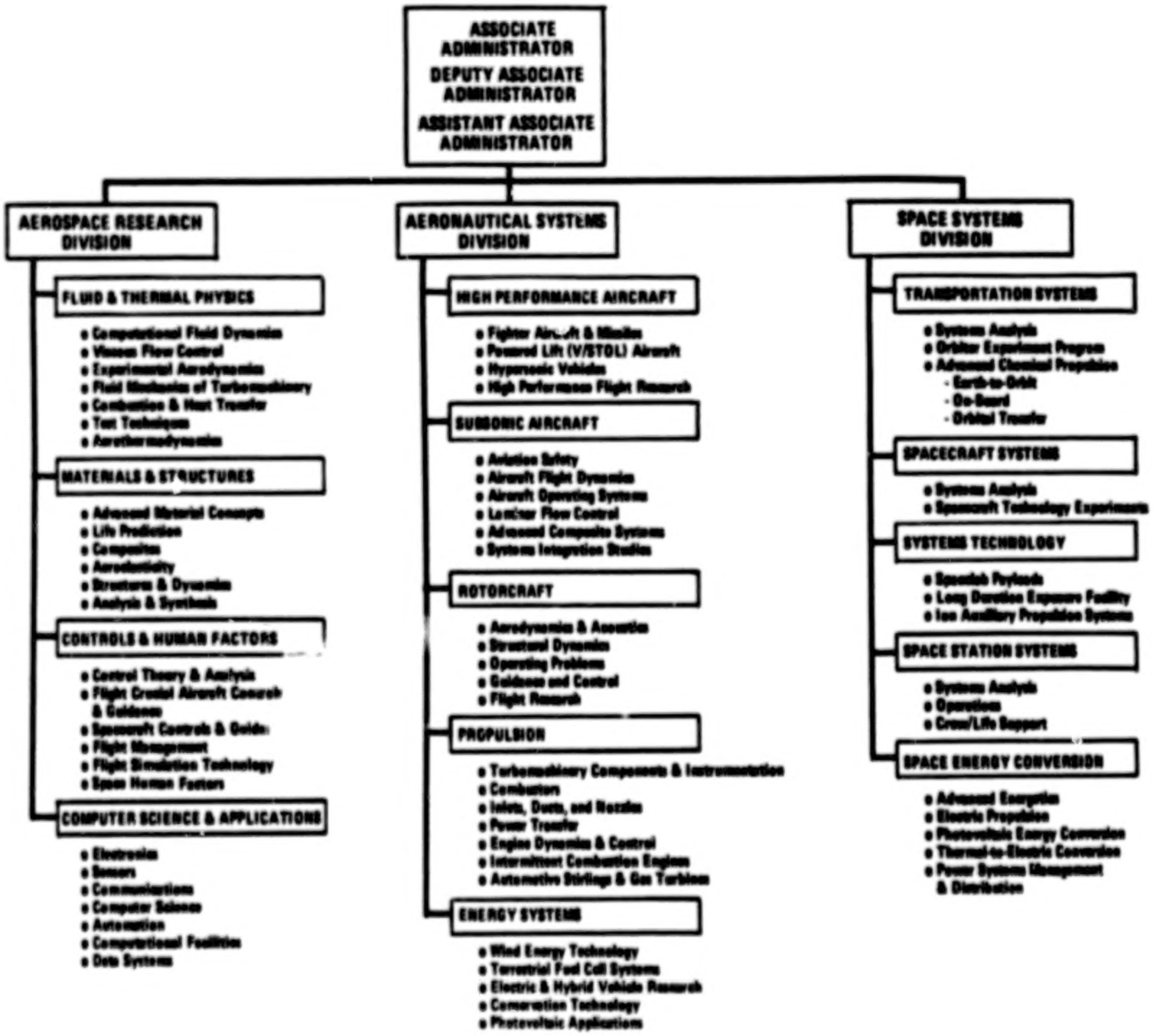
ASSOCIATE ADMINISTRATOR
DEPUTY ASSOCIATE ADMINISTRATOR
ASSISTANT ASSOCIATE ADMINISTRATOR
AEROSPACE RESEARCH DIVISION
FLUID & THERMAL PHYSICS
• Computational Fluid Dynamics
• Viscous Flow Control
• Experimental Aerodynamics
• Fluid Mechanics of Turbomachinery
• Combustion & Heat Transfer
• Test Techniques
• Aerothermodynamics
MATERIALS & STRUCTURES
• Advanced Material Concepts
• Life Prediction
• Composites
• Aeroelasticity
• Structures & Dynamics
• Analysis & Synthesis
CONTROLS & HUMAN FACTORS
• Control Theory & Analysis
• Flight Crucial Aircraft Controls & Guidance
• Spacecraft Controls & Guidance
• Flight Management
• Flight Simulation Technology
• Space Human Factors
COMPUTER SCIENCE & APPLICATIONS
• Electronics
• Sensors
• Communications
• Computer Science
• Automation
• Computational Facilities
• Data Systems
AERONAUTICAL SYSTEMS DIVISION
HIGH PERFORMANCE AIRCRAFT
• Fighter Aircraft & Missiles
• Powered Lift (V/STOL) Aircraft
• Hypersonic Vehicles
• High Performance Flight Research
SUBSONIC AIRCRAFT
• Aviation Safety
• Aircraft Flight Dynamics
• Aircraft Operating Systems
• Laminar Flow Control
• Advanced Composite Systems
• Systems Integration Studies
ROTORCRAFT
• Aerodynamics & Acoustics
• Structural Dynamics
• Operating Problems
• Guidance and Control
• Flight Research
PROPULSION
• Turbomachinery Components & Instrumentation
• Combustors
• Inlets, Ducts, and Nozzles
• Power Transfer
• Engine Dynamics & Control
• Intermittent Combustion Engines
• Automotive Stirlings & Gas Turbines
ENERGY SYSTEMS
• Wind Energy Technology
• Terrestrial Fuel Cell Systems
• Electric & Hybrid Vehicle Research
• Conservation Technology
• Photovoltaic Applications
SPACE SYSTEMS DIVISION
TRANSPORTATION SYSTEMS
• Systems Analysis
• Orbiter Experiment Program
• Advanced Chemical Propulsion
- Earth-to-Orbit
- On-Board
- Orbital Transfer
SPACECRAFT SYSTEMS
• Systems Analysis
• Spacecraft Technology Experiments
SYSTEMS TECHNOLOGY
• Spacelab Payloads
• Long Duration Exposure Facility
• Ion Auxiliary Propulsion Systems
SPACE STATION SYSTEMS
• Systems Analysis
• Operations
• Crew/Life Support
SPACE ENERGY CONVERSION
• Advanced Energetics
• Electric Propulsion
• Photovoltaic Energy Conversion
• Thermal-to-Electric Conversion
• Power Systems Management & Distribution

Figure 4

AIRCRAFT CONTROLS AND GUIDANCE

The three main areas of research sponsored by the Controls and Human Factors Office in the areas of aircraft controls and guidance are: applied control theory, flight-crucial systems, and flight path management and guidance (fig. 5). The goal of the applied control theory research is to provide the general tools for designing active control systems for many categories of aircraft. The flight-crucial systems research is attempting to develop analytical and mathematical models for ascertaining the validity and probability of failure of electronic active control systems and avionics in general. The overall goal is to provide a methodology for designing and verifying electronic active control systems which have the reliability of primary structural surfaces. The flight path guidance research program is aimed at providing fuel-efficient trajectories for commercial transports, time-optimal intercept guidance for tactical aircraft, and new enhanced display media for improving the cockpit environment.

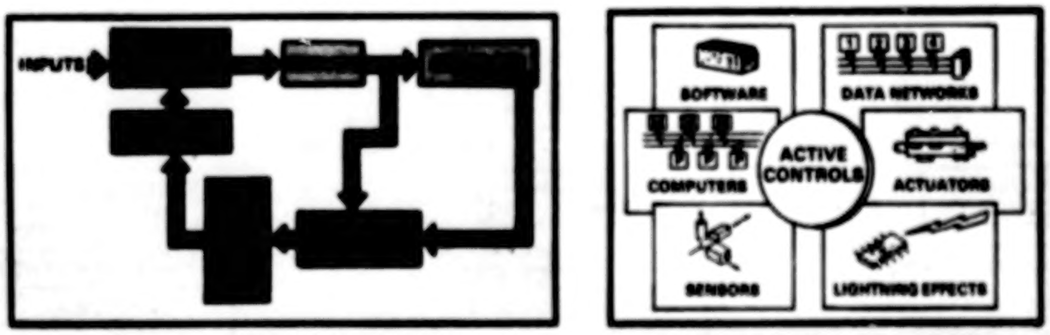

APPLIED CONTROL THEORY

FLIGHT CRUCIAL SYSTEMS

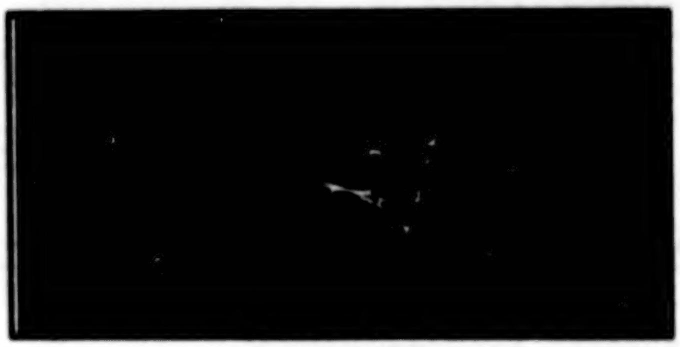

FLIGHT PATH

Figure 5

ACTIVE CONTROL TECHNOLOGY

Active control research at NASA embodies many important elements (fig. 6). There is a significant effort involved in the development of synthesis tools for control laws which account for structural flexibility. Several different approaches are being investigated. The control system designs are then evaluated using a variety of analysis tools. Successful candidates are then tested in the wind tunnel or in flight. This process provides a validation of synthesis techniques, analysis tools, and experimental facilities. The goal of active controls research is to improve mission effectiveness by reducing weight, increasing performance, and enhancing passenger acceptance.

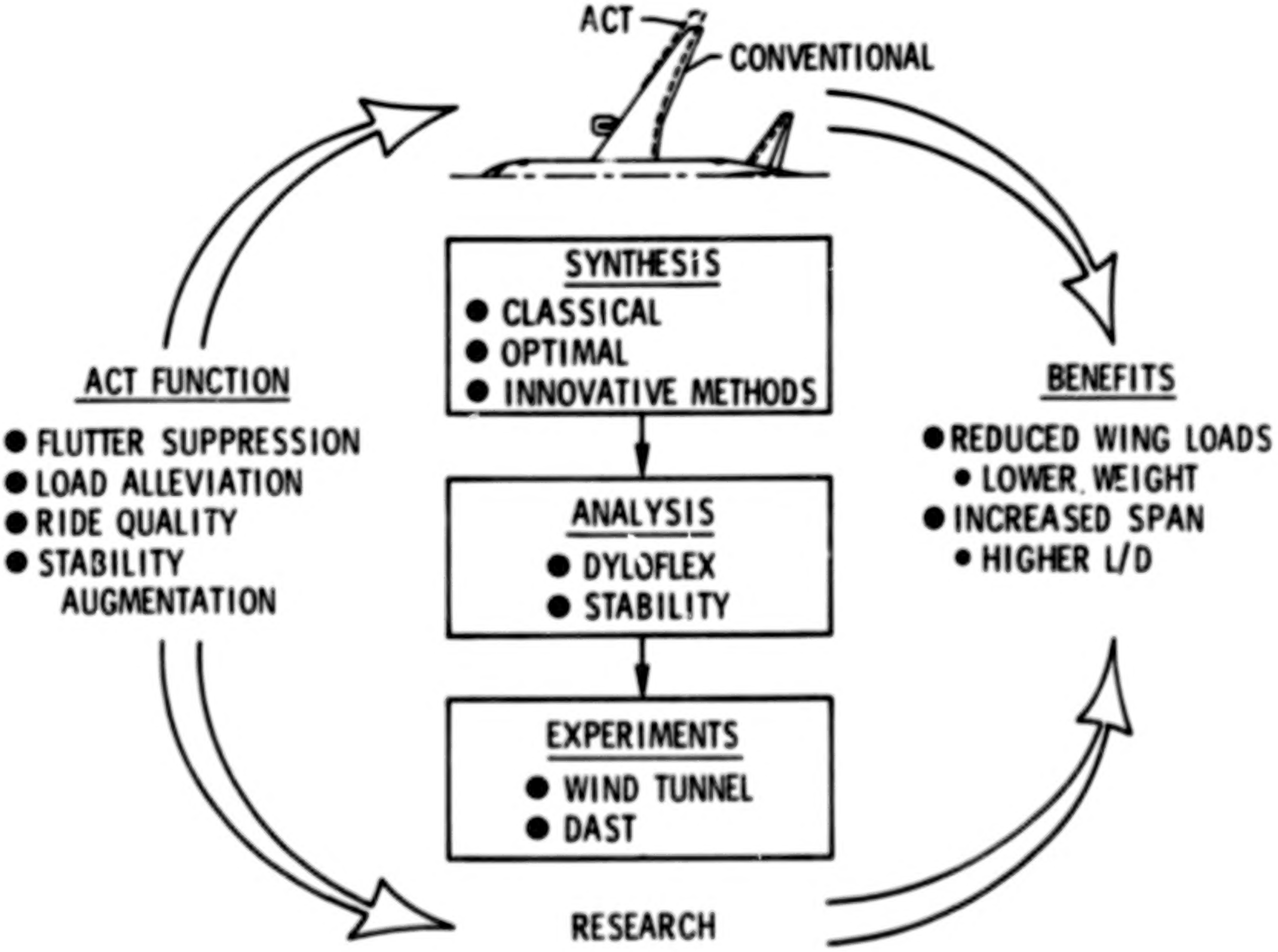
ACT
CONVENTIONAL
SYNTHESIS
● CLASSICAL
● OPTIMAL
● INNOVATIVE METHODS
ACT FUNCTION
● FLUTTER SUPPRESSION
● LOAD ALLEVIATION
● RIDE QUALITY
● STABILITY AUGMENTATION
BENEFITS
● REDUCED WING LOADS
• LOWER WEIGHT
● INCREASED SPAN
• HIGHER L/D
ANALYSIS
● DYLOFLEX
● STABILITY
EXPERIMENTS
● WIND TUNNEL
● DAST
RESEARCH

Figure 6

PARAMETER ESTIMATION

Parameter estimation is an important part of the control research program (fig. 7). Control system performance is greatly enhanced by having the most accurate model of the aircraft possible. Modelling work includes linear and nonlinear analysis of general aviation, commercial transport, and tactical aircraft. Recent cooperative agreements for exchange of data and information with Boeing and with Israel serve to illustrate the importance such work has in the eye of industry and the role that NASA plays in this area.

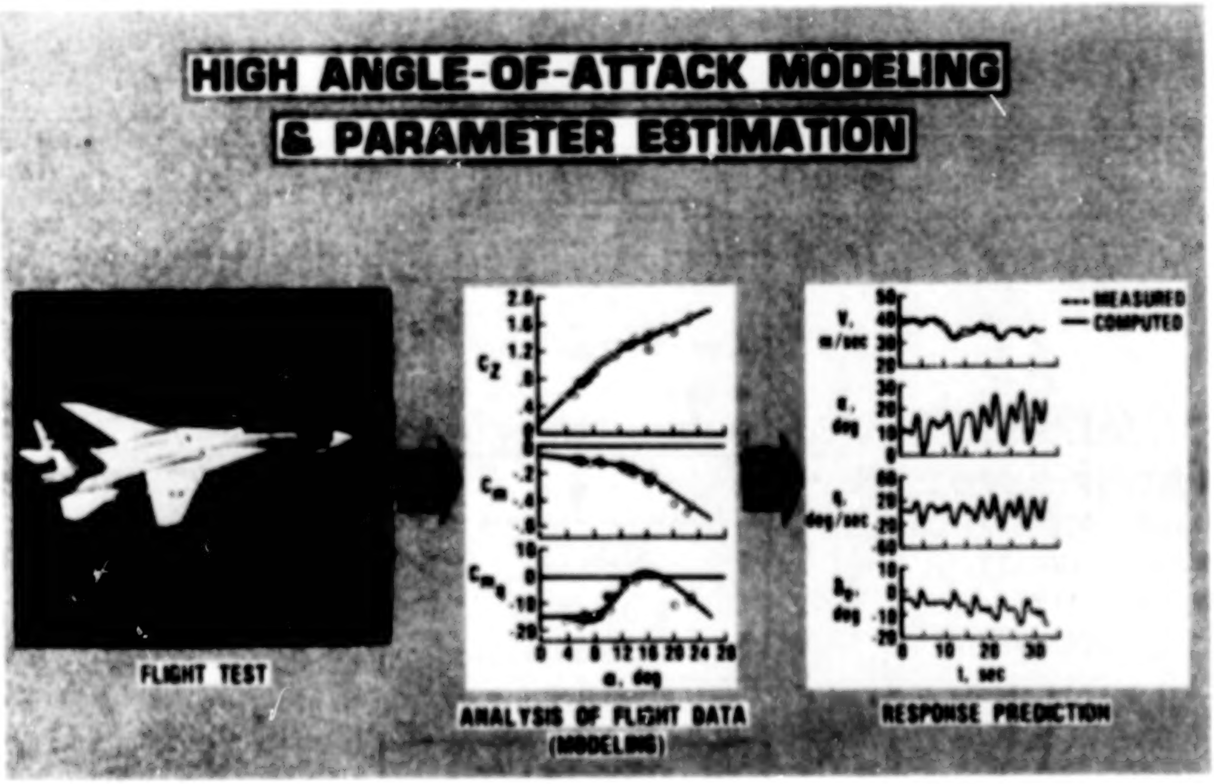

HIGH ANGLE-OF-ATTACK MODELING
& PARAMETER ESTIMATION

FLIGHT TEST

ANALYSIS OF FLIGHT DATA
(MODELING)

RESPONSE PREDICTION

Figure 7

FAULT-TOLERANT COMPUTERS

Research for fault-tolerant computers is the prime focus of the flight-crucial controls program (fig. 8). Two pioneering computer concepts have been constructed. The SIFT (Software Implemented Fault Tolerance) computer and the FTMP (Fault-Tolerant Multi-Processor) computer are currently undergoing evaluation in AIRLAB (Avionics Integration Research Laboratory). It is hoped that the experience gained with studying these concepts will provide an ultimate system reliability that has a probability of failure per flight hour of less than 10^{-9}.

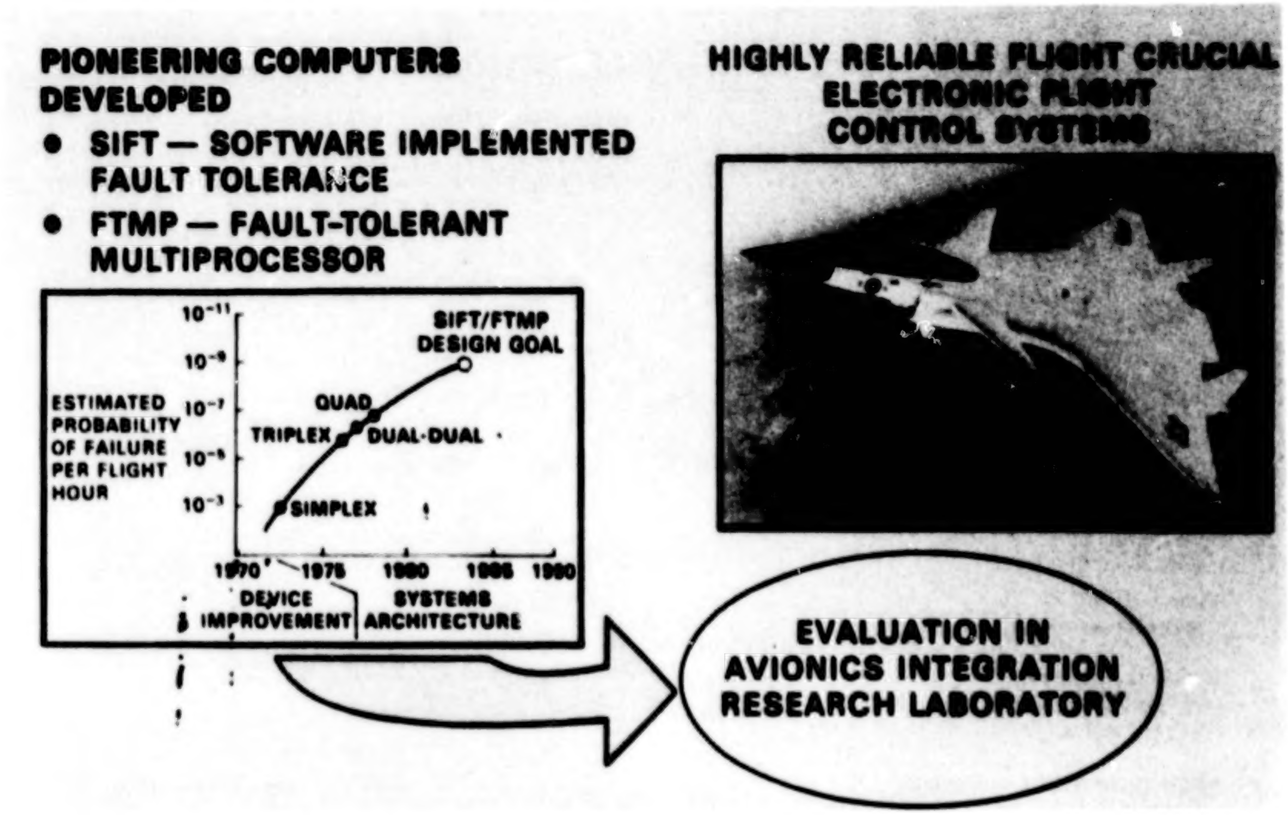

PIONEERING COMPUTERS DEVELOPED

- SIFT — SOFTWARE IMPLEMENTED FAULT TOLERANCE
- FTMP — FAULT-TOLERANT MULTIPROCESSOR

HIGHLY RELIABLE FLIGHT CRUCIAL ELECTRONIC FLIGHT CONTROL SYSTEMS

EVALUATION IN AVIONICS INTEGRATION RESEARCH LABORATORY

ESTIMATED PROBABILITY OF FAILURE PER FLIGHT HOUR
10^{-11}
10^{-9}
10^{-7}
10^{-5}
10^{-3}
SIFT/FTMP DESIGN GOAL
QUAD
TRIPLEX
DUAL-DUAL
SIMPLEX
1970
1975
1980
1985
1990
DEVICE IMPROVEMENT
SYSTEMS ARCHITECTURE

Figure 8

AIRLAB

AIRLAB (fig. 9) is a new facility which brings online an impressive set of capabilities for performing fault-tolerant research. System transient response and recovery rates are investigated during the injection of artificial faults at the gate, component, and functional levels. Through the study of actual state-of-the-art concepts physically located at AIRLAB, the development of analytical models and emulation methods are a near-term objective. With tools available for analyzing architectures and hardware component selection, design methodologies can be developed. Additionally, new efforts are underway to model and understand software reliability.

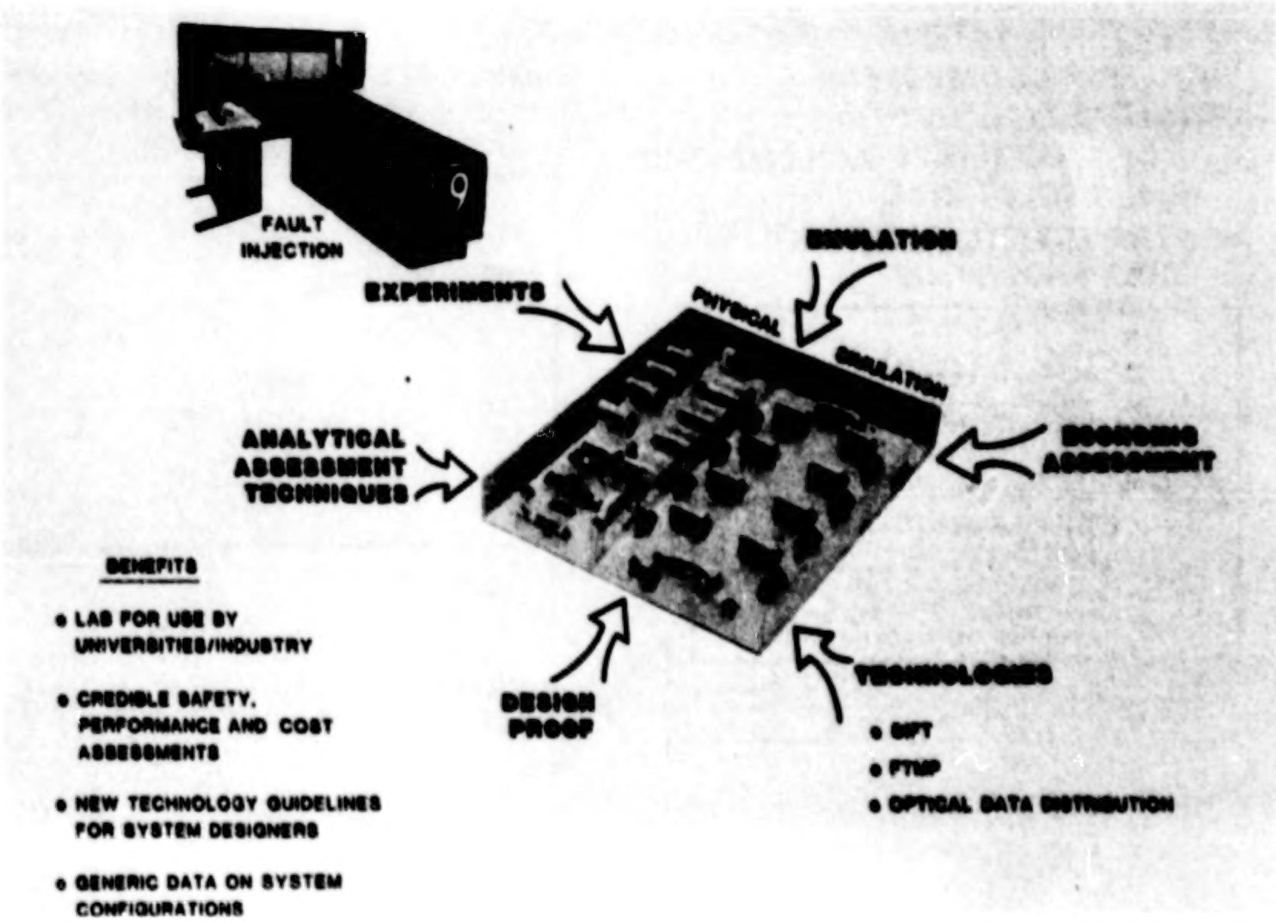
FAULT INJECTION
EMULATION
EXPERIMENTS
PHYSICAL
EMULATION
ANALYTICAL ASSESSMENT TECHNIQUES
ECONOMIC ASSESSMENT
BENEFITS
• LAB FOR USE BY UNIVERSITIES/INDUSTRY
• CREDIBLE SAFETY, PERFORMANCE AND COST ASSESSMENTS
• NEW TECHNOLOGY GUIDELINES FOR SYSTEM DESIGNERS
• GENERIC DATA ON SYSTEM CONFIGURATIONS
DESIGN PROOF
TECHNOLOGIES
• SIFT
• FTMP
• OPTICAL DATA DISTRIBUTION

Figure 9

CONTROLS AND GUIDANCE--FLIGHT PATH GUIDANCE

In the area of flight path guidance (fig. 10) there is research in three major segments underway. Tools for computing optimal guidance laws for transport, V/STOL, rotorcraft, and tactical aircraft are being refined. Current emphasis is on trying to integrate such concepts into the air traffic control (ATC) system and provide 4-D traffic flow management. Additionally, there is an effort to develop advanced display media concepts for cockpits of the future.

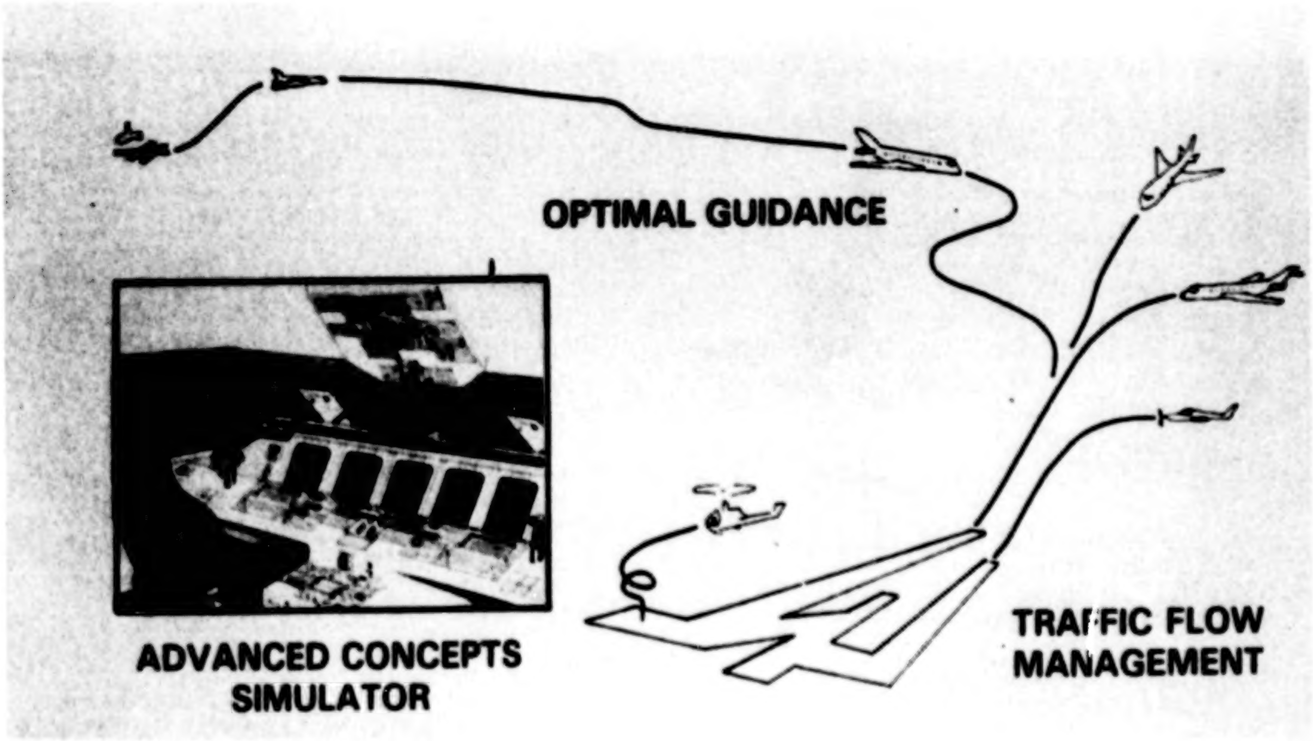
OPTIMAL GUIDANCE
ADVANCED CONCEPTS SIMULATOR
TRAFFIC FLOW MANAGEMENT

Figure 10

COCKPIT AVIONICS PROGRAM

Cockpit avionics research (fig. 11) in the controls and guidance program emphasizes the development of advanced display concepts. The prime users of this research will be the avionics manufacturers. Active areas of research include advanced display media, display generation techniques, data input/output technology, and cockpit systems integration. The goal of most research is toward thin panels which are required for the "All-Glass Cockpit" concept where electromechanical display devices are replaced by computer-generated images. It should be noted that the human factors research program at NASA is cooperating with industry in developing fundamental guidelines for deciding what should be displayed to the pilots.

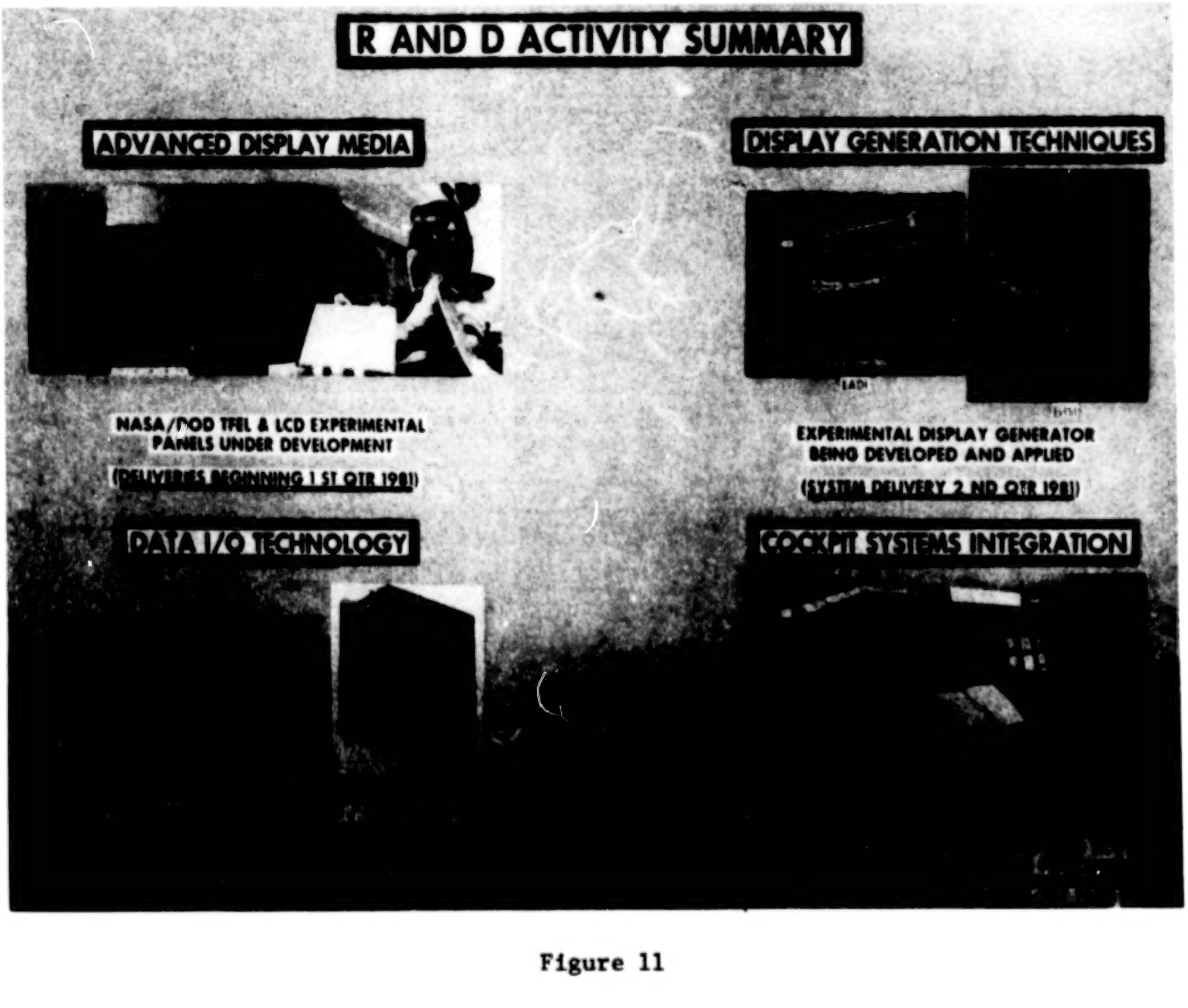

R AND D ACTIVITY SUMMARY

ADVANCED DISPLAY MEDIA

NASA/DOD TFEL & LCD EXPERIMENTAL PANELS UNDER DEVELOPMENT

(DELIVERIES BEGINNING 1 ST QTR 1981)

DISPLAY GENERATION TECHNIQUES

EXPERIMENTAL DISPLAY GENERATOR BEING DEVELOPED AND APPLIED

(SYSTEM DELIVERY 2 ND QTR 1981)

DATA I/O TECHNOLOGY

COCKPIT SYSTEMS INTEGRATION

Figure 11

VEHICLE SPECIFIC CONTROLS AND GUIDANCE TECHNOLOGY

Up to now, most of the research that was described was sponsored by the Aerospace Research Division at NASA Headquarters and represents vehicle independent or generic developments. Figure 12 shows some of the vehicle specific research that is sponsored by the Aeronautical Systems Division at NASA Headquarters. Active controls research is performed in transport, general aviation, high-performance, V/STOL, and rotorcraft classes of airplanes. A natural development process would be the development of general design tools which are then used to synthesize control systems for a specific vehicle. The direct application to a particular problem and the experience gained can be used to refocus research in control theory as new challenges are presented.

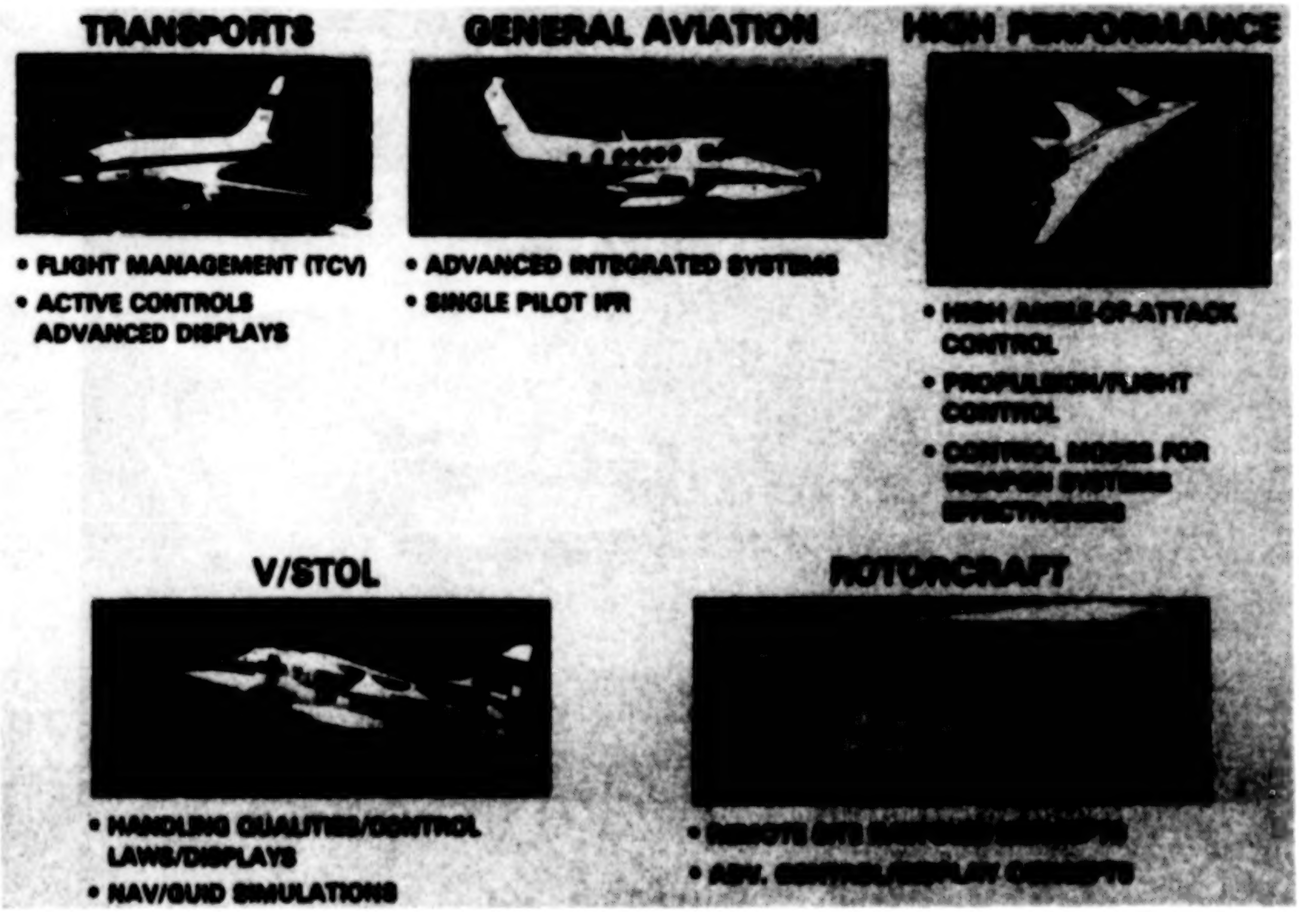

TRANSPORTS

- FLIGHT MANAGEMENT (TCV)
- ACTIVE CONTROLS ADVANCED DISPLAYS

GENERAL AVIATION

- ADVANCED INTEGRATED SYSTEMS
- SINGLE PILOT IFR

HIGH PERFORMANCE

- HIGH ANGLE-OF-ATTACK CONTROL
- PROPULSION/FLIGHT CONTROL
- CONTROL MODES FOR WEAPON SYSTEMS EFFECTIVENESS

V/STOL

- HANDLING QUALITIES/CONTROL LAWS/DISPLAYS
- NAV/GUID SIMULATIONS

ROTORCRAFT

- REMOTE SITE [illegible] CONCEPTS
- ADV. CONTROL/DISPLAY CONCEPTS

Figure 12

FLIGHT TEST OF ACTIVE CONTROLS TECHNOLOGY

NASA has had an aggressive program in cooperation with industry to investigate and demonstrate the application of active controls technology to commercial transports. One aspect of the program was a flight test demonstration of maneuver load alleviation and relaxed static stability on a Lockheed L-1011 (fig. 13). Analysis and piloted simulations of the technology were validated using the flight test results.

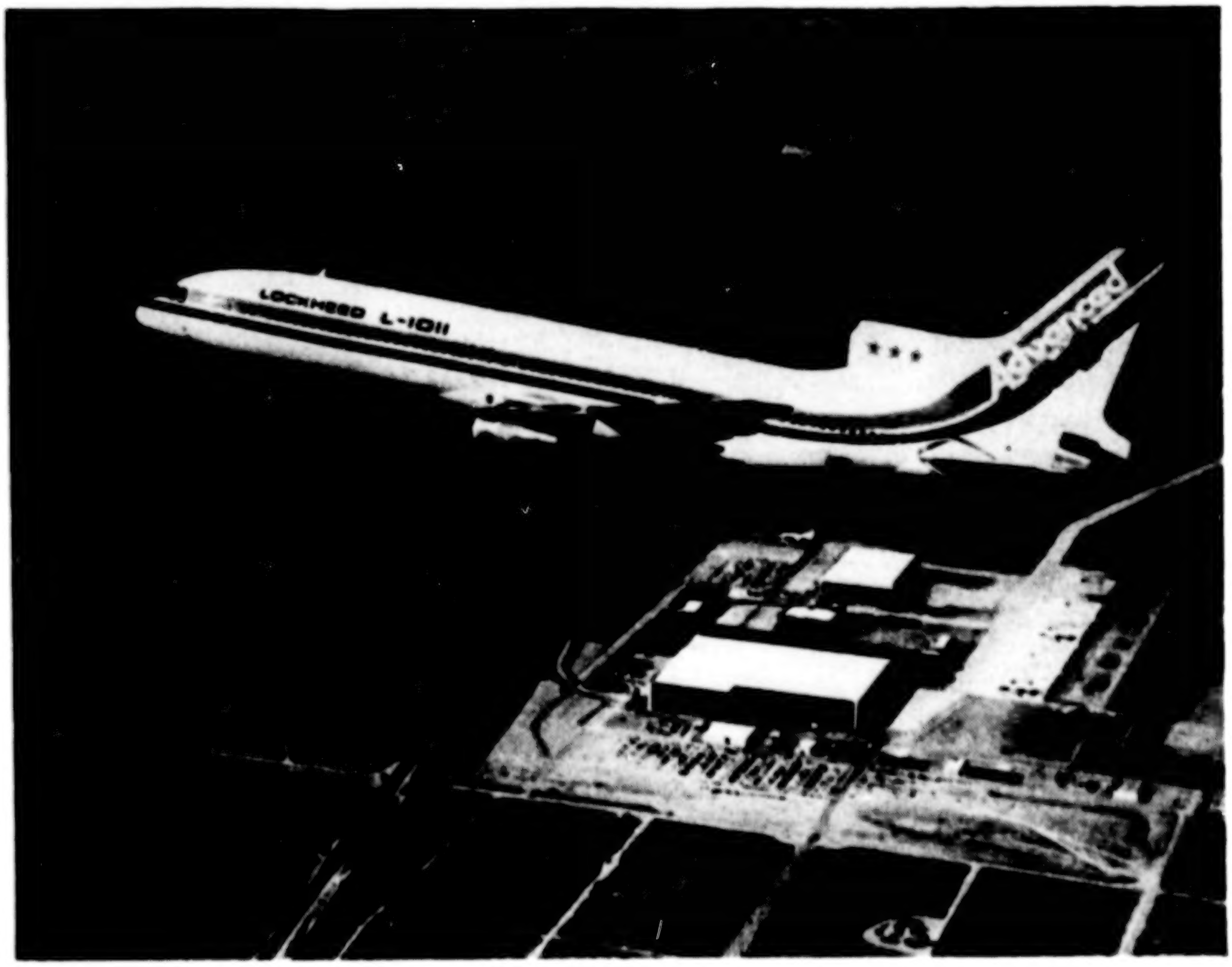

Figure 13

ROTORCRAFT CONTROLS RESEARCH

A number of controls activities are being focused upon V/STOL aircraft and rotorcraft (fig. 14). The nonlinear, inverse control theory presented in this conference was sponsored with generic controls research money. Now the tools that have been developed are being used to design control laws which are being flown on the NASA Ames UH-1H. This is a good example of the ideal flow of NASA research in controls: theory enhancement; tool development; simulation and analysis; followed by verification and validation through flight test.

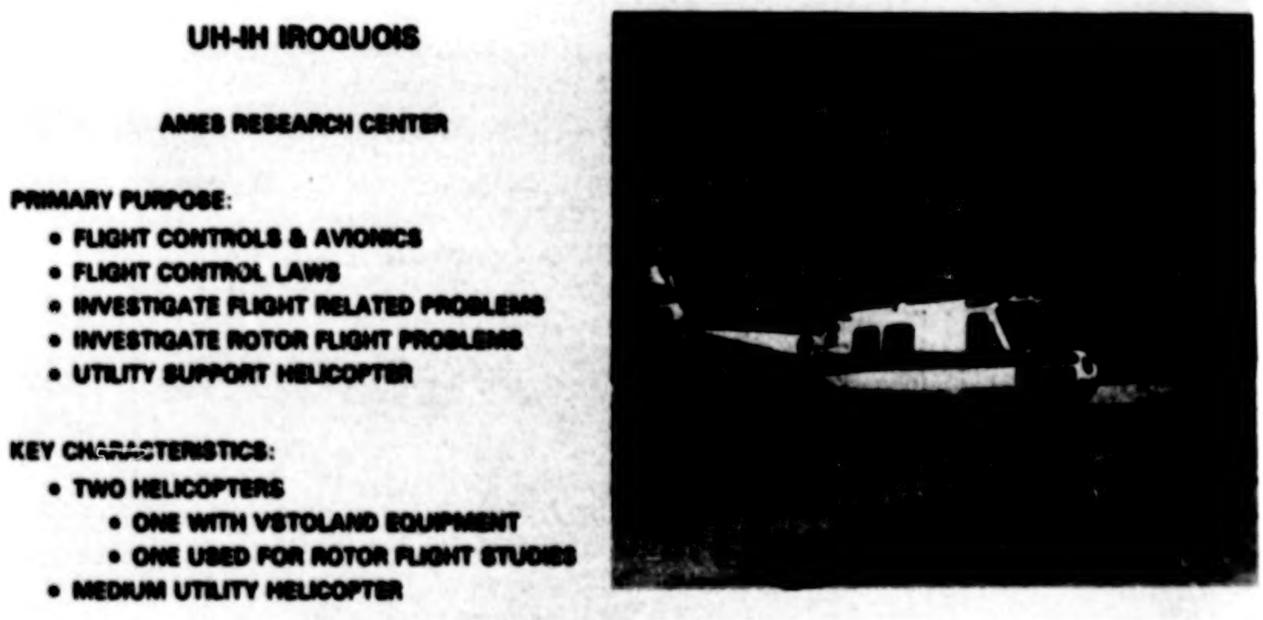

UH-1H IROQUOIS

AMES RESEARCH CENTER

PRIMARY PURPOSE:
- FLIGHT CONTROLS & AVIONICS
- FLIGHT CONTROL LAWS
- INVESTIGATE FLIGHT RELATED PROBLEMS
- INVESTIGATE ROTOR FLIGHT PROBLEMS
- UTILITY SUPPORT HELICOPTER

KEY CHARACTERISTICS:
- TWO HELICOPTERS
  - ONE WITH VSTOLAND EQUIPMENT
  - ONE USED FOR ROTOR FLIGHT STUDIES
- MEDIUM UTILITY HELICOPTER

Figure 14

AFTI/F-16 ADVANCED TEHCNOLOGIES

The AFTI/F-16 program (fig. 15) has joint military and NASA funding. It has been a tremendous success in terms of demonstrating what can be accomplished through the aggressive use of integrated controls technologies. The addition of vertical canards and multi-purpose trailing-edge flaps allowed the addition of new control modes including translational flight, nose pointing, and flat turns. Other systems concepts have been evaluated including voice command, heads-up displays, and multi-purpose advanced panel displays. Work is continuing with the evaluation of advanced combat and maneuvering systems taking advantage of the new operational control modes.

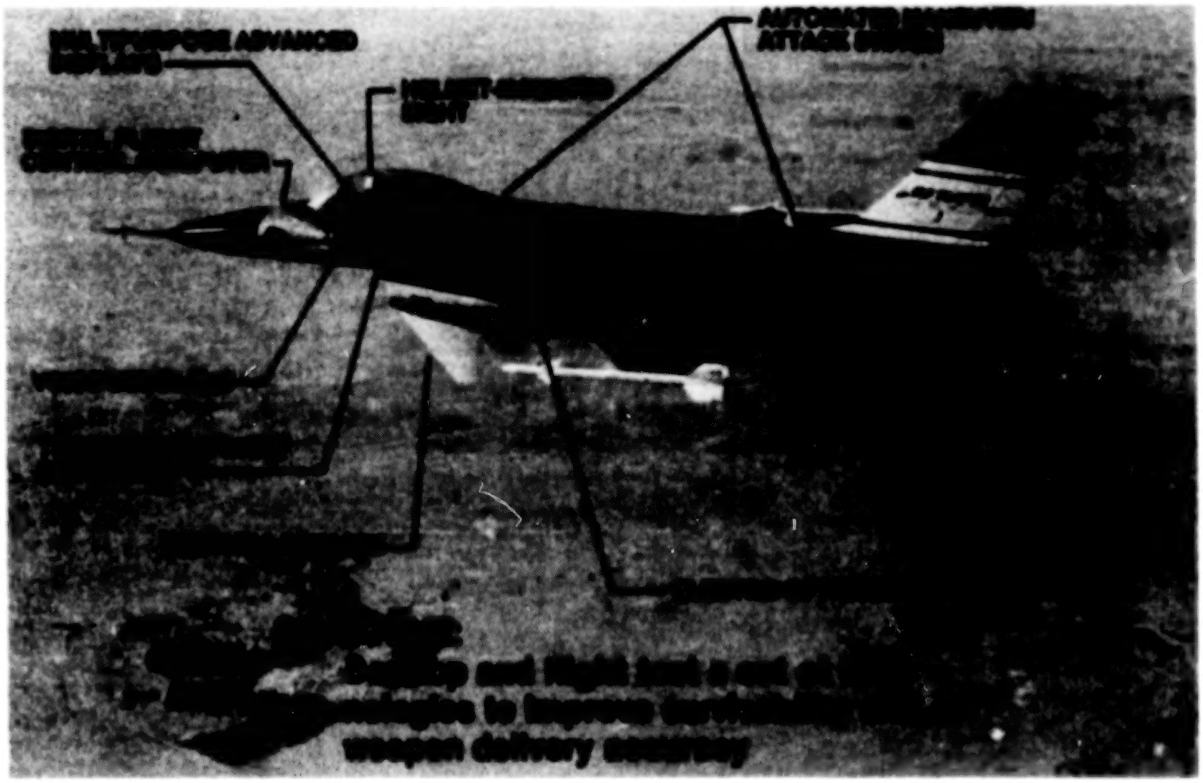
MULTIPURPOSE ADVANCED DISPLAYS
HELMET-MOUNTED SIGHT
DIGITAL FLIGHT CONTROL COMPUTER
AUTOMATED MANEUVERING ATTACK SYSTEM
Develop and flight test a set of
to improve
weapon delivery accuracy

Figure 15

HIGHLY MANEUVERABLE AIRCRAFT TECHNOLOGY (HiMAT)

The HiMAT technology demonstration program (fig. 16) has recently been completed and was jointly funded by the USAF and NASA. It was used to assess the effectiveness of integrated aircraft design with an emphasis on maximizing transonic maneuvering without compromising supersonic performance. Additionally, composites were used to aeroelastically tailor the lifting surfaces to allow deflection into optimal aerodynamic shape under any load. HiMAT is an RPV (Remotely Piloted Vehicle) which permitted the use of risky and advanced technologies in a flight vehicle at greatly reduced cost.

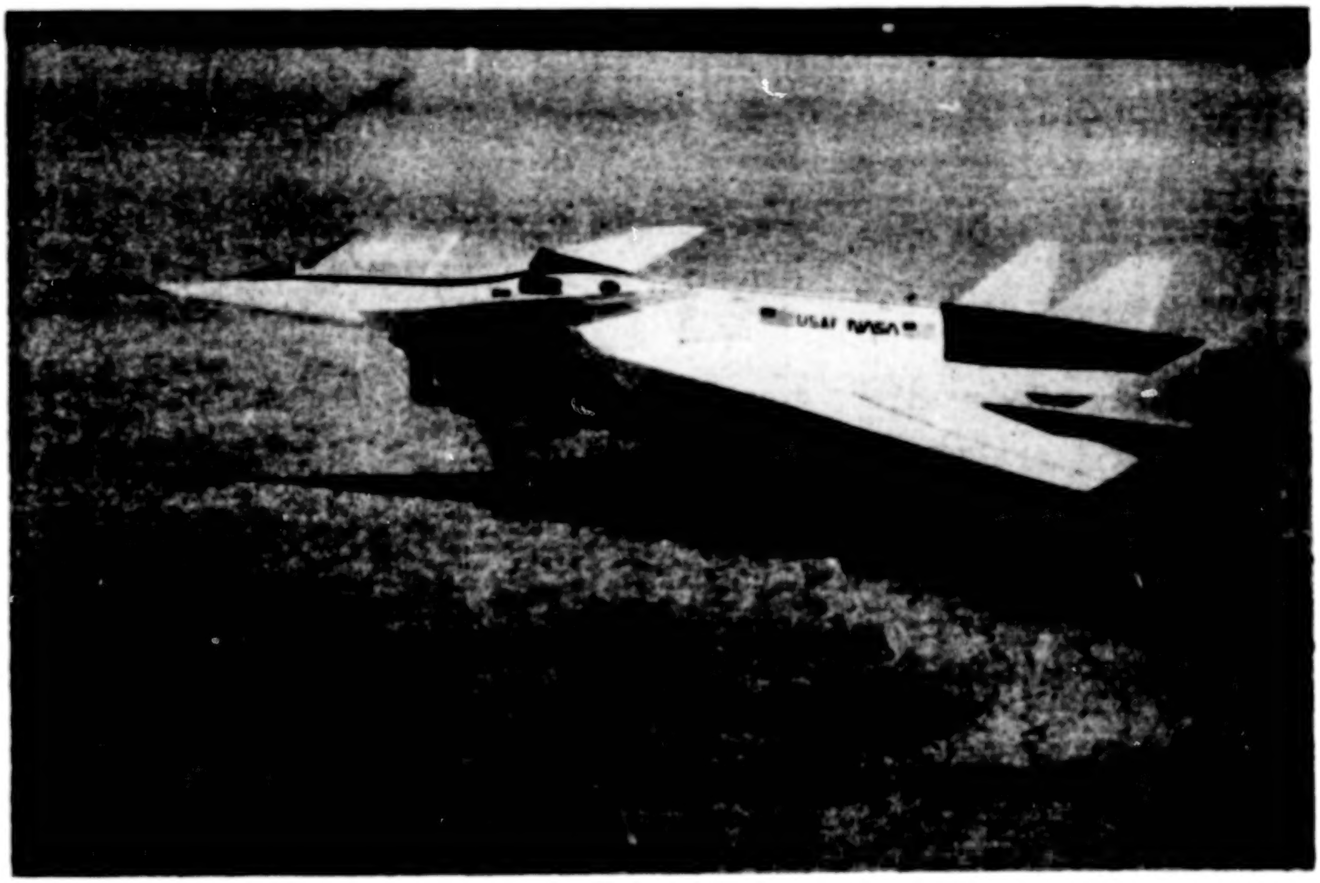

Figure 16

X-29A RESEARCH PROGRAM

Another joint program between DARPA, USAF, and NASA is the X-29A Flight Research Vehicle (fig. 17). It is being used to investigate aeroelastically tailored, forward-swept-wing technology. It features a closely coupled canard, multiple longitudinal control surfaces, and a static margin of 35 percent unstable. Because of these features, it has become a major technical challenge for the controls specialists. When the joint military/NASA flight tests have been completed, the aircraft will be retained by NASA and will be used for continuing flight research with respect to integrated control systems.

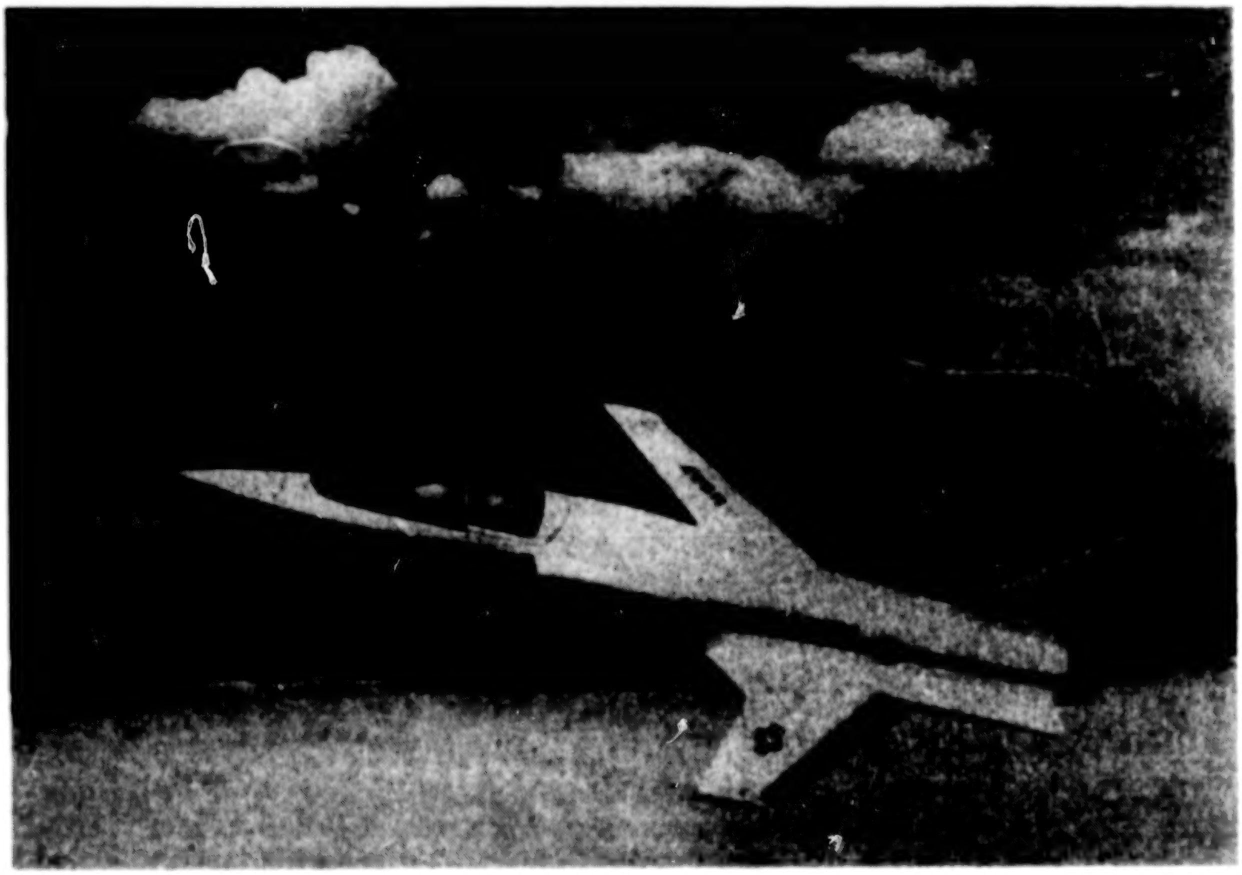

Figure 17

SUPERAUGMENTED AIRCRAFT CRITERIA

The X-29 and Shuttle (fig. 18) are prime examples of highly augmented aircraft. This level of what is sometimes termed "superaugmentation" results from the requirements for low observables, ultra-high maneuverability, and the extended flight envelope. However, since the dynamic response of these vehicles is dominated by the control system characteristics, as opposed to conventional airplane dynamics, the interfacing with pilots becomes an issue. Early results indicate that flying qualities criteria need to be reconsidered for this category of aircraft. Such criteria are important for being able to design effective controls for piloted vehicles. Significant research envisioned for the future will undoubtedly be aimed at developing design guidelines through expanding the data base and constructing handling quality criteria for application superaugmented aircraft.

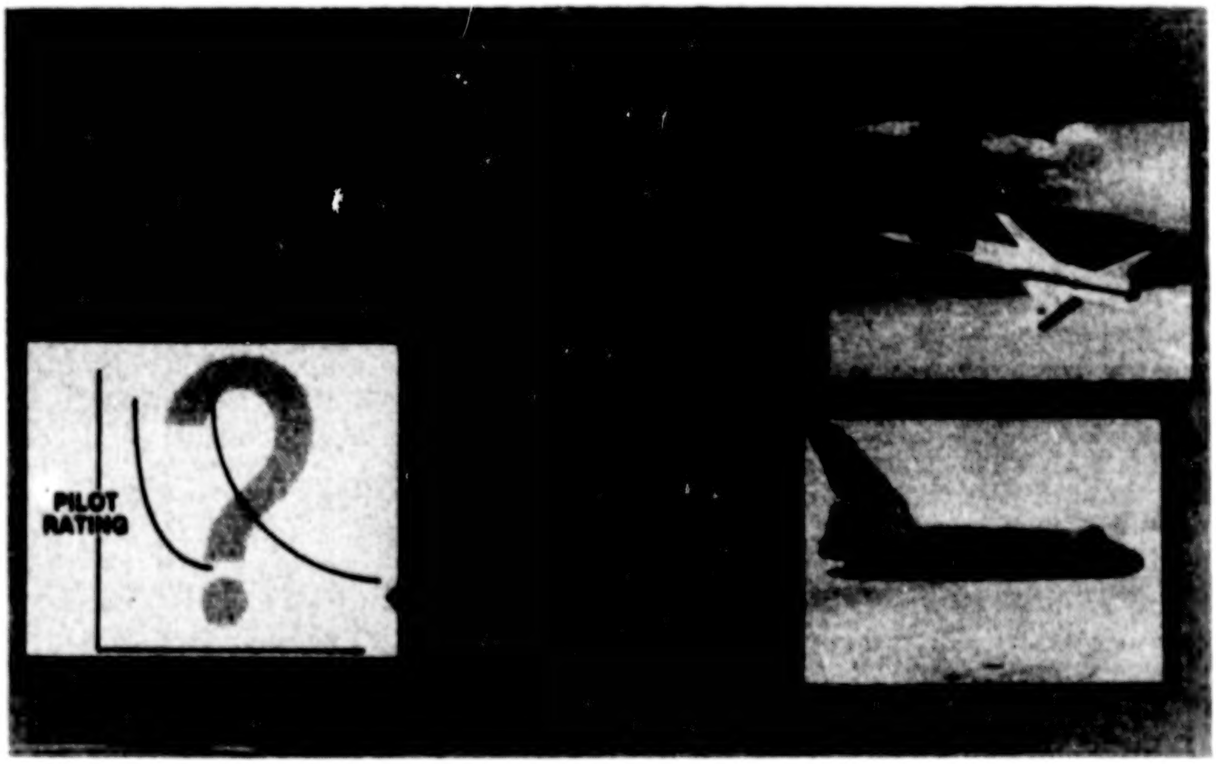

Figure 18

RESEARCH OPPORTUNITIES FOR THE FUTURE

What NASA research will be performed in the future? The answer to this question is a major goal of this workshop. The papers presented should yield a good scope of what the current NASA-sponsored aeronautical controls program is. The panel discussions and interactions with participants will hopefully serve to guide the future directions. Because of this, active participation by all attending the workshop is encouraged and is, in fact, essential for the continued United States preeminence in the area of aircraft controls.

SESSION I

CONTROL SYSTEM DESIGN REQUIREMENTS

Ray V. Hood
Session Chairman

N84
20569

UNCLAS

N84 20569

FLYING QUALITIES CRITERIA FOR SUPERAUGMENTED AIRCRAFT

Donald T. Berry
NASA Ames Research Center
Dryden Flight Research Facility
Edwards, California

First Annual NASA Aircraft Controls Workshop
NASA Langley Research Center
Hampton, Virginia
October 25-27, 1983

PRECEDING PAGE BLANK NOT FILMED

SUPERAUGMENTED AIRCRAFT

Before proceeding with a review of superaugmented aircraft activities, it would be prudent to define what we mean by superaugmented aircraft. The term is defined below. Early applications of feedback control tended to enhance the basic static and dynamic stability of aircraft in a way that was equivalent to augmenting the basic aerodynamic stability derivatives. The resulting responses were improved but conventional. As basic aircraft stability levels became weaker and the augmentation became more elaborate, aircraft began to depart significantly from classical behavior.

Certain characteristics are highly typical of superaugmented aircraft and are also indicated below.

Definition

- **Aircraft with flying qualities that are dominated by the closed-loop control system rather than aerodynamic stability**

Dominant characteristics

- **Large time delays**
- **Unconventional longitudinal response**
- **Small, effective roll time constants**

AIRCRAFT PITCH RATE POLE/ZERO CONFIGURATIONS

An example of a difference between a classical and superaugmented aircraft is illustrated below in terms of pitch rate transfer functions in the s plane. These diagrams are highly idealized but the basic features are quite representative. The classical aircraft typically is augmented primarily in damping so the closed-loop configuration is similar to an aircraft with good aerodynamic damping. Superaugmentation is normally required for aircraft with a basic static instability. Proportional plus integral compensation is typically used to stabilize the aircraft and provide good closed-loop frequency and damping. However, the high gains required result in the conventional attitude numerator being cancelled by a basic aircraft pole and the effective attitude lead being determined by the zero of the proportional plus integral compensation.

Classical

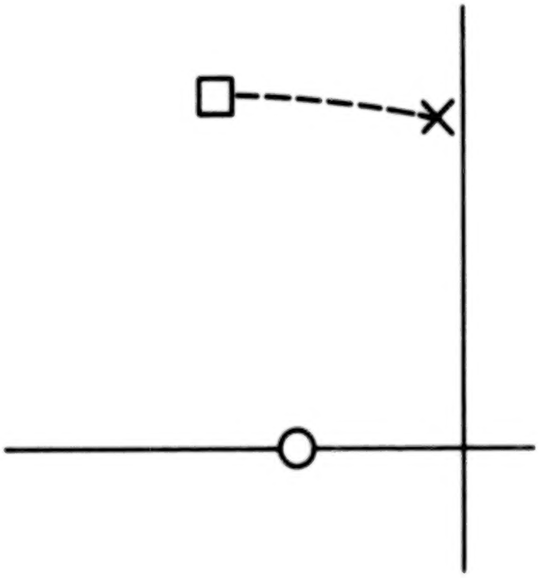

Superaugmented

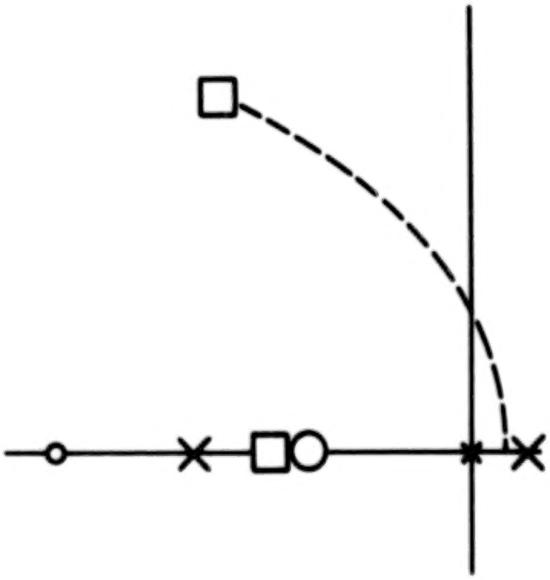

DRYDEN SUPERAUGMENTED AIRCRAFT FLYING QUALITIES RESEARCH

Current activities of the Dryden Flight Research Facility that pertain to flying qualities of superaugmented aircraft are listed here in chronological order of their initiation. It can be seen that a variety of programs are underway. The highlights of these programs will be covered in the ensuing discussion. However, the descriptions will be brief because of the number of activities and the space available. This paper, then, will be an overview of Dryden superaugmented aircraft flying qualities research.

Program	Implementation
• F-8 DFBW Experiments	In house
• Orbiter flying qualities	In house, contractor (STI)
• Shuttle FCS improvements	In house, contractor (CALSPAN)
• Nonconventional vehicle flying qualities	Grant - Purdue
• AFTI/F-16	In house, Air Force
• Flying qualities and control system alternatives	Contractor study (STI)
• Pilot model measurements	Grant - U. Cal. Davis
• VMS Shuttle evaluation	In house, JSC
• TIFS pitch rate criteria	Contractor (CALSPAN)

ORIGINAL PAGE IS
OF POOR QUALITY

F-8 DIGITAL FLY-BY-WIRE (DFBW) FLIGHT EXPERIMENTS

The F-8 DFBW was the world's first fully fly-by-wire airplane. Initial program emphasis was on system reliability and redundancy management. In recent years, the vehicle has been used to investigate flying qualities associated with advanced control laws and superaugmentation, as listed below. The time delay studies investigated the effect of transport delay on flying qualities in landing, formation flying, and in-flight refueling. Highly augmented aircraft typically have large values of equivalent transport delay. The nonlinear control law investigation was a cooperative program with the British and studied control laws that varied prefilter time constants as a function of feedback error and changed loop structure as a function of task. The PIO suppression filters study (ref. 4) was an extension of concepts developed for the Space Shuttle.

- **Time delays**
- **Nonlinear control laws (CADRE)**
- **PIO suppression filters**

OEX ORBITER FLYING QUALITIES EXPERIMENT

This effort is under the sponsorship of the Orbiter Experiments Program (OEX). The purpose is to use Shuttle data and flight experience to develop flying qualities criteria for next generation Shuttlecraft and to improve existing Shuttles where feasible. The Shuttle has some unique characteristics and mission tasks; nevertheless, it is a superaugmented vehicle, and there is much technology transfer between it and high-performance aircraft.

- **Generate flight data base for criteria for current and future Space Shuttlecraft**
- **Establish flying qualities data "pipeline"**
- **Use flight data to validate analytic/simulator studies**

ORIGINAL PAGE IS
OF POOR QUALITY

DRYDEN GRANT ACTIVITIES

Grants under the direction of Dryden that pertain to superaugmented aircraft are outlined below.

The investigator for the Purdue grant is Dr. Dave Schmidt. The integrated pilot-optimal control synthesis simultaneously utilizes an optimal control pilot model and modern control theory to produce control system designs with optimum flying qualities. The optimal control approach to the Neal/Smith flying qualities criteria uses an optimal control pilot model instead of the classical pilot compensation model. The pilot parameter identification techniques study is looking at the use of time series analysis to measure pilot dynamics, strategy, and workload from flight-test time histories.

Principal investigator for the University of California-Davis grant is Dr. Ron Hess. This effort is aimed at using existing pilot measurement techniques to obtain data from ongoing flight experiments and obtain a flight-validated data base of pilot math model parameters. Both classical and optimal control models will be used.

Purdue University: (Schmidt)

Develop prediction techniques for flying qualities of complex, nonconventional vehicles

- **Integrated pilot-optimal control synthesis**
- **Optimal control approach to Neal/Smith**
- **Pilot parameter identification techniques**

University of California - Davis (Hess)

Establish flight-validated pilot model data base

- **Analyze F-8 DFBW flight experiments**

AFTI/F-16 FLYING QUALITIES FLIGHT EXPERIENCE

The AFTI/F-16 is a superaugmented aircraft with direct lift and side force control and a task-tailored multimode flight control system. It is a very ambitious program that is striving to evaluate highly advanced control system mechanizations and architectures as well as unconventional control laws. Initial program emphasis has been on checkout of the digital flight control system and functional evaluation of the flight control concepts. Much qualitative flying qualities information has been obtained, and the highlights of this experience are indicated below.

- **Utility of task-tailored flying qualities demonstrated**
- **Technology not available to optimize control modes**
- **PIO and roll ratchet tendencies persist**

AMES VMS SHUTTLE FLIGHT CONTROL IMPROVEMENT STUDY

The Ames Vertical Motion Simulator (VMS) was used in a recent program to study Shuttle flying qualities in approach and landing. This program was sponsored by the Johnson Space Center. Dryden participated because of its background in previous Shuttle approach and landing studies. The program is outlined below.

Objectives

Evaluate proposed changes to Shuttle FCS to improve flying qualities in approach and landing

Configurations

- Baseline Shuttle
- Shaped pitch rate
- Lead/lag prefilter
- Slapdown system
- Rate command/att hold
- Sink rate command
- C*

Results

- Shaped pitch rate, slapdown, and C* best of mods

- Slapdown and C* eliminated after aggravated maneuvers due to rate limiting

- Pilots with extensive Shuttle training preferred baseline system

- Test pilots without Shuttle training preferred shaped pitch rate

TIFS PITCH RATE CRITERIA FLIGHT RESEARCH PROGRAM

The Air Force/Calspan Total In-Flight Simulator (TIFS) very recently completed a program under joint Dryden/Langley sponsorship to investigate flying qualities criteria for pitch rate command systems. The objectives of the program and configurations tested are outlined below. Preliminary results indicate that superaugmented configurations were rated level two or three. Prefilters that tended to restore more classical aircraft response improved the ratings.

Objectives

- Generate flight data base for improved pitch rate command systems
- Emphasis on superaugmented aircraft

Configurations

- 200,000 lb class advanced aircraft
- Negative static stability
- Neutral static stability
- Proportional + integral augmentation
- With/without prefilters
- Pitch rate augmentation

SUMMARY

This review can be summarized as follows.

- Additional data needed to develop superaugmented aircraft flying qualities criteria
- Dryden activities aimed at increased understanding of superaugmentation and providing flight-validated data base
- Current effort involves F-8 DFBW, Space Shuttle, AFTI/F-16 and X-29

BIBLIOGRAPHY

1. Radford, R. C., Smith, R. E., and Bailey, R. E., "Landing Flying Qualities Evaluation for Augmented Aircraft," NASA CR-163097, Aug. '80.

2. Schmidt, D. K., and Innocenti, M., "Pilot Optimal Multivariable Control Synthesis by Output Feedback," NASA CR-163112, Jul. '81.

3. Teper, G. L. et al., "Analysis of Shuttle Orbiter Approach and Landing Conditions," NASA CR-163108, Jul. '81.

4. Powers, B. G., "An Adaptive Stick-Gain to Reduce Pilot-Induced Oscillation Tendencies," Journ. of Guid., Contr., and Dynam., Mar.-Apr. '82, pp. 138-142.

5. Weingarten, N. C., and Chalk, C. R., "In-Flight Investigation of the Effects of Pilot Location and Control System Design on Airplane Flying Qualities for Approach and Landing," NASA CR-163115, Jan. '82.

6. Bacon, B. J., and Schmidt, D. K., "A Modern Approach to Pilot/Vehicle Analysis and the Neal Smith Criteria," AIAA Paper No. 82-1357, Aug. '82.

7. Berry, D. T., "Flying Qualities: A Costly Lapse in Flight Control Design?," Astronautics and Aeronautics, vol. 20, no. 4, Apr. '82, pp. 35,54-57.

8. Berry, D. T. et al., "In-Flight Evaluation of Control System Pure Time Delays," Journ. of Aircraft, vol. 19, no. 4, Apr. '82, pp. 318-323.

9. Meyers, T. T., Johnston, D. E., and McRuer, D., "Space Shuttle Flying Qualities and Flight Control Assessment Study," Phase 1, NASA CR-170391, Jun. '82; Phase 2, NASA CR-170406; Phase 3, NASA CR-17040

10. Shafer, M. F., Smith, R. E., and Stewart, J. F., "Flight Test Experience with Pilot-Induced Oscillation Suppression Filters," AIAA Paper No. 83-2107, Aug. '83.

11. Larson, R. R., Smith, R. E., and Krambeer, K. D., "Flight Test Results Using Non-Linear Control With the F-8 Digital Fly-By-Wire Aircraft," AIAA Paper No. 2174, Aug. '83.

12. Weingarten, N. C., and Chalk, C. R., "Application of Calspan Pitch Rate Control System to the Space Shuttle for Approach and Landing," NASA CR-170402, May '83.

N84
20570

UNCLAS

N84 20570

LARGE AIRCRAFT HANDLING QUALITIES

William D. Grantham
NASA Langley Research Center
Hampton, Virginia

First Annual NASA Aircraft Controls Workshop
NASA Langley Research Center
Hampton, Virginia
October 25-27, 1983

The point to be made here is that some of the present-day longitudinal handling qualities criteria for transport class aircraft do not apply to very large (G.W. = 2,000,000 lbf) transport aircraft. In fact, of the four criteria indicated here, only the short-period frequency requirements of MIL-F-8785C could be said to be in agreement with the present very large aircraft simulation study results. Moreover, if it is conceded that the C-5A has satisfactory longitudinal handling characteristics, then it might be concluded that none of these criteria are applicable to very large aircraft.

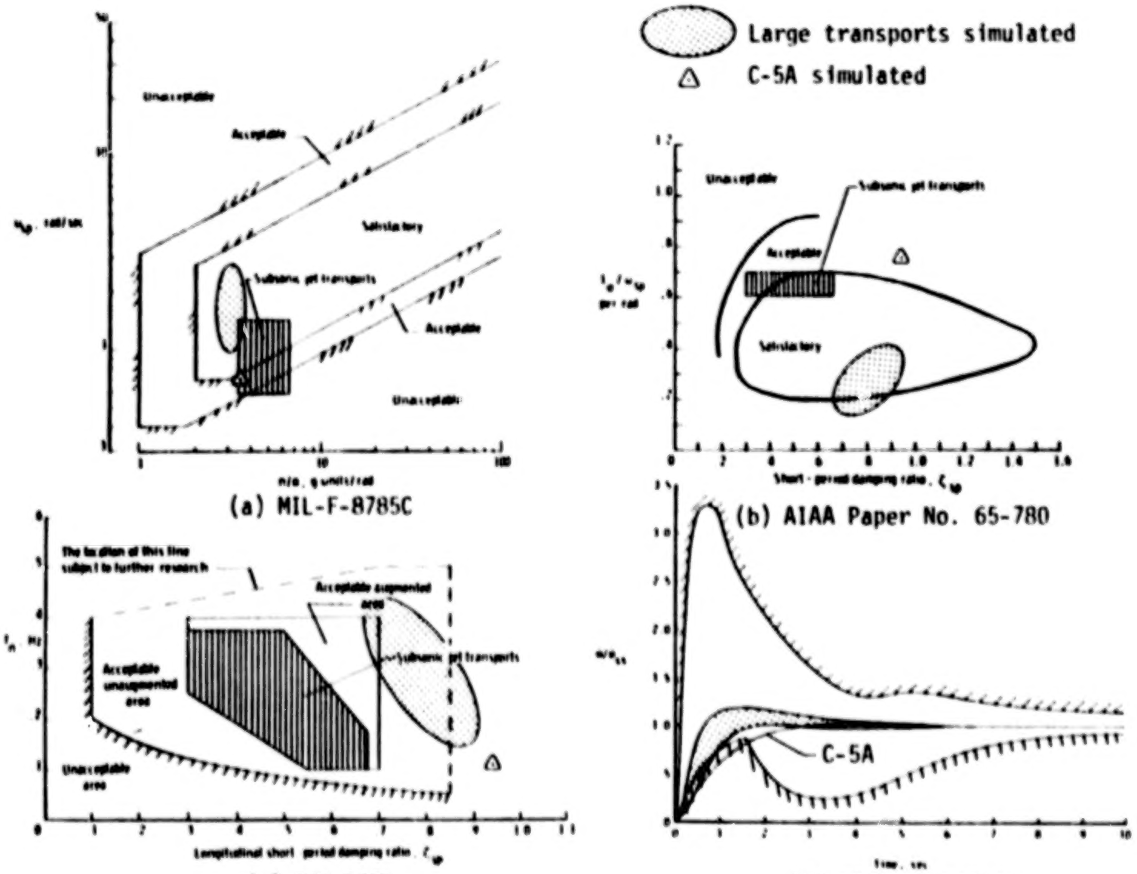

(a) MIL-F-8785C

(b) AIAA Paper No. 65-780

(c) ARP 842B

(d) NASA CR-137635

EFFECTIVE TIME DELAY t_1 IN COMMAND PATH
(PILOT ω_{BW} = 1.5 RAD/SEC)

These pitch rate response criteria were developed by Chalk (NASA CR-159236) and address such parameters as "effective time delay (t_1);" "transient peak ratio ($\Delta q_2/\Delta q_1$);" and "effective rise time ($\Delta t = t_2 - t_1$);" and apply to the dynamic response with the pilot in the loop. This table indicates that the effective time delays of the simulated large transports meet the requirements of this reference for pitch, roll, and yaw. Also, although it is not indicated in this chart, the pitch transient peak ratio ($\Delta q_2/\Delta q_1$) requirement was met for all large transports simulated.

None of the large aircraft simulated met the suggested pitch requirements for Δt (effective rise time parameter). This is quite disconcerting since the referenced limits on Δt are derived from or related to the constant limits on $\omega_n{}^2/n/\alpha$ used in MIL-F-8785C, and as shown earlier in the first figure of this presentation, all of the simulated large aircraft met the level 1 requirement for $\omega_n{}^2/n/\alpha$.

It should be noted that NASA CR-159236 lists no requirements for "transient peak ratio" or "effective rise time" for the roll and yaw axes.

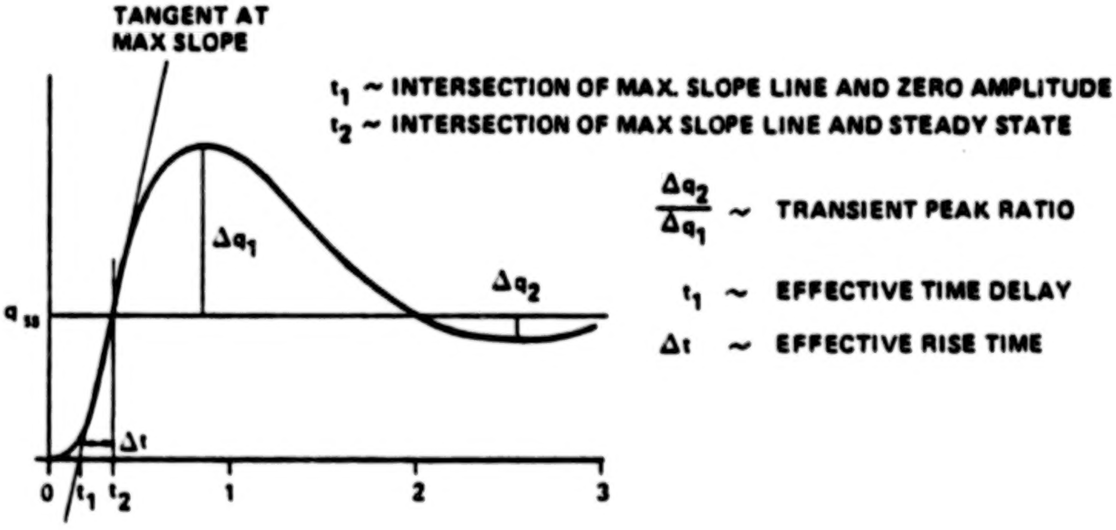
TANGENT AT MAX SLOPE
t_1 ~ INTERSECTION OF MAX. SLOPE LINE AND ZERO AMPLITUDE
t_2 ~ INTERSECTION OF MAX SLOPE LINE AND STEADY STATE
$\frac{\Delta q_2}{\Delta q_1}$ ~ TRANSIENT PEAK RATIO
t_1 ~ EFFECTIVE TIME DELAY
Δt ~ EFFECTIVE RISE TIME
Δq_1
Δq_2
q_{ss}
Δt
0
t_1
t_2
1
2
3

Requirements-NASA CR-159236			Large Aircraft Simulation Results				
				Unaugmented Ave		Augmented Ave	
Level	Pitch	Roll and Yaw	Level	Pitch	Roll	Pitch	Roll
1	≤ .200 sec	≤ .283 sec	1	.053	.103	.120	.133
2	≤ .283 sec	≤ .400 sec	2	✓	✓	✓	✓
3	≤ .350 sec	≤ .467 sec	3	✓	✓	✓	✓

COMPARISON OF SIX LAHOS CONFIGURATIONS TO THE SPACE SHUTTLE SUBSONIC PITCH RATE REQUIREMENTS

Because the Shuttle is always operated as a closed-loop system, the conventional MIL-F-8785C open-loop aircraft modal format for flying qualities was considered to be inappropriate. Instead, Shuttle pitch axis flying qualities were specified in the time domain by the response boundaries indicated in this chart. However, the Shuttle specification itself does not correlate well with much of the recent flying qualities experimental data. For example, some selected LAHOS configurations (AFFDL-TR-78-122) were compared to the Shuttle criterion. Note that it was possible to select some LAHOS configurations that exceeded the boundaries and yet had good (level 1) flying qualities, while others that met the requirements had poor (level 2) flying qualities. (Similar results were found for correlations of the Neal and Smith data of AFFDL-TR-70-74.)

LAHOS Config.	Pilot Rating	
	Overall	Approach
2-1	Level 1	-
3-C	Level 1	-
4-C	Level 1	Level 1

LAHOS Config.	Pilot Rating	
	Overall	Approach
4-0	Level 2	-
4-3	Level 2	Level 1
4-4	Level 2	Level 2

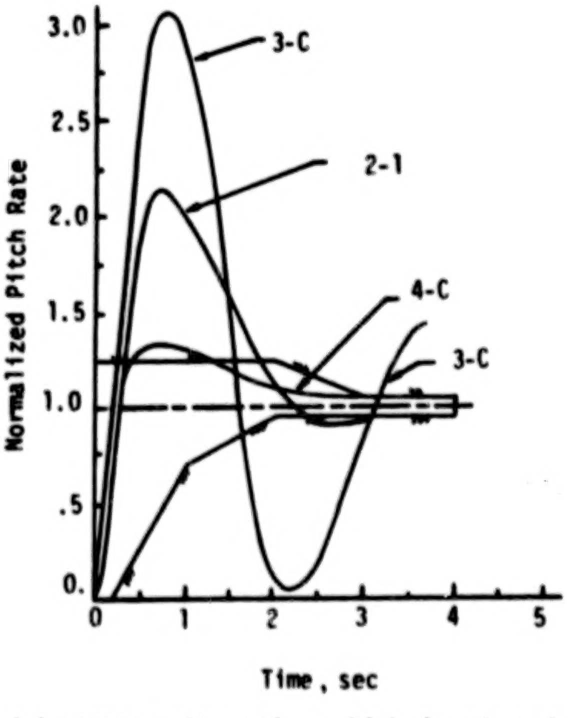

(a) LAHOS configurations which do not meet the Shuttle pitch-rate requirements.

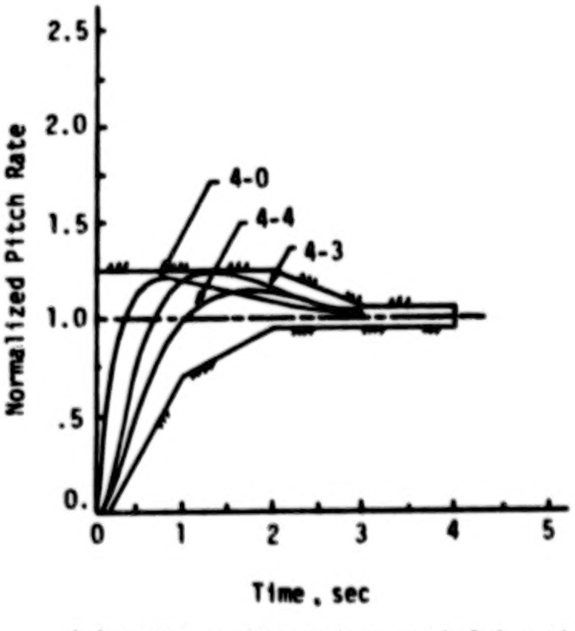

(b) LAHOS configurations satisfying the Shuttle pitch-rate requirements.

COMPARISON OF SIX LAHOS CONFIGURATIONS TO THE SPACE SHUTTLE SUBSONIC PITCH RATE ENVELOPE, BUT USING NORMALIZED α RESPONSE

It has been suggested that the original Shuttle time-history envelope was developed for angle of attack instead of pitch rate. The figure on the left of this chart shows the α response of LAHOS configurations 2-1, 4-C, and 3-C plotted in the Shuttle time-history response envelope. The responses now fall approximately within the Shuttle envelope with level 1 flying qualities.

The figure on the right of this chart shows a plot of the α responses of LAHOS configurations 4-0, 4-3, and 4-4 on the same Shuttle time-history envelope, and all three configurations have level 2 flying qualities. Although the pitch rate responses of these three configurations were shown to be within the Shuttle envelope in the previous figure, the angle-of-attack responses shown here indicate a very sluggish, unacceptably responsive vehicle.

* CALSPAN suggests that normalized α should be used instead of normalized pitch rate.

LAHOS	Pilot Rating	
Config.	Overall	Approach
2-1	Level 1	-
3-C	Level 1	-
4-C	Level 1	Level 1

LAHOS	Pilot Rating	
Config.	Overall	Approach
4-0	Level 2	-
4-3	Level 2	Level 1
4-4	Level 2	Level 2

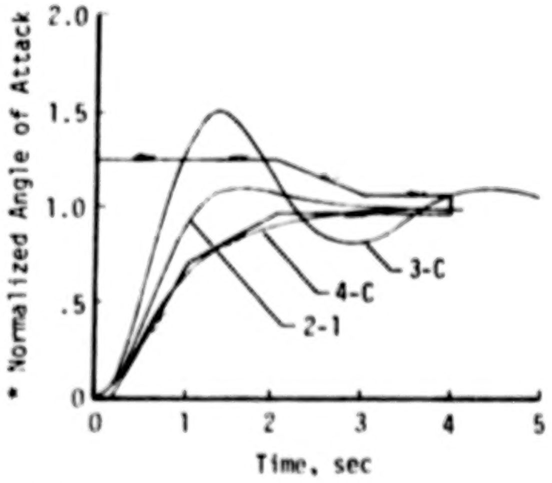

(a) Configurations which satisfy Shuttle $\dot{\theta}$ envelope when α is used.

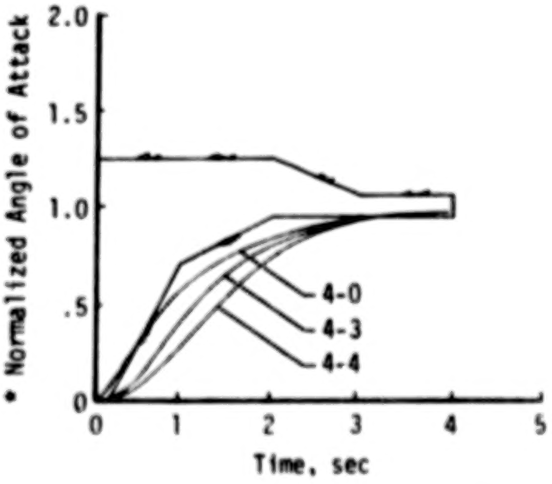

(b) Configurations which do not satisfy Shuttle $\dot{\theta}$ envelope when α is used.

COMPARISON OF LARGE TRANSPORT AIRCRAFT SIMULATED TO SHUTTLE PITCH RATE CRITERION ENVELOPE, BUT USING NORMALIZED α RESPONSE

This chart presents a comparison of the "angle-of-attack" response for the simulated large transport aircraft to the "pitch rate" response criterion developed for the Space Shuttle.

These large aircraft do not correlate well with the Shuttle criterion, even when normalized α is substituted for normalized $\dot{\theta}$. The figure on the right presents the augmented dynamic response for four large aircraft configurations, all of which were assessed by the pilots as having satisfactory (level 1) approach and landing flying qualities. However, when compared to the Shuttle time-history envelope, it would be concluded that these large aircraft had unacceptably sluggish responses, which was not the case.

Large A/C Config.	Pilot Rating, Landing Task
1	Level 2
2	Level 2
3	Level 2
4	Level 1

Large A/C Config.	Pilot Rating, Landing Task
1	Level 1
2	Level 1
3	Level 1
4	Level 1

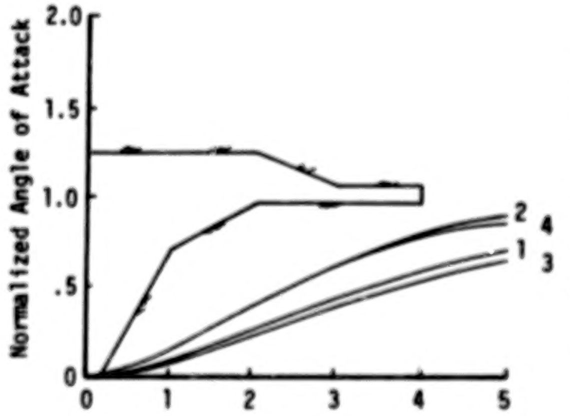

(a) Unaugmented large transports simulated.

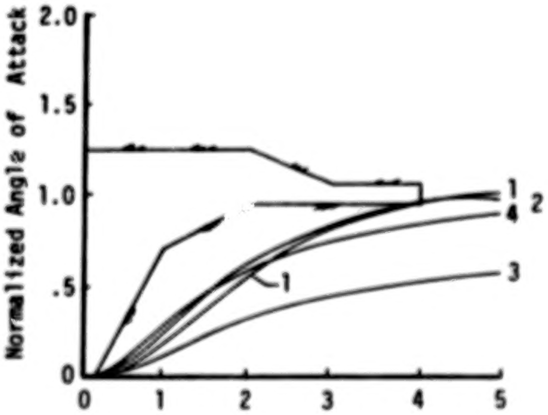

(b) Augmented large transports simulated.

COMPARISON OF LARGE TRANSPORT SIMULATED AIRCRAFT TO BOEING PITCH RATE REQUIREMENTS

The low-speed pitch rate response criterion indicated in this chart and reported in NASA CR-137635 was developed by the Boeing Company for application to the handling qualities requirements for supersonic transports. It should be noted that this Boeing criterion differs from the Shuttle pitch rate response criterion presented earlier in that this Boeing criterion allows for much more pitch rate overshoot, and allows for much less initial pitch rate delay.

Upon comparing this pitch rate response and pilot opinion of the very large "subsonic" jet transport of the present ground-based simulation study, it can be seen that the simulated large aircraft results agree reasonably well with the Boeing-developed SST landing approach criterion. Indications are, however, that the minimum satisfactory level of "initial" pitch rate response allowed by this criterion could probably be relaxed for very large (G.W. = 2,000,000 lbf) transport aircraft.

Large A/C Config.	Pilot Rating, Landing Task
1	Level 2
2	Level 2
3	Level 2
4	Level 1

Large A/C Config.	Pilot Rating, Landing Task
1	Level 1
2	Level 1
3	Level 1
4	Level 1

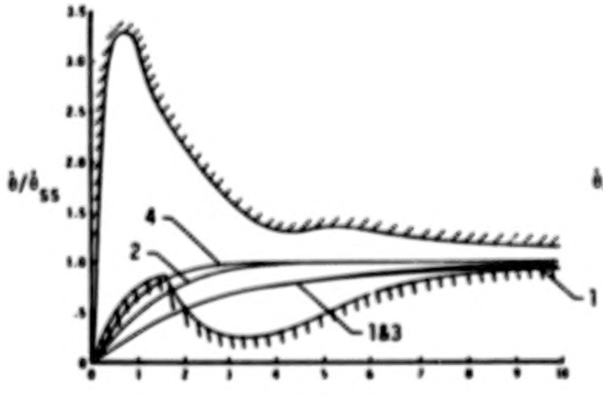

(a) Unaugmented large transports simulated.

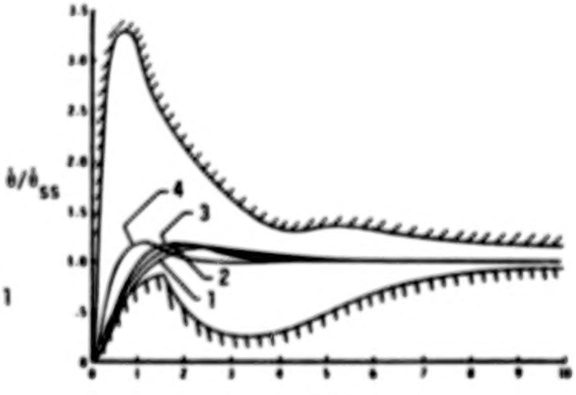

(b) Augmented large transports simulated.

COMPARISON OF SHORT-TERM PITCH RESPONSE OF SIMULATED LARGE TRANSPORT AIRCRAFT WITH CATEGORY C REQUIREMENTS OF PROPOSED MIL HANDBOOK

The short-period frequency requirement of 8785C was based upon the premise that the normal acceleration response to attitude changes is a primary factor affecting the pilot's perception of the minimum allowable ω_{sp} [that is, limits are placed on $\omega_{sp}^2/(n/\alpha)$]. Likewise, the physical interpretation of the so-called "control anticipation parameter" [CAP $= \omega_{sp}^2/(n/\alpha)$] assumes that the dominant concern for a pilot pitch control input is normal acceleration response.

It is, of course, also true that the pitch attitude response to pitch control inputs is of paramount importance, and, whether the appropriate correlating parameter is n/α or $1/T_{\theta_2}$ is a moot point in that data that correlate with $1/T_{\theta_2}$ generally also correlate with n/α. However, it was observed in AIAA Paper No. 69-898 that the product $\omega_{sp}T_{\theta_2}$ provided a slightly better correlation than CAP. (Physically, $\omega_{sp}T_{\theta_2}$ represents the separation in phase between aircraft response in path and pitch attitude.)

Thus, the $\omega_{sp}T_{\theta_2}$, in combination with ζ_{sp}, criterion of AFWAL-TR-82-3081 is presented in this chart along with the characteristics of the simulated very large aircraft of the present study. And, since the pilots' opinion of these configurations during approach and landing were, in general, level 2 when unaugmented and level 1 when augmented, it is concluded that the results of the present 6-DOF ground-based simulator results are in good agreement with this $\omega_{sp}T_{\theta_2}$ vs. ζ_{sp} criterion.

NOTE: $1/T_{\theta_2} \doteq n_\alpha(g/V)$ IN THIS INSTANCE

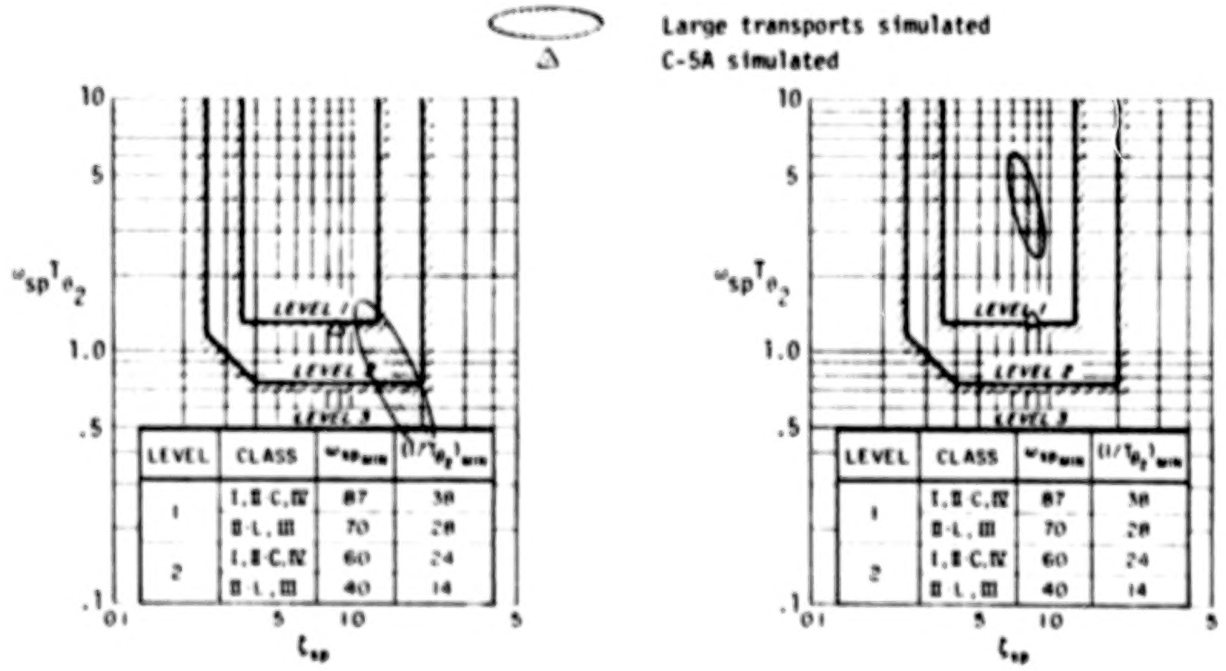

LEVEL	CLASS	$\omega_{sp_{min}}$	$(1/T_{\theta_2})_{min}$
1	I, II-C, IV	87	38
	II-L, III	70	28
2	I, II-C, IV	60	24
	II-L, III	40	14

(a) Large aircraft, unaugmented.

(b) Large aircraft, augmented.

COMPARISON OF SIMULATED LARGE TRANSPORT AIRCRAFT TO LOCKHEED C-5A AND BOUNDARIES FROM FLIGHT TEST

The boundary indicated as taken from TN D-7062 was derived using a general purpose airborne simulator (Lockheed Jetstar) with a model-controlled, variable-stability system installed to provide simulation capability. This boundary presents the pilot ratings (PR) for the maximum "roll acceleration" commanded by the pilots for the various roll time constants investigated. The boundary indicates that a roll acceleration capability of approximately 0.12 rad/sec^2 or greater was considered to be satisfactory (PR < 3.5) by the pilots; and that the pilot ratings rapidly became unacceptable (PR > 6.5) when the roll acceleration capability was decreased below 0.10 rad/sec^2.

The boundary indicated for the large transports (G.W. = 2,000,000 lbf) simulated in the present study (on a 6-DOF ground-based simulator) indicates that a roll acceleration capability as low as 0.09 rad/sec^2 was evaluated as being satisfactory (PR < 3.5). Similar piloting tasks were used in both studies.

Note that the C-5A ground-based simulation results indicate a pilot rating of 4.0 (level 2) for the lateral-directional handling qualities and yet the roll acceleration capability was greater than 0.2 rad/sec^2, indicating that the roll control power was not the reason for the level 2 lateral-directional pilot rating.

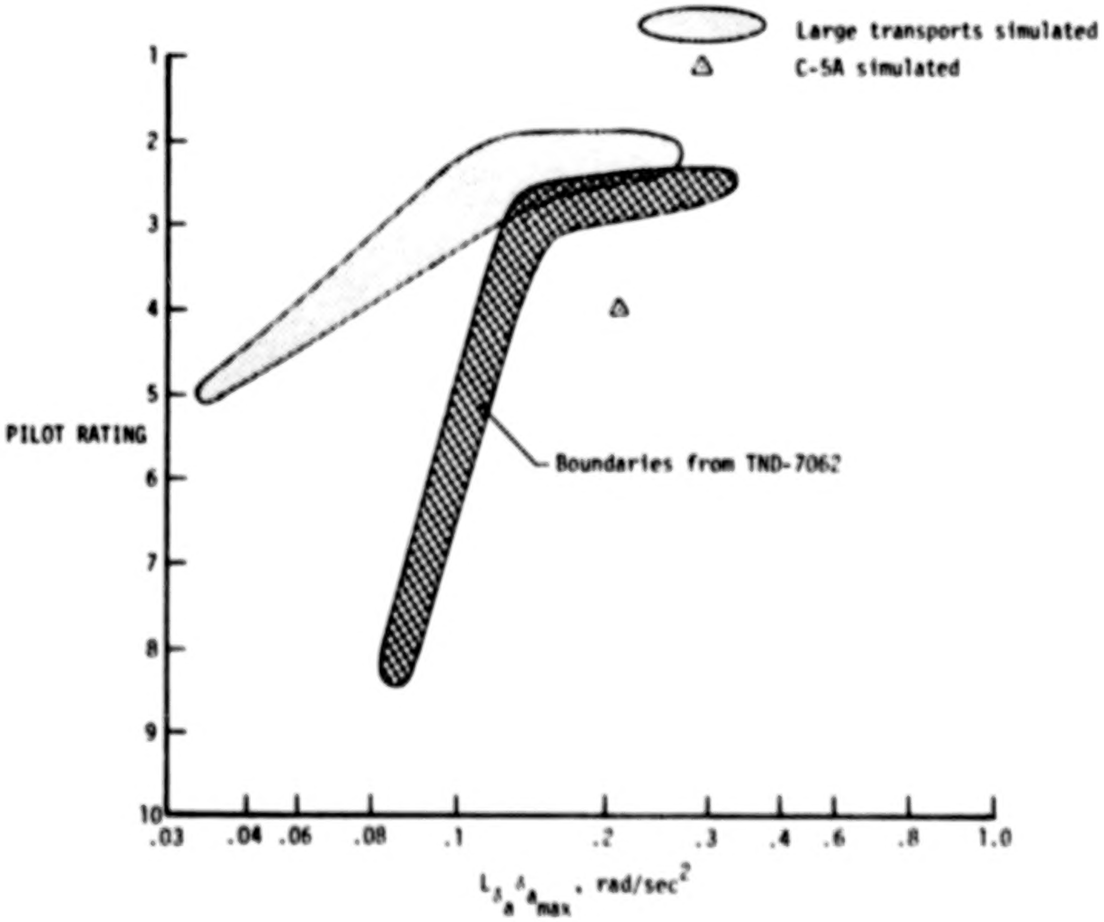

COMPARISON OF RESULTS FROM LARGE AIRCRAFT SIMULATIONS WITH REFERENCED RESULTS

This chart relates pilot opinion of an aircraft's roll response to the parameter ϕ_1. (The term ϕ_1 is defined as the maximum bank angle that can be achieved in one second.) The results of the present large aircraft simulation study (6-DOF ground-based simulator) are compared to the results of TN D-7062 and CR-635 (both reporting results obtained from airborne simulators).

None of these simulation results agrees as to the minimum satisfactory level (PR < 3.5) of ϕ_1. The results from TN D-7062 indicate that ϕ_1 must be greater than approximately 6° for level 1 roll response; the results of CR-635 indicate that ϕ_1 must be greater than approximately 3° for level 1 roll response; and the results from the present ground-based simulation study indicate that the ϕ_1 for very large transport aircraft could be as low as approximately 1° and still be considered to have satisfactory (level 1) roll response.

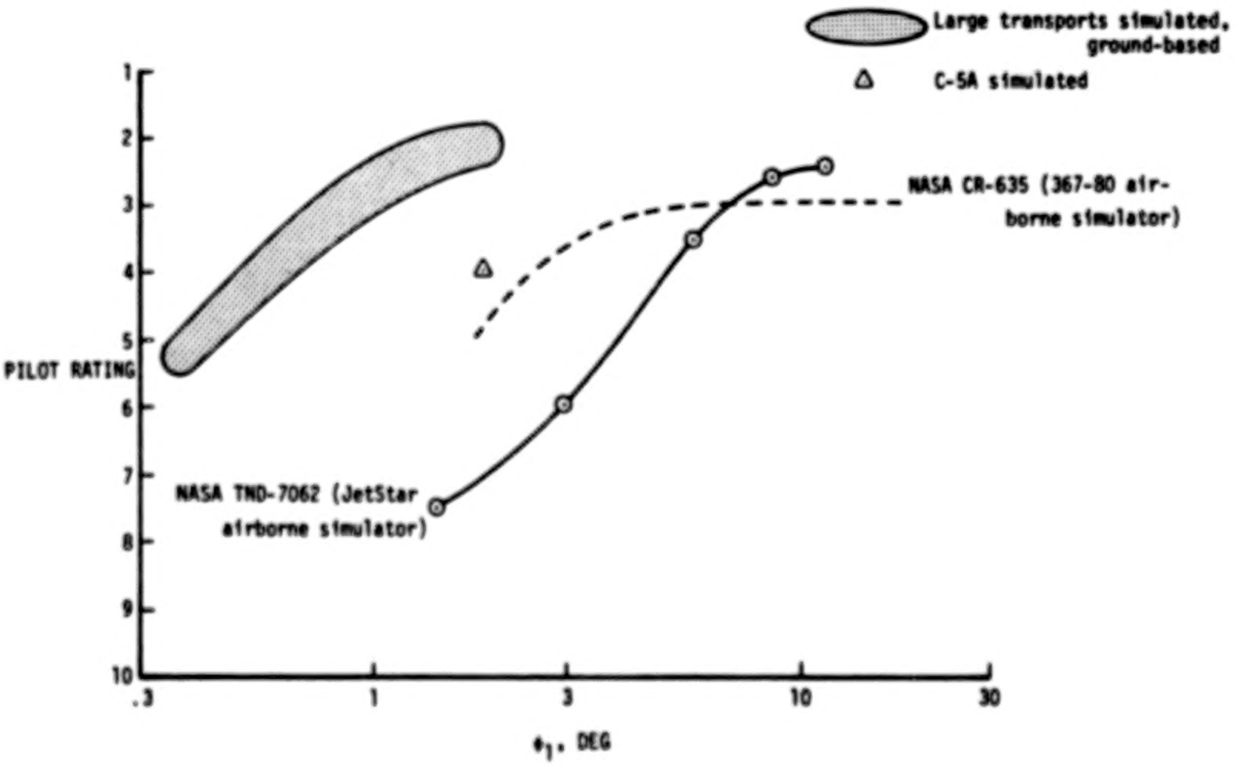

VARIATION OF PILOT RATING WITH BANK ANGLE ATTAINED IN THE FIRST SECOND

Maximum bank angle in the first second after initiation of wheel deflection ($\phi_{1_{max}}$) has been suggested as a figure of merit for roll control systems. The variation of pilot rating with $\phi_{1_{max}}$ for the ground-based simulator results reported in CR-635 are indicated in this chart to be a function of effective wheel angle, $\delta_{w_{eff}}$. (The term $\delta_{w_{eff}}$ is defined as the wheel angle for maximum rolling moment.)

These indicated lines of constant effective wheel angle suggest that the pilot is rating the bank angle per wheel deflection or roll response sensitivity, more so, or instead of, the parameter $\phi_{1_{max}}$. Another interesting point to be seen from this chart is that a constant pilot rating of 3 (level 1) was obtained at the constant value of $\phi_{1_{max}}/\delta_{\omega} = 0.1$, while $\phi_{1_{max}}$ varied from 3° ($\delta_{w_{eff}} = 30°$) to 9° ($\delta_{w_{eff}} = 90°$). Note also the results of the present large aircraft simulation study. Although values of $\phi_{1_{max}}$ of these large aircraft configurations were much smaller than those of the referenced data, the large aircraft $\delta_{w_{eff}}$ was also smaller and the overall results were the same; a pilot rating of 3 was obtained when $\phi_1/\delta_w = 0.1$ ($\phi_{1_{max}} = 1.5°$ for $\delta_{w_{eff}} = 15°$).

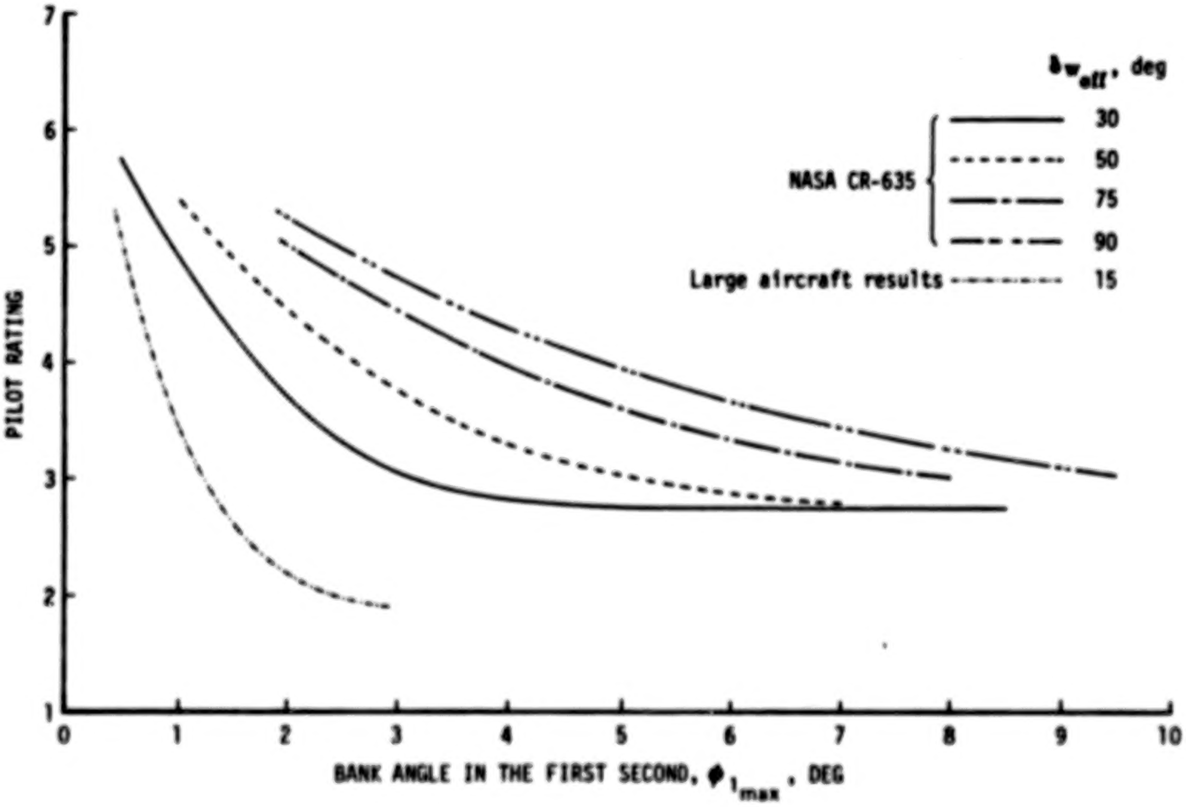

ORIGINAL PAGE IS
OF POOR QUALITY

COMPARISON OF ROLL PERFORMANCE FROM LARGE AIRCRAFT SIMULATED WITH REFERENCED RESULTS

An inadequate "large aircraft data base" has led to handling qualities specification problems, and, as a result, there is a risk that future aircraft will be overdesigned, unnecessarily expensive, or possibly inadequate to perform the design mission. For example, considerable effort and expense were initially expended on the C-5A in an attempt to meet a requirement for rolling to an 8° bank angle in one second. It was later determined from flight tests that the handling qualities of the C-5A were totally acceptable with less than one-half such roll capability.

All four of the figures on this chart relate pilot opinion to the time required to bank 30° ($t_{\phi=30°}$). Figure (a) shows C-5A roll performance compared to the 8785C requirement. Although this aircraft is considered to have satisfactory roll performance, it would be evaluated as less than satisfactory by the military specification criterion. Boeing suggested a few years ago that the $t_{\phi=30°}$ criterion should be a function of aircraft landing weight (fig. (b)). Several aircraft in service today meet this criteria but do not meet the MIL-SPEC criteria. Extrapolation of the Boeing criteria indicates that the $t_{\phi=30°}$ requirement should be relaxed for heavier Class III aircraft.

Current results of the ongoing large aircraft simulation study are summarized in figures (c) and (d). Results shown in figure (c) indicate that a $t_{\phi=30°}$ of less than 6 sec should result in "acceptable" roll response characteristics, and that a $t_{\phi=30°}$ of less than 4.0 sec results in "satisfactory" roll response. Figure (d) indicates that the present large aircraft ground-based simulation results are in good agreement with the airborne simulation results of TN D-7062, wherein smaller Class III aircraft were simulated.

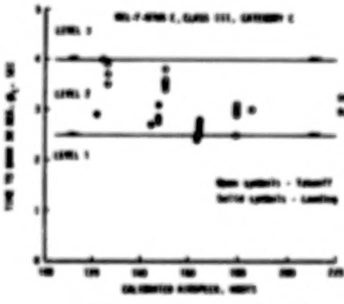

(a) C-5A roll performance (PR=3.5).

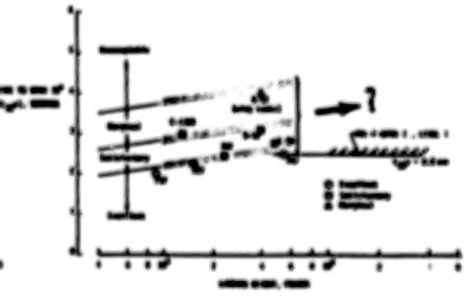

(b) Roll performance of various aircraft at landing approach.

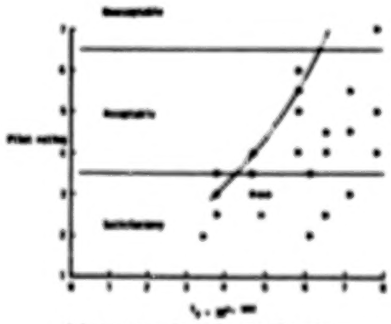

(c) Large aircraft simulated roll performance for landing task.

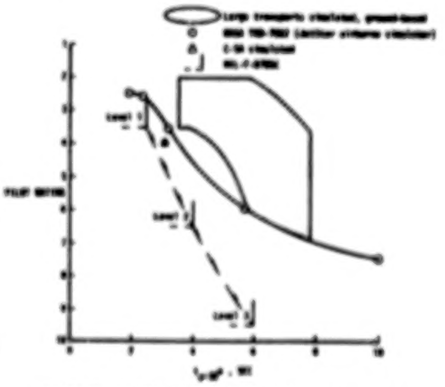

(d) Large aircraft simulated roll performance compared to other results and MIL-F-8785C.

SUMMARY

- The short-period frequency requirements of MIL-F-8785C are applicable to the very large transport aircraft simulated.

- The large aircraft simulated in this study meet the requirements of NASA CR-159236 for effective time delay and pitch transient peak ratio. However, the requirements of this reference for the effective rise time parameter are believed to be too conservative for very large transport aircraft.

- These large aircraft simulation results are in very good agreement with the $\omega_{SP}T_{\theta_2}$ vs. ζ_{sp} criterion of AFWAL-TR-82-3081.

- A value of the parameter $L_{\delta_A}\delta_{A_{max}}$, which is an indication of the roll accleration capability, as low as 0.09 rad/sec^2 was considered to be satisfactory for the very large transports simulated. This compares to a value of approximately 0.12 rad/sec^2 desired for smaller transports.

- A minimum satisfactory level of the parameter ϕ_1 was determined to be much lower for the large aircraft simulated in this study compared to the values determined in previous studies for smaller transport aircraft. However, the magnitude of ϕ_1/δ_W required for these large transports was determined to be the same as that required for smaller transports; thus, $\phi_1/\delta_W \approx 0.1$ produces satisfactory roll characteristics.

- Data obtained to date as well as other data indicate that MIL-SPEC requirements for the parameter $t_{\phi=30°}$ are too conservative for very large transport aircraft. The results of the present study indicate that a $t_{\phi=30°}$ of less than 6 sec should result in "acceptable" roll response characteristics, and a $t_{\phi=30°}$ of less than 4.0 sec should result in "satisfactory" roll response.

BIBLIOGRAPHY

1. Military Specification Flying Qualities of Piloted Airplanes, MIL-F-8785C, Nov. 1980.

2. Shomber, H. A.; and Gertsen, W. M.: Longitudinal Handling Qualities Criteria: An Evaluation. AIAA Paper No. 65-780, Nov. 1965.

3. Aerospace Recommended Practice: Design Objectives for Flying Qualities of Civil Transport Aircraft. ARP 842B, Soc. Automat. Eng., Aug. 1, 1964. Revised Nov. 30, 1970.

4. Sudderth, Robert W.; Bohn, Jeff G.; Caniff, Martin A.; and Bennett, Gregory R.: Development of Longitudinal Handling Qualities Criteria for Large Advanced Supersonic Aircraft. NASA CR-137635, March 1975.

5. Chalk, C. R.: Recommendations for SCR Flying Qualities Design Criteria. NASA CR-159236, April 1980.

6. Smith, Rogers E.: Effects of Control System Dynamics on Fighter Approach and Landing Longitudinal Flying Qualities. AFFDL-TR-78-122, vol. 1, March 1978.

7. Neal, T. Peter; and Smith, Rogers E.: An In-Flight Investigation to Develop Control System Design Criteria for Fighter Airplanes. AFFDL-TR-70-74, vol. 1, Dec. 1970.

8. Ashkenas, I. L.: Summary and Interpretation of Recent Longitudinal Flying Qualities Results. AIAA Paper No. 69-898, Aug. 1969.

9. Hoh, Roger H.; Mitchell, David G.; Ashkenas, Irving L.; Klein, Richard H.; Heffley, Robert K.; and Hodgkinson, John: Proposed MIL Standard and Handbook - Flying Qualities of Air Vehicles, vol. 2: Proposed MIL Handbook. AFWAL-TR-82-3081, vol. 2, Nov. 1982.

10. Holleman, Euclid C.; and Powers, Bruce G.: Flight Investigation of the Roll Requirements for Transport Airplanes in the Landing Approach. NASA TN D-7062, Oct. 1972.

11. Condit, Philip M.; Kimbrel, Laddie G.; and Root, Robert G.: Inflight and Ground-Based Simulation of Handling Qualities of Very Large Airplanes in Landing Approach. NASA CR-635, Oct. 1966.

N84
20571

UNCLAS

N84 20571

A SUMMARY OF ROTORCRAFT HANDLING QUALITIES RESEARCH AT NASA AMES RESEARCH CENTER

Robert T. N. Chen
NASA Ames Research Center
Moffett Field, California

First Annual NASA Aircraft Controls Workshop
NASA Langley Research Center
Hampton, Virginia
October 25-27, 1983

OBJECTIVES AND SCOPE

The objectives of the rotorcraft handling qualities research program at Ames Research Center, as shown in figure 1, are twofold: (1) to develop basic handling qualities design criteria to permit cost-effective design decisions to be made for helicopters, and (2) to obtain basic handling qualities data for certification of new rotorcraft configurations. The research on the helicopter handling qualities criteria has focused primarily on military nap-of-the-Earth (NOE) terrain flying missions, which are flown in day visual meteorological conditions (VMC) and instrument meteorological conditions (IMC), or at night. The Army has recently placed a great deal of emphasis on terrain flying tactics in order to survive and effectively complete the missions in modern and future combat environments. Unfortunately, the existing Military Specification MIL-H 8501A (ref. 1), which is a 1961 update of a 1951 document, does not address the handling qualities requirements for terrain flying. The research effort is therefore aimed at filling the void and is being conducted jointly with the Army Aeromechanics Laboratory at Ames. The research on rotorcraft airworthiness standards with respect to flying qualities requirements has been conducted in collaboration with the Federal Aviation Administration (FAA). This effort focused, in the recent past, on helicopter instrument flight rules (IFR) airworthiness criteria and is now addressing the airworthiness concerns for such new rotorcraft configurations as tilt-rotor aircraft.

OBJECTIVES

DEVELOP FLYING QUALITIES AND CERTIFICATION CRITERIA

SCOPE

- **NOE OR TERRAIN FLIGHT IN VMC AND IMC/NIGHT (ARMY)**
- **TERMINAL AREA IFR OPERATIONS (FAA)**

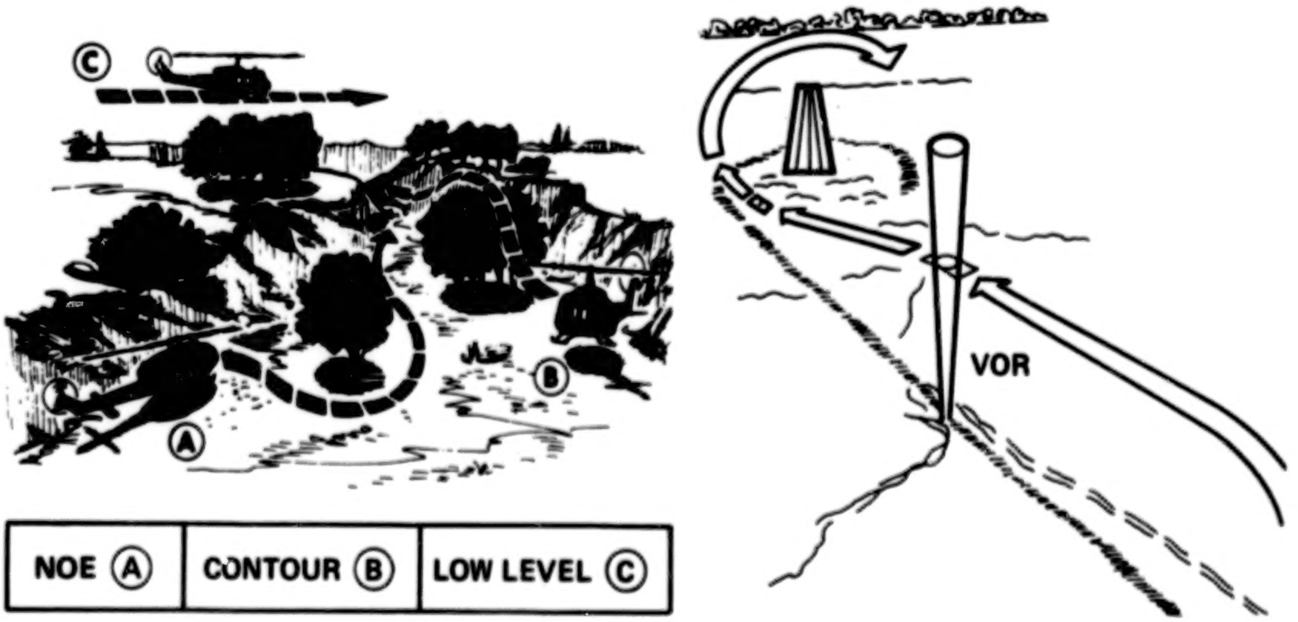

Figure 1

FACTORS INFLUENCING AGILITY FOR TERRAIN FLIGHT

In terrain flight, the pilot is often called upon to fly complicated and rapidly changing trajectories to avoid obstacles and to unmask and quickly remask. The characteristics of the helicopter that permit the pilot to fly these complex trajectories quickly, precisely, and easily are essential to safe and successful operations, and we may define this aggregate of characteristics as agility. Factors influencing agility are many: basic performance potential of the aircraft, engine/governor dynamics, stability and control characteristics, and cockpit interface (fig. 2). For quickness, the helicopter must be able to change rapidly the magnitude and direction of its velocity vector. Adequate control powers in pitch, roll, and yaw are required for a quick rotation of the thrust vector; adequate installed power and responsiveness of the engine/governor system together with adequate rotor thrust capability are needed to meet the demand for rapid changes in thrust magnitude. For precision and ease with which the pilot flies those complex trajectories, the helicopter must have good stability and control characteristics. Interaxis coupling must be minimized so that unnatural or complicated control coordination is not required. Also, proper controller characteristics, flight director displays, and vision aids are needed to assist the pilot in flying the missions in adverse weather conditions or at night.

AGILITY: THE QUALITIES PERMITTING PILOTS TO FLY COMPLEX TRAJECTORIES QUICKLY, PRECISELY, AND EASILY

QUICKNESS ⇨ ABILITY TO RAPIDLY CHANGE MAGNITUDE AND DIRECTION OF AIRCRAFT VELOCITY VECTOR

- INSTALLED POWER, RESPONSIVENESS OF ENGINE/GOVERNOR SYSTEM
- ADEQUATE CONTROL POWER IN PITCH, ROLL, YAW
- ADEQUATE ROTOR THRUST CAPABILITY

EASE AND PRECISION ⇨ GOOD COMBINATIONS OF STABILITY AND CONTROL, AND ADEQUATE PILOT AIDS

- ADEQUATE DAMPING, PROPER CONTROL SENSITIVITY
- SMALL INTERAXIS COUPLING
- ADEQUATE STABILITY
- PROPER COCKPIT INTERFACE AND PILOT AIDS
  - CONTROLLER CHARACTERISTICS
  - DISPLAYS (IMC)
  - VISION AIDS (NIGHT)

Figure 2

EFFECT OF ENGINE DYNAMICS ON HANDLING QUALITIES

The effects of engine dynamics and thrust-response characteristics on helicopter handling qualities have until recently remained largely undefined. A multiphase program is being conducted to study, in a generic sense, the effects of engine response, rotor inertia, rpm control, excess power, and vertical sensitivity and damping on helicopter handling qualities in hover and representative low-speed NOE operations. To date, three moving-based piloted simulations have been conducted on the Vertical Motion Simulator (VMS) at Ames. This series of investigations concentrates specifically on the helicopter configuration with an rpm-governed gas-turbine engine. It was found (ref. 2) that variations in the engine governor response time can have a significant effect on helicopter handling qualities as shown in figure 3. For the tasks evaluated, satisfactory handling qualities and rpm control were achieved only with a highly responsive governor (which for the model in the study was $w_n > 7$ rad/sec). The results indicate that for satisfactory handling qualities, there is a qualified trade-off between engine response time and vehicle vertical damping; however, increases in engine time constant are limited by poor rpm overspeed and underspeed control.

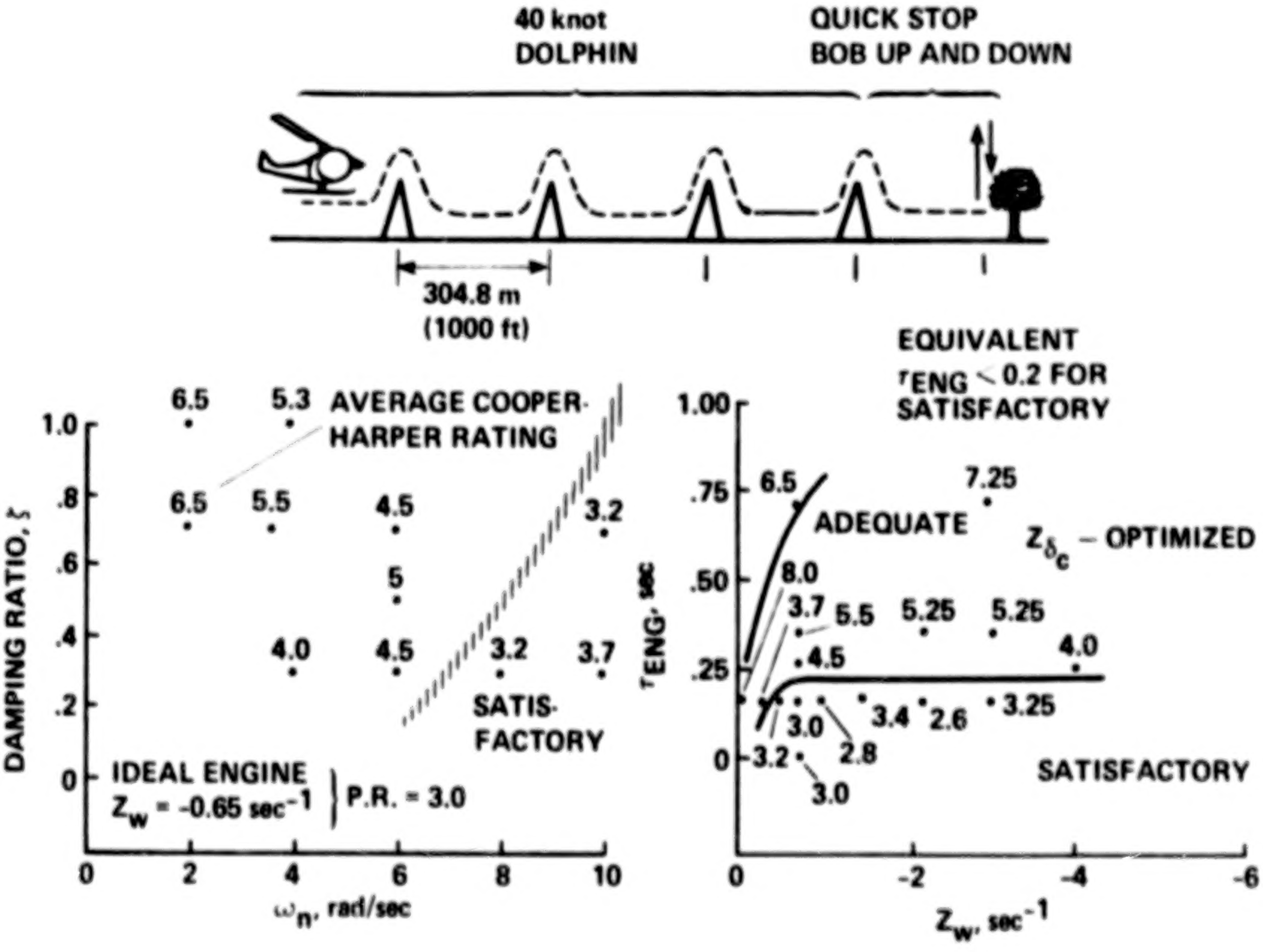

Figure 3

EFFECT OF EXCESS THRUST, ROTOR INERTIA, AND RPM CONTROL ON HELICOPTER HANDLING QUALITIES

The excess power requirements (T/W) for the NOE tasks were investigated with various levels of vehicle vertical damping Z_w. Results indicated that the required level of T/W is a strong function of Z_w as shown in figure 4, and is minimized at a Z_w value around -0.8 rad/sec. In addition to the required engine response time (as previously shown in fig. 3), an excess power level of T/W = 1.1 is required to achieve satisfactory handling qualities for the bob-up task evaluated. The thrust response of a helicopter, unlike that of fixed-wing VTOL aircraft, is influenced by several factors, including (1) engine governor dynamics, (2) vertical damping resulting from rotor inflow, and (3) the energy stored in the rotor, which is a function of rotor inertia. The experimental results (ref. 3) indicate, however, that increases in rotor inertia (thus the stored kinetic energy) have only a minor and desirable effect on handling qualities. The effect on handling qualities of requirements for pilot monitoring and control of rotor rpm can be significant. For a slow engine governor, the degradation in pilot rating in the bob-up tasks was as much as two ratings. It may therefore warrant consideration of techniques to relieve the pilot of the task and concern for monitoring proper rpm.

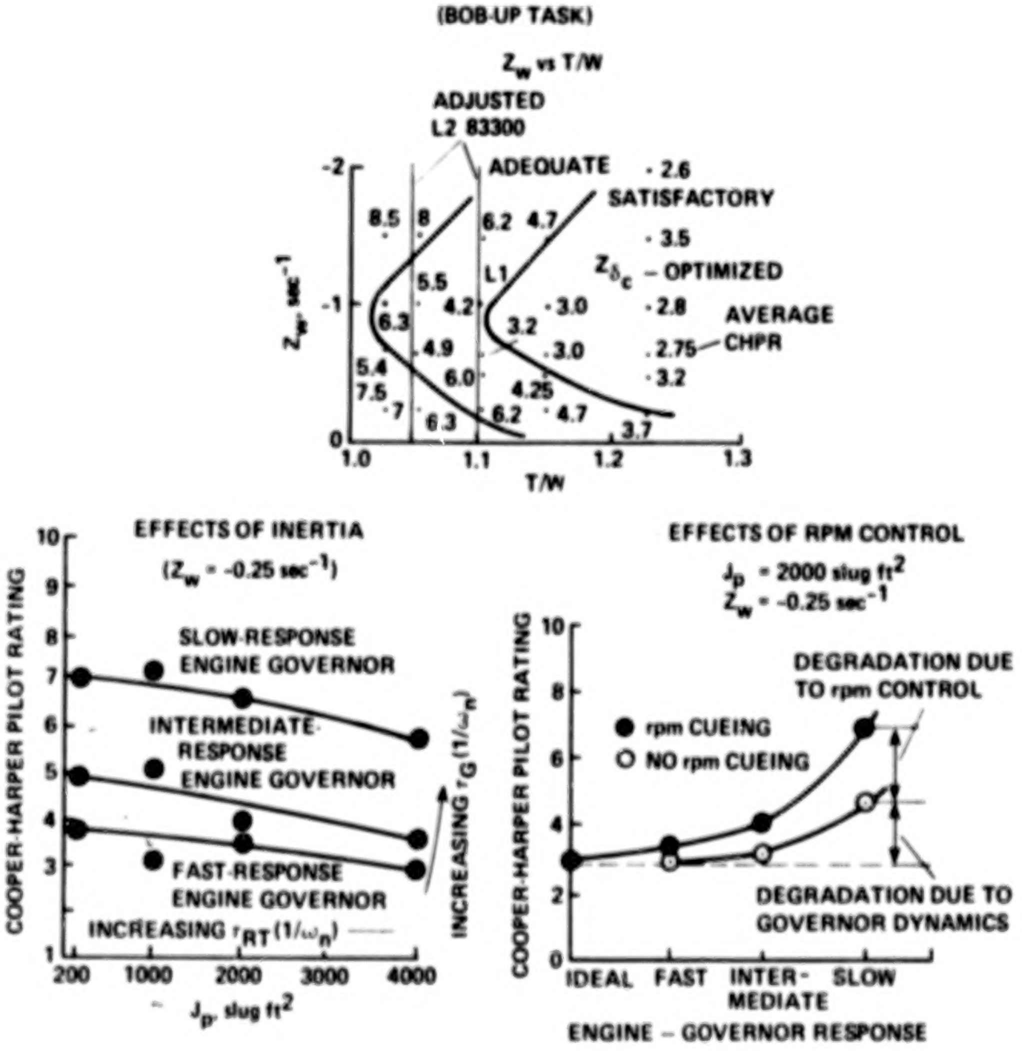

Figure 4

EFFECTS OF INTERAXIS COUPLING ON HELICOPTER HANDLING QUALITIES

One unique characteristic of the handling qualities problems associated with the single main rotor helicopter is the cross coupling between the longitudinal- and lateral-directional motions such as yawing, rolling, and pitching moments due to collective pitch input, and the pitch-roll cross coupling caused by aircraft angular rate in pitch and roll. Recent design trends of augmenting control power with increased flapping hinge offset or with a stiffened flapping hinge to increase low-g maneuverability can aggravate those undesirable interaxis cross couplings. To quantify their influences on the handling qualities, piloted simulation experiments (refs. 4, 5) and a flight experiment have been conducted (ref. 6). Some of the results are shown in figure 5, which indicates the trends of pilot rating as influenced by the level of yawing moment due to collective input N_{δ_c}, the ratio of pitching moment caused by collective input to pitch damping M_{δ_c}/Mq, and the ratio of the rolling moment caused by pitch rate to roll damping Lq/Lp. Means of reducing the interaxis coupling through either proper selection of rotor system design parameters or use of stability and control augmentation systems to improve the handling qualities have also been investigated (ref. 7).

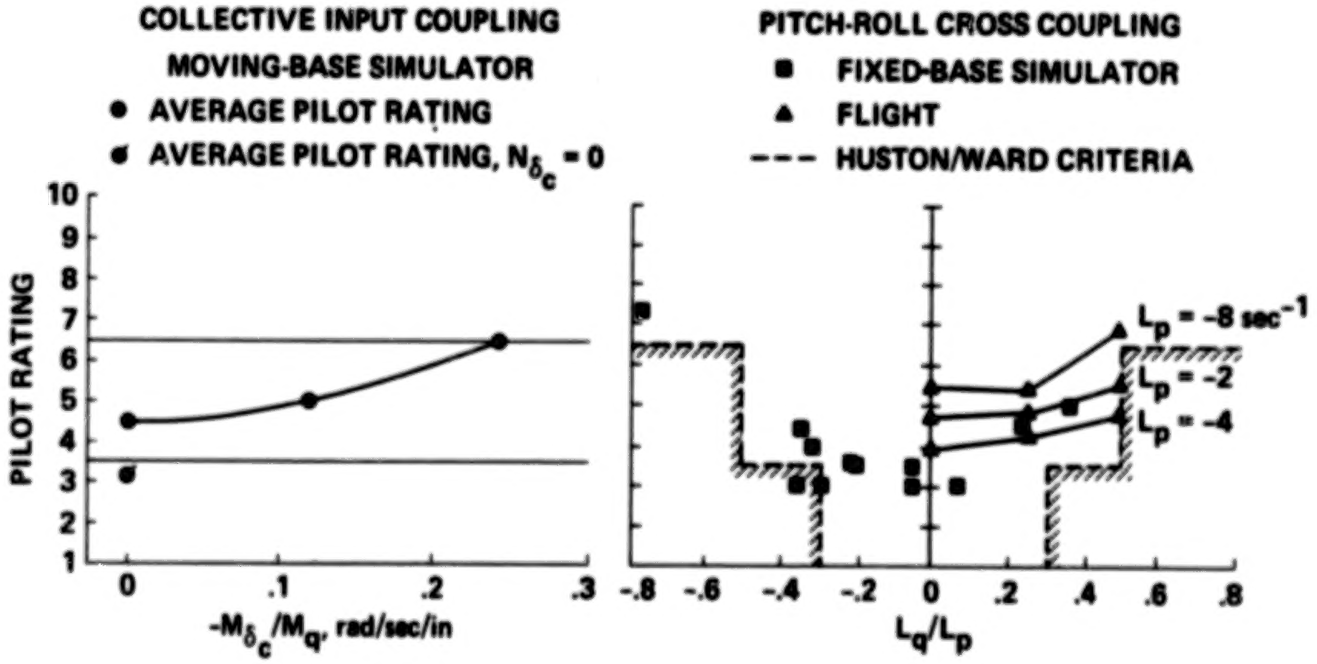

Figure 5

ORIGINAL PAGE IS
OF POOR QUALITY

INTERACTION OF CONTROLLER CHARACTERISTICS, CONTROL LAW, AND DISPLAY

In support of the Army's Advanced Digital/Optical Control System (ADOCS) program, a series of piloted simulations (refs. 8-11) were conducted both at the Boeing Vertol facility and in-house on the VMS at Ames to assess the interactive influences of side-stick controller characteristics, level of stability and control augmentation, and a helmet-mounted display which provided a limited field-of-view image with superimposed flight control symbology. A wide range of stability and control augmentation system (SCAS) designs, ranging from the basic UH60A helicopter SCAS to a SCAS with translational rate command/translational rate stabilization, was investigated. Variations in controller force-deflection characteristics and the number of axes controlled through an integrated side-stick controller as shown in figure 6 were studied. The handling qualities data base developed from this series of experiments for both day visual and night/adverse weather terrain flying tasks will be used not only for the design of the ADOCS demonstrator helicopter but also as design data for future military rotorcraft such as JVX and LHX.

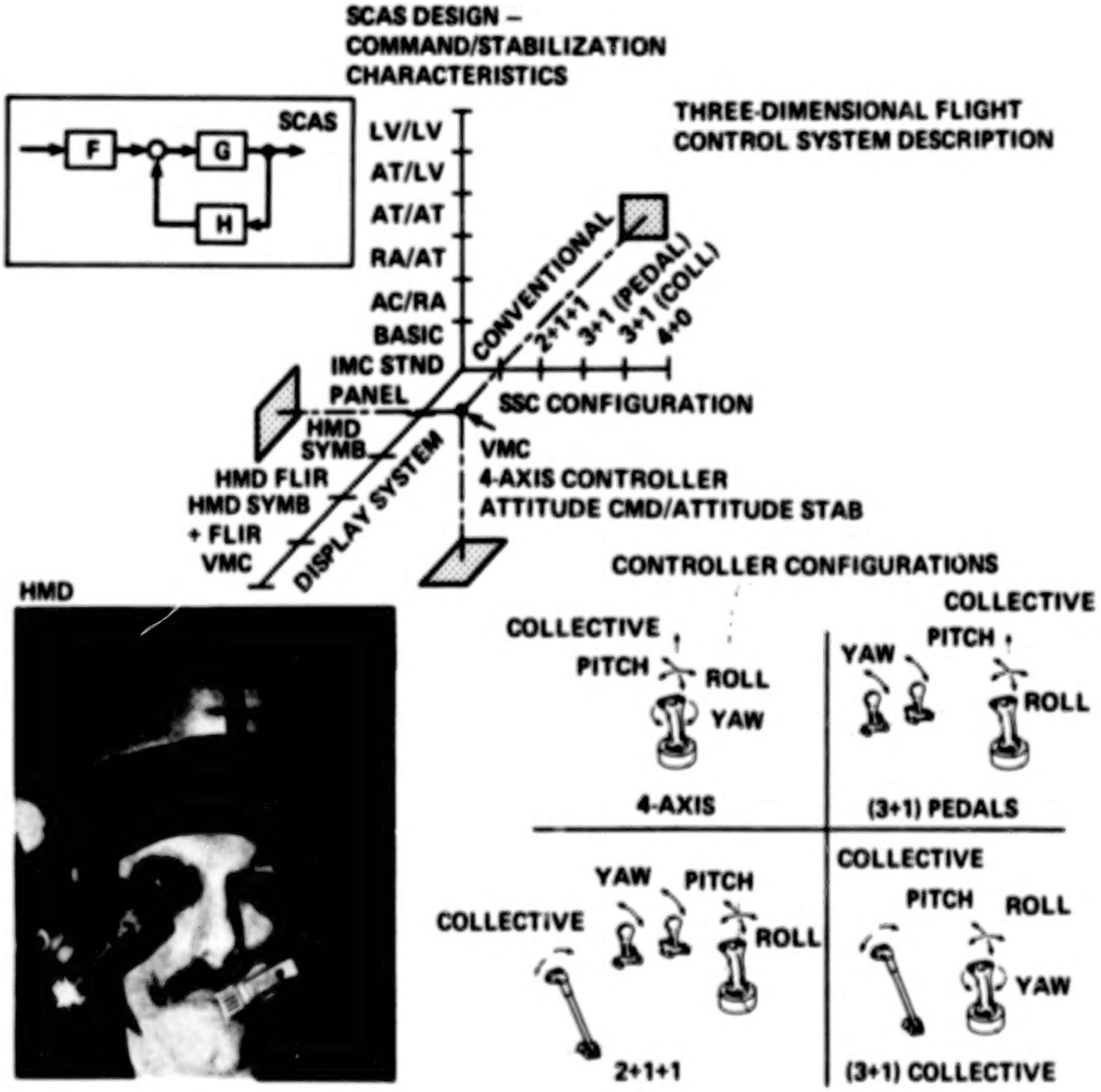
SCAS DESIGN –
COMMAND/STABILIZATION
CHARACTERISTICS
F
G
H
SCAS
LV/LV
AT/LV
AT/AT
RA/AT
AC/RA
BASIC
THREE-DIMENSIONAL FLIGHT
CONTROL SYSTEM DESCRIPTION
CONVENTIONAL
2+1+1
3+1 (PEDAL)
3+1 (COLL)
4+0
IMC STND
PANEL
HMD
SYMB
SSC CONFIGURATION
VMC
4-AXIS CONTROLLER
ATTITUDE CMD/ATTITUDE STAB
HMD FLIR
HMD SYMB
+ FLIR
VMC
DISPLAY SYSTEM
HMD
CONTROLLER CONFIGURATIONS
COLLECTIVE
PITCH
ROLL
YAW
4-AXIS
COLLECTIVE
YAW
PITCH
ROLL
(3+1) PEDALS
YAW
PITCH
COLLECTIVE
ROLL
2+1+1
COLLECTIVE
PITCH
ROLL
YAW
(3+1) COLLECTIVE

Figure 6

COMPARISON OF IMC AND VMC PILOT RATINGS

The results of this series of simulation experiments show that an integrated four-axis force controller with small deflection in all axes was preferred to other four-axes devices with no deflection (stiff stick). With small deflection, the pilot's ability to modulate single-axis forces was improved and the tendency to overcontrol or to produce input coupling was reduced. The results also indicate (ref. 9) that level of stability and control augmentation has a dominant effect on NOE handling qualities. With a high level of augmentation, satisfactory handling qualities for NOE tasks were achieved for all the three levels (two to four axes) of integrated force controllers having small deflection as shown in figure 7. However, the fully integrated (four-axis) controller degraded handling qualities compared to separate controllers for such large-amplitude multiaxis control tasks as a decelerating turning approach to hover and a high-speed slalom maneuver. Mission tasks flown under the simulated reduced visibility conditions received pilot ratings two or more rating points worse than the identical tasks flown under day VMS conditions.

NOE TASK

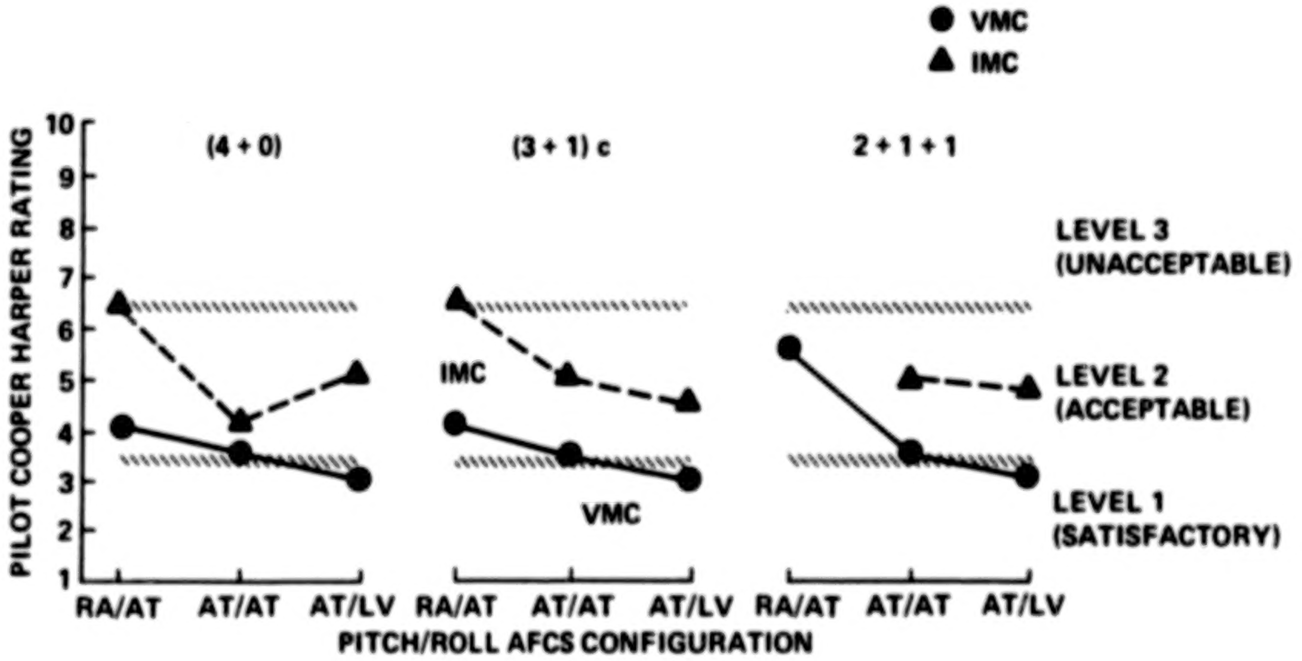

Figure 7

INFLUENCE OF LOAD FACTOR AND TURN DIRECTION ON MODE SHAPE

With ever-increasing military demands for agility and maneuverability of rotorcraft, there is a need to better understand the flight dynamics of rotorcraft in such large-amplitude, asymmetric maneuvers as steep, high-g turns. To meet this need, an analytical procedure has been developed to permit a systematic investigation of rotorcraft dynamic characteristics in steep, high-g turns (refs. 12-14). Numerical examinations of a tilt-rotor aircraft and several single-rotor helicopters with different types of main-rotor systems have been conducted. It has been found that strong coupling exists, particularly at low speeds, between the longitudinal- and the lateral-directional motions in high-g turns for both the symmetrical and asymmetrical-type rotorcraft; flying qualities and flight-control design analyses based on small disturbances from straight flight are grossly inadequate for predicting flight dynamics in high-g maneuvers. For example, for single-rotor helicopters the direction of turn has a significant influence on the flight dynamic characteristics in high-g turns. Figure 8 illustrates the effects of load factor and turn direction on the eigenvector of the Dutch-roll mode for a study hingeless rotor helicopter in level turns at 60 knots.

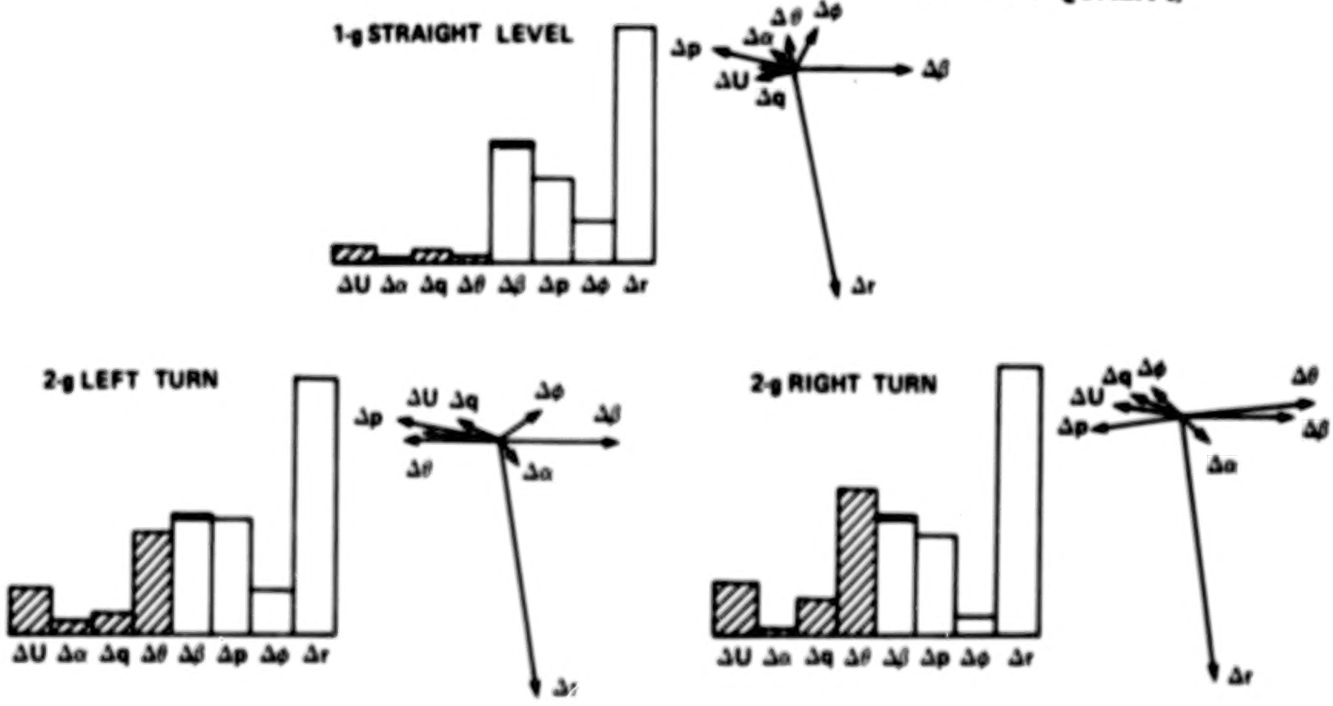

Figure 8

EFFECT OF LOAD FACTOR, TURN DIRECTION, AND UNCOORDINATION ON CONTROL RESPONSE

The developed analytical procedure also permits a systematic examination of statics and flight dynamics of rotorcraft in various levels of uncoordinated high-g turning maneuvers. Examinations of several rotorcraft indicate (1) that the aircraft trim attitudes in uncoordinated high-g turns can be grossly altered from those for coordinated turns, and (2) that within the moderate range of uncoordinated flight (side force up to ±0.1 g), the dynamic stability of these rotorcraft is relatively insensitive. However, the coupling between the longitudinal- and the lateral-directional motions is strong, and it becomes somewhat stronger as the sideslip increases. Examinations of the effect of uncoordinated high-g turns on the performance of a stability and control augmentation system designed using linear quadratic synthesis techniques indicate that the aircraft response with the SCAS on can degrade as sideslip increases. The influence of sideslip, however, is found to be less drastic than that of either load factor or turn direction as illustrated in figure 9 (ref. 14). In addition, the study also assessed the individual effects of the aerodynamic, kinematic, and inertial coupling on the flight dynamics of rotorcraft in steep turns.

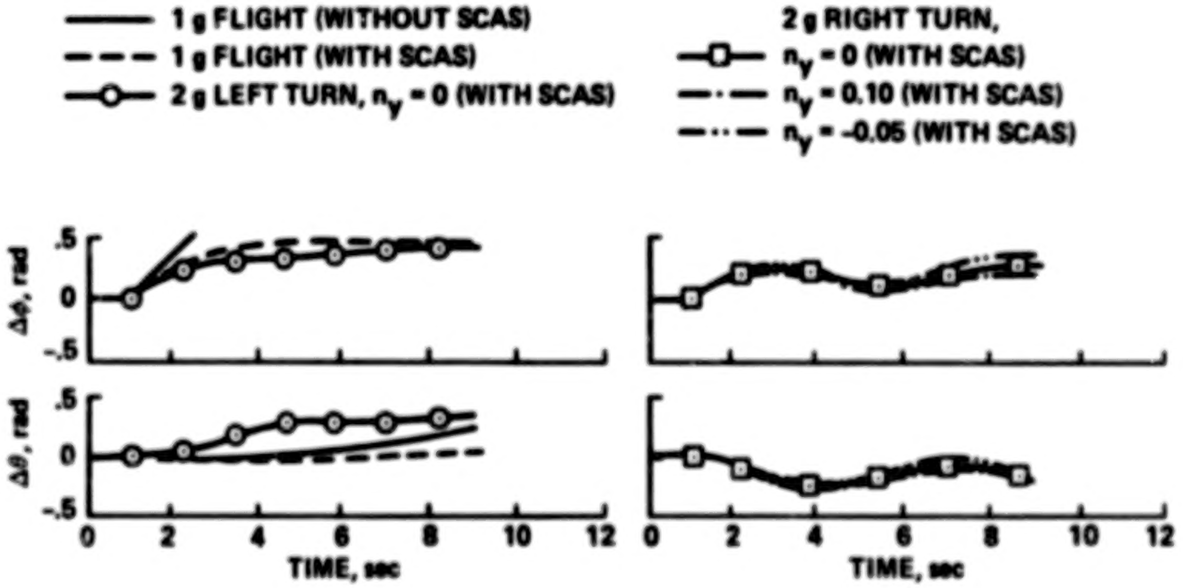

Figure 9

HELICOPTER IFR AIRWORTHINESS CRITERIA

We now turn to the rotorcraft certification criteria research. The rapid expansion of civil helicopter operations has led to increasing efforts to assess problem areas in civil helicopter design, certification, and operation. A joint NASA-FAA program was instituted at Ames to investigate the influence of the helicopter's inherent flight dynamics, flight control system, and display complement on flying qualities for IFR flight, both in terms of design parameters to ensure a good IFR capability and with regard to the characteristics that should be required for certification. The specific areas of concern that were addressed include (1) the requirements for stable force or position control gradients; (2) the difference in criteria for normal-category rotorcraft, depending on whether the aircraft is to be certified single or dual pilot; and (3) the SCAS and display requirements for decelerating instrument approach to exploit the helicopter's unique capability to fly at very low speeds. Five ground-based piloted simulations and one flight experiment were conducted during a 3-yr period beginning in 1978 (refs. 15 and 16). These experiments were summarized in figure 10 in terms of the specific objectives, the task evaluated, and the facility used.

EXPERIMENT SUMMARY

EXPERIMENT	TASK	OBJECTIVES	FACILITY	DATE
1	• CONST. SPEED VOR • DUAL PILOT	• HELICOPTER MODELS • SCAS IMPLEMENTATION	FSAA	NOV 78
2	• CONST. SPEED VOR • DUAL PILOT	• STATIC STABILITIES • SCAS IMPLEMENTATION	FSAA	MAR 79
3	• CONST. SPEED MLS • SINGLE AND DUAL PILOT	• FLIGHT DIRECTORS AND CONTROL-DISPLAY • CREW LOADING	FSAA	MAR 80
4	• CONST. SPEED MLS • DUAL PILOT	• VALIDATE GRD. SIM. RESULTS FOR STATICS, SCAS, AND FLIGHT DIRECTORS	FLIGHT: UH-IH	SEP 80
5	• CONST. SPEED MLS • DUAL PILOT	• LONGITUDINAL DOF • STATIC AND DYNAMIC CRITERIA	VMS	NOV 80
6	• DECELERATING MLS • DUAL PILOT	• INSTRUMENT DECELERATION • ELECTRONIC DISPLAYS	VMS	OCT 81

Figure 10

INFLUENCE OF LONGITUDINAL CONTROL GRADIENT

Regulations (ref. 17) require positive longitudinal control force stability at approach speeds for both transport and normal-category helicopters, regardless of crew loading. This requirement is probably justifiable for rate-damping types of SCAS, although little significant degradation has been shown with neutral or slightly unstable gradients; hence, the neutral gradient, at least, could be considered marginally acceptable. Figure 11 shows the results of this series of experiments, which indicate the trend of handling qualities as influenced by static longitudinal stability for the rate-damping type of SCAS. Note that with this type of SCAS, average ratings in the satisfactory category were not achieved, even at the most stable level. In commenting about these configurations, the pilots noted increasing difficulties in maintaining trim and controlling speed precisely as the static stability was decreased, but they also noted that the instrument tracking performance was still adequate at least to neutral stability. It should be emphasized that a rate-command attitude-hold type of SCAS results in a neutral longitudinal gradient; this type of SCAS was generally rated in the satisfactory category. Hence the requirement of control gradient may have to be linked to the type of SCAS employed, which it currently is not.

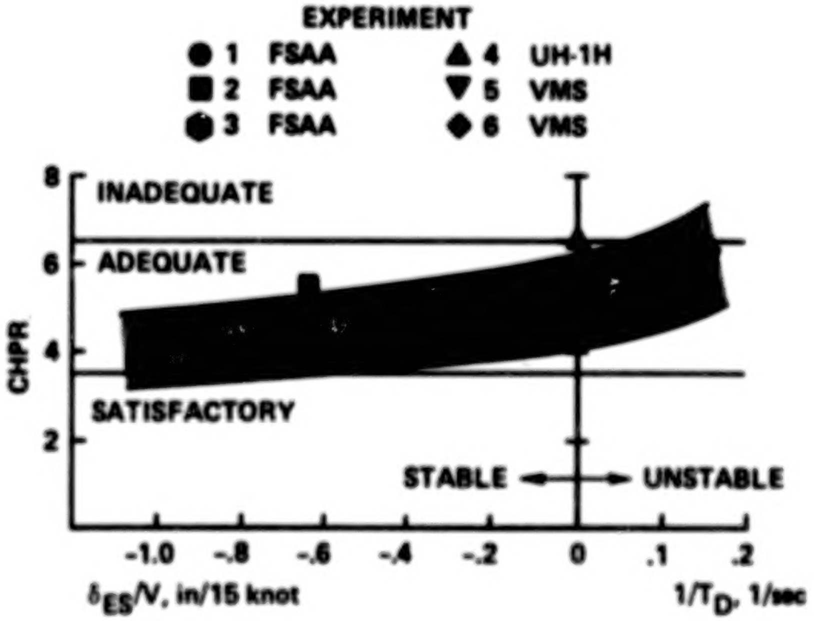

Figure 11

INFLUENCE OF SCAS

Most helicopters currently certified for single-pilot IFR operations employ advanced SCAS or displays or both. Of concern is the level of complexity of the SCAS required to achieve a good IFR capability because of the cost, control authority, and reliability factors the SCAS introduces. The influence of SCAS on the IFR handling qualities was therefore investigated. As shown in figure 12, three types of pitch and roll SCAS, among others, were considered: rate damping with input decoupling, rate command-attitude-hold (RCAH), and attitude command (AC). These cases are primarily for the SCAS incorporated on a machine with neutral basic longitudinal stability. Note that a rate-damping SCAS does not alter the control position gradient, a RCAH SCAS results in a neutral gradient (as described earlier), and the attitude SCAS stabilizes the gradient because of the M_θ term. As indicated in figure 12, rate-damping augmentation, even at a fairly high level and with input decoupling, generally has received pilot ratings from marginally adequate to just worse than satisfactory. Attitude augmentation in pitch and roll (implemented either as RCAH or AC) is required to achieve satisfactory handling qualities for IFR operations in turbulence. With attitude augmentation, the interaxis coupling and turbulence excitation are reduced and short-term and long-term dynamics are improved.

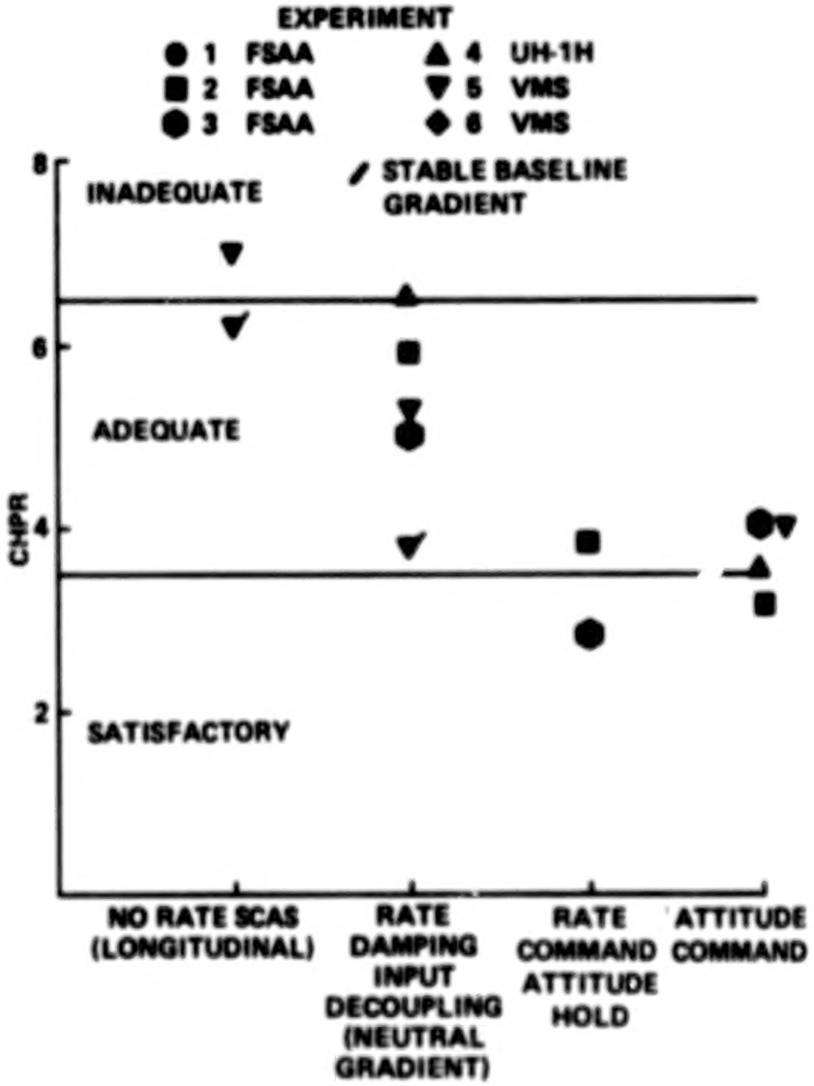

Figure 12

INFLUENCE OF TASK DIFFICULTY

Since the pilot rating applies to a control/display combination for a specific task, and since the evaluation tasks varied somewhat across this series of experiments, it is instructive to show the influence of task on the ratings. Ratings from these experiments are compared in figure 13 for similar SCAS characteristics (rate SCAS and attitude-command SCAS) and displays (with and without three-cue flight director displays) as a function of the task evaluated. It is noted that the addition of three-cue flight directions generally improves ratings. Also, an increase in the task difficulty (e.g., single pilot or inclusion of an instrument deceleration) results in degraded ratings for equivalent configurations. Specifically, the difference between the dual-pilot and single-pilot tasks is seen to be almost one pilot rating point. A difference in requirements for single- and dual-pilot operations is warranted. In addition, it may also be seen from figure 13 that a decelerating instrument approach leads to worse ratings than even the single-pilot task with a constant-speed approach. More stringent criteria may therefore be required for decelerating instrument operations.

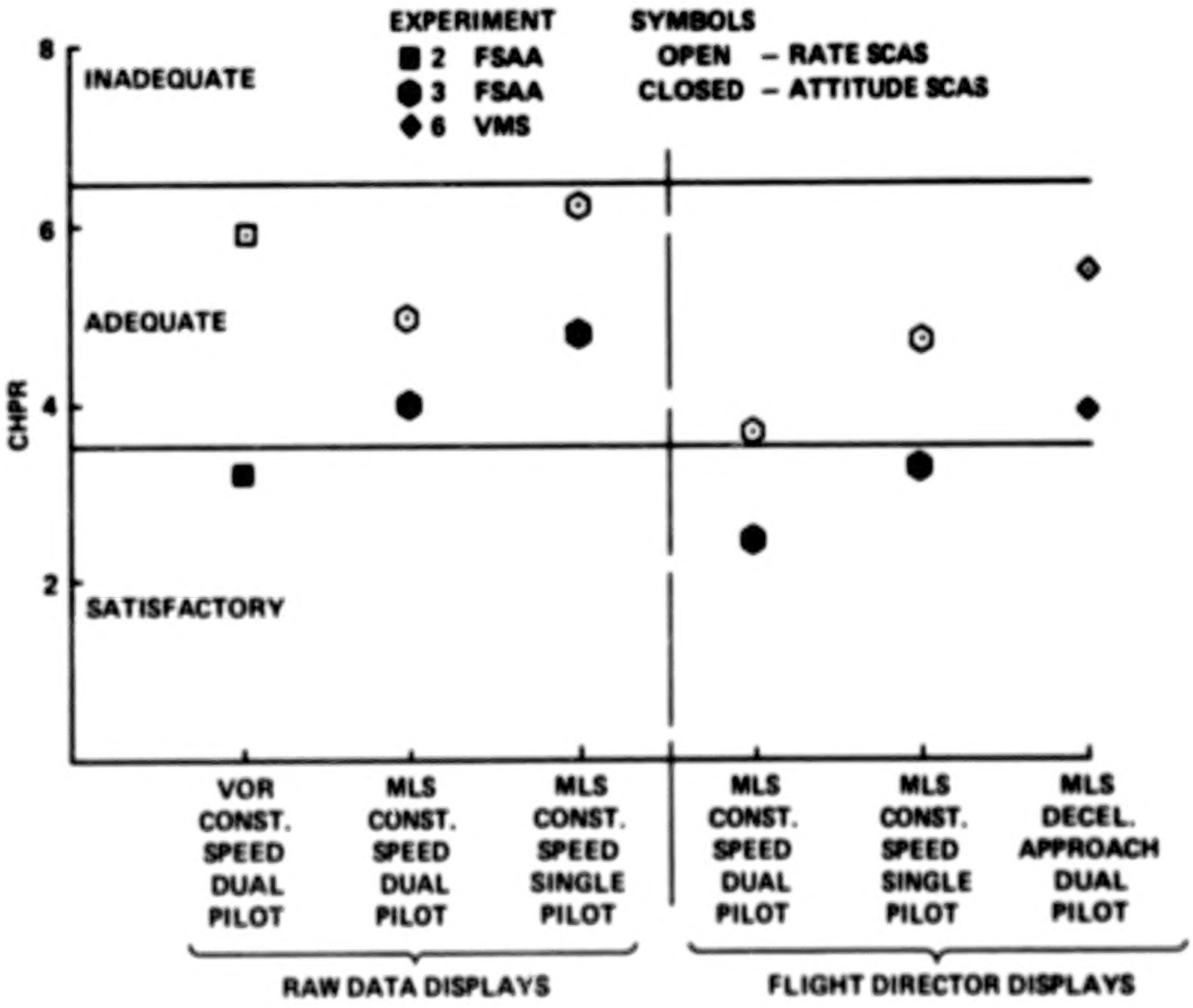

Figure 13

PILOT EVALUATIONS OF TILT-ROTOR TRANSITION

The first ground-based simulation experiment in a projected series of investigations was conducted by NASA and the FAA on the VMS at Ames to perform a preliminary assessment of airworthiness considerations for tilt-rotor aircraft in terminal area operations (fig. 14). Principal variables of the experiment were (1) visual versus instrument approaches, (2) the type of stability and control augmentation, and (3) three conversion profiles ranging from full conversion before the glide slope to full conversion on the glide slope. The results obtained in a recent study indicated that, for visual approaches, satisfactory performance within moderate pilot compensation was generally achievable irrespective of the conversion profile used; crosswinds and a moderate level of turbulence had a noticeably degrading effect with the baseline XV-15 SCAS but minimal influence with an attitude SCAS. For instrument approaches, the desired performance could be achieved with the attitude SCAS and the conversion profile having all conversion prior to the glide slope. It was also found that the marginally inadequate performance for the profile having all the conversion on the glide slope could be improved to the satisfactory level by adding automatic thrust tilt and three-cue flight directors.

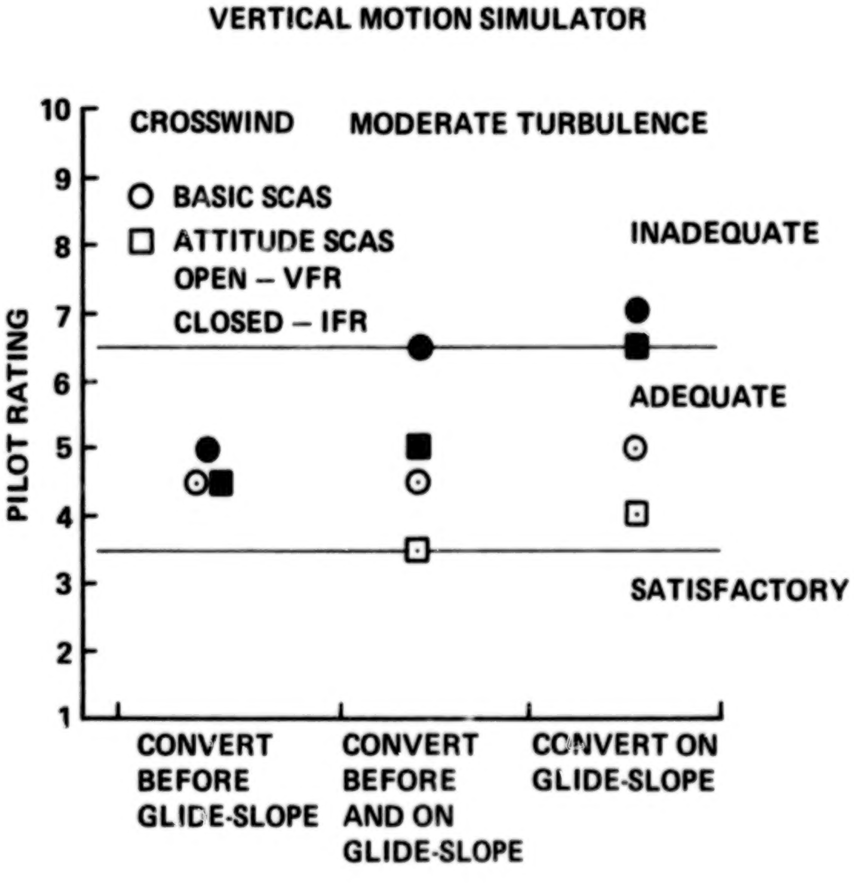

Figure 14

SUMMARY

In summary, we have briefly reviewed some major rotorcraft handling qualities research projects at Ames Research Center (fig. 15). They were grouped into two categories: (1) military rotorcraft handling qualities research, and (2) civil rotorcraft certification criteria research. In the first category, the research efforts that focus on determining the effects of engine and thrust response characteristics, interaxis coupling, controller characteristics control law/display interaction, and large-amplitude maneuvers were highlighted. In the second category, efforts to develop IFR airworthiness handling qualities criteria for helicopters and tilt-rotor aircraft were discussed. Before concluding this discussion, it may be worth noting that a joint Army/Navy program is currently under way to update MIL-H-8501A. The objective is to develop mission-oriented handling qualities requirements for military rotorcraft (ref. 18). NASA's role related to the program is (1) to continue working with the Army (Aeromechanics Laboratory) to establish a comprehensive handling qualities data base and design guidelines for land-based military rotorcraft, and (2) to expand the scope to include research on developing rotorcraft handling qualities criteria for Navy shipboard mission tasks.

- **MILITARY ROTORCRAFT HANDLING QUALITIES RESEARCH**
  - **EFFECTS OF ENGINE AND THRUST RESPONSE CHARACTERISTICS**
  - **EFFECTS OF INTERAXIS COUPLING**
  - **INTERACTIVE EFFECTS OF CONTROLLER/CONTROL LAW/DISPLAY**
  - **EFFECTS OF LARGE AMPLITUDE (HIGH-g) MANEUVERS**
- **ROTORCRAFT CERTIFICATION CRITERIA RESEARCH**
  - **HELICOPTER IFR TERMINAL AREA OPERATIONS**
  - **TILT-ROTOR AIRCRAFT**

Figure 15

REFERENCES

1. General Requirement for Helicopter Flying and Ground Handling Qualities. Military Specification MIL-H-8501A, Bureau of Naval Weapons, 7 Sept. 1961.

2. Corliss, L. D.: The Effects of Engine and Height-Control Characteristics on Helicopter Handling Qualities. J. AHS, vol. 28, no. 3, July 1983, pp. 56-62.

3. Corliss, L. D.; Blanken, C. L.; and Nelson, K.: Effects of Rotor Inertia and RPM Control on Helicopter Handling Qualities. AIAA Paper 83-2070, 1983.

4. Chen, R. T. N.; and Talbot, P. D.: An Exploratory Investigation of the Effects of Large Variations in Rotor System Dynamics Design Parameters on Helicopter Handling Characteristics in Nap-of-the-Earth Flight. J. AHS, vol. 24, no. 3, July 1978, pp. 23-36.

5. Chen, R. T. N.; Talbot, P. D.; Gerdes, R. M.; and Dugan, D. C.: A Piloted Simulator Study on Augmentation Systems to Improve Helicopter Flying Qualities in Terrain Flight. NASA TM-78571, 1979.

6. Corliss, L. D.; and Carico, G. D.: A Preliminary Flight Investigation of Cross-Coupling and Lateral Damping for Nap-of-the-Earth Helicopter Operations. AHS Paper 81-28, 1981.

7. Chen, R. T. N.: Unified Results of Several Analytical and Experimental Studies of Helicopter Handling Qualities in Visual Terrain Flight. Helicopter Handling Qualities, NASA CP-2219, 1982, pp. 59-74.

8. Landis, K. H.; and Aiken, E. W.: An Assessment of Various Side-Stick Controller/Stability and Control Augmentation Systems for Night Nap-of-the Earth Flight Using Pilot Simulation. Helicopter Handling Qualities, NASA CP-2219, 1982, pp. 75-96.

9. Landis, K. H.; Dunford, P. J.; Aiken, E. W.; and Hilbert, K. B.: A Piloted Simulator Investigation of Side-Stick Controller/Stability and Control Augmentation System Requirements for Helicopter Visual Flight Tasks. AHS Paper A-83-39-59-4000, 1983.

10. Aiken, E. W.: Simulator Investigation of Various Side-Stick Controller/ Stability and Control Augmentation Systems for Helicopter Terrain Flight. AIAA Paper 82-1522, 1982.

11. Aiken, E. W.; Landis, K. H.; Glusman, S. I.; and Hilbert, K. B.: An Investigation of Side-Stick Controller/Stability and Control Augmentation System Requirements for Helicopter Terrain Flight Under Reduced Visibility Conditions. AIAA Paper 84-0235, Jan. 1984.

12. Chen, R. T. N.; and Jeske, J. A.; Influence of Sideslip on the Kinematics of the Helicopter in Steady Coordinated Turns. J. AHS, vol. 27, no. 4, Oct. 1982, pp. 84-92.

13. Chen, R. T. N.: Flight Dynamics of Rotorcraft in Steep High-g Turns. AIAA Paper 82-1345, 1982.

14. Chen, R. T. N.; Jeske, J. A.; and Steinberger, R. H.: Influence of Sideslip on the Flight Dynamics of Rotorcraft in Steep Turns at Low Speeds. 39th Annual Forum of the AHS, St. Louis, Mo., May 9-11, 1983 (Paper No. A-83-39-56-4000).

15. Lebacqz, J. V.: A Ground Simulation Investigation of Helicopter Decelerating Instrument Approaches. AIAA Paper 82-1346, 1982.

16. Lebacqz, J. V.; Chen, R. T. N.; Gerdes, R. M.; and Weber, J. M.: A Summary of NASA/FAA Experiments Concerning Helicopter IFR Airworthiness Criteria. J. AHS, vol. 28, no. 3, July 1983, pp. 63-70.

17. Rotorcraft Regulatory Review Program Notice, No. 1; Proposed Rulemaking, Federal Register, vol. 45, no. 245, Dec. 18, 1980.

18. Key, D. L.: The Status of Military Helicopter Handling Qualities Criteria. AGARD Criteria for Handling Qualities of Military Aircraft, AGARD CP-333, June 1982, pp. 11-1 to 11-9.

N84
20572

UNCLAS

N84 20572

FLEXIBLE AIRCRAFT FLYING AND RIDE QUALITIES

Irving L. Ashkenas, Raymond E. Magdaleno, and Duane T. McRuer
Systems Technology, Incorporated
Hawthorne, California

First Annual NASA Aircraft Controls Workshop
NASA Langley Research Center
Hampton, Virginia
October 25-27, 1983

REPORT CONTENTS

This presentation covers some of the highlights of NASA CR-172201, "Flight Control and Analysis Methods for Studying Flying and Ride Qualities of Flexible Transport Aircraft." The report itself contains the chapters listed in Fig. 1, and we'll follow this order in our discussion. Of course, we'll have to limit ourselves to the more significant aspects and forego many of the details that are in the report.

We'll start with a block diagram representative of a generalized FCS, go into a brief analytic exposition to illustrate a central principle in flexible mode control, list and discuss some of the pertinent pilot-centered requirements, expose the desired features of the control methodology, and select the methodology to be used.

Then we'll discuss the example Boeing-supplied characteristics and show how we approximated these with a reduced-order model and a simplified treatment of unsteady aerodynamics. The closed-loop flight control system design follows, along with first-level assessments of resulting handling and ride quality characteristics. Some of these do not meet the postulated requirements and remain problems to be solved possibly by further analysis or future simulation.

I. INTRODUCTION

II. GENERAL ASPECTS OF FLEXIBLE VEHICLE CONTROL

III. SYSTEM DESIGN REQUIREMENTS AND DESIRES

IV. METHODOLOGY CONSIDERATIONS FOR FLEXIBLE AIRCRAFT CONTROLS AND FLYING QUALITIES ANALYSIS

V. FLEXIBLE AIRPLANE CHARACTERIZATION AND SIMPLIFICATION

VI. FLIGHT CONTROL DESIGN AND ASSESSMENTS

VII. CONCLUSIONS AND RECOMMENDATIONS

REFERENCES

Figure 1

GENERALIZED FLIGHT CONTROL SYSTEM FOR TRANSPORT AIRCRAFT INCLUDING FLEXIBLE MODES

This block diagram (Fig. 2) illustrates primarily the multiple feedback paths acting on the sensor array and the possible use of secondary control points and limited forward loop elements. The primary FCS design task, of course, is to formulate the sensor equalization complex to yield a stable, robust system which meets the direct and implied requirements.

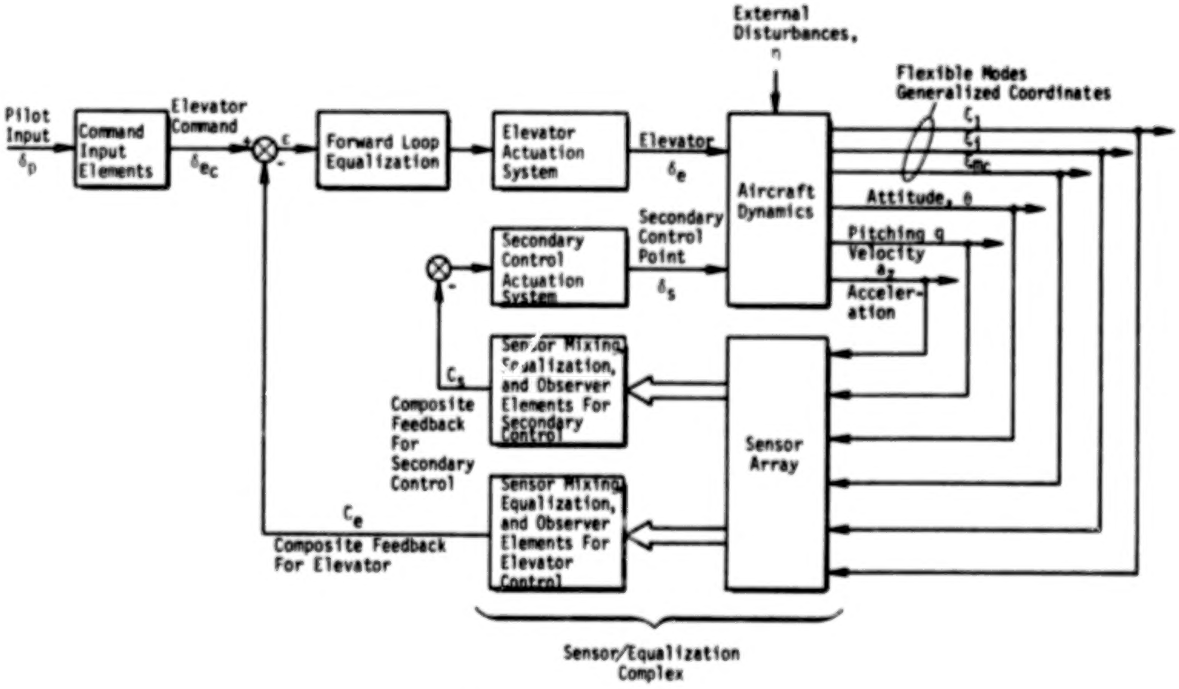
External Disturbances, η
Flexible Modes Generalized Coordinates
ζ_1
$\dot{\zeta}_1$
ζ_{nc}
Pilot Input δ_p
Command Input Elements
Elevator Command δ_{e_c}
+
-
ε
Forward Loop Equalization
Elevator Actuation System
Elevator δ_e
Aircraft Dynamics
Attitude, θ
Pitching Velocity q
Acceleration a_z
Secondary Control Actuation System
Secondary Control Point δ_s
-
C_s
Sensor Mixing, Equalization, and Observer Elements For Secondary Control
Composite Feedback For Secondary Control
Sensor Array
C_e
Composite Feedback For Elevator
Sensor Mixing, Equalization, and Observer Elements For Elevator Control
Sensor/Equalization Complex

Figure 2

ELEMENTARY FLEX MODE CONSIDERATIONS

These equations (Fig. 3) constitute a simplified treatment of the considerations involved in synthesizing a suitable sensor-equalization response.

The first equation represents the rigid-body attitude rate response; the second is the first oscillatory flexible mode response where ϕ' is the slope of the first bending mode at the sensor station.

Adding these responses yields the third equation with the simplified numerator/denominator ratios shown. The point is that selection of the sensor location and corresponding mode slope ϕ' can be used to directly affect these ratios or the equivalent pole-zero ordering.

$$\frac{q_o}{\delta_e} \doteq \frac{\phi_o'}{s}$$

$$\frac{q_{flex}}{\delta_e} \sim \frac{\phi_1'(x)s}{s^2 + 2(\zeta\omega)_D s + \omega_D^2}$$

$$G(s) = \frac{C_e}{E} = \frac{K[s^2 + 2\zeta_N\omega_N s + \omega_N^2]}{s[s^2 + 2\zeta_D\omega_D s + \omega_D^2]}$$

$$\omega_N = \sqrt{\frac{\phi_o'}{\phi_o' + \phi_1'}}\,\omega_D$$

$$\zeta_N = \sqrt{\frac{\phi_o'}{\phi_o' + \phi_1'}}\,\zeta_D$$

Figure 3

If the zero is greater than the pole, the root locus progresses into the right half-plane as in a); if less, it stays in the left half-plane as in b) and the proper choice of feedback gain will then provide enhanced structural mode damping.

This is a simplified explanation of a well-known general principle of flexible mode control, i.e., the desirability of synthesizing a sensor-equalization characteristic which exhibits an alternating numerator/denominator ordering of quadratic pairs (a sawtooth Bode) which creates leading phase "blips" for those modes which are to be controlled. For those modes which are to be largely ignored by the control system, appropriate notch or low-pass filtering might be considered if the modes are not so high in frequency relative to actuator and other dynamics as to make them insignificant anyway. (See Fig. 4.)

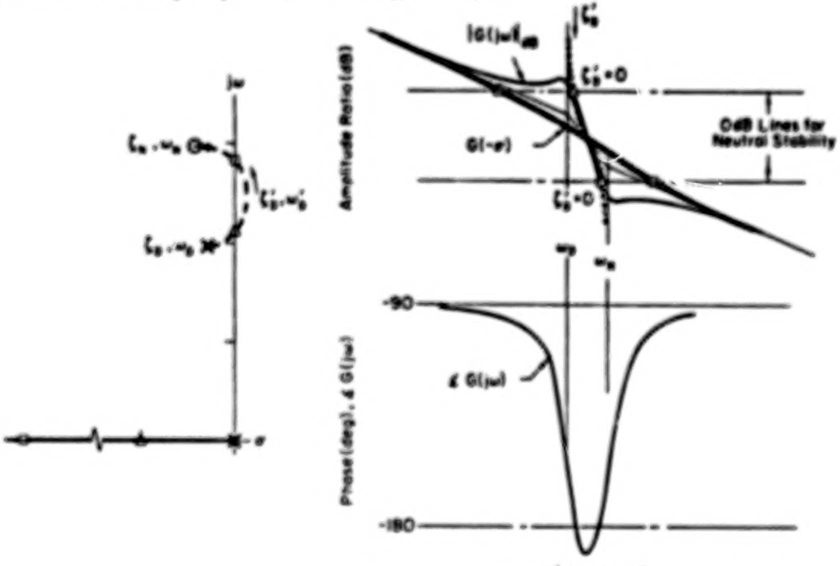
jω
ζ_a, ω_a
ζ_b', ω_b'
ζ_b, ω_b
σ
$|G(j\omega)|_{dB}$
ζ_b'
$\zeta_b' = 0$
G(−σ)
0dB Lines for Neutral Stability
$\zeta_b' = 0$
Amplitude Ratio (dB)
ω_b
ω_a
-90
∠ G(jω)
Phase (deg), ∠ G(jω)
-180
ω, σ, ω_b' (log scale)

a) Log-Lead Dipole $\left(\frac{\omega_a}{\omega_b} > 1\right)$

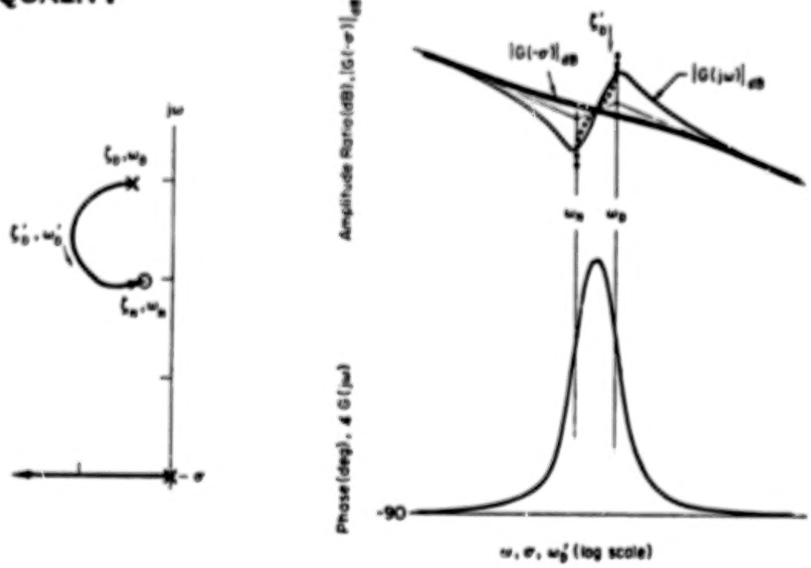
jω
ζ_b, ω_b
ζ_b', ω_b'
ζ_a, ω_a
σ
ζ_b'
$|G(-\sigma)|_{dB}$
$|G(j\omega)|_{dB}$
Amplitude Ratio (dB), $|G(-\sigma)|_{dB}$
ω_a
ω_b
Phase (deg), ∠ G(jω)
-90
ω, σ, ω_b' (log scale)

b) Lead-Lag Dipole $\left(\frac{\omega_a}{\omega_b} < 1\right)$

Figure 4

PILOT-CENTERED COMMAND REQUIREMENTS AND FLYING QUALITIES

In addition to the foregoing implied requirement, there are direct requirements for minimum satisfactory flying and ride qualities. The flying qualities list shown here pertains to pilot's attitude and acceleration response to elevator input (Fig. 5).

The first two headings refer primarily to attitude control and reflect the possible use of either frequency- or time-domain assessment criteria.

The third heading relates mostly to unwanted acceleration responses which can be excited directly by the pilot's remnant, self-excited by feedthrough to, and amplification resulting from, the pilot's body-arm-controller induced motions, or directly excited by normal closed-loop piloted operation.

The final heading generally relates to either attitude or acceleration responses, although attitude is the more common culprit. Both synchronous behavior and the PIO syndrome are assessed later for the derived system, as are pertinent aspects of the preceding items.

FREQUENCY DOMAIN

- **EQUIVALENT** $\frac{\theta}{\delta}(s) = \frac{M_\delta(s+1/T_{\theta_2})e^{-\tau s}}{s(s^2+2\zeta\omega s+\omega^2)}$
- **BANDWIDTH**
- **CLOSED LOOP**

TIME DOMAIN

- **ENVELOPE**
- **BOUNDED TIME PARAMETERS**
- **TRP**

FLEXIBLE MODE EFFECTS

- **REMNANT EXCITATION**
- **VIBRATION FEEDTHROUGH**
- **PILOT CLOSED-LOOP EXCITATON OF FLEX MODES**

PIO CONSIDERATIONS

- **SYNCHRONOUS BEHAVIOR**
- **PIO SYNDROME**

Figure 5

FQ AND FLEX A/C CONTROL CONSIDERATIONS GOVERNING CONTROL DESIGN TECHNIQUE SELECTION

The summation of certain of the foregoing and of the more complete considerations in the report as they pertain to the selection of appropriate design methodology is listed here (Fig. 6).

In the first place, we have to consider uncertainties and variations in the airframe poles and zeros due to changes in flight conditions and loading.

Second, we have to utilize and consider many elements which are basically expressed in frequency-domain formulations.

Third are the direct and implied control design criteria which can be in time- or frequency-domain formulations, or simply expressed as desirable qualities.

Based on these and other considerations, the basic control methodology selected comprises conventional, classical, multivariable, frequency-domain analysis techniques.

1. KEY AIRCRAFT PARAMETERS
   - POLES, ZEROS { WIDE RANGING (LO FREQ)
   - NARROW RANGES (HI FREQ)
2. FREQUENCY DOMAIN FORMULATIONS
   - PILOT I/O CONTROL ACTIVITIES, REMNANT, VIBRATION FEEDTHROUGH, PIO BEHAVIOR
   - UNSTEADY AERODYNAMICS
   - MODAL FORMULATIONS → FREQUENCY-IDENTIFIED POLES AND ZEROS
   - CONTROL ACTIVITY RANGE
   - RIDE AND HABITABILITY CONSIDERATIONS AND CRITERIA
   - RANDOM GUST INPUTS
3. CONTROL SYSTEM DESIGN CRITERIA
   - FLYING QUALITIES REQUIREMENTS
   - FLEX MODE POLE, ZERO SEQUENCING FOR CONTROLLED MODES
   - GAIN STABILIZATION FOR IGNORED MODES
   - ENHANCED DAMPING FOR MODES POSSIBLY CAUSING EXCESSIVE REMNANT PILOT FEEDTHROUGH, PILOT SYNCHRONOUS BEHAVIOR
   - PIO SUSCEPTIBILITY
   - CONTROLLER SIMPLICITY
   - CONTROLLER ROBUSTNESS

Figure 6

THREE VIEWS OF SUPERSONIC CRUISE AIRCRAFT

Before applying these techniques, it was necessary to derive a simplified representation of the Boeing-supplied data base for the delta wing supersonic cruise aircraft (SCRA), shown in Fig. 7, which included:

a. Modal equations of motion (EOM) - 25 × 25

b. Computer printouts of EOM matrix elements for 6 reduced-frequency sets of unsteady aerodynamics for each of 4 flight conditions

c. Mode shape data in a variety of formats: tabulated, interpolated displacements and slopes at selected locations on the fuselage centerline; pictorial or perspective views; and contour plots for wing relative displacements out-of-plane

d. Numerical frequency response data at 149 discrete frequencies supplied on magnetic tapes for four flight conditions. These "data" are the result of interpolation among the 6 reduced-frequency sets of unsteady aerodynamics

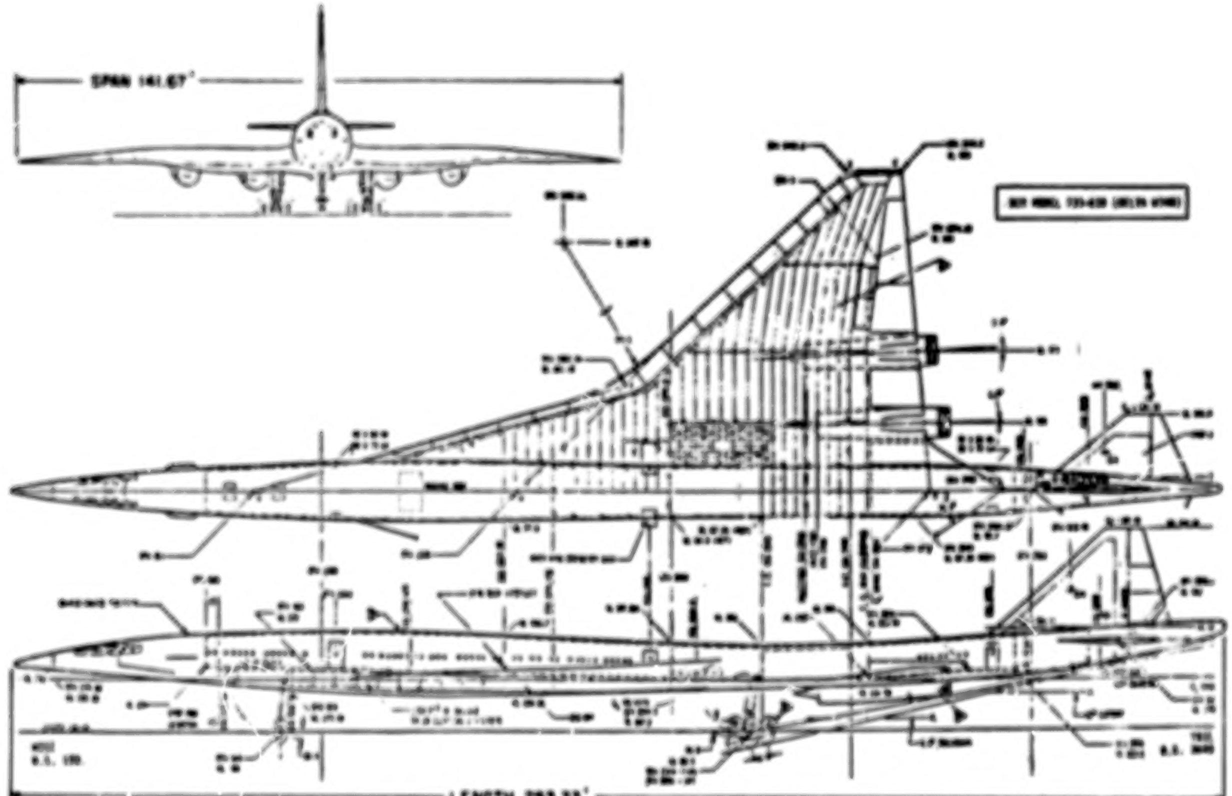

Figure 7

ORIGINAL PAGE IS OF POOR QUALITY

MODE SHAPES FOR TAKEOFF WEIGHT DISTRIBUTION

To afford an appreciation for the scope of the complete model formulation, the total set of centerline elastic mode shapes for the take-off case is shown in Fig. 8 in the form of displacement normalized to maximum deflection. In general, the modes are 3-dimensional, and Fig. 8 shows just the cut along the fuselage centerline. In many cases the maximum deflection is not along the centerline, and there is no corresponding unity value shown for those modes.

Modes one and two (Fig. 8) are rigid-body modes, respectively heave and pitching motion. Mode three is the first structural (bending) mode, and the structural modes go up in complexity and frequency as the numbers go up. The in-vacuo frequencies in Hz are as follows.

Mode	Frequency (Hz)	Mode	Frequency (Hz)	Mode	Frequency (Hz)
3	1.14	9	4.44	15	6.44
4	1.60	10	4.82	16	6.89
5	2.49	11	5.15	17	7.06
6	2.95	12	5.45	18	7.24
7	3.81	13	5.92	19	7.44
8	4.28	14	6.11	20	7.56

For a transport aircraft, this list has a remarkably large number of low-frequency closely spaced modes which can interfere, in one way or another, with piloted control.

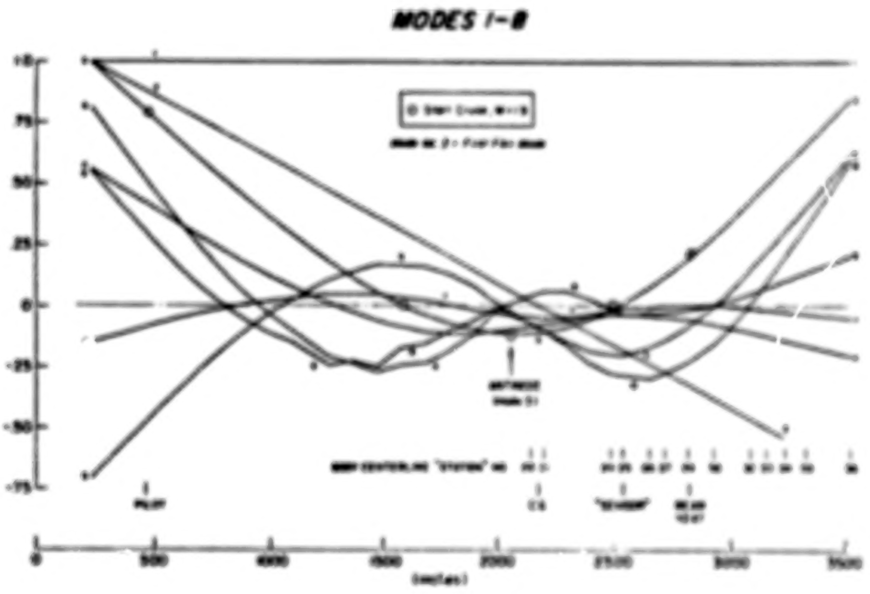

Figure 8

MODE SHAPES FOR TAKEOFF WEIGHT DISTRIBUTION (CONCLUDED)

Various body centerline stations and physical points are identified along the bottom of each plot. The "sensor station" is one chosen by Boeing as being in a fairly stiff region as evident by the fairly flat shape of the various modes in this area. The open circle symbols in Fig. 8 show that there is little change in mode three for the start cruise condition.

Modes nine through fourteen in Fig. 9 are characterized by more lumps and bumps than the first set, and modes fifteen through twenty in Fig. 9 are even lumpier and include some very large spikes. These anomalies appear to be due to ill-conditioned lumped parameters, that is, the mass and stiffness elements chosen for the analysis are not necessarily well conditioned and apparently lead to local resonances which give rise to the discontinuities shown.

However, notice that the area in the "sensor" region, where the structure is relatively stiff, is pretty smooth for all modes.

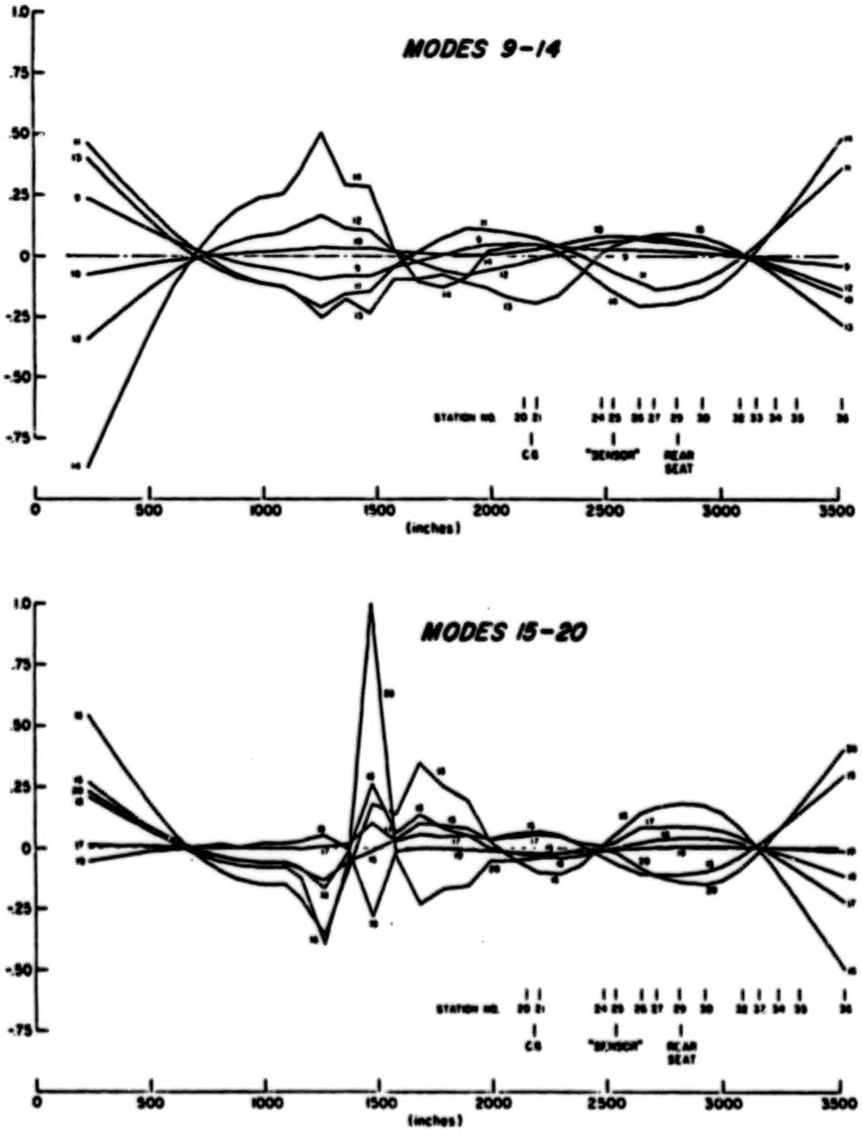

Figure 9

C-2

COMPARISON OF MODEL C WITH COMPLETE DISCRETE BOEING DATA

The number of elastic modes selected for final retention in the simplified model underwent a gradual increase from three to seven to ten largely to account for the acceleration response shown in Fig. 10. The reduced-order (10 mode) model "C" shown retains modes 3 to 6, 8, and 11 to 15, and is effected through progressive elimination of successive elastic modes by neglecting dynamic (s^2 and s) terms relative to (constant) stiffness terms in each successive modal column. The generalized coordinate to be eliminated, now characterized by only a stiffness term, is expressed in terms of the remaining coordinates. Notice that some of the retained modal equations are for higher frequency modes than those eliminated. This poses no mathematical problem, the progressive elimination of the equations in question proceeds as described above. However, there is no good physical rationale for neglecting the dynamic (s^2 and s) terms of certain lower frequency modes and retaining those for some higher frequency modes, except that it produces an excellent match as illustrated in Fig. 10, where the high-frequency behavior is reproduced with sufficient fidelity to permit accurate ride quality analyses to proceed on the basis of the reduced-order model.

This match is also based on simplified, "distributed" unsteady aerodynamics, meaning that for each degree of freedom, or matrix column, the corresponding flexible mode frequency was used to assign constant aerodynamics consistent with that value of reduced frequency.

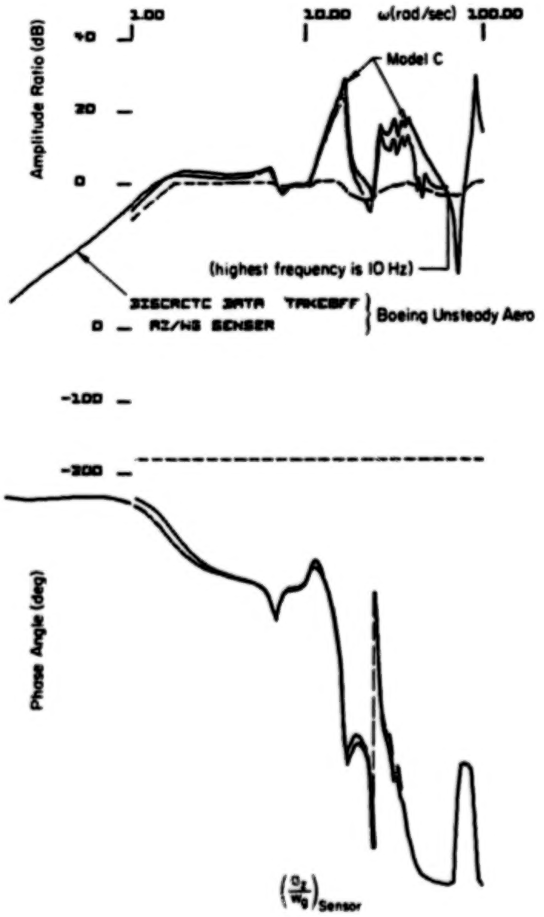

Figure 10

MODEL D TAKEOFF BODES OF PITCH ATTITUDE

A final correction was applied to eliminate perceived inconsistencies in the supplied numerical elevator inertial properties and produce the "final" (Fig. 11) model "D" attitude responses for two locations. The rear seat location provides the better sawtooth and is so labeled.

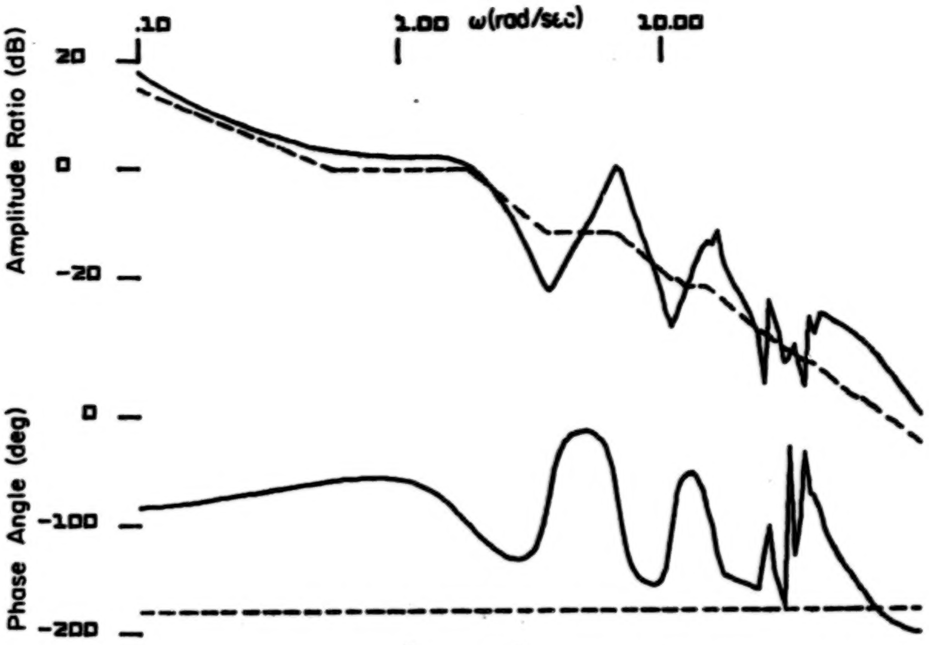

a) $\left.\frac{\theta_{\text{Rear Seat}}}{-\delta_{ec}}\right]_{2825}$ "Sawtooth" Bode

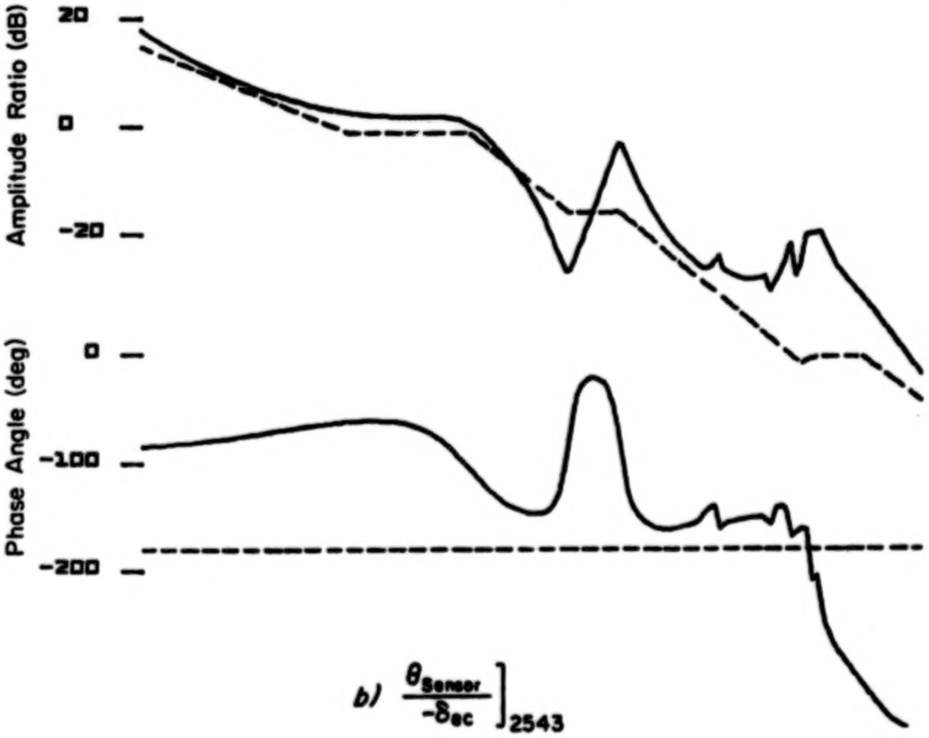

b) $\left.\frac{\theta_{\text{Sensor}}}{-\delta_{ec}}\right]_{2543}$

Figure 11

MODEL D TAKEOFF BODE WITH PITCH RATE GYRO

Figure 12 shows the Bode for a rate gyro, with typical dynamics, at the rear seat station with a suggested closure gain of 0.5.

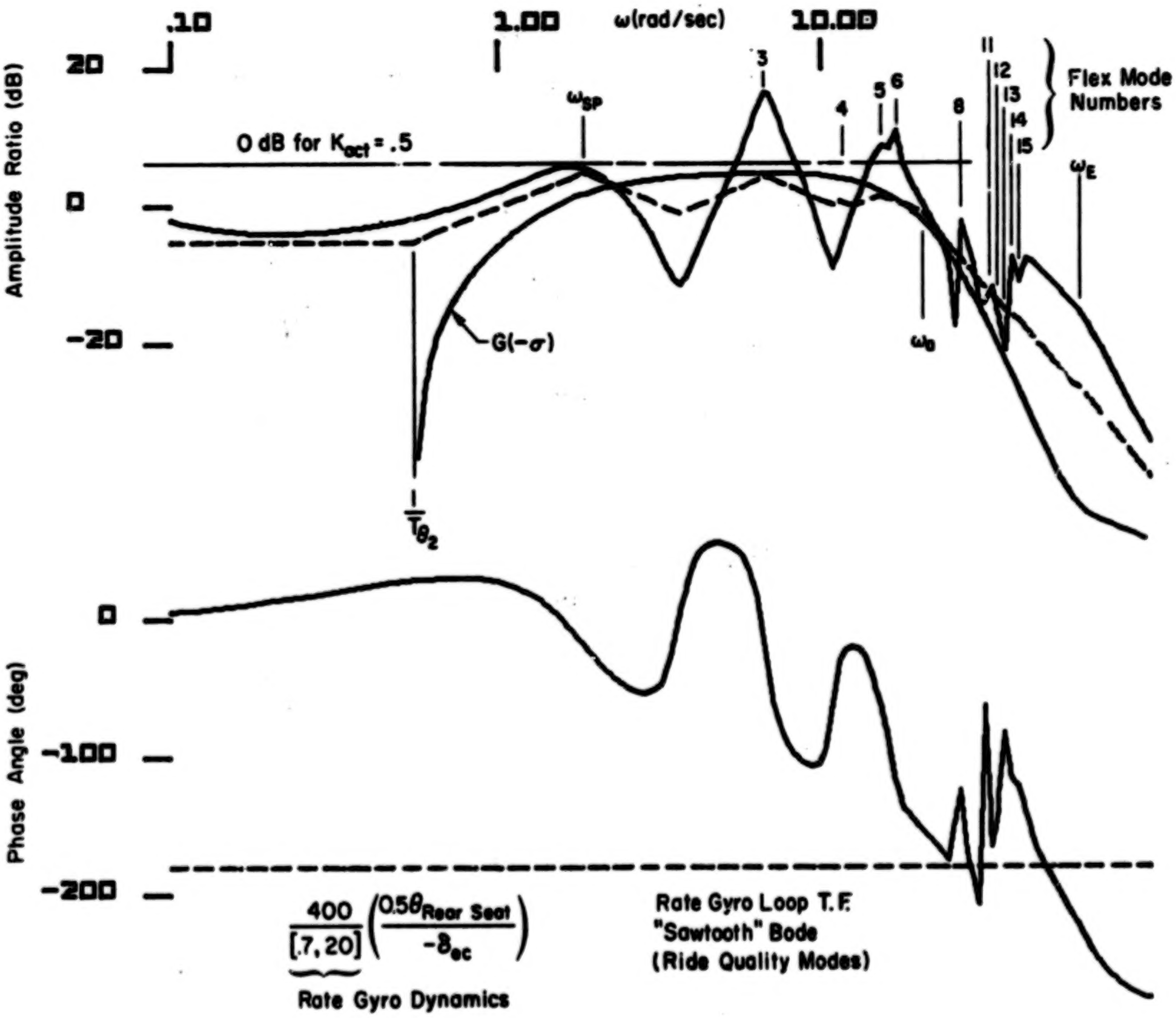

Figure 12

ROOT LOCUS PLOT OF FIGURE 12 SYSTEM

The corresponding root locus plot in Fig. 13 shows the resulting improved damping of all modes except 11, 13, and 14, which are slightly degraded.

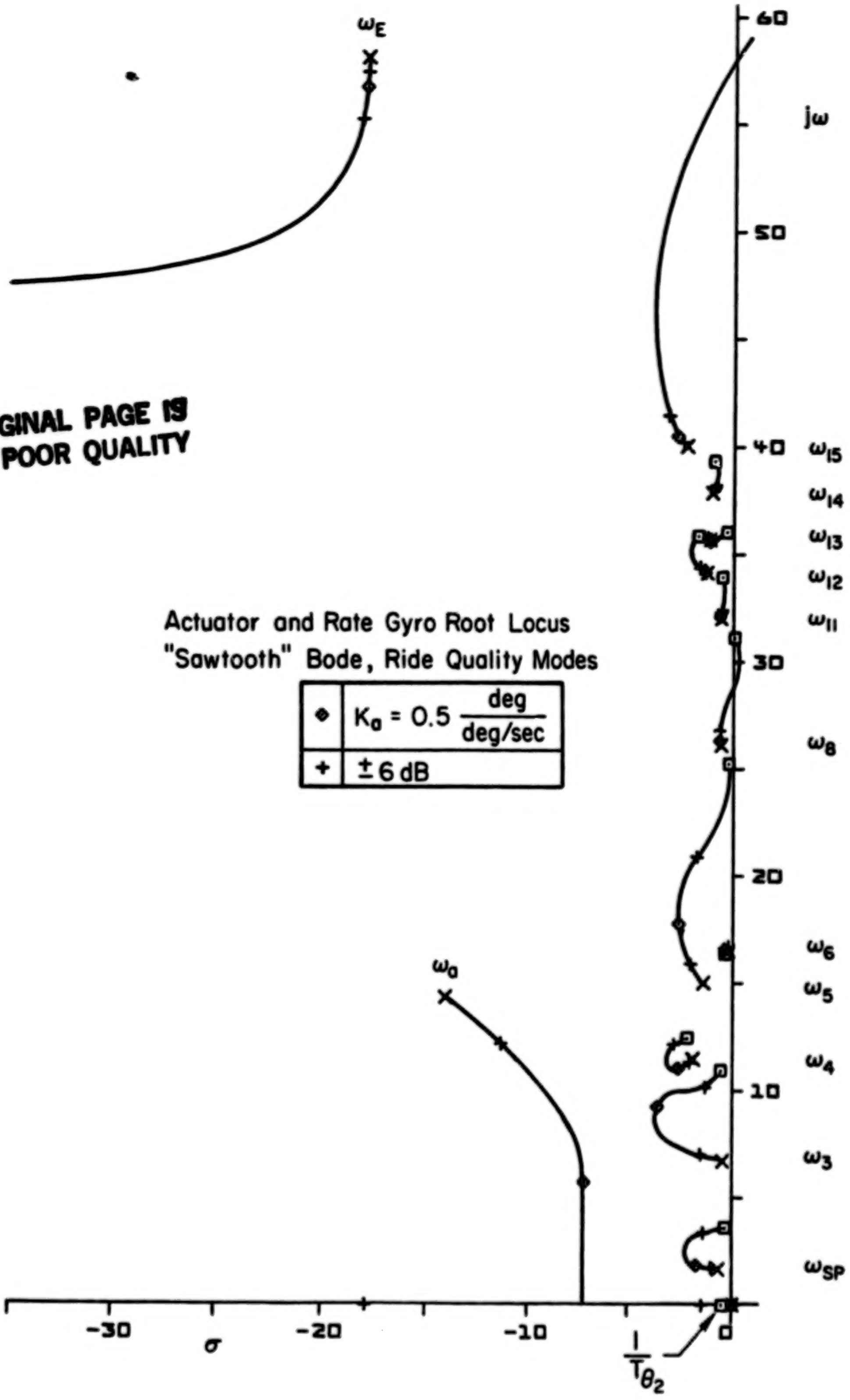

Figure 13

PILOT STATION AUGMENTED ATTITUDE RESPONSE TO ELEVATOR, $\frac{\theta'_{pilot}}{\delta_e}$

We also looked at a_z feedbacks to δ_e but they were not very effective in providing additional damping of the lower frequency modes. In fact, the higher frequency modes, 6, 8, and 11 to 15, are essentially unobservable by a centerline accelerometer. Accordingly, vertical acceleration feedback to the elevator appears to be unnecessary to slightly undesirable; it was therefore eliminated as a primary closure possibility. The remaining basic elevator control loop structure shown below is simple indeed (Fig. 14).

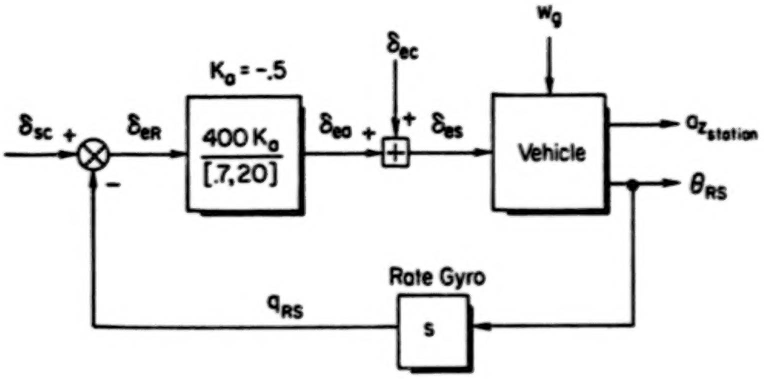

w_g
δ_{ec}
$K_a = -.5$
δ_{sc} +
δ_{eR}
$\frac{400K_a}{[.7,20]}$
δ_{ea} +
+
δ_{es}
Vehicle
$a_{z_{station}}$
θ_{RS}
-
Rate Gyro
q_{RS}
s

Figure 14

ELEVATOR CONTROL LOOP STRUCTURE

The basic FCS-augmented attitude response at the pilot's station to control inputs using this system is given in Fig. 15. The effective bandwidth, set in this case by a 6 dB gain margin requirement, is about 0.9 to 1.0 rad/sec which corresponds to satisfactory handling for this flight condition.

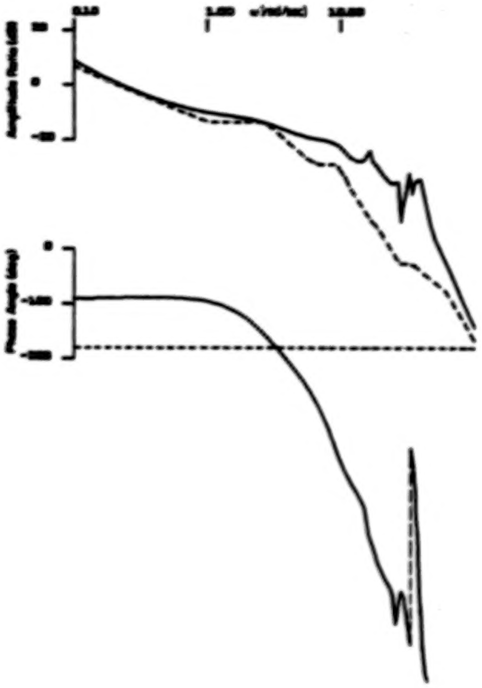

Figure 15

θ' RESPONSE TO 10-DEG STEP ELEVATOR

However, the pilot's station attitude response to a step input in Fig. 16 shows an effective time delay of about 0.55 sec, greater than allowable even using the most optimistic data. This quite large time delay is also apparent in the Fig. 15 phase characteristics (i.e., using the simple approximation $\tau\omega$ = 90 deg = 1.57 rad where $\omega \sim \phi$ = 180 deg, $\tau_{eff} \doteq 1.57/3.2 \doteq 0.49$). It is directly traceable to bending mode effects as shown at the bottom of Fig. 16, which shows only about a 0.10 sec delay in the pitch response at the rear seat where the mode slopes are all either basically smaller than, or opposite in sign to, those at the pilot station. Thus the difference is attributable to the natural change in sign of the mode slopes in going from the rear seat to the pilot's station. The change in sign is a result of the inherent bending mode shapes of a slender flexible body. In this sense, the associated additional time delay of the pilot's attitude response to a step control aft-surface input is fundamental. Before we decide what, if anything, can be done to eliminate or reduce such additional delay, we need to make further assessments.

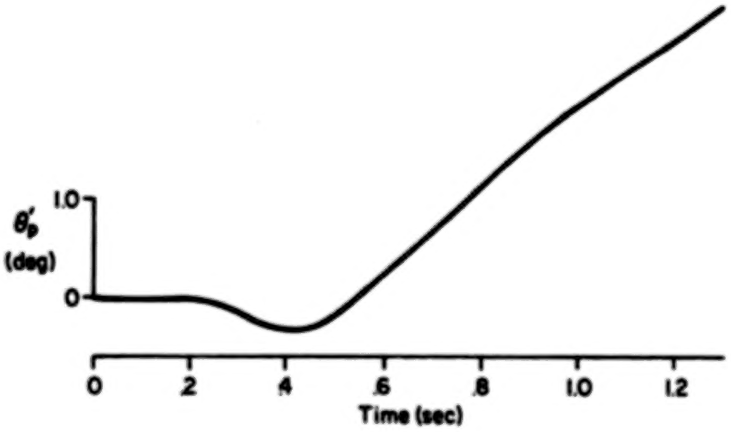

At Pilot Station

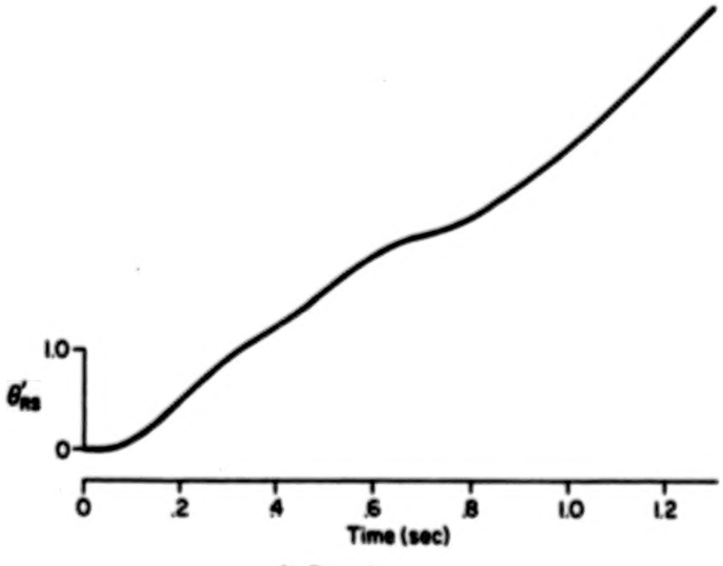

At Rear Seat

Figure 16

"SYNCHRONOUS" PIO POSSIBILITY

Relative to PIO proneness, the Fig. 15 pilot's attitude Bode is such that loop closure can be easily effected with pure gain adaptation on the part of the pilot. Accordingly, there is no tendency for the "PIO syndrome" which is characterized by required low-frequency lag adaptation for normal closed-loop operations. Such lag is an easy to accomplish, low-workload behavioral pattern described by pilots as a "smooth, trim-like control action." The trouble arises when, in an attempt to regain control after an upset or other stressful occurrence, the pilot regresses to a pure gain type of proportional control. Then the pilot-vehicle (with the suddenly changed pilot equalization) may temporarily have too small a gain margin at a "high" frequency oscillatory mode (short period or conceivably a flexible mode).

The lightly damped peak at about 16.5 rad/sec (Fig. 15) could conceivably be excited momentarily by "synchronous" pilot behavior at this frequency. The resulting PIO would not be unstable at the more probable lower gain shown in the fragmentary root locus of Fig. 17, but could have quite low damping. Of course, the level of pilot gain involved can only be sustained for a short time before the system diverges at the lower frequency corresponding to the -180 deg phase crossover in Fig. 15. Thus, at best, synchronous PIO would occur in "bursts" rather than in a sustained oscillation.

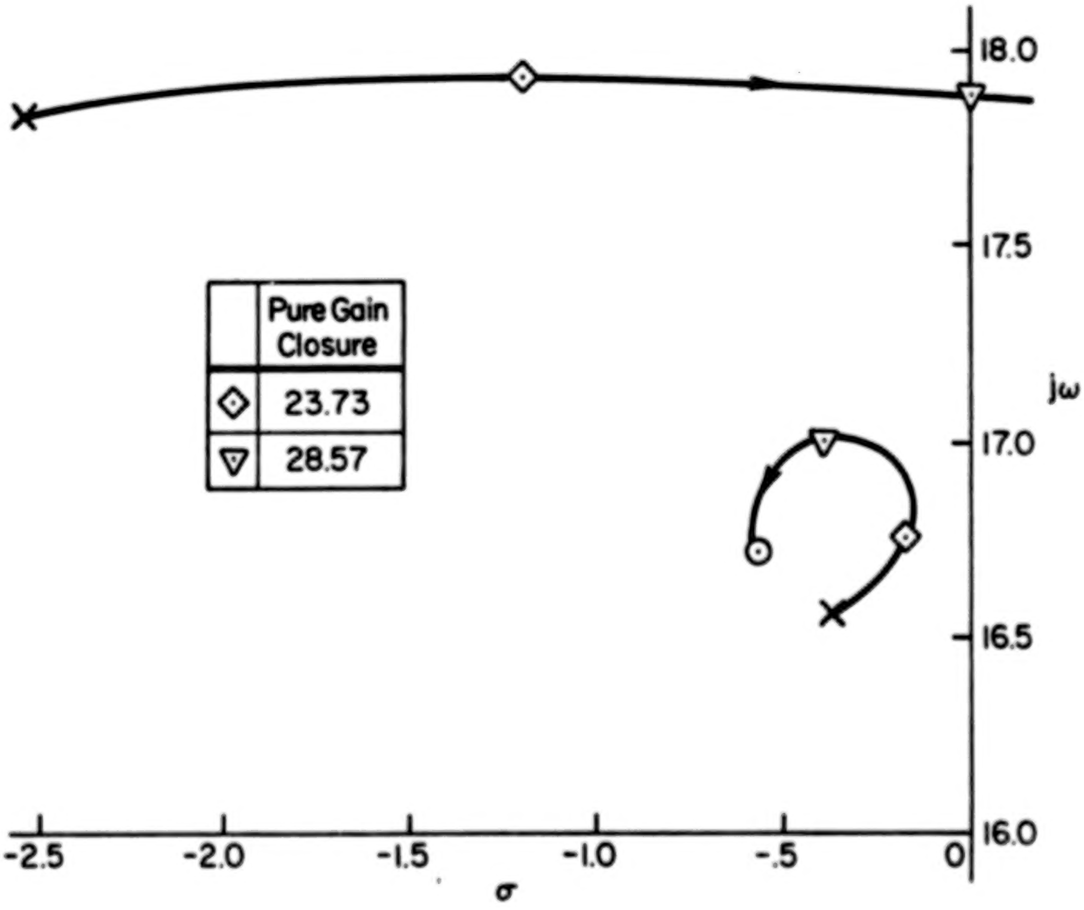

Figure 17

PILOT STATION ACCELERATION (a'_{z_p}) RESPONSE TO ELEVATOR INPUTS

With respect to vibration feedthrough to the pilot, the excitation at the pilot's station due to step and ramp elevator inputs is shown in Fig. 18. Clearly, the alleviating influence of a rate limited surface input is desirable to avoid the high-frequency ringing at about 40 rad/sec and to reduce the amplitude and frequency of the 16 rad/sec mode. However, for a 10-deg elevator ramped in at 30 deg/sec, the effective time delay increment (half of the time to ramp to 10 deg) is 0.17 sec. Therefore the effects of realistic surface rate limits will be to accentuate the effective time delay problem which is already possibly critical. A better solution to the vibration feedthrough problem than low surface rate saturation is desirable.

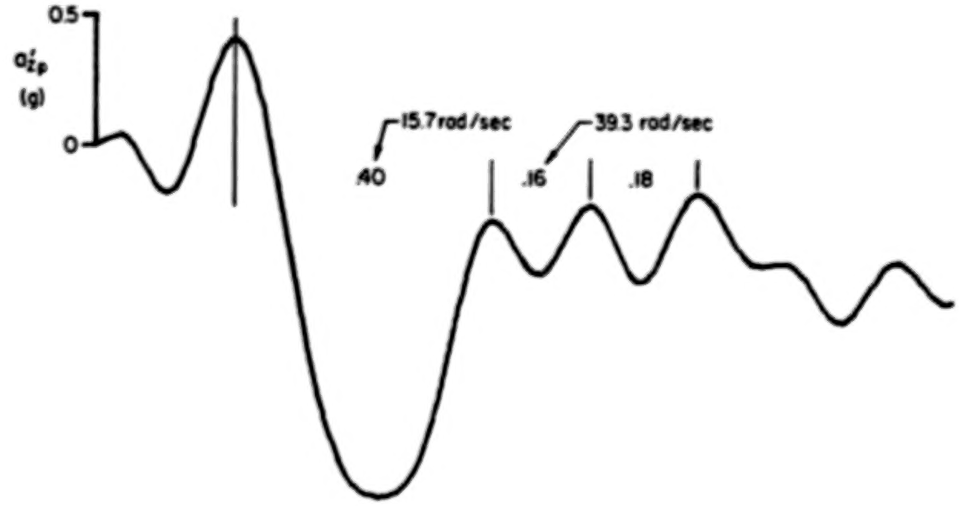

a) 10 deg Step

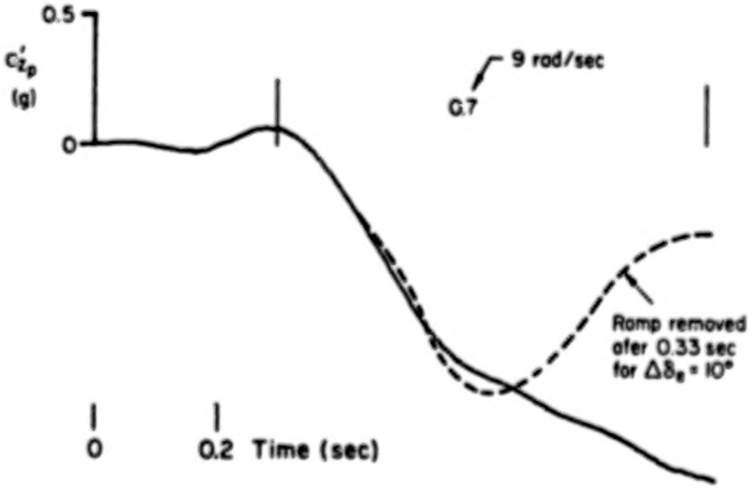

b) 30 deg/sec Ramp

Figure 18

$\left.\frac{a_z}{w_g}\right]'$ AMPLITUDES WITH SENSOR LOCATION

Turning now to ride qualities and Fig. 19, we have to recognize first that the usual Dryden turbulence spectra effectively flatten the asymptotic amplitude response to random gust inputs over almost the entire frequency range. This is indicated by the long dashed lines in Fig. 19 which represent the zero dB line for a σ_w unity gust, still leaving large spikes in the pilot's a_z response at about 16 and 36 rad/sec. As shown in the figure, these same spikes are generally evident along the entire cabin area. This means that ride quality is a general problem, not necessarily peculiar to pilot location. Accordingly, a general solution must be found. This could conceivably take one of two forms: use of a secondary control point to damp the offending modes or seat motion attenuation and damping.

The ride mode most evident in Fig. 19 is that at roughly 16 rad/sec, mode 6. The largest amplitude spike above the zero dB gust lines at 16 rad/sec is about 34 dB (at the rear node) or an amplification factor of 50. This is far too large to be effectively damped by passive seat suspension and cushioning systems.

Mode 6's three-dimensional character is predominantly of a wing torsional nature so it's not surprising that a centerline control has no effect on it. It is also clear that the wing lift due to such torsional deflection will apply more or less uniformly along the fuselage, which explains the Fig. 19 results. The obvious way to damp this motion is to use the outboard wing movable surfaces responding to motion also sensed at an outboard location. The Boeing data, unfortunately, do not cover symmetric aileron or flaperon inputs to the longitudinal mode, so this option remains as a possible future exercise.

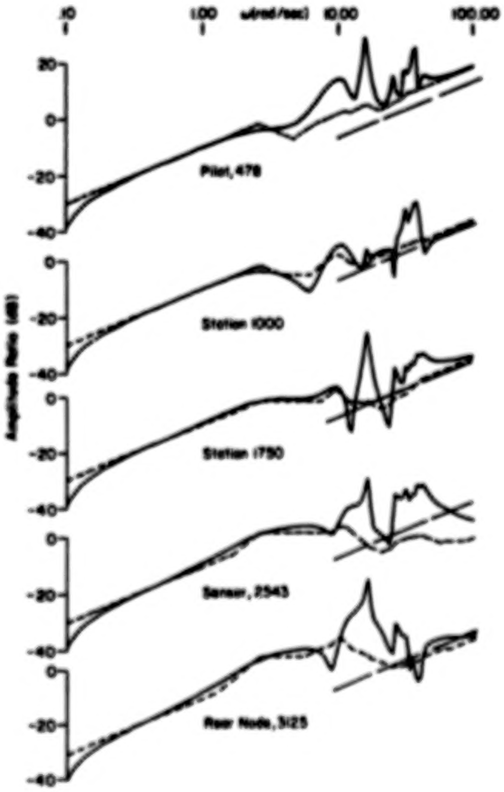

Figure 19

RESULTS AND CONCLUSIONS: GENERAL

- Systematically exposed all design-centered factors to consider (1)(Fig. 20)
  - Control system functions and roles
  - Flexible mode control principles
    - FCS criteria and desires for
      - Pilot-centered command and flying qualities
      - Ride qualities
      - Controller-centered requirements and design implications
  - Available design methodologies and selection of recommended methods
- Established fundamental requirements on effective vehicle characteristics (aircraft/controller combination) consistent with simple robust controllers — i.e., pole-zero ordering (2)
- Translated above into system and subsystem requirements (1)
- Confirmed a simplified treatment of unsteady aerodynamics which compared very well with the complete treatment (3)
- Developed and demonstrated considerations for selective inclusion/deletion of significant/insignificant modes within reduced-order systems (3)
- Demonstrated systematic design/analysis methods to meet requirements; derived a very simple robust system (4)

(1) ASSEMBLED REQUIREMENTS AND DESIRES

(2) REITERATED A CENTRAL PRINCIPAL IN FLEXIBLE MODE CONTROL

(3) DERIVED AND UTILIZED A SIMPLIFIED FLEXIBLE AIRPLANE MODEL

(4) DEMONSTRATED SYSTEMATIC DESIGN METHODS

(5) IDENTIFIED CERTAIN PROBLEMS ENDEMIC TO FLEXIBLE VEHICLES OF TYPE STUDIED

Figure 20

CONCLUSIONS: SPECIFIC "PROBLEMS"

- The effective time delay in θ_p response to elevator appears to be a generic problem due to low-frequency bending mode(s) as seen at the pilot station (Fig. 21).
- Vertical acceleration feedthrough at the pilot's station can be reduced by lowering the saturation rate of the elevator. However, this adds to the θ response lag and may not be a viable solution.
- Vertical acceleration response to w_g is high in general and must be reduced for good ride qualities. Analysis indicates that secondary, outboard surface(s), and off-centerline located sensors offer a probable solution which should also decrease vertical acceleration feedthrough.
- The above "prominent" mode is also involved in "synchronous PIO" possibilities, but these are evident in the pilot's pitch attitude response and may or may not be reduced by the above-suggested secondary control surfaces.
- Because of its prominence in ride, synchronous PIO, and vibration feedthrough, response characteristics similar to those of the "prominent" mode are likely candidates for simulation research.

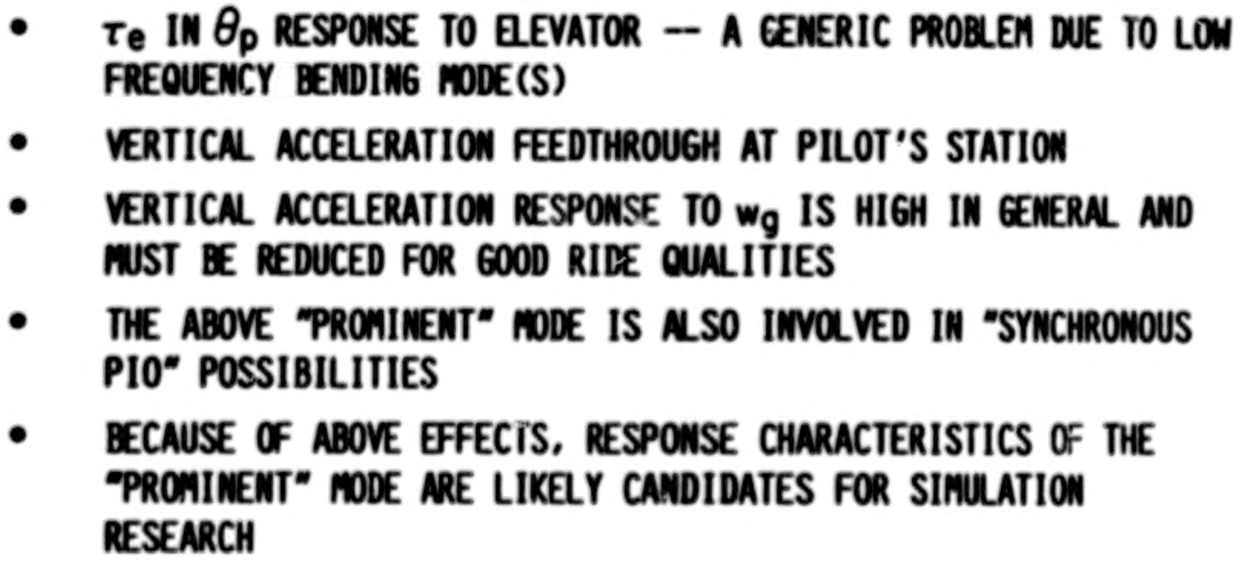

- τ_e IN θ_p RESPONSE TO ELEVATOR -- A GENERIC PROBLEM DUE TO LOW FREQUENCY BENDING MODE(S)
- VERTICAL ACCELERATION FEEDTHROUGH AT PILOT'S STATION
- VERTICAL ACCELERATION RESPONSE TO w_g IS HIGH IN GENERAL AND MUST BE REDUCED FOR GOOD RIDE QUALITIES
- THE ABOVE "PROMINENT" MODE IS ALSO INVOLVED IN "SYNCHRONOUS PIO" POSSIBILITIES
- BECAUSE OF ABOVE EFFECTS, RESPONSE CHARACTERISTICS OF THE "PROMINENT" MODE ARE LIKELY CANDIDATES FOR SIMULATION RESEARCH

Figure 21

RECOMMENDATIONS

- Expand present study to include off-center line symmetric controls (Fig. 22)
- Plan and conduct moving base simulation to investigate:
  - (a) Low-frequency time delays in pilot station attitude response associated with fuselage bending modes
  - (b) Motion feedthrough and potential synchronous PIO due to high-frequency centerline motion
- Develop more-automated means to achieve simple controllers which exhibit robust characteristics demonstrated herein, e.g.:

  Automated numerator synthesis for minimum (fixed-form) sensor/equalization complexes which assure desired zero, pole order, and permit maximum spacing between a limited (specified) number of zero, pole pairs

  Frequency domain optimal performance indices and procedures which preordain an optimal controller/aircraft combination satisfying the sawtooth Bode requirements

- STUDY OFF-CENTER LINE SYMMETRIC CONTROLS
- PLAN AND CONDUCT MOVING BASE SIMULATION TO INVESTIGATE:
  - (A) TIME DELAYS DUE FUSELAGE BENDING MODES
  - (B) FEEDTHROUGH AND POTENTIAL SYNCHRONOUS PIO DUE TO HIGH-FREQUENCY COCKPIT ACCELERATION
- DEVELOP MORE-AUTOMATED MEANS TO ACHIEVE SIMPLE, ROBUST CONTROLLERS

Figure 22

BIBLIOGRAPHY

1. Ashkenas, I. L., Magdaleno, R. E., and McRuer, D. T.: Flight Control and Analysis Methods for Studying Flying and Ride Qualities of Flexible Transport Aircraft, NASA CR-172201, August 1983.

N84
20573

UNCLAS

N84 20573

IMPLICATIONS OF CONTROL TECHNOLOGY ON AIRCRAFT DESIGN

Steven M. Sliwa and P. Douglas Arbuckle
NASA Langley Research Center
Hampton, Virginia

First Annual NASA Aircraft Controls Workshop
NASA Langley Research Center
Hampton, Virginia
October 25-27, 1983

ABSTRACT

New controls technologies are now available for implementation with aircraft systems. Many aircraft with state-of-the-art technology in the fields of aerodynamics, structures, and propulsion require extensive augmentation merely for safety of flight considerations in addition to potential performance improvements. The actual performance benefits of integrating the new controls concepts with other new technologies can be optimized by including such considerations early in the design process. Recently, several advanced aircraft designs have run into considerable problems related to control systems and flying qualities during flight test, requiring costly redesign and fine-tuning efforts. It is no longer possible for the aircraft design to be completed prior to getting the controls specialists involved. The challenge to the control system designer has become so great that his concerns must be considered at the conceptual design level. A computer program developed at NASA for evaluating the economic payoffs of integrating controls into the design of transport aircraft at the beginning will be described.

- NEW CONTROLS TECHNOLOGIES ARE AVAILABLE
- MANY NEW AIRCRAFT REQUIRE ADVANCED CONTROLS
- EXPENSE OF FINE TUNING CONTROL SYSTEMS FOR CURRENT STATE-OF-THE-ART AIRCRAFT HAS RISEN DRAMATICALLY
- INTEGRATING CONTROLS INTO DESIGN PROCESS IS BENEFICIAL
- A TOOL HAS BEEN DEVELOPED TO EVALUATE THE PAYOFFS OF CONTROLS INTEGRATION

INCREASE IN CONTROLS COMPLEXITY

ORIGINAL PAGE IS
OF POOR QUALITY

During the past 20 years, the control systems being used on state-of-the-art aircraft have improved significantly. In the 1950's and 1960's, simple control laws were being applied to improve the flying qualities. In contrast, current configurations may require extensive augmentation for safety of flight as well as for good flying qualities. Because of this, and because of the increased complexity of all aircraft systems, it has become extremely difficult to fine-tune or adjust control laws during flight test. Redesign efforts currently require significant amounts of engineering, which result in costly delays. Previously, very simple control schemes were used merely for improving flying qualities, and mechanical back-up systems were always utilized in the event of electronic component failure. Now, highly complex laws which rely on the improved reliability of digital and analog circuits use redundant systems for back-up modes. These examples illustrate some of the fundamental issues facing a control system design engineer today.

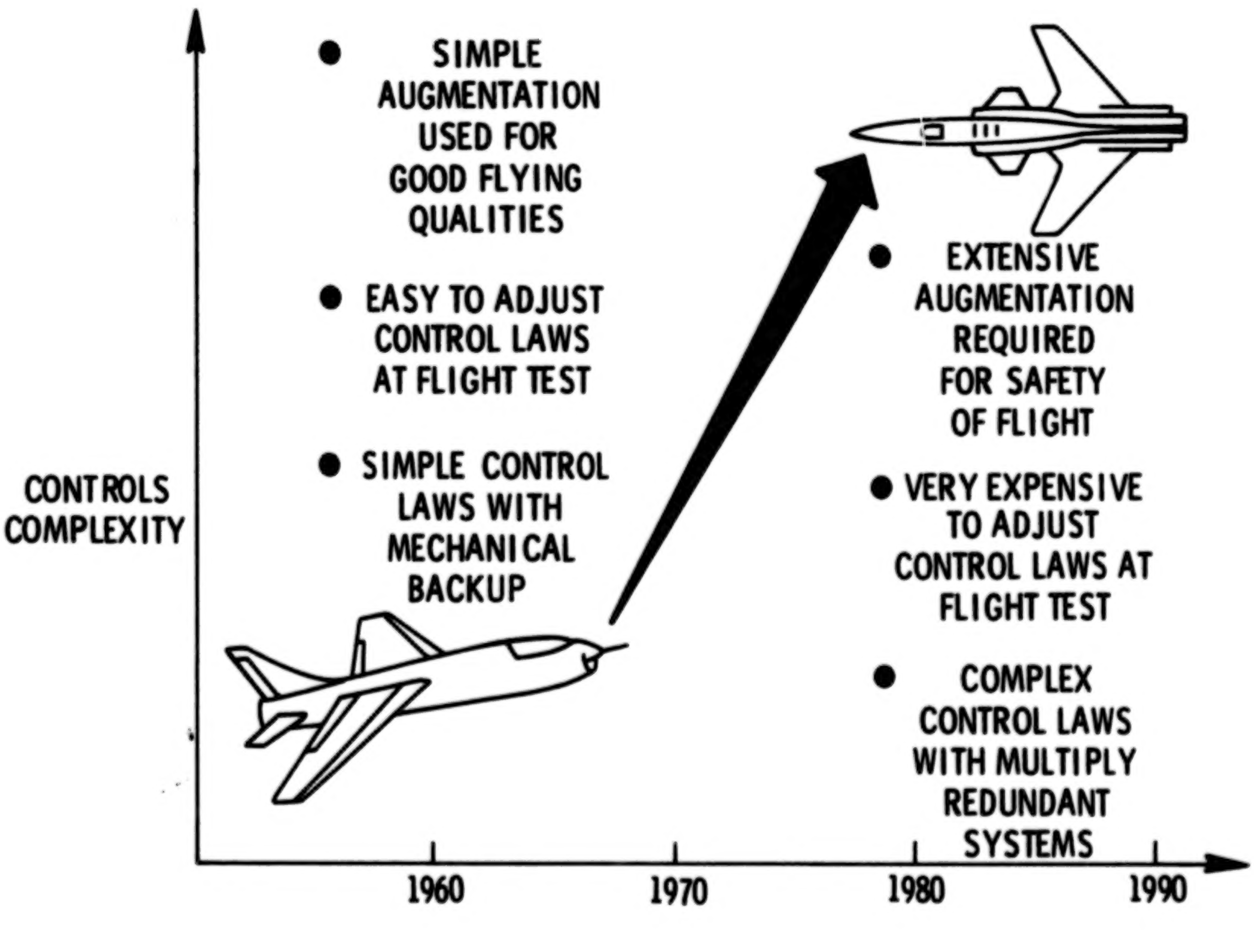
• SIMPLE AUGMENTATION USED FOR GOOD FLYING QUALITIES
• EASY TO ADJUST CONTROL LAWS AT FLIGHT TEST
• SIMPLE CONTROL LAWS WITH MECHANICAL BACKUP
CONTROLS COMPLEXITY
• EXTENSIVE AUGMENTATION REQUIRED FOR SAFETY OF FLIGHT
• VERY EXPENSIVE TO ADJUST CONTROL LAWS AT FLIGHT TEST
• COMPLEX CONTROL LAWS WITH MULTIPLY REDUNDANT SYSTEMS
1960
1970
1980
1990

COMPARISON OF CONTROLS TECHNOLOGY

A comparison of some of the characteristics of early automatic control systems for aircraft and those being applied to current configurations is shown below. Initially, control systems were designed using simple single-loop analyses for aircraft with limited envelopes where rigid airframe assumptions were adequate. Now flexible aircraft with expanded envelopes have significant aeroservoelastic interactions that cannot be ignored during control system design. The current tendency is to develop digital fly-by-wire control systems utilizing complex multi-input, multi-output design techniques with sophisticated redundancy management. Clearly, to achieve the full potential of applying these technologies, the controls integration must occur early in the design process.

THEN	NOW
● MECHANICAL LINKAGES	● DIGITAL 6 DOF FLY BY WIRE
● SIMPLE YAW DAMPER WAS ONLY AUGMENTATION	● COMPLEX CONTROL LAWS WITH HIGH-ORDER COMPENSATORS
● SIMPLE SISO DESIGN TECHNIQUES USED DURING CONTROL SYSTEM DESIGN	● COMPLEX MIMO DESIGN TECHNIQUES USED DURING CONTROL SYSTEM DESIGN
● RIGID AIRFRAME ASSUMPTION GOOD	● AEROSERVOELASTIC INTERACTIONS IMPORTANT
● LIMITED ENVELOPE	● EXPANDED ENVELOPE
● SIMPLE CONTROL MODES	● NEW, COMPLEX CONTROL MODES
● REDUNDANCY THROUGH MECHANICAL STRENGTH	● REDUNDANCY THROUGH MULTIPLE SYSTEMS
	● NEED FOR CONTROLS INTEGRATION EARLY IN DESIGN EFFORT

EVOLUTION OF CONTROL SYSTEMS

The control system components have undergone considerable change and refinement. Originally, simple mechanical linkages using cables, pulleys, and push rods were used. As hydraulic boost became popular, it became possible to improve the flying qualities in certain flight regimes by feeding back a sensed variable, such as yaw rate. The control system with simple augmentation still maintained full authority through mechanical connections between the pilot and the control surface. In the event of a failure of a control system component, the pilot still maintained control, but with reduced flying qualities. The current trend of fly-by-wire control systems requires redundancy of critical elements since there will no longer be mechanical connections between the pilot and control system as a backup. The concepts of fault tolerance, detection, and isolation are new areas of important research.

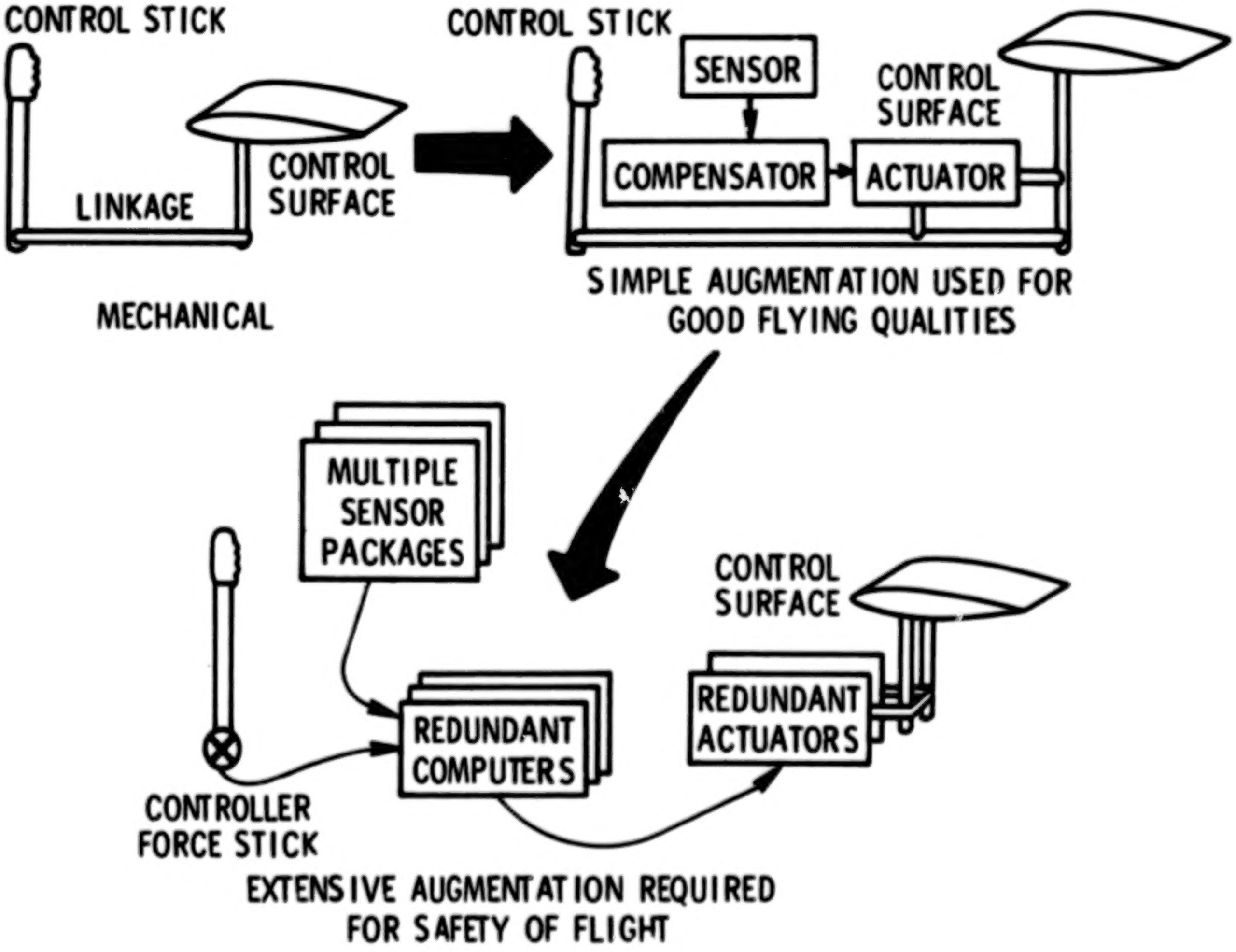
CONTROL STICK
LINKAGE
CONTROL SURFACE
MECHANICAL
CONTROL STICK
SENSOR
CONTROL SURFACE
COMPENSATOR
ACTUATOR
SIMPLE AUGMENTATION USED FOR GOOD FLYING QUALITIES
MULTIPLE SENSOR PACKAGES
CONTROL SURFACE
REDUNDANT ACTUATORS
REDUNDANT COMPUTERS
CONTROLLER FORCE STICK
EXTENSIVE AUGMENTATION REQUIRED FOR SAFETY OF FLIGHT

APPLICATION OF RSSAS TO A CURRENT TRANSPORT CONFIGURATION

Relaxed Static Stability Augmentation Systems (RSSAS) for transport configurations is one application of advanced control systems that may result in significant benefits. Immediate performance gains can usually be realized through a reduction in trim drag. Further gains can be achieved by resizing the horizontal tail due to a reduction in the stability constraint for the inherent aerodynamic stability of the aircraft. Good flying qualities will be achieved by the active control system. The reduction in tail area results in a decrease in aircraft operating weight and drag. All of these benefits yield fuel savings of 2 to 4 percent for most transport configurations.

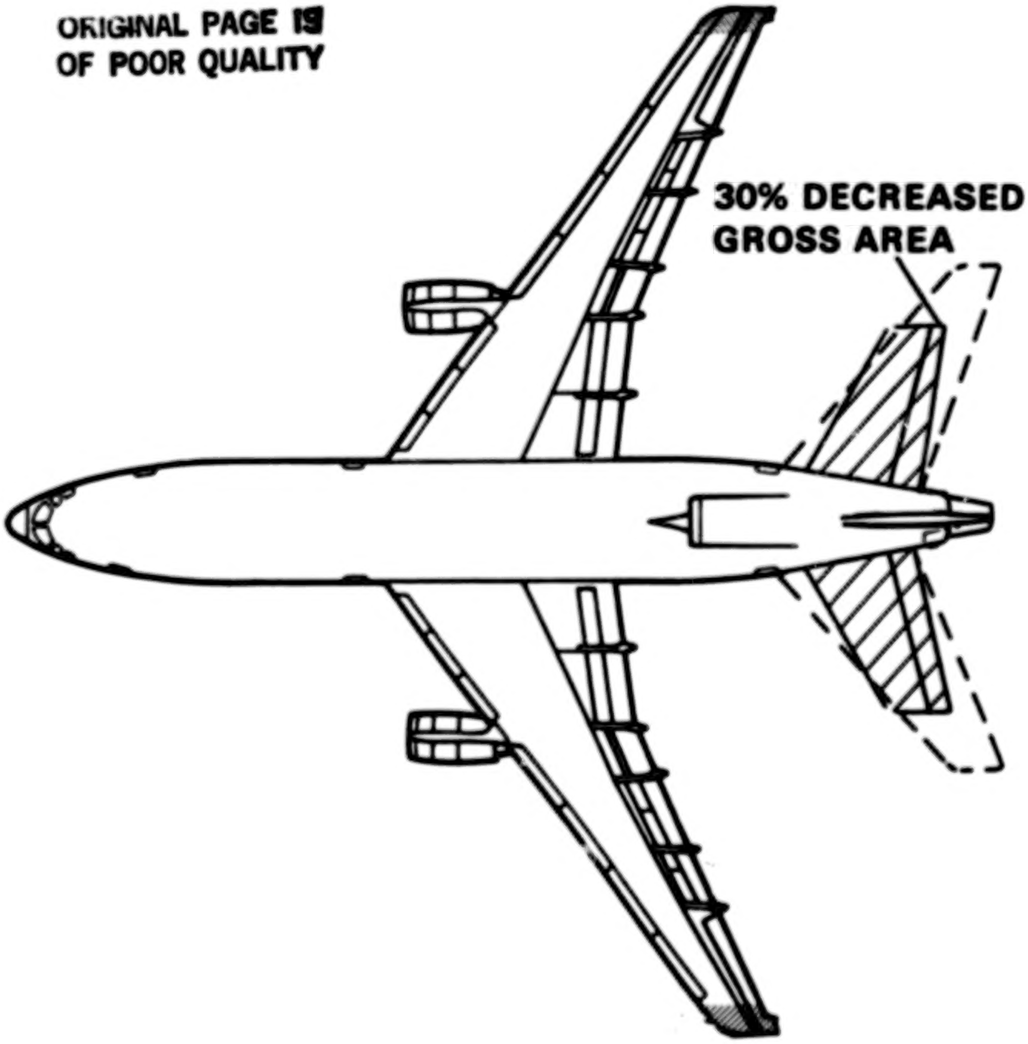

ORIGINAL PAGE IS
OF POOR QUALITY

RESIZED TRANSPORT TO TAKE ADVANTAGE OF RSSAS

The greatest benefits of utilizing a RSSAS system can be achieved by introducing the concept at the conceptual design stages. A reduction in tail area results in weight and drag savings. Hence, the wing and engine can be resized, resulting in more weight savings. Additionally, the fuselage and landing gear structure can be redesigned for the lighter weight. In fact, after the airframe modifications, a further reduction in tail area may be possible, resulting in another round of changes. These benefits continue to cascade through the design but generally converge rapidly, resulting in a design which takes maximum, synergistic advantage of applying this new technology. If the concept is not introduced soon enough, the full benefits of RSSAS cannot be achieved. In the case of transport aircraft, fuel savings of 6 to 9 percent are possible.

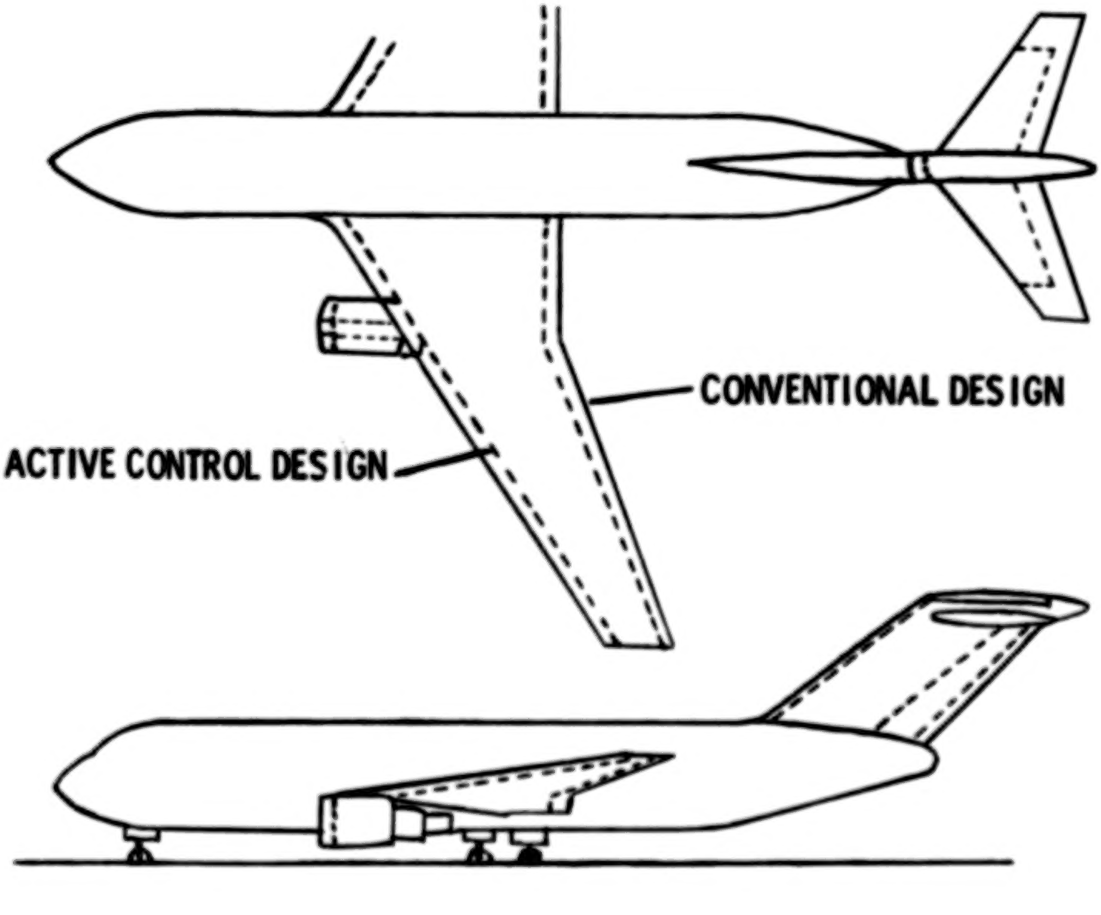

PROGRESS IN DESIGN

The actual integration of multiple decentralized control systems into a single centralized control system has also been a recent development which will result in augmented operational safety, performance, and capability as well as improved economy. In present practice, each component of the vehicle is designed independently. Certain advanced designs require control systems for various aspects, such as flying qualities, engine performance, structural damping, and weapon control. Each subsystem typically has an independent controller which is directed by the crew or flight management computer. It is conceivable that independent controllers could work in harmony; but, it is just as likely that they will conflict with each other. A preferred approach is to integrate all the controls and design each subsystem controller simultaneously. Such a system will tend to work in harmony in response to crew or computer commands.

COMPONENT DESIGN OF
PROPULSION, AERODYNAMICS,
STRUCTURES AND CONTROLS

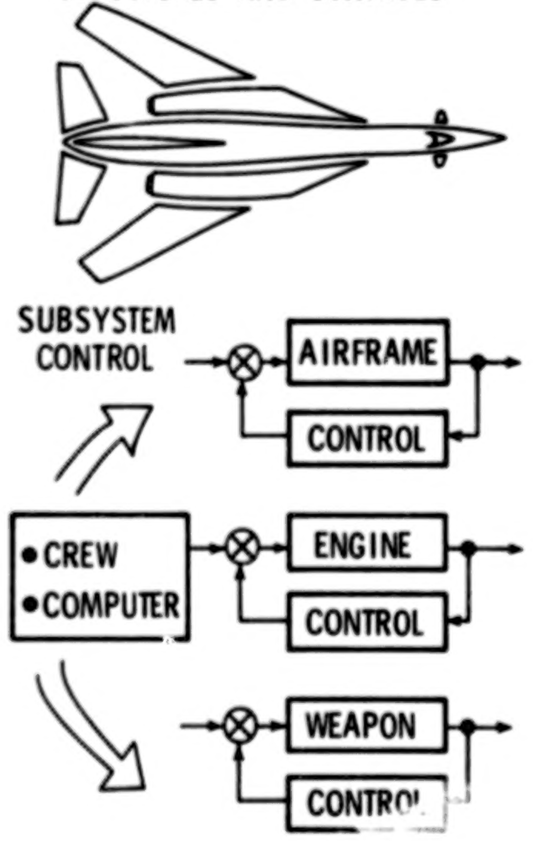
SUBSYSTEM CONTROL
AIRFRAME
CONTROL
• CREW
• COMPUTER
ENGINE
CONTROL
WEAPON
CONTROL

INTEGRATED DESIGN OF
PROPULSION, AERODYNAMICS,
STRUCTURES AND CONTROLS

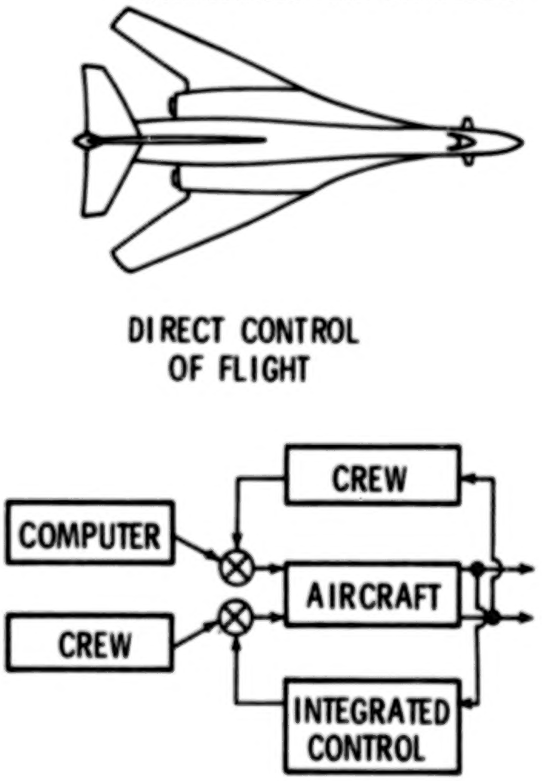
DIRECT CONTROL
OF FLIGHT
CREW
COMPUTER
AIRCRAFT
CREW
INTEGRATED CONTROL

FULL POTENTIAL OF INTEGRATED USE OF CONTROLS

Once the use of advanced integrated controls has been hypothesized, there are many avenues that can be explored. Modern control theory allows the use of multiple effectors allowing such things as wing warping, rolling tails, spoilers, leading-edge devices, and thrust vectoring for control and performance enhancements. Unconventional flight modes, such as target alignment independent of flight path or side force excursions, can then be contemplated. All of these functions cannot be properly used if a separate controller is designed for each. Instead, a total integrated control system design approach should be used to minimize the conflicts and optimize the overall performance.

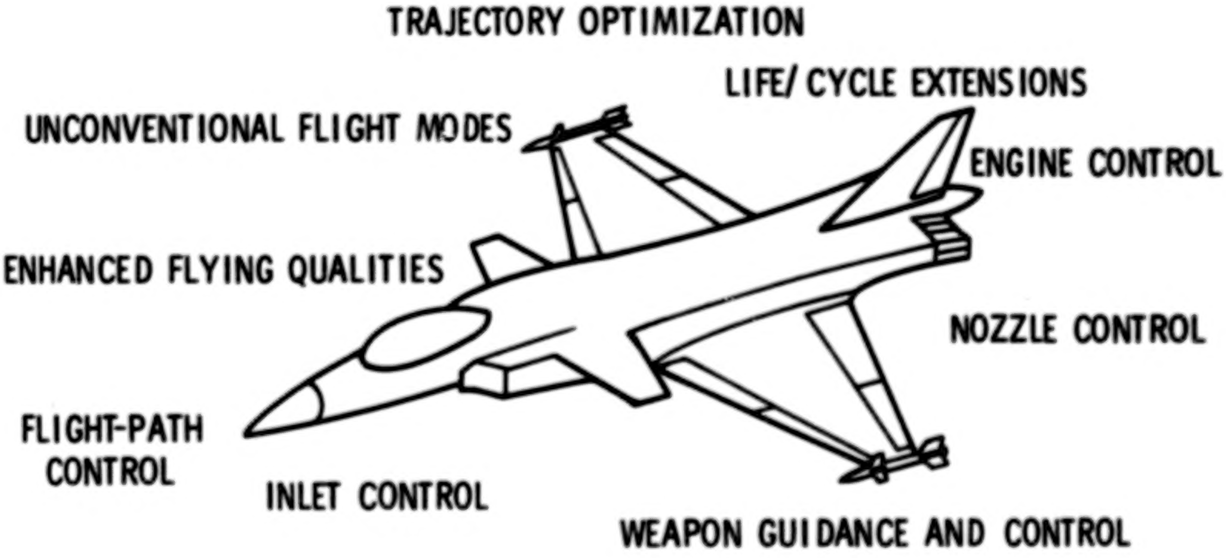
TRAJECTORY OPTIMIZATION
LIFE/ CYCLE EXTENSIONS
UNCONVENTIONAL FLIGHT MODES
ENGINE CONTROL
ENHANCED FLYING QUALITIES
NOZZLE CONTROL
FLIGHT-PATH CONTROL
INLET CONTROL
WEAPON GUIDANCE AND CONTROL

CONFIGURATION BENEFITS

OPTIMUM PRELIMINARY DESIGN OF TRANSPORTS

OPDOT (Optimum Preliminary Design of Transports) is a computer program developed at NASA Langley Research Center for evaluating the impact of new controls technologies upon transport aircraft (see reference 1). It provides the capability to look at configurations which have been resized to take advantage of active controls and provide an indication of economic sensitivity to its use or the requisite assumptions. Although this tool returns a conceptual design configuration as its output, it does not have the accuracy, in absolute terms, to yield satisfactory point designs for immediate use by aircraft manufacturers. However, the relative accuracy of comparing generated configurations while varying technology assumptions has been demonstrated to be highly reliable making OPDOT a useful tool for ascertaining the synergistic benefits of active controls, composite structures, improved engine efficiencies, and other advanced technology developments.

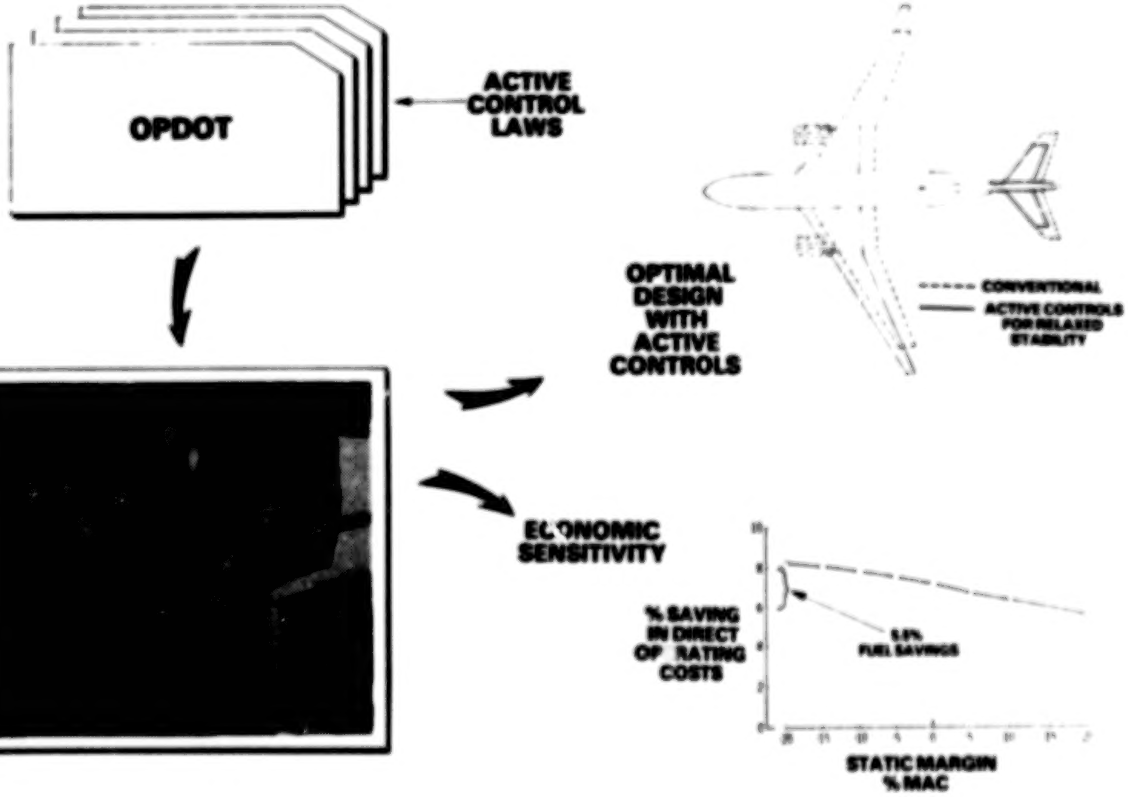
OPDOT
ACTIVE CONTROL LAWS
OPTIMAL DESIGN WITH ACTIVE CONTROLS
CONVENTIONAL
ACTIVE CONTROLS FOR RELAXED STABILITY
ECONOMIC SENSITIVITY
% SAVING IN DIRECT OPERATING COSTS
10
8
6
4
2
0
5.8% FUEL SAVINGS
20
15
10
5
0
5
10
15
20
STATIC MARGIN % MAC

OPTIMAL DESIGN METHODOLOGY

The approach that is used by OPDOT is direct numerical optimization of an economic performance index. A set of independent design variables is iterated given a set of design constants and data. The design variables include wing geometry, tail geometry, fuselage size, engine size, etc. This iteration continues until the optimum performance index is found which satisfies all the constraint functions. The analyst interacts with OPDOT by varying the input parameters to the contraint functions or to the design constants. The optimization of aircraft geometry features is equivalent to finding the ideal aircraft size, but with more degrees of freedom than classical design procedures will allow.

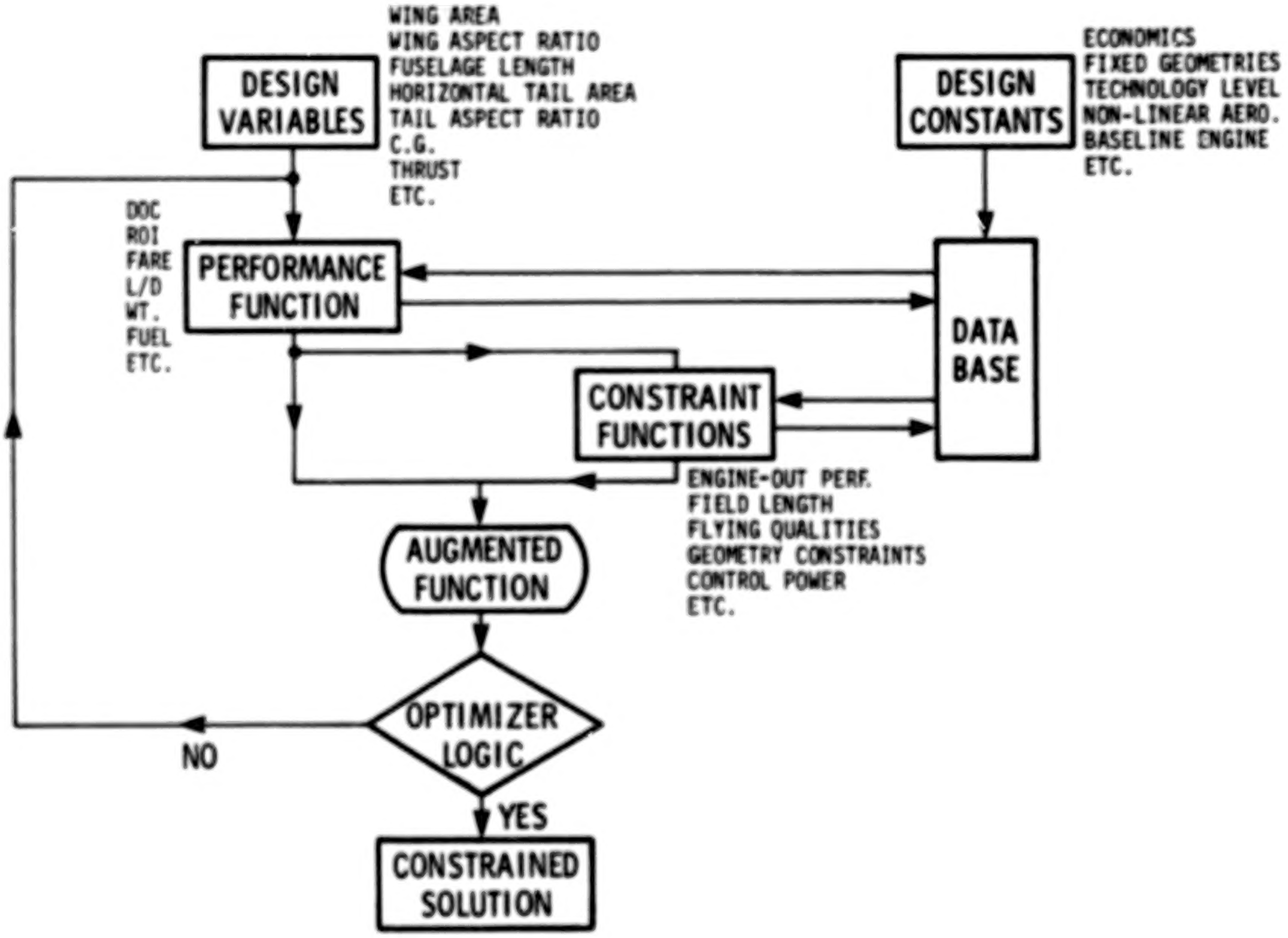
DESIGN VARIABLES
WING AREA
WING ASPECT RATIO
FUSELAGE LENGTH
HORIZONTAL TAIL AREA
TAIL ASPECT RATIO
C.G.
THRUST
ETC.
DESIGN CONSTANTS
ECONOMICS
FIXED GEOMETRIES
TECHNOLOGY LEVEL
NON-LINEAR AERO.
BASELINE ENGINE
ETC.
DOC
ROI
FARE
L/D
WT.
FUEL
ETC.
PERFORMANCE FUNCTION
DATA BASE
CONSTRAINT FUNCTIONS
ENGINE-OUT PERF.
FIELD LENGTH
FLYING QUALITIES
GEOMETRY CONSTRAINTS
CONTROL POWER
ETC.
AUGMENTED FUNCTION
OPTIMIZER LOGIC
NO
YES
CONSTRAINED SOLUTION

PERFORMANCE FUNCTION FLOW DIAGRAM

The performance index in OPDOT is computed by having a candidate configuration "fly" an entire mission while satisfying reserve fuel requirements. Industry statistics are used for estimating weights and costs. The stability and control analysis is similar to Datcom-type capabilities, and the program computes the interference drag in a general way, making OPDOT sensitive to tail sizing considerations. The flight profile is a multiple-step model of a suboptimal cruise/climb for optimum fuel efficiency. The program is fairly flexible to use and has graphics output to illustrate each configuration.

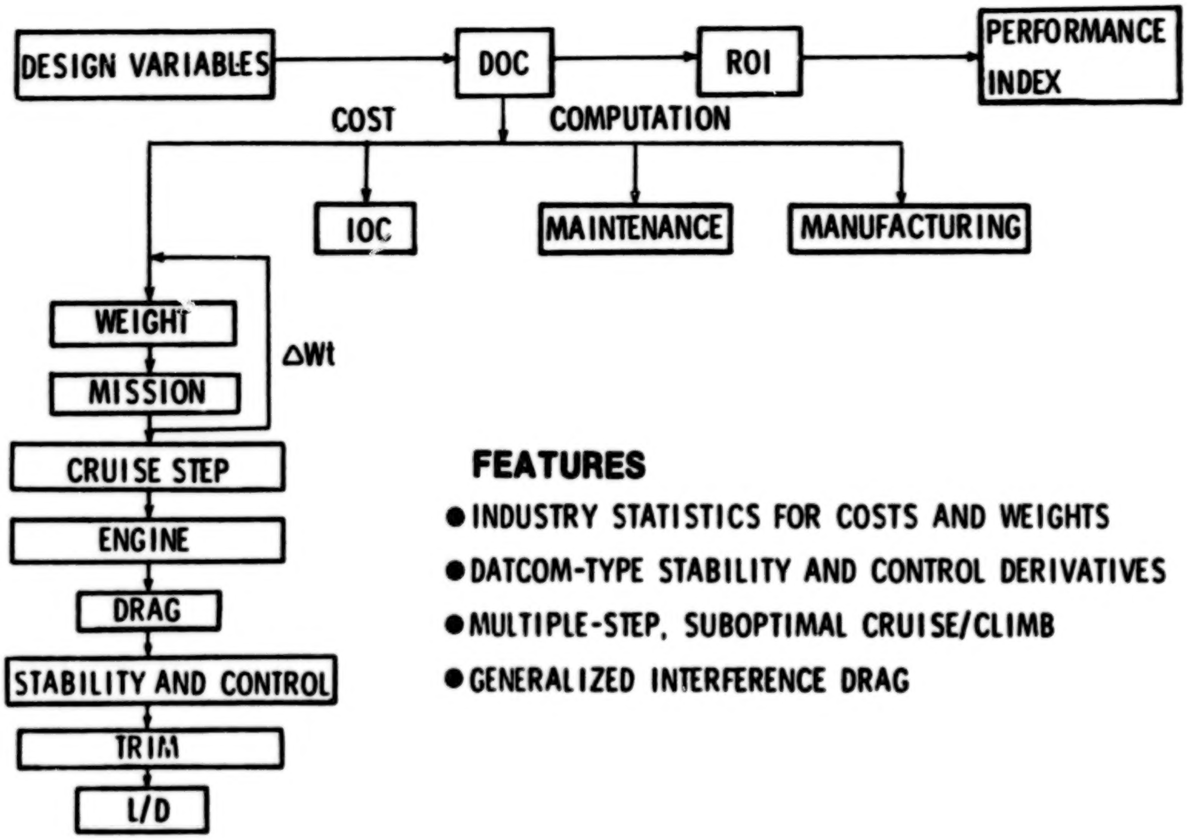
DESIGN VARIABLES
DOC
ROI
PERFORMANCE INDEX
COST
COMPUTATION
IOC
MAINTENANCE
MANUFACTURING
WEIGHT
ΔWt
MISSION
CRUISE STEP
ENGINE
DRAG
STABILITY AND CONTROL
TRIM
L/D

FEATURES

- INDUSTRY STATISTICS FOR COSTS AND WEIGHTS
- DATCOM-TYPE STABILITY AND CONTROL DERIVATIVES
- MULTIPLE-STEP, SUBOPTIMAL CRUISE/CLIMB
- GENERALIZED INTERFERENCE DRAG

METHODOLOGY FOR CONDUCTING SENSITIVITY STUDIES

A study is performed by inputting a set of problem parameters and selecting an initial set of independent design variables. OPDOT finds a solution, and that configuration is saved for later comparison. The analyst then systematically varies a design constant or constraint function, and each optimum design is stored. Then a locus of optimum designs can be plotted as a function of the parameter in question. This plot can be used to determine the sensitivity of a design to applying a new technology, for example, and each point includes the maximum synergistic benefits available for the set of inputs specified.

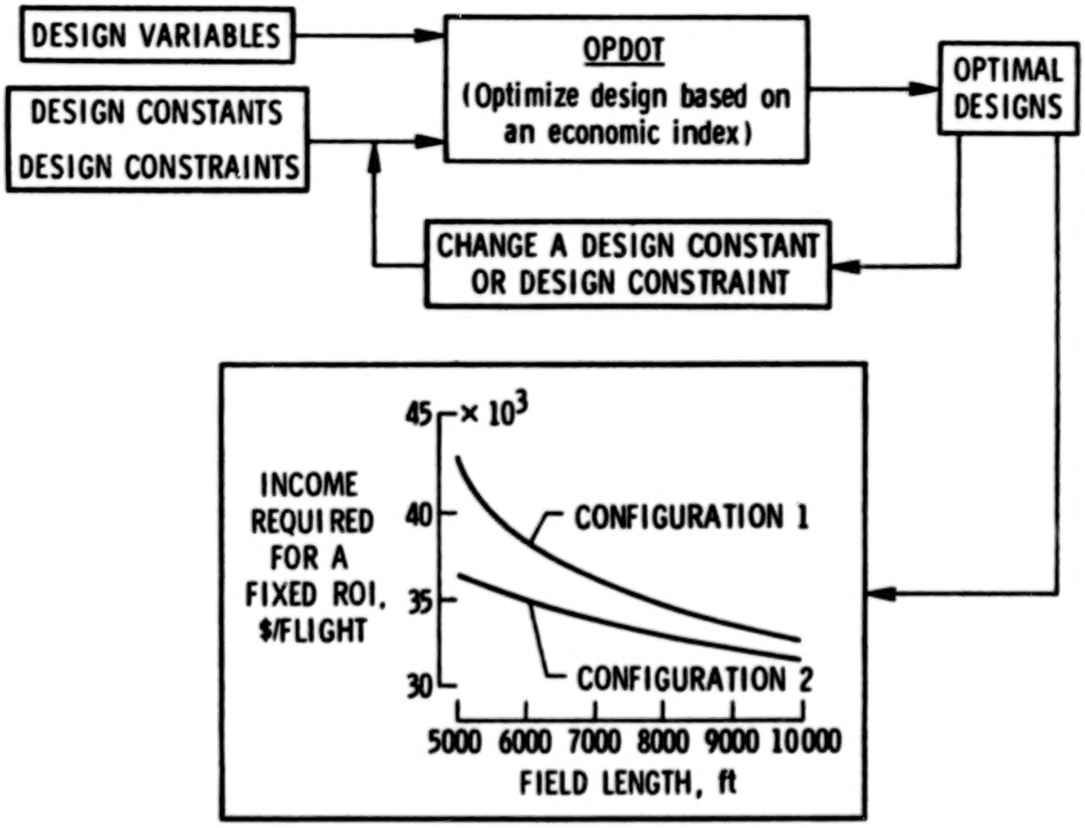
DESIGN VARIABLES
DESIGN CONSTANTS
DESIGN CONSTRAINTS
OPDOT
(Optimize design based on an economic index)
OPTIMAL DESIGNS
CHANGE A DESIGN CONSTANT OR DESIGN CONSTRAINT
INCOME REQUIRED FOR A FIXED ROI, $/FLIGHT
45
× 10³
40
35
30
CONFIGURATION 1
CONFIGURATION 2
5000
6000
7000
8000
9000
10000
FIELD LENGTH, ft

FLYING QUALITIES STUDY

One study that was made with OPDOT (references 2,3) was the evaluation of the impact of minimum acceptable flying qualities upon aircraft design. This is the prime factor which influences aircraft design when RSSAS systems are considered. It is assumed that an RSSAS system will augment the flying qualities up to more than acceptable levels, but provisions must be made in the event the autopilot/augmentation system fails. Transport aircraft will generally have mechanical backups, so they should have sufficient unaugmented stability to assure the flight can be completed after a set of failures. Clearly these requirements, in effect, specify the inherent aerodynamic stability characteristics of the configuration. OPDOT will give the designer and regulators economic sensitivities to these criteria, enabling a proper compromise between safety and economy to be made. During the course of this study, it was found that many of the criteria being considered for unaugmented flying qualities of transports with RSSAS were inadequate or inappropriate for specifying airplane design parameters.

- LEVEL OF UNAUGMENTED FLYING QUALITIES DETERMINES INHERENT STABILITY CHARACTERISTICS
- ECONOMIC SENSITIVITIES FOR THESE CRITERIA WERE FOUND
- MANY CRITERIA WERE INADEQUATE FOR PROPERLY SPECIFYING THE UNAUGMENTED FLYING QUALITIES

IMPACT OF STATIC MARGIN

ORIGINAL PAGE IS OF POOR QUALITY

A study was made considering the impact of relaxing the static stability requirement for transport aircraft. A locus of optimum designs is plotted. For the configuration being considered, a savings of 2.5 percent in direct operating cost is possible when compared to a baseline configuration with 5-percent static margin. This corresponds to a fuel savings of 6 percent. At a certain point, in this case at -7 percent static margin, reducing the static stability constraint yields no further improvements. This is because the control constraints (typically nose-gear unstick during takeoff) override the tendency to make the tail smaller. A certain minimum size tail is required for control, and the center-of-gravity cannot be moved any further aft without sacrificing nose gear steering traction.

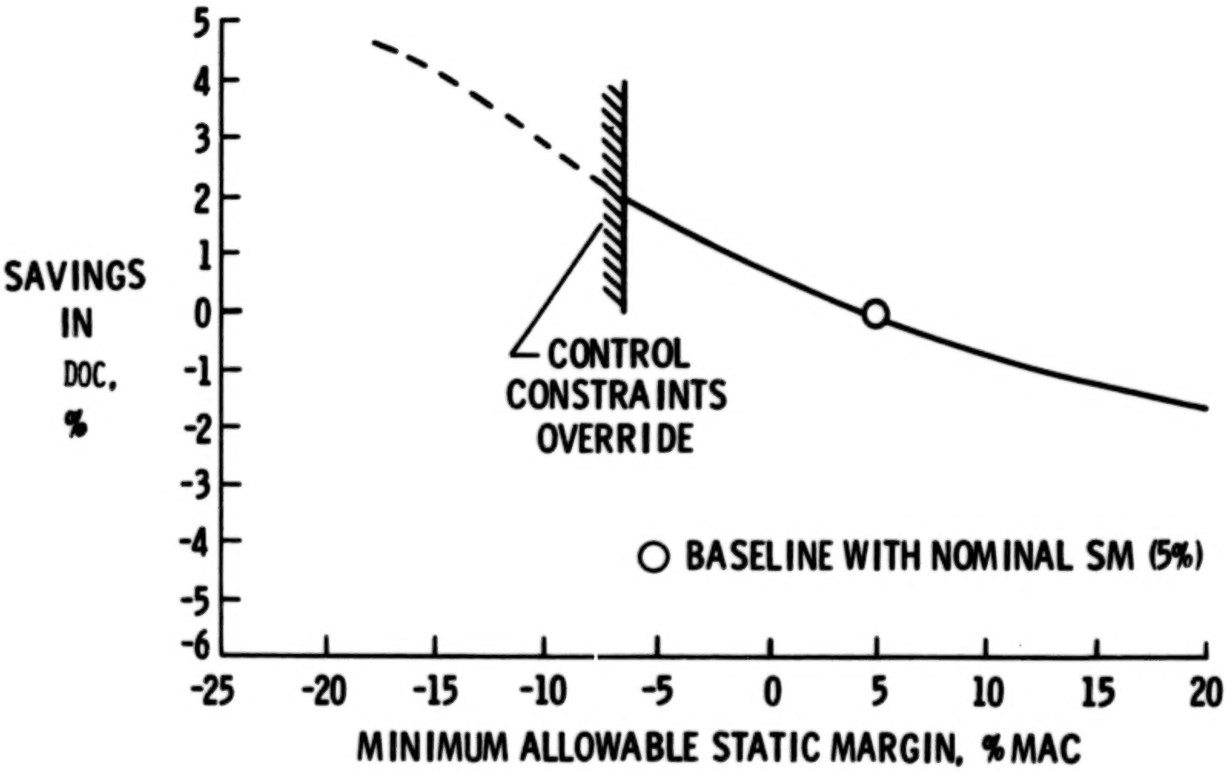

IMPACT OF LOADABILITY UPON DOC

Implied in the static margin sensitivity study was a range of allowed center-of-gravity travel. The control constraints are usually critical on the forward c.g. limit, and the stability constraints are usually critical on the aft c.g. limit. Reducing this range results in savings for all static margins under consideration. However, most benefits are achieved during the first 50 percent of reduction, indicating that if more careful center-of-gravity control is possible, a fuel savings of 2 percent or more is possible.

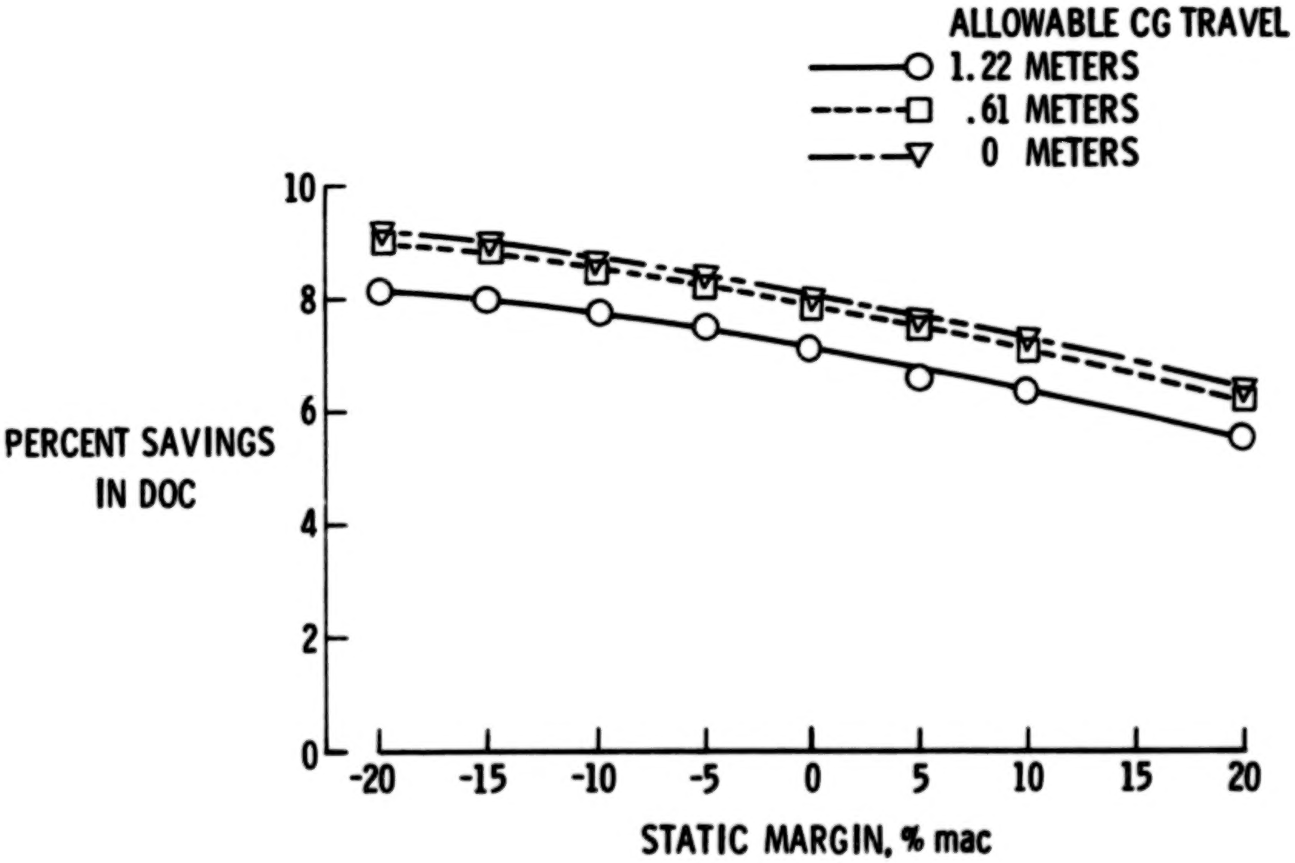

IMPACT OF LANDING GEAR LOCATION UPON DOC

Also implied in the static margin study was an aft limit for placing the landing gear. Studies have shown that the maximum aft placement for transport aircraft, where the gear and wing are collocated for structural efficiency, is about 65 percent of the mean aerodynamic chord. This is a critical constraint for RSSAS aircraft since it limits how far aft the center of gravity can travel before traction for nose gear steering is lost. Savings of nearly 1 percent in direct operating cost are possible if the gear could be located further aft without structural weight penalty. This corresponds to a fuel savings of over 2 percent.

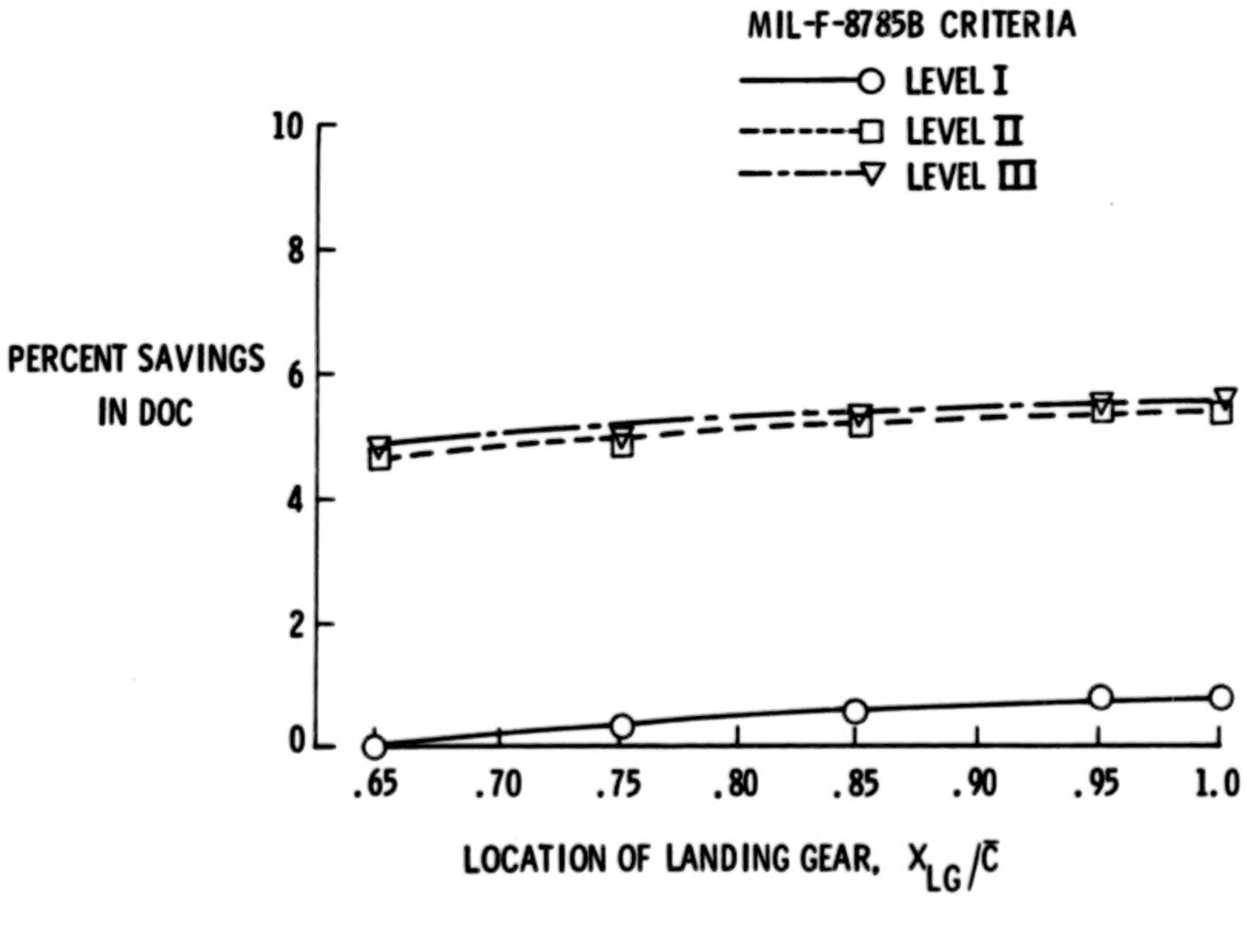

DOC SAVINGS VERSUS TIME-TO-DOUBLE

Another unaugmented flying qualities criterion that may be of interest is time-to-double amplitude. This plot illustrates the possible importance of economic sensitivity to a proposed criteria. If a designer or regulator is considering applying a constraint of 30 or 40 seconds, it is easy to see that the economic benefits of relaxing the constraint from 30 to 40 seconds is of little economic consequence. However, the opposite is true if considering an arbitrary boundary ranging between 2 and 6 seconds. The economic sensitivity information should be used before establishing the flight qualities criteria boundary since it significantly impacts the aircraft design.

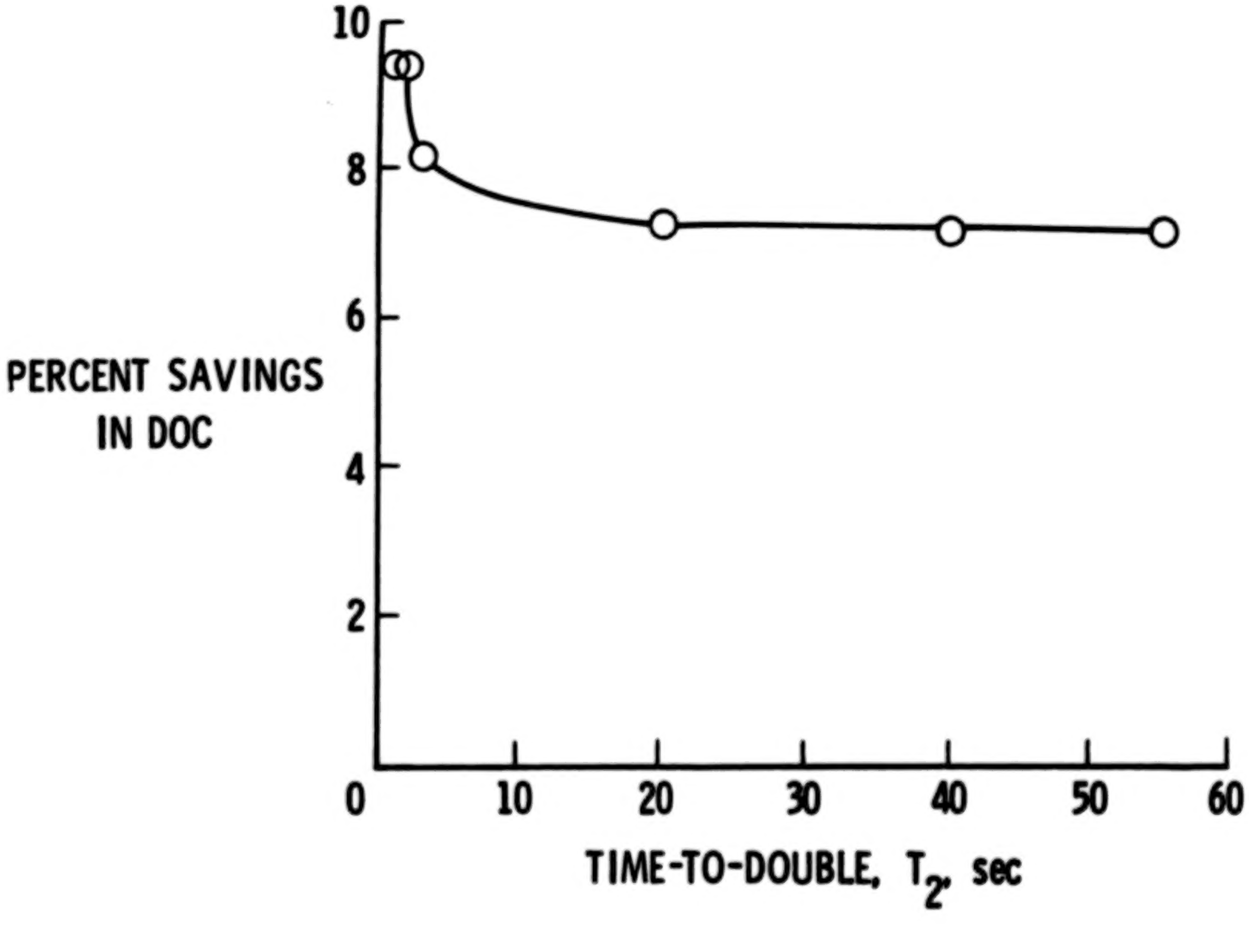

ORIGINAL PAGE IS
OF POOR QUALITY

IMPACT OF LOAD ALLEVIATION

Gust load alleviation and maneuver load alleviation are active controls concepts that have potential economic payoff. Utilization of these technologies impacts the design because the structure could be designed to a lower limit load factor resulting in a weight savings. Plotted is the savings in empty weight and direct operating cost for incremental reduction in limit load factor. The dotted line just reflects benefits of the lighter structure for the baseline configuration. The solid line includes resizing the airframe to take advantage of the weight savings from active controls.

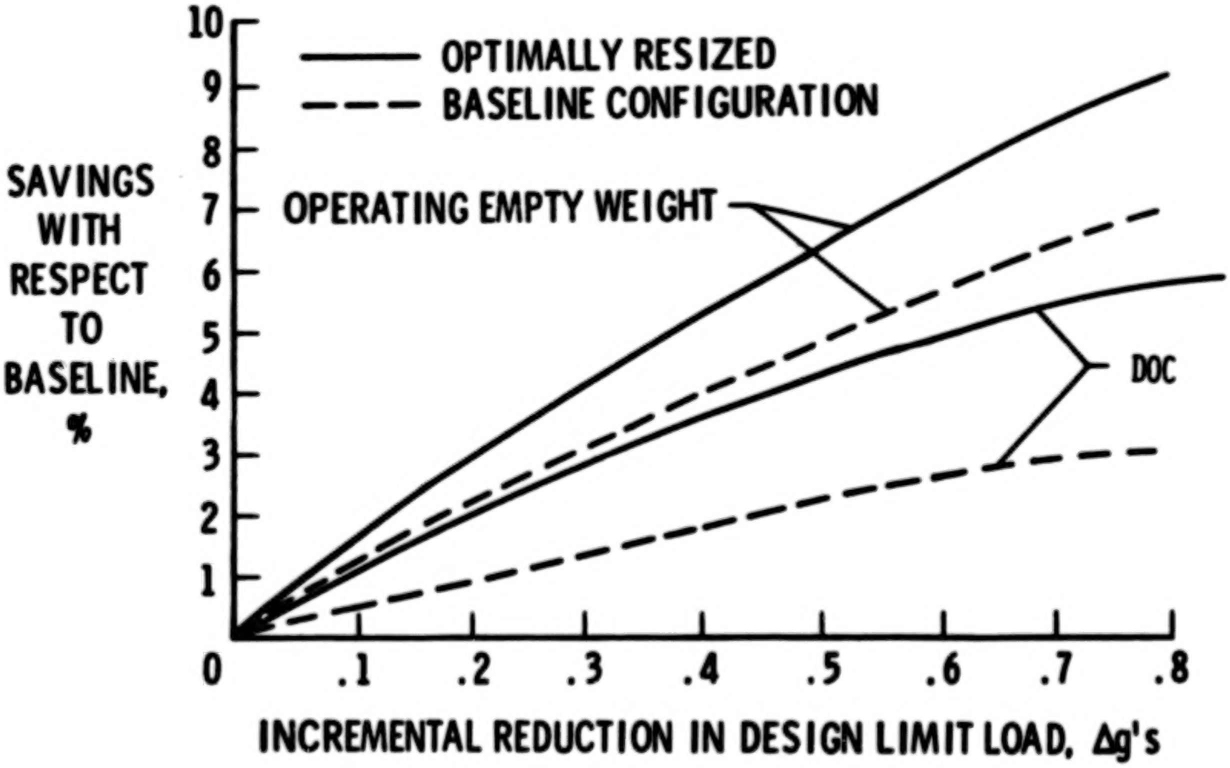

RESEARCH USING OPDOT

Other studies have been performed using OPDOT, including the investigation of the relative benefits of applying general technology improvements to transports and the evaluation of required economic and mission assumptions. Recently, a study was completed which determined the economic viability of canard transports when compared to conventional aft tail configurations. Future studies planned include the completion of vectored thrust integration for transports; multi-body and multi-surface configuration with canard, wing, and aft tail evaluation; and commuter transport technology requirements.

OTHER STUDIES

- RANKING OF OTHER GENERIC TECHNOLOGY IMPROVEMENTS
  (REFS. 4,5)
- EVALUATION OF ECONOMIC AND MISSION ASSUMPTION
  (REF. 5)
- DETERMINATION OF ECONOMIC VIABILITY OF CANARD TRANSPORTS
  (REF. 6)

FUTURE STUDIES

- COMPLETION OF VECTORED THRUST STUDIES
- MULTI-BODY AND MULTI-SURFACE TRANSPORT EVALUATION
- STUDY COMMUTER TRANSPORT TECHNOLOGY REQUIREMENTS
- EXTEND PROGRAM TO OTHER AIRCRAFT TYPES

SUMMARY

The integration of controls early in the design process is important because the implication of unaugmented flying qualities during control system failures impacts the aerodynamic design; because it is a requisite for the proposed technology improvements to achieve their full, synergistic potential; and, because flight test expense can be saved. Adjustments to the control laws after an advanced technology prototype has been built is no longer an easy proposition. Hence, it has become increasingly important to include control technologist and design considerations during conceptual design. In this discussion, a computer program developed at NASA Langley was described which utilizes optimization techniques to evaluate economic sensitivities of applying new technologies at the preliminary design level of transport aircraft.

- IT IS BENEFICIAL TO INTEGRATE CONTROLS CONSIDERATIONS INTO BEGINNING OF DESIGN PROCESS

    CONTROL SYSTEM AND FAILURE MODE ASSUMPTIONS IMPACT INHERENT AERODYNAMIC DESIGN

    FULL POTENTIAL OF ALL TECHNOLOGIES CAN BE REALIZED

    FLIGHT TEST EXPENSE WITH RESPECT TO FLYING QUALITIES CAN BE SAVED

- A TOOL USING OPTIMIZATION TECHNIQUES HAS BEEN DEVELOPED FOR TRANSPORT AIRCRAFT

REFERENCES

1. Sliwa, Steven M.; and Arbuckle, P. Douglas: OPDOT: A Computer Program for the Optimum Preliminary Design of a Transport Airplane. NASA TM-81857, 1980.

2. Sliwa, Steven M.: Impact of Longitudinal Flying Qualities Upon the Design of a Transport With Active Controls. AIAA Paper No. 80-1570, Aug. 1980.

3. Sliwa, Steven M.: Economic Evaluation of Flying-Qualities Design Criteria for a Transport Configured With Relaxed Static Stability. NASA TP-1760, 1980.

4. Sliwa, Steven M.: Sensitivity of the Optimal Design Process to Design Constraints and Performance Index for a Transport Airplane. AIAA Paper No. 80-1895, Aug. 1980.

5. Sliwa, Steven M.: Use of Constrained Optimization in the Conceptual Design of a Medium-Range Subsonic Transport. NASA TP-1762, December, 1980.

6. Arbuckle, P. Douglas; and Sliwa, Steven M.: Parametric Study of Critical Constraints for a Canard Configured Medium Range Transport Using Conceptual Design Optimization. AIAA Paper No. 83-2141, Aug. 1983.

N84
20574

UNCLAS

N84 20574

RELIABILITY AND MAINTAINABILITY ASSESSMENT FACTORS FOR RELIABLE FAULT-TOLERANT SYSTEMS

Salvatore J. Bavuso
NASA Langley Research Center
Hampton, Virginia

First Annual NASA Aircraft Controls Workshop
NASA Langley Research Center
Hampton, Virginia
October 25-27, 1983

ABSTRACT

A long-term goal of the NASA Langley Research Center is the development of a reliability assessment methodology of sufficient power to enable the credible comparison of the stochastic attributes of one ultrareliable system design against others. This methodology, developed over a 10-year period, is a combined analytic and simulative technique. An analytic component is the Computer-Aided Reliability Estimation capability, third generation, or simply CARE III. A simulative component is the Gate Logic Software Simulator capability, or GLOSS.

This paper focuses on the numerous factors that potentially have a degrading effect on system reliability and the ways in which these factors that are peculiar to highly reliable fault-tolerant systems are accounted for in credible reliability assessments. Also presented are the modeling difficulties that result from their inclusion and the ways in which CARE III and GLOSS mitigate the intractability of the heretofore unworkable mathematics.

RELIABILITY ASSESSMENT GOAL

A long-term goal of the NASA Langley Research Center is the development of a reliability assessment methodology of sufficient power to enable the credible comparison of the stochastic attributes of one ultrareliable system design against others (fig. 1). This methodology, developed over a 10-year period, is a combined analytic and simulative technique.

OBJECTIVE: DEVELOP A CAPABILITY TO ASSESS THE RELIABILITY OF ANY FAULT-TOLERANT DIGITAL COMPUTER-BASED SYSTEM, INCLUDING THE SYSTEM EFFECTS OF SOFTWARE

Figure 1

COMBINED ANALYTIC SIMULATIVE METHODOLOGY

The methodology for performing reliability assessments is based on the utilization of an analytic model that accounts for the long time constants of hardware and/or software failures and a separate analytic model that tracks the short time constants of system fault-handling mechanisms. These models, which are embodied in computer programs, in conjunction with a simulative model, make possible the reliability assessment of large, practical fault-tolerant systems (fig. 2).

The CARE III computer program (codeveloped by the Raytheon Company and the Langley Research Center (ref. 1)) provides an analytic capability. The GLOSS is a simulative capability that provides CARE III with stochastic fault-handling data. The GLOSS concept was demonstrated by application to the CPU of an avionic processor. A generalized GLOSS that provides a user-friendly hardware description language interface is currently being developed. The GLOSS was codeveloped by the Bendix Corporation and the Langley Research Center (refs. 2, 3).

```
CCCC      A    RRR    EEEE   !!!!!!!!!         GGGGG  L     00000  SSSSS  SSSSS
C        A A   R  R   E        ! ! !           G      L     0   0  S      S
C       AAAAA  RRR    EEE      ! ! !           G  GG  L     0   0  SSSSS  SSSSS
C      A     A R  R   E        ! ! !           G   G  L     0   0      S      S
CCCC   A     A R    R EEEE   !!!!!!!!!         GGGGG  LLLLL 00000  SSSSS  SSSSS
```

COMPUTER-AIDED RELIABILITY ESTIMATION   GATE LOGIC SOFTWARE SIMULATION

AN ANALYTIC CAPABILITY   A SIMULATIVE CAPABILITY

Figure 2

TECHNOLOGICAL DEVELOPMENT LEADING TO CARE III

The motivation for developing the combined analytic simulative methodology dates back to 1973. The long-term development of CARE III is depicted in figure 3. State-of-the-art reliability evaluators were typical of CARE, a computer program developed by the Jet Propulsion Laboratory, and TASRA (Tabular System Reliability Analysis), developed by Battelle Memorial Laboratories. The Raytheon Company and Langley jointly developed the CARE II, which provided a superset CARE model with an extensive fault-handling model. Langley was also involved in the development of CAST (Combined Analytic Simulative Technique), which provides the current Langley modeling concept. CAST was developed by the Ultra Systems, Inc. CARSRA (Computer-Aided Redundant System Reliability Analysis) was a spin-off from the Boeing ARCS (Advanced Reconfigurable Computer System) study. Langley has also been involved in numerous technology development studies, some of which are depicted in the figure. This long-term involvement has culminated in the development of the CARE III.

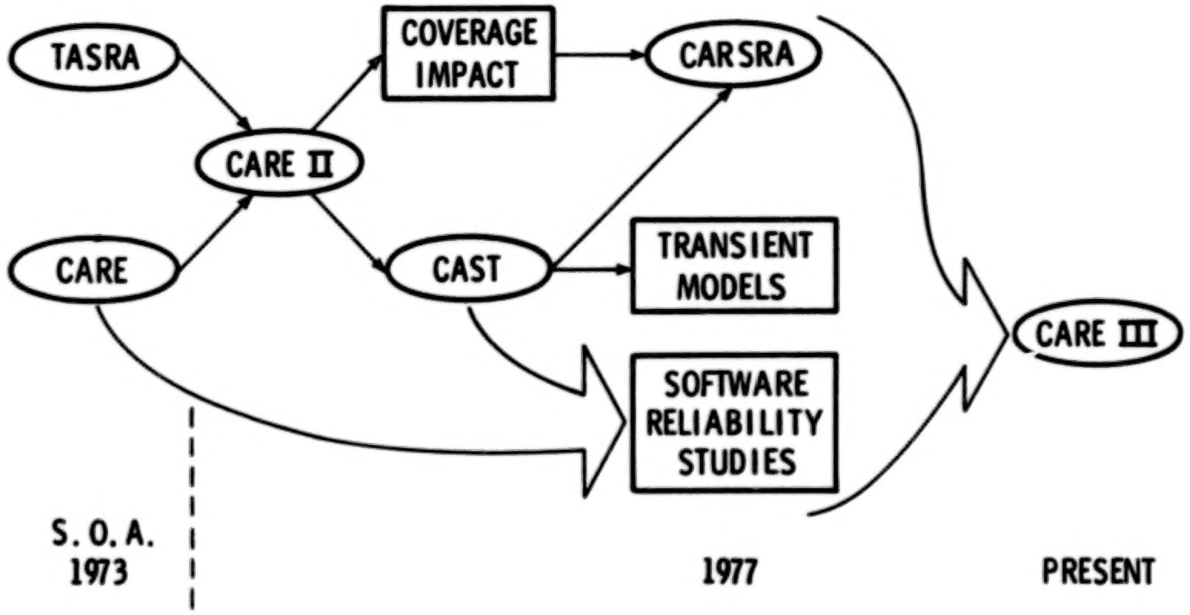

FLIGHT CONTROL
COMPUTER ASSESSMENT

- FLIGHT CONTROL SYSTEM ASSESSMENT
- TRANSIENT-FAULT MODELING
- SOFTWARE-ERROR AND REDUNDANCY MODELING

Figure 3

PROFOUND OBSERVATIONS

On our way toward developing the specifications for CARE III, we found that for ultrareliable systems certain factors that previously were of little interest to the reliability analyst now potentially have a significant effect (fig. 4). This is particularly true of systems with a flight crucial probability of failure of less than 10^{-9} in a 1- to 10-hour mission. An example of this observation is the latent (undetected) fault. We also realized that even complex assessment capabilities must be user-friendly; this is always a difficult task for complex capabilities.

PROBLEMS:

1. **EVERYTHING IMPORTANT WHEN $P_F < 10^{-1}$**
2. **PROGRAM VERSATILITY vs CONVENIENCE AND EFFICIENCY**

Figure 4

ORIGINAL PAGE IS
OF POOR QUALITY

HIGHLY RELIABLE FAULT-TOLERANT SYSTEMS TO WHICH CARE III IS APPLICABLE

The class of fault-tolerant systems of most interest currently utilizes off-the-shelf processors or computers (fig. 5). These systems rely heavily on the ability of the processors to detect system faults/errors, to identify the fault/error to the smallest reconfigurable unit, and to effect recovery.

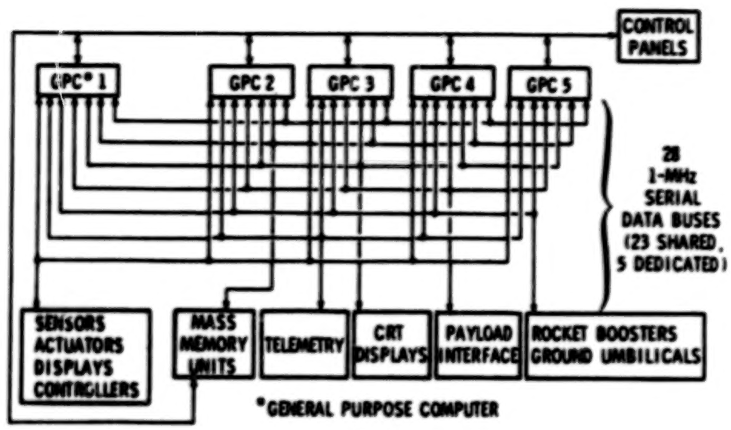
CONTROL PANELS
GPC* 1
GPC 2
GPC 3
GPC 4
GPC 5
28 1-MHz SERIAL DATA BUSES (23 SHARED, 5 DEDICATED)
SENSORS ACTUATORS DISPLAYS CONTROLLERS
MASS MEMORY UNITS
TELEMETRY
CRT DISPLAYS
PAYLOAD INTERFACE
ROCKET BOOSTERS GROUND UMBILICALS
*GENERAL PURPOSE COMPUTER

SPACE SHUTTLE SYSTEM

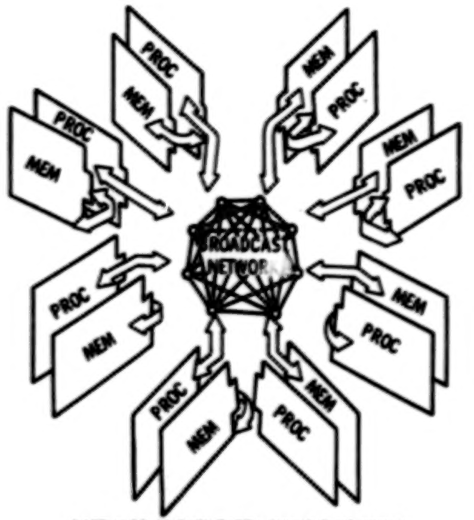
PROC
MEM
BROADCAST NETWORK

SOFTWARE IMPLEMENTED FAULT TOLERANCE (SIFT)

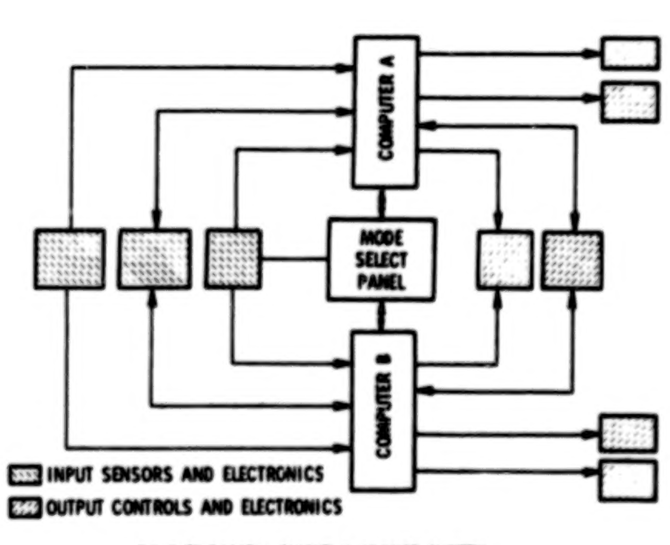
COMPUTER A
MODE SELECT PANEL
COMPUTER B
▨ INPUT SENSORS AND ELECTRONICS
▨ OUTPUT CONTROLS AND ELECTRONICS

DC-9-80 DIGITAL FLIGHT GUIDANCE SYSTEM

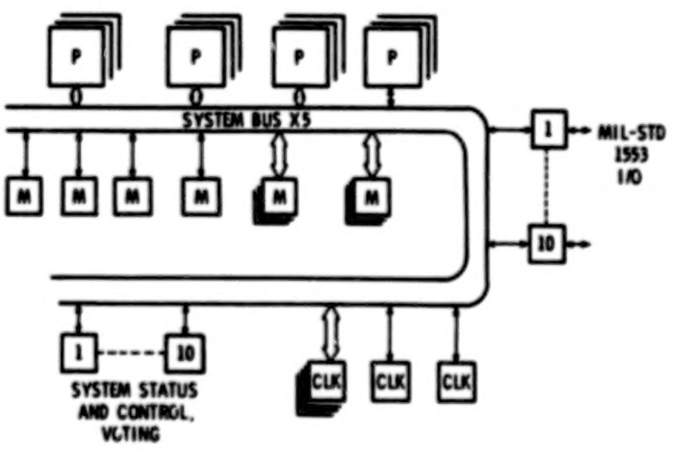
P
P
P
P
SYSTEM BUS X5
M
M
M
M
M
M
1
10
MIL-STD 1553 I/O
1
10
SYSTEM STATUS AND CONTROL, VOTING
CLK
CLK
CLK

FAULT-TOLERANT MULTIPROCESSOR

Figure 5

COVERAGE - A MAJOR RELIABILITY DRIVER

In ultrareliable fault-tolerant systems, the inability of a system to achieve perfect fault/error handling is often the dominant cause of system failure (fig. 6). The major contributor of diminished fault/error handling is the latent fault/error. The long-term (latent) accumulation of faults/errors poses a severe threat to the system's ability to detect and mask out anomalies. The modeling of fault/error handling adds a tremendous amount of additional complexity to the reliability assessment task.

THE PREDOMINANT CAUSE OF FAILURE IN ULTRARELIABLE
DIGITAL SYSTEMS HAS BEEN SHOWN TO BE ATTRIBUTED TO
FACTORS OTHER THAN HARDWARE SPARES DEPLETION

COVERAGE - MEASURE OF SYSTEM'S ABILITY TO HANDLE FAULTS ⟹ SYSTEM

- FAULT DETECTION
- FAULT ISOLATION
- RECONFIGURATION AND RECOVERY

UNDETECTED FAULT - LATENT FAULT

Figure 6

DELINEATION OF HARDWARE AND SOFTWARE FAILURE AND ERROR MODELS

The increased complexity is indicated by the number of additional fault/error models that now must be considered. The increase in the number of fault/error models that must be accounted for is largely attributed to use of the digital computer (which possess extensive memory capability) and very high system reliability requirements. An extensive memory capability is a two-edged sword in that not only are computational capability and flexibility enhanced, but the likelihood of latent faults and errors occurring is also increased. Ultrareliability necessitates the consideration of design errors, which previously were considered to be insignificant. Each branch in the trees in figure 7 represents a fault/error model. Faults are hardware generated, whereas errors are caused by a fault or by software design anomalies. Either one may be permanent or may appear to be transient or intermittent. The common piece-parts reliability analysis is shown as a permanent random hardware failure.

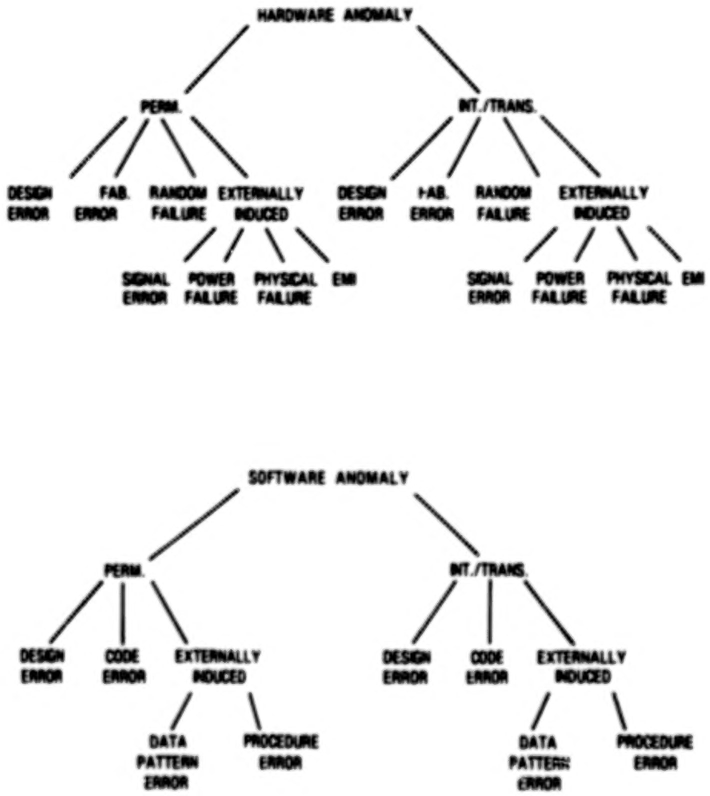
HARDWARE ANOMALY
PERM.
INT./TRANS.
DESIGN ERROR
FAB. ERROR
RANDOM FAILURE
EXTERNALLY INDUCED
DESIGN ERROR
FAB. ERROR
RANDOM FAILURE
EXTERNALLY INDUCED
SIGNAL ERROR
POWER FAILURE
PHYSICAL FAILURE
EMI
SIGNAL ERROR
POWER FAILURE
PHYSICAL FAILURE
EMI
SOFTWARE ANOMALY
PERM.
INT./TRANS.
DESIGN ERROR
CODE ERROR
EXTERNALLY INDUCED
DESIGN ERROR
CODE ERROR
EXTERNALLY INDUCED
DATA PATTERN ERROR
PROCEDURE ERROR
DATA PATTERN ERROR
PROCEDURE ERROR

Figure 7

ORIGINAL PAGE IS
OF POOR QUALITY

FUNCTIONAL DEPENDENCY TREE FOR A NEAR-FUTURE PROPOSED FLIGHT CONTROL SYSTEM

Ultrareliable fault-tolerant systems increase the system reliability by employing redundancy, which further compounds the modeling task. A typical proposed advanced reconfigurable flight control system would utilize triple voting of units for the sensors, processor memories, and actuator electronics (fig. 8). In this example, the number of units increased from 22 for a nonredundant system to 64 for the fault-tolerant architecture.

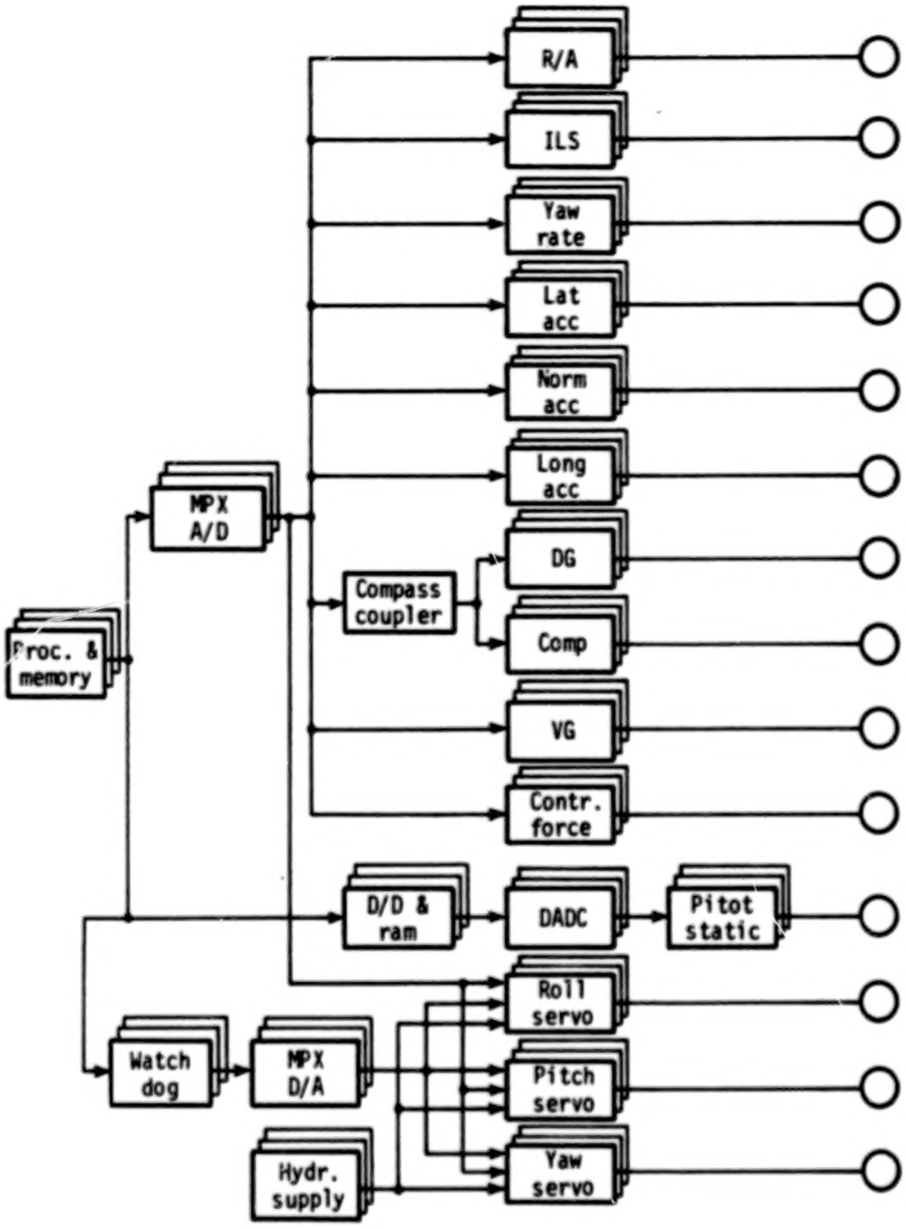
R/A
ILS
Yaw rate
Lat acc
Norm acc
Long acc
MPX A/D
DG
Compass coupler
Comp
Proc. & memory
VG
Contr. force
D/D & ram
DADC
Pitot static
Roll servo
Watch dog
MPX D/A
Pitch servo
Hydr. supply
Yaw servo

Figure 8

POSSIBLE STOCHASTIC MODELING APPROACHES

Until recently, the reliability analyst was forced to compromise the analysis of such large systems either by modeling sections of the problem at a time and/or by making simplifying assumptions to keep the size of the reliability model tractable (fig. 9). The difficulty in this approach is that it is time consuming and complex. Perhaps more important, it is prone to error and is often unreproducible. Reliability models for the advanced reconfigurable system example shown in figure 8, which would include the details previously discussed (fig. 7), would require on the order of millions of states in the Markov modeling sense. For each state, there exists an ordinary differential equation. Thus, a Markov model for this system would require the solution of millions of differential equations, a task that is expensive, if not impossible.

- ⟶ MARKOV (CAST, ARIES, CARSRA, SURF)
- COMBINATORIAL (CARE, CARE II)
- KOLMOGOROV (CARE III) (REF. 4)

Figure 9

ALTERNATE STOCHASTIC MODELING APPROACHES

Aside from using the popular Markov technique, two other approaches come to mind. The combinational method is the traditional piece-parts technique (fig. 10). In applying this technique to a fault-tolerant system with a reasonable degree of complexity, one soon learns, as in the development of CARE II, that the computational aspects become unmanageable and involve nested integrals four or more deep. The Kolmogorov method, in conjunction with a state aggregation technique, overcomes the computational difficulties of both the Markov and combinatorial techniques.

- MARKOV (CAST, ARIES, CARSRA, SURF)
- → COMBINATORIAL (CARE, CARE II)
- → KOLMOGOROV (CARE III)

Figure 10

THE CARE III APPROACH

The ability of CARE III to provide extensive fault occurrence and fault-handling models is largely attributed to its ability to cope with large state spaces and is made possible by the observation that the time constants associated with fault occurrence are on the order of 10^4 hours, whereas the time constants of the fault-handling model are on the order of 10^{-5} hours. This wide time separation allows the fault occurrence model to be treated as being independent of the fault-handling model. Thus, the fault-handling model is evaluated without regard to fault occurrences (fig. 11). The results of the fault-handling model are then combined with the fault occurrence model to produce the desired reliability outputs. The fault occurrence model is solved using Kolmogorov's forward differential equations. The Kolmogorov technique is used because the state reduction process discussed above necessarily requires the solution of a nonhomogenous (time-dependent failure rates) Markov process.

APPROACH

- DEFINE SYSTEM STATE ONLY IN TERMS OF NUMBER OF EXISTING FAULTS
- INDEPENDENTLY EVALUATE TRANSITION PARAMETERS AS A FUNCTION OF DISTRIBUTION OF POSSIBLE FAULT TYPES AND STATES
- DETERMINE RELIABILITY USING KOLMOGOROV'S FORWARD DIFFERENTIAL EQUATIONS

TASK

- NUMBER OF STATES DRASTICALLY REDUCED, TRANSITION RATES NECESSARILY TIME DEPENDENT

Figure 11

A MIXED MARKOV MODEL AND ITS STATE-REDUCED AGGREGATED RELIABILITY MODEL

An illustration of the state reduction technique can be seen by observing the reliability model of a two-unit system (fig. 12(a)). States 0, 1, and F are the fault occurrence states. The states enclosed in the dashed lines are the fault-handling states. The two-unit model is a mixture of a nonhomogenous and a semi-Markov model, which is the type of model CARE III was designed to evaluate. The model that CARE III actually evaluates is the aggregated reliability model shown in Figure 12(b). The aggregated model is a nonhomogeneous Markov model. CARE III approximates the mixed process with a nonhomogeneous Markov process and can do so because of the wide separation in time constants in the fault occurrence and fault-handling models. In the aggregate model, the states are strictly fault occurrence states (defines number of failed units). The fault-handling model information contained in the dashed box of the two-unit system is mapped into the time-varying transition rate a'(t). The nonhomogeneous aggregated Markov model is solved using the Kolmogorov solution technique to produce time-varying probabilities of being in states 0, 1', and F (the failure state) over the desired mission time. Although the state reduction wasn't too dramatic for this simple example, in practical assessments, state reductions of 6 orders of magnitude have been estimated.

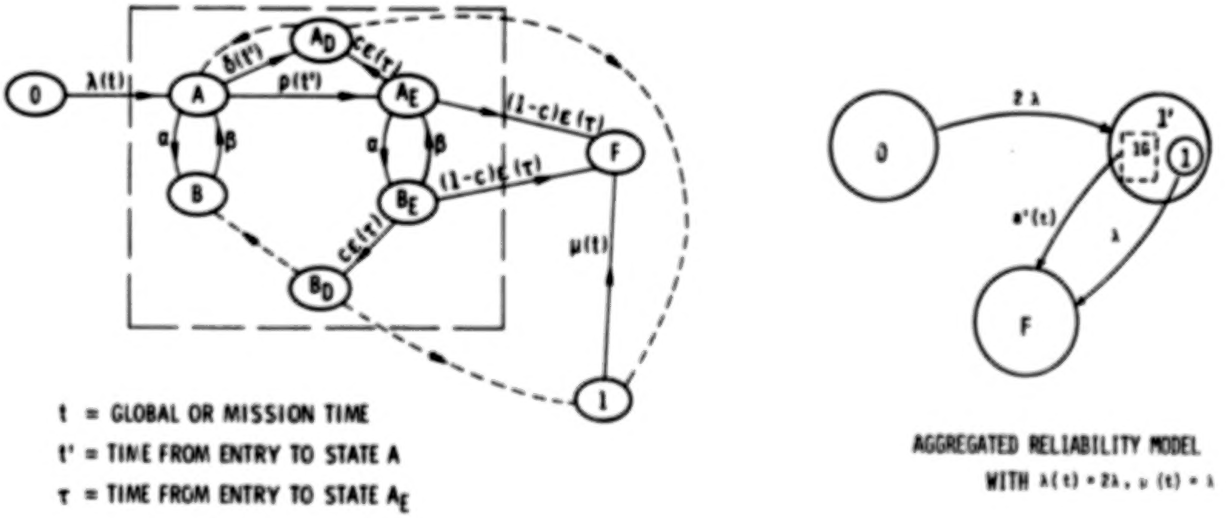

t = GLOBAL OR MISSION TIME
t' = TIME FROM ENTRY TO STATE A
τ = TIME FROM ENTRY TO STATE A_E

AGGREGATED RELIABILITY MODEL
WITH $\lambda(t) = 2\lambda$, $\mu(t) = \lambda$

(a) (b)

Figure 12

CARE III FAULT-HANDLING MODEL

The ability of CARE III to model the fault/error models delineated in figure 7 is made possible by CARE III's single- and double-fault models through the judicious selection of the appropriate transition rates and/or state holding probability density functions. The double fault model accounts for critically coupled coexisting failures, which are user defined. The critically coupled failures, when they exist, are defined by certain combinations of pairs of states in the single-fault model (e.g., failure of two critically coupled units each in state A will cause system failure). The structure of the single-fault model can be grasped by referring to figure 13, the reliability model of a two-unit system.

Initially, the system is in state 0 and has experienced no failures. When a failure occurs, the system enters state A, the active latent state. This arrival is governed by the arrival density $\lambda(t)$. Depending upon the nature of the failure (i.e., permanent, transient, intermittent, etc.), the fault-handling model will be defined differently. For example, if the failure is intermittent, $\lambda(t)$ would be the probability density function (pdf) for the arrival of an intermittent, and states A and B define the intermittent model where α and β are constant transition rates into and out of state B. When the system is in state B, the benign state, the failed unit appears to have healed itself, that is, the manifestation of the failure, a fault, vanishes. However, when the failed manifestation is once again resumed (the fault reappears), the system enters state A, where the failure looks like a permanent failure. It could be detected by a self-test program with pdf $\delta(t')$, and the system would enter state A_D, the active detected state. If a spare exists, the system will purge the faulty unit and switch in the spare (dashed arc to state 1). Alternatively, while in the active state, the fault could generate errors with pdf $\rho(t')$. The system then will enter A_E, the active error state. The intermittent failure could manifest its intermittent state again, and the system would then enter state B_E, the benign error state. Although the failure is benign, the error may not be benign and may cause system failure which is denoted by the B_E to F transition $(1-c)\varepsilon(\tau)$.

The error detection density is $\varepsilon(\tau)$, and 1-C is the proportion of errors from which the system is unable to recover. While in state B_E, the error could be detected and corrected. In this event, the system enters state B_D (benign detected) by transition $c\varepsilon(\tau)$. At this point, the system may choose to do nothing further with the detected and corrected error and so move to the benign state, or the system may choose to reconfigure out the module containing the error and therefore move to state 1. The dashed arcs are instantaneous transitions. The other transition out of state A_E is to state F, the single-point failure transition $(1-c)\varepsilon(\tau)$. This transition is similar to the B_E to F transition. In a well-designed fault-tolerant system, $(1-c)\varepsilon(\tau)$ should be near zero. If $\lambda(t)$ is the pdf for the arrival of a transient, α would be set to a value greater than zero and β would be equal to zero. The pdf $\lambda(t)$ for the arrival of a permanent failure would be defined so that $\alpha = \beta = 0$. The dashed arc going from state A_D to A enables the analyst to include the effects of the system decision that the detected fault which took the system from state A to A_D was, in fact, a transient. In this regard, the system would not reconfigure out a nonfailed module.

ORIGINAL PAGE IS
OF POOR QUALITY

The reader will note that the reliability model has three measures of time associated with it, which necessarily makes the model a semi-Markov process. This added complexity is required because the behavior of the system is dependent on the onset of the various fault-behavior events. The availability of data for the fault-handling models is unfortunately still poor at best and is often nonexistent altogether. The creation of the data is the subject of a considerable amount of current research. The GLOSS capability alluded to in figure 2 was used to estimate $\delta(t')$ and $\varepsilon(\tau)$ for permanent faults in the CPU of an avionic miniprocessor. (See fig. 13.)

Although the literature has often reported that transient faults are by far the most frequently occurring anomaly, virtually no test data exist that can be used for modeling transient occurrences or transient fault handling. Test data for intermittent faults are also sparse (ref. 5).

In view of the extreme sensitivity that reliability assessments of ultrareliable systems show to best-guess transient and intermittent failure occurrence data, one can only wonder why such data are not abundant.

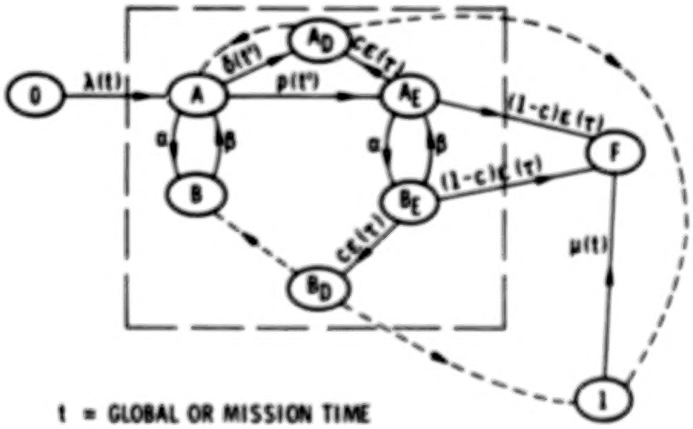

t = GLOBAL OR MISSION TIME
t' = TIME FROM ENTRY TO STATE A
τ = TIME FROM ENTRY TO STATE A_E

Figure 13

CONCLUDING REMARKS

The reliability assessment of ultrareliable fault-tolerant systems adds new dimensions of complexity to the assessment methodology (fig. 14). New tools are emerging to assist the reliability analyst to cope with the additional modeling complexities.

The availability of data for these novel tools is, however, slow in coming and will no doubt stunt the progress of developing ultrareliable fault-tolerant systems.

- NOVEL POWERFUL ASSESSMENT METHODOLOGIES ARE EMERGING: CARE III AND GLOSS
- AVAILABILITY OF DATA IS SPARSE
- LACK OF SUFFICIENT DATA WILL STUNT THE GROWTH OF ULTRARELIABLE DIGITAL SYSTEMS

Figure 14

REFERENCES

1. Bavuso, S. J.: Advanced Reliability Modeling of Fault-Tolerant Computer-Based Systems. Electronic Systems Effectiveness and Life Cycle Costing, J. K. Skwirzynski ed., Springer-Verlag, 1983, pp. 279-302.

2. McGough, J. G.; and Swern, F. L.: Measurement of Fault Latency in a Digital Avionic Processor Part II. NASA CR-145371, 1983.

3. Bavuso, S. J.; McGough, J. G.; and Swern, F. L.: Latent Fault Modeling and Measurement Methodology for Application to Digital Flight Controls. Advanced Flight Control Symposium, USAF Academy, Colorado Springs, Colo., August 1981.

4. Feller, William: Introduction to Probability Theory and Its Applications. Third ed. Wiley and Sons, 1968.

5. O'Neill, E. J.; and Halverson, J. R.: Study of Intermittent Field Hardware Failure Data in Digital Electronics. NASA CR-159268, 1980.

SESSION II

PARAMETER AND STATE ESTIMATION AND OPTIMAL GUIDANCE TECHNIQUES

Lawrence W. Taylor, Jr.
Session Chairman

N84
20575

UNCLAS

N84 20575

PRACTICAL ASPECTS OF MODELING AIRCRAFT DYNAMICS FROM FLIGHT DATA

Kenneth W. Iliff and Richard E. Maine
Ames Research Center
Dryden Flight Research Facility
Edwards, California

First Annual NASA Aircraft Controls Workshop
NASA Langley Research Center
Hampton, Virginia
October 25-27, 1983

PRECEDING PAGE BLANK NOT FILMED

The purpose of parameter estimation, a subset of system identification, is to estimate the coefficients (such as stability and control derivatives) of the aircraft differential equations of motion from sampled measured dynamic responses. Model structure determination, which is another aspect of systems identification, is discussed elsewhere.

Statement of Aircraft Parameter Estimation Problem

Estimate the coefficients (parameters) of the aircraft differential equations of motion from sampled measured dynamic responses

In the past, the primary reason for estimating stability and control derivatives from flight tests was to make comparisons with wind tunnel estimates. As aircraft became more complex, and as flight envelopes were expanded to include flight regimes that were not well understood, new requirements for the derivative estimates evolved. For many years, the flight-determined derivatives were used in simulations to aid in flight planning and in pilot training. The simulations were particularly important in research flight-test programs in which an envelope expansion into new flight regimes was required. Parameter estimation techniques for estimating stability and control derivatives from flight data became more sophisticated to support the flight-test programs. As knowledge of these new flight regimes increased, more complex aircraft were flown. Much of this increased complexity was in sophisticated flight control systems. The design and refinement of the control system required higher fidelity simulations than were previously required.

Uses of Flight-Determined Estimates

- Correlation studies
- Handling qualities documentation
- Design compliance
- Simulation
  - Flight planning (envelope expansion)
  - Pilot training
- Control system design
  - Linear analysis
  - Nonlinear simulation
  - Pilot in the loop

The maximum likelihood estimator is used to obtain the stability and control derivatives from flight data. This is done by minimizing the cost function $J(\xi)$ where the unknown derivatives to be estimated are in the vector ξ. The term J is the weighted outer product of the difference between the measured response and the computed response, based on the current value of ξ. For the stability and control derivative problem, we can assume the state and measurement equations are linear, although they need not be for maximum likelihood estimators in general.

Maximum Likelihood Estimator

State Equation

$$\dot{x} = Ax + Bu + \eta$$

Observation Equation

$$z_i = Cx_i + Du_i + n_i$$

Minimize Cost Function

$$J(\zeta) = \sum_{i=1}^{N} [z_i - \tilde{z}_i(\zeta)]^{*} R^{-1} [z_i - \tilde{z}_i(\zeta)] + \tfrac{1}{2} N \ln |R|$$

Where

$\tilde{z}_i$ is computed estimate of z_i

ζ is vector of unknowns

ORIGINAL PAGE IS
OF POOR QUALITY

If we look at the case where the vector of unknowns ξ contains only the roll-damping and the roll-control power, we can see some of the essential features of the minimization of the cost function. The cost function is shown here as a function of these two unknowns for a set of simulated data with added measurement noise. The minimum is shown, as well as the true value used in simulation. The reason for the difference is the measurement noise. This is also true for the case of real-flight data, where the measurement error may also be caused by modeling error. The maximum likelihood estimate is at the minimum of the cost function.

Cost Function Surface Near Minimum

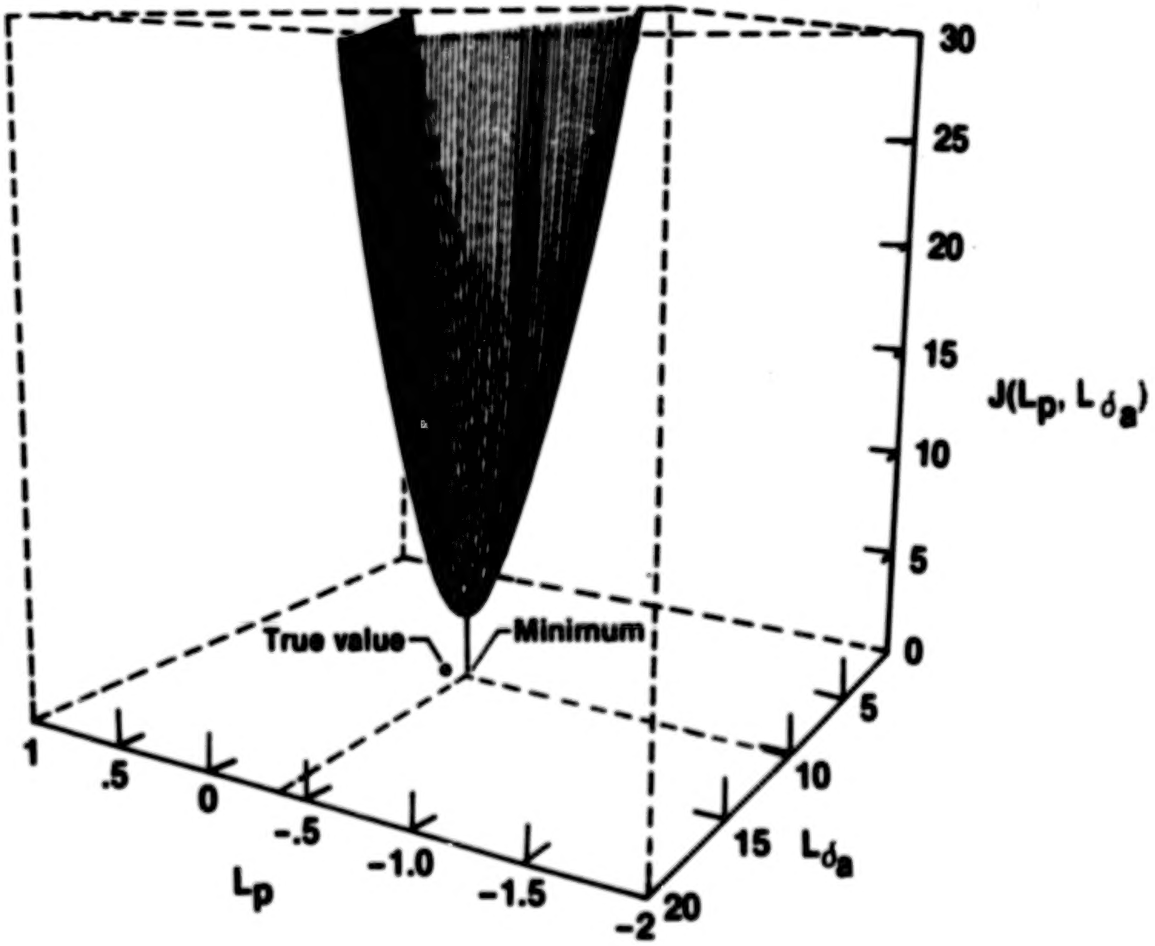

ORIGINAL PAGE IS
OF POOR QUALITY

If we slice through the surface at constant values of the cost function, we can depict the cost function with isoclines. If we are far from the minimum (lowest isocline value), the isoclines are not elliptical. As we approach the minimum, the isoclines become more closely elliptical or nearly quadratic. Most minimization techniques take advantage of the quadratic nature of the cost function near the minimum.

Cost Function Isoclines

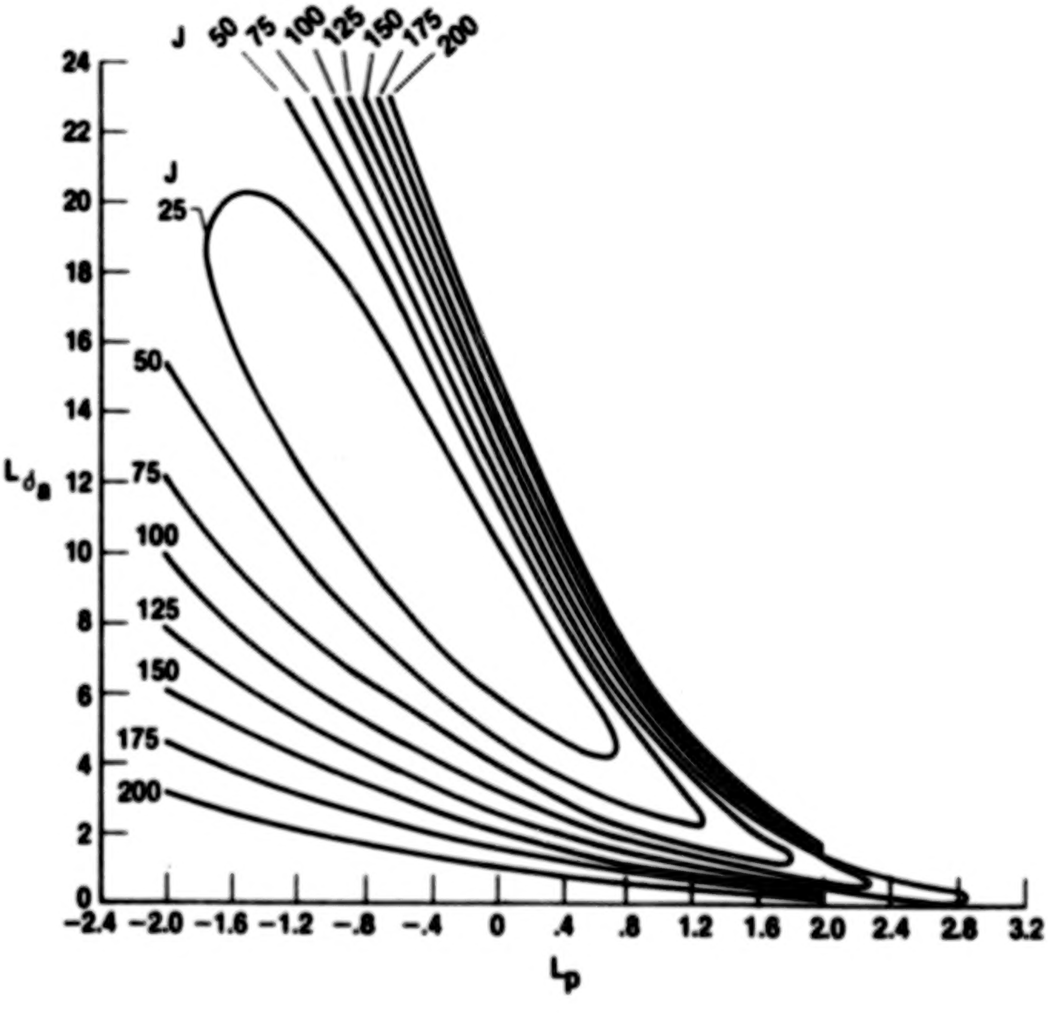

The F-14 is a twin-engine, high-performance fighter aircraft that has variable wing sweep capability. The F-14 program addressed improvement of airplane handling qualities at high angles of attack by incorporating a number of control system techniques. The first part of the program was dedicated to obtaining flight-determined stability and control derivatives. The flight conditions covered the subsonic envelope of the F-14, which is the complete trimmed angle-of-attack range for Mach numbers of 0.9 and below.

F-14 AIRPLANE CONFIGURATION

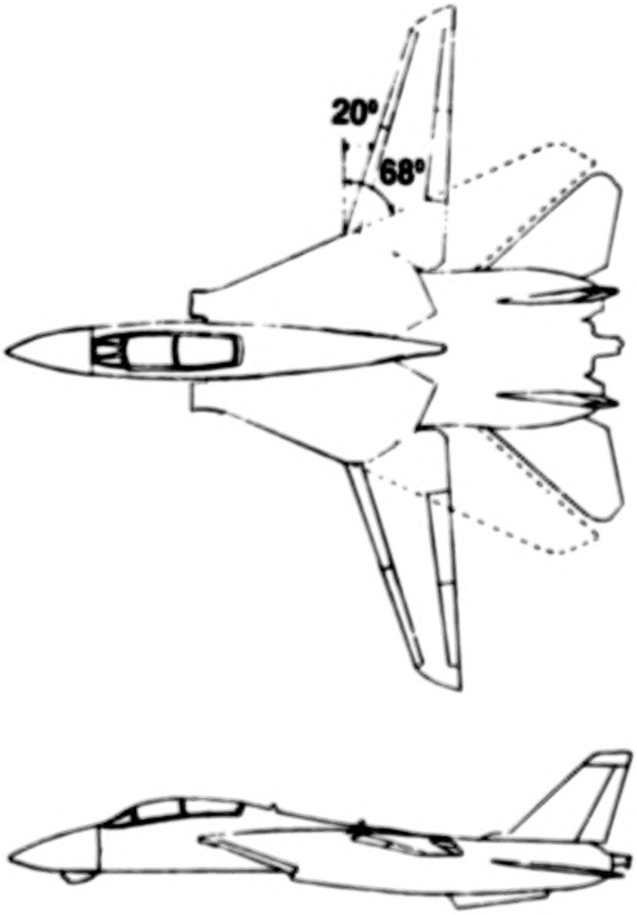

ORIGINAL PAGE IS
OF POOR QUALITY

This figure shows the flight-determined damping in roll (C_{l_p}) as a function of angle of attack (α) for low Mach numbers (<0.55) and for a Mach number of 0.9. There was some uncertainty in the accuracy of the wind tunnel predictions of C_{l_p} because the tunnel model configuration was different from the flight configuration. These flight data agreed with the trends found in the tunnel; with the proper interpretation, even the magnitudes were in fair agreement.

DAMPING-IN-ROLL ESTIMATES

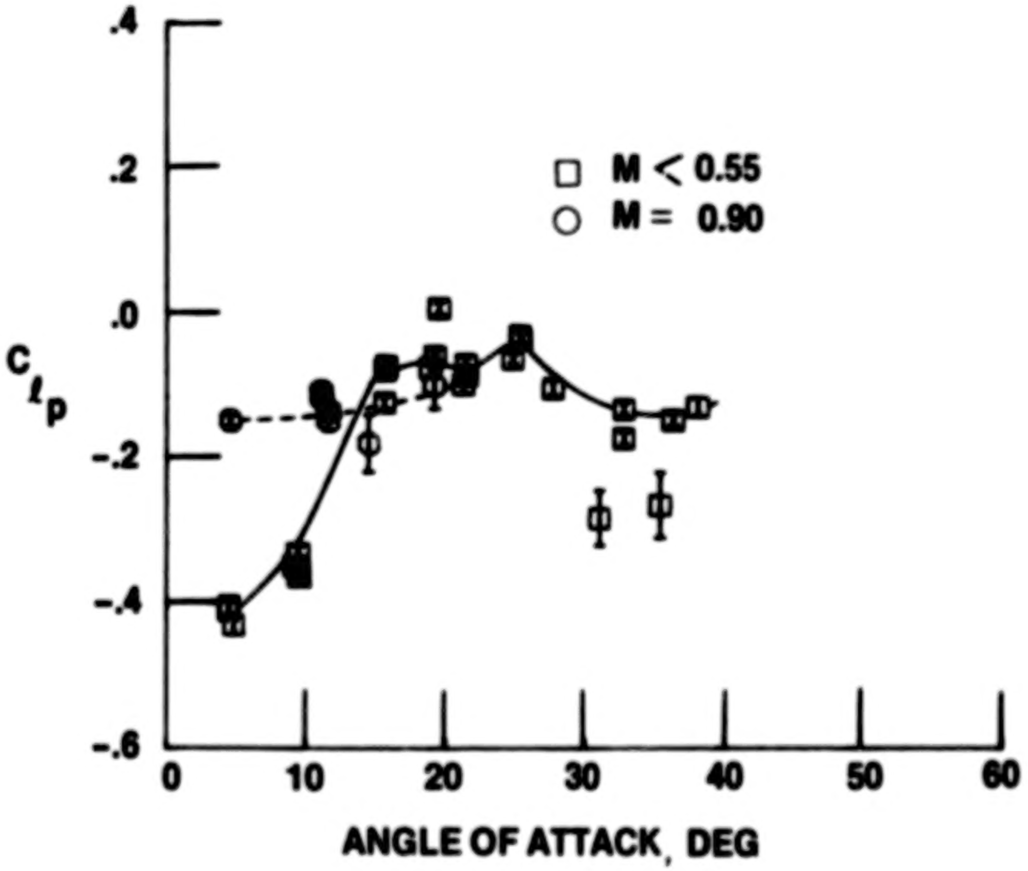

ORIGINAL PAGE IS
OF POOR QUALITY

This figure shows the flight-determined values of dihedral effect (C_{l_β}) as a function of α compared with the results of two different sets of wind tunnel results. There was some concern about the disagreement of the two sets of wind tunnel results before flight. At low angles of attack, the three sets of estimates are in fair agreement; however, at angles of attack above 15°, the flight data lie between the sets of tunnel data.

DIHEDRAL EFFECT ESTIMATES

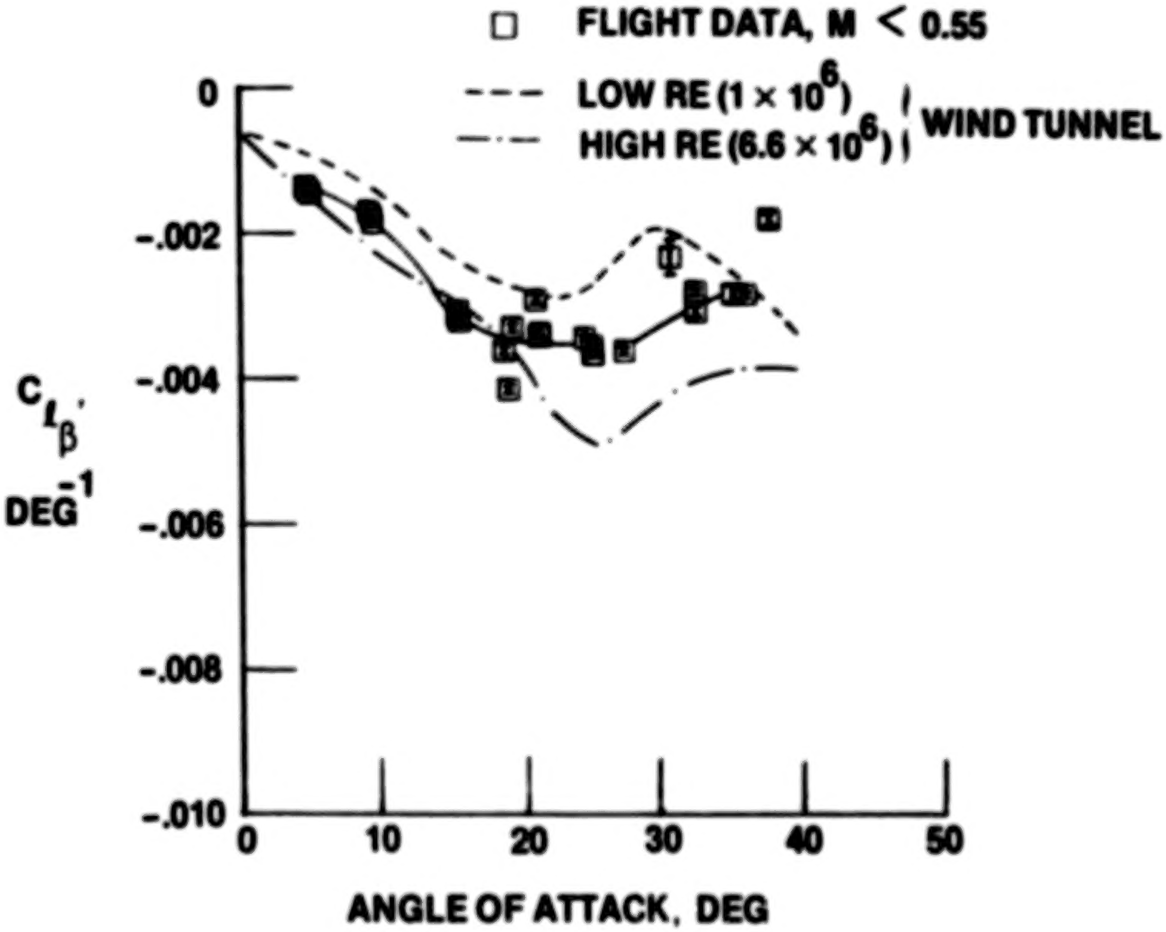

ORIGINAL PAGE IS
OF POOR QUALITY

The F-14 data in this figure show the sensitivity with which we can determine stability and control derivatives. Rolling-moment coefficient as a result of differential spoiler deflection ($C_{\ell_{\delta_{sp}}}$) is shown as a function of angle of attack. It is apparent that there is about 10 percent to 20 percent more effectiveness with the direct lift control (DLC) off. The difference between DLC on and DLC off is a small configurational change. With the DLC on, the spoilers are positioned 4° above the wing contour; with the DLC off, the spoilers are positioned along the wing contour. Therefore, the 4° change in position results in a significant change in spoiler effectiveness, demonstrating the sensitivity with which the parameter estimation method can detect changes in vehicle characteristics that result from changes in configuration.

DIFFERENTIAL SPOILER EFFECTIVENESS ESTIMATES

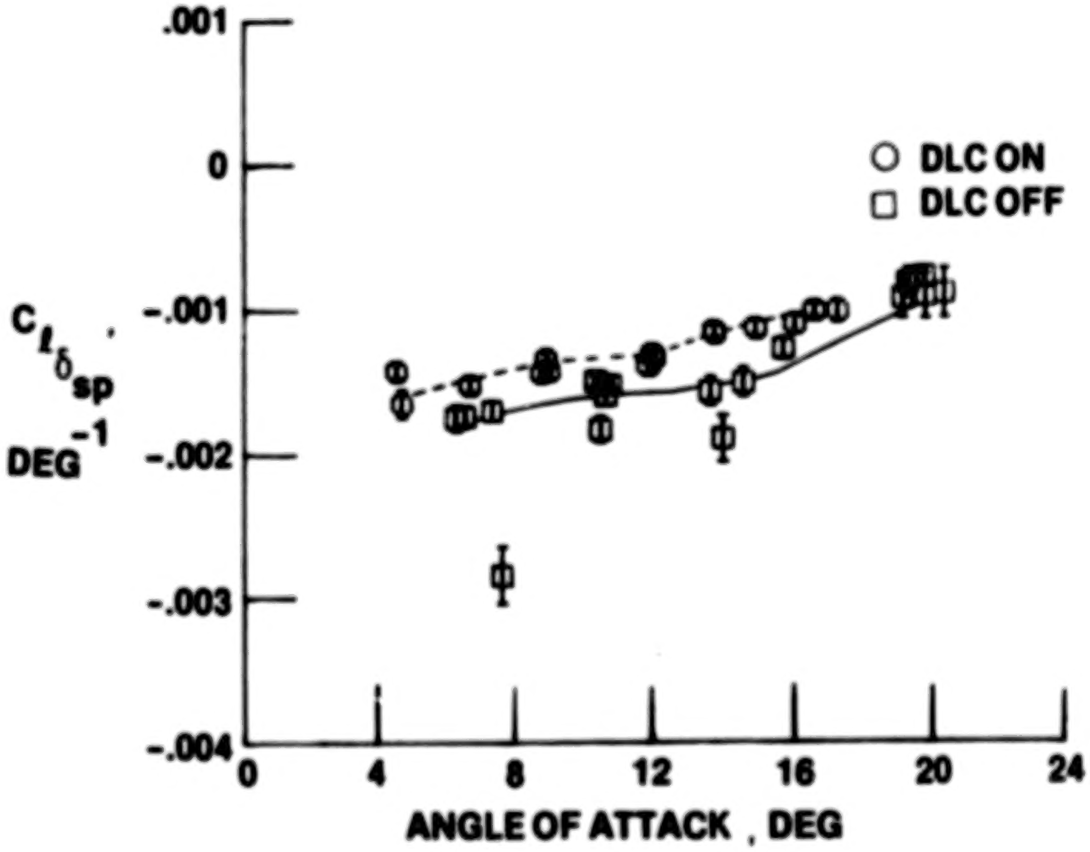

The highly maneuverable aircraft technology (HiMAT) vehicle is a remotely piloted research vehicle with advanced close-coupled canards, wing-type winglets, and provisions for variable leading-edge camber. The flight-test philosophy was to fly the vehicle in a stable condition, with the control feedbacks set to zero, to obtain stability and control derivatives. While these data were being gathered, a control system suitable for unstable flight was being designed, based on wind tunnel tests. Then, with the flight-determined derivatives, the simulator could be updated and the control system adjusted for this update so that the vehicle could be flown safely at a negative static margin. Stability and control maneuvers were performed at Mach numbers from 0.40 to 0.92, at angles of attack up to 10°, and at altitudes from 15,000 ft to 45,000 ft. A complete set of stability and control characteristics was obtained for both the longitudinal and lateral-directional degrees of freedom.

HiMAT RPRV BASELINE CONFIGURATION

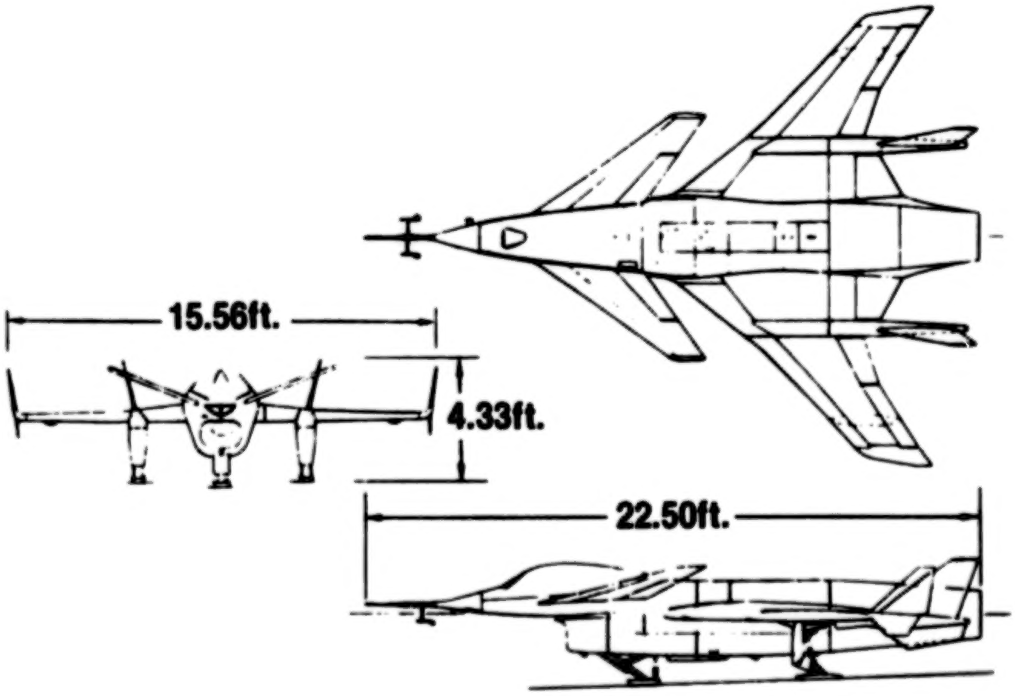

The HiMAT vehicle is constructed of advanced composite materials to allow for aeroelastic tailoring and to minimize weight. It is to be flown with a relaxed static margin because the wing deformation then results in a desirable camber shape at high load factor and the time drag is reduced. The vehicle was designed to fly with a sustained 8-g turn capability at a Mach number of 0.9 and an altitude of 25,000 ft, and to demonstrate supersonic flight to a Mach number of 1.4. To attain the Mach 0.9 condition, it is predicted that the vehicle must be flown at a 10-percent mean aerodynamic chord (MAC) negative static margin (unstable). The philosophy for testing HiMAT is somewhat different from that for testing production aircraft. Flight-determined stability and control derivatives are to be relied on to keep the wind tunnel program to a minimum. The original simulation data base contained the wind tunnel data, supplemented with some computed characteristics.

HiMAT TECHNOLOGY DEMONSTRATION

- VEHICLE CONCEPT
  - REMOTELY PILOTED
  - CLOSE-COUPLED CANARD
  - ADVANCED COMPOSITES
  - AEROELASTICALLY TAILORED
  - NEGATIVE STATIC MARGIN

- DESIGN POINT DEMONSTRATION
  - SUSTAINED 8-G CAPABILITY
  - SUPERSONIC FLIGHT TO MACH OF 1.4

The results of the flight test program showed that damping in yaw (C_{n_r}) was twice the predicted value, yawing moment with respect to roll rate (C_{n_p}) was the opposite sign, and rolling moment with respect to yaw rate (C_{ℓ_r}) was a small fraction of the predicted value. Rudder effectiveness ($C_{n_{\delta r}}$) was 25 percent of the prediction, rolling moment due to rudder deflection ($C_{\ell_{\delta r}}$) was twice the prediction, and both yawing moment with respect to aileron deflection ($C_{n_{\delta a}}$) and yawing moment with respect to elevon deflection ($C_{n_{\delta_{DE}}}$) were more positive than the prediction. Using the value found from flight data, the control system was changed markedly from the original control system, which was based on data from the limited wind tunnel program.

FLIGHT TO PREDICTION COMPARISON (LATERAL-DIRECTIONAL)

(MINIMAL WIND TUNNEL PROGRAM)

DAMPING

C_{n_r}	TWICE PREDICTION
C_{n_p}	OPPOSITE SIGN OF PREDICTION
C_{l_r}	SMALL FRACTION OF PREDICTION

CONTROL

$C_{n_{\delta_r}}$	25% LESS THAN PREDICTION
$C_{l_{\delta_r}}$	TWICE PREDICTION
$C_{n_{\delta_a}}$	AND $C_{n_{\delta_{DE}}}$ MORE POSITIVE THAN PREDICTION

ORIGINAL PAGE IS
OF POOR QUALITY

The Space Shuttle is a large double-delta-winged vehicle designed to enter the atmosphere and land horizontally. The entry control system consists of 12 vertical reaction control system (RCS) jets (six up-firing and six down-firing) and eight horizontal RCS jets (four left-firing and four right-firing), four elevon surfaces, a body flap, and a split rudder surface. The locations of these devices are shown in this figure. The vertical jets and the elevons are used for both pitch and roll control. The jets and elevons are used symmetrically for pitch control and asymmetrically for roll control.

Shuttle Configuration

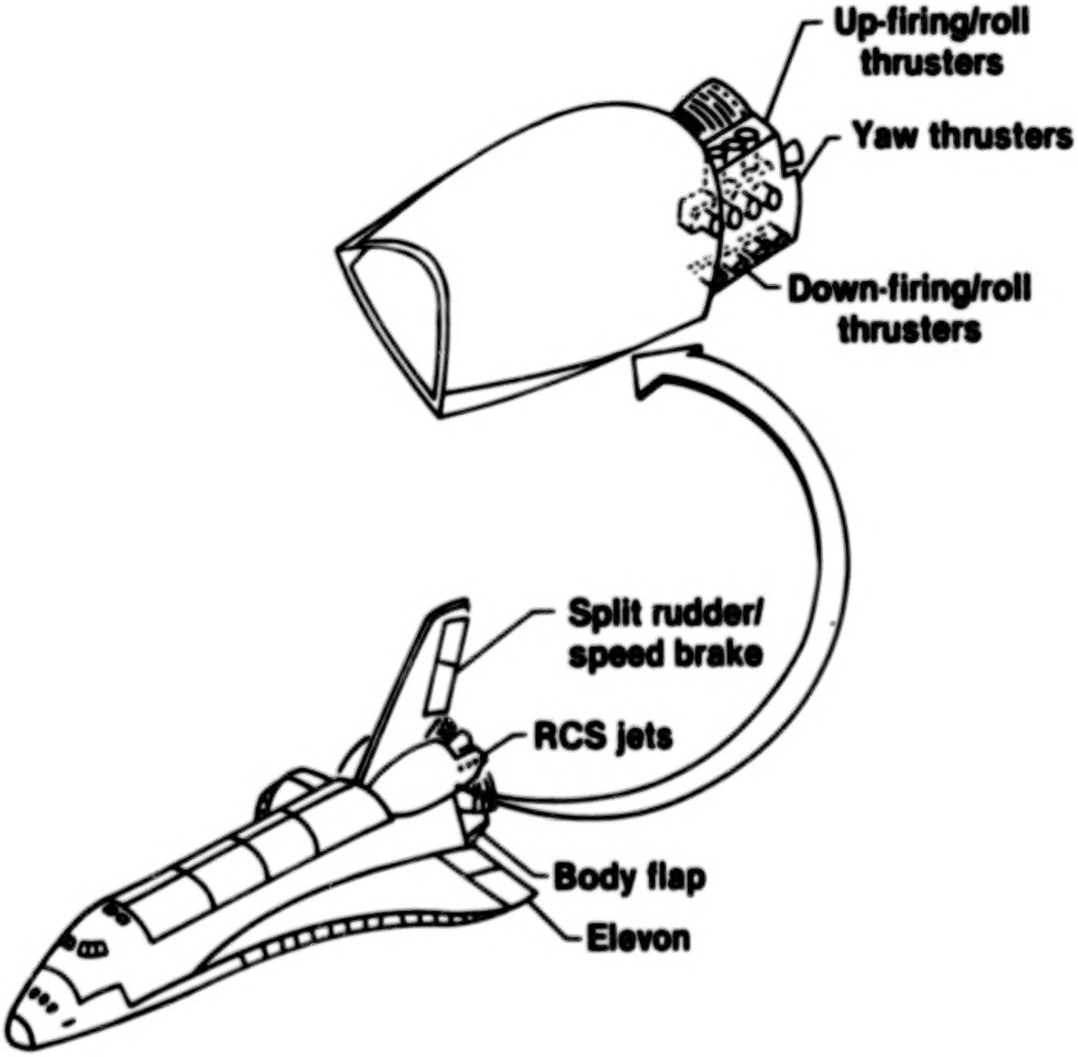
Up-firing/roll thrusters
Yaw thrusters
Down-firing/roll thrusters
Split rudder/ speed brake
RCS jets
Body flap
Elevon

The flight-determined stability and control derivatives are used to update and improve simulations, refine the control system, modify flight envelope restrictions (placards), and improve flight procedures.

Uses of Estimates From Shuttle

Improve simulation

Control system refinement

Modify placard

Improve flight procedures

One of the interesting examples of where parameter estimation played an important role in the Shuttle program occurred during the first energy management bank maneuver on the first entry of the Shuttle (STS-1). The computed response to the automated control inputs with the predicted stability and control derivatives is shown in this figure. The control inputs shown here are the closed-loop commands from the Shuttle control laws. The maneuver was to be made at a velocity of 24,300 ft/sec and at a dynamic pressure of about 12 lb/ft^2.

PREDICTED BANK
MANEUVER FOR STS-1

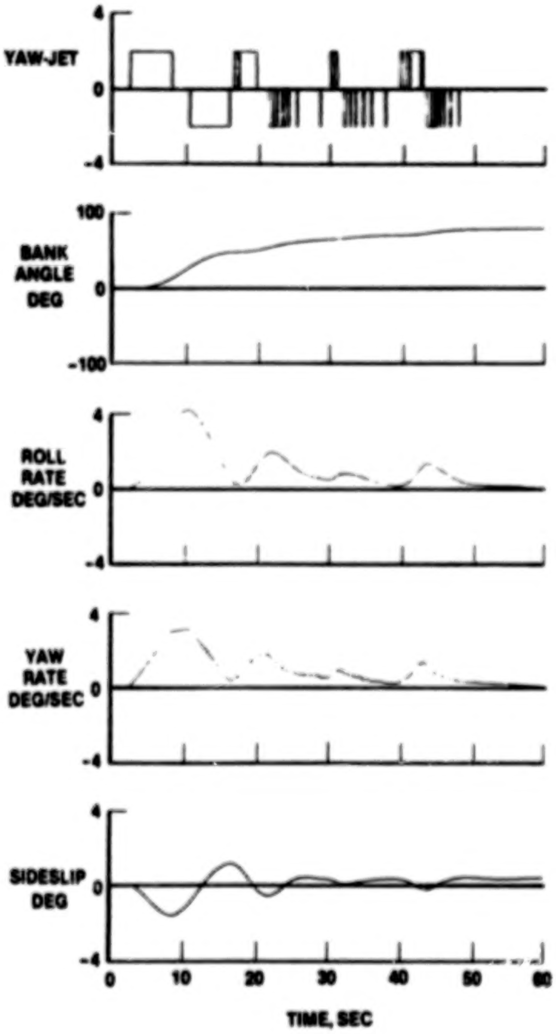

The actual maneuver from STS-1 that occurred at this flight condition is shown in this figure. The flight data show a more hazardous maneuver than was predicted. At this flight condition, the excursions must be kept small. The flight maneuver resulted in twice the sideslip peaks predicted and in a somewhat higher roll rate than predicted. In addition, there was more yaw-jet firing than was predicted, and the motion was more poorly damped than predicted. It is obvious from comparing the predictions with the results of the actual maneuver that the stability and control derivatives are significantly different. Although the flight maneuver resulted in excursions greater than planned, the control system did manage to damp out the oscillation in less than 1 min. With a less conservative design approach, the resulting entry could have been much worse.

Actual Bank Maneuver for STS-1

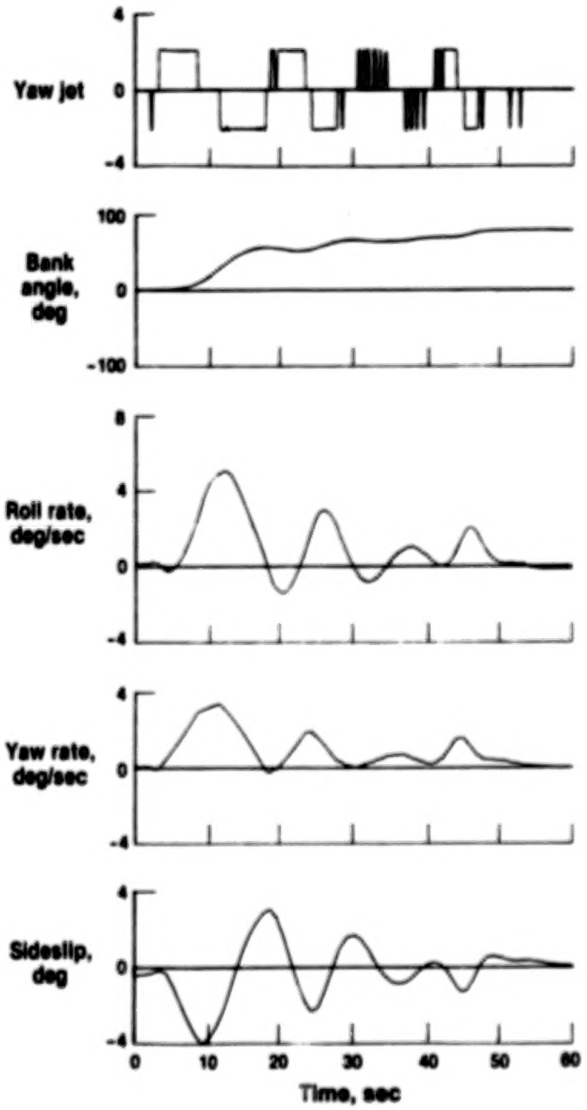

ORIGINAL PAGE IS
OF POOR QUALITY

The obvious way to assess the problem with the first bank maneuver is to compare the flight-determined stability and control derivatives with the predictions. Of all the derivatives obtained from STS-1, the most important one that differed most from predictions at the flight condition being discussed was L_{YJ}, which is the rolling moment due to the firing of a single yaw jet. Since the entry tends to monotonically decrease in Mach number, the derivative can best be portrayed as a function of the guidance system "Mach number," which is V/1000. This figure shows L_{YJ} as a function of guidance "Mach number." Only the estimates from STS-1 are shown in these figures. The prediction is shown by the solid line. The symbols designate the estimates, and the vertical bars, the uncertainties. The dashed line is the fairing of the flight data.

Roll Due to Yaw Jet Estimates

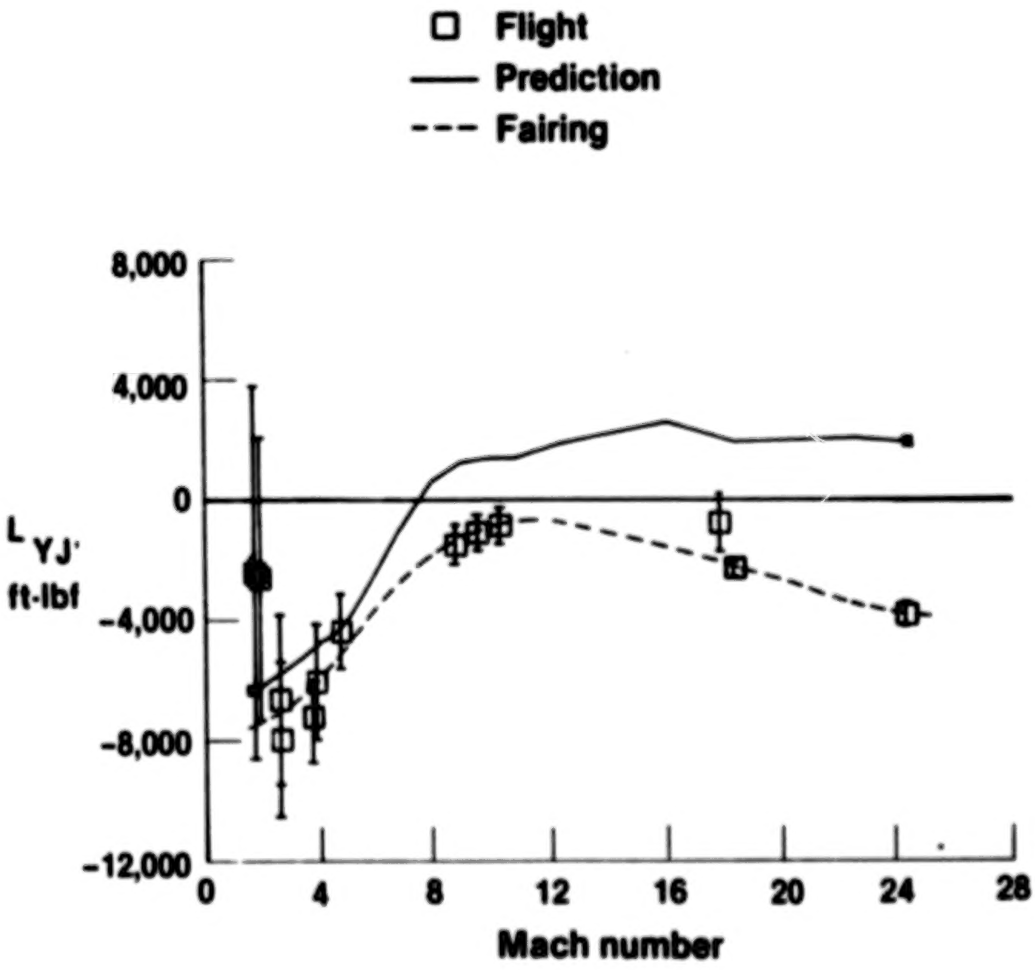

ORIGINAL PAGE IS
OF POOR QUALITY

The control system software is very complex; it cannot be changed and verified between STS missions, so an interim approach was taken to eliminate large excursions on future flights. The flight-determined derivatives were put into the simulation data base, and the Shuttle pilots practiced performing the maneuver manually to attain a smaller response within more desirable limits. The maneuver was performed manually on STS-2 and STS-3. This figure shows the manually flown maneuver from STS-2. The maneuver appears to be much better behaved, for roll rate (p), yaw rate (r), and angle of sideslip (β) are within the desired limits. The maneuver does not look like the original predicted response, because the derivatives and the input are different, and the basic control system remains unchanged. Since the response variables are kept low and the inputs are slower and smaller, the flight responses on STS-2 through STS-4 do not show a tendency to oscillate. For STS-5 through STS-8, the control system automatically inputs the commands. The resulting maneuvers look nearly identical to the maneuver shown in this figure.

Bank Maneuver After Problem Solved

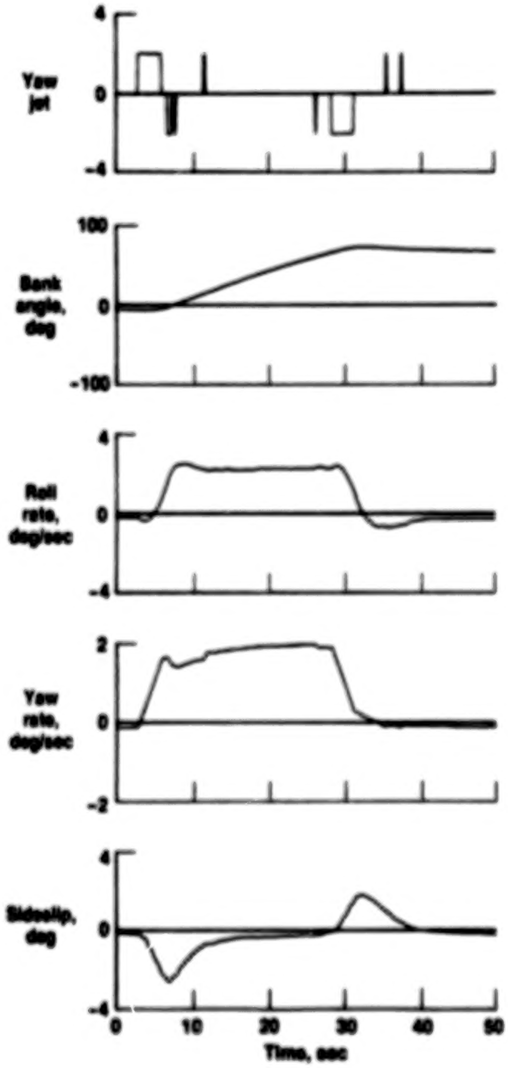

Maximum likelihood parameter estimation techniques were used in the F-14 program to effect control system changes that improved the handling qualities of the aircraft at high angles of attack. The same techniques provided the primary source of information for the refinement of the control system for the HiMAT vehicle at negative static margin. The energy management maneuvers have been redefined for the Space Shuttle, based on simulations using flight-determined stability and control estimates. Moreover, parameter estimation techniques are being relied on for future control system design, placard modification or removal, and flight procedures for the Space Shuttle.

CONCLUSIONS

PARAMETER ESTIMATION IMPORTANT IN FLIGHT TEST

PARAMETER ESTIMATES USED TO
- IMPROVE HANDLING QUALITIES
- REFINE CONTROL SYSTEMS
- UPDATE SIMULATIONS
- MODIFY PLACARDS

CAREFUL SCRUTINY OF ESTIMATE NECESSARY

N84
20576

UNCLAS

N84 20576

APPLICATIONS OF MODEL STRUCTURE DETERMINATION TO FLIGHT TEST DATA

James G. Batterson
NASA Langley Research Center
Hampton, Virginia

and

Vladislav Klein
George Washington University
Hampton, Virginia

First Annual NASA Aircraft Controls Workshop
NASA Langley Research Center
Hampton, Virginia
October 25-27, 1983

SYSTEM IDENTIFICATION DEFINED

The following definition of system identification was suggested by Zadeh[1] in 1968 and is widely accepted today. The three main objects that this definition connects are boxed. The harmonic content of the input to the system should be rich enough to excite the important modes of that system. A class of systems from which the model will be chosen is selected through engineering judgment or on the basis of a priori knowledge. Finally, the decision must be made about a decision criterion specifying which model from the class is equivalent to the physical system under test.

IDENTIFICATION IS THE DETERMINATION, ON THE BASIS OF INPUT

AND OUTPUT OF A SYSTEM WITHIN A SPECIFIED CLASS OF SYSTEMS,

TO WHICH THE SYSTEM UNDER TEST IS EQUIVALENT.

IDENTIFICATION APPLICATIONS

The benefits of airplane identification are shown here. The results of this procedure can be used in several areas indicated. They are especially important today, since modern airplanes rely upon digital control and, hence, a good mathematical model.

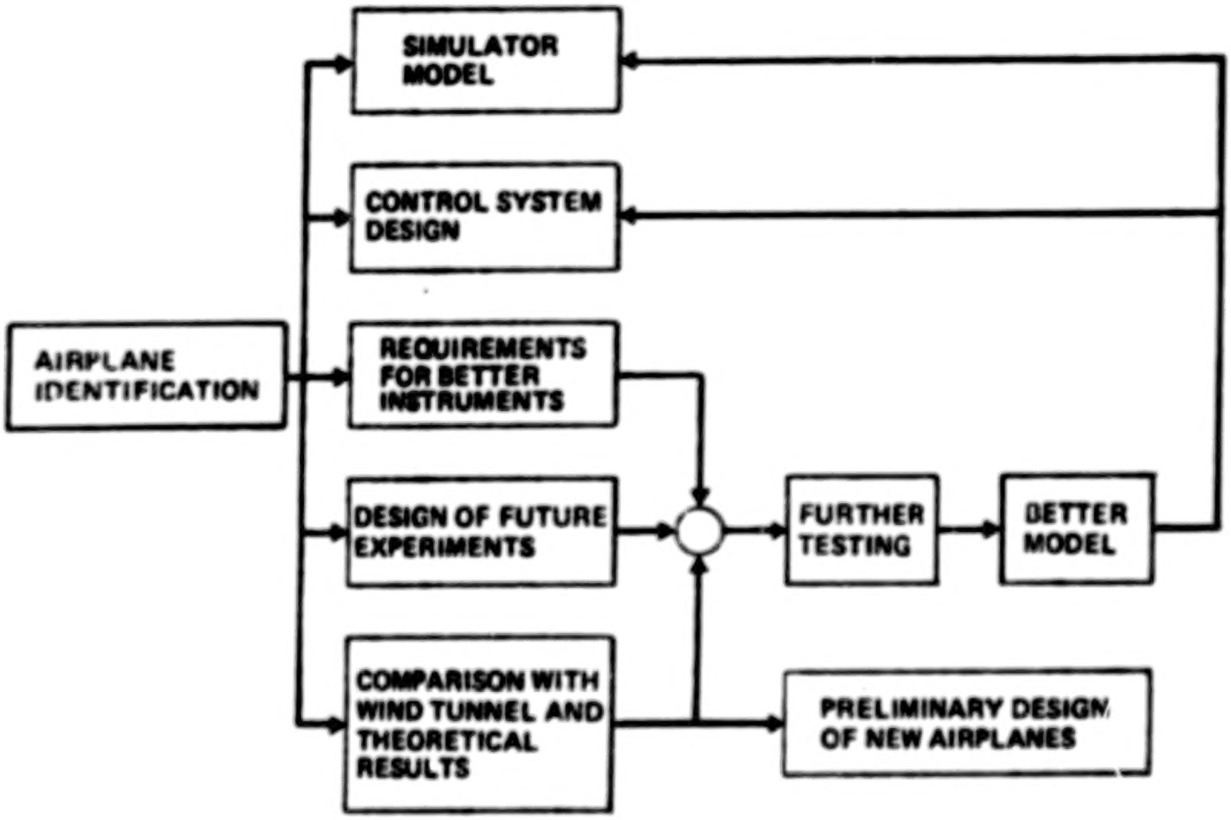
SIMULATOR MODEL
CONTROL SYSTEM DESIGN
AIRPLANE IDENTIFICATION
REQUIREMENTS FOR BETTER INSTRUMENTS
DESIGN OF FUTURE EXPERIMENTS
FURTHER TESTING
BETTER MODEL
COMPARISON WITH WIND TUNNEL AND THEORETICAL RESULTS
PRELIMINARY DESIGN OF NEW AIRPLANES

BLOCK SCHEME OF AIRPLANE IDENTIFICATION

Airplane identification requires several steps. This presentation will concentrate on model structure determination.

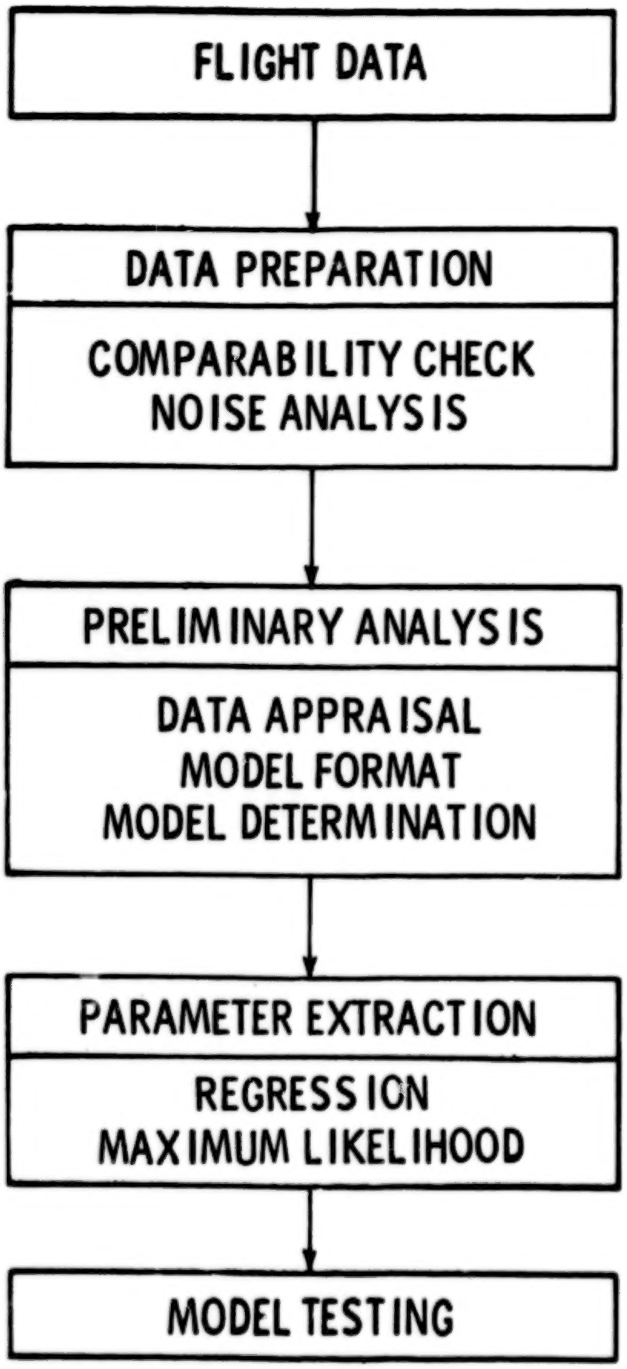
FLIGHT DATA
DATA PREPARATION
COMPARABILITY CHECK
NOISE ANALYSIS
PRELIMINARY ANALYSIS
DATA APPRAISAL
MODEL FORMAT
MODEL DETERMINATION
PARAMETER EXTRACTION
REGRESSION
MAXIMUM LIKELIHOOD
MODEL TESTING

STEPWISE REGRESSION

The stepwise regression is developed from the "classical" linear regression. It allows for the selection of important terms in the aerodynamic model equation. It can show the adequacy of a linear model or a necessity for adding some nonlinear terms.

ASSUME THE GENERAL FORM OF THE AERODYNAMIC MODEL EQUATIONS CAN BE WRITTEN AS

$$y(t) = \theta_0 + \theta_1 X_1(t) + \theta_2 X_2(t) + - - - + \theta_{Q-1} X_{Q-1}^{(t)}$$

THEN FOR EACH OF N OBSERVATIONS

$$y(i) = \theta_0 + \theta_1 X_1(i) + \theta_2 X_2(i) + - - - + \theta_{Q-1} X_{Q-1}^{(i)} + n(i)$$

WHERE $n(i)$ IS THE EQUATION ERROR AT THE i^{th} OBSERVATION

AS APPLIED TO THE VERTICAL FORCE EQUATION:

$$\frac{2mg}{\rho V^2 S} a_Z = C_Z = C_{Z_0} + C_{Z_\alpha} (\alpha - \alpha_0)$$

$$+ C_{Z_q} \frac{q\bar{c}}{2V} + C_{Z_{\delta_e}} (\delta e - \delta e_0)$$

$$+ \text{HIGHER ORDER TERMS}$$

For the data from large amplitude maneuvers it can be beneficial to approximate the aerodynamic functions by splines rather than Taylor's series expansion. The polynomial splines are written as functions of the "+" function, $(\alpha - \alpha_i)_+^m$ for knots of α_i. This function has value $(\alpha - \alpha_i)^m$ for $\alpha \geq \alpha_i$ and has value 0 for $\alpha < \alpha_i$. In case of a function in two variables, a two-dimensional spline should be used or the data can be partitioned in one of the two variables. Data partitioning leads to a simplified model.

- ANOTHER REPRESENTATION OF NONLINEAR MODEL IS A SPLINE REPRESENTATION:

$$C_Z = C_{Z_0} + C_{Z_\alpha}\alpha + \sum_{i=1}^{k} C_{Z_{\alpha_i}} (\alpha - \alpha_i)_+$$

$$+ C_{Z_q}\frac{q\bar{c}}{2V} + \sum_{i=1}^{k} C_{Z_{q_i}} (\alpha - \alpha_i)_+^0 \frac{q\bar{c}}{2V}$$

$$+ C_{Z_{\delta_e}}\delta e + \sum_{i=1}^{k} C_{Z_{\delta_{e_i}}} (\alpha - \alpha_i)_+^0 \delta e$$

- COMBINE DATA FROM SEVERAL MANEUVERS AND APPLY STEPWISE REGRESSION WITH POLYNOMINAL SPLINES TO COMBINED DATA SET
- COMBINE DATA FROM SEVERAL MANEUVERS AND PARTITION AS A FUNCTION OF ANGLE OF ATTACK, SIDESLIP, etc.

MODEL STRUCTURE COMPARISON AT DIFFERENT ENTRIES

The model building using stepwise regression and spline approximation is demonstrated in fitting of the vertical force coefficient. The first three entries into the regression show the effect of each term selected and the improvement in the fit to the data.

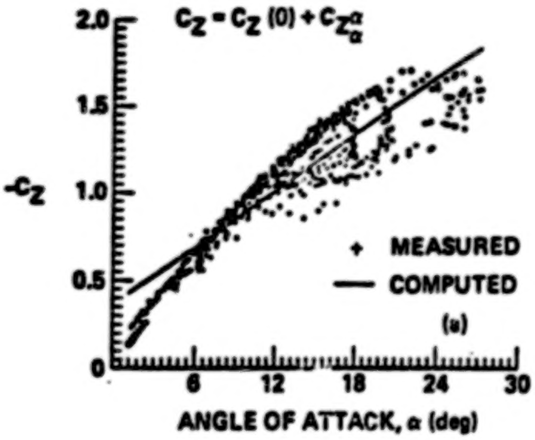

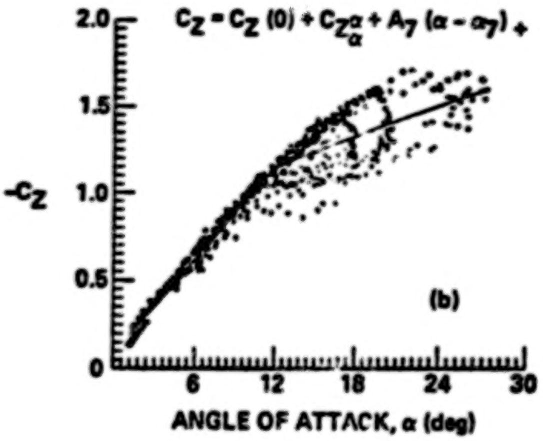

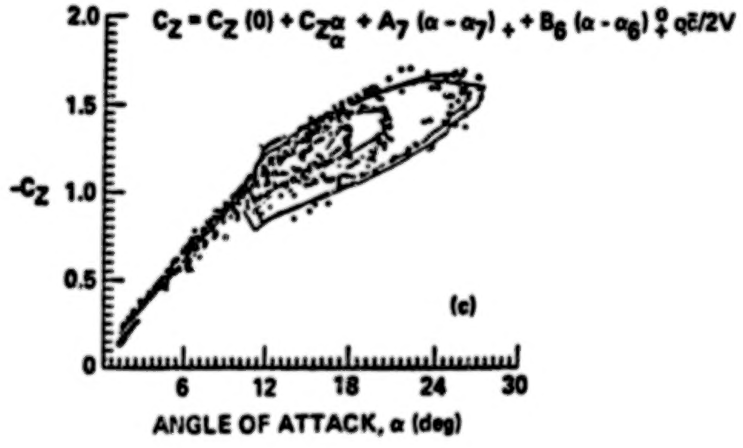

MODEL SELECTION CRITERIA

The stepwise procedure continues in selecting terms as long as they are statistically significant. But for the selection of an adequate model several criteria should be considered.

THE ACTUAL TERMS SELECTED FOR THE FINAL MODEL DEPEND ON SEVERAL CRITERIA:

- THE PARTIAL F VALUE F_p OF EACH TERM SHOULD BE GREATER THAN 5
- THE F STATISTIC SHOULD BE MAXIMUM FOR THE FINAL MODEL
- R^2, THE SQUARED MULTIPLE CORRELATION COEFFICIENT, SHOULD BE CLOSE TO 100 PER CENT FOR THE FINAL MODEL
- THE RESIDUAL SEQUENCE SHOULD BE RANDOM AND UNCORRELATED

LONGITUDINAL PARAMETERS FROM DIFFERENT MANEUVERS
GENERAL AVIATION AIRPLANE

The comparison of results from small and large amplitude maneuvers is presented for the vertical force coefficient. The spline of first, second, and zero degree was used for the three functions shown.

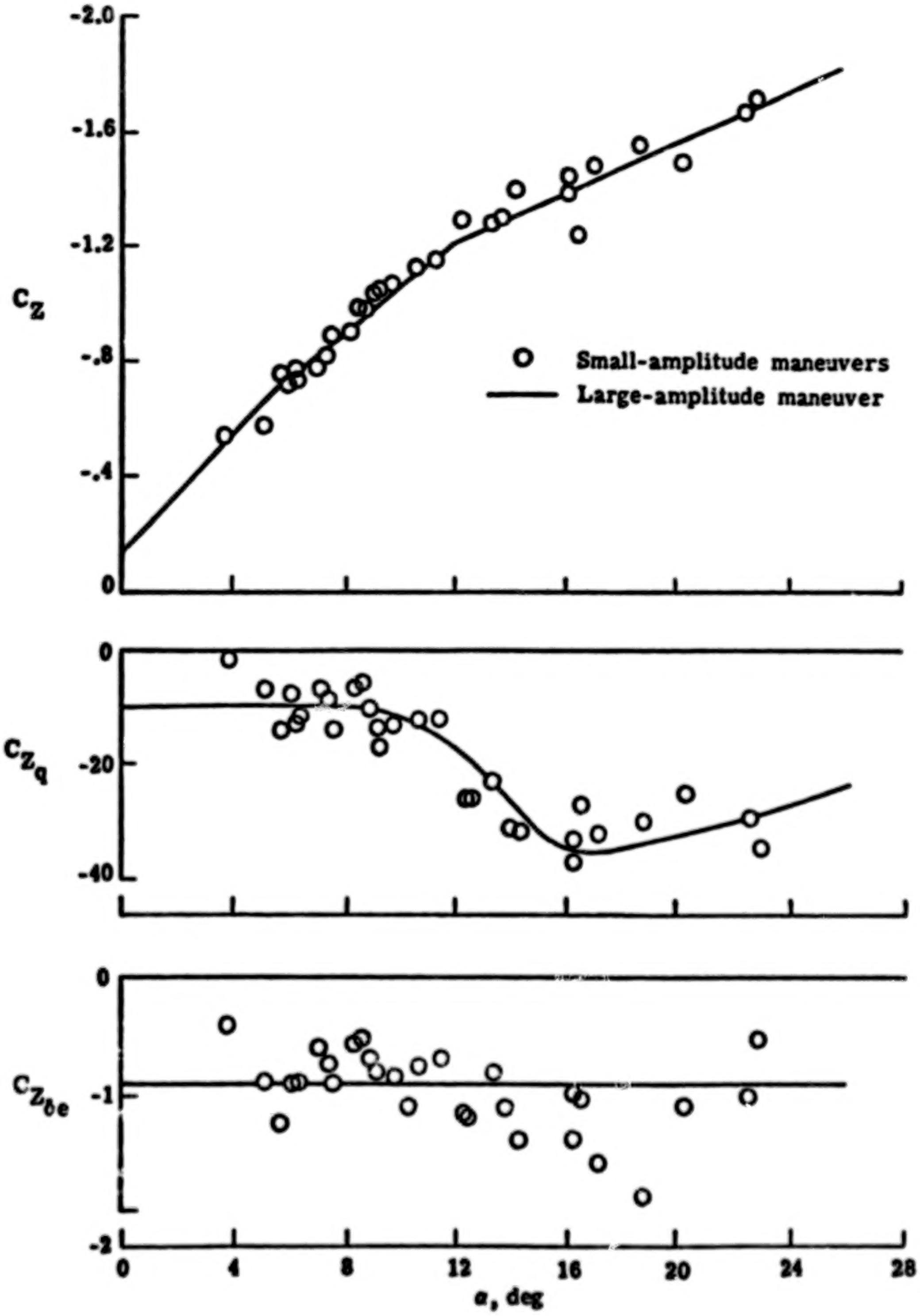

ORIGINAL PAGE IS
OF POOR QUALITY

MODEL VALIDATION
GENERAL AVIATION AIRPLANE

The model determined by stepwise regression from the data of a single large amplitude maneuver is validated by numerically integrating the equations of motion and comparing with the measured data of an independent set.

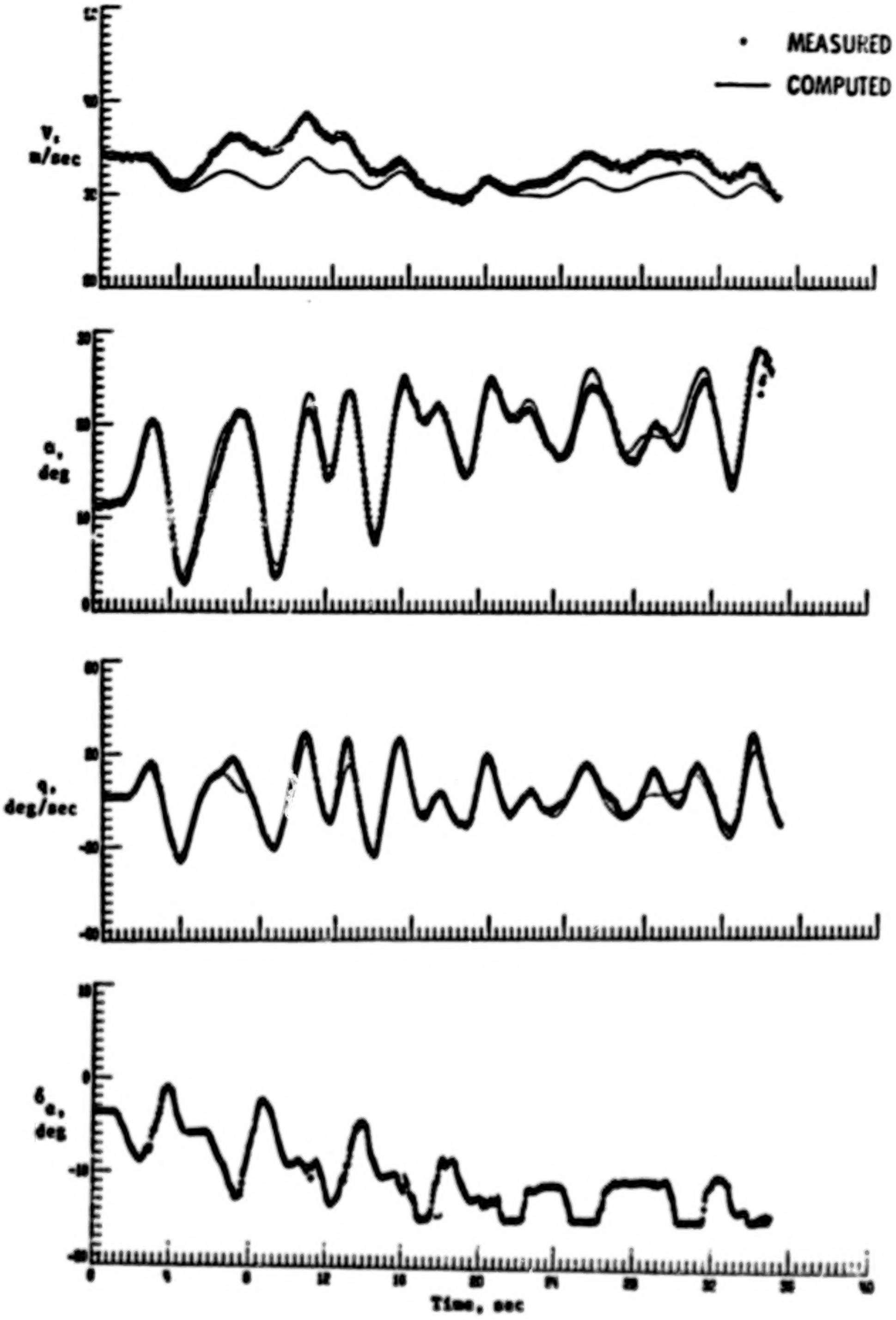

DIRECTIONAL STABILITY PARAMETER FROM LOW-AMPLITUDE MANEUVERS AND WIND TUNNEL MEASUREMENTS - ADVANCED FIGHTER

Nonlinearities in aerodynamics parameters of high-performance airplanes can be detected from the measured data by the application of stepwise regression. These results can be compared with wind tunnel measurements. The example shows the directional stability parameter plotted against the angle of attack as obtained from small amplitude maneuvers and wind tunnel measurements.

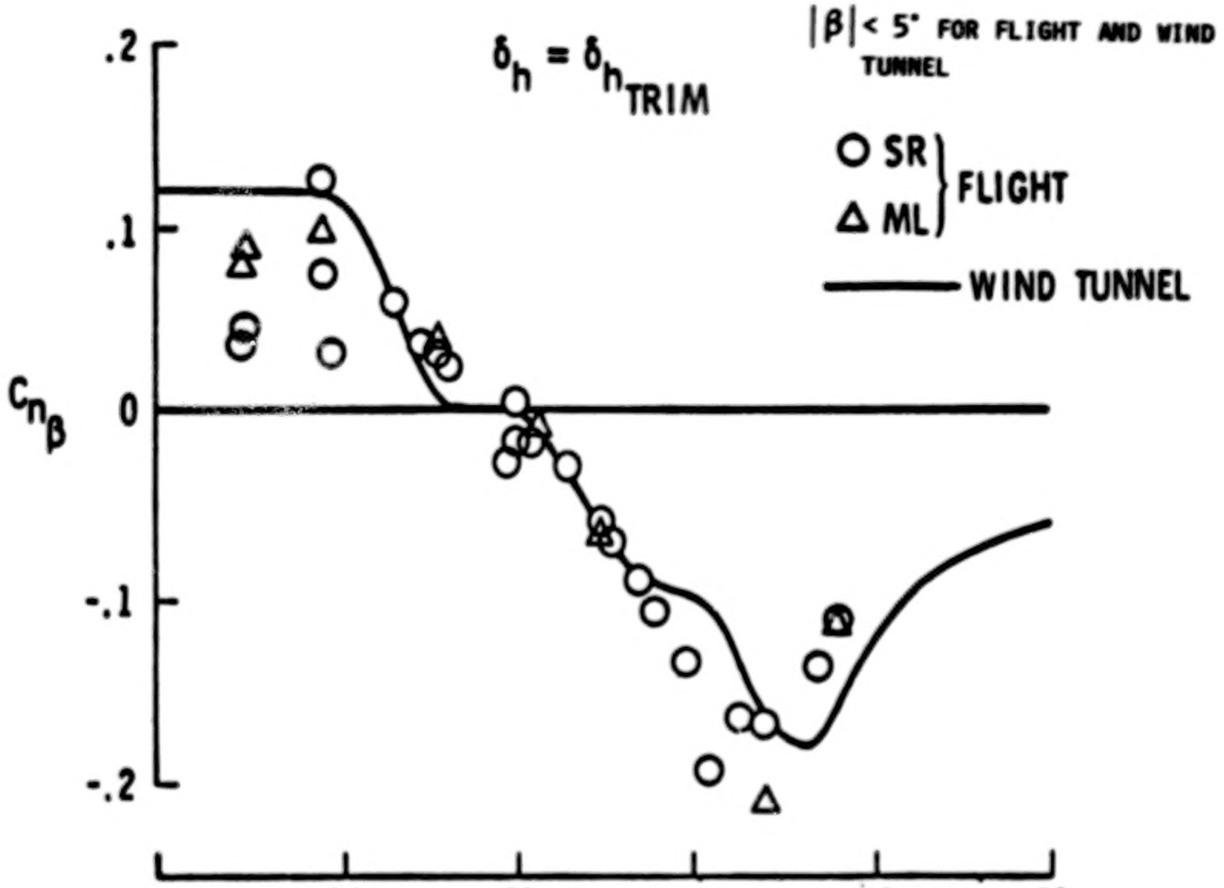

ORIGINAL PAGE IS
OF POOR QUALITY

DIRECTIONAL STABILITY PARAMETER FROM LOW-AMPLITUDE MANEUVERS AND WIND TUNNEL MEASUREMENTS - ADVANCED FIGHTER (CONTINUED)

The directional stability parameter determined from five large amplitude maneuvers is compared with wind tunnel measurements.

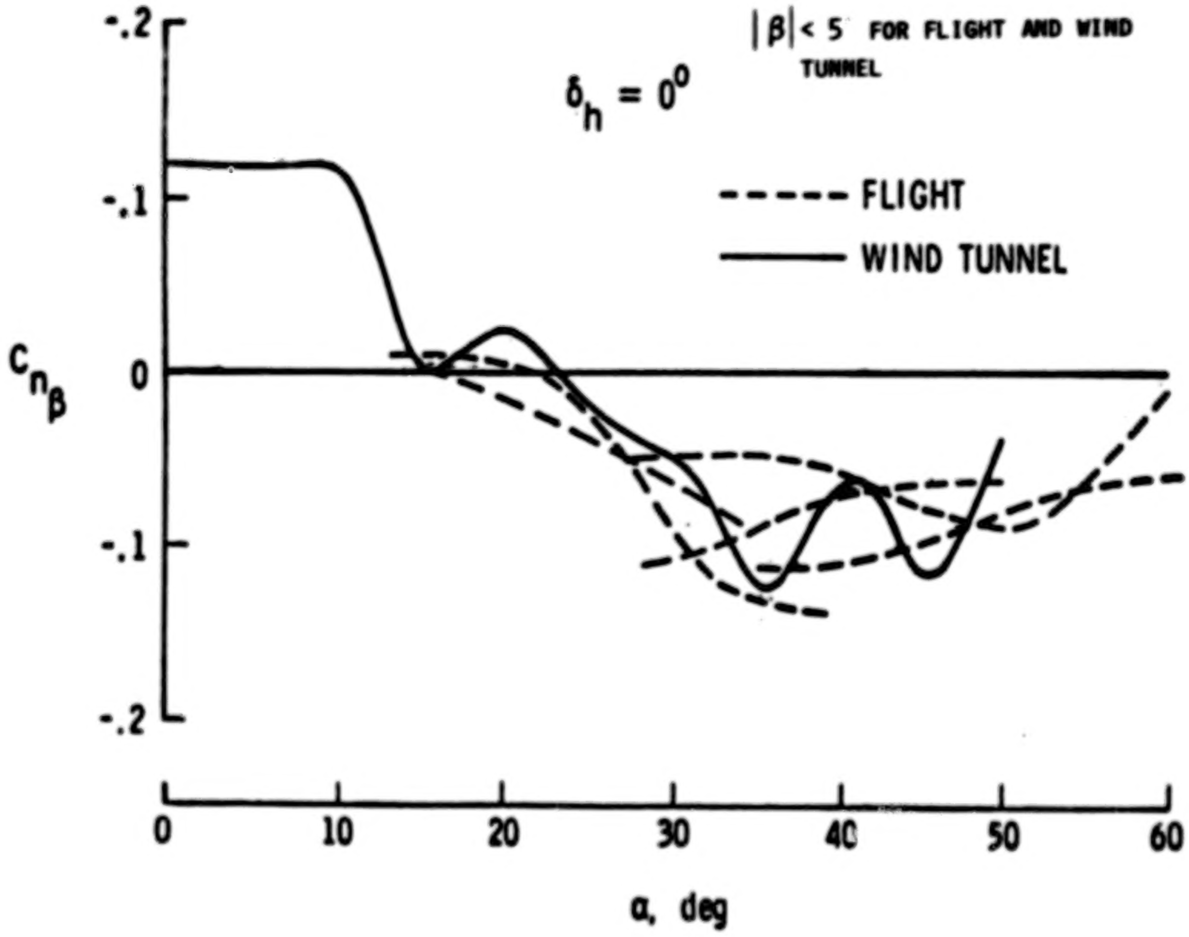

ORIGINAL PAGE IS
OF POOR QUALITY

DIRECTIONAL STABILITY PARAMETER FROM LOW-AMPLITUDE MANEUVERS AND WIND TUNNEL MEASUREMENTS - ADVANCED FIGHTER (CONCLUDED)

The directional stability parameter determined from partitioned data is compared with wind tunnel measurements.

ORIGINAL PAGE IS
OF POOR QUALITY

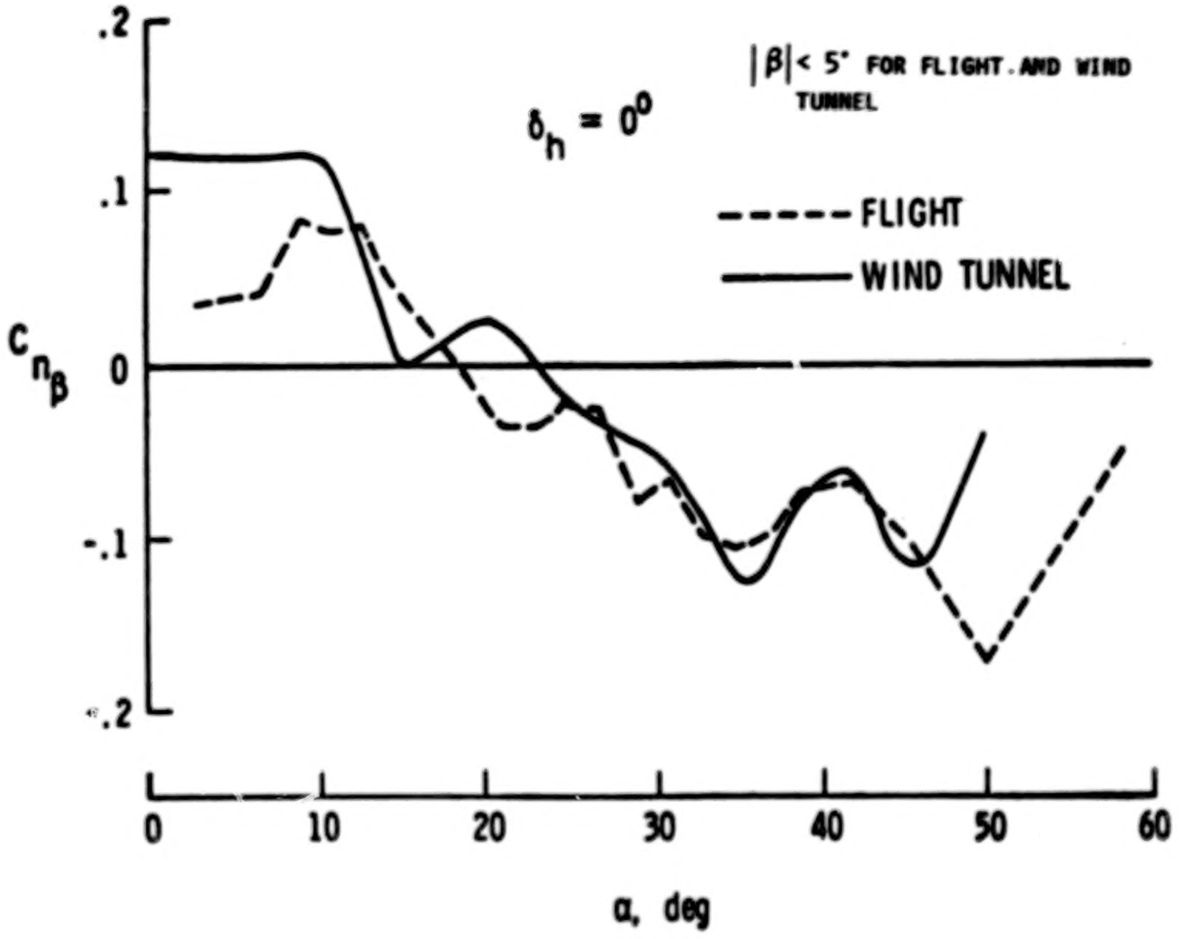

ESTIMATED LIFT CURVE FROM WIND UP TURNS — JET TRANSPORT

For the jet transport, nonlinearities in the lift curve can occur at relatively low angles of attack. Therefore, even for small perturbed maneuvers it can be necessary to use nonlinear aerodynamic model equations. The example shows the results from the wind up turns which were flown for airplane certification.

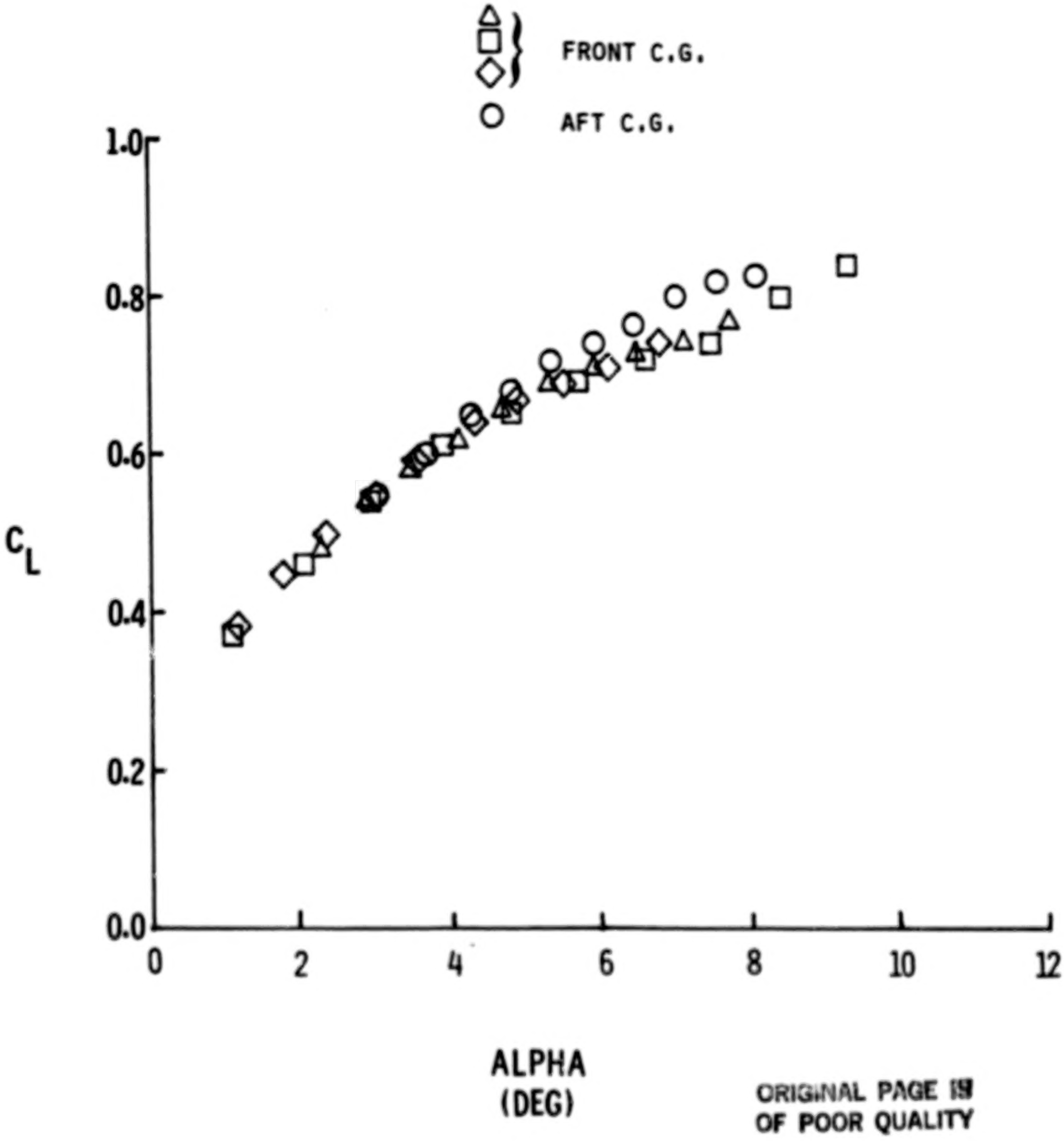

ORIGINAL PAGE IS OF POOR QUALITY

SUMMARY

The technique presented in this paper has been published in references 2 and 3.

- o INCORRECT STABILITY AND CONTROL DERIVATIVES CAN RESULT FROM AN INADEQUATE AERODYNAMIC MODEL STRUCTURE.
- o STEPWISE REGRESSION CAN BE USED TO DETERMINE THE STRUCTURE FOR AN ADEQUATE MODEL.
- o SEVERAL STATISTICAL AND INFORMATION CRITERIA NEED TO BE CONSIDERED WHEN SELECTING AN ADEQUATE MODEL.
- o FLIGHT DATA WHICH COVERS A NONLINEAR AERODYNAMIC MODEL RANGE MAY BE ANALYZED AS A SINGLE DATA SET OR PARTITIONED INTO SEVERAL DISTINCT SETS.
- o STEPWISE REGRESSION FOR MODEL STRUCTURE DETERMINATION AND PARAMETER ESTIMATION HAS BEEN SUCCESSFULLY APPLIED TO THREE AIRCRAFT TYPES (SINGLE ENGINE GENERAL AVIATION, UNAUGMENTED MODERN JET FIGHTER, JET TRANSPORT).

REFERENCES

1. Zadeh, L. A.: From Circuit Theory to System Theory. Proceedings of I.R.E., vol. 50, no. 5, May 1962, pp. 856-865.

2. Klein, Vladislav, Batterson, James G., and Murphy, Patrick C.: Determination of Airplane Model Structure From Flight Data by Using Modified Stepwise Regression. NASA TP-1916, October 1981.

3. Klein, Vladislav and Batterson, James G.: Determination of Airplane Model Structure From Flight Data Using Splines and Stepwise Regression. NASA TP-2126, March 1983.

N84
20577

UNCLAS

N84 20577

MIXING 4D-EQUIPPED AND UNEQUIPPED AIRCRAFT IN THE TERMINAL AREA

L. Tobias, H. Erzberger, and H. Q. Lee
NASA Ames Research Center
Moffett Field, CA 94035

and

P. J. O'Brien
FAA Technical Center
Atlantic City, NJ

First Annual NASA Aircraft Controls Workshop
NASA Langley Research Center
Hampton, Virginia
October 25-27, 1983

*

c-3

INTRODUCTION

On-board 4D guidance systems, which can predict and control the touchdown time of an aircraft to an accuracy of a few seconds throughout the descent, have been developed and demonstrated in several flight test programs. However, in addition to refinements of the on board system, two important issues still need to be considered. First, in order to make effective use of these on-board systems, it is necessary to understand and develop the interactions of the airborne and air traffic control (ATC) system in the proposed advanced environment. Unless the total system is understood, the advanced on-board system may prove unusable from an ATC standpoint. Second, in planning for a future system in which all aircraft are 4D equipped, it is necessary to confront the transition situation in which some percentage of traffic must still be handled by conventional means. In terms of 4D, this means that some traffic must still be given radar vectors and speed clearances (that is, be spaced by conventional distance separation techniques), while the 4D-equipped aircraft need to be issued time assignments. How to reconcile these apparent differences and develop an efficient ATC operation is the subject of this paper.

MIXING 4D EQUIPPED AND UNEQUIPPED AIRCRAFT IN THE TERMINAL AREA

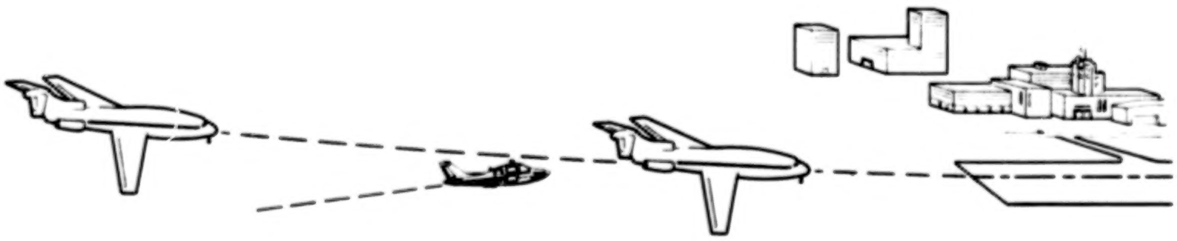

OBJECTIVES

The objectives of this study are to develop efficient algorithms and operational procedures for time scheduling a mix of 4D-equipped and unequipped aircraft in the terminal area, and, using the NASA Ames real-time air traffic control (ATC) simulation facility, to evaluate the system operation under various mix conditions.

- **DEVELOP CANDIDATE OPERATIONAL PROCEDURES AND TIME-SCHEDULING ALGORITHMS FOR CONTROLLING A MIX OF 4D-EQUIPPED AND UNEQUIPPED AIRCRAFT IN THE TERMINAL AREA**
- **EVALUATE THE SYSTEM OPERATION UNDER VARIOUS MIX CONDITIONS**

OPERATIONAL PROCEDURES

The basic operational procedure is as follows: the ATC computer generates time assignments for all aircraft as they enter the greater terminal area. For the 4D-equipped aircraft, the controller assigns the aircraft a route and a touchdown time. The 4D-equipped aircraft generates and flies the 4D route. The controller was instructed not to alter this assigned time unless necessary for safety reasons. The unequipped aircraft must still be controlled by radar vectors. However, the controllers can use the position of the 4D aircraft to achieve the time assignments for the unequipped aircraft.

ATC COMPUTER GENERATES TIME ASSIGNMENTS

- 4D EQUIPPED:
  - CONTROLLER ASSIGNS TOUCHDOWN TIME
  - AIRCRAFT GENERATES AND FLIES 4D ROUTE
  - ASSIGNED TIME NOT ALTERED
- UNEQUIPPED:
  - CONTROLLER ISSUES RADAR VECTORS
  - CONTROLLER USES 4D AIRCRAFT POSITIONS TO ACHIEVE TIMES FOR UNEQUIPPED

ON-BOARD SYSTEM

A complete on-board 4D guidance system is a complex entity involving interaction between numerous guidance, control, and navigation subsystems in an aircraft. The integrated collection of these subsystems augmented with special algorithms to provide fuel-efficient time control essentially constitutes the 4D flight management system of an equipped aircraft. The basic steps in the trajectory synthesis are shown below. For a number of years, NASA has designed and flight tested research systems incorporating various types of time control methods for both STOL and conventional aircraft. These tests have demonstrated the ability to predict and control arrival time accurately under varied operational conditions, achieving arrival time accuracies of ±10 sec.

- **AIRCRAFT SYNTHESIZES TRAJECTORY**
  1. **HORIZONTAL PROFILE: TURNS AND STRAIGHT LINES**
  2. **VERTICAL PROFILE: LEVEL FLIGHT AND CONSTANT DESCENT ANGLE SEGMENTS**
  3. **AIRSPEED PROFILE: CONSTANT CAS AND DECELERATION SEGMENTS**
- **ARRIVAL TIME ACCURACIES OF ±10 sec ACHIEVABLE**
- **CONTROLLER CAN VECTOR AIRCRAFT; THEN ASSIGN NEW TIME VIA CAPTURE**

CAPTURE TRAJECTORIES

A 4D-equipped aircraft which has been vectored off its 4D route can be assigned a revised time and a waypoint to capture the 4D route. This figure shows two aircraft positions P_1 and P_2. A capture trajectory is shown by a dotted line from position P_1 to the capture waypoint 3. If the touchdown time associated with this trajectory is too early, the aircraft continues to fly according to its last vector clearance until it reaches position P_2, where the pilot captures the 4D route via the trajectory shown.

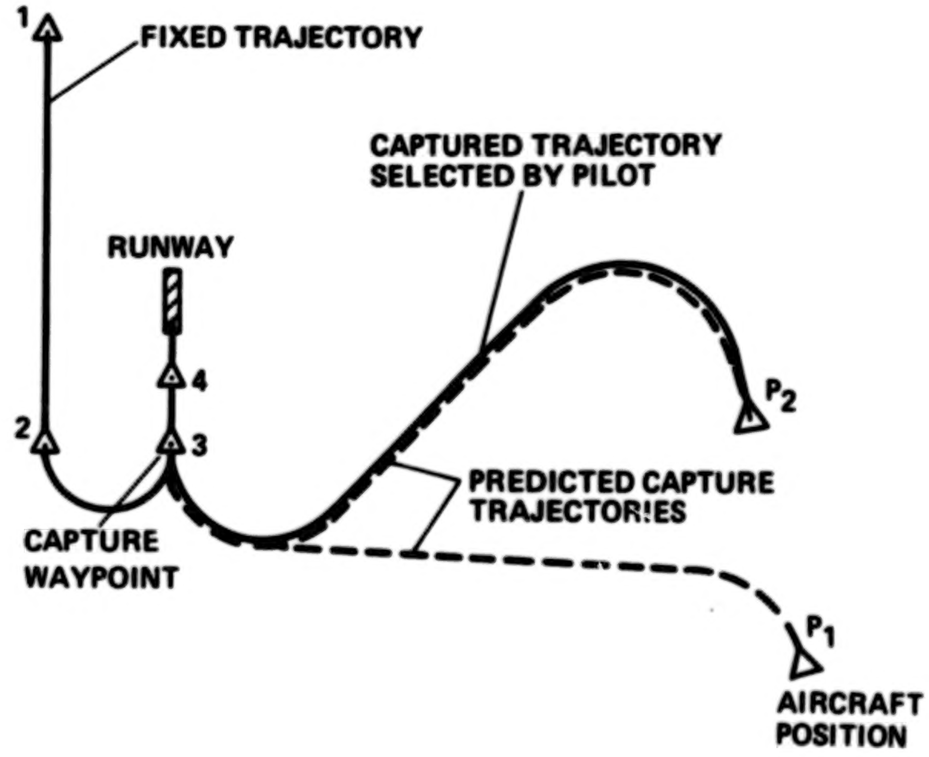
1
FIXED TRAJECTORY
CAPTURED TRAJECTORY SELECTED BY PILOT
RUNWAY
4
2
3
P2
PREDICTED CAPTURE TRAJECTORIES
CAPTURE WAYPOINT
P1
AIRCRAFT POSITION

TIME-SCHEDULING ALGORITHMS

The 4D-equipped aircraft have the capability of meeting a touchdown-time assignment to an accuracy of a few seconds. It is now desired to use this capability to formulate efficient operational procedures for the time scheduling of all aircraft in the terminal area. This will be developed in three parts: (1) determine the minimum time separation conditions given the minimum distance separations; (2) determine the interarrival time separations for two consecutive aircraft to be used in aircraft scheduling; and (3) develop a scheduling algorithm for assigning landing times.

- **TRANSLATION OF DISTANCE SEPARATIONS TO TIME**
- **TIME SEPARATIONS AT TOUCHDOWN**
- **INTERACTIVE SCHEDULING ALGORITHMS**

TRANSLATION OF DISTANCE SEPARATIONS TO TIME

The minimum separation distance rules depend on aircraft weight category and are summarized in this figure. These distances can be converted to minimum separation times using speed profile data. The result is the matrix T, where each element is the minimum separation time at touchdown so that at no time when aircraft are along a common path is the separation distance rule violated.

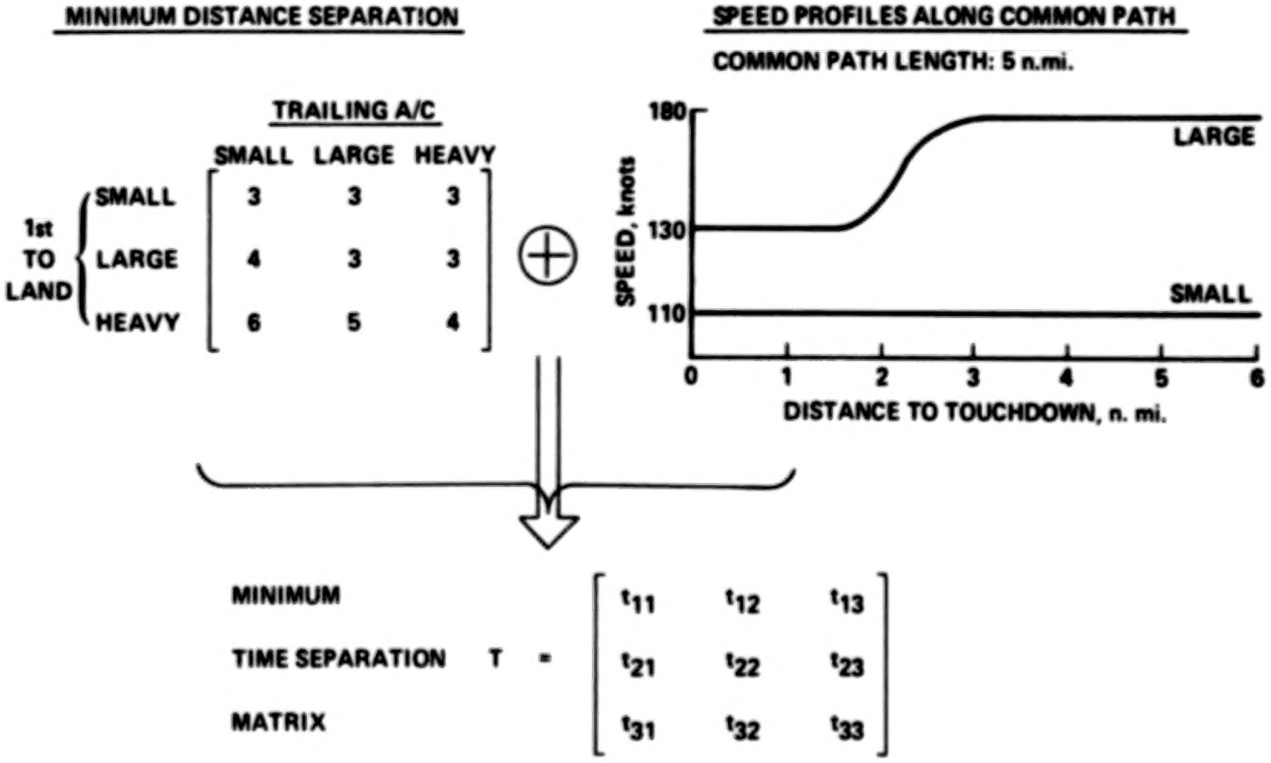
MINIMUM DISTANCE SEPARATION
SPEED PROFILES ALONG COMMON PATH
COMMON PATH LENGTH: 5 n.mi.
180
130
110
SPEED, knots
LARGE
SMALL
0
1
2
3
4
5
6
DISTANCE TO TOUCHDOWN, n. mi.

		TRAILING A/C		
		SMALL	LARGE	HEAVY
1st TO LAND	SMALL	3	3	3
	LARGE	4	3	3
	HEAVY	6	5	4

$\oplus$

MINIMUM TIME SEPARATION MATRIX

$$T = \begin{bmatrix} t_{11} & t_{12} & t_{13} \\ t_{21} & t_{22} & t_{23} \\ t_{31} & t_{32} & t_{33} \end{bmatrix}$$

TIME SEPARATIONS AT TOUCHDOWN

It is assumed that, if two consecutive aircraft are 4D-equipped, the interarrival times given by T can be used for scheduling purposes. However, unequipped aircraft will need additional time buffers to prevent separation distance violations. If the probability density function of an unequipped aircraft meeting an assigned time via controller vectoring is known (this can be determined in the specific experimental context), then time buffers can be determined to keep the probability of separation distance violation below a desired level. These time buffers result in a revised time separation matrix T' described below.

BUFFERS ADDED TO PREVENT MINIMUM SEPARATION VIOLATIONS

FOR TWO CONSECUTIVE AIRCRAFT AT TOUCHDOWN:

IF BOTH EQUIPPED, $T' = (t'_{ij}) = (t_{ij} + \delta_a)$

IF ONE EQUIPPED, $T'' = (t''_{ij}) = (t_{ij} + \delta_b)$

IF BOTH UNEQUIPPED, $T''' = (t'''_{ij}) = (t_{ij} + \delta_c)$

WHERE $0 \leq \delta_a < \delta_b < \delta_c$

INTERACTIVE SCHEDULING ALGORITHMS

The previous discussion established the time separation matrix at touchdown shown as a function of weight category, and whether or not aircraft are 4D equipped. It is assumed that the feeder fix time for each aircraft is known. Based on this time and on the desired time to traverse the route, a desired touchdown time for each aircraft can be determined. This information can be used to generate an initial time schedule, as described in reference 1. However, in addition to setting up an initial schedule, algorithms are required to revise the schedule. Missed approaches need to be accommodated. Also, the controllers may need to change the aircraft arrival rate. It may be that they also are required to block out specific time periods from the computer schedule to accommodate a missed approach or a priority landing. These are important aspects of the complete scheduling problem.

WITH TIME SEPARATION CONSTRAINTS CAN NOW GENERATE SCHEDULE

- ESTABLISH TOUCHDOWN ORDER
- PROVIDE FOR REVISIONS
  - CHANGE ARRIVAL RATE
  - MISSED APPROACHES
  - EMERGENCIES

EVALUATION OF SYSTEM OPERATION UNDER VARIOUS MIX CONDITIONS

The candidate operational procedures and time schedule algorithms previously described were used in a real-time ATC simulation study of operations under various mix conditions.

- **SIMULATION FACILITY**
- **SCENARIO AND TEST CONDITIONS**
- **RESULTS**

SIMULATION FACILITY

The simulation was conducted using the NASA Ames ATC Simulation Facility shown in this figure. It includes two air traffic controller positions, each having its own color computer graphics display. In this study, one was designated arrival control and the other, final control. The controllers each communicate with one or two keyboard pilots. Each keyboard pilot can control up to 10 computer-generated aircraft simultaneously. The clearance vocabulary includes standard heading, speed, and altitude clearances as well as special clearances for 4D-equipped aircraft. This figure also depicts piloted simulators. Previous studies have utilized one or two piloted simulators which were connected by voice and data link to the ATC Simulation Facility; however, in this study, no piloted simulator was used.

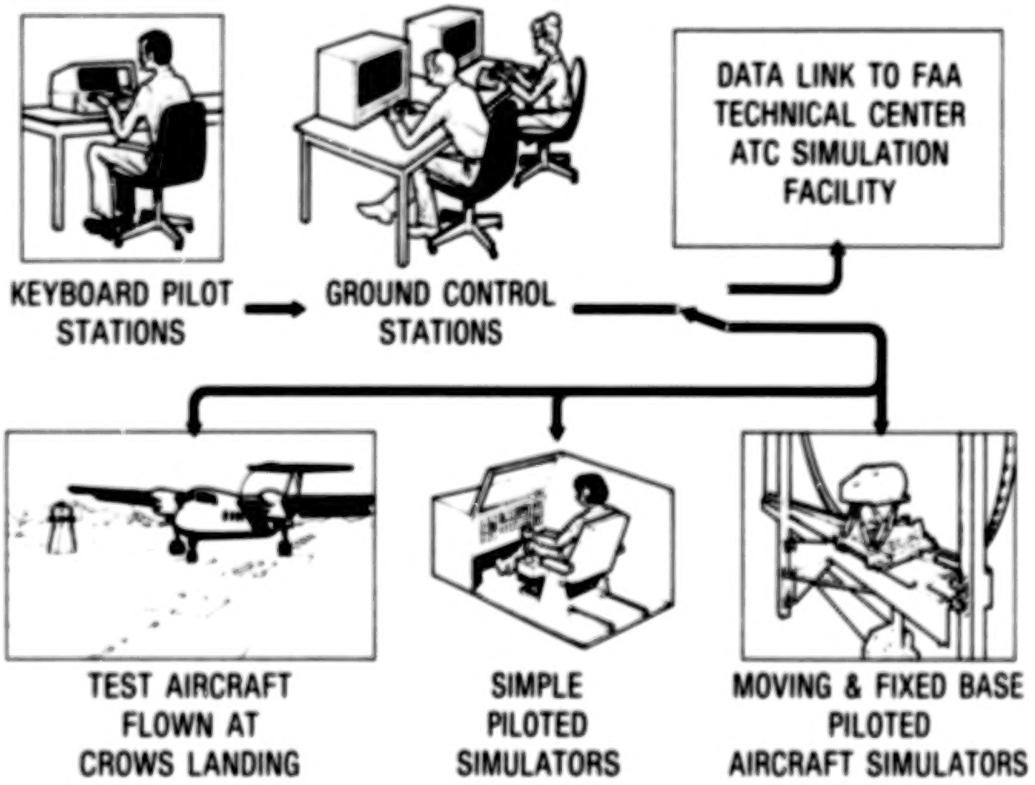
DATA LINK TO FAA TECHNICAL CENTER ATC SIMULATION FACILITY
KEYBOARD PILOT STATIONS
GROUND CONTROL STATIONS
TEST AIRCRAFT FLOWN AT CROWS LANDING
SIMPLE PILOTED SIMULATORS
MOVING & FIXED BASE PILOTED AIRCRAFT SIMULATORS

APPROACH CONTROLLER DISPLAY

The route structure and runway configuration investigated are shown in this figure. Two routes, Ellis, from the north, and Sates, from the south, are high-altitude routes flown by large or heavy jet transport-type aircraft. Aircraft on these routes fly profile descent procedures, but may or may not be 4D equipped. Hence, there is a mix of 4D-equipped and unequipped aircraft of the same speed class along the same route. In addition, low-speed aircraft were considered which flew the Deerpark route from the east, but shared a 5 n. mi. common path length and used the same runway as the jet traffic. The Deerpark traffic was unequipped, and always constituted 25% of the traffic mix. To assist the controller in integrating the 4D-equipped and unequipped traffic, a flight data table (FDT) was provided to the left of the route structure. The information supplied includes aircraft type, route, scheduled touchdown time, and anticipated delay. The main test variable was the mix of traffic. Three mix cases were run: 25, 50, and 75% 4D equipped.

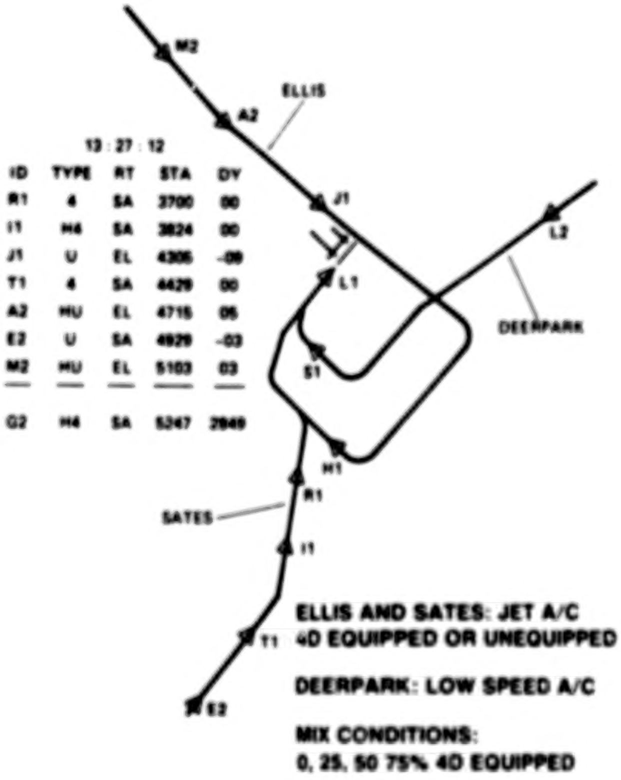

13 : 27 : 12

ID	TYPE	RT	STA	DY
R1	4	SA	3700	00
I1	H4	SA	3824	00
J1	U	EL	4306	-09
T1	4	SA	4429	00
A2	HU	EL	4715	05
E2	U	SA	4929	-03
M2	HU	EL	5103	03
G2	H4	SA	5347	2949

ELLIS AND SATES: JET A/C
4D EQUIPPED OR UNEQUIPPED

DEERPARK: LOW SPEED A/C

MIX CONDITIONS:
0, 25, 50 75% 4D EQUIPPED

ORIGINAL PAGE IS
OF POOR QUALITY

EXPERIMENT CONDITIONS

In this study, a saturated arrival traffic flow was used. It is assumed that instrument flight rule (IFR) conditions prevail, and that all aircraft use runway 4R; furthermore, no departures, winds, or navigation errors are simulated. For purposes of this study, it was assumed that all aircraft depart the feeder fix at their scheduled departure times. Magnitude departure errors that can be tolerated as well as the means to provide ground computer assists to nullify departure errors are main issues addressed by current research.

- **SATURATED ARRIVAL TRAFFIC FLOW**
- **NO WINDS, NO NAVIGATION ERRORS**
- **ALL AIRCRAFT DEPART AT SCHEDULED TIMES**

CONTROLLER EVALUATIONS

Three research air traffic controllers from the FAA Technical Center participated in this study. Controllers were asked to compare operations under the traffic mix conditions. The 25% equipped case was rated the condition with the heaviest workload. The main difficulty seemed to be that the controllers were establishing distance spacing of most of the traffic, and they felt that by not altering the flight path of the 4D-equipped aircraft, they were occasionally losing some slot time. They were, however, quite pleased with the 50% 4D-equipped case, which allowed for easy handling of the unequipped aircraft. The 75% 4D-equipped case was rated most orderly by all the controllers, but when this many aircraft were 4D-equipped (the only unequipped aircraft were the Deerpark arrivals, which always constituted 25% of the traffic sample), there was "basically nothing to do." The controllers were asked if there was any difficulty in handling the mix of speed classes, the slow traffic on Deerpark and the jet traffic on Ellis and Sates. They indicated that spacing behind the low-speed aircraft was sometimes a problem, since they had to allow for a large initial separation along the common path length. The controllers indicated that the time order information displayed on the flight data table was useful; however, the touchdown time and delay information was not used.

- **COMPARISON OF MIX CONDITIONS**
- **CONTROLLING THE MIX**
- **USE OF DISPLAYED TIME DATA**

AVERAGE NUMBER OF CLEARANCES

This figure provides the average number of clearances/aircraft. It can be seen that as more aircraft are 4D equipped, the average number of clearances per aircraft decreases. This is fairly obvious in the experiment context described, since 4D-equipped aircraft were not vectored. They were assigned a touchdown time which was not altered in most cases.

% EQUIPPED	AVERAGE NUMBER OF CLEARANCES/AIRCRAFT
0	5.2
25	4.5
50	2.7
75	2.4

EFFECT OF 4D ON LOW-SPEED TRAFFIC

The previous figure shows the decrease in the average number of controller clearances as a greater percentage of aircraft are 4D equipped. A major concern is: does the average number of clearances for the unequipped aircraft increase as the percentage of equipped aircraft increases? The answer to that question is provided in the figure below, which gives the average number of clearance/aircraft for the Deerpark route only. Recall that the Deerpark traffic was always 25% of the traffic sample, and that all Deerpark is unequipped aircraft. This figure indicates that the average number of clearances given to the Deerpark unequipped aircraft is the same, independent of the mix condition. Also shown is the average time in the system (in minutes) for the Deerpark traffic, which is also seen to be independent of the mix condition.

LOW-SPEED (DEER PARK) TRAFFIC IS 25% OF ALL TRAFFIC IN EACH TEST CONDITION

MIX	AVG. TIME IN SYSTEM, min:sec	AVG. # OF CLEARANCES PER AIRCRAFT
0	19:16	6.9
25	18:56	6.5
50	19:05	6.2
75	19:05	6.4

LOSS OF 4D SCHEDULING

There was a desire to examine how traffic handling is disrupted if a breakdown of the 4D scheduling computer occurs. To investigate this, during a 75% 4D-equipped run, the FDT was removed from the screen so that the controllers no longer had a display of schedule times and order for aircraft in their sector. Furthermore, all feeder-fix departures from then on would not have any 4D time assignment, and would have to be vectored. The map display which showed aircraft positions was not removed. Initially, there was no change. The 4D-equipped aircraft already in the control sector could still be left alone since they would continue to follow their previously assigned 4D route. This is in contrast to a totally ground-based 4D system in which the ground system generates clearances for every aircraft; when that type of system fails, all aircraft are affected in a short time. The only difficulty experienced with the system tested was that after the failure occurred, controllers continued to allow traffic to depart the feeder fixes at the higher arrival rate for the 75% equipped case, rather than to adjust to the baseline vector arrival rate. If the flow-rate adjustment for new feeder-fix departures is made when the failure occurs, then it seems clear that the use of the on-board 4D system provides a safe transition to the standard vector mode.

OBJECTIVE: DETERMINE EFFECTS OF ATC COMPUTER OUTAGE

ACTION: DURING A 75% 4D RUN, FLIGHT DATA TABLE REMOVED

OBSERVATION: NO INITIAL CHANGE (BUSY PERIOD). SOME PROBLEMS WITH HIGH ARRIVAL RATE OF NEW ARRIVALS

CONCLUSIONS: ONBOARD 4D PROVIDES SAFE TRANSITION TO VECTOR MODE. NEED TO ESTABLISH AS PART OF PROCEDURE AN IMMEDIATE CHANGE OF FLOW RATE FOR NEW DEPARTURES

ORIGINAL PAGE IS OF POOR QUALITY

CONCLUSIONS

Algorithms were developed to obtain an initial time schedule and to provide for revisions for a mix of 4D-equipped and unequipped aircraft in the terminal area. These algorithms were used to develop a candidate set of operational procedures for mixing 4D-equipped and unequipped jet aircraft along the same route, and for mixing different speed classes along merging routes. A basic rule established was not to alter the 4D equipped aircraft once they were assigned a landing time. This procedure resulted in the controllers learning to use the 4D aircraft positions to effectively vector the unequipped aircraft to their assigned landing slot. However, procedures were also demonstrated to vector the equipped aircraft and to reassign touchdown times. In addition, it was shown that a loss of the ground based 4D system results in a smooth transition to vector operations. Controller evaluations indicated that the 25%-equipped case was the most difficult to handle. Nevertheless, quantitative data actually showed a decrease in the number of controller clearances with respect to the 0% 4D-equipped case. Controllers felt that the procedure of not altering the 4D-equipped aircraft when so few were equipped was workable, but that it was a more complex task. Nevertheless, fuel was saved even in this case, compared to 0% 4D-equipped aircraft. The controller workload as measured by the average number of clearances per aircraft decreased as the percentage of 4D-equipped aircraft increased. Moreover, this average decrease was not accomplished at the expense of the unequipped aircraft. The number of clearances for the unequipped aircraft as well as the time delays was independent of mix condition.

- **DEVELOPED SCHEDULING ALGORITHMS AND OPERATIONAL PROCEDURES**
- **ALL MIX CONDITIONS EFFECTIVELY CONTROLLED**
- **REDUCED CLEARANCES AS PERCENTAGE 4D INCREASED**
- **UNEQUIPPED NOT PENALIZED BY 4D**

REFERENCE

1. Tobias, L.: Time Scheduling of a Mix of 4D Equipped and Unequipped Aircraft, NASA TM-84327, 1983.

N84
20578

UNCLAS

N84 20578

APPLICATION OF FUEL/TIME MINIMIZATION TECHNIQUES TO ROUTE PLANNING AND TRAJECTORY OPTIMIZATION

Charles E. Knox
NASA Langley Research Center
Hampton, VA

First Annual NASA Aircraft Controls Workshop
NASA Langley Research Center
Hampton, Virginia
October 25-27, 1983

ABSTRACT

Rising fuel costs combined with other economic pressures have resulted in industry requirements for more efficient air traffic control and airborne operations. NASA has responded with an on-going research program to investigate the requirements and benefits of using new airborne guidance and pilot procedures that are compatible with advanced air traffic control systems and that will result in more fuel efficient flight. This paper summarizes the results of flight testing an airborne computer algorithm designed to provide either open-loop or closed-loop guidance for fuel efficient descents while satisfying time constraints imposed by the air traffic control system. The paper will also describe some of the potential cost and fuel savings that could be obtained with sophisticated vertical path optimization capabilities.

DIRECT OPERATING COST

Between 1970 and 1980, the average price paid by airlines for fuel rose approximately 1000%. In 1970, fuel costs represented about 25% of the flights' direct operating costs. In 1980, this percentage rose to between 60 and 70 percent. In addition, inflation has caused crew costs and other non-fuel airline operating costs to increase. These increased operating costs combined with lower revenue levels arising from recessionary trends in the economy have led to an emphasis on achieving more economical operations through changes in procedures, flight operations, airborne equipment capability, and in air traffic control (ATC) operations.

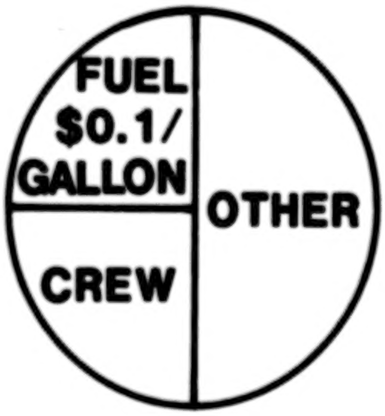

1970

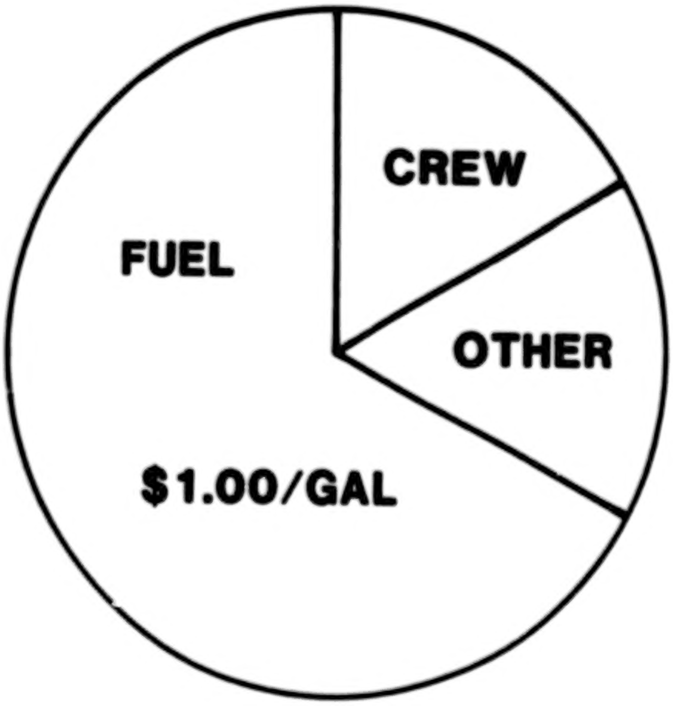

1980

TIME-BASED METERING PROCEDURES

In response to the fuel crisis, the Federal Aviation Administration developed several programs to save fuel including an automated time-based metering (TMB) form of air traffic control for arrivals into the terminal area. This TBM concept provides fleet-wide (all users) fuel savings through time control by matching the airplane arrival rate into the terminal area to the airport's arrival acceptance rate. This procedure reduces the need for holding and for low-altitude vectoring for sequencing to land. Fuel savings are also achieved on an individual airplane basis by permitting the pilot to descend at his discretion from cruise altitude to a designated metering fix in a fuel-efficient manner. Substantial fuel savings have resulted but air traffic control workload is high since the radar controller maintains time management for each airplane through either speed commands or path stretching with radar vectors. Pilot workload is increased since the pilot must plan for a fuel-efficient descent usually by using various rules of thumb.

NASA has flight-tested in its Transportation System Research Vehicle (TSRV) Boeing B-737 airplane a flight management descent algorithm designed to increase fuel savings by reducing the time dispersion of airplanes crossing the metering fix at an ATC-designated time by transferring the responsibility of time navigation from the radar controller to the flight crew. Time and path (4-D) closed-loop guidance were provided to the pilot for an idle-thrust, clean-configured, constant Mach descent with transition to a constant airspeed descent to arrive at the metering fix at a time, altitude, and airspeed predetermined by ATC.

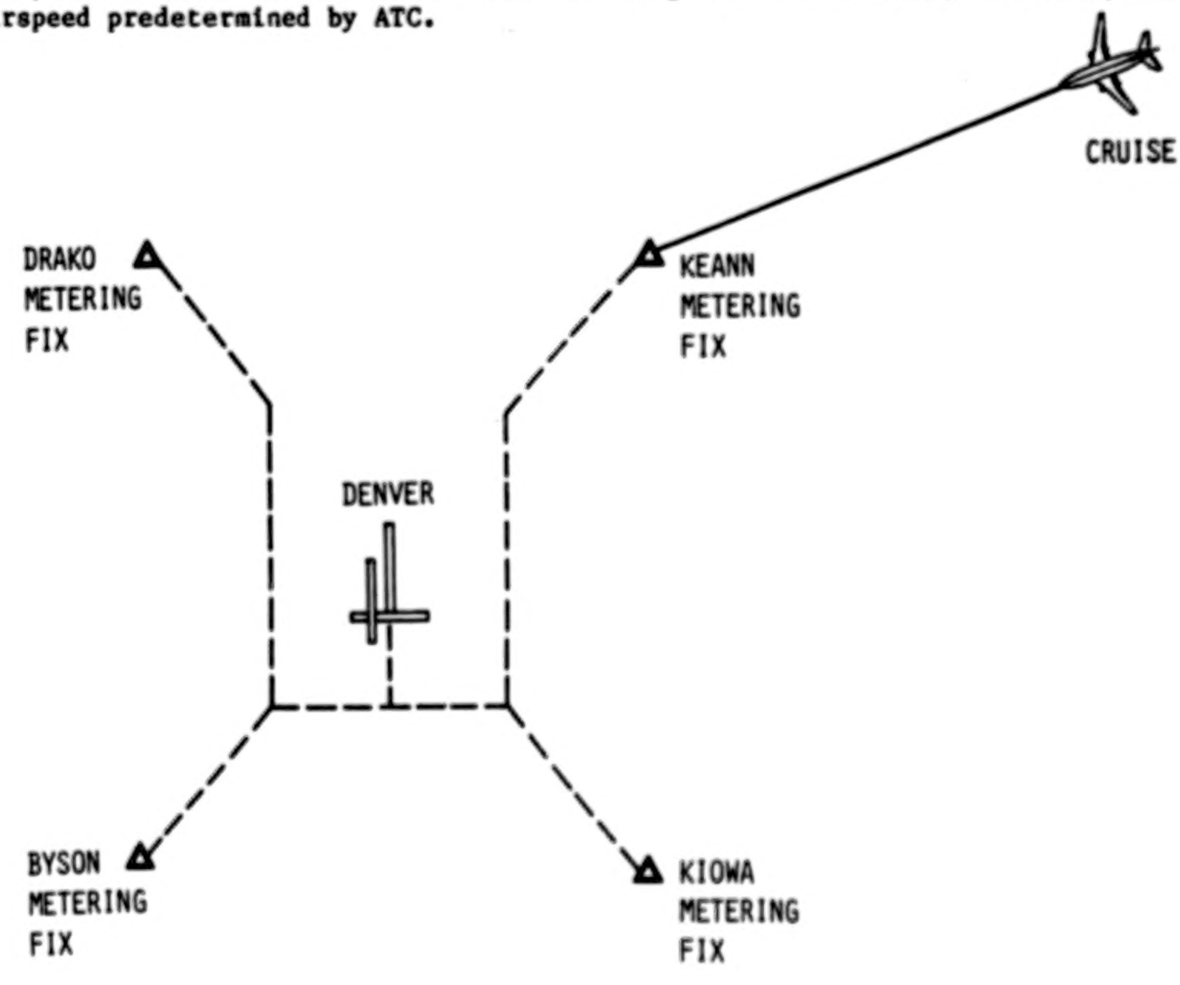

AIRBORNE COMPUTED DESCENT PATH

The NASA airborne flight management descent algorithm computes the parameters required to describe a seven-segment cruise and descent profile between an arbitrarily located entry fix to an ATC-defined metering fix. (Segments 2 and 3 are computed if the flight will be restricted by the ATC 250 knot airspeed limit below 10,000 feet.) The computed parameters are then used by the airplane's navigation and display systems to present guidance to the pilot and/or autopilot.

The descent profile is based on linear approximations of airplane performance for an idle-thrust, clean-configured descent. Airplane gross weight, wind, and nonstandard temperature and pressure effects are also considered in these calculations. To be compatible with standard airline operating practices, the path is calculated based upon the descent being flown at a constant Mach number with transition to a constant calibrated airspeed and speed changes being flown at a constant altitude.

The flight management descent algorithm may be used in either of two modes. In the first mode, the pilot may input the Mach/airspeed descent schedule to be flown, and the descent profile is calculated independent of an assigned metering fix time. If a metering fix time is subsequently assigned, some time error, which must be nulled by the pilot, may result since an arbitrary specification of the descent speed schedule may not satisfy both the initial and final time boundary conditions.

The second mode was designed for time-metered operations. In this mode, pilot inputs include the estimated time of arrival to the entry fix and the ATC specified metering fix arrival time. The descent profile is then calculated based on a Mach/airspeed descent schedule, computed through an iterative process, that will closely satisfy the crossing times for both of these way points.

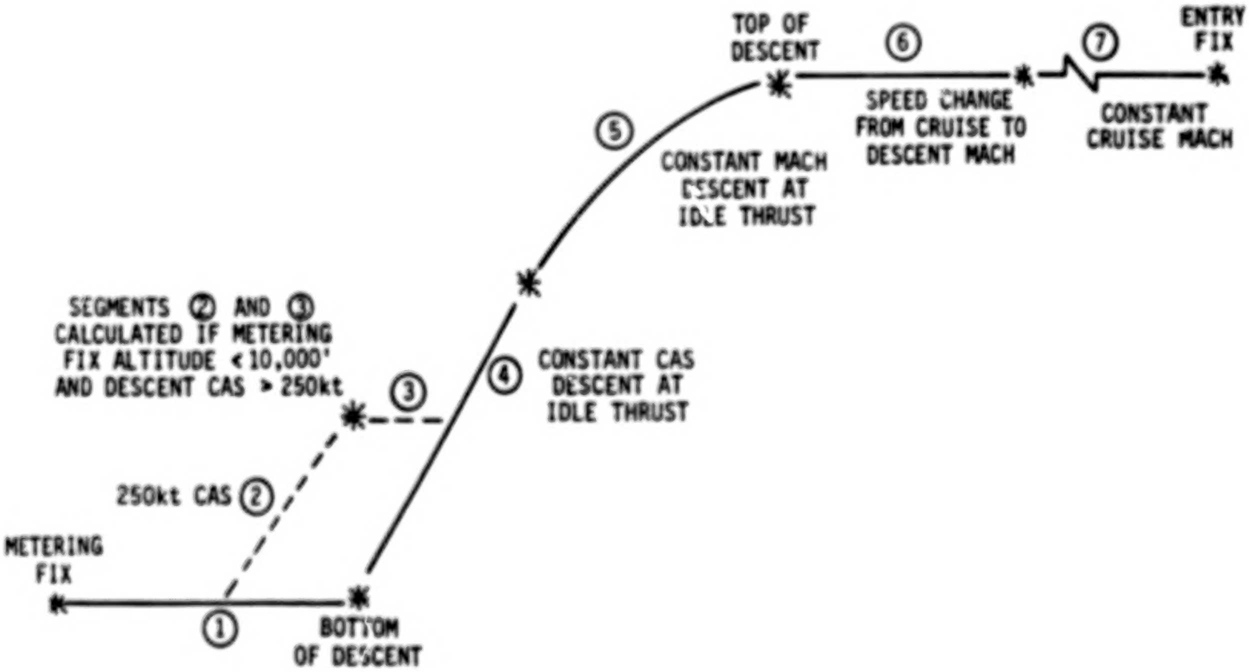
TOP OF DESCENT
⑥
⑦
ENTRY FIX
SPEED CHANGE FROM CRUISE TO DESCENT MACH
CONSTANT CRUISE MACH
⑤
CONSTANT MACH DESCENT AT IDLE THRUST
SEGMENTS ② AND ③ CALCULATED IF METERING FIX ALTITUDE < 10,000' AND DESCENT CAS > 250kt
③
④
CONSTANT CAS DESCENT AT IDLE THRUST
250kt CAS ②
METERING FIX
①
BOTTOM OF DESCENT

RESULTS AND FUTURE INVESTIGATION

Research flight tests of the NASA flight management descent algorithm in the Denver Air Route Traffic Control Center time-based metered air traffic environment demonstrated that time guidance and control in the cockpit were acceptable to both the pilots and the ATC controllers. Descent guidance presented on the airborne CRT flight instrumentation allowed the test airplane to be flown across the metering fix at the proper altitude and speed and significantly reduced the time dispersion occurring with other airplanes at the metering fix. The concept of closed-loop guidance time control in the cockpit could be readily extended, with similar results, to other aircraft with integrated electronic navigation and guidance/display systems. However, many airplanes flying in the time-based metering ATC environment do not have these integrated electronic guidance and display systems. This research was then extended to provide the pilots of unequipped airplanes with simplified open-loop 4-D guidance. The issues in this research are a trade-off between performance and pilot workload and acceptance.

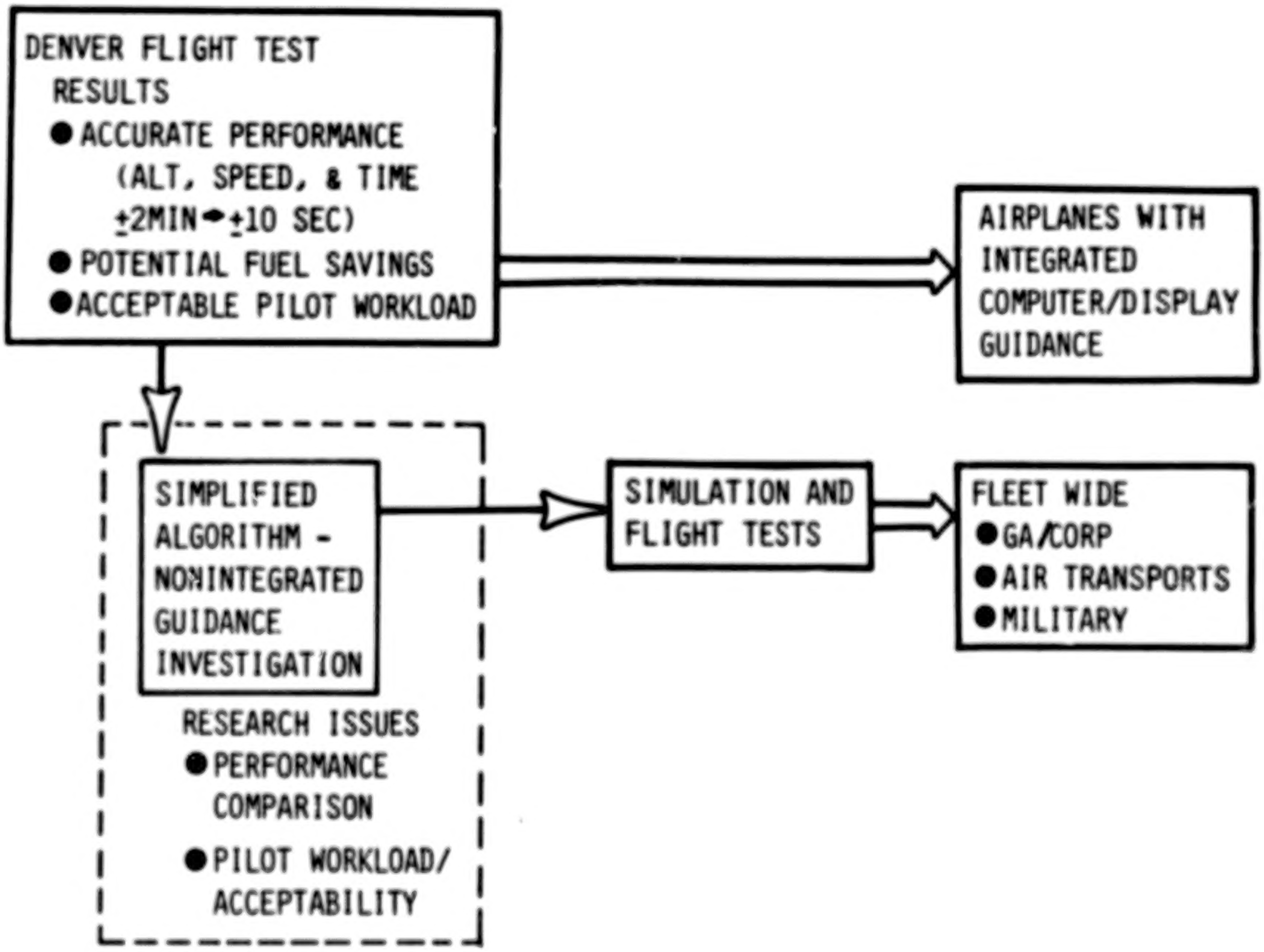
DENVER FLIGHT TEST
RESULTS
● ACCURATE PERFORMANCE
(ALT, SPEED, & TIME
±2MIN → ±10 SEC)
● POTENTIAL FUEL SAVINGS
● ACCEPTABLE PILOT WORKLOAD
AIRPLANES WITH
INTEGRATED
COMPUTER/DISPLAY
GUIDANCE
SIMPLIFIED
ALGORITHM -
NONINTEGRATED
GUIDANCE
INVESTIGATION
RESEARCH ISSUES
● PERFORMANCE
COMPARISON
● PILOT WORKLOAD/
ACCEPTABILITY
SIMULATION AND
FLIGHT TESTS
FLEET WIDE
● GA/CORP
● AIR TRANSPORTS
● MILITARY

PROFILE DESCENT HAND-HELD CALCULATOR

To determine the feasibility of providing open-loop guidance to the flight crew to make fuel-conservative, time—constrained descents to the metering fix, the NASA descent algorithm was programmed on a small, hand-held programmable calculator. All inputs required by the algorithm are made by the pilot through the keyboard. All outputs are shown in the calculator display.

Flight tests conducted with NASA test pilots in a T-39A (Sabreline) airplane indicated that it was feasible to fly the descents with open-loop guidance provided to the pilot in the form of a DME indication to define the top-of-descent point and the appropriate Mach and airspeed indications to use during the descent. The resulting mean distance and time errors to actually achieve the predicted speed and altitude conditions at the end of the descent profile were 1.2 n. mi. long and 1.4 seconds early. A question remained, however, if open-loop guidance provided by a hand-held calculator would be pilot acceptable in an operational environment.

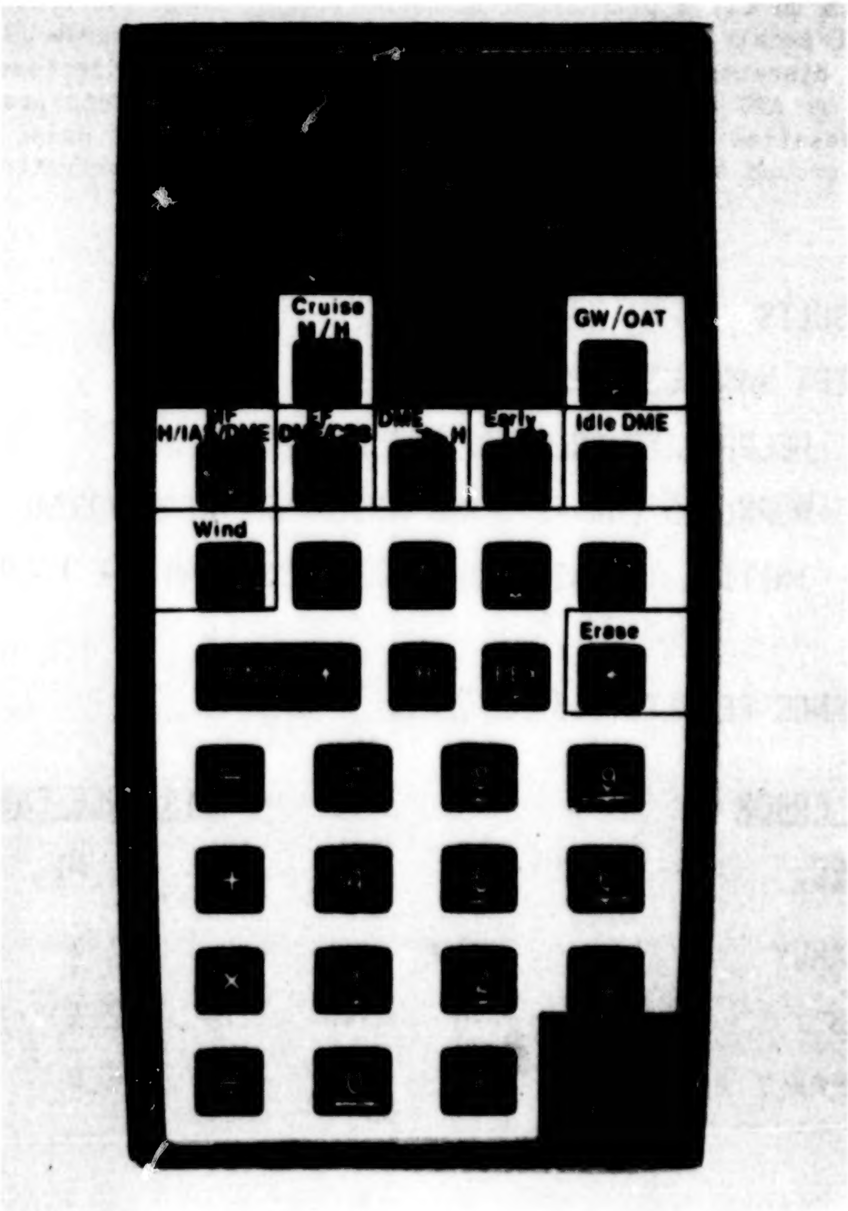

PROFILE DESCENT HAND-HELD CALCULATOR
UNITED AIRLINES FLIGHT TESTS

Joint flight tests were conducted with United Airlines to determine if the concept of using open-loop guidance for fuel-conservative descents with a hand-held calculator during routine flight operations was acceptable to the pilots. The results of these tests showed that the majority of the pilots participating in the tests felt that the open-loop guidance concept of the calculator provided useful information. Several test subjects felt that they could mentally compute the top-of-descent point and would not save additional fuel through use of the calculator. However, all of the test subjects agreed that the computations necessary to satisfy the metering fix crossing time constraints were too difficult for mental calculation and would require other means (such as the calculator) to provide guidance. All subjects agreed that the workload associated with using the calculator was low and would not interfere with normal crew tasks.

All of the test subjects expressed a concern that the ATC system would not allow them to fly a preplanned descent without being interrupted and thus suffer a fuel penalty. This concern was realized during these flight tests: 68% of the descents were modified with altitude restrictions or speed restrictions by ATC and required recomputation of the descent profile. This statistic emphasizes the requirement that compatibility must exist between the airborne and ground systems to realize significant fuel conservation.

- TEST RESULTS:

  CONCEPT WAS ACCEPTABLE TO PILOTS

  - HELPFUL TO CREW FOR DESCENT PLANNING
  - WORKLOAD LOW--DID NOT INTERFERE WITH NORMAL CREW TASKS
  - INITIAL TRAINING REQUIRED LESS THAN ONE HOUR

- PERFORMANCE RESULTS--16 DESCENTS

TIME ERROR SEC.		DISTANCE ERROR N. MI.
1 EARLY	MEAN	1.7
20.8	σ	2.1
39 EARLY	MAX	6.4

ADVANCED FLIGHT MANAGEMENT CONCEPTS

The NASA flight management research activities also include defining the interface and guidance requirements necessary for practical implementation of sophisticated optimal path trajectory calculations. One of the corner stones of this research effort is the "OPTIM" computer program. This program generates a full vertical path profile including climb, cruise, and descent based upon one of three selectable objectives: minimum cost, minimum fuel, or fixed time/minimum fuel.

The OPTIM computed profile is generated from solutions of an energy state approach in which range and specific energy are used to describe aircraft state. A cost functional, which expresses the quantity (fuel or operating cost) which is to be minimized, is combined with the aircraft state equations to form a Hamiltonian with energy as the independent variable. As energy is incremented along the trajectory, airspeed and thrust are chosen to minimize the Hamiltonian. In this manner a complete vertical profile is generated along a pre-specified horizontal path.

This program presently is being used in a fast-time mode to examine parametric sensitivities and to define potential fuel and cost savings. The program has also been implemented into a real-time piloted simulation to define interface requirements between the pilot, the airborne guidance systems, and the ground-based ATC systems to ensure compatibility and efficiency.

"OPTIM" GENERATES VERTICAL FLIGHT PROFILES THAT MINIMIZE DOC AND SATISFY EXTERNALLY IMPOSED TIME CONSTRAINTS

- MINIMUM COST
- MINIMUM FUEL
- FIXED TIME, MINIMUM FUEL

● FAST-TIME ANALYSIS

- PARAMETRIC SENSITIVITY
- FLIGHT PLANNING TOOL
- DEFINE POTENTIAL TRIP FUEL AND COST SAVINGS

● REAL-TIME SIMULATION

- PILOT/AIRPLANE SYSTEMS INTERFACE REQUIREMENTS FOR PRACTICAL OPTIMAL FLIGHT PATHS
- INTERFACE REQUIREMENTS TO ENSURE A/G COMPATIBILITY AND EFFICIENCY

DIRECT OPERATING COST MINIMIZATION

The direct operating cost (DOC) function used in the OPTIM program is a function of the cost of operation per hour K_1 and the cost per pound of fuel K_2. The geometry (speed, altitude, and flight path angle) of the trajectory is a function of the ratio of K_1 and K_2 rather than the absolute magnitudes. The selection of the value of fuel cost is relatively straightforward. However, the selection of the operating costs per hour is much more complex to establish. These costs must be truely time variant costs rather than cyclic costs (i.e., costs associated with take-off and landing are cyclic, not trip time variant). The magnitude of the operating cost may also be biased higher or lower to change trip times (changes airspeed and altitude) to reflect corporate policy. Airline management should select the proper values for K_1 and K_2 to reflect both optimal flight operations and corporate policy for each flight.

$$\text{DOC} = K_1\ (\text{HOURS}) + K_2\ (\text{FUEL USED})$$

$$K_1 = \$/\text{HOUR} \qquad K_2 = \$/\text{POUND FUEL}$$

- DOC IS A FUNCTION OF K_1 AND K_2
- TRAJECTORY IS A FUNCTION OF THE RATIO OF K_1 AND K_2
- INTERACTIVE SELECTION OF K_1 AND K_2 IS DESIRABLE

AIRLINE TRIP PLANNING

An actual flight planning example will illustrate the potential fuel and cost savings that can be achieved by using an optimal path trajectory program like OPTIM. In this example, an airline has 11 different pre-specified routes between Chicago and Phoenix to allow the flight dispatcher to select the most favorable route considering winds and other atmospheric conditions. Typically, a flight dispatcher will choose the highest cruise altitude possible, for the given airplane gross weight and ambient temperature, that is consistent with ATC altitude constraints. For this flight, a route slightly north of the shortest route (designated ATC route) was chosen to take advantage of lower head winds. Even though this route is nine miles longer than the shortest route, the fuel required to complete the trip and the resulting trip cost were reduced since the time to complete the trip was reduced.

TYPICAL CHICAGO - PHOENIX ROUTE STRUCTURE

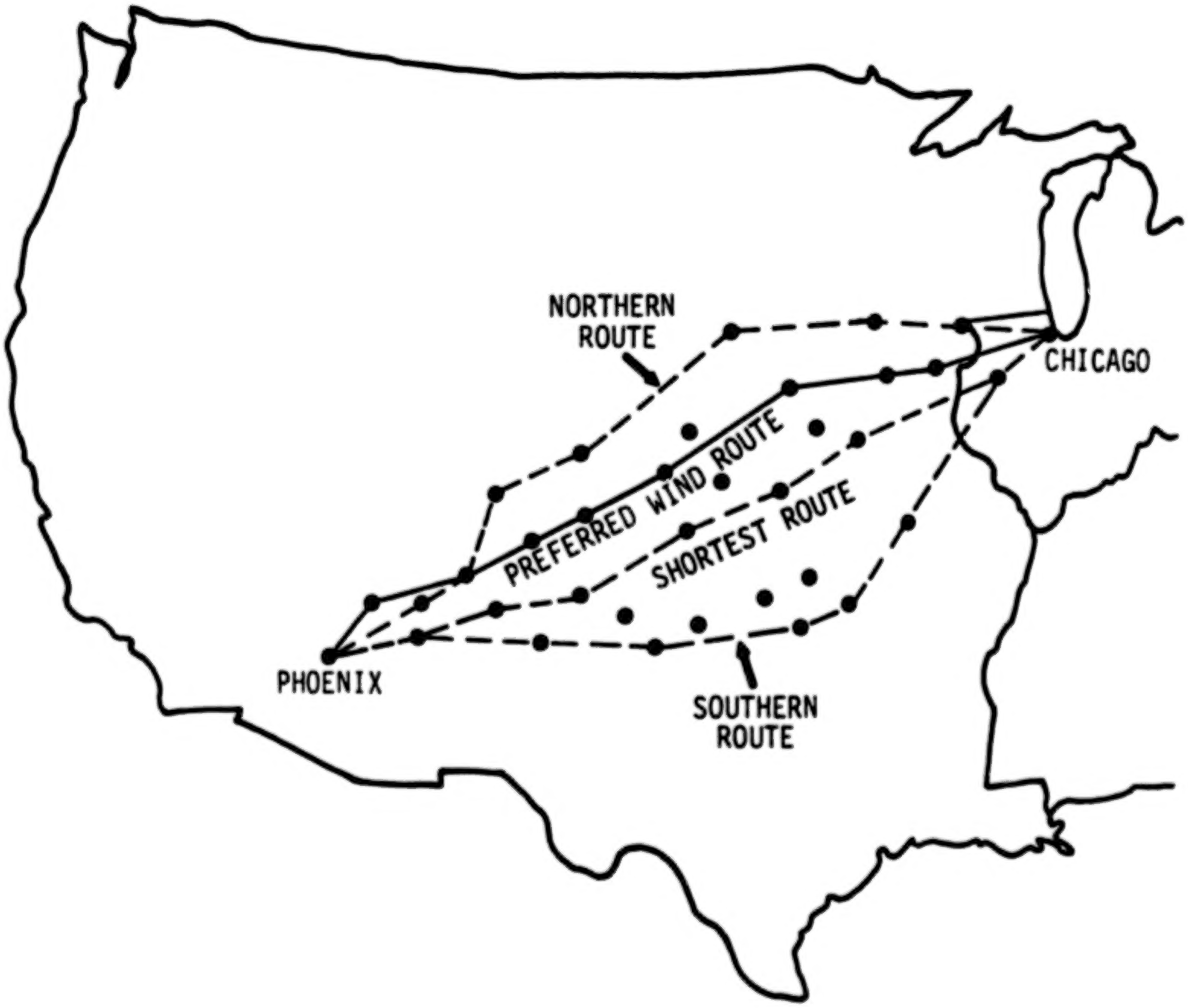

ORD - PHX ROUTE SELECTION

This figure shows the magnitude of trip time, fuel required, and cost to complete the Chicago to Phoenix trip using a generic commercial tri-jet transport airplane with time variant costs of $600 per hour and fuel costs of 15 cents per pound. The first two cases show a comparison of the trip flown at a cruise altitude of 35,000 feet (chosen by the flight dispatcher) for the shortest distance route and the preferred wind route. By flying the preferred wind route, the trip time was reduced by 3 minutes and 39 seconds resulting in a corresponding decrease of 404 pounds of fuel used and a reduction of $97.10 to the trip cost.

To illustrate how much further trip costs could be reduced, the OPTIM program was run in a minimum cost mode for the preferred wind routing. The results of this run, listed in the third case, indicate that a cruise altitude of 24,000 feet should be used. Even though this lower altitude resulted in more fuel used to complete the trip (742 pounds), the total trip cost was reduced by $147.55 due to a 25 minute 44 second reduction of trip time.

It should be stressed at this point that the trip profile (airspeed and cruise altitude) will change as the time cost and the fuel cost ratio is changed. As time costs are reduced or fuel costs increase, the trip profile will change towards a minimum fuel trajectory.

It was interesting to note that with the OPTIM program run in the minimum cost mode on the ATC preferred route, further trip time, fuel, and cost reductions were obtained. This illustrates the fact that to achieve truly optimal cost and fuel savings, both horizontal and vertical path optimization must be obtained together.

TRI-JET AIRPLANE

TIME COST $600/HR -- FUEL COST $.15/LB

ROUTE DESCRIPTION	TIME H:M:S	FUEL LB	COST $
1. SHORTEST GROUND DISTANCE (1263 nmi RANGE); CRUISE ALTITUDE 35,000 FT	3:46:04	29,100	6625.75
2. PREFERRED WIND ROUTE (1272 nmi RANGE); CRUISE ALTITUDE 35,000 FT	3:42:25	28,696	6528.65
3. PREFERRED WIND ROUTE (1272 nmi RANGE); CRUISE OPTIM PROFILE (~24,000 FT)	3:16:41	29,438	6381.10
4. SHORTEST GROUND DISTANCE (1263 nmi RANGE); CRUISE OPTIM PROFILE (~24,000 FT)	3:15:01	29,134	6320.37

TRIP COST COMPARISON

This figure shows trip cost expressed in $/mile as a function of trip length for a generic commercial twin-jet transport airplane operating on three different vertical profiles. The three profiles presented are a standard handbook profile, a minimum cost profile which satisfies current ATC vertical path constraints, and an unconstrained minimum cost profile. The minimum cost profiles each represent a significant savings relative to the handbook profile which calls for a constant airspeed/Mach climb, cruise at a fixed altitude and Mach number, and a constant Mach/airspeed descent. The cost-optimized profile with ATC constraints complies with the ATC-imposed speed limit of 250 knots under 10,000 feet and maintains a fixed cruise altitude. The second cost-optimized profile does not comply with the 250-knot speed limit and gradually increases the cruise altitude as fuel is burned.

The difference in trip costs between the optimized profiles and the handbook profiles are significant — increasing from 3.1% to 3.8% as trip length increases from 500 to 1500 n. mi. for the ATC-constrained profile. For the unconstrained profile, the trip costs range from 4.3% to 4.5% less than handbook.

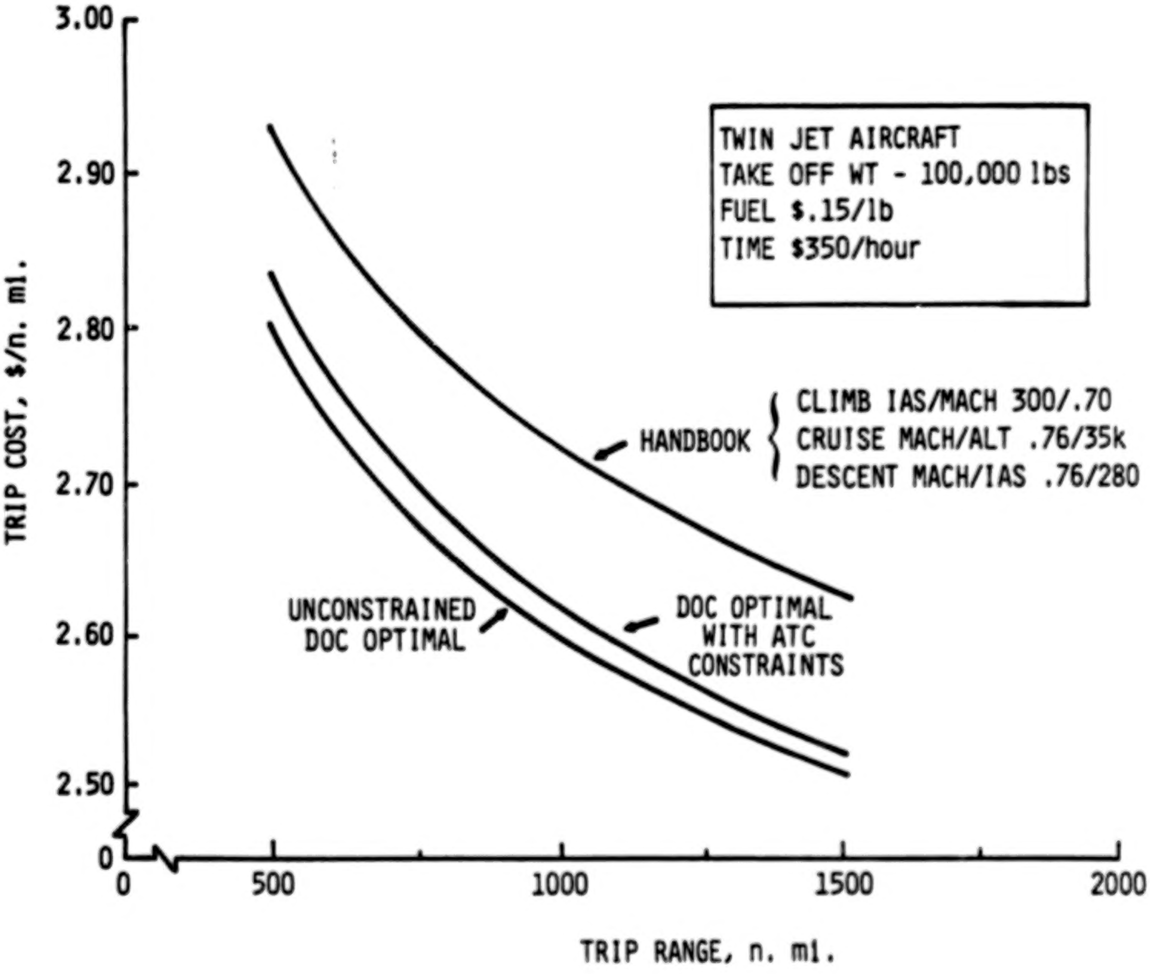

ORIGINAL PAGE IS
OF POOR QUALITY

TRIP FUEL USAGE COMPARISON

This figure shows fuel used to complete the trip expressed as pounds/mile as a function of trip distance for the same generic commercial twin-jet used in the previous figure. The three profiles presented are the handbook profile and the optimized profiles, with and without the ATC vertical path constraints. However, the optimized paths were computed based on minimizing fuel usage rather than cost. The resulting fuel savings between the handbook profile and the minimum fuel profile with ATC constraints ranged between 7.4% for a 500-mile trip to 8.8% for a 1500-mile trip. If the ATC vertical profile and speed constraints were eliminated the total savings would range between 8% and 9.5%.

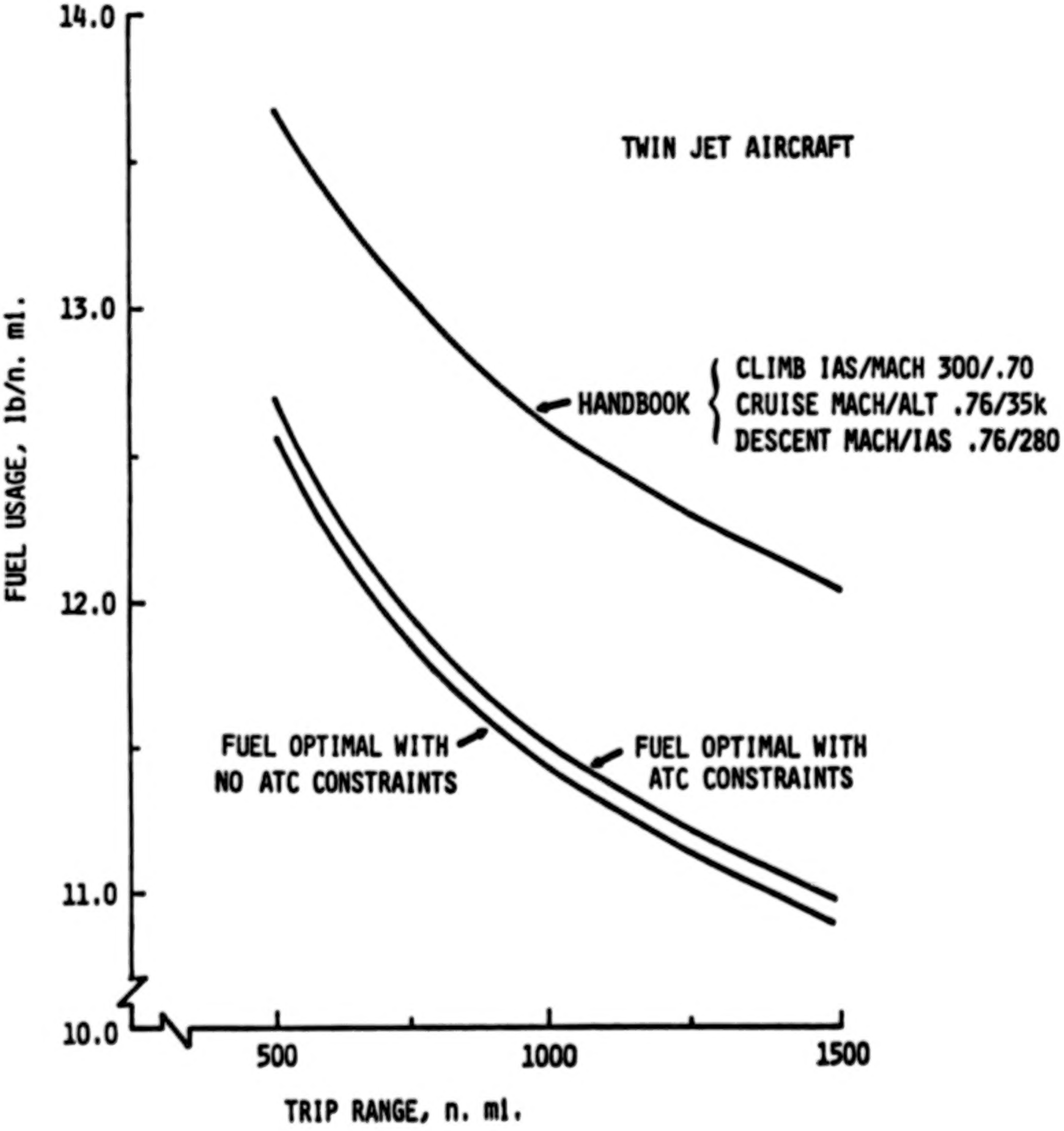

FUEL SAVED VIA FIXED-TIME OPTION

Another option in the OPTIM program is the minimum fuel, fixed-time mode. This mode will be used when a fixed trip time, for either airline or ATC purposes, is desired. This chart shows the percentage of fuel saved by absorbing known time delays through reduced speeds during the cruise and descent flight segments instead of maintaining normal cruise speeds and absorbing the delay in a holding pattern prior to descent. Curves for 500 n. mi., 1000 n. mi., and 1500 n. mi. trips are plotted to show the percentage of fuel saved for each trip as a function of the amount of time to absorb. The assumption is made that the delay is known at the beginning of the cruise segment, although the OPTIM program can reoptimize the profile later in the cruise to absorb the delay. However, the later in the flight that the pilot knows his delay, the smaller the delay that can be absorbed by using speed control. Significant fuel savings can be obtained with this capability, but may require modification of some ATC procedures and policies to obtain arrival time assignments early in the trip.

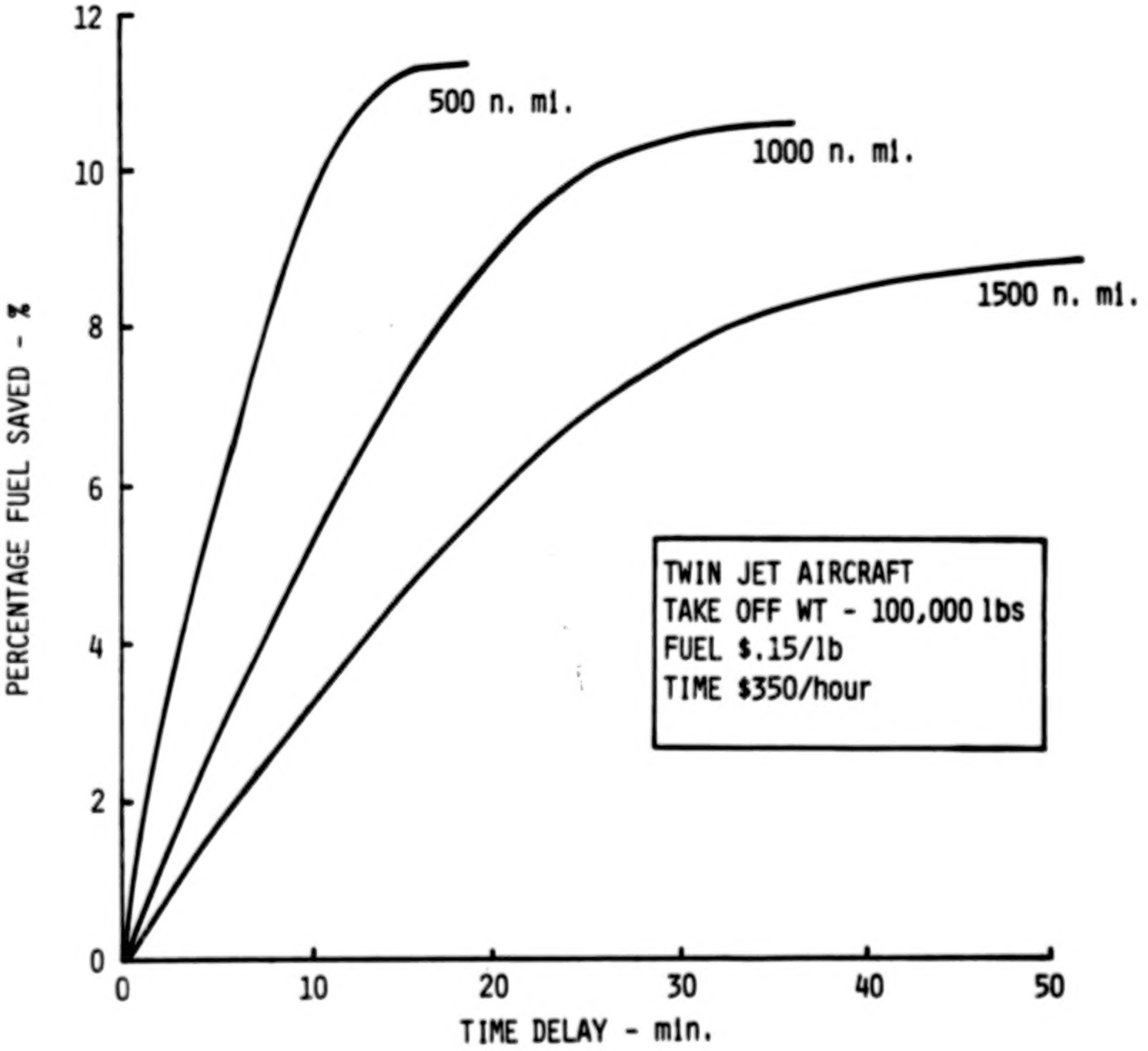

SPEED/ALTITUDE FOR CONVENTIONAL AND MINIMUM COST PROFILES

A significant problem that must be addressed in the practical implementation of the optimized flight paths is to provide adequate guidance for the pilot or autopilot to fly the vertical profiles computed by the optimization routines. This figure illustrates this problem by comparing the speed and altitude profiles of a conventional handbook climb, cruise, and descent with one computed for a minimum cost flight.

The piloting techniques employed on a conventional "handbook" profile are manageable by the pilot since thrust is generally set to a predetermined value and the vertical flight path controlled by adjusting the pitch attitude of the airplane in reference to maintaining a constant value in either the altimeter, airspeed indicator, or the Machmeter. As shown in this figure, during a conventional profile (heavy dashed line), the airplane is accelerated to 250 knots indicated airspeed (KIAS) shortly after take-off. A constant 250 KIAS climb is maintained until reaching 10,000 feet. Then the airplane is accelerated to 300 KIAS while remaining at approximately 10,000 feet. A constant 300-knot climb is maintained until the desired .70 Mach number is obtained. At this point a constant .70 Mach is flown until reaching cruise altitude. Then the airplane is accelerated at constant altitude to the cruise Mach number (.76 in this example). The descent is flown at a constant Mach number (.76) with a transition to a constant 280 KIAS between 23,000 and 24,000 feet. At 10,000 feet, a constant altitude is maintained until the airspeed is slowed to 250 KIAS. This speed is maintained until entering the terminal area for landing.

The minimum cost speed and altitude profile (heavy solid line) may be contrasted to the conventional profile. When unconstrained by the ATC-imposed 250-KIAS limit (above 10,000 feet) neither airspeed, Mach number, nor altitude is constant during the climb or descent. Conventional guidance and pilot techniques are not adequate to fly these profiles. These profiles may not be acceptable due to increased pilot workload and the uncomfortable feeling of not being in control of the airplane.

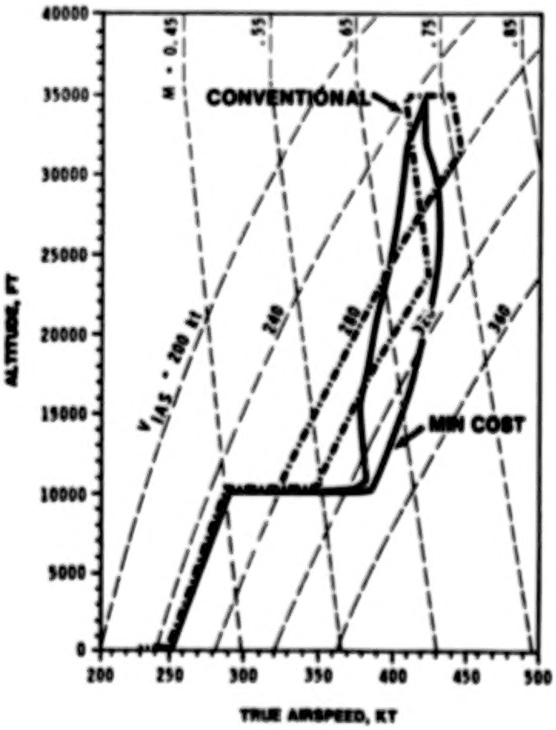

The flight path profiles of the optimized trajectories may differ significantly from conventional profiles as illustrated in the previous figure. Many questions arise about the interface required for the flight crew to fly the airplane along optimal trajectories, particularly, in an airline environment. There are additional concerns about obtaining the full benefits of optimal trajectories within an ATC environment with other air traffic.

NASA is engaged in an advanced flight management concepts research effort. This research will be conducted in two phases. The first phase will be aimed at defining the interface requirements between the flight crew and the airborne systems necessary for executing practical optimal flight paths. This will essentially be a single airplane problem with no external influences from ATC or adverse weather. The emphasis in this phase will be on guidance and control requirements and pilot and passenger acceptability from an airline operations point of view.

The second phase of this research will be aimed at defining the interface requirements between the airborne system (including the flight crew and airborne electronic systems) and the ATC system. This will be a systems problem in that additional constraints such as ATC requirements, other air traffic, or adverse weather will be considered. The emphasis in this phase of research will be an airborne system flexibility and air/ground communication requirements.

PILOT/ AIRPLANE SYSTEMS
INTERFACE REQUIREMENTS FOR
PRACTICAL OPTIMAL FLIGHT PATHS

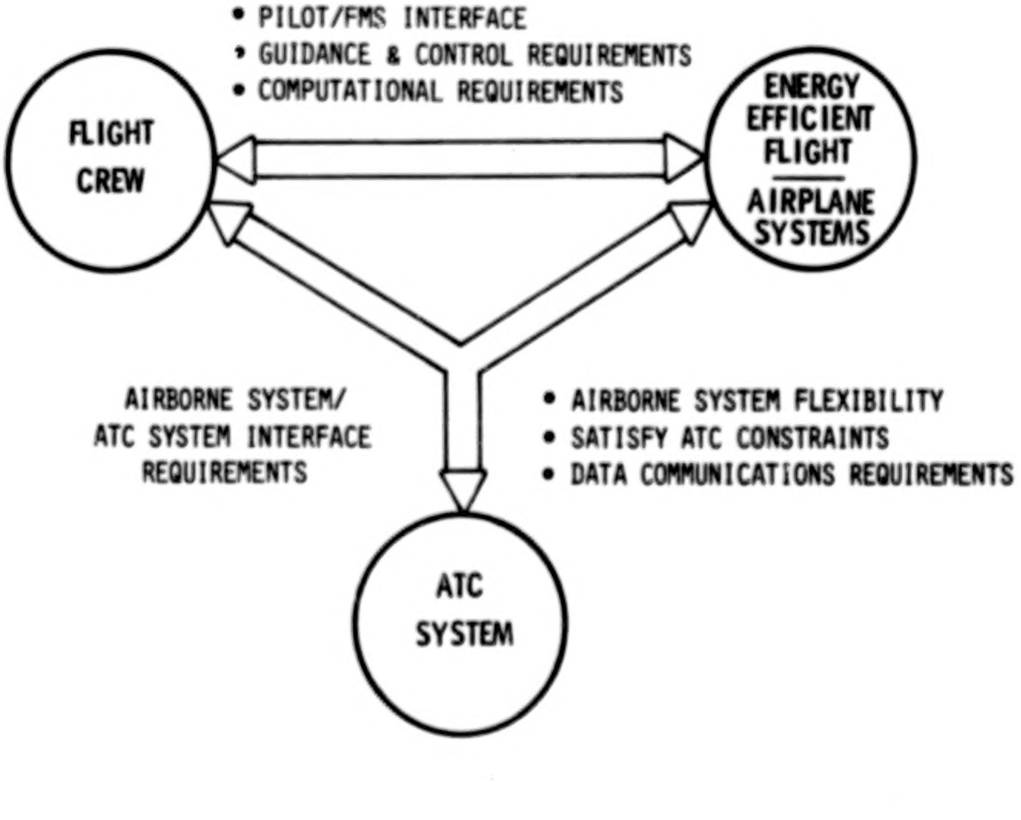
• PILOT/FMS INTERFACE
• GUIDANCE & CONTROL REQUIREMENTS
• COMPUTATIONAL REQUIREMENTS
FLIGHT CREW
ENERGY EFFICIENT FLIGHT
AIRPLANE SYSTEMS
AIRBORNE SYSTEM/ ATC SYSTEM INTERFACE REQUIREMENTS
• AIRBORNE SYSTEM FLEXIBILITY
• SATISFY ATC CONSTRAINTS
• DATA COMMUNICATIONS REQUIREMENTS
ATC SYSTEM

SUMMARY

Potential fuel savings and subsequent cost reductions have been demonstrated with the simplified computations of the programmable calculator with open-loop guidance. Additional savings may be obtained from closed-loop guidance and with the more complex trajectory computations that can be provided with an integrated flight system.

Regardless of the sophistication of the airborne system, however, compatibility must exist with the air traffic system. Airborne derived optimal trajectories must retain the profile qualities that produce the desired optimization, but also fit the path constraints necessary for safe air traffic control.

Flight crew response due to external influences, such as other air traffic or adverse weather, will be a key issue in the acceptance and usefulness of future flight optimization airborne systems. Attention must be paid to the air/ground communication interface and the airborne system flexibility to ensure a high degree of systems efficiency.

- POTENTIAL FUEL SAVINGS AND COST REDUCTIONS HAVE BEEN DEMONSTRATED WITH BOTH SIMPLIFIED AND COMPLEX TRAJECTORY COMPUTATIONS.
- INCREASED OPERATING COSTS HAVE NECESSITATED INCREASED EFFICIENCY AND COMPATIBILITY BETWEEN AIR TRAFFIC CONTROL AND FLIGHT OPERATIONS.
- PILOT AND AIRBORNE/GROUND SYSTEMS INTERFACE REQUIREMENTS RESULTING FROM FLIGHT ON NON-STANDARD, OPTIMIZED TRAJECTORIES MUST BE DEFINED.

N84
20579

UNCLAS

N84 20579

FEEDBACK LAWS FOR FUEL MINIMIZATION FOR TRANSPORT AIRCRAFT

Douglas B. Price and Christopher Gracey
NASA Langley Research Center
Hampton, Virginia

First Annual NASA Aircraft Controls Workshop
NASA Langley Research Center
Hampton, Virginia
October 25-27, 1983

TRAJECTORY OPTIMIZATION

The Theoretical Mechanics Branch has as one of its long-range goals to work toward solving real-time trajectory optimization problems on board an aircraft. This is a generic problem that has application to all aspects of aviation from general aviation through commercial to military. Our overall interest is in the generic problem, but we must focus on specific problems to achieve concrete results. The problem is to develop control laws that will generate approximately optimal trajectories with respect to some criteria such as minimum time, minimum fuel, or some combination of the two. These laws must be simple enough to be implemented on a computer that can be flown on board an aircraft, which implies a major simplification from the two-point boundary value problem generated by a standard trajectory optimization problem. In addition, the control laws must allow for changes in end conditions during the flight, and changes in weather along a planned flight path. Therefore, a feedback control law that generates commands based on the current state rather than a precomputed open-loop control law is desired. This requirement, along with the need for order reduction, argues for the application of singular perturbation techniques.

- Solve Trajectory Optimization Problems on board the aircraft in real time
- Allow for changing conditions
  - Weather
  - Air traffic control changes
- Feedback control law
- Singular perturbation techniques

SINGULAR PERTURBATIONS

Singular perturbation techniques can sometimes be used to break a big problem down into more manageable parts. For example, a large-order numerical optimization problem can frequently be divided into a series of smaller subproblems that can be solved one by one in a serial fashion. The solutions to these subproblems are then combined to generate an approximation to the solution of the original large-order problem. This technique is very valuable and has been used successfully in a number of different areas. The validity of the technique depends on a separation of time scales for (or a decoupling of) the various states involved in the problem. For some problems, this separation of the states occurs naturally, and may even be made obvious by one or more small parameters of the problem. For flight problems, some of the time-scale separations are fairly easy to find and agree upon, but others are controversial at best. Another problem with the technique is that while stable feedback laws can be generated for the initial boundary layers which correspond to the ascent portion of a trajectory, the feedback laws are unstable in the descent portion.

- Subdivide large-scale numerical optimization problem into series of smaller subproblems
- Solve subproblems serially then put solutions together to approximate solution to original problem
- Difficulties with the technique:
  - Time-scale ordering / separation
  - Terminal boundary layers - descent

FUEL OPTIMAL TRANSPORT PROBLEM

The particular problem to be discussed here is a fuel optimization problem for a transport aircraft in the vertical plane. The cost function which is to be minimized is the integral over the flight time of fuel flow rate f. The state vector consists of range x; total energy per unit weight E; altitude h; and flight path angle γ. The controls for the problem are thrust T; and lift L. The remaining parameters are velocity V; the force of gravity g; drag D; and weight W (which is considered a constant for the problem). The fuel flow rate is modelled as a quadratic in thrust with coefficients that are, in general, functions of energy and altitude. The drag is modelled as a quadratic in lift with coefficients that are also functions of energy and altitude. The ε's on the left-hand sides of the state equations are "small" numbers that determine the ordering and separation of the states in the singular perturbation formulation of the problem.

Minimize $\quad J = \int_{t_0}^{t_f} f(h, E, T)\, dt$

subject to:

$$\dot{x} = V \cos \gamma$$

$$\varepsilon_1 \dot{E} = (T - D)\, V/W$$

$$\varepsilon_2 \dot{h} = V \sin \gamma$$

$$\varepsilon_3 \dot{\gamma} = g(L - W \cos \gamma)/WV$$

where

$$f = \alpha_0(E,h) + \alpha_1(E,h)\, T + \alpha_2(h)\, T^2$$

$$D = \beta_0(E,h) + \beta_1(E,h)\, L + \beta_2(E,h)\, L^2$$

SEPARATION OF STATES

One way to approach the question of the separation of the various states in the problem is to assume that they can be separated into mutually exclusive time scales, each consisting of one state. This is, of course, ad hoc and does not bother with the realities of the aircraft dynamics, but has the virtue that it makes the equations easy to solve. The resulting feedback control law is easy to implement, at least for the initial boundary layers. The modelling of the aircraft dynamics under this assumption is unsatisfactory because altitude and flight path angle are highly coupled. An alternate approach is to recognize this coupling and separate the states into three groups: range as the outer layer, energy as the first boundary layer, and altitude and flight path angle as the second boundary layer. The equations for altitude and flight path angle are linearized about the solution from the first boundary layer subproblem so that a feedback solution can still be obtained.

- "Straight" Singular Perturbations – separate layers for altitude and flight path angle
  - $\varepsilon_3 \ll \varepsilon_2$
  - leads to implementable feedback law
  - unsatisfactory modelling of A/C dynamics
- Linearize altitude/flight-path angle subproblem about solution from first boundary layer
  - $\varepsilon_3 = \varepsilon_2$
  - Implementable feedback law
  - good model of dynamics

LINEARIZED BOUNDARY LAYERS

This figure shows a plot of the solution for altitude from the separate boundary layers discussed on the previous slide for a trajectory with initial altitude at point A. The curve labeled C is the altitude solution from the outer layer and represents the cruise altitude for a transport trajectory. It is a horizontal line because the outer layer solution is a constant altitude cruise. The curve labeled B represents the first boundary layer solution for altitude. It converges to the cruise equilibrium nicely but does not meet the initial condition. The actual altitude for the trajectory comes from the second boundary layer solution and is shown as the curve starting at A. It meets the initial condition and approaches the first boundary layer solution as they both converge to the cruise altitude.

ASCENT

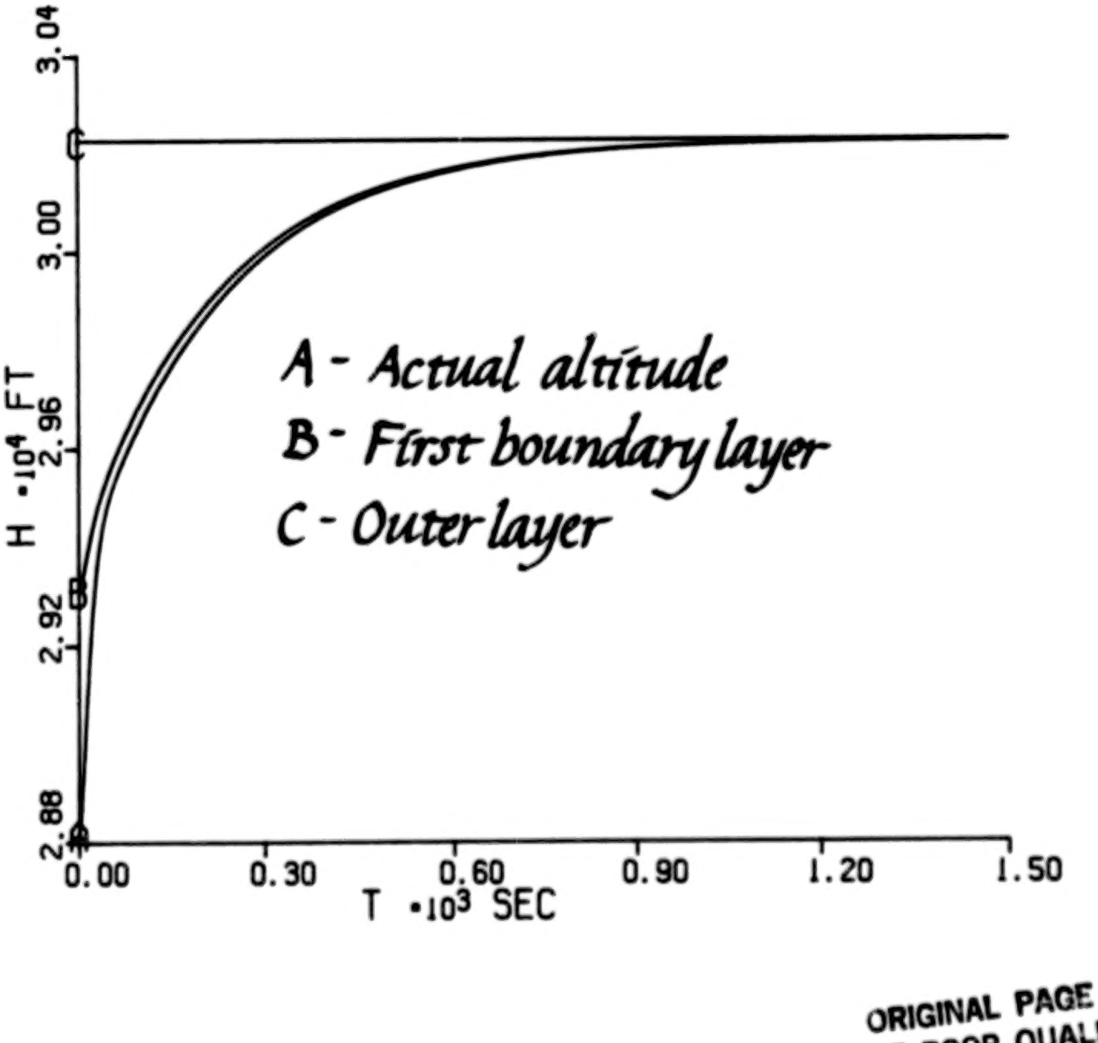

The difficulty with singular perturbation techniques for descent trajectories can be shown in this figure which shows the altitude resulting from a singularly perturbed solution for a descent. The horizontal line again represents the cruise altitude and is an equilibrium for the boundary layer equations. The other two curves are the altitude solutions from the first and second layer subproblems computed in the backward direction from the endpoint. However, for descent (and for any terminal boundary layer), the trajectory is moving away from the stable equilibrium as time increases. For this reason, the feedback law that was stable for ascent is unstable for descent. Therefore, any inaccuracies at the beginning of or along the trajectory will result in very large errors at the endpoint. The only reliable way to use the same control law for descent as ascent is to precompute the descent in the negative direction from the desired endpoint. This precludes taking into account any changes in the end conditions after the descent is initiated.

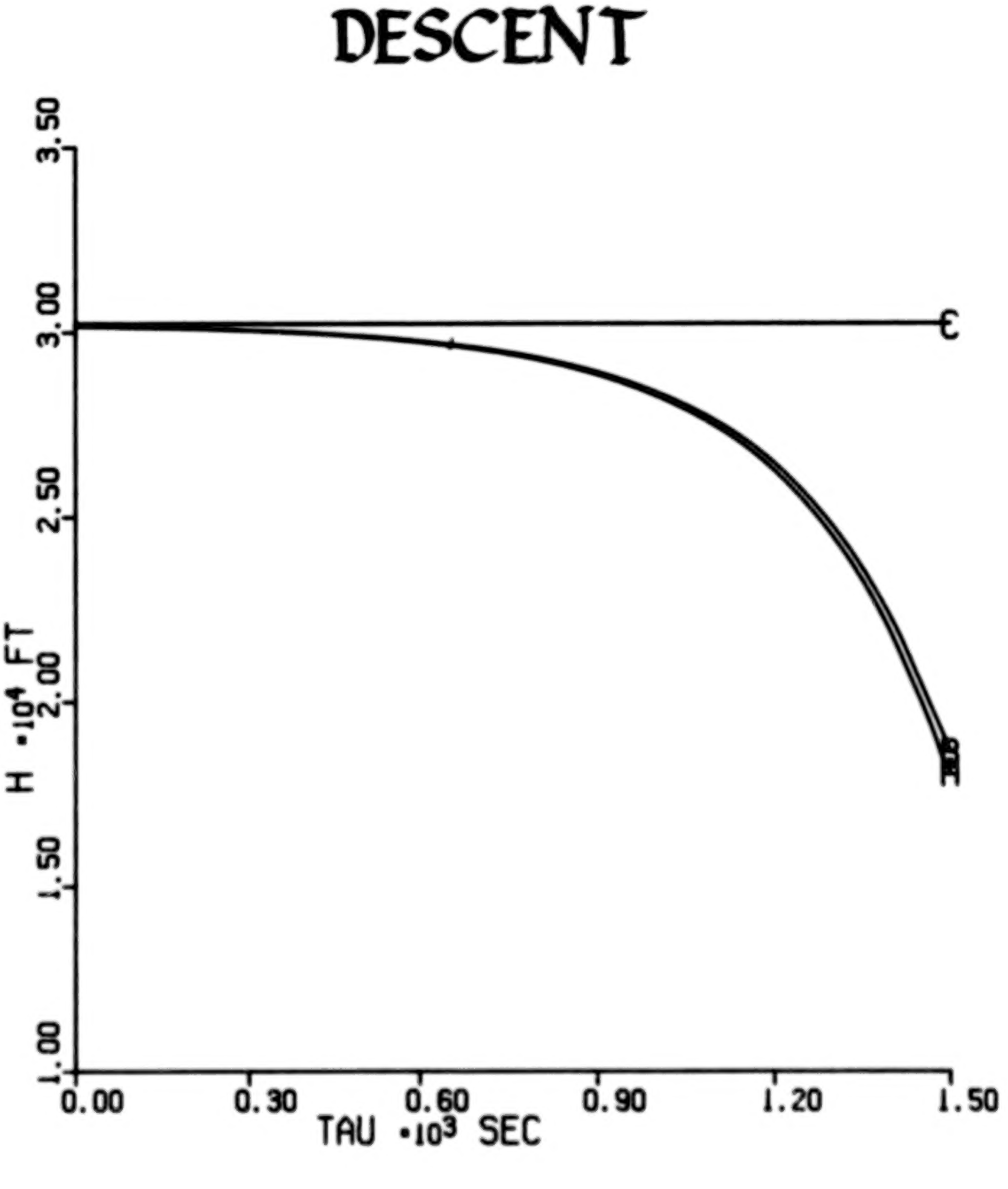

ANOTHER APPROACH FOR DESCENT

In order to accommodate the terminal part of a trajectory while maintaining commonality with the analysis used so far, it was decided to change the problem statement by modifying the cost function to include an altitude term multiplied by an adjustable coefficient. The cost function becomes the integral of a convex combination of the fuel flow rate, as before, and the additional altitude term. When the weighting parameter k is zero, this is the original cost function for the problem. Values of k between 0 and 1 change the equilibrium altitude for the problem to a value lower than that for the original cruise. Thus, the aircraft can be made to descend by changing the parameter k to a nonzero value. The desirable property of always approaching a stable equilibrium is maintained with this technique, and it becomes just an extension of the technique used for ascent. The cost function is no longer that for a fuel optimal problem when k is not zero, but the fuel flow rate is still a part of the cost function. This cost function represents a trade-off between fuel optimization and simplicity of the overall control law.

- Change problem to get stable feedback law for descent trajectory
- Change cost function - add altitude term

$$J = \int_{t_0}^{t_1} [(1-k)\, f(E,h,T) + kh]\, dt$$

- Different values of k give different values for equilibrium altitude

EQUILIBRIUM ALTITUDES

This figure demonstrates that the equilibrium altitude may be changed in an almost linear fashion by changing the constant k multiplying altitude in the cost function. The equilibrium altitude for this problem is a function of cruise velocity. The outer layer subproblem (with k = 0) consists of determining the cruise altitude that corresponds to a given cruise velocity. The choice of cruise velocity must be made from other considerations. This figure shows equilibrium altitudes for four different cruise velocities plotted against the constant k. It can be seen that as k varies butween 0 and .4, the equilibrium altitude changes from the fuel optimal altitude to the ground. The variation for each value of velocity is nearly linear, but the change with velocity is obviously nonlinear. These curves were generated by solving the outer layer subproblem for four different values of cruise velocity for different values of the parameter k.

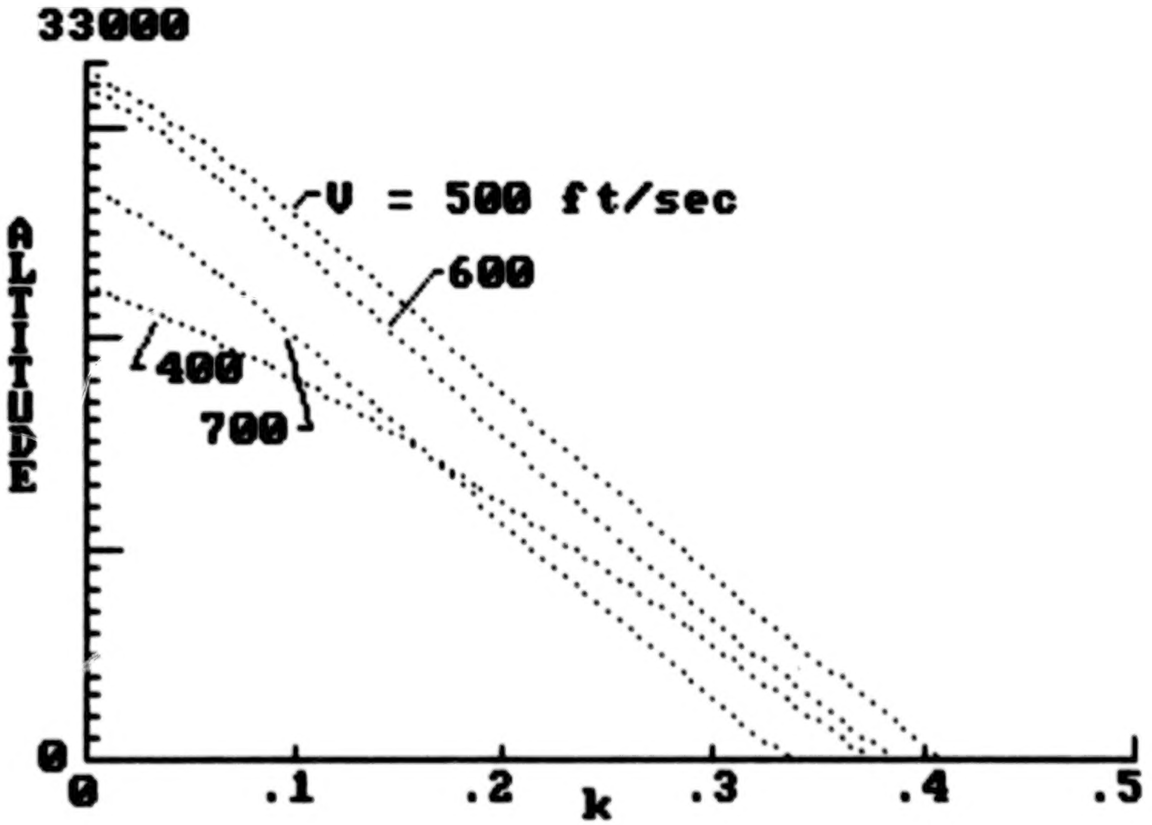

DESCENT TRAJECTORY

This figure shows a descent trajectory generated by the technique described previously. It is a plot of altitude vs time with three different curves plotted. The curve with the straight line segments represents the altitude from the outer layer subproblem. It starts at the fuel optimal cruise level with k = 0. At 100 seconds into the flight, k is varied linearly from 0 to .15, and the equilibrium altitude follows it down almost in a straight line. The other two curves are the altitude from the first and second boundary layers. The secondary boundary layer altitude represents the actual altitude achieved by the simulated aircraft using the feedback control law under discussion. By changing the way the parameter k is varied, descents with different characteristics can be achieved. One common characteristic is that the bottom of the descent is always an exponentially stable approach to the new equilibrium altitude.

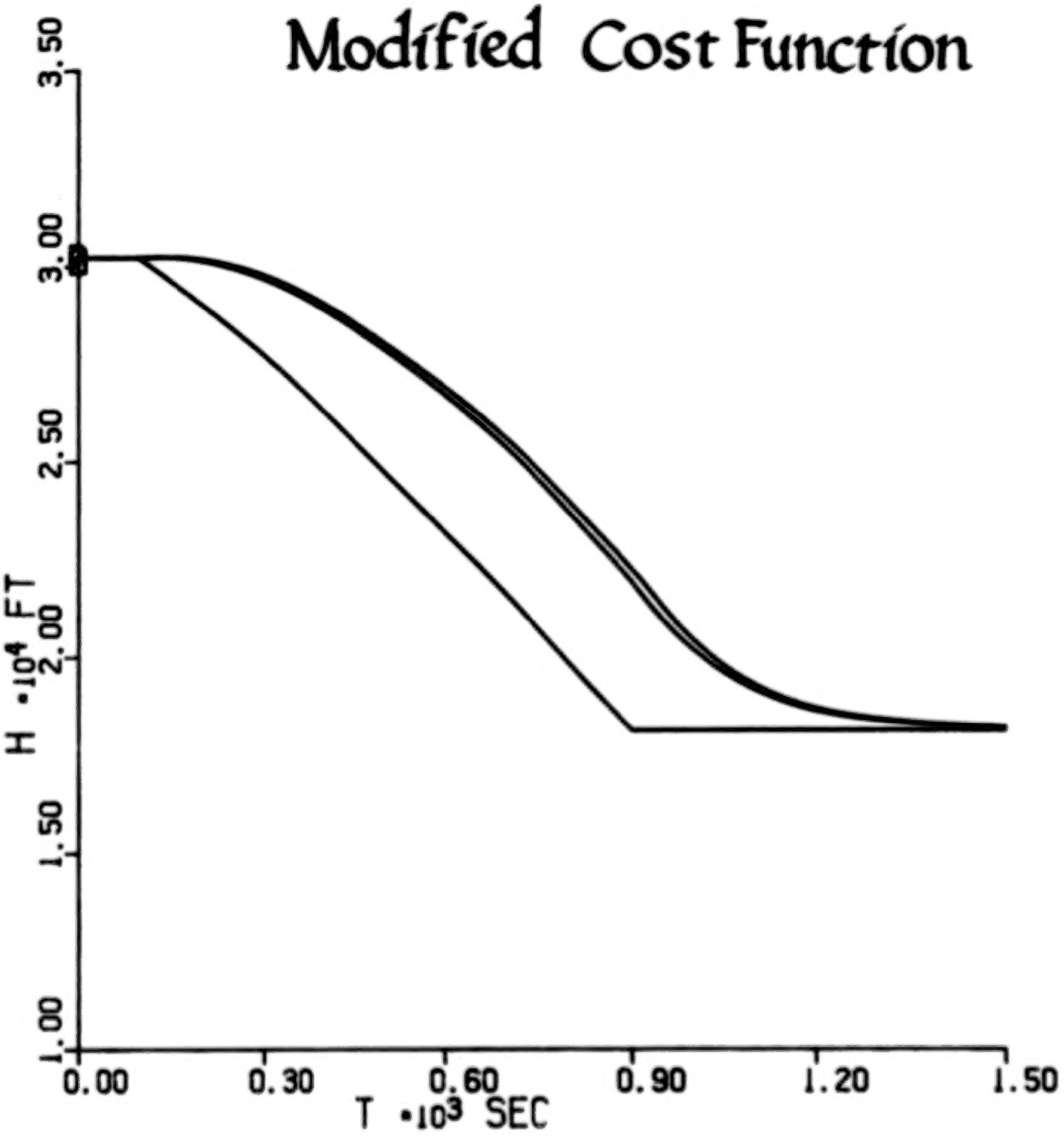

COMMENTS

The general area of singular perturbation techniques has been shown to offer a good framework for on-board optimal trajectory control. The large numerical problem of computing optimal trajectories requires some simplification and order reduction in order to hope for an on-board solution. The haphazard use of order reduction techniques without considering the implications of separating states which may actually change on the same time scale can lead to control laws based on an improper model of flight dynamics. In particular, altitude and flight path angle must be considered on the same time scale for the fuel optimal transport problem, since they are highly coupled. By linearizing the altitude and flight path angle equations about the solution to the first boundary layer subproblem, they can be considered on the same time scale, and a feedback control law can be developed that accurately reflects the dynamics of the aircraft.

A major problem with singular perturbation techniques has been the inability to derive stable feedback laws for terminal layers without precommuting the terminal boundary layer trajectory. It has been shown that by adding an altitude term to the cost function with a variable multiplier, feedback laws can be generated that always fly toward a stable equilibrium. These laws, though ad hoc in nature, can be used to approximate optimal trajectories. A nice feature of this technique is that the control law used for ascent is continued throughout the trajectory with the only change for descent being a nonzero multiplier on the altitude term.

Singular perturbation techniques offer a good framework for on-board optimal trajectory control

Altitude and flight-path angle must be considered on same time scale

Altitude term in cost function leads to feedback law that is good for whole trajectory

Need optimal trajectories for comparisons

N84
20580

UNCLAS

N84 20580

IDENTIFICATION OF MULTIVARIABLE HIGH-PERFORMANCE TURBOFAN ENGINE DYNAMICS FROM CLOSED-LOOP DATA

Walter C. Merrill
NASA Lewis Research Center
Cleveland, Ohio

First Annual NASA Aircraft Controls Workshop
NASA Langley Research Center
Hampton, Virginia
October 24-26, 1983

PRECEDING PAGE BLANK NOT FILMED

A typical engine control design cycle consists of developing a dynamic engine simulation from steady-state component performance data, designing a control based upon this simulation, and then testing and modifying the control in an engine test cell to meet performance requirements. This design cycle has been successful for state-of-the-art engines. However, for more advanced multivariable engines that exhibit strong variable interactions, this procedure will result in substantial trial and error modification of the control during the testing phase. One method to automate the design process and reduce control modification testing and development cost would be to identify accurate dynamic models directly from the closed-loop test data. These identified models would then be used in conjunction with a synthesis procedure to systematically refine the control. Recent advances in closed-loop identifiability (Ref. 1) present a methodology for this direct identification of engine model dynamics from closed-loop test data. This paper describes the application of an identification method (Ref. 2) to simulated and actual closed-loop F100 engine data (Ref. 3). This study was undertaken to determine if useful dynamic engine models could be identified directly from closed-loop engine test data (Ref. 4). (See fig. 1.)

Determine Multivariable Engine Models
Directly From Closed-Loop Engine Test Data

Figure 1.- Identification objective.

The F100 engine was tested in the Lewis Research Center altitude test facility to evaluate the F100 Multivariable Control (MVC) law (Ref. 3). During the same test period the "Bill of Material" (BOM) control was also evaluated as a baseline/backup control model. Thus, there were a variety of closed-loop operating records obtained throughout the flight envelope with a number of different power input requests. (See fig. 2.)

Note that direct control of the engine controls inputs is not possible. Since this is a closed-loop process, input and output noise will be correlated. Normally, this precludes the use of open-loop indentification techniques which require independence of the inputs and outputs. However, sufficient independence can be guaranteed if the PI control changes during a transient or if the simplified engine model generates a full rank, independent desired input. This latter condition is the case for the F100 MVC structure and thus allows a direct application of open-loop identification methodology.

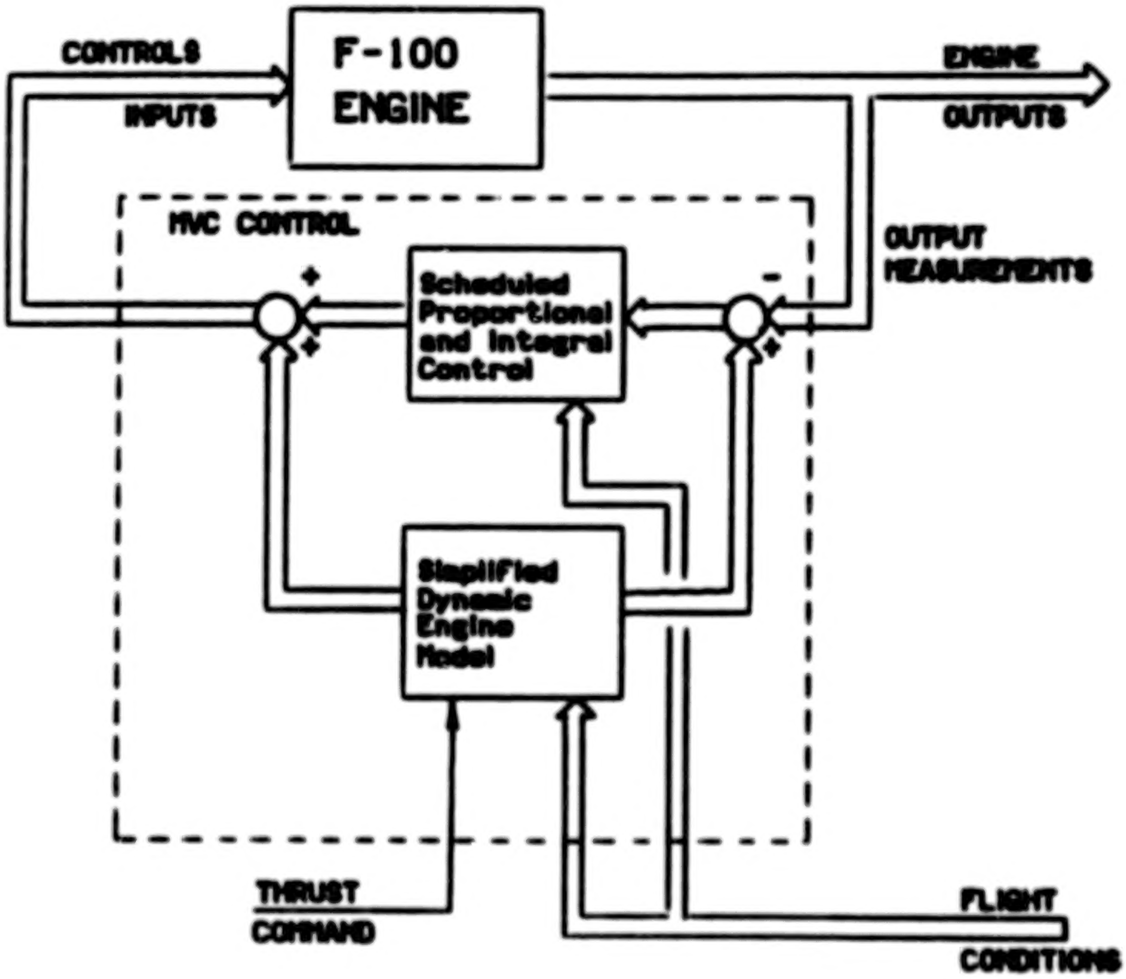
CONTROLS
INPUTS
F-100
ENGINE
ENGINE
OUTPUTS
MVC CONTROL
OUTPUT
MEASUREMENTS
+
+
-
+
Scheduled Proportional and Integral Control
Simplified Dynamic Engine Model
THRUST
COMMAND
FLIGHT
CONDITIONS

Figure 2.- F100 multivariable control structure.

The Instrumental Variable/Approximate Maximum Likelihood (IV/AML) method is an output error method of time series analysis. It was implemented in a combined iterative/recursive form. The IV/AML method was selected because the method exhibits reasonable convergence for a small number of samples. The IV/AML method is based upon an approximate decomposition of the maximum likelihood solution to the identification problem (fig. 3).

Approach

IV/AML Method of Recursive Time Series Analysis Directly Applied to Closed-Loop Data

Figure 3.- Identification approach.

Engine dynamics at a steady-state operating point are adequately modeled by a linear state space system. For the F100 engine a three-output four-input model written with the "transfer function" form given in Ref. 2 is shown. Engine speeds (N1 and N2) are important dynamic engine variables. Engine exhaust nozzle pressure (PT6) is an indicator of engine thrust. The engine inputs are fuel flow (WF), nozzle area (AJ), compressor inlet variable guide vane position (CIVV) and rear compressor variable stator vane position (RCVV). (See fig. 4.)

$$(zI + A_1)x_k = B_1 u_k$$

$$(zI + C_1)q_k = e_k$$

$$y_k = x_k + q_k$$

$$y = (N1, N2, PT6)^T$$

$$u = (WF, AJ, CIVV, RCVV)^T$$

Figure 4.- Engine model equations.

The initial values for the A, B, and C matrices of the model were determined from SISO open-loop identification tests performed on an engine simulation. These values were used to start the closed-loop identification procedure. The model structure was taken from a third-order behavioral model developed in Ref. 5. Signal-to-noise ratios were determined from actual closed-loop data. Analysis showed the noise levels to be very low. (See fig. 5.)

- A,B,C Initial Values from Simulation
- Structure from Behavioral Model
- Noise Estimates from Data
  - MVC Data $7<SNR<35$
  - BOM Data $22<SNR<600$

Figure 5.- Engine model definition.

The IV/AML method was originally applied to SISO simulated data to determine initial parameter values. The method was then applied to open-loop MIMO simulated data. From these MIMO tests an additional element of A_1 was found to be necessary to satisfactorily model PT6. Also, the noise model was found to be very close to the plant model. The engine model found from this MIMO test was then used to predict engine behavior based upon actual closed-loop engine data.

The F100 engine was tested in the Lewis Research Center altitude test facility to evaluate the F100 Multivariable Control (MVC) law (Ref. 3). During the same test period the "Bill of Material" (BOM) control was also evaluated as a baseline/backup control mode. Thus, there are a variety of closed-loop operating records obtained throughout the flight envelope with a number of different power input requests. The two multivariable data sets used in this report were recorded at an ALT = 10,000 ft, MN = 0.9 condition as the power request was varied (step change) in a small (hopefully linear) range about intermediate engine power. One set corresponds to an MVC control test, the other to a BOM test. Data were sampled at T = 0.05 sec for 10-second transients, which yields 200 points for each record in the data sets. (See fig. 6.)

- Simulation (Open Loop)
    - SISO
    - MIMO
- Test Data (Closed Loop)
    - BOM Control
    - MVC Control
    - T=.05; 200 Points

Figure 6.- Application of instrumental variable/approximate maximum liklihood method.

Normalized WF from the BOM and MVC control tests is shown in figure 7. This is typical of the engine inputs in these tests. Power spectrum analysis of these inputs shows a slightly higher frequency component in the MVC inputs, although more total power is contained in the BOM inputs. However, for both the BOM and MVC inputs most of the power is concentrated below 6 radians/sec.

Note that these inputs are not persistently exciting.

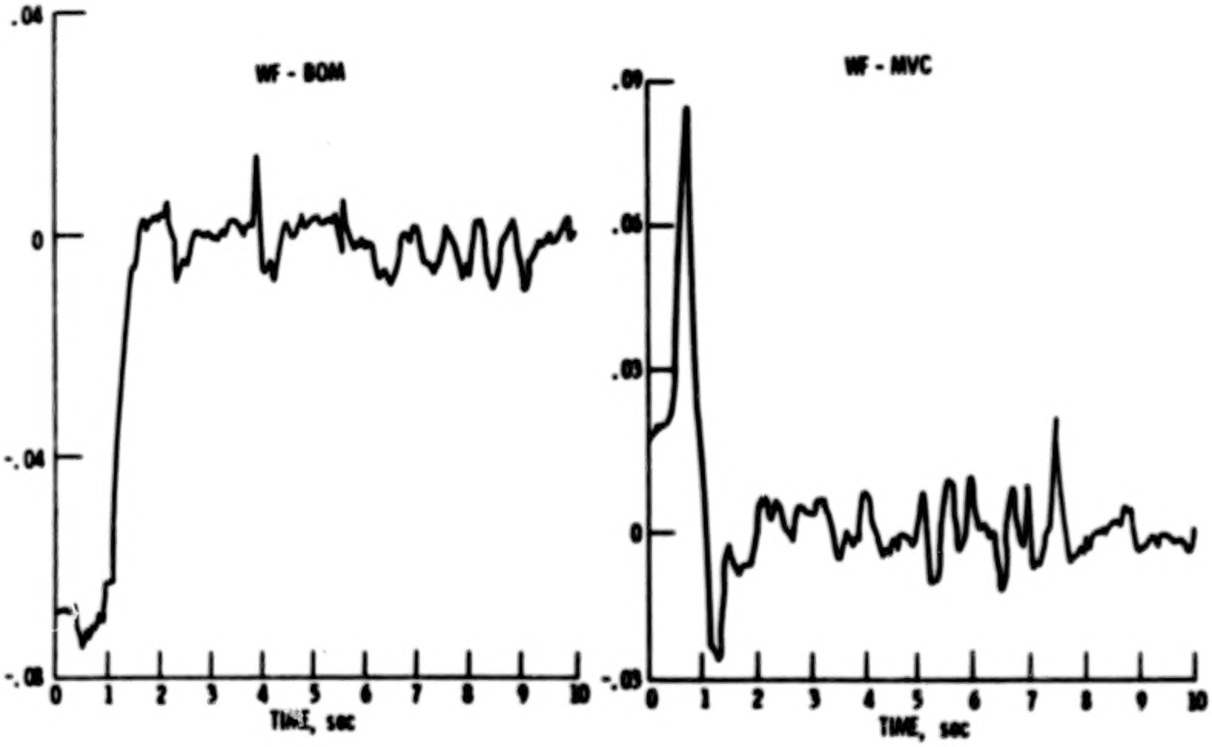

Figure 7.- Typical test inputs.

ORIGINAL PAGE IS
OF POOR QUALITY

The control inputs of figure 7 were used in conjunction with the MIMO model indentified from the simulation (Model 1) to predict engine output.

Comparing the predicted outputs of model 1 with the actual outputs, it was apparent that model 1 was unacceptable. No output was predicted well for either BOM or MVC data. Figure 8 is typical of the comparison. Slight discrepancies between simulation and test data cannot account for large discrepancies between predicted and actual outputs.

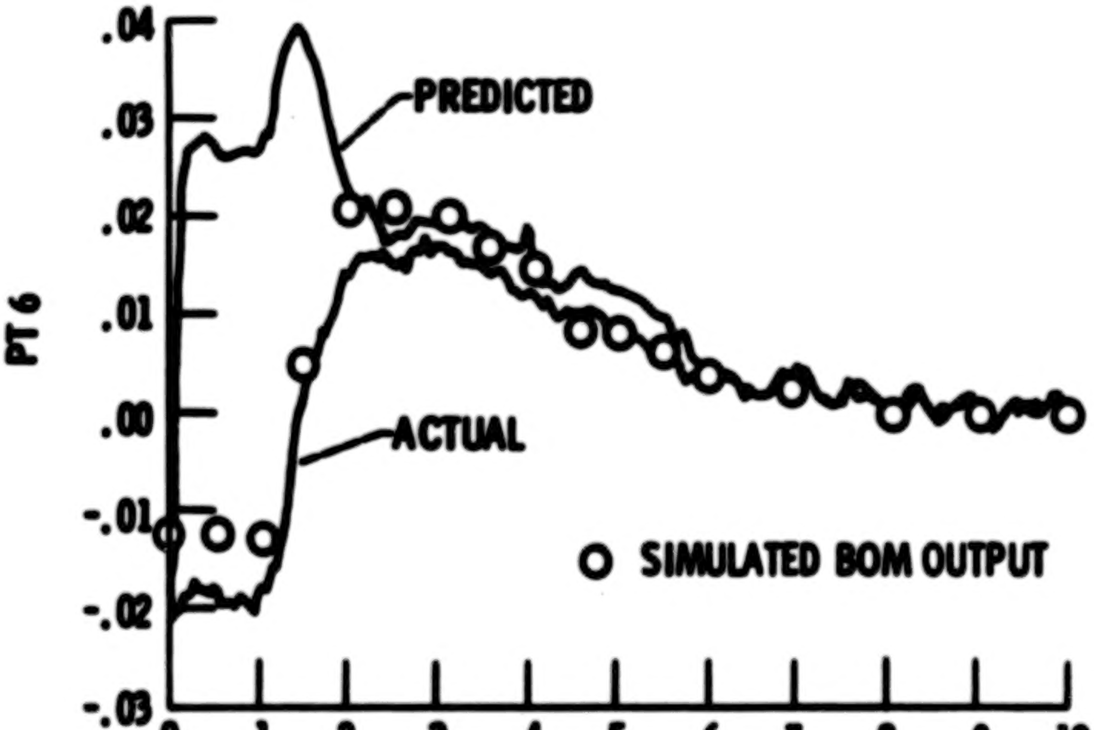

Figure 8.- Identification results for model 1.

To investigate this inability to predict engine response, the IV/AML method was applied directly to the closed-loop data producing models 2 (MVC) and 3 (BOM).

Model 1 was used as a starting point. As illustrated in figure 9, model 3 accurately reproduces the data from which it was generated (BOM). Model 2 results are similar. In fact, the error of all the outputs for models 1, 2, and 3 is less than 1%. However, comparing parameters for models 1, 2, and 3 it can be seen that while A_1 remains essentially unchanged, elements of B_1 do change substantially. This implies a slightly overparameterized model structure which does account for the inability of model 1 to predict BOM and MVC engine data.

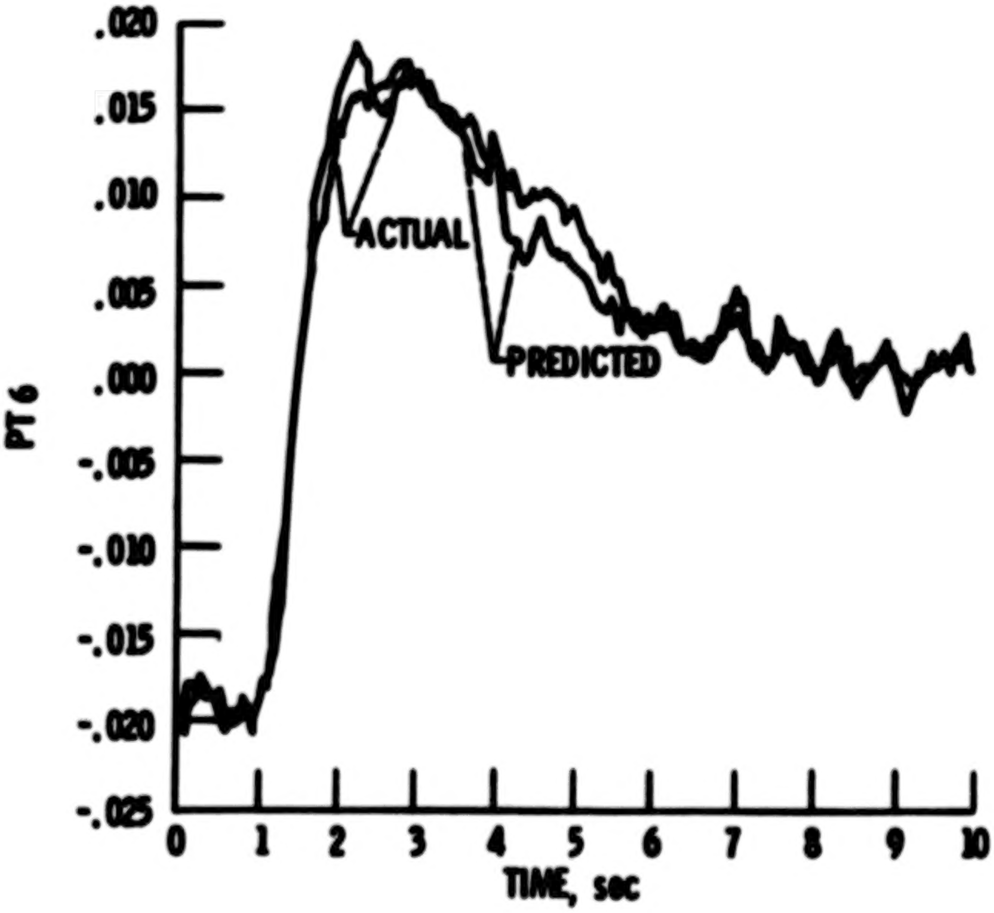

Figure 9.- Identification results for model 3.

A procedure was developed to remove the overparameterization. Three parameters were eliminated and this new structure was applied to the simulation data. The resultant IV/AML identified model is given as model 4. (See fig. 10.)

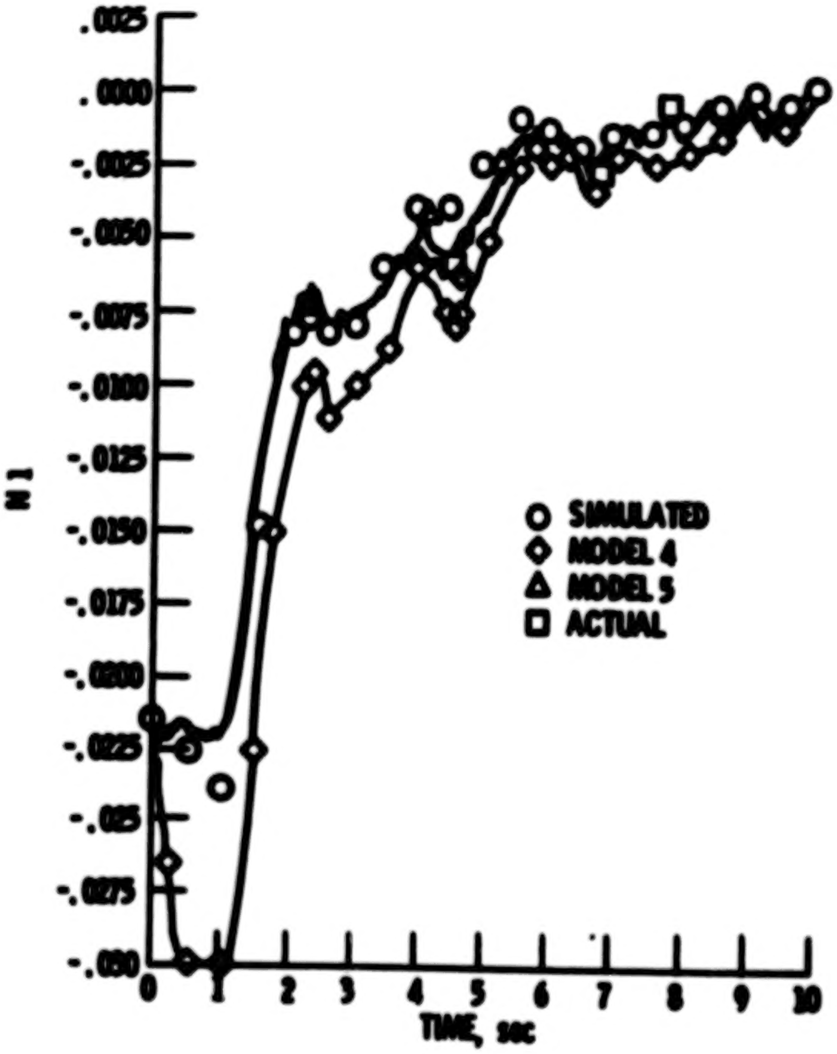

Figure 10.- Identification results for models 4 and 5.

When used to predict BOM and MVC output data, model 4 was still unsatisfactory. Model 4 did predict N1(MVC), N2(MVC), and N2(BOM). However, N1(BOM) and especially PT6 for both data sets were not predicted well. The error in PT6 is somewhat expected from sensor and input bandwidth consideration. The N1(BOM) error was not expected, however. Figure 11 compares predicted N1 data using model 4 to actual closed-loop N1(BOM) data. Model 4 predicted N1 grossly follows the trend of the simulated data. Thus, it appears that the dynamic portion of model 4 is correct. However, there must then be large discrepancies in some of the model 4 gain terms. These discrepancies are somewhat perplexing since model 4 predicted N1(MVC) but not N1(BOM).

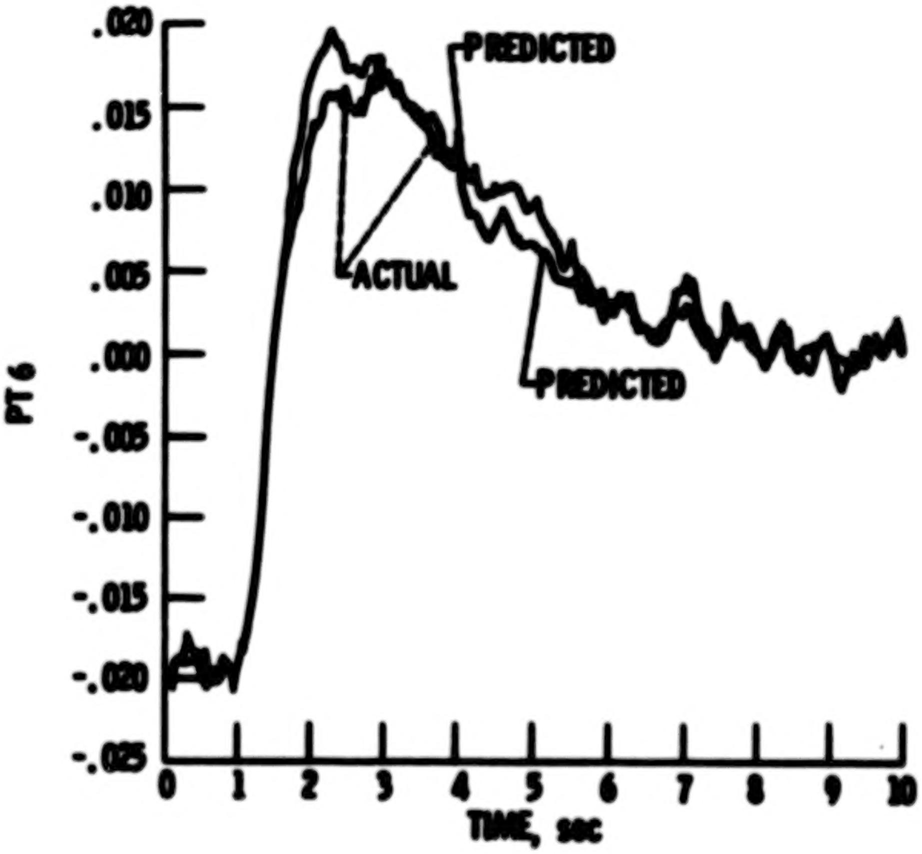

Figure 11.- Identification results for model 5, PT6.

ORIGINAL PAGE IS
OF POOR QUALITY

Recall, however, that the BOM inputs are larger in magnitude than the MVC inputs and that model 4 represents linearized dynamics. Thus, some nonlinear effects may be inherent in the BOM data. This explanation is not entirely satisfactory since N2(BOM) and N2(MVC) were both predicted. Further work to resolve this problem is required. The IV/AML identification method was again utilized to further refine the model parameters for the structure of model 4 using the two sets of experimental closed-loop data. The purpose of this final iteration is to identify a single model that can accurately predict both sets of engine test data and, hopefully, simulation data as well. (See fig. 12.)

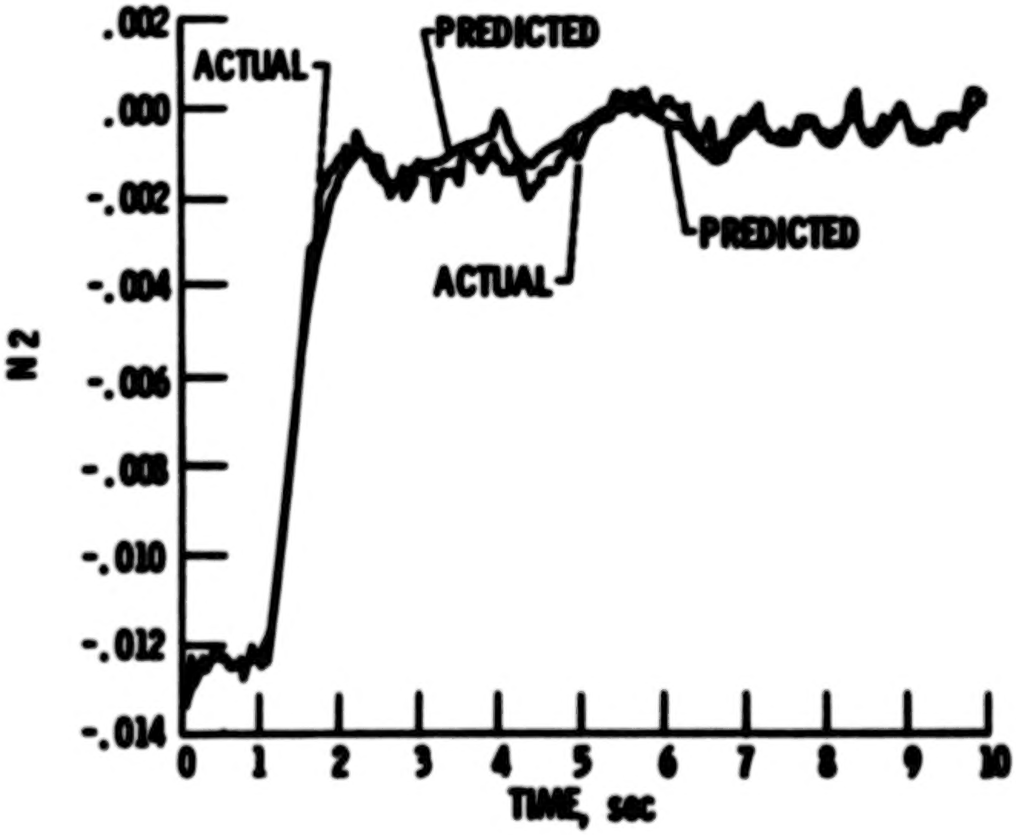

Figure 12.- Identification results for model 5, N2.

Again model 4 was used as an initial condition in the IV/AML method applied to the BOM and MVC data. Models 5 and 6 resulted. Both models 5 and 6 fit their respective data sets quite well. Figures 10 to 12, for example, show a good fit of the BOM data by outputs predicted using model 5. Similar comparisons to MVC data were obtained using model 6. More importantly, when the BOM model 5 is used to predict the MVC data, the comparison given in Figures 13 to 15 is quite reasonable. Thus, model 5 (or equivalently model 6) represents a model which predicts a class of inputs and can be used with confidence in a control design procedure.

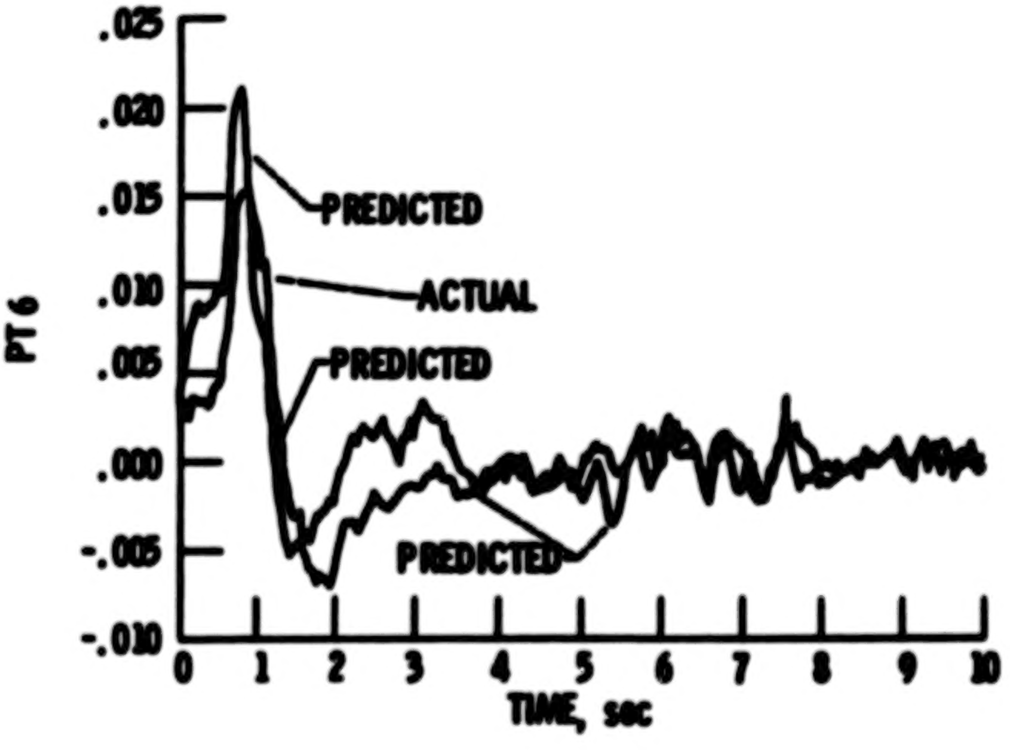

Figure 13.- Identification results for model 5 predicting multivariable control data, PT6.

ORIGINAL PAGE IS
OF POOR QUALITY

The IV/AML method was applied to both open-loop simulation and closed-loop test data of an F100 turbofan engine. The method accurately and consistently identified models from both the simulation and test data. Due to the structure of the BOM and MVC control laws, the engine model is strongly system identifiable and consequently a direct identification approach was used on the closed-loop data.

A third-order model structure was derived and found to be overparameterized. Three parameters were eliminated by sensitivity considerations. The simplified structure was found acceptable for fitting both simulation and test data. Test model accuracy is limited to 6 radians/sec since spectral analysis of the inputs shows limited signal strength above this frequency.

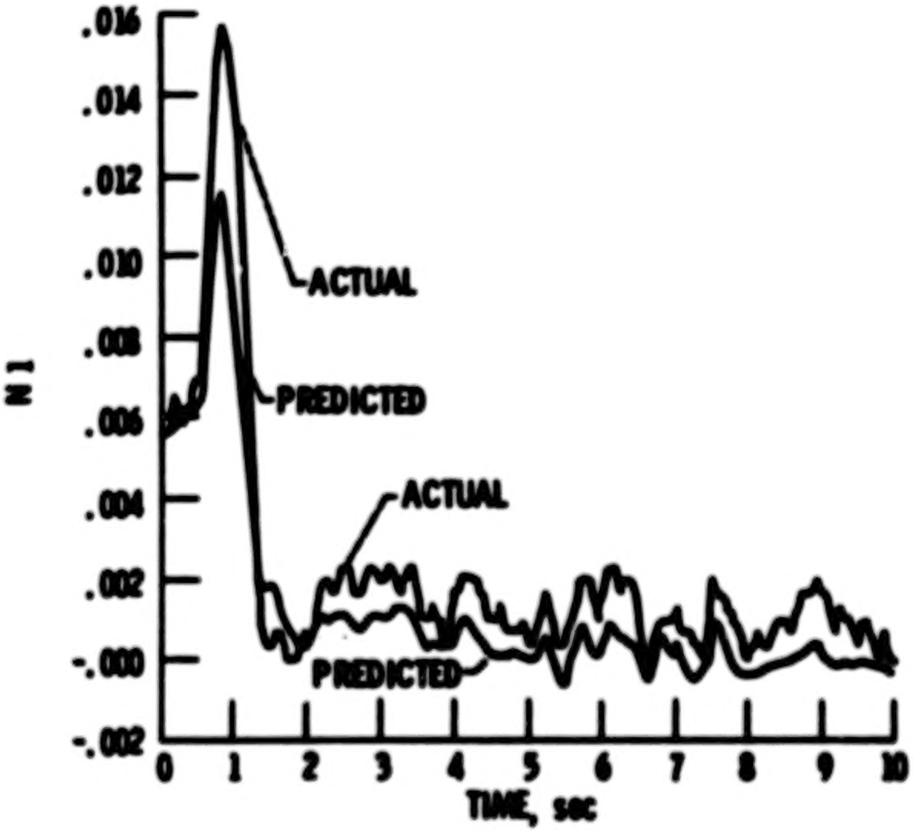

Figure 14.- Identification results for model 5 predicting multivariable control data, N1.

Comparisons showed that models identified from simulated data generally predicted N1(MVC), N2(MVC), and N2(BOM) test response adequately. However, predictions of PT6(MVC) and PT6(BOM) were poor and N1(BOM) showed some discrepancies in dynamics. The PT6 differences are attributed to the low-frequency content of the test input signals (~6 radians/sec), the bandwidth of the sensor, and the high-frequency nature of the PT6 mode. However, the difference in N1 is attributable to a difference in simulated versus actual engine performance. This conclusion is accurately portrayed in a comparison of identified models.

ORIGINAL PAGE IS
OF POOR QUALITY

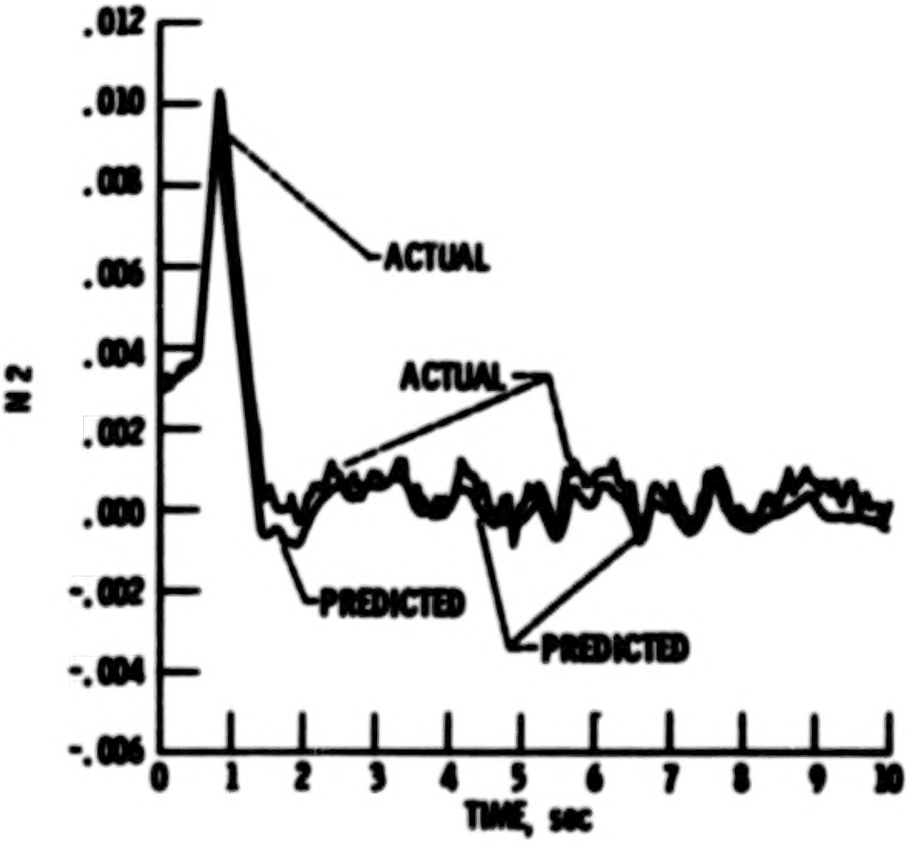

Figure 15.- Identification results for model 5 multivariable control data, N2.

Finally, a simplified model determined from BOM data accurately predicted not only BOM but also MVC test response data. This ability to predict engine performance for a class of inputs generates confidence in controls designed from this model. Thus, it is concluded that useful dynamic engine models can be obtained from closed-loop test data using the IV/AML identification method. This identification technique, then, represents the first step in an automated engine control design process. (See fig. 16.)

- Basic IV/AML Worked Well
- Engine Model is SSI
- Third-Order Model Structure
- Simulation Predicts Test Data
- Models from Simulation do not Predict N1(BOM) and PT6(BOM & MVC)
- BOM Model Predicts MVC Data

Figure 16.- Conclusions.

REFERENCES

1. Soderstrom, T.; Ljung, L.; and Gustavsson, I.: Identifiability Conditions for Linear Multivariable Systems Operating Under Feedback. IEEE Trans. of Autom. Control, Vol. AC-21, No. 6, Dec. 1976, pp. 837-840.

2. Jakeman, A.; and Young, P.: Refined Instrumental Variable Methods of Recursive Time-Series Analysis - Part II, Multivariable Systems. Int. J. Control, Vol. 29, No. 4, 1979, pp. 624-644.

3. Lehtinen, F.K.B; Costakis, W.G.; Soeder, J.F.; and Seldner, K.: Altitude Test of a Multivariable Control System for the F100 Engine. NASA TMS-83367, July 1983.

4. Merrill, W.: Identification of Multivariable High Performance Turbofan Engine Dynamics from Closed-Loop Data. NASA TM 82785, June 1982.

5. DeHoff, R.L.; Hall, W.E., Jr.; Adams, R.J.; and Gupta, N.K.: F100 Multivariable Control Synthesis Program. Vols. I and II, AFAPL-TR-77-35, June 1977. (AD-A052420 and AD-A052346.)

SESSION III

CONTROL SYSTEM DESIGN TECHNIQUES

Jarrell R. Elliott
Session Chairman

N84
20581

UNCLAS

N84 20581

EIGENSPACE DESIGN TECHNIQUES FOR ACTIVE FLUTTER SUPPRESSION

William L. Garrard and Bradley S. Liebst
Dept. of Aerospace Engineering and Mechanics
University of Minnesota
Minneapolis, MN

First Annual NASA Aircraft Controls Workshop
NASA Langley Research Center
Hampton, Virginia
October 25-27, 1983

PRECEDING PAGE BLANK NOT FILMED

OBJECTIVE

The objective of this discussion is to examine the application of eigenspace design techniques to an active flutter suppression system for the DAST ARW-2 research drone. Eigenspace design techniques allow the control system designer to determine feedback gains which place controllable eigenvalues in specified configurations and which shape eigenvectors to achieve desired dynamic response. Eigenspace techniques have been applied to the control of lateral and longitudinal dynamic response of aircraft [1,2]. However, little has been published on the application of eigenspace techniques to aeroelastic control problems.

This discussion will focus primarily on methodology for design of full-state and limited-state (output) feedback controllers. We do not intend to address the significant difficulties associated with the realization of full- and limited-state controllers. Most of the states in aeroelastic control problems are not directly measurable, and some type of dynamic compensator is necessary to convert sensor outputs to control inputs. Compensator design can be accomplished by use of a Kalman filter modified if necessary by the Doyle-Stein procedure for full-state loop transfer function recovery [3], by some other type of observer, or by transfer function matching.

EIGENSPACE DESIGN TECHNIQUES

Eigenspace techniques allow the designer to place closed-loop eigenvalues (λ_i) and shape closed-loop eigenvectors (v_i). We will briefly review the theory. For a more detailed discussion see Refs. 1, 2, and 4. First we assume the system is controllable and observable and the matrices B and C are of full rank. (In the case of full-state feedback, C = I.) Later the controllability assumption will be relaxed. The above assumptions yield the results shown below. If we have full-state feedback and n controls, we can arbitrarily place all eigenvalues and shape all eigenvectors to any desired form. If we have full-state feedback and a single control, only pole placement is possible. Since any attainable eigenvector is in the subspace spanned by $(\lambda I-A)^{-1}B$, it is impossible to exactly achieve a desired eigenvector in most aircraft control problems. In practice this does not appear to be a serious problem.

Uncontrollable eigenvalues cannot be moved but an additional element in each eigenvector associated with these eigenvalues can be shaped.

$$\dot{x} = Ax + Bu$$

$$y = Cx$$

$\text{Dim}(x) = n$

$\text{Dim}(u) = m$

$\text{Dim}(y) = r$

(1) max (m,r) closed-loop eigenvalues can be assigned

(2) max (m,r) closed-loop eigenvectors can be shaped

(3) min (m,r) elements of each eigenvector can be arbitrarily chosen

Attainable eigenvector in space spanned by

$$(I\lambda_i-A)^{-1}B$$

CALCULATION OF GAIN MATRIX-I

We will first describe the eigenspace design technique for full-state feedback for a system described in standard state-space form. The design procedure consists of determining a gain matrix K such that for all closed-loop eigenvalue and eigenvector pairs

$$(A+BK)v_i = \lambda_i v_i$$

where λ_i is the desired closed-loop eigenvector and v_i is the associated closed-loop eigenvector. This is equivalent to finding w_i such that

$$(I\lambda_i - A)\, v_i = Bw_i$$

Once all the w_i's have been found, the gain matrix can be calculated.

In order to arbitrarily place all the λ_i's and v_i's, the control vector will have to be of the same order as the state vector and B would have to be invertible. In general this is not the case, and the achievable eigenvalues must lie in the subspace spanned by

$$(\lambda_i I - A)^{-1}B$$

In general, the desired eigenvector v_i^d will not reside in this subspace.

$$\dot{x} = Ax + Bu$$

$$y = Cx$$

$$u = Ky$$

$$x = \sum_{i=1}^{n} a_i v_i e^{\lambda_i t}$$

$$(A + BK)v_i = \lambda_i v_i$$

$$(I\lambda_i - A)v_i = Bw_i$$

$$v_i = L_i w_i$$

$$L_i = (\lambda_i I - A)^{-1}B$$

$$K = W[CV]^{-1}$$

ORIGINAL PAGE IS
OF POOR QUALITY

CALCULATION OF GAIN MATRIX-II

Since the desired eigenvalues are in general not achievable, the w_i's are selected to minimize the weighted sum of the squares of the difference between the elements of the desired and attainable eigenvectors given by the performance index J_i. The term P_i is a positive definite symmetric matrix whose elements can be chosen to weight the difference between certain elements of the desired and attainable eigenvalues more heavily than others. Setting the derivative of J_i with respect to w_i equal to zero gives w_i. The notation * denotes complex transpose. Once w_i is calculated, the achievable eigenvector v_i is obtained. If an eigensolution is not to be altered, setting $w_i = 0$ assures that the associated v_i and λ_i remain in their open-loop configurations. If we desire output feedback, the procedure is easily modified as shown.

In case of a complex eigenvalue, a real-gain matrix results from a simple transformation [1, 2, 4].

$$J_i = (v_i^d - v_i)^* P_i (v_i^d - v_i)$$

$$\frac{\partial J_i}{\partial w_i} = 0$$

$$w_i = (L_i^* P_i L_i)^{-1} L_i^* P_i v_i^d$$

If an eigensolution is not to be altered,

$$w_i = 0$$

UNCONTROLLABLE EIGENVALUES-I

In aeroelastic control problems, the states associated with the gust model are uncontrollable. Moore [4] showed that it is possible to use feedback to assign some components of eigenvectors associated with uncontrollable eigenvalues. An algorithm for performing such an assignment is given. For an uncontrollable eigenvalue λ_g,

$$[I\lambda_g - A]$$

is singular. We can partition the eigenvector v_g associated with this eigenvalue as shown below where v_g^{II} contains only the uncontrollable states.

λ_g uncontrollable

Partition v_g such that

$$[\lambda_g I - A]v_g = Bw_g$$

Becomes

$$\left[\begin{array}{c|c} I\lambda_g - A^I & Q \\ \hline 0 & R \end{array}\right] \left[\begin{array}{c} v_g^{I} \\ \hline v_g^{II} \end{array}\right] = \left[\begin{array}{c} B^I \\ \hline 0 \end{array}\right] w_g$$

v_g^{II} contains only uncontrollable states

UNCONTROLLABLE EIGENVALUES-II

The equation

$$Rv_g^{II} = 0$$

is automatically satisfied if we select v_g^{II} to be equal to the open-loop portion of v_g which contains the uncontrollable states. Since λ_g is not an eigenvalue of A^I, $[\lambda_g I - A^I]$ is nonsingular, and by performing the indicated calculations, w_g can be determined in much the same way as for the controllable eigenvalues.

$$Rv_g^{II} = 0$$

$$v_g^I = [\lambda_g I - A^I]^{-1} B^I w_g - [\lambda_g I - A^I]^{-1} P v_g^{II}$$

or

$$v_g^I = L_g w_g + \Delta v_g$$

minimizing

$$J_g = (v_g^{Id} - v_g^I)^* P_g (v_g^{Id} - v_g^I)$$

yields

$$w_g = (L_g^* P_g L_g)^{-1} L_g^* P_g (v_g^{Id} - \Delta v_g)$$

DAST ARW-2 FLIGHT TEST VEHICLE

The DAST ARW-2 flight test vehicle shown below is a Firebee II Drone which has been modified by replacing the conventional wing with a high aspect ratio supercritical wing designed to flutter within the flight envelope. Two control surfaces, an inboard and outboard aileron, are available on the wing. Current plans are to use the outboard aileron for flutter control and gust load alleviation and to use the inboard aileron for maneuver load control. Since two control inputs are needed if eigenvector shaping is to be accomplished, it was decided to use both the inboard and outboard control surfaces for flutter control. As will be shown, the inboard aileron is not effective for flutter suppression. However, it is possible to demonstrate eigenspace techniques using this control surface. Research currently in progress uses the elevator for control of rigid-body modes and the outboard aileron for control of flutter. Planned research will incorporate a leading-edge and a trailing-edge surface.

DAST ARW-2 SENSOR AND CONTROL SURFACE LOCATIONS

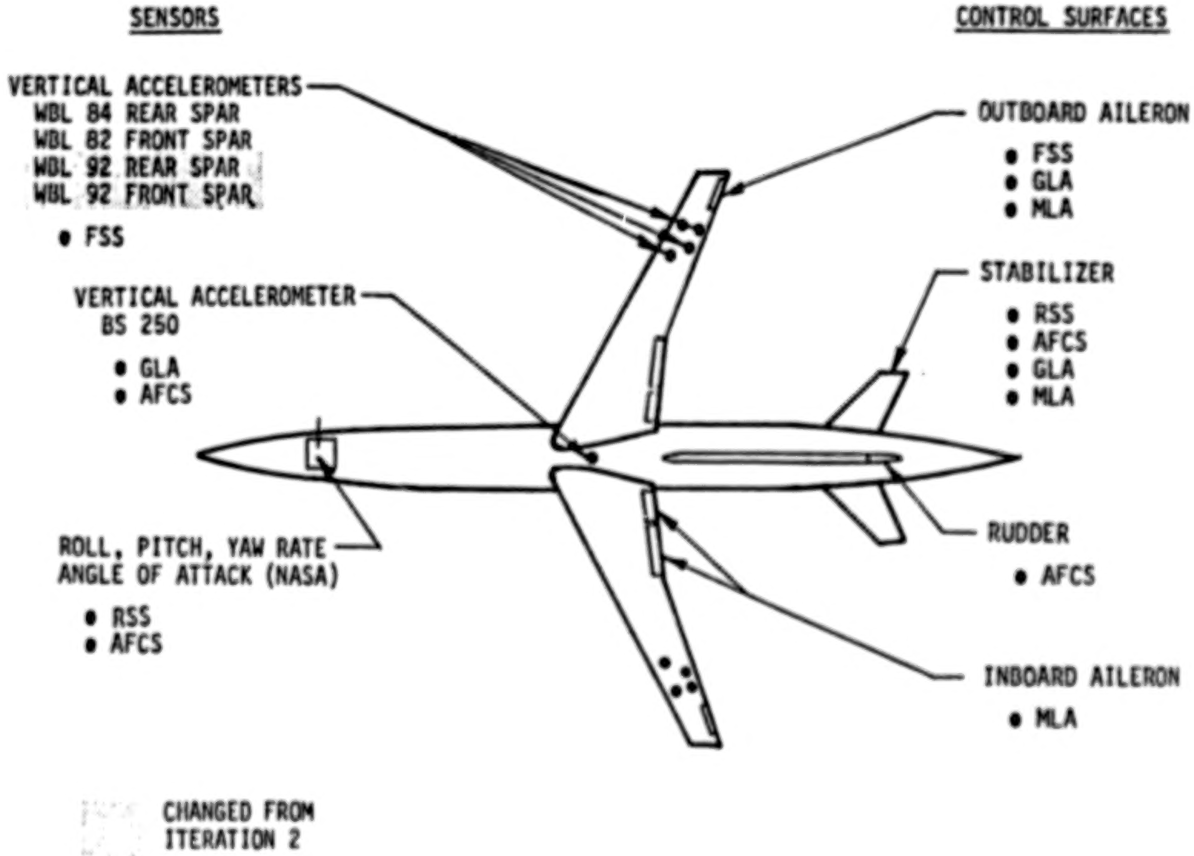
SENSORS
VERTICAL ACCELEROMETERS
WBL 84 REAR SPAR
WBL 82 FRONT SPAR
WBL 92 REAR SPAR
WBL 92 FRONT SPAR
• FSS
VERTICAL ACCELEROMETER
BS 250
• GLA
• AFCS
ROLL, PITCH, YAW RATE
ANGLE OF ATTACK (NASA)
• RSS
• AFCS
CONTROL SURFACES
OUTBOARD AILERON
• FSS
• GLA
• MLA
STABILIZER
• RSS
• AFCS
• GLA
• MLA
RUDDER
• AFCS
INBOARD AILERON
• MLA
CHANGED FROM
ITERATION 2

PERFORMANCE SPECIFICATIONS

The design flight condition for the flutter control system is $M=0.86$ (275 m/s or 908 ft/s) and an altitude of 15000 ft (475 m). At this flight condition, the uncontrolled wing flutters, and the flutter control system is required to stabilize the wing without exceeding specified limits on rms control surface activity. The control surfaces saturate if these limits are exceeded. Gain and phase margins must be adequate. The wing flutters at $M=0.75$ at this altitude, and the flutter control system must be activated at $M=0.7$. It must be verified that activation of the control system does not destabilize the wing at this flight condition. Also the flutter controller must not result in excessive increases in bending, shear, or torsional loads compared with the uncontrolled wing.

Design Condition

$M = 0.86$ $h = 15000$ ft.

Maximum RMS Control Surface Activity for 12 ft/s Gust

	Deflection	Deflection Rate
Inboard	10°	130°/s
Outboard	15°	740°/s

Mininum Stability Margins

Gain - 6 dB

Phase - 45°

No large increases in bending, torsion, and shear at $M = 0.7$

AEROELASTIC MODEL

In the aeroelastic model of the wing given below, y_f is the vector of displacements of the various flexural modes, y_c is the vector of control surface deflections, y_g is the gust velocity, M_s is the structural mass matrix, C_s is the structural damping matrix, K_s is the structural stiffness matrix, q is dynamic pressure, and Q_c is the matrix of aerodynamic influence coefficients. Q_c is calculated as a function of reduced frequency by a doublet-lattice procedure and is approximated by Q_A, a matrix of rational polynomials in the Laplace operator s. The matrices A_i are selected to give the best least-squares fit to Q_c over a range of reduced frequencies.

$$([M_s]s^2 + [C_s]s + [K_s])\ [y_f] + q[Q_c(s)]\begin{bmatrix} y_f \\ y_c \\ y_g \end{bmatrix} = 0$$

$$[Q_c(s)] \simeq [A_0] + [A_1]\frac{cs}{2v} + [A_2]\left[\frac{cs}{2v}\right]^2 + \sum_{m=1}^{L} \frac{[A_{m+2}]s}{s+\frac{2v}{c}K_m}$$

FLEXURAL MODES

Initially, seven structural modes were used in the math model of the wing; however, by comparing eigenvalues calculated using lower order models with eigenvalues resulting from a model which included seven structural modes, it was found that flutter could accurately be modeled by including only three modes. These modes are shown below. The first mode will be labeled first mode bending, the second mode will be labeled second mode bending although it contains some torsion, and the third mode will be labeled first mode torsion. Rigid-body modes were not included.

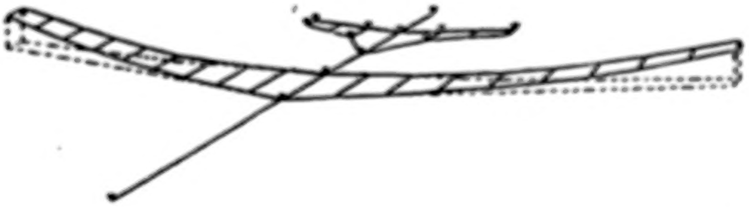

First Bending

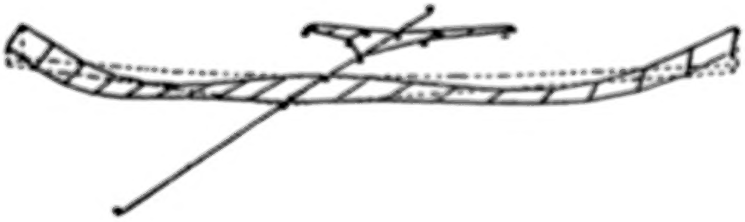

Second Bending

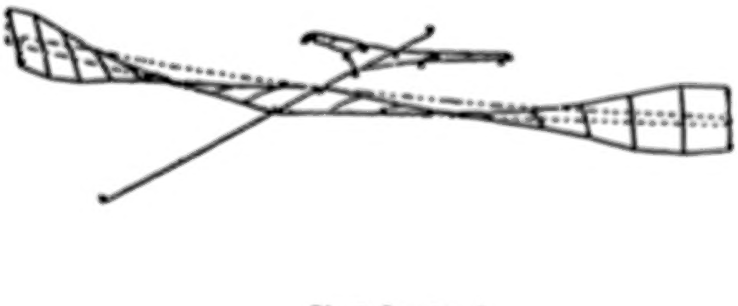

First Torsional

ORIGINAL PAGE IS
OF POOR QUALITY

OPEN-LOOP ROOT LOCUS

The locus of the roots associated with the flexure modes is shown below. The lowest frequency mode is associated with first mode bending, the next highest with second mode bending and the highest with first mode torsion. It can be seen that first mode bending is the unstable mode while second mode damping increases with velocity. The frequencies of these modes approach one another with increasing velocity. The first torsion mode is not affected by velocity as much as the other two modes, but it is necessary to include this mode in order for the system to flutter. The wing flutters at a velocity of 787 ft/s (240 m/s). This is about Mach 0.75.

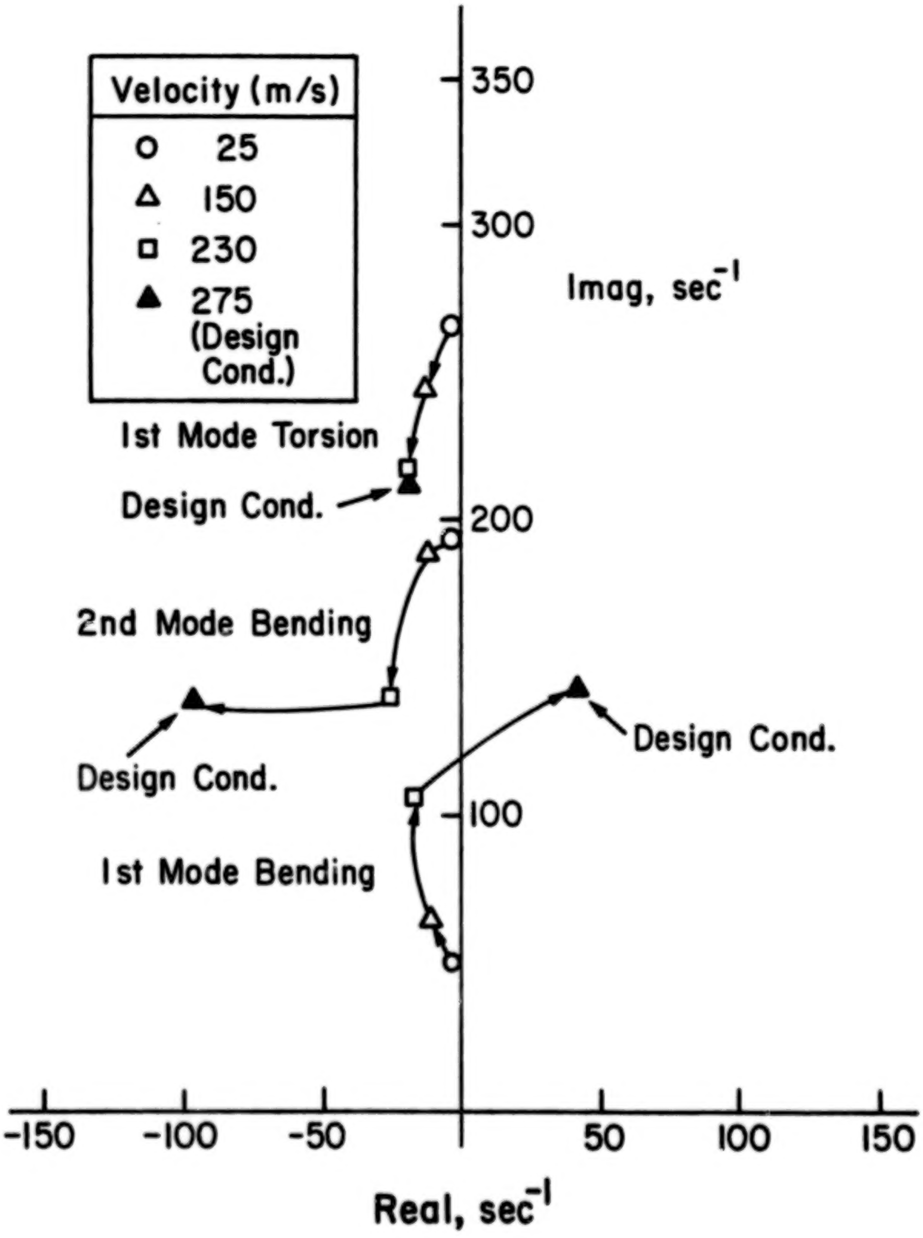

WIND GUST AND ACTUATOR MODELS
AND STATE SPACE FORMULATION

A second-order model forced by white noise was used to simulate the vertical gust. Both inboard and outboard ailerons are driven by high bandwidth actuators. In the range of frequencies covered by the three-mode structural model, a fourth-order transfer function was shown to give a very close approximation of the actual inboard actuator/aileron transfer function. A third-order transfer function was used for the outboard aileron. The details of these models are given in Ref. 5. The state space model of the combined system is given below. The vector X_F includes the displacements and velocities associated with flexure modes and the aerodynamic lag states. The vector X_c includes the states associated with the inboard and outboard actuator models. The vector X_g includes the states associated with the gust model. The vector U is the control input to the actuators, and w is the scalar white noise input to the gust model. The total system model is 18th order. Note that the open-loop responses of the actuators are decoupled from one another and are not influenced by the motion of the wing (small inertial cross-coupling terms have been neglected) and that the gust states are uncontrollable.

$$y_g/w = G_g(s)$$

$$y_{c_i}/u_i = G_i(s)$$

$$y_{c_o}/u_o = G_o(s)$$

$$\begin{bmatrix} \dot{X}_F \\ \dot{X}_c \\ \dot{X}_g \end{bmatrix} = \begin{bmatrix} A_{11} & A_{12} & A_{13} \\ 0 & A_{22} & 0 \\ 0 & 0 & A_{33} \end{bmatrix} \begin{bmatrix} X_F \\ X_c \\ X_g \end{bmatrix} + \begin{bmatrix} 0 \\ B \\ 0 \end{bmatrix} U_c + \begin{bmatrix} 0 \\ 0 \\ G \end{bmatrix} w$$

EIGENSPACE DESIGN APPROACHES

The initial eigenspace controller was designed by rotating the unstable eigenvalues about the imaginary axis and leaving all other eigenvalues and eigenvectors in their open-loop positions. The results are shown in the table on the following page. Although this initial design stabilized the wing at both the flutter test condition (M=0.86) and at the condition at which the flutter controller would be initially activated (M=0.7), the rms inboard deflection rate is near its maximum (saturation) value at the flutter condition. It was felt that the performance might be enhanced by redesign of the control system to reduce the inboard deflection rate. Also the initial design approach did not use the capability of eigenspace techniques to shape eigenvectors as well as assign eigenvalues, and it was desired to exercise this capability. Since the aircraft exhibits satisfactory response at velocities less than the flutter speed, it was decided to force the closed-loop response of the wing at the design condition to approach the open-loop response of the wing at a velocity 656 ft/s (20% less than the flutter speed). The closed-loop eigenvalues associated with the flexure modes and aerodynamic lag states were moved to their open-loop positions at 656 ft/s. The open-loop actuator eigenvalues were the same for both flight conditions and were not moved, and the gust eigenvalues were uncontrollable and could not be moved. The desired eigenvectors were selected to be the open-loop eigenvectors of the wing at 656 ft/s. The weighting matrices in the performance index were initially set at one. This procedure reduced all surface activity only slightly. It was decided to use eigenvector shaping to shift control surface activity from the inboard to the outboard actuator. The components of the open-loop aeroelastic eigenvectors in the actuator directions are zero for all flight conditions. Since the desired eigenvectors were chosen to be the open eigenvectors, penalizing the difference between the achievable and desired aeroelastic eigenvectors in the direction of the inboard actuator would reduce inboard activity. This was accomplished by increasing the weights on these components to 2.5×10^3 while all other weights remained at one. The results are shown in the table on the following page.

COMPARISON OF RMS CONTROL SURFACE ACTIVITY FOR THE EIGENSPACE CONTROLLERS

The performance of the initial and final eigenspace controllers is summarized in the table below. The inboard actuator rate for the initial eigenspace design is almost saturated while, with eigenvector shaping, the control effort is shifted from the inboard to the outboard control surface. Failure of both the inboard and outboard aileron was simulated. When the inboard actuator failed, performance was not affected very much; however, failure of the outboard actuator resulted in an unstable response. This indicates that the inboard actuator is not a good choice for use in flutter suppression.

Controller Design	Inbd Defl	Inbd Rate	Outbd Defl	Outbd Rate
Unstable Roots Rotated About Imag Axis (Initial Design)	0.5	108.0	3.3	509.0
Eigenvector Shaping to Reduce Inbd Rate (Final Design)	0.9	86.0	4.7	612.0
Initial Design Inbd Failed	-	-	3.5	519.0
Final Design Inbd Failed	-	-	4.4	572.0
Max Allowable	10	130	15	740

CLOSED-LOOP ROOT LOCUS

The root locus of the aeroelastic modes for the final eigenspace design is shown below. The wing goes unstable at about 1017 ft/s (M=0.96). The open-loop flutter speed is 787 ft/s (M=0.75); therefore, the control system results in an increase in flutter speed of about 29%. As in the open-loop case, the first bending mode goes unstable, but in the closed-loop case, the eigenvalues associated with this mode move to the real axis where one real root goes unstable. The roots associated with the second bending mode are almost unstable at this velocity.

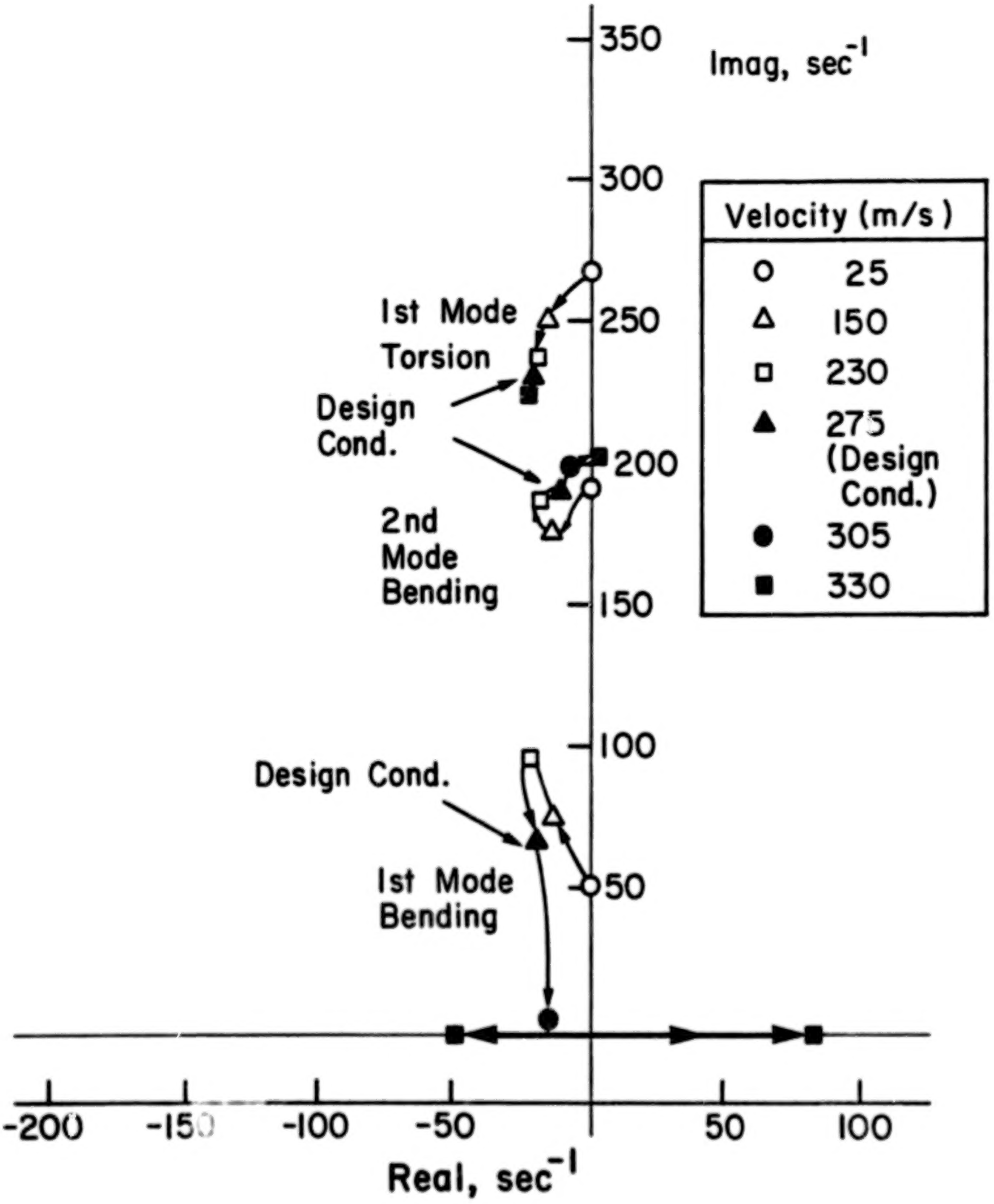

FLUTTER BOUNDARY

The results of varying altitude while maintaining Mach number constant are used to define the flutter boundary for the open-loop wing and the wing controlled with the final eigenspace design. At M=0.86, the uncontrolled wing is unstable until an altitude of 6700 m is reached. At the same Mach number, the controlled wing is stable for altitudes above 2900 m. At M=0.7, the uncontrolled wing is stable for altitudes above 1800 m, whereas the controlled wing is stable for altitudes above 2100 m.

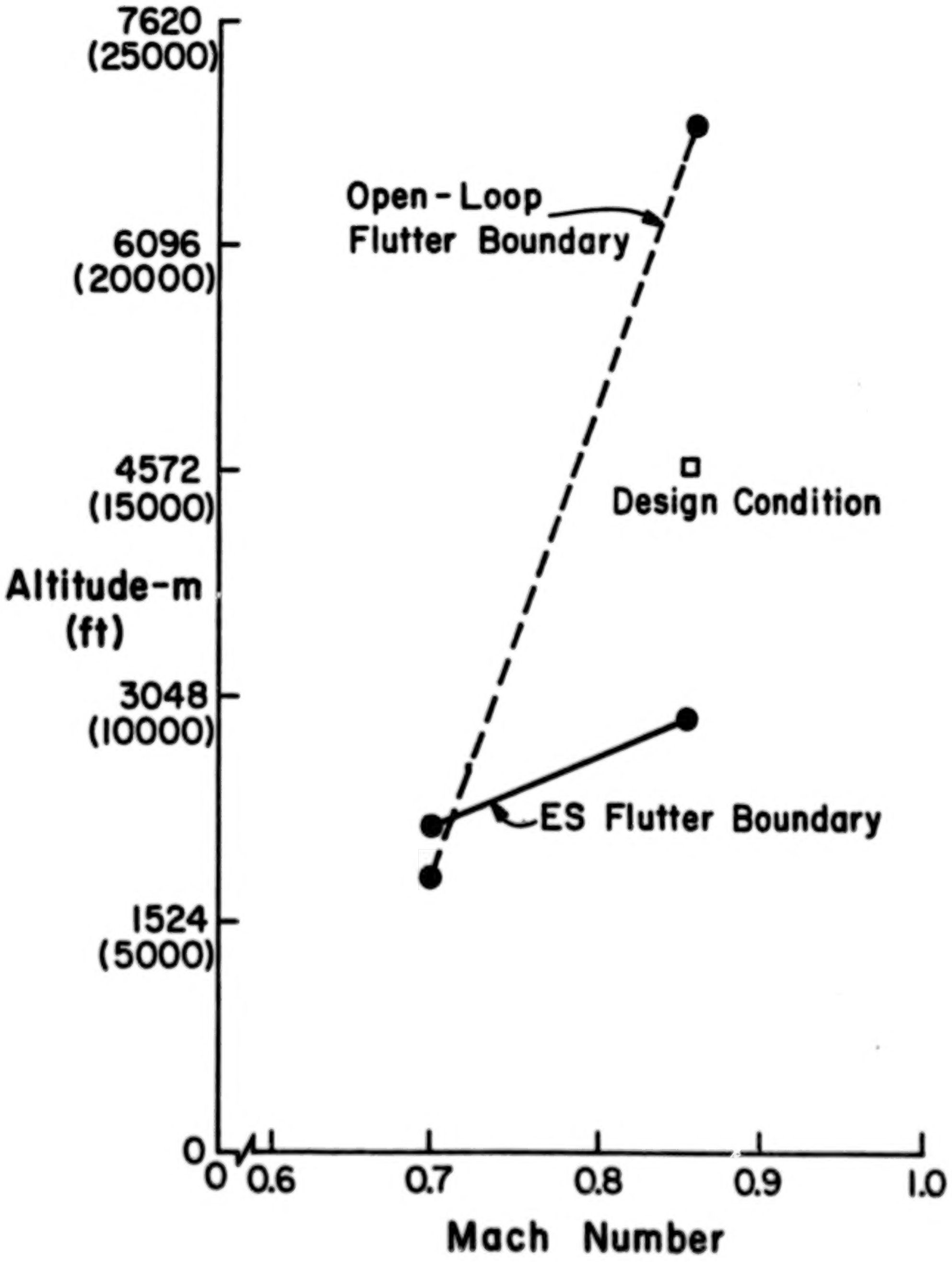

STABILITY MARGINS

Since the inboard aileron was ineffective in stabilizing the wing, and the outboard aileron is critical, stability margins with only the outboard loop closed are shown below. The initial eigenspace design results from rotating the unstable eigenvalues about the imaginary axis and, with the inboard aileron inactive, this is identical to a design resulting from linear quadratic regulator theory. This is guaranteed to have excellent stability margins (Ref. 6). The gain margin is 6 dB, and phase margins are greater than 60°. The frequency response characteristics of the final eigenspace design are considerably different from those of the initial design. Gain margins are 6 dB or better, but phase margins are less than 20°. The solid lines represent the initial eigenspace design, and the dotted lines represent the final eigenspace design.

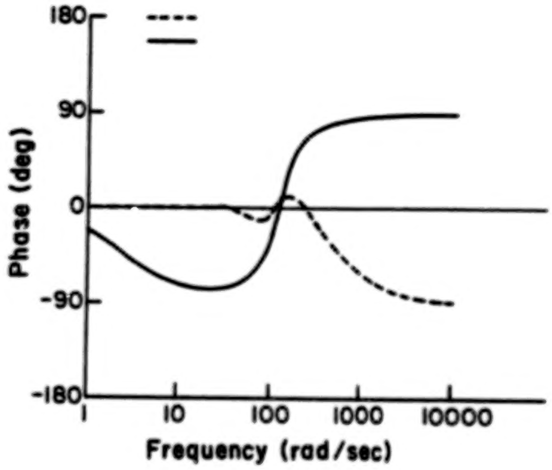

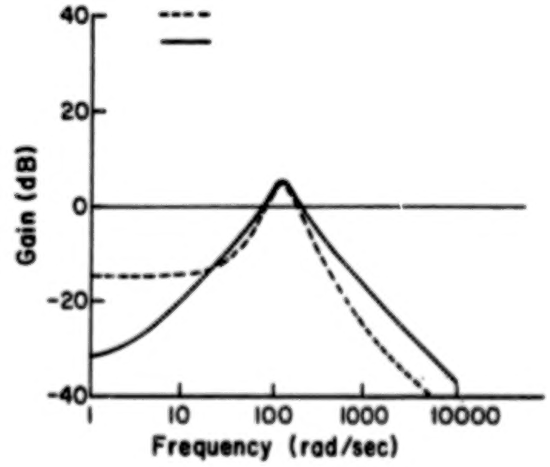

OUTPUT FEEDBACK

Since the inboard actuator was ineffective for flutter control, it was eliminated from the design. This resulted in a system with a single control input and allowed only eigenvalue assignment. An accelerometer was used to measure the motion of the wing, and a feedback compensator that approximated the frequency response characteristics of the full-state loop transfer function was designed. Also the effects of restricting the number of states in the feedback controller were investigated. The design approach was to treat this as a problem in output feedback as described earlier. The C matrix was selected to eliminate various states from the output, and a feedback controller was designed using eigenvalue placement techniques. Since the gust states are uncontrollable if P states are fed back, only P-2 eigenvalues could be placed. The following sets of states were eliminated from being fed back: (a) gust (2 states), (b) aerodynamic lags (3 states), (c) actuator (3 states), (d) first bending (2 states), (e) second bending (2 states), (f) first torsion (2 states), and (g) first torsion and aerodynamic lags (5 states). Except in the case where the first bending mode was eliminated, unstable eigenvalues were rotated about the imaginary axis, and eigenvalues associated with the retained states were maintained in their open-loop positions. The positions of the other eigenvalues were not assigned. Since the eigenvalues of the first bending mode were unstable, these eigenvalues were rotated, and the eigenvalues of the first torsional mode were not assigned. This mode then went unstable. The results are summarized below. The rms response was very sensitive to the gust states, and attempts to remove these states or alter their eigenvectors resulted in large rms responses. Loads at the wing root were reduced using the full-state design. Note a slightly different gust model was used so the rms results below are not directly comparable with those presented earlier.

States Eliminated	Otbd Defl	Otbd Rate	Gain Margin Db	Phase Margin (Degrees)
Gust	32	456	6.0	±60
Actuators	2.0	265	4.1	±36
Aero. Lags	6.6	394	5.7	-50,60
Mode 1	Unstable	Unstable	Unstable	Unstable
Mode 2	2.0	260	2.8	-27,18
Mode 3	2.0	271	5.8	-63,+54
Mode 3 + Aero. Lags	6.6	430.0	6.1	-54,+72 +81,+45
Full State	2.0	259	6	±60
Compensator	2.72	250.8	6.0	±60

RMS Responses M = .86

ORIGINAL PAGE IS
OF POOR QUALITY

CONCLUSIONS

Eigenspace techniques can provide a powerful tool for the design of feedback control systems for aircraft. The design techniques described in this paper are easily implemented and are computationally inexpensive. The basic problems facing the designer are those of determining where to place eigenvalues and of selecting appropriate eigenvectors. This usually requires some insight into the system to be controlled; however, in this respect all control system design techniques are the same. Stability margins must be carefully examined since there are no guaranteed margins as is the case for linear quadratic regulators. On the other hand, modal decoupling is easily achieved, and certain roots can be maintained in their open-loop configurations if desired. Output or limited-state controllers can easily be designed.

	Shear ($lbs \times 10^2$)	Torsion ($in - lbs \times 10^2$)	Bending ($in - lbs \times 10^4$)
Open Loop	4.131	6.928	2.365
Closed Loop	3.775	1.029	2.321

Wing Root Loads M = 0.7

REFERENCES

1. Andry, A. N., Shapiro, E. Y., and Chung, J. C., "On Eigenstructure Assignment for Linear Systems," IEEE Trans Aerospace and Electronic Systems, vol. 19, no. 5, Sept. 1983, pp. 711-729.

2. Cunningham, T. B., "Eigenspace Selection Procedures for Closed Loop Response Shaping with Modal Control," Proceedings IEEE Conference on Decision and Control, vol. 1, Dec. 1980, pp. 178-186.

3. Doyle, J. C., and Stein, G., "Multivariable Feedback Design: Concepts for a Classical/Modern Synthesis," IEEE Trans Auto. Control, vol. AC-26, no. 1, Feb. 1981, pp. 4-18.

4. Moore, B. C., "On the Flexibility Offered by Full-State Feedback in Multivariable Systems Beyond Closed Loop Eigenvalue Assignment," IEEE Trans Auto. Control, vol. AC-21, Oct. 1976, pp. 682-691.

5. Garrard, W. L., and Liebst, B. S., "Active Flutter Suppression Using Eigenspace and Linear Quadratic Design Techniques," Proceedings AIAA Guidance and Control Conference, Aug. 1983, pp. 423-431.

6. Safanov, M. G., and Athans, M., "Gain and Phase Margins of Multi-Loop LQG Regulators," IEEE Trans Auto. Control, vol. AC-22, no. 2, April 1977, pp. 173-179.

N84
20582

UNCLAS

N84 20582

TOOLS FOR ACTIVE CONTROL SYSTEM DESIGN

William M. Adams, Jr., Sherwood H. Tiffany,
and Jerry R. Newsom
NASA Langley Research Center
Hampton, Virginia

First Annual NASA Aircraft Controls Workshop
NASA Langley Research Center
Hampton, Virginia
October 25-27, 1983

PRECEDING PAGE BLANK NOT FILMED

RESEARCH OBJECTIVES

The objective of the research reported here is to develop efficient control law analysis and design tools which properly account for the interaction of flexible structures, unsteady aerodynamics and active controls. The next two figures indicate how such tools can be employed to incorporate active controls into the aircraft design process.

DEVELOPMENT. APPLICATION. VALIDATION AND DOCUMENTATION OF EFFICIENT MULTIDISCIPLINARY COMPUTER PROGRAMS FOR ANALYSIS AND DESIGN OF ACTIVE CONTROL LAWS

UTOPIAN DESIGN PROCESS

The optimum airplane for a given mission can only be achieved when full advantage is taken of the economic and/or performance benefits that are achievable from each discipline. One could argue that these benefits can best be realized when the design variables from each discipline are varied simultaneously in the search for an optimum design. Currently, however, the process is to perform the optimization separately, but not independently, in each discipline. A given discipline, e.g. aerodynamics, may relax certain design criteria and assume that other disciplines, e.g. structures and controls, can make up deficits in stability, safety margins, etc., that result.

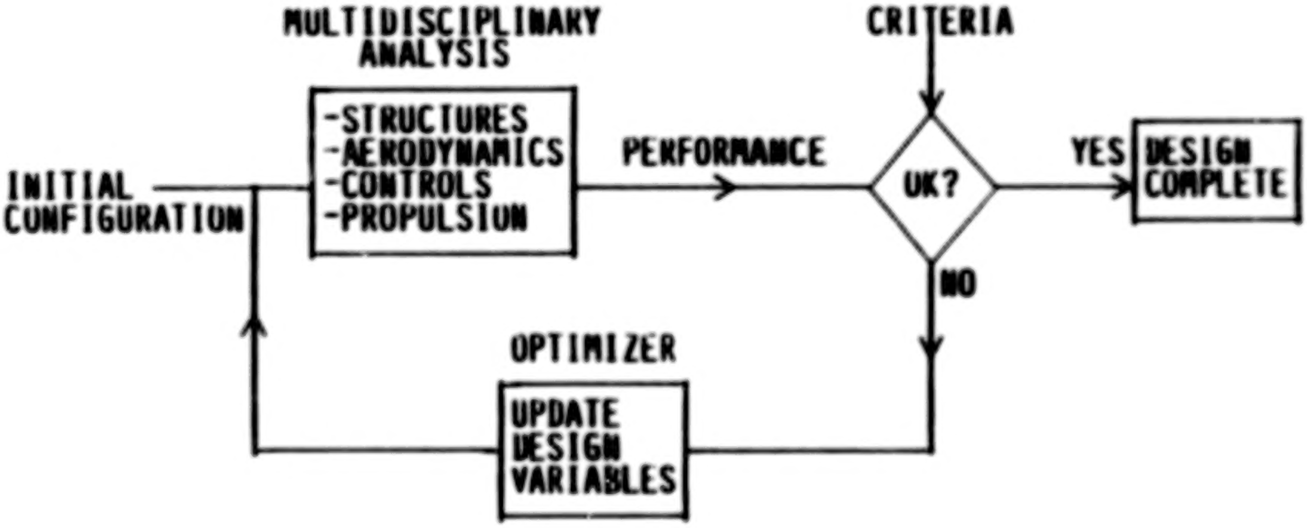
MULTIDISCIPLINARY ANALYSIS
CRITERIA
-STRUCTURES
-AERODYNAMICS
-CONTROLS
-PROPULSION
PERFORMANCE
OK?
YES
DESIGN COMPLETE
INITIAL CONFIGURATION
NO
OPTIMIZER
UPDATE DESIGN VARIABLES

PRESENT CONTROL LAW DESIGN PROCESS

ORIGINAL PAGE IS
OF POOR QUALITY

The following diagram illustrates the current active control law design process. Fixed models are received from the structures and aerodynamic disciplines. These models may have been purposely designed with deficits in stability, strength and flutter margins. The controls specialists initially determine an estimate of the control law that is required to remove the deficits. An iterative process is then initiated to refine the control law to remove the deficits while satisfying robustness, control power and other criteria. If the design criteria cannot be met, or if they can easily be satisfied, the other disciplines repeat their portion of the design process with appropriately modified design criteria and supply the controls discipline with updated models. This process is repeated until it converges upon an optimum design. The remainder of the paper will describe techniques for obtaining initial estimates of the control laws, performing aeroelastic analyses and optimizing the control laws subject to specified design criteria.

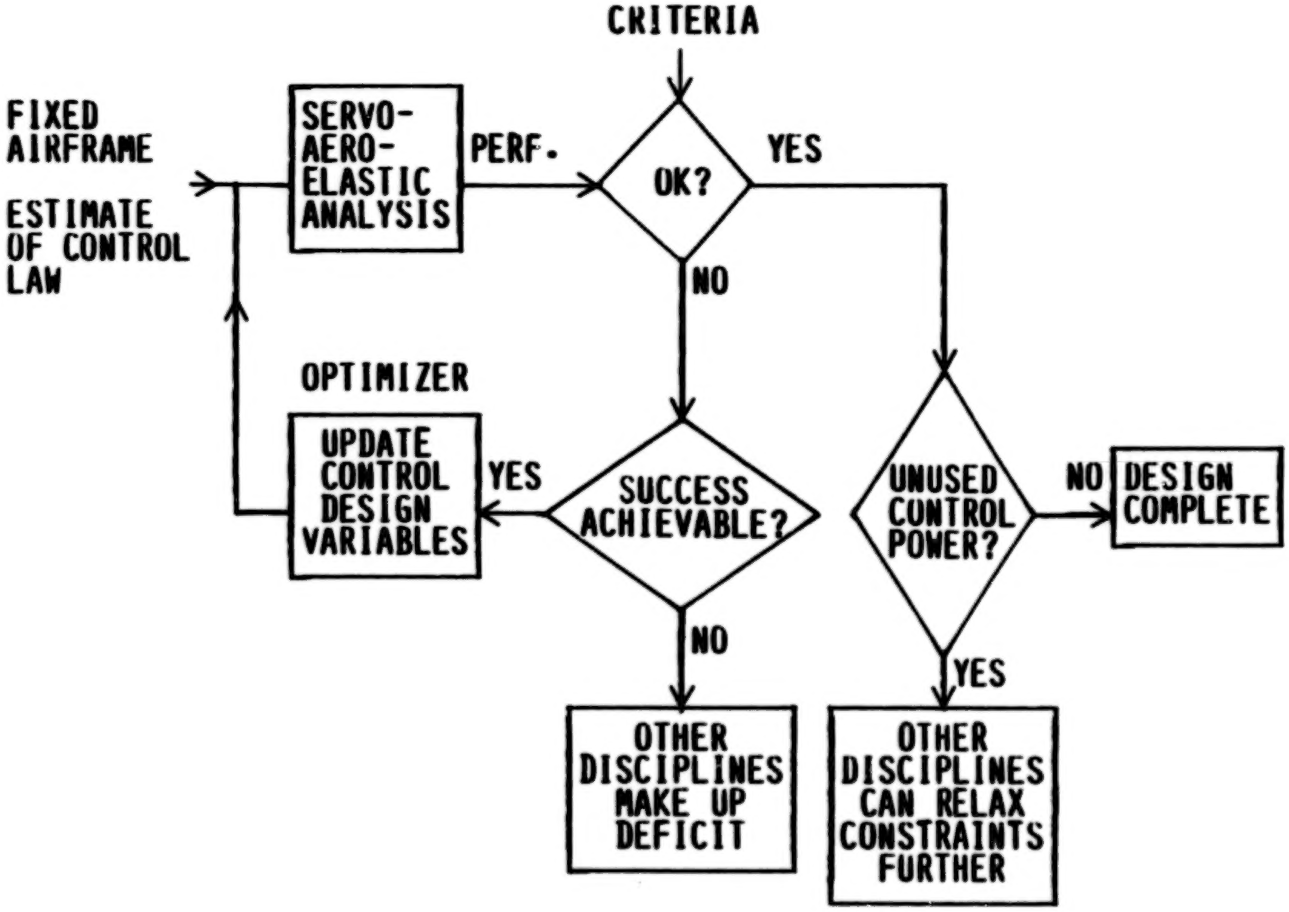
CRITERIA
FIXED AIRFRAME
ESTIMATE OF CONTROL LAW
SERVO-AERO-ELASTIC ANALYSIS
PERF.
OK?
YES
NO
OPTIMIZER
UPDATE CONTROL DESIGN VARIABLES
YES
SUCCESS ACHIEVABLE?
NO
OTHER DISCIPLINES MAKE UP DEFICIT
UNUSED CONTROL POWER?
NO
DESIGN COMPLETE
YES
OTHER DISCIPLINES CAN RELAX CONSTRAINTS FURTHER

C-4

ANALYSIS TOOLS

Efficient tools for the analysis of stability and response characteristics of aeroelastic vehicles are necessary before active control law design can be contemplated. Such tools must properly consider the interactions between flexible structures, unsteady aerodynamics and active control systems. Several computer programs were developed in the 1970's either by NASA or under NASA sponsorship. DYLOFLEX is an integrated system of stand-alone computer programs which was developed primarily to perform dynamic loads analyses of flexible airplanes with active controls (ref. 1); it also has stability analysis capability. DYLOFLEX was developed under contract by the Boeing Company and is available from COSMIC (Computer Software Management and Information Center). Several years ago an aeroelastic capability was incorporated into NASTRAN by the MacNeal-Schwendler Corporation (ref. 2). This addition gave NASTRAN the capability to compute unsteady aerodynamic forces and stability and dynamic response characteristics of aeroelastic vehicles with active controls. NASTRAN is available from COSMIC. The aerodynamic forces are expressed in transcendental form in both DYLOFLEX and NASTRAN. Consequently, the equations of motion are not in a form that can be used in linear system analysis. One final tool, ISAC, developed at Langley (ref. 3) is described in more detail on the next chart.

o DYLOFLEX (DYNAMIC LOADS OF FLEXIBLE STRUCTURES WITH ACTIVE CONTROLS)

o NASTRAN (NASA STRUCTURAL ANALYSIS PROGRAM)

o ISAC (INTERACTION OF STRUCTURES AERODYNAMICS AND CONTROLS)

Flexible structures are represented in ISAC in terms of a modal characterization that is input from an external source such as NASTRAN. Unsteady aerodynamic forces can be either accepted as input or computed internally using a doublet lattice code (ref. 4). An option is included to make a rational s-plane approximation to the unsteady aerodynamic forces (ref. 5). This allows the equations of motion to be written in time-invariant state space form amenable to linear systems analysis and design techniques (refs. 5,6). Stability and dynamic response calculations can be made and displayed graphically that include the effects of sensor dynamics, actuator dynamics and multi-input/multi-output control laws. The ISAC program is operable in either a batch or an interactive mode. Its use is greatly facilitated by the presence of a data complex and data complex manager for reading, writing, storing, and cataloging of data. The ISAC program is regularly used in NASA Langley-related research. It is partially documented and has been distributed to several users outside Langley.

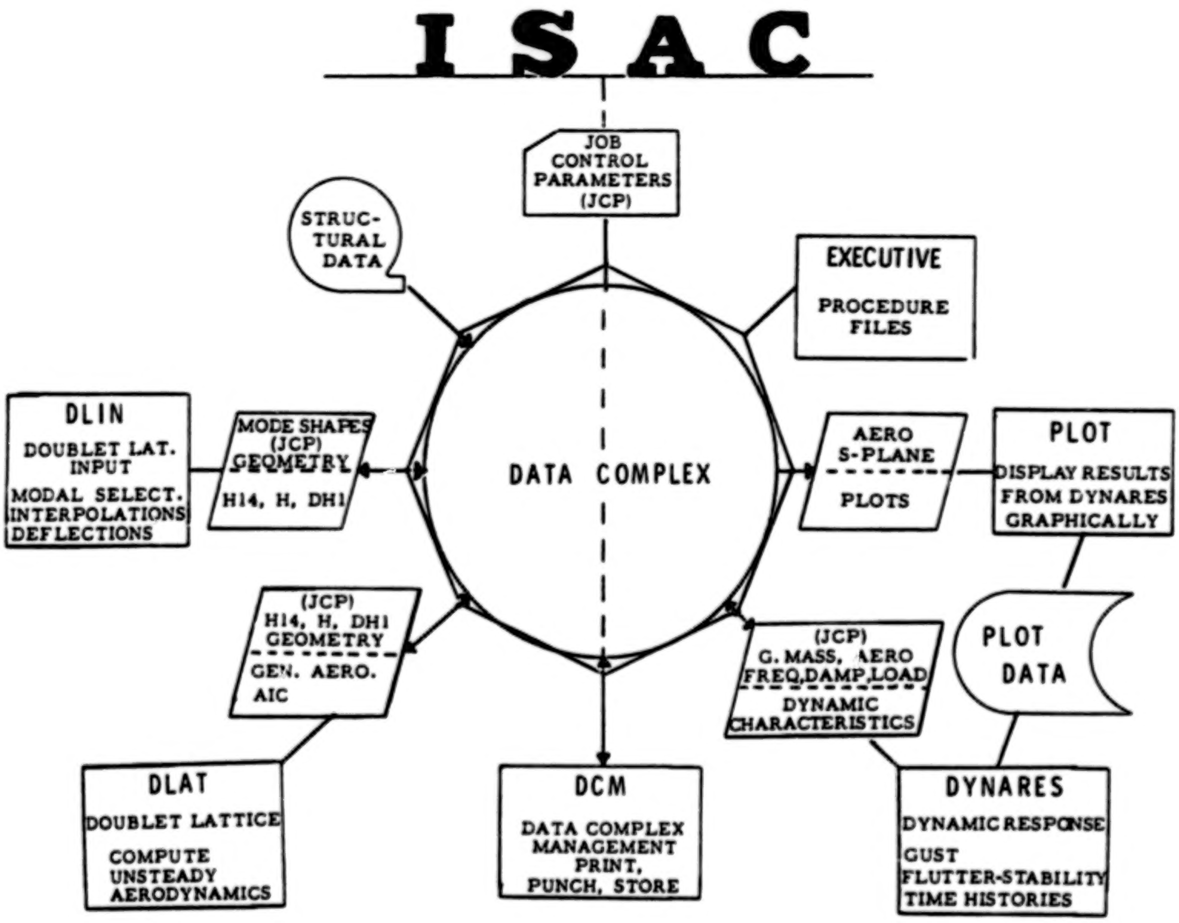
ISAC
JOB CONTROL PARAMETERS (JCP)
STRUC-TURAL DATA
EXECUTIVE
PROCEDURE FILES
DLIN
DOUBLET LAT. INPUT
MODAL SELECT.
INTERPOLATIONS
DEFLECTIONS
MODE SHAPES (JCP)
GEOMETRY
H14, H, DH1
DATA COMPLEX
AERO
S-PLANE
PLOTS
PLOT
DISPLAY RESULTS FROM DYNARES GRAPHICALLY
PLOT DATA
(JCP)
H14, H, DH1
GEOMETRY
GEN. AERO.
AIC
(JCP)
G. MASS, AERO
FREQ,DAMP,LOAD
DYNAMIC CHARACTERISTICS
DLAT
DOUBLET LATTICE
COMPUTE UNSTEADY AERODYNAMICS
DCM
DATA COMPLEX MANAGEMENT
PRINT, PUNCH, STORE
DYNARES
DYNAMIC RESPONSE
GUST
FLUTTER-STABILITY
TIME HISTORIES

DAST ARW-2 PROJECT SUPPORT

The ISAC program is being used to support the DAST (Drones for Aerodynamic and Structural Testing) ARW-2 (Aeroelastic Research Wing Number 2) project. The ARW-2, scheduled for flight tests in calendar year 1985, is dependent upon several active control functions for safety of flight in some regions of its flight envelope. Initial support involved comparison of NASA and Boeing Wichita analytic predictions of stability and response characteristics. These comparisons were valuable in that they pointed out the need for modeling improvements in both ISAC and the Boeing Wichita programs. The NASA/Boeing predictions are now in reasonably good agreement although differences remain in predicted gain and phase margins in the flutter suppression control law. Ultimately, the correlation of measured and analytically predicted performance will be documented. These comparisons will, hopefully, provide information that will help to improve current mathematical modeling techniques. Reference 7 in these workshop proceedings presents the results of several experimental tests involving active controls for which analytical modeling and prediction of control law performance were done in part using ISAC. This chart also depicts some of the graphical outputs that can be obtained by use of ISAC.

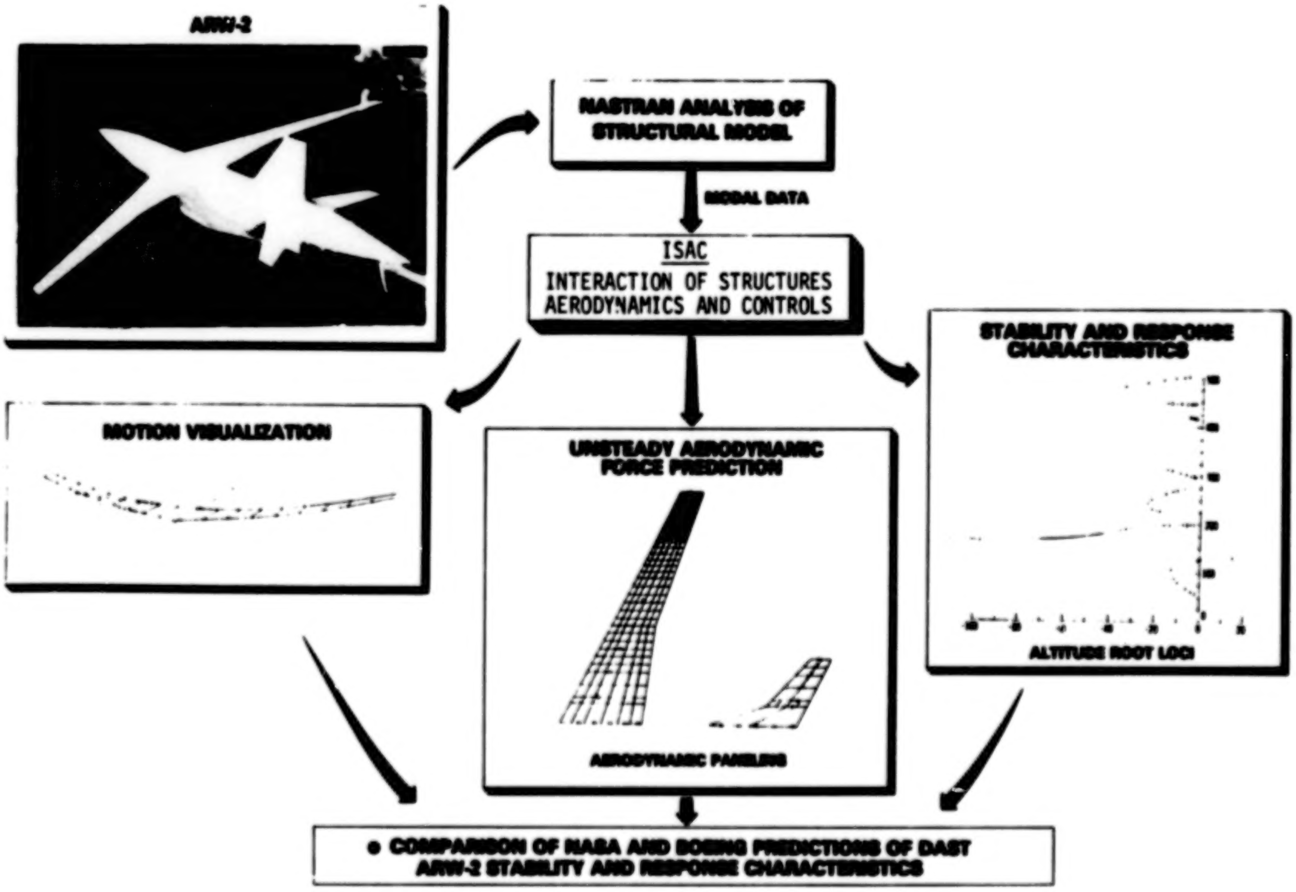
ARW-2
NASTRAN ANALYSIS OF STRUCTURAL MODEL
MODAL DATA
ISAC
INTERACTION OF STRUCTURES AERODYNAMICS AND CONTROLS
MOTION VISUALIZATION
UNSTEADY AERODYNAMIC FORCE PREDICTION
AERODYNAMIC PANELING
STABILITY AND RESPONSE CHARACTERISTICS
ALTITUDE ROOT LOCI
• COMPARISON OF NASA AND BOEING PREDICTIONS OF DAST ARW-2 STABILITY AND RESPONSE CHARACTERISTICS

DESIGN TOOLS

A number of control law design tools have been developed at Langley:

ORACLS (ref. 8) is a system of algorithms for designing linear feedback control laws for linear time-invariant multivariable differential or difference equation state vector models. ORACLS applies some of the most efficient numerical linear algebra procedures to implement Linear Quadratic Gaussian (LQG) methodology. The ORACLS system can be obtained from COSMIC.

MICAD (refs. 9-11) uses goal-oriented strategies to obtain pareto-optimal solutions that satisfy multiple objectives for either deterministic plants or plants with random parameters. MICAD is, to some degree, a special purpose tool that was developed to design control laws for the lateral degrees of freedom of rigid aircraft. It is, nevertheless, generalizable to a wider class of problems. Documentation of MICAD is planned but a completion date has not been identified. A. A. Schy is directing the development of MICAD. Since the 1960's he has advocated the explicit inclusion of design criteria in the design process.

PADLOCS (refs. 12-14) and SYNPAC (refs. 15,16) are two collections of algorithms which provide the capability to design implementable low order active control laws for high order aeroelastic aircraft. They allow direct inclusion of design criteria and, consequently, are similar in structure to MICAD. The three programs do, however, differ substantially internally in performance function and constraint formulations and in options for obtaining constrained optimization solutions. Documentation of SYNPAC is now in progress.

- ORACLS (OPTIMAL REGULATOR ALGORITHMS FOR THE CONTROL OF LINEAR SYSTEMS)
- MICAD (MULTIOBJECTIVE INSENSITIVE COMPUTER AIDED DESIGN)
- PADLOCS (PROGRAMS FOR ANALYSIS AND DESIGN OF LINEAR OPTIMAL CONTROL SYSTEMS)
- SYNPAC (SYNTHESIS PACKAGE FOR ACTIVE CONTROLS)

ISAC/ORACLS/SYNPAC INTERFACE

An approach to control law design commonly employed at Langley in active control applications is illustrated using the ISAC, ORACLS and SYNPAC programs. A model of the plant is defined using ISAC and stored on the data complex. TRANSFR, a module of SYNPAC, is used to examine pole-zero locations associated with candidate feedback paths and to prepare input to an interactive version of ORACLS. These input data include the model of the plant and estimates of the intensities of noise sources in the plant and in the sensor outputs. Full order controllers are designed using ORACLS. The Doyle-Stein (ref. 17) procedure of adding ficticious process noise at the input is employed where necessary to improve the robustness characteristics of the full order controller. Modal residualization/truncation is employed to select an implementable reduced order controller. Within SYNPAC, or other similar design algorithms, the reduced order controller is optimized as shown in the next chart.

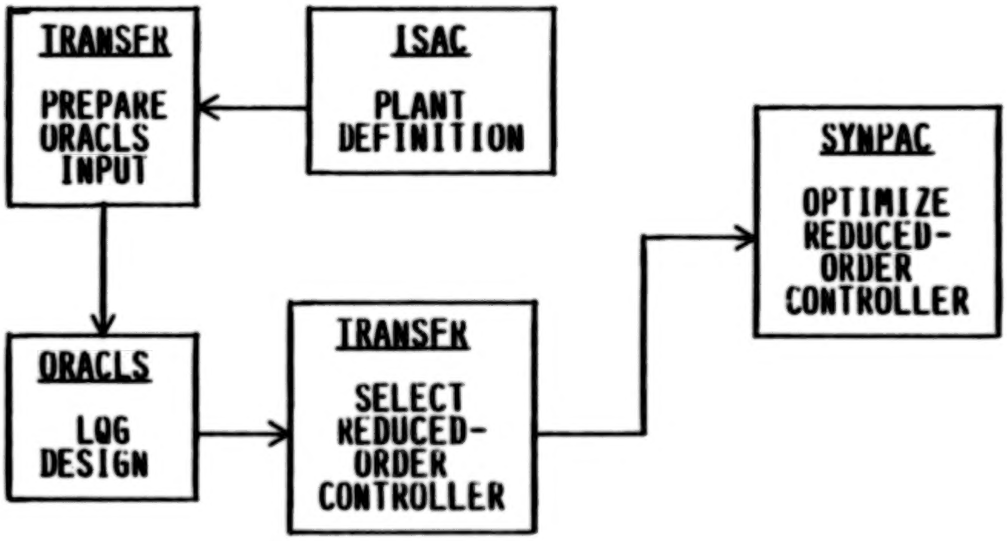
TRANSFR
PREPARE ORACLS INPUT
ISAC
PLANT DEFINITION
SYNPAC
OPTIMIZE REDUCED-ORDER CONTROLLER
ORACLS
LQG DESIGN
TRANSFR
SELECT REDUCED-ORDER CONTROLLER

SYNTHESIS PACKAGE FOR ACTIVE CONTROLS

This chart illustrates the phase of the design cycle initiated after a candidate control law form has been selected. The selection process has been illustrated on the previous page for the modified LQG approach. Other techniques could have been employed to select the control law form such as Nissim's energy method (ref. 18), eigenspace methods (refs. 19 and 20), classical methods, etc. Constrained optimization techniques are employed to determine values for the free parameters in the fixed form control law which optimize a measure of goodness and allow the design criteria to be satisfied.

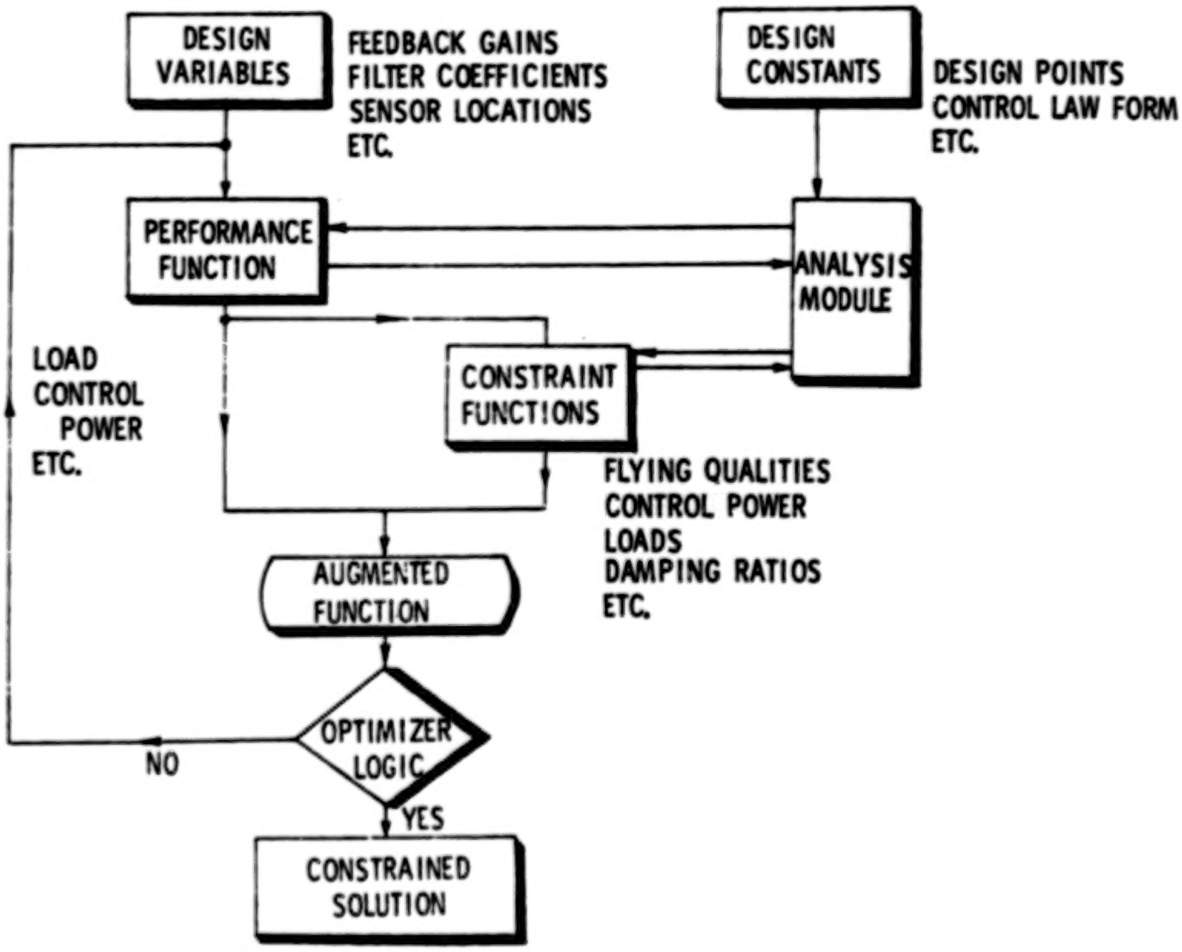
DESIGN VARIABLES
FEEDBACK GAINS
FILTER COEFFICIENTS
SENSOR LOCATIONS
ETC.
DESIGN CONSTANTS
DESIGN POINTS
CONTROL LAW FORM
ETC.
PERFORMANCE FUNCTION
ANALYSIS MODULE
LOAD
CONTROL
POWER
ETC.
CONSTRAINT FUNCTIONS
FLYING QUALITIES
CONTROL POWER
LOADS
DAMPING RATIOS
ETC.
AUGMENTED FUNCTION
OPTIMIZER LOGIC
NO
YES
CONSTRAINED SOLUTION

SENSOR SIGNAL IPUTS TO SYMMETRIC FLUTTER SUPPRESSION CONTROL LAW

This and the next three charts show the application of SYNPAC to improve the robustness characteristics of a control law for suppression of symmetric flutter of the DAST ARW-2 aircraft. A more complete description is presented in reference 16. This chart depicts the sensors (vertical accelerometers) and control surfaces that were employed and defines how the sensor signals are separated into symmetric components. Note that the control law is single-input/single-output.

ORIGINAL PAGE IS
OF POOR QUALITY

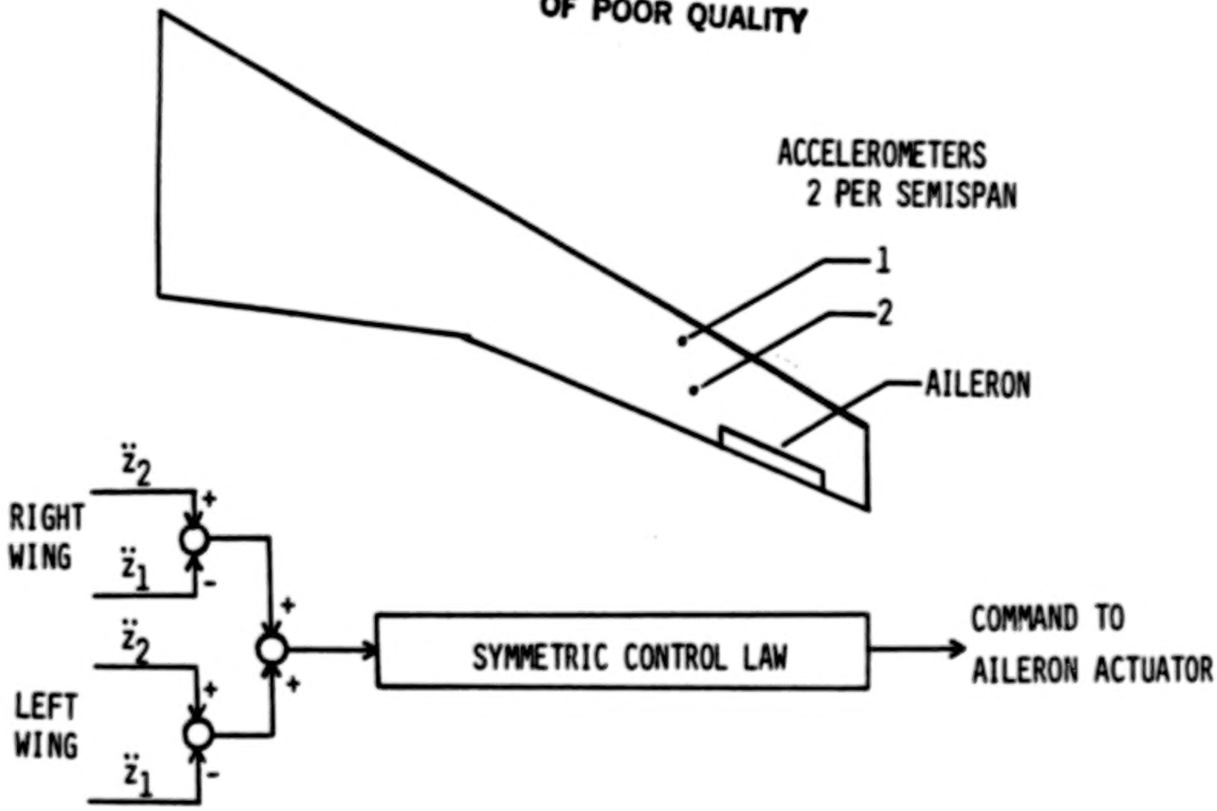
ACCELEROMETERS
2 PER SEMISPAN
1
2
AILERON
RIGHT WING
$\ddot{z}_2$
$\ddot{z}_1$
LEFT WING
$\ddot{z}_2$
$\ddot{z}_1$
+
-
+
-
+
+
SYMMETRIC CONTROL LAW
COMMAND TO
AILERON ACTUATOR

ROBUSTNESS MAXIMIZATION

In reference 16 a full order controller (25th order) was designed using ORACLS for a design point at a Mach number of 0.86 and an altitude of 15,000 ft. Order reduction techniques were used to obtain an implementable 9th order approximation to this controller of the form indicated below. The controller exhibited poor robustness characteristics at an off design point at a Mach number of 0.91 and an altitude of 15,000 ft. SYNPAC was employed to improve the robustness characteristics. Design variables D_i (i=1,2,...,9) were found which maximized the minimum singular value of the return difference transfer function subject to the indicated constraints.

FIND VALUES FOR THE DESIGN VARIABLES, D_I, WHERE

$$(U_{FS}/Y) = D_1 \frac{(S+D_2)(S+D_3)}{(S^2+D_4S+D_5)} \frac{(S^2+D_6S+D_7)}{(S^2+D_8S+D_9)} T(S)$$

AND T(S) IS A FIXED FILTER

SUCH THAT

- MINIMUM SINGULAR VALUE IS MAXIMIZED
- CONTROL POWER CONSTRAINTS ARE SATISFIED
- +6dB ≤ GAIN MARGIN ≤ -6dB
- 40° ≤ PHASE MARGIN ≤ -40°

ORIGINAL PAGE IS
OF POOR QUALITY

ORIGINAL PAGE IS
OF POOR QUALITY

CLOSED LOOP BLOCK DIAGRAM

The performance of the controller optimized for robustness will be exhibited by showing Nyquist plots for the initial and optimized controllers. This chart identifies the loop breaking point and symbols employed to represent the pertinent transfer functions.

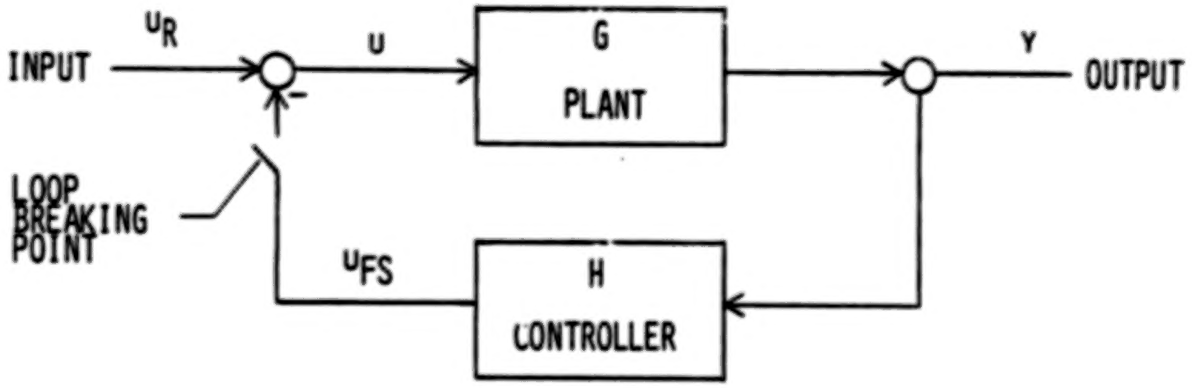
INPUT
u_R
u
G
PLANT
Y
OUTPUT
-
LOOP BREAKING POINT
u_{FS}
H
CONTROLLER

NYQUIST PLOTS OF HG TRANSFER FUNCTION (M = 0.91, H = 15,000 FEET)

The plant is unstable (a complex conjugate pair of unstable poles) at the indicated flight condition. Consequently, for stability the Nyquist plot must encircle the (-1) point once in a counterclockwise direction as frequency varies from 0 to $+\infty$. Increasing frequency is indicated by arrows on the figure. The initial controller stabilized the system but exhibited poor gain and phase margins with an accompanying small minimum singular value (the point at which the minimum singular values occurs is indicated by the heavy solid line). After optimization the minimum singular value was increased by 26 percent, control power constraints (not shown) were satisfied and gain and phase margin constraints were met to within a 2.5-percent tolerance.

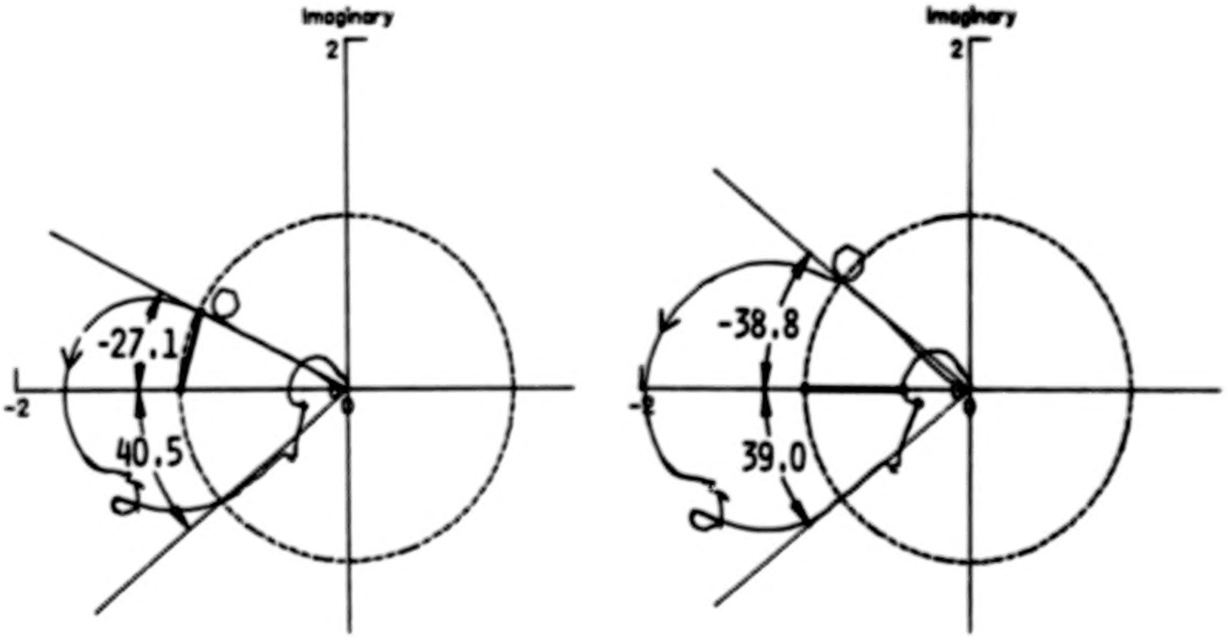

INITIAL CONTROLLER

OPTIMIZED CONTROLLER

CONCLUDING REMARKS

Several tools applicable to analysis and design of control laws for aeroelastic vehicles have been identified. DYLOFLEX and NASTRAN are available from COSMIC. ISAC, developed primarily for in-house research, is only partially documented and would require substantial modification for use on a computer complex differing from the one at Langley. It has, nevertheless, been distributed to several off-site users. ORACLS is the only design tool that is sufficiently well documented for distribution. Linear potential flow aerodynamic theory is employed in computing aerodynamic forces. Consequently, the modeling accuracy becomes doubtful at analysis and design points approaching the transonic region. Improvement is needed in the aerodynamic modeling.

- ANALYSIS AND DESIGN TOOLS IDENTIFIED
- CRITERIA EXPLICITLY INCLUDED IN DESIGN PROCEDURE
- CONCERN ABOUT UNMODELED NONLINEAR AERODYNAMIC EFFECTS
- DOCUMENTATION OF ANALYSIS AND DESIGN TOOLS IS UNDERWAY

REFERENCES

1. Perry, B. III; Kroll, R. I.; Miller, R. D.; and Goetz, R. C.: DYLOFLEX: A Computer Program for Flexible Aircraft Flight Dynamic Loads Analysis with Active Controls. Journal of Aircraft, Vol. 17, No. 4, April 1980, pp. 275-282.

2. Harder, Robert L.; MacNeal, Richard H.; and Rodden, William P.: A Design Study for the Incorporation of Aeroelastic Capability into NASTRAN. NASA CR 111918, May 1971.

3. Peele, Ellwood L.; and Adams, William M., Jr.: A Digital Program for Calculating the Interaction Between Flexible Structures, Unsteady Aerodynamics, and Active Controls. NASA TM 80040, January 1979.

4. Albano, E.; and Rodden, W. P.: A Doublet Lattice Method for Calculating Lift Distributions on Oscillating Surfaces in Subsonic Flows. AIAA Journal, Vol. 7, No. 2, February 1969, pp. 279-285.

5. Roger, Kenneth L.: Airplane Math Modeling Methods for Active Control Design. AGARD CR 228, August 1977.

6. Mahesh, J. K.; Stone, C. R.; Garrard, W. L.; and Hausman, P. D.: Active Flutter Control for Flexible Vehicles. NASA CR 159160, November 1979.

7. Newsom, Jerry R.; and Abel, Irving: Experiences With the Design and Implementation of Flutter Suppression Systems. NASA Aircraft Controls Research - 1983, NASA CP-2296, 1984, pp. 489-509.

8. Armstrong, Ernest S.: ORACLS - A Design System for Linear Multivariable Control. Marcel Dekker, Inc., c.1980.

9. Schy, Albert A.: Nonlinear Programming in Design of Control Systems with Specified Handling Qualities. Proceedings of 1972 IEEE Conference on Decision and Control and 11th Symposium on Adaptive Processes, December 1972, pp. 272-279.

10. Schy, A. A.; Adams, William M., Jr.; and Johnson, K. G.: Computer-Aided Design of Control Systems to Meet Many Requirements. NATO AGARD Conference Proceedings No. 137 on Advances in Control Systems, May 1974, pp 6-1 to 6-7.

11. Schy, A. A.; and Giesy, D. P.: Tradeoff Studies in Multiobjective Insensitive Design of Airplane Control Systems. AIAA Paper No. 83-2273, August 1983.

12. Newsom, J. R.: A Method for Obtaining Practical Flutter Control Laws Using Results of Optimal Control Theory. NASA TP 1471, August 1979.

13. Mukhopadhyay, V.; Newsom, J. R.; and Abel, I.: A Method for Obtaining Reduced Order Control Laws for High Order Systems Using Optimization Techniques. NASA TP 1876, 1981.

14. Newsom, Jerry R.; and Mukhopadhyay, V.: The Use of Singular Value Gradients and Optimization Techniques to Design Robust Controllers for Multiloop Systems. AIAA Paper No. 83-2191, August 1983.

15. Adams, William M., Jr.: and Tiffany, Sherwood H.: Control Law Design to Meet Constraints Using SYNPAC--Synthesis Package for Active Controls. NASA TM 83264, January 1982.

16. Adams, William M., Jr.; and Tiffany, Sherwood, H.: Design of a Candidate Flutter Suppression Control Law for DAST ARW-2. AIAA Paper No. 83-2221, August 1983.

17. Doyle, J. C.; and Stein, G.: Robustness with Observers. IEEE Transactions on Automatic Control, Vol. AC-24, No. 4, August 1979, pp. 607-611.

18. Nissim, E.; and Abel, I.: Development and Application of an Optimization Procedure for Flutter Suppression Using the Aerodynamic Energy Concept. NASA TP 1137, February 1978.

19. Garrard, William L.; and Liebst, Bradley S.: Active Flutter Suppression Using Eigenspace and Linear Quadratic Design Techniques. AIAA Paper No. 2222, August 1983.

20. Ostroff, A. J.; and Pines, S.: Application of Modal Control to Wing-Flutter Suppression. NASA TP 1983, May 1982.

N84
20583

UNCLAS

N84 20583

ALGORITHMS FOR OUTPUT FEEDBACK, MULTIPLE-MODEL, AND DECENTRALIZED CONTROL PROBLEMS

Nesim Halyo and John R. Broussard
Information and Control Systems, Incorporated
Hampton, Virginia

First Annual NASA Aircraft Controls Workshop
NASA Langley Research Center
Hampton, Virginia
October 25-27, 1983

PRECEDING PAGE BLANK NOT FILMED

ABSTRACT

The optimal stochastic output feedback, multiple-model, and decentralized control problems with dynamic compensation are formulated and discussed. Algorithms for each problem are presented, and their relationship to a basic output feedback algorithm is discussed. An aircraft control design problem is posed as a combined decentralized, multiple-model, output feedback problem. A control design is obtained using the combined algorithm. An analysis of the design is presented.

ADVANTAGES OF STOCHASTIC OUTPUT FEEDBACK

The stochastic optimal output feedback problem [1-8] is a significant extension of the "full-state feedback" LQG problem [9]. Its formulation addresses some important limitations encountered in practical systems and provides a flexibility useful in configuring the control law for ease of implementation. Some of the advantages of the stochastic output feedback problem are shown below. Output feedback introduces a rich class of control law structures which can be used in modern control designs.

- DESIGNER CAN SELECT THE STATES FOR FEEDBACK
- PROVIDES A METHOD TO DESIGN OUTER LOOP CONTROL LAWS
- ACCOUNTS FOR ACTUATOR DYNAMICS WITHOUT NECESSITY FOR ACTUATOR STATE FEEDBACK
- ACCOUNTS FOR PHASE SHIFTS INTRODUCED BY PREFILTERS AND OTHER ESTIMATORS WITHOUT NECESSITY OF FEEDBACK
- PROVIDES A SYSTEMATIC METHOD TO INCREASE OR DECREASE GAINS BY ADJUSTING PLANT AND MEASUREMENT NOISE COVARIANCES
- PROVIDES CONSIDERABLE FLEXIBILITY IN THE CONTROL STRUCTURE IN A MODERN CONTROL SETTING

FORMULATION OF THE STOCHASTIC OUTPUT FEEDBACK PROBLEM

The discrete stochastic optimal output feedback problem is formulated below. The control U_k feeds back the output Y_k through a constant gain matrix K. The term $\mathcal{D}$ is the set of gains K for which $J_N(K)$ converges to a finite value $J(K)$. The term $\mathcal{S}$ is the set of gains which stabilizes the closed-loop system. The optimization problem can be posed as: Find a stabilizing gain K^* (K^* e $\mathcal{S}$) which minimizes the cost $J(K)$, i.e., $J(K^*) \leq J(K)$, $K \in \mathcal{D}$.

$$X_{k+1} = \phi X_k + \Gamma U_k + W_k$$

$$Y_k = C X_k + V_k$$

$$U_k = - K Y_k$$

$$E(W_k \ W_i^T) = W\delta_{ki} \qquad E(V_k \ V_i^T) = V\delta_{ki} \qquad E(X_o \ X_o^T) = S_o$$

$$E(W_k) = 0 \qquad E(V_k) = 0 \qquad E(W_k \ V_j^T) = E(W_k \ X_o^T) = E(V_k \ X_o^T) = 0$$

$$J_N(K) = \frac{1}{2(N+1)} \sum_{K=0}^{N} E(X_{k+1}^T Q X_{k+1} + U_k^T R U_k)$$

$$J(K) = \lim J_N(K) < \infty \qquad K \in \mathcal{D}$$

EXAMPLE

**ORIGINAL PAGE IS
OF POOR QUALITY**

Some important characteristics of the stochastic optimization problem posed are illustrated in a simple first-order example. In this example, the domain of optimization $\mathcal{D}$ is the semi-open interval (0, 2), while the set of stabilizing gains S consists of the open interval (0, 2). The system is completely controllable and output stabilizable. However, as illustrated by the example, output stabilizability alone does not guarantee the existence of a solution to the optimization problem. The cost function $J(K)$, for this example, has no minimum in $\mathcal{D}$ or in S. Furthermore, the example illustrates that the continuity of the cost function $J(K)$ over its domain $\mathcal{D}$ is not guaranteed, as $K = 0$ is a point of discontinuity. Therefore, it is desirable to determine conditions under which an optimal solution exists.

$$X_{k+1} = X_k + U_k \qquad Y_k = X_k + V_k$$

$$Q = 1 \qquad R = 0 \qquad V = 1 \qquad W = 0 \qquad S_o = 1$$

$$\Gamma^T Q \Gamma + R = 1 > 0 \qquad C W C^T + V = 1 > 0$$

$$J(K) = \begin{cases} \frac{K}{2-K} & 0 < K < 2 \\ 1 & K = 0 \end{cases}$$

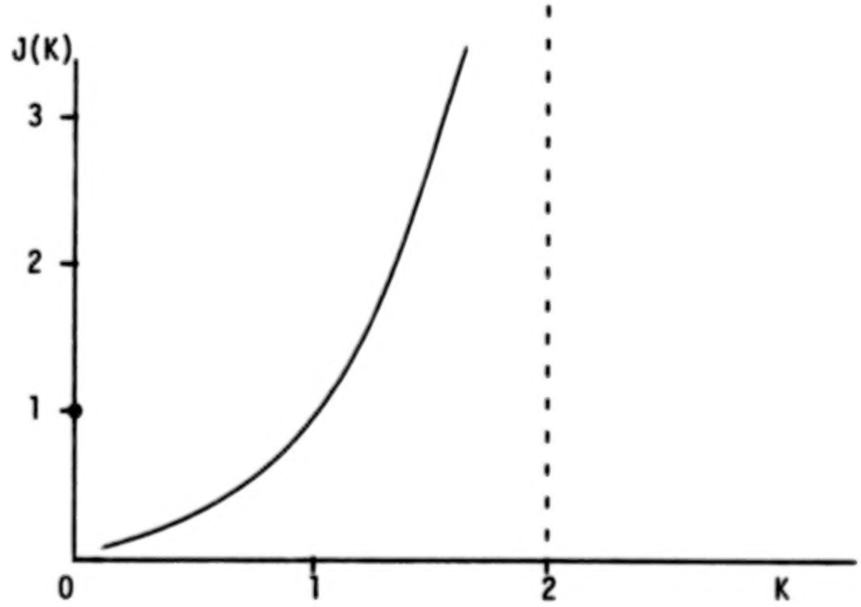

OUTPUT FEEDBACK EXISTENCE CONDITIONS

As illustrated by the example, the domain of optimization is not necessarily a closed set, and can be unbounded, although *S* is always open. Thus, it is necessary to determine conditions under which the minimum cost is attained at an interior point of *S*. Such conditions which guarantee the existence of a solution to the optimization problem are shown below. Under these conditions, the domain of optimization $\mathcal{D}$ coincides with the stability set *S*, which insures that the optimal gain stabilizes the closed-loop system. On the other hand, it can be shown that the cost function $J(K)$ is always continuous on *S* [10]. Note that the example considered previously fails to satisfy the condition $W \geq \varepsilon\, \Gamma\, \Gamma^T$, but satisfies all the remaining conditions. While the conditions 1, 2, and 3 ensure the existence of a stable global minimum, they are not necessary for the existence of a solution to the optimization problem. However, the class of optimization problems covered is quite broad, and because the existence conditions are expressed in terms of known system parameter matrices, verification is a simple task. Note that the measurement noise and control penalty terms are not necessary for existence, which is a major difference between the discrete and continuous output feedback problems. Also note that Q and W need not be positive definite, but must satisfy 1. Condition 1 is intriguing, as it corresponds to a method of improving robustness in control and filter designs [11]. The uniqueness of the solution is not ensured, except for special cases such as **full-state** feedback.

SUFFICIENT CONDITIONS FOR EXISTENCE:

1. FOR SOME $\varepsilon > 0 \quad Q \geq \varepsilon\, C^T C \quad W \geq \varepsilon\, \Gamma\, \Gamma^T$

2. $\Gamma^T Q\, \Gamma + R > 0 \quad C\, W\, C^T + V > 0$

3. (C, ϕ, Γ) IS OUTPUT STABILIZABLE

LET 1 AND 2 HOLD. $J(K)$ HAS A STABLE MINIMUM IF, AND ONLY IF, (C, ϕ, Γ) IS OUTPUT STABILIZABLE

For gains which stabilize the closed-loop system, the cost function $J(K)$ can be expressed more explicitly in terms of K, as shown below. An expression which provides more insight can be obtained by considering the incremental cost $\Delta J(K, \Delta K)$. As the incremental cost is the total change in the cost due to a change ΔK in the gain, the optimization problem can also be treated as that of finding a ΔK^* which minimizes the incremental cost for a fixed $K \epsilon S$. Due to the almost quadratic form of the incremental cost, a "natural" direction is the one which would minimize the incremental cost if it were actually quadratic in ΔK. The following theorem exploits this direction, $d(K)$.

Theorem: Let the existence conditions 1, 2, and 3 hold, and K_0 be in S. Then there exist $\beta > 0$, a sequence $\{K_i, i \geq 0\}$, and a limit point, say K^*, of the sequence such that

$$J(K_i) \downarrow J(K^*) \quad \text{and} \quad \frac{\partial J}{\partial K}(K_i) \to \frac{\partial J}{\partial K}(K^*) = 0$$

$$K_{i+1} = K_i + \alpha\, d(K_i)$$

$$d(K) = \hat{P}(K)^{-1}\, \Gamma^T\, P(K)\, \phi\, S(K)\, C^T\, \hat{S}(K)^{-1} - K$$

whenever $0 < \alpha \leq \beta$.

$$J(K) = \frac{1}{2}\, \mathrm{tr}\{P(K)\, W\} + \frac{1}{2}\, \mathrm{tr}\{K^T\, \hat{P}(K)\, K\, V\} \qquad K \epsilon S$$

$$P(K) = \phi(K)^T\, P(K)\, \phi(K) + C^T\, K^T\, R\, K\, C + Q$$

$$S(K) = \phi(K)\, S(K)\, \phi(K)^T + \Gamma\, K\, V\, K^T\, \Gamma^T + W$$

$$\hat{P}(K) = \Gamma^T\, P(K)\, \Gamma + R \qquad \hat{S}(K) = C\, S(K)\, C^T + V$$

$$\begin{aligned} \Delta J(K,\Delta K) &= J(K+\Delta K) - J(K) \\ &= \frac{1}{2}\, \mathrm{tr}\{2\, \Delta K^T [\hat{P}(K+\Delta K)\, K\, \hat{S}(K) - \Gamma^T\, P(K+\Delta K)\, \phi\, S(K)\, C^T] \\ &\quad + \Delta K^T\, \hat{P}(K+\Delta K)\, \Delta K\, \hat{S}(K)\} \qquad K,\ K+\Delta K \epsilon S \end{aligned}$$

NECESSARY CONDITIONS

$$\hat{P}(K^*)\, K^*\, \hat{S}(K^*) = \Gamma^T\, P(K^*)\, \phi\, S(K^*)\, C^T \qquad K^* \epsilon S$$

OUTPUT FEEDBACK ALGORITHM

Convergence Theorem: Let $\{K_i,\ i \geq 0\}$ be a sequence of gains obtained from the algorithm, starting with $K_0 \in S$. Then, any limit point, say K^*, satisfies the necessary conditions for optimality, stabilizes the closed-loop system, and $J(K_i) \downarrow J(K^*)$.

```
1.  CHOOSE  $K_0 \in S$    $\alpha_0 = 1$    $z > 1$    $i = 0$

2.  SOLVE THE LYAPUNOV EQUATIONS
    $P(K_i) = \phi(K_i)^T P(K_i) \phi(K_i) + C^T K_i^T R K_i C + Q$
    $S(K_i) = \phi(K_i) S(K_i) \phi(K_i)^T + \Gamma K_i V K_i^T \Gamma^T + W$
    IF $P(K_i)$ OR $S(K_i)$ IS NOT NON-NEGATIVE DEFINITE GO TO 5

3.  COMPUTE $d(K_i)$, $K_{i+1}$
    $d(K_i) = \hat{P}(K_i)^{-1} \Gamma^T P(K_i) \phi S(K_i) C^T \hat{S}(K_i)^{-1} - K_i$
    $K_{i+1} = K_i + \alpha_i d(K_i)$

4.  COMPUTE THE COST $J(K_i)$
    $J(K_i) = \frac{1}{2} tr\{P(K_i) W\} + \frac{1}{2} tr\{K_i^T P(K_i) K_i V\}$
    IF $i = 0$,  SET $i = 1$    AND GO TO 2.
    IF $J(K_i)-J(K_{i-1}) < -\frac{1}{4} \alpha_{i-1}(2-\alpha_{i-1})\, tr\{d(K_{i-1})^T \hat{P}(K_{i-1}) d(K_{i-1}) \hat{S}(K_{i-1})\}$ GO TO 6

5.  REDUCE $\alpha$
    $\alpha_i = \alpha_i/z$    $K_i = K_{i-1}$    $d(K_i) = d(K_{i-1})$
    $K_{i+1} = K_i + \alpha_i d(K_i)$    $\alpha_{i+1} = \alpha_i$    $i = i+1$    GO TO 2

6.  COMPUTE GRADIENT
    $\frac{\partial J}{\partial K}(K_i) = - \hat{P}(K_i) d(K_i) \hat{S}(K_i)$
    IF $\left\| \frac{\partial J}{\partial K}(K_i) \right\| > \epsilon_1$ OR $|J(K_i) - J(K_{i-1})| > \epsilon_2$, $\alpha_{i+1} = \alpha_i$,  $i = i+1$,  GO TO 2

7.  STOP
```

OPTIMAL DYNAMIC COMPENSATION

Most control systems for complex plants use some form of dynamic compensation. The dynamic compensator may simply consist of an integral feedback or a rate command structure, or may be a Kalman filter or an observer. Classical control designs make considerable use of dynamic compensation in the form of various filters, washout loops, etc. The basic form of a digital control system making use of dynamic compensation is shown below. The design of dynamic compensation in an optimal control setting can be imbedded into the optimal output feedback formulation by augmenting the state with the compensator states [12,13]. In this form, the order of the dynamic compensator is a design parameter and can be selected so as to obtain a low order, easily implemented compensator. For systems which are not stabilizable with the available measurements, such as some cases of flutter suppression, dynamic compensation is a necessary rather than a simply desirable structure [14]. The design of the dynamic compensator can be obtained using the output feedback algorithm presented earlier.

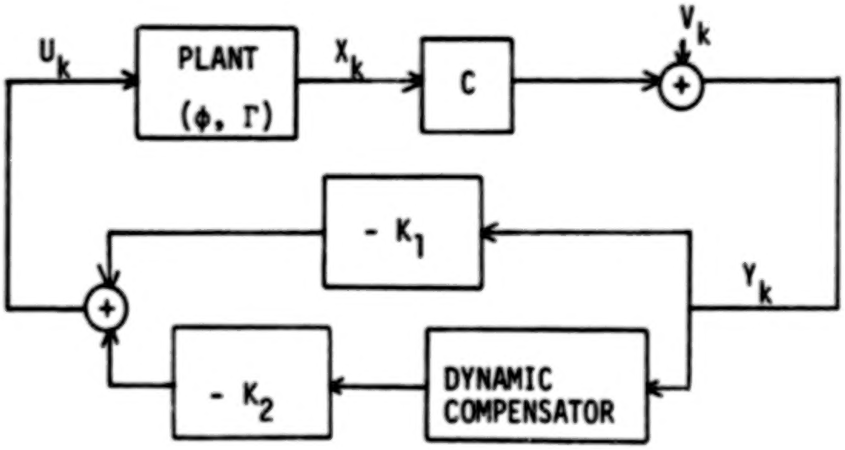

$$X_{k+1} = \phi\, X_k + \Gamma\, U_k + W_k \qquad Y_k = C\, X_k + V_k$$

$$Z_{k+1} = \phi_z\, Z_k + \Gamma_z\, Y_k \qquad U_k = -\, K_1\, Y_k - K_2\, Z_k$$

$$\begin{pmatrix} X_{k+1} \\ Z_{k+1} \end{pmatrix} = \begin{pmatrix} \phi & 0 \\ 0 & \phi_{zo} \end{pmatrix} \begin{pmatrix} X_k \\ Z_k \end{pmatrix} + \begin{pmatrix} \Gamma & 0 \\ 0 & I \end{pmatrix} \begin{pmatrix} U_k \\ \mu_k \end{pmatrix} + \begin{pmatrix} W_k \\ W_{zk} \end{pmatrix}$$

$$\bar{Y}_k = \begin{pmatrix} C & 0 \\ & I \end{pmatrix} \begin{pmatrix} X_k \\ Z_k \end{pmatrix} + \begin{pmatrix} V_k \\ 0 \end{pmatrix} \qquad \begin{pmatrix} U_k \\ \mu_k \end{pmatrix} = - \begin{pmatrix} K_1 & K_2 \\ -\Gamma_z & -(\phi_z - \phi_{zo}) \end{pmatrix} \bar{Y}_k$$

ADVANTAGES OF THE **MULTIPLE-MODEL** OUTPUT FEEDBACK APPROACH

While output feedback introduces significant flexibility in the structure of a control law, it does not directly address some of the objectives and requirements encountered in designing control laws. The **multiple-model** output feedback approach provides a design method which can be used to obtain important design requirements while preserving all the advantages inherent in output feedback. Some of the advantages of the approach follow.

- PRESERVES ALL THE ADVANTAGES OF OUTPUT FEEDBACK
- PROVIDES A DESIGN METHOD FOR ROBUST CONTROL LAWS
- PROVIDES A DESIGN METHOD FOR MULTIPLE CRITERIA
- PROVIDES A DESIGN METHOD FOR ACTUATOR FAILURE ACCOMMODATION
- PROVIDES A DESIGN METHOD FOR SENSOR FAILURE ACCOMMODATION

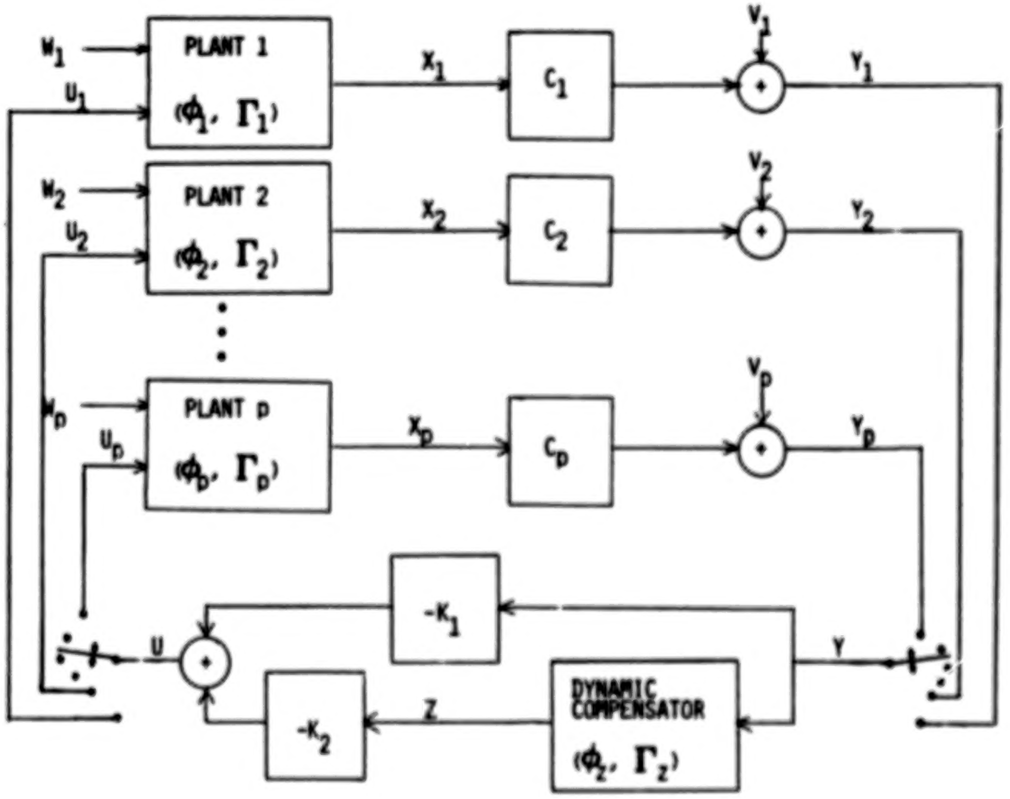
W1
U1
PLANT 1
(Φ1, Γ1)
X1
C1
V1
+
Y1
W2
U2
PLANT 2
(Φ2, Γ2)
X2
C2
V2
+
Y2
Wp
Up
PLANT p
(Φp, Γp)
Xp
Cp
Vp
+
Yp
-K1
U
+
Y
-K2
Z
DYNAMIC COMPENSATOR
(Φz, Γz)

FORMULATION OF THE MULTIPLE-MODEL OUTPUT FEEDBACK PROBLEM

The multiple-model output feedback formulation considers the problem of designing a fixed control law to meet design objectives expressed in terms of various plant models, measurement models, and performance criteria as shown below. The control law structure can contain dynamic compensation and output feedback. For example, the design objective of insensitivity to variations in some plant parameters can be addressed by selecting plant models (ϕ_j, Γ_j) which include these variations. Some types of actuator, sensor, or other plant subsystem failures can be addressed in the design by appropriate selection of the parameters Γ_j, C_j, ϕ_j, V_j, and W_j. Various other design objectives can be addressed in a similar manner.

Let S_j be the set of gains which stabilizes the j^{th} plant model, while $\mathcal{D}_j$ is the set of gains for which the j^{th} cost remains finite. The intersection S of the S_j's determines the control gains which stabilize all the plant models, while the intersection $\mathcal{D}$ of the $\mathcal{D}_j$'s is the set on which the total cost $J(K)$ is finite. The optimization problem can be posed as: Find a gain K^* which stabilizes all the models (i.e., $K^* \in S$) and minimizes the cost $J(K)$, i.e., $J(K^*) \le J(K)$, $K \in \mathcal{D}$.

$$X_{jk+1} = \Phi_j X_{jk} + \Gamma_j U_{jk} + W_{jk} \qquad 1 \le j \le p$$

$$Y_{jk} = C_j X_{jk} + V_{jk} \qquad 1 \le j \le p$$

$$U_{jk} = - K Y_{jk} = - K C_j X_{jk} - K V_{jk}$$

$$J_j(K) = \lim_{N\to\infty} \frac{1}{2(N+1)} \sum_{k=0}^{N} E(X_{jk+1}^T Q_j X_{jk+1} + U_{jk}^T R_j U_{jk}) < \infty \qquad K \in \mathcal{D}_j$$

$$J(K) = \sum_{j=1}^{p} \gamma_j J_j(K) \qquad \gamma_j > 0 \qquad K \in \mathcal{D}$$

$$\mathcal{D} = \bigcap_{j=1}^{p} \mathcal{D}_j \qquad S = \bigcap_{j=1}^{p} S_j$$

MULTIPLE-MODEL OUTPUT FEEDBACK EXISTENCE CONDITIONS

As for the case of the (single-model) output feedback problem, the existence of a solution to the optimal control problem posed is not always ensured. However, as seen by the sufficient conditions given below, a solution does exist for a large class of optimization problems. It should be noted that the constraint that the optimal gain **stabilizes the closed-loop models excludes** problems where no stabilizing gain exists, so that this class of problems must be treated separately. The sufficient conditions for the problem posed can be obtained by extending the results for output feedback. It can be shown that the cost function $J(K)$ is always continuous on $\mathcal{S}$, but not necessarily on $\mathcal{D}$. However, for the class of problems satisfying the sufficient conditions, $\mathcal{D}$ and $\mathcal{S}$ are equal. The conditions given here are not necessary for the existence of a stable global minimum, and the uniqueness of a solution is not ensured. Nevertheless, the class of problems included is broad enough to cover most parameter sensitivity objectives, control, or sensor failure accommodation objectives, as well as other significant objectives.

SUFFICIENT CONDITIONS FOR EXISTENCE

1. FOR SOME $\varepsilon > 0$, AND ALL $j \le p$ $\quad Q_j \ge \varepsilon C_j^T C_j \quad W_j \ge \varepsilon \Gamma_j \Gamma_j^T$

2. $\Gamma_j^T Q_j \Gamma_j + R_j > 0 \qquad C_j W_j C_j^T + V_j > 0 \qquad 1 \le j \le p$

3. $\mathcal{S}$ IS NON-NULL

LET 1 AND 2 HOLD. $J(K)$ HAS A STABLE MINIMUM IF, AND ONLY IF,

$\mathcal{S} = \bigcap_{j=1}^{p} \mathcal{S}_j$ CONTAINS AN ELEMENT

ORIGINAL PAGE IS
OF POOR QUALITY

MULTIPLE-MODEL INCREMENTAL COST AND NECESSARY CONDITIONS

For gains which stabilize all the plant models, the cost function $J(K)$ can be expressed in terms of the gain K, as shown. Similarly, the incremental cost $\Delta J(K,\Delta K)$ or the change in the cost due to a change in the gain, is seen to resemble a quadratic form in ΔK. The necessary conditions can be easily obtained from the incremental cost by letting ΔK approach zero. The direction $d(K)$, which would minimize the incremental cost if it were a true quadratic form, is selected to obtain an algorithm. It is seen that the direction $d(K)$ is the solution of a linear equation which requires a larger number of computations than the output feedback case. Also note that setting p equal to one results in the output feedback equations.

$$J(K) = \frac{1}{2} \sum_{j=1}^{p} \gamma_j \Big[\mathrm{tr}\{P_j(K)\, W_j\} + \mathrm{tr}\{K^T\, \hat{P}_j(K)\, K\, V_j\} \Big] \qquad K \in S$$

$$P_j(K) = \phi_j(K)^T\, P_j(K)\, \phi_j(K) + C_j^T\, K^T\, R_j\, K\, C_j + Q_j$$

$$S_j(K) = \phi_j(K)\, S_j(K)\, \phi_j(K)^T + \Gamma_j\, K\, V_j\, K^T\, \Gamma_j^T + W_j$$

$$\hat{P}_j(K) = \Gamma_j^T\, P_j(K)\, \Gamma_j + R_j \qquad \hat{S}_j(K) = C_j\, S_j(K)\, C_j^T + V_j$$

$$\Delta J(K,\Delta K) = \frac{1}{2}\, \mathrm{tr}\Big\{2\, \Delta K^T \sum_{j=1}^{p} \gamma_j \Big[\hat{P}_j(K+\Delta K)\, K\, \hat{S}_j(K) - \Gamma_j^T\, P_j(K+\Delta K)\, \phi_j\, S_j(K)\, C_j^T\Big]$$

$$+ \sum_{j=1}^{p} \gamma_j\, \Delta K^T\, \hat{P}_j(K+\Delta K)\, \Delta K\, \hat{S}_j(K)\Big\} \qquad K \quad K+\Delta K \in S$$

$$\frac{\partial J}{\partial K}(K) = \sum_{j=1}^{p} \gamma_j\, \hat{P}_j(K)\, K\, \hat{S}_j(K) - \Gamma_j^T\, P_j(K)\, \phi_j\, S_j(K)\, C_j^T$$

$$\sum_{j=1}^{p} \gamma_j \quad \hat{P}_j(K)\, d(K)\, \hat{S}_j(K) = -\frac{\partial J}{\partial K}(K)$$

NECESSARY CONDITIONS

$$\sum_{j=1}^{p} \gamma_j\, \hat{P}_j(K^*)\, K^*\, \hat{S}_j(K^*) = \sum_{j=1}^{p} \gamma_j\, \Gamma_j^T\, P_j(K^*)\, \phi_j\, S_j(K^*)\, C_j^T \qquad K^* \in S$$

MULTIPLE-MODEL OUTPUT FEEDBACK ALGORITHM

```
1.  CHOOSE $K_0 \epsilon S$,  $\alpha_0 = 1$,  $z > 1$,  $i = 0$
2.  SOLVE THE LYAPUNOV EQUATIONS FOR $j = 1, \ldots, p$
        $P_j(K_i) = \phi_j(K_i)^T P_j(K_i) \phi_j(K_i) + C_j^T K_k^T R_j K_i C_j + Q_j$
        $S_j(K_i) = \phi_j(K_i) S_j(K_i) \phi_j(K_i)^T + \Gamma_j K_i V_j K_i^T \Gamma_j^T + W_j$
        IF $P_j(K_i)$ OR $S_j(K_i)$ IS NOT NON-NEGATIVE DEFINITE GO TO 5
3.  SOLVE FOR $d(K_i)$, $K_{i+1}$
        $\sum_{j=1}^{p} \gamma_j \hat{P}_j(K_i) d(K_i) \hat{S}_j(K_i) = - \frac{\partial J}{\partial K}(K_i)$
        $K_{i+1} = K_i + \alpha_i d(K_i)$
4.  COMPUTE THE COST $J(K_i)$
        $J(K_i) = \frac{1}{2} \sum_{j=1}^{p} \gamma_i \left[ tr\left\{P_j(K_i) W_j + tr\left\{K_i^T P_j(K_i) K_i V_j\right\}\right\}\right]$
        IF $i = 0$,  SET $i = 1$ AND GO TO 2
        IF $J(K_i)-J(K_{i-1}) < -\frac{1}{4} \alpha_{i-1}(2-\alpha_{i-1}) \sum_{j=1}^{p} \gamma_j tr\left\{d(K_{i-1})^T \hat{P}_j(K_{i-1}) d(K_{i-1}) \hat{S}_j(Ki-1)\right\}$
            GO TO 6
5.  REDUCE $\alpha$
        $\alpha_i = \alpha_i/z$    $K_i = K_{i-1}$    $d(K_i) = d(K_{i-1})$
        $K_{i+1} = K_i + \alpha_i d(K_i)$    $\alpha_{i+1} = \alpha_i$    $i = i+1$    GO TO 2
6.  CHECK CONVERGENCE
        IF $\left\| \frac{\partial J}{\partial K}(K_i) \right\| > \epsilon_1$ OR $|J(K_i) - J(K_{i-1})| > \epsilon_2$, $\alpha_{i+1} = \alpha_i$,  $i = i+1$,  GO TO 2
7.  STOP
```

DECENTRALIZED CONTROL FORMULATION

It is well known that the optimal decentralized control problem for linear plants with Gaussian statistics and quadratic cost criteria does not necessarily result in a linear system, and when constrained to linear systems may result in infinite order systems [15-17]. Given these negative results, it is natural to constrain the class of decentralized controllers to linear systems of fixed finite order, i.e., the class of decentralized controllers with fixed-order dynamic compensators as local controllers [18]. However, since the dynamic compensator problem can be imbedded into the output feedback problem, it suffices to consider the class of decentralized output feedback controllers. Furthermore, the decentralized output feedback problem can be posed as a constrained output feedback problem, where the gain K is restricted to block diagonal form [18]. Let $\mathcal{S}$ be the collection of block diagram gains (of appropriate dimensions) which stabilize the decentralized system, while $\mathcal{D}$ is the set of block diagonal gains for which the cost $J(K)$ is finite. Then the problem can be posed as: Find a stabilizing gain $K^* \epsilon \mathcal{S}$ which minimizes the cost function over $\mathcal{D}$, i.e., $J(K^*) \le J(K)$, $K \epsilon \mathcal{D}$. It can be shown that **if a block diagonal stabilizing gain exists with $\Gamma^T Q\Gamma + R$ and $CWC^T + V$ positive definite, and if there exists some $\epsilon > 0$ such that $Q > \epsilon C^TC$ and $W > \epsilon \Gamma \Gamma^T$, then the optimal decentralized control problem posed has a solution. The necessary conditions are easily obtained from the incremental cost** [18].

$$X_{k+1} = \phi X_k + \sum_{\ell=1}^{L} \Gamma_\ell U_{\ell k} + W_k$$

$$Y_{\ell k} = C_\ell X_k + V_{\ell k} \qquad 1 \le \ell \le L$$

$$U_{\ell k} = - K_\ell U_{\ell k} \qquad 1 \le \ell \le L$$

$$J(K) = \lim_{N\to\infty} \frac{1}{2(N+1)} \sum_{k=0}^{N} \sum_{\ell=1}^{L} E(X_{k+1}^T Q_\ell X_{k+1} + U_{\ell k}^T R_\ell U_{\ell k})$$

$$X_{k+1} = \phi X_k + \Gamma U_k + W_k \qquad Y_k = C X_k + V_k$$

$$U_k = - K Y_k$$

$$C = \begin{pmatrix} C_1 \\ \vdots \\ C_L \end{pmatrix} \qquad \Gamma = (\Gamma_1, \ldots, \Gamma_L)$$

$$K = \text{BLOCK DIAG} \left\{ K_\ell \quad 1 \le \ell \le L \right\}$$

$$J(K) = \lim_{N\to\infty} \frac{1}{2(N+1)} \sum_{k=0}^{N} E(X_{k+1}^T Q X_{k+1} + U_k^T R U_k) < \infty \qquad K \epsilon \mathcal{D}$$

MULTIPLE-MODEL DECENTRALIZED CONTROL ALGORITHM

One approach to obtain an algorithm for the decentralized control problem posed is to close the control loop over all the local controllers, except one, solve the resulting unconstrained output feedback problem, then iterate on the next local controller. While this method does not make use of some of the analytical tools developed, which would result in a more efficient algorithm, a solution to the combined decentralized **multiple-model** output feedback can be obtained using the previously developed algorithm for **multiple-model** problems.

```
1.  CHOOSE A BLOCK DIAGONAL $K^o$ in $S$    $i = 1$    $\ell = 1$

2.  SOLVE THE MULTIPLE-MODEL OUTPUT FEEDBACK PROBLEM FOR THE SYSTEMS
        $\left\{(C_{\ell j}, \phi_j - \sum_{\ell' \neq \ell} \Gamma_{\ell' j} K^i_{\ell'} C_{\ell' j}, \Gamma_{\ell j}) \quad j = 1, 2, \ldots, p\right\}$
    WITH WEIGHTING MATRICES $\left\{Q_j + \sum_{\ell' \neq \ell} C^T_{\ell' j} K^{i^T}_{\ell'} R_{\ell' j} K^i_{\ell'} C_{\ell'} \quad j = 1, \ldots, p\right\}$
    $\left\{R_{\ell j}, \; j = 1, \ldots, p\right\}$ AND STATISTICS $\left\{V_{\ell j} \quad j = 1, 2, \ldots, p\right\}$
        $\left\{W_j - \sum_{\ell' \neq \ell} \Gamma^T_{\ell' j} K^{i^T}_{\ell'} V_{\ell' j} K^i_{\ell'} \Gamma_{\ell' j} \quad j = 1, \ldots, p\right\}$ TO OBTAIN $K^{i+1}$

3.  IF $\ell = L$,   GO TO 4
    SET $K^i_\ell = K^{i+1}_\ell$    $\ell = \ell + 1$    GO TO 2

4.  SET $K^{i+1}_\ell = K^i_\ell$    $1 \leq \ell \leq L$
    IF $|J(K^{i+1}) - J(K^i)| \leq \varepsilon_1$  AND  $\left\|\frac{\partial J}{\partial K}(K^{i+1})\right\| \leq \varepsilon_2$    STOP

5.  $i = i + 1$  $\ell = 1$    GO TO 2
```

AN APPLICATION TO RESTRUCTURABLE CONTROLS

The optimal stochastic multiple-model, decentralized control, output feedback and dynamic compensation problems formulated provide powerful techniques to investigate a large class of control system design problems. The stochastic output feedback, dynamic compensation, and decentralized control problems provide a wealth of control structures; however, the "best" structure(s) for a given design problem are not determined and depend on the practical constraints. On the other hand, the multiple-model formulation provides a powerful technique to describe design objectives in an optimal control setting, with computable algorithms and implementable structures.

As an illustration, the combined multiple-model decentralized control algorithm is used to design a simple aircraft control law which accommodates some types of control actuator failures. While the performance of a control law under normal conditions is a primary design goal, a practical control design must also consider the implications of various scenarios, such as actuator failures. The restructurable control problem addresses methods of modifying the structure of the law to accommodate failures. However, the detection of the exact nature of the failure requires a period of time. Depending on the actual failure, during this period of time the aircraft may be forced into a condition from which recovery is difficult, and sometimes not possible. Therefore, it is reasonable to restructure the control system in stages. As soon as the existence of a failure is known, or even highly likely, the system may be restructured into a control law which can accommodate a large number of failed components. This first stage restructuring can provide the valuable time necessary to identify the exact failure, decide the best second-stage structure, and implement it before the aircraft is forced into a possibly irrecoverable condition. The multiple-model formulation provides a control design method where the law is at least stable in the failed condition as well as under normal circumstances, when possible. Since the control law is stable for the case of no failure, a false alarm does not produce harmful effects. In the following example, a wing leveler with dynamic compensation and a decentralized structure is modeled with normal and failed aileron for failure accommodation, and at two airspeeds to provide insensitivity.

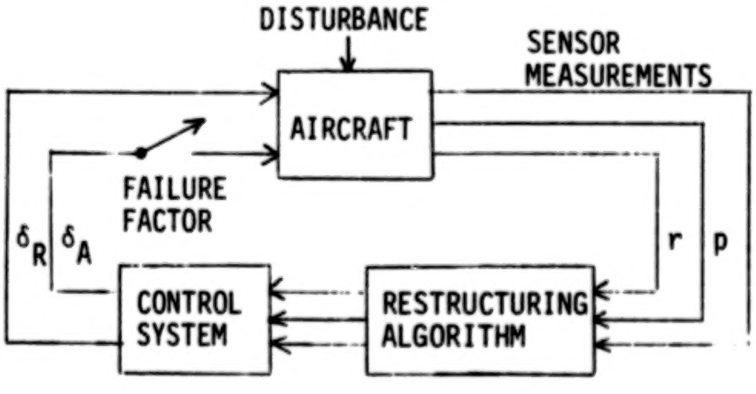

FAILURE ACCOMMODATION

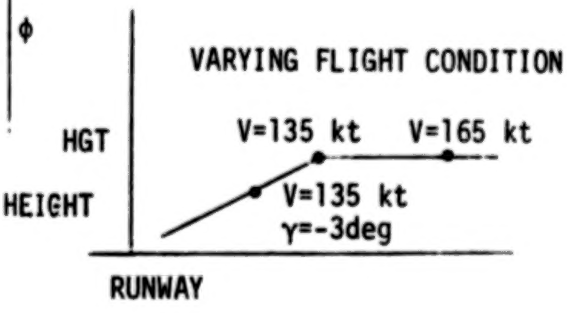
VARYING FLIGHT CONDITION

FLIGHT CONTROL DESIGN EXAMPLE

The advantages offered by the multiple-model decentralized approach are demonstrated using an aircraft digital flight control system design problem. The control problem is the simplified design of the lateral dynamics, inner-loop control system for the NASA ATOPS research aircraft (a Boeing 737). The aircraft model includes the body-axis states, v, p, r, and ϕ. Also included in the model are aileron and rudder actuators dynamics, a one-state dynamic compensator, and aileron and rudder control states caused by weighting the control difference in the quadratic cost function. Noisy sensor measurements are p, r, and ϕ. The dynamic compensator state and control states are noise-free measurements. The dynamic compensator state is quadratically weighted to "follow" the aircraft v state. The closed-loop eigenvalues using optimal output feedback at one trimmed flight condition (V_o = 135 kn, Wt = 85,000 lbs, h_o = 1,000 ft) are shown below. The other table shows the closed-loop eigenvalues for the multiple-model, decentralized design at the same flight condition with the same quadratic weights and noise covariances. The Dutch roll mode has the lowest damping in both designs.

OUTPUT FEEDBACK DESIGN

MAPPED EIGENVALUES (135 KN)	
REAL	IMAG.
- .521	0.00
- .903	1.47
- .903	-1.47
- 1.53	1.72
- 1.53	-1.72
- 1.25	0.92
- 1.25	-0.92
-14.4	0.00
-36.5	0.00

MULTIPLE-MODEL DECENTRALIZED DESIGN

MAPPED EIGENVALUES (135 KN)	
REAL	IMAG.
- .436	0.00
- .925	1.93
- .925	-1.93
- 1.08	1.22
- 1.08	-1.22
- 1.23	0.00
- 2.62	0.00
-13.4	0.00
-42.1	0.00

FEEDBACK GAINS FOR SINGLE- AND MULTIPLE-MODEL DESIGNS

The lateral dynamics flight control design for the multiple-model case uses four models: two models at 135 kn and 165 kn with the aileron operational, and two models at 135 kn and 165 kn with the aileron failed. The design is decentralized as four gains in the output feedback gain matrix are forced to be zero. The controls are the dynamic compensator control μ, aileron rate $\dot{\delta}A$, and rudder rate $\dot{\delta}R$. In the multiple-model decentralized design, no control states are fed back to the dynamic compensator, and aileron and rudder control state crossfeed gains are forced to be zero. The primary differences in the two gain matrices are the ϕ and p gains to $\dot{\delta}R$ which change sign. The **fixed-gain multiple-model** design stabilizes all four models. The **single-model** design causes the closed-loop system with the aileron failed to be unstable.

OUTPUT FEEDBACK DESIGN

CONTROL GAIN MATRIX						
	COMP.	p	r	ϕ	δA	δR
$\delta\mu$	-0.769	0.0032	-3.47	0.829	0.661	0.721
$\dot{\delta}A$	1.92	-3.94	-7.09	-3.96	-2.94	0.698
$\dot{\delta}R$	-0.250	-0.499	3.77	-0.447	0.0055	-2.77

MULTIPLE-MODEL DECENTRALIZED DESIGN

CONTROL GAIN MATRIX						
	COMP.	p	r	ϕ	δA	δR
$\delta\mu$	-0.80	-0.527	-4.58	0.731	0.	0.
$\dot{\delta}A$	0.104	-2.49	-4.51	-1.96	-1.94	0.
$\dot{\delta}R$	-0.516	0.721	7.74	0.860	0.	-4.05

SINGLE-MODEL DESIGN SIMULATION - NO FAILURES

A linear simulation of the **single-model** optimal output feedback design is shown below. Roll attitude is initially 5 deg at the beginning of the simulation and is smoothly returned to zero by the control system. Lateral velocity v is kept small, and the dynamic compensator state is similar to v.

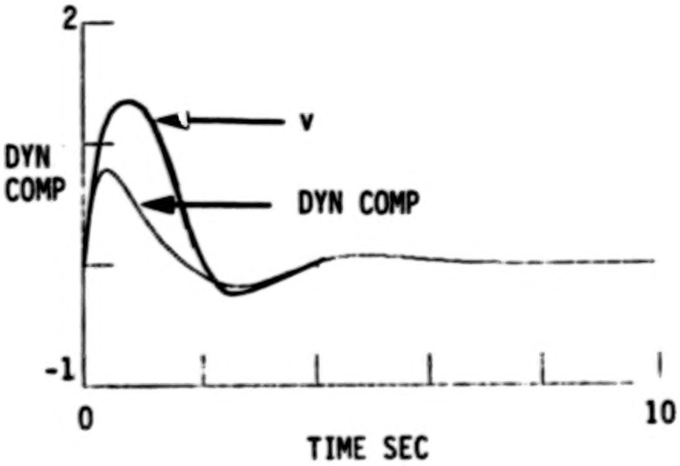

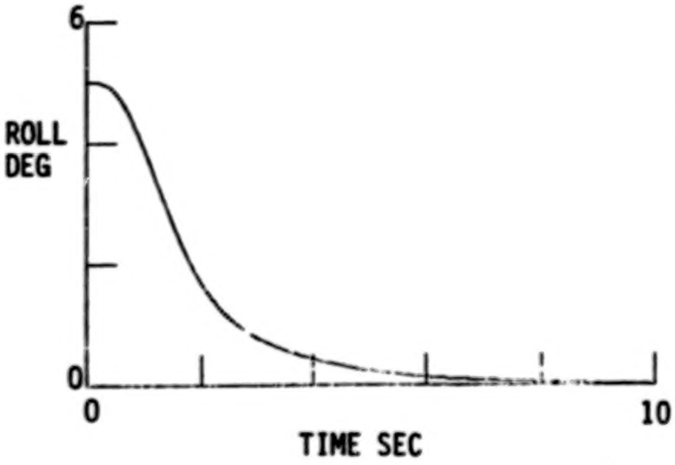

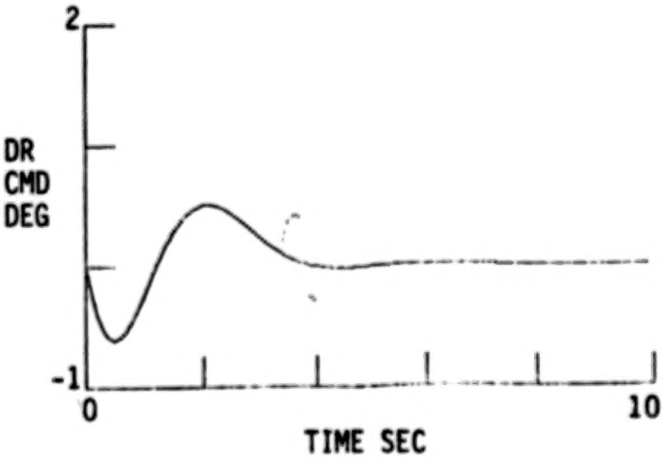

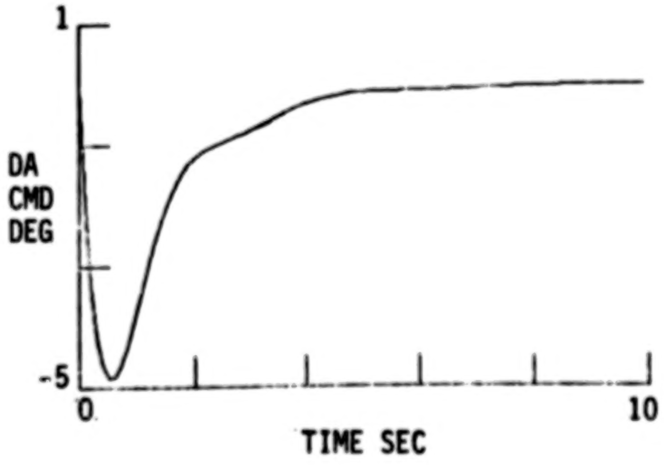

SINGLE-MODEL DESIGN SIMULATION - FAILED AILERON

The linear simulation shows the aileron failing 1.5 sec into the simulation and remaining fixed at approximately 2 deg. The closed-loop aircraft system is unstable and roll attitude is seen to diverge.

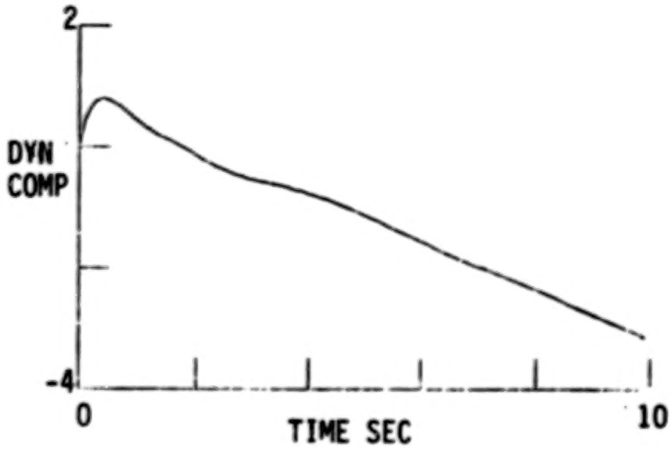

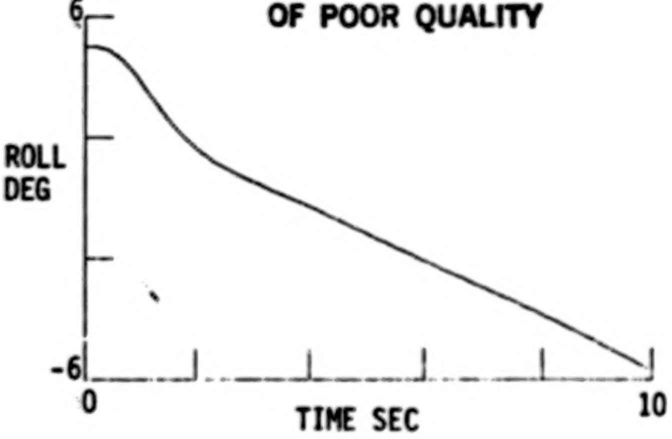

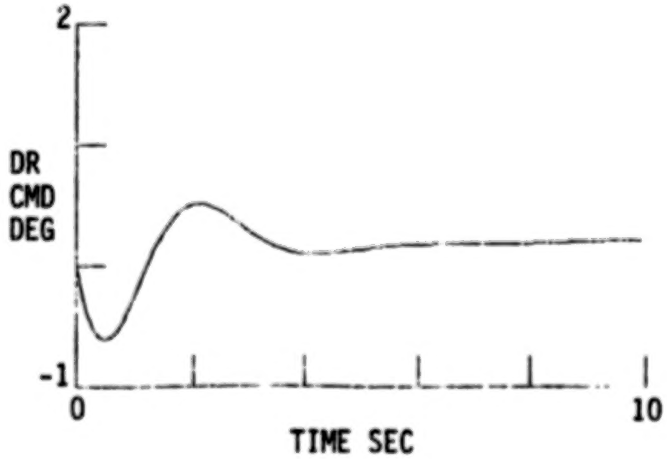

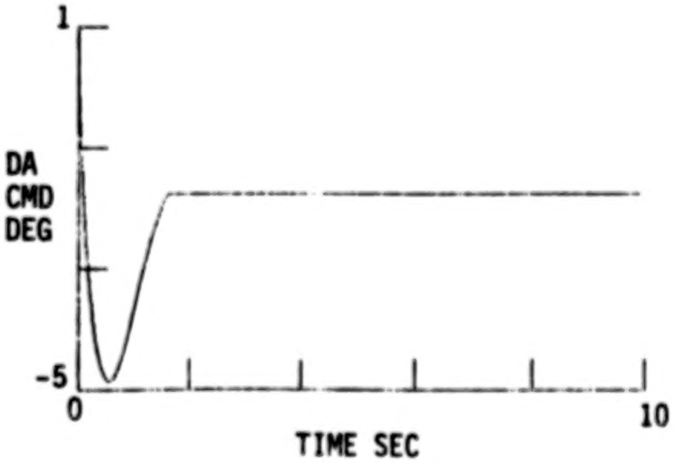

FIRST-STAGE RESTRUCTURING: MULTIPLE-MODEL DECENTRALIZED DESIGN - FAILED AILERON

The linear simulation shows the aileron failing at 1.5 sec into the simulation and remaining fixed at that level in the following period. The **single-model** output feedback design controls the aircraft until 10 sec. As the closed-loop system is unstable in this condition, the aircraft continues to roll past the level wings condition. It is assumed that by 10 sec., or 8.5 sec. after the aileron failure, the decision that a failure has occurred is made, and the first stage restructuring is engaged. The control law simulated after 10 sec. is the **multiple-model** decentralized design. As shown by the simulation, the restructured control arrests the roll of the aircraft, and brings it to a **non-zero but** easily manageable and stable bank angle, providing the time necessary for the **second-stage** restructuring.

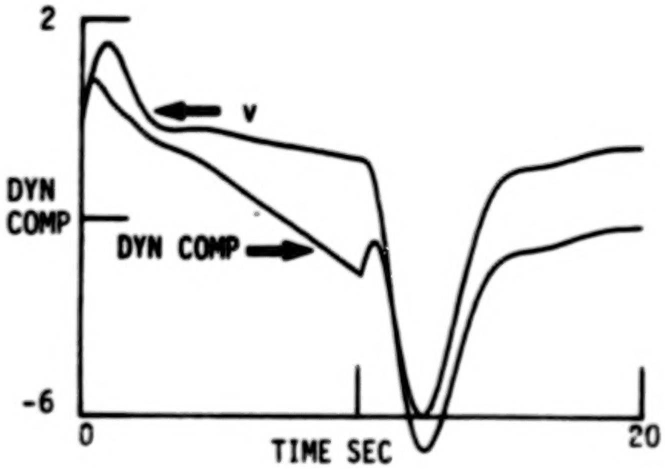

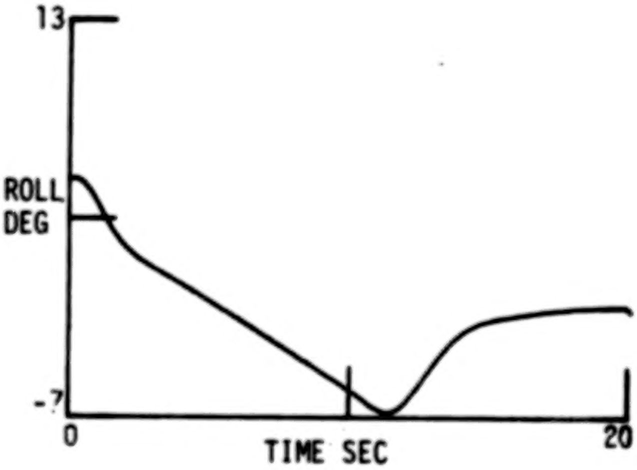

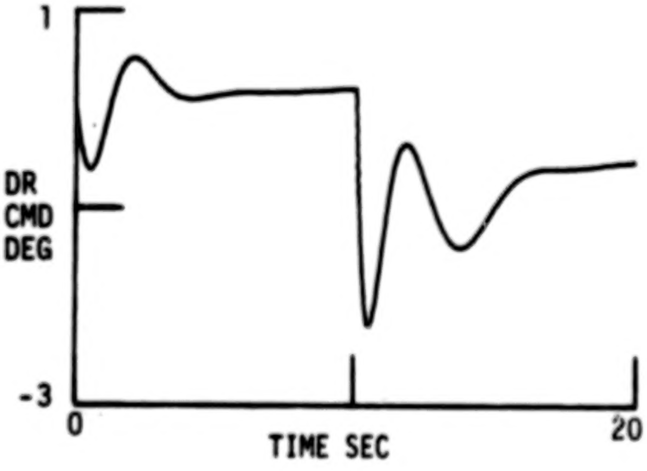

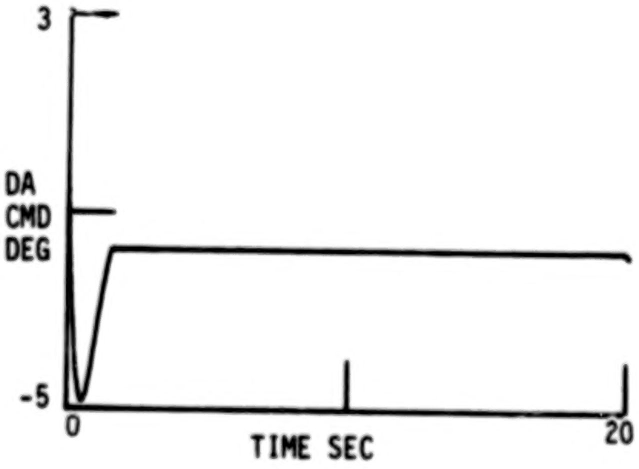

REFERENCES

1. Axaster, S., "Sub-Optimal Time Variable Feedback Control of Linear Dynamic Systems with Random Inputs", Inter. J. of Control, Vol. 4, No. 6, Dec. 1966, pp. 549-566.

2. Rekasius, Z. V., "Optimal Linear Regulators with Incomplete State Feedback", IEEE Trans. Automatic Control, Vol. AC-12, June 1967, pp. 296-299.

3. Kosut, R. L., "Suboptimal Control of Linear Time-Invariant Systems Subject to Control Structure Constraints", IEEE Trans. Automatic Control, Vol. AC-15, October 1970, pp. 557-563.

4. Levine, W. S., and Athans, M., "On the Determination of the Optimal Constant Output Feedback Gains for Linear Multivariable Systems", IEEE Trans. Automatic Control, Vol. AC-15, February 1970, pp. 44-48.

5. Kurtaran, B., and Sidar, M., "Optimal Instantaneous Output-Feedback Controllers for Linear Stochastic Systems", Inter. J. of Control, Vol. 19, No. 4, April 1974, pp. 154-157.

6. O'Reilly, J., "Optimal Instantaneous Output-Feedback Controllers for Discrete-Time Linear Systems with Inaccessible State", Inter. J. of System Science, Vol. 9, No. 1, Jan. 1978, pp. 9-16.

7. Sobel, K., and Kaufman, H., "Application of Stochastic Optimal Reduced State Feedback Gain Computation Procedures to the Design of Aircraft Gust Alleviation Controllers", Proc. of IFAC Conference, vol. 2, Helsinki, Finland, 1978, pp. 1127-1233.

8. Horisberger, H. P., and Belanger, P. R., "Solution of the Optimal Constant Output Feedback Problem by Conjugate Gradients", IEEE Trans. Automatic Control, Vol. AC-19, No. 4, August 1974, pp. 434-435.

9. Athans, M., "The Role and Use of the Stochastic Linear-Quadratic-Gaussian Problem in Control System Design", IEEE Trans. Automatic Control, Vol. AC-16, December 1971, pp. 529-552.

10. Halyo, N., and Broussard, J. R., "A Convergent Algorithm for the Stochastic Infinite-Time Discrete Optimal Output Feedback Problem", Proc. of the 1981 JACC, Charlottesville, VA, June 1981, p. WA-1E.

11. Doyle, J. C., and Stein, G., "Robustness with Observers", IEEE Trans. Automatic Control, Vol. AC-24, August 1979, pp. 607-611.

12. Johnson, T. L., and Athans, M., "On the Design of Optimal Constrained Dynamic Compensators for Linear Constant Systems", IEEE Trans. Automatic Control, Vol. AC-15, December 1970, pp. 658-660.

13. Mendel, J. M., and Feather, J., "On the Design of Optimal Time-Invariant Compensators for Linear Stochastic Time-Invariant Systems", IEEE Trans. Automatic Control, Vol. 20, No. 5, October 1975, pp. 653-656.

14. Broussard, J. R., and Halyo, N., "Active Flutter Suppression Using Optimal Output Feedback Digital Controllers", NASA CR-165939, May 1982.

15. Witsenhausen, H. S., "A Counterexample in Stochastic Optimum Control", SIAM J. of Control, Vol. 6, No. 1, Feb. 1968, pp. 131-147.

16. Whittle, P., and Rudge, J. F., "The Optimal Linear Solution of a Symmetric Team Control Problem", J. of Applied Probability, Vol. 11, No. 2, June 1974, pp. 337-381.

17. Sandell, N. R., Varaiya, P., Athans, M., and Safonov, M. G., "Survey of Decentralized Control Methods for Large Scale Systems", IEEE Trans. on Automatic Control, Vol. AC-23, No. 2, April 1978, pp. 108-128.

18. Caglayan, A. K., Halyo, N., and Broussard, J. R., "The Use of the Optimal Output Feedback Algorithm in Integrated Control System Design", Proceedings of the IEEE 1983 National Aerospace and Electronics Conference NAECON 1983, Vol. 2, 1983, pp. 1242-1251.

N84
20584

UNCLAS

N84 20584

PILOT MODELING, MODAL ANALYSIS, AND CONTROL OF LARGE FLEXIBLE AIRCRAFT

David K. Schmidt
School of Aeronautics and Astronautics
Purdue University
West Lafayette, IN

First Annual NASA Aircraft Controls Workshop
NASA Langley Research Center
Hampton, Virginia
October 25-27, 1983

INTRODUCTION

The issues to be addressed in this presentation are threefold. The first deals with the question of whether dynamic aeroelastic effects can significantly impact piloted flight dynamics. If so, when and how does this come about, and is there a potential design problem? For example, if one were to explore this problem experimentally, what mathematical model would be appropriate to use in the simulation? What modes, for example, should be included in the simulation, or what linear model should be used in the control synthesis? The second question deals with the appropriate design criteria or design objectives. In the case of active control, for example, what should be the design objectives for the control synthesis if aeroelastic effects are a problem. Finally, if unacceptable characteristics are to be eliminated through active control, what is the achievable performance improvement for practical systems? (See fig. 1.)

The outline of the topics to be presented includes a description of a model analysis methodology aimed at answering the question of the significance of higher order dynamics. Secondly, a pilot vehicle analysis of some experimental data will be presented that addresses the question of "What's important in the task?" The experimental data will be presented briefly, followed by the results of an open-loop modal analysis of the generic vehicle configurations in question. Finally, one of the vehicles will be augmented via active control and the results presented.

ISSUES

- CAN DYNAMIC AEROELASTIC EFFECTS SIGNIFICANTLY IMPACT (PILOTED) AIRCRAFT FLIGHT DYNAMICS?

  WHEN - HOW?

  IS THERE A POTENTIAL PROBLEM?

- WHAT ARE APPROPRIATE DESIGN CRITERIA OR OBJECTIVES?

- WHAT IS THE ACHIEVABLE PERFORMANCE IMPROVEMENT VIA ACTIVE CONTROL?

Figure 1

WHAT AFFECTS VEHICLE TIME RESPONSE

Linear system theory tells us that a system's response to a particular input may be represented mathematically as the summation of contributions from each of the system's modes. Each mode's contribution, furthermore, may be analytically thought of as a term in the partial-fraction expansion of the transform of the system's response. The significance of the eigenvalues of the system to its response is well known. However, equally significant is the residue associated with each system eigenvalue. For real vehicles, the response theoretically includes an infinite summation over all of the system's modes. However, practically speaking, only a finite number of these modes contributed significantly to the vehicle response. Furthermore, for a conventional aircraft and considering a short period approximation, for example, only one mode is used to approximate the vehicle's response. Furthermore, stating handling qualities specifications in terms of the modal damping and frequency was sufficient in this case to specify acceptable and unacceptable time responses. It is clear then that when the higher order modes of the system (or the eigenvalues and residues of those modes) are such that they significantly contribute to the time response of the system, those modal contributions must be considered to accurately reflect the system's dynamics. (See fig. 2.)

CLASSICAL EXAMPLE:

RIGID BODY $\dot{\theta}(s)/\alpha_g(s)$ (E.G. GUST PULSE)

$$\dot{\theta}(s) = \frac{R_1}{s + \lambda_1} + \frac{R_2}{s + \lambda_2} + \left[\sum_{i=i}^{\infty} \frac{R_i}{s + \lambda_i}\right]$$

R_i'S FUNCTIONS OF λ'S AND ZEROS (EIGENVECTORS)

AND FOR CONVENTIONAL VEHICLES THE EFFECTS OF

λ'S ON R_i'S WAS ENOUGH TO ALLOW STATING HANDLING

QUAL. SPECS. ON λ'S ONLY

Figure 2

VEHICLE TIME RESPONSE (CONTINUED)

Now consider the same example response, that is, pitch rate to a gust pulse, represented mathematically in the time domain with the usual state equations. Transforming these equations into modal coordinates and expressing the partial-fraction expansion of the transform of the response, we see that the expansion may be determined directly from the parameters in the system's time-domain modal state representation. Specifically, in fact, the residues associated with each mode are simply a product of the elements obtained from the modal observability matrix and the elements obtained from the modal disturbability or controllability matrix, depending upon which input is being considered. All these results are developed for the input represented mathematically as an impulse, or the residues are the system's impulse-response residues for the input selected. (See fig. 3.)

LET $\frac{\dot{\theta}(s)}{\alpha_g(s)} = K\,N(s^m)/D(s^n)$

or $\dot{\bar{x}} = A\,\bar{x} + B\,\alpha_g \qquad \dot{\theta}(t) = [1,\ \ldots\ 0]\,\bar{x}$

IN MODAL COORDINATES

$$\dot{\bar{q}} = \Lambda\,\bar{q} + D\,\alpha_g \qquad \dot{\theta}(t) = Y(t) = C\bar{q}$$

$$D = T^{-1}B \qquad C = [1,\ 0\ \ldots\ 0]T \qquad T = [\bar{\nu}_1 \vdots \bar{\nu}_2 \cdots\ \nu_n$$

Now $\dot{\theta}(s) = Y(s) = C[sI - \Lambda]^{-1}D = \sum_{i=i}^{n} \left[\frac{c_i d_i}{s-\lambda_i}\right]$

AND $\dot{\theta}(t) = \sum_{i=i}^{n} c_i d_i\, e^{-\lambda_i t}$

$$= \sum_{i=1}^{n} R_i\, e^{-\lambda_i t} \quad \text{where} \quad \underline{R_i = c_i d_i}$$

Figure 3

VEHICLE TIME RESPONSE (CONCLUDED)

Furthermore, the residues associated with the system's step response are easily obtained in terms of the previously determined impulse residues and the eigenvalues for the particular mode. Finally, this system's step response and each mode's contribution to that response may alternatively be considered as the area under the impulse response, and the contribution of each mode to that term is shown in figure 4.

- RESIDUES FOR THE SYSTEM'S STEP RESPONSE ARE

$$R_S^i = R_I^i/\lambda_i \qquad i = 1, \ldots, n$$

λ_i = eigenvalue

R_I^i = impulse residue

- AREA UNDER IMPULSE RESPONSE DUE TO MODE I IS

$$A_i(t) = R_I^i/\lambda_i \quad (e^{\lambda_i t}-1)$$

Figure 4

APPLICATION OF THE METHODOLOGY

To apply the technique presented, one must determine the appropriate system inputs that are important in the application, as well as determine the significant physical response variables of the system that are important in the piloted task. Inputs in question include the pilot stick input and atmospheric turbulence. Important vehicle responses might include rigid-body attitude and rate, sensed attitude and rate including elastic deformation effects, flight path angle, acceleration at various locations on the vehicle, and so forth. Furthermore, the inputs just cited may not be well modeled by white noise, for example. Therefore, evaluating the pure impulse response of the aircraft is not as meaningful as the response evaluated with appropriate input characteristics included. The input characteristics that are significant are the limited bandwidth properties of the pilot's input as well as the atmospheric gust spectrum. These input characteristics may be incorporated with the vehicle math model to form what might be referred to as an integrated dynamic model. Modal analysis is then performed on this model such that controllability, disturbability, observability, and, in particular, modal residues may be assessed. (See fig. 5.)

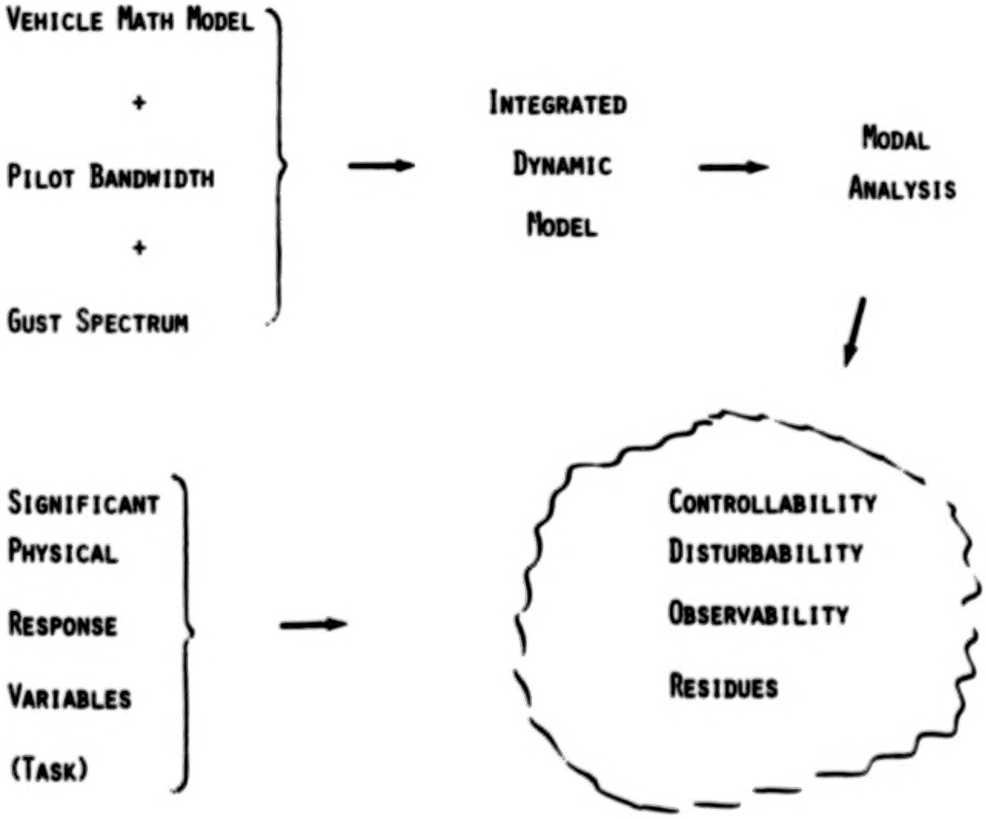
Vehicle Math Model
+
Pilot Bandwidth
+
Gust Spectrum
Integrated
Dynamic
Model
Modal
Analysis
Significant
Physical
Response
Variables
(Task)
Controllability
Disturbability
Observability
Residues

Figure 5

SYSTEM RESPONSES OF IMPORTANCE

The question now turns to what vehicle responses are significant in this problem. As shown in figure 6, both rigid-body attitude as well as indicated attitude, which includes the local elastic deformation of the vehicle, may be considered significant response variables. Determining the important vehicle responses in a longitudinal task will now be considered.

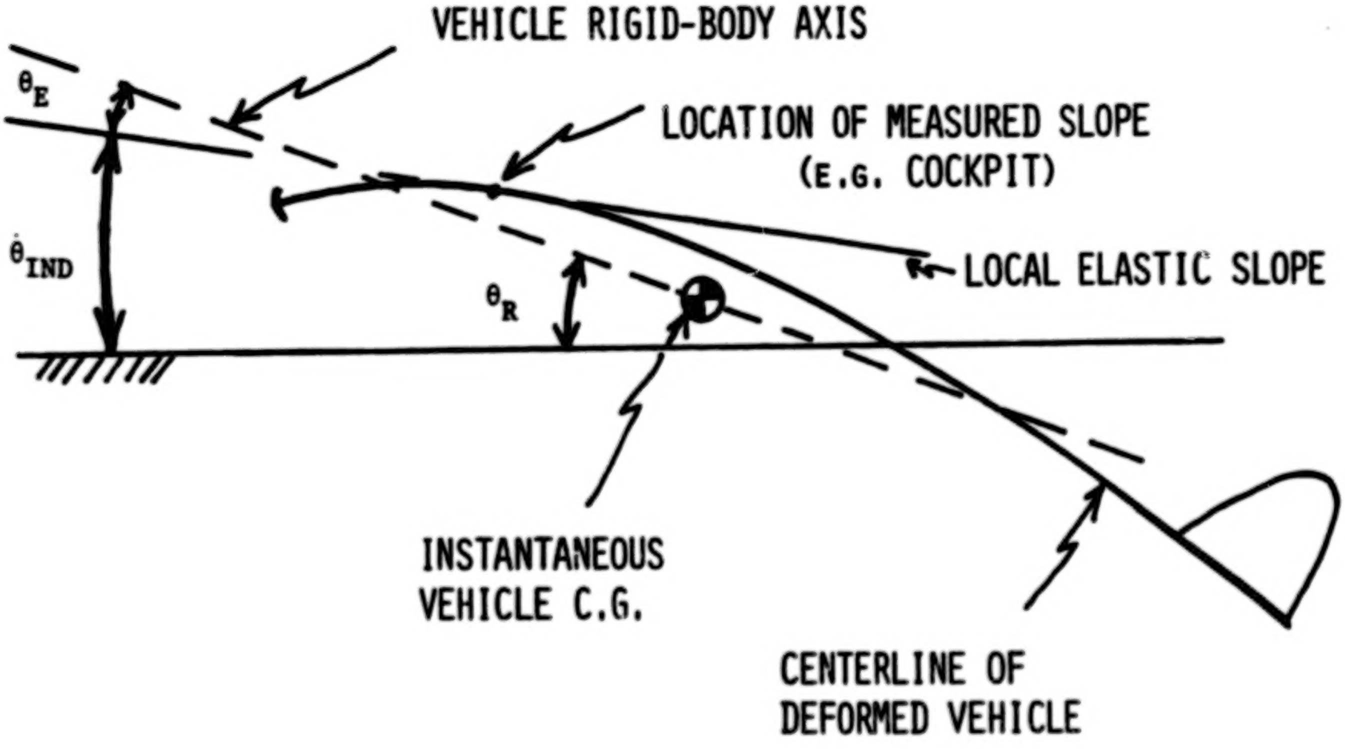
VEHICLE RIGID-BODY AXIS
θ_E
LOCATION OF MEASURED SLOPE
(E.G. COCKPIT)
θ_{IND}
LOCAL ELASTIC SLOPE
θ_R
INSTANTANEOUS
VEHICLE C.G.
CENTERLINE OF
DEFORMED VEHICLE

Figure 6

PILOT VEHICLE ANALYSIS

To better understand the important vehicle responses in the longitudinal axis, a pilot vehicle analysis was performed on a set of generic vehicle dynamics. An optimal-control pilot model was used in this evaluation with essentially "standard" model parameters. Details of this analysis may be found in reference 1. The pilots in the experimental setting were to perform a pitch-attitude tracking task, and this same task was evaluated analytically as well. The observations available to the pilots were both the indicated attitude of the vehicle, as measured at the cockpit, as well as the commanded attitude that the subjects were to follow. The issue is the selection of the appropriate pilot objective, or the appropriate vehicle response that the pilot was attempting to control. Was the pilot attempting to minimize indicated attitude, which included the elastic deformation of the vehicle, or is rigid-body attitude the response that he is attempting to control? The geometry of the basic vehicle may be considered to be as shown in figure 7. Seven different sets of generic vehicle dynamics were evaluated, where the first configuration represents a vehicle similar to the B-1. The remaining configurations may be thought of as having the same geometric characteristics, but the material properties of the structure are changed such that the in-vacuo mode frequencies of the structure are modified from Configuration 1, or the baseline. The resulting eigenvalues of the dynamic configurations are represented in Table 1.

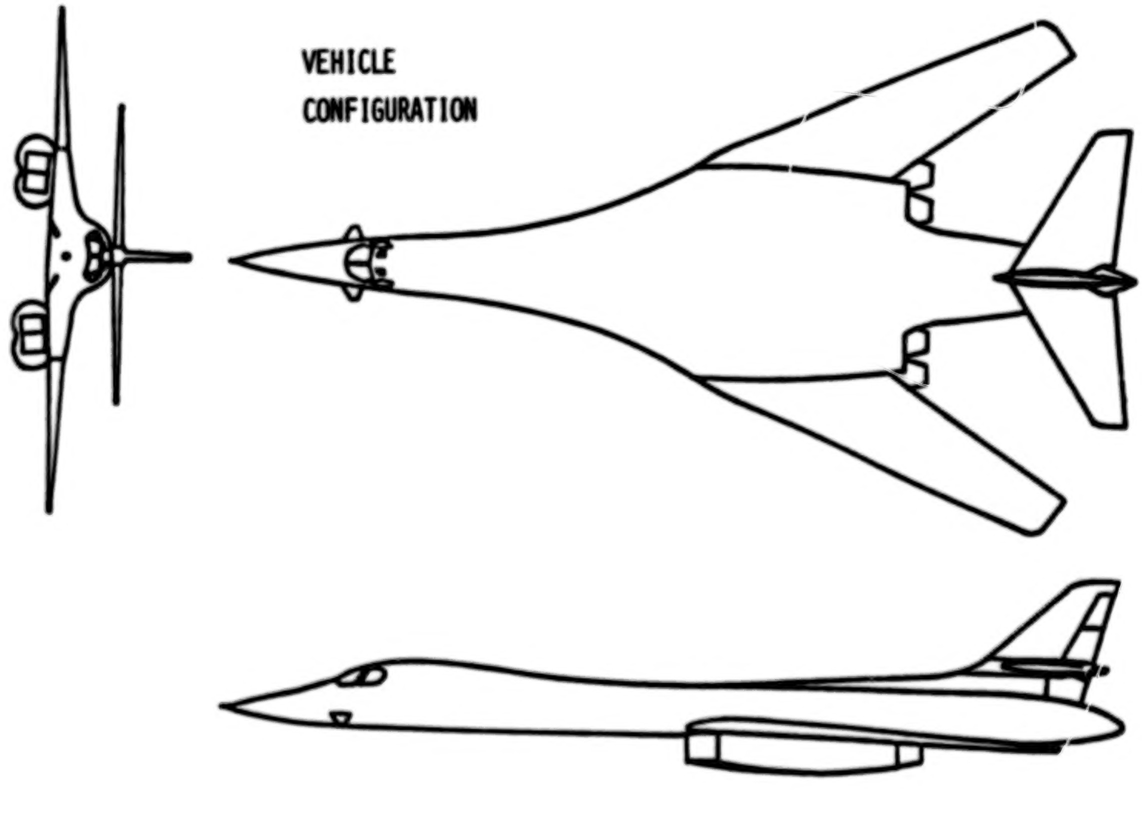

Figure 7

CONFIGURATION SUMMARY

Shown in Table 1 are the in-vacuo mode frequencies of the first two elastic modes included in the vehicle models. Mode 1 represents the first fuselage bending mode, while mode 2 has a mode shape that would correspond to the second fuselage bending mode. These mode frequencies were varied parametrically, and the resulting aeroelastic vehicle model was obtained in each case. The eigenvalues of the vehicle are listed in the table as well. Each of the modes was identified from its eigenvector or mode shape. Note, in particular, the first four configurations. Configurations 1-3 arise from a monotonic reduction in vibration frequency of the first fuselage mode. Configuration 4 (although perhaps unrealistic physically) has a reduced mode frequency associated with the other elastic mode. Furthermore, comparing Configurations 3 and 4 in terms of their eigenvalues indicates that both have unstable phugoid modes and approximately equivalent short period eigenvalues, and also they exhibit roughly similar aeroelastic mode eigenvalues.

Table 1

CONFIGURATION	IN-VACUO FREQUENCIES		PHUGOID	SHORT PERIOD	ELASTIC MODES	
	MODE 1	MODE 2	MODE*	MODE*	FIRST*	SECOND*
1(BASELINE)	13.7	21.2	(.02, .08)	(.53, 2.8)	(.05, 13.3)	(.02,21.4)
2	9.2	21.2	(0., .06)	(.52, 2.6)	(.09, 8.8)	(.02,21.4)
3	6.2	21.2	(+.09)(-.08)	(.52, 1.8)	(.20, 5.9)	(.02,21.4)
4	13.7	4.8	(+.15)(-.13)	(.69, 1.6)	(.05, 13.3)	(.11, 6.0)
5	10.7	9.3	(+.05, -.03)	(.55, 2.4)	(.11, 10.3)	(0.0, 9.8)
6	11.7	11.7	(0., .05)	(.54, 2.6)	(.08, 11.7)	(0.0,11.6)
7	6.9	6.9	(+.18)(-.15)	(.70, 1.4)	(.19, 7.3)	(0.0, 6.9)

*MODAL PARAMETER NOTATION, COMPLEX (ζ, ω_N), REAL (-P), ALL FREQUENCIES IN RAD/SEC

SUMMARY OF EXPERIMENTAL RESULTS

Shown in Table 2 is the summary of tracking scores and subjective rating associated with the seven dynamic configurations. Of significant importance is the pilot comment associated with Configuration 5. He specifically stated that he was attempting to ignore the oscillation that he observed in the display, and he attempts to control the rigid-body attitude. Note in the results a monotonic degradation in tracking performance and subjective rating as the elastic mode frequencies in Configurations 1-3 are reduced.

Table 2

Configuration	RMS Error (deg) (mean ± 1σ)	Cooper-Harper Rating (mean ± 1σ)	Comments
1	1.2 ± 0.6	1.6 ± 0.4	Very nice; No problem.
2	1.0 ± 0.5	2.0 ± 0.3	Little oscillation; More difficult than C1; Slight control response lag.
3	5.7 ± 1.1	5.9 ± 1.9	Difficult; Required high concentration; PIO problem; Extreme response lag.
4	1.9 ± 0.3	3.1 ± 1.1	Little more difficult than C1; Slightly sluggish attitude response.
5	1.2 ± 0.5	1.9 ± 0.4	Not difficult, little more oscillation, but could ignore it and fly rigid-body; Like config. 2.
6	1.5 ± 0.7	2.0 ± 0.5	Pretty good; Same as 2.
7	7.6 ± 2.8	6.7 ± 1.6	With severe oscillations, virtually uncontrollable. Abrupt control inputs led to disaster.

COMPARISON OF ANALYTICAL AND EXPERIMENTAL RESULTS

Shown in figure 8 is the comparison of the tracking performance obtained analytically with the pilot/vehicle analysis and the performance obtained experimentally, shown in the previous table. Note in the case of Configuration 3, for example, the low tracking score predicted from the model under the assumption that the subjects were attempting to control the displayed error. This error, as you recall, included the elastic contribution to the displayed attitude. On the other hand, modeling the task as a rigid-body attitude control task results in the analytical tracking errors as shown in the figure.

ORIGINAL PAGE IS OF POOR QUALITY

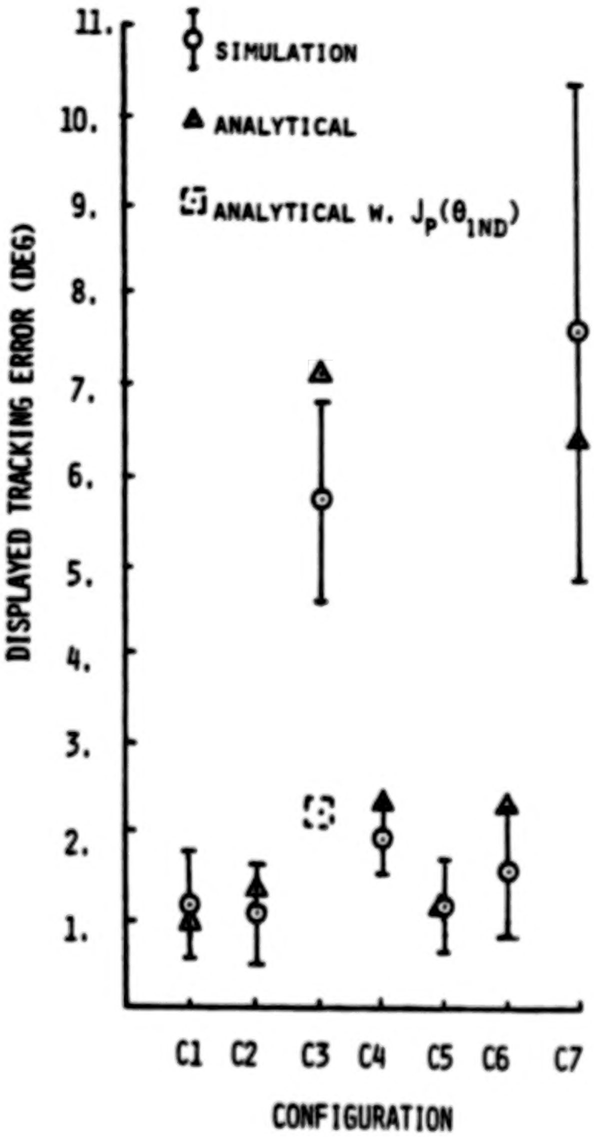

Figure 8

COMPARISON OF ANALYTICAL AND EXPERIMENTAL SUBJECTIVE RATINGS

Shown in figure 9 is the excellent correlation between experimental subjective ratings and the ratings obtained analytically from a model-based metric. The metric used was simply the magnitude of the quadratic cost function obtained naturally in the modeling process. These results, and the results of the previous figure, indicate that rigid-body attitude is the primary control variable in the closed-loop pitch tracking task. Also, experimental and analytical results indicate clearly that as elastic mode frequencies coalesce with the rigid-body modes, the tracking performance is significantly degraded.

ORIGINAL PAGE IS
OF POOR QUALITY

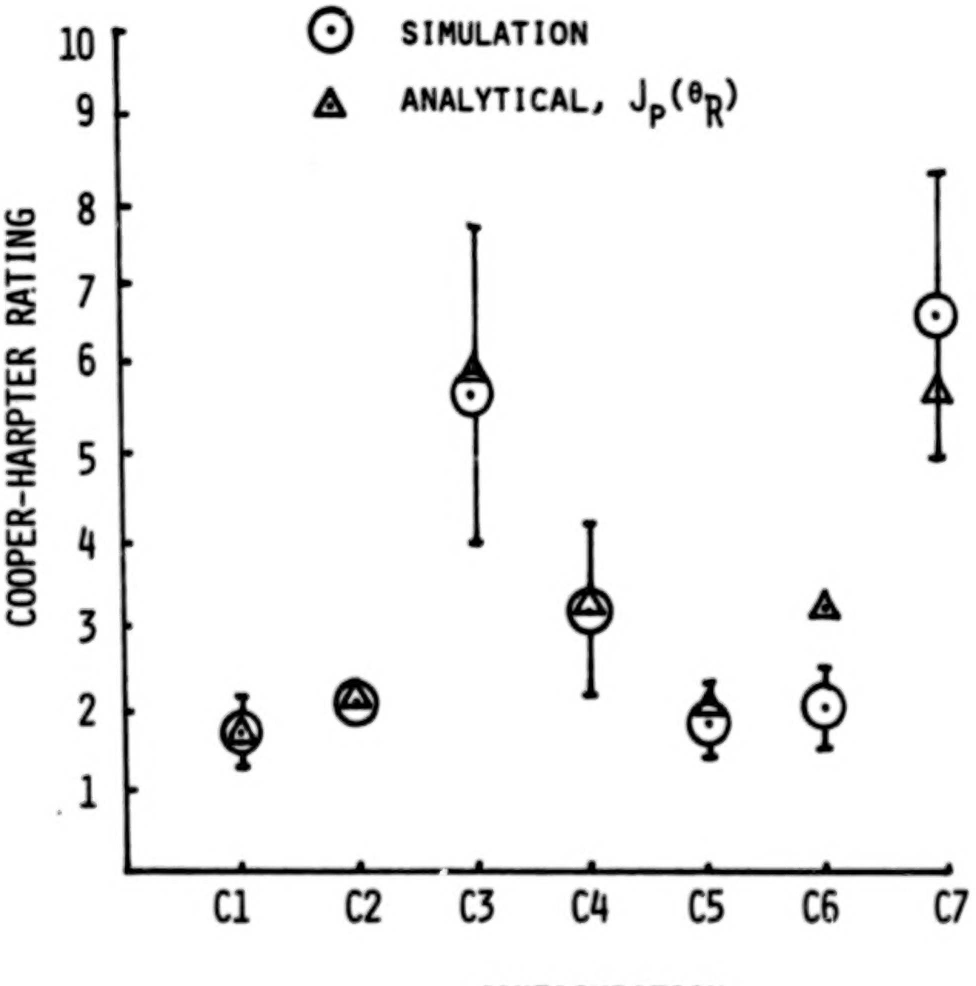

Figure 9

OPEN-LOOP VEHICLE ANALYSIS

Performing the modal analysis outlined previously on the seven configurations results in the modal residues shown in figures 10-13 for Configurations 1-4. (See Ref. 2 for complete results.) Along with other system's responses, these results indicate clearly the contribution of the first aeroelastic mode to the rigid-body pitch rate ($\dot{\theta}_R$) pilot impulse response. We refer to these residues as pilot impulse residues because they include the important characteristic of limited pilot bandwidth. This is modeled simply as an impulse passed through a first-order lag with time constant representative of that of the pilot. Note the monotonic increase in the residue in the rigid-body pitch rate associated with the first aeroelastic mode, as the frequency of this mode is reduced (Conf. 1-3). This residue in the case of Configuration 3 is actually larger than the residue associated with the "rigid-body" short period mode. Reiterating, in the case of Configuration 3, the rigid-body pitch rate response is dominated by the first aeroelastic mode, where dominance is defined in terms of residue magnitude.

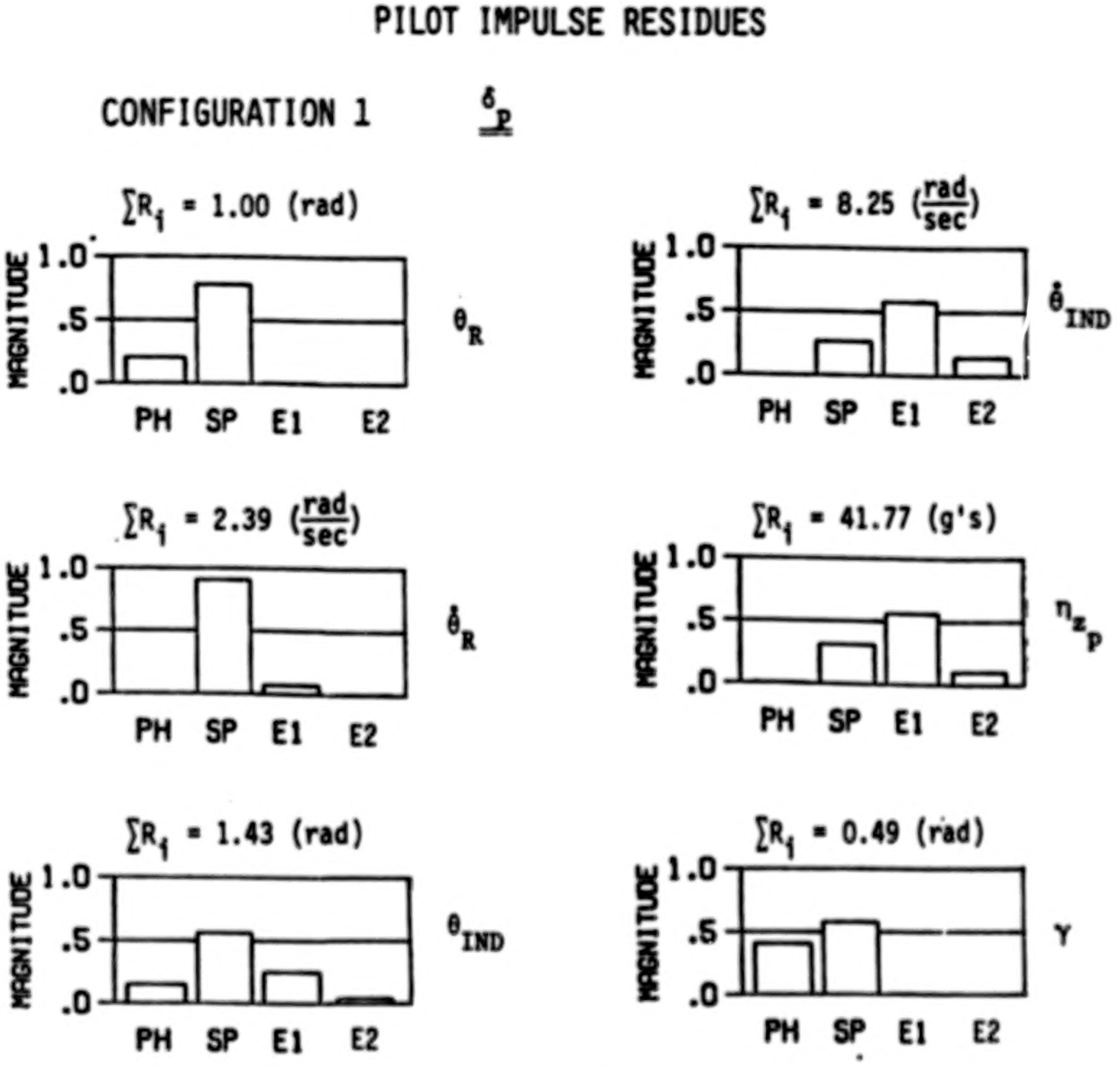

Figure 10

PILOT IMPULSE RESIDUES

CONFIGURATION 2 $\underline{\delta_P}$

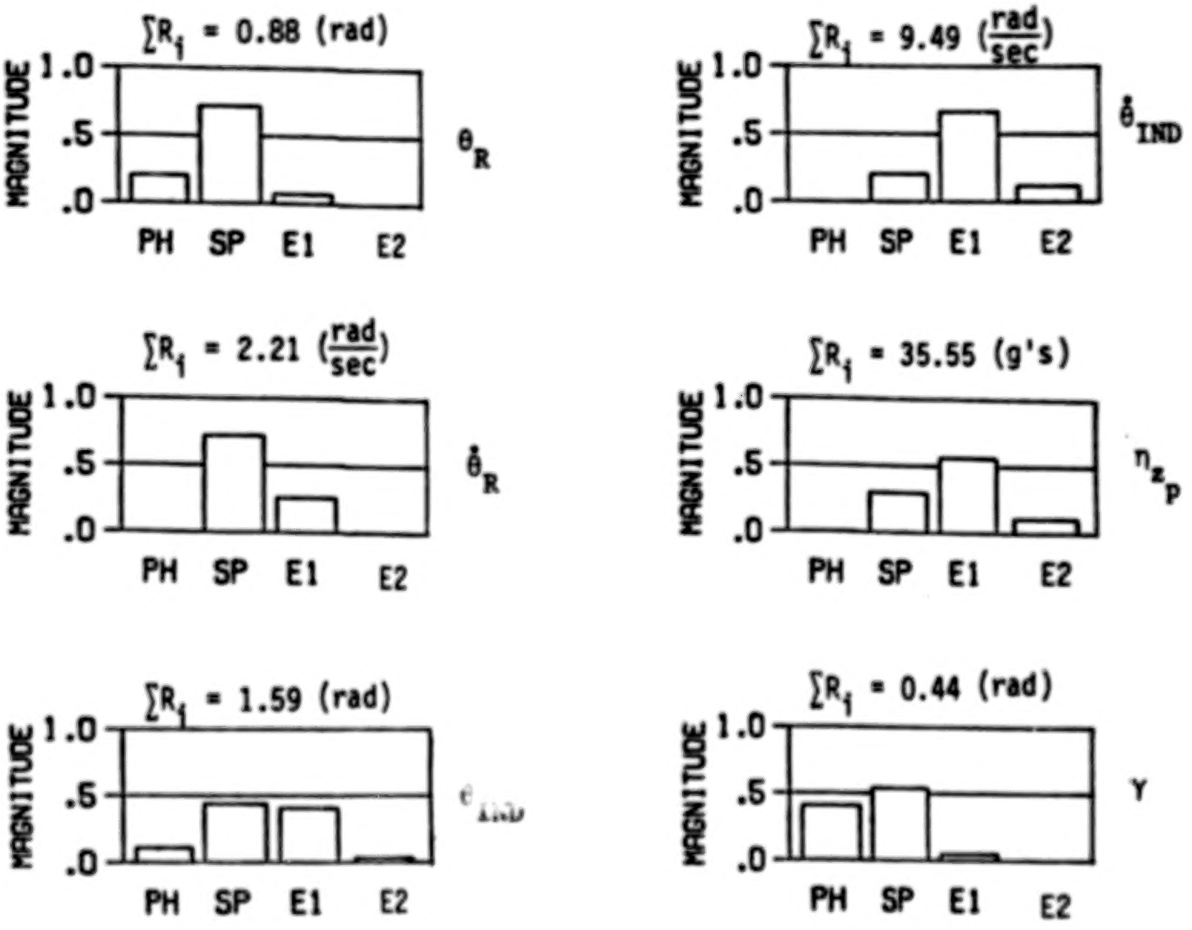

Figure 11

PILOT IMPULSE RESIDUES

CONFIGURATION 3 $\underline{\delta_p}$

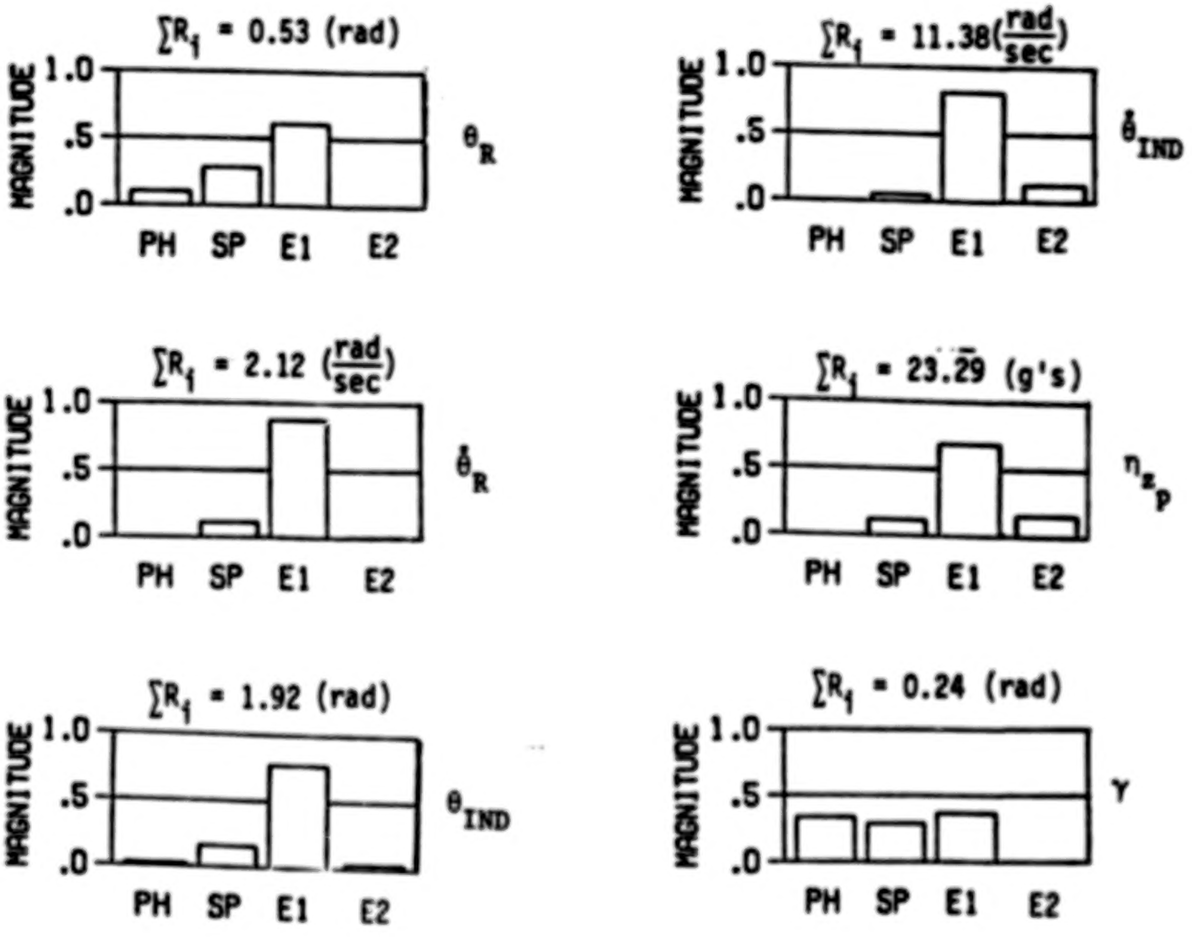

$\sum R_i = 0.53$ (rad)

$\sum R_i = 11.38 (\frac{rad}{sec})$

$\sum R_i = 2.12 (\frac{rad}{sec})$

$\sum R_i = 23.29$ (g's)

$\sum R_i = 1.92$ (rad)

$\sum R_i = 0.24$ (rad)

Figure 12

OPEN-LOOP VEHICLE ANALYSIS (CONCLUDED)

Note, on the other hand, the residues for rigid-body pitch rate for Configuration 4. Although the contribution of this elastic mode to the response is measurable, the response is still dominated by the short-period mode. This result, along with the results for Configuration 3, explains why the tracking performance and subjective rating for Configuration 3 were so drastically inferior to those of Configuration 4. This was true in spite of the fact that these two configurations had roughly comparable eigenvalues. Clearly, the eigenvalues alone do not completely explain the results obtained experimentally.

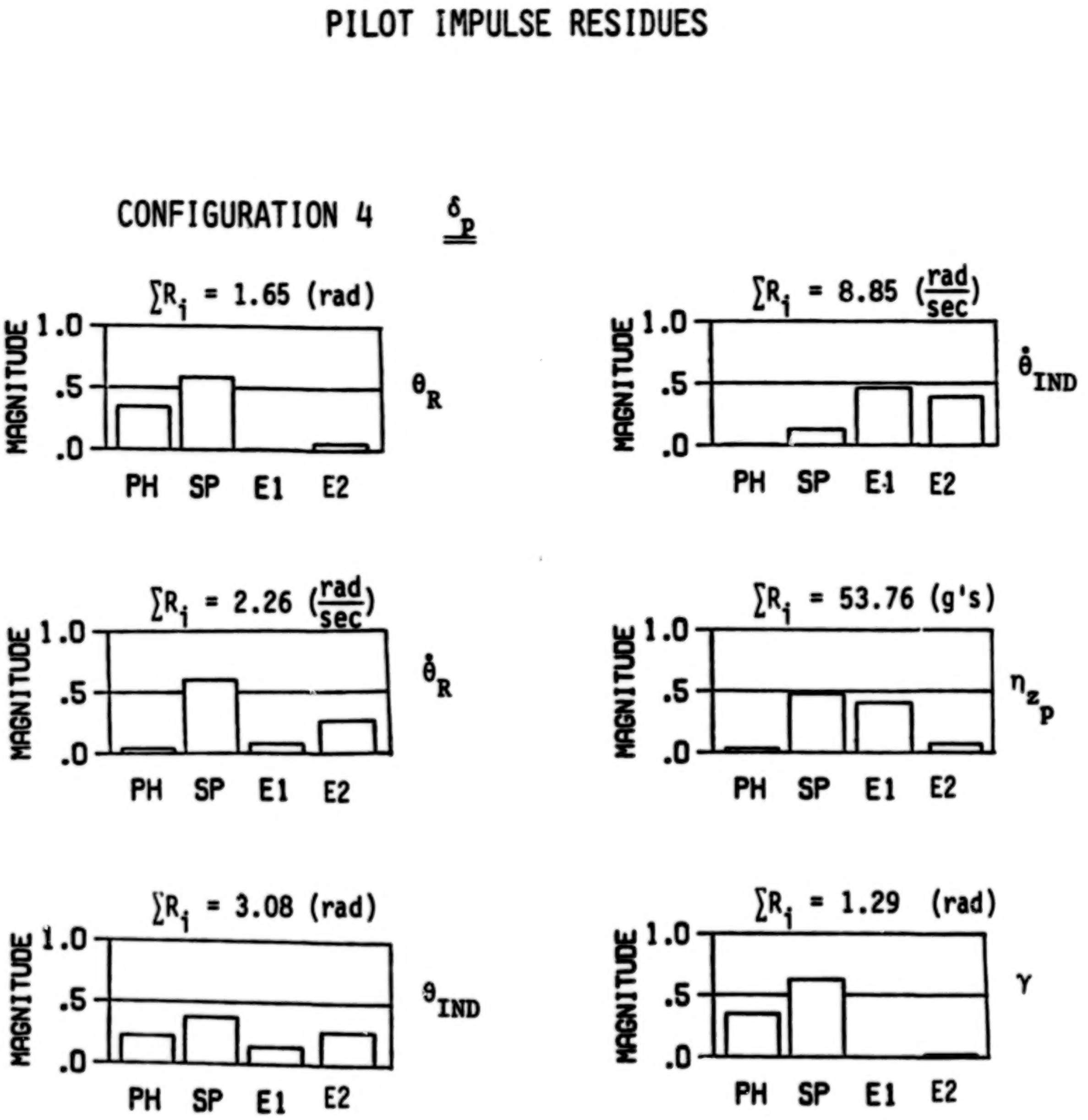

Figure 13

MODIFICATION THROUGH MODAL CONTROL

Given a linear system's dynamics, a control law can be determined such that the closed-loop eigenvalues and eigenvectors are modified to exhibit more desirable characteristics (fig. 14). The number of closed-loop or augmented system modes that may be "placed" is equal to the number of measurements available for feedback, and the freedom to specify the mode shapes, or eigenvectors associated with these modes, depends on the rank of the control vector. (See Refs. 3, 4). Control laws based on this theoretical concept may be implemented with constant gain measurement-feedback architecture, or they may be synthesized with linear quadratic Gaussian (LQG) optimal control (Ref. 5). In the case of measurement feedback, if insufficient measurements are available, the unspecified system modes may be unstable. Conversely, control synthesis using LQG invokes the asymptotic properties of such controllers and theoretically guarantees augmented system stability. To explore the achievable performance that might be obtained through such modal control concepts, we have augmented one of the seven vehicle configurations considered previously (Configuration 2) with a constant gain feedback controller with gains determined directly from the eigenspace assignment goal.

EIGENSPACE ASSIGNMENT

(MODAL CONTROL)

GIVEN THE LINEAR SYSTEM

DYNAMICS $\dot{X} = AX + BU$

MEASUREMENTS $Z = CX$; DIM $Z = M$

CONTROLS $U = GZ$; DIM $U = R$

A GAIN G MAY BE FOUND SUCH THAT IF

$(A + BGC)\bar{v}_i = \lambda_i \bar{v}_i$

λ_i AND $\bar{v}_i$; $i = 1 . . . M$

HAVE DESIRABLE CHARACTERISTICS

Figure 14

UNAUGMENTED VEHICLE MODES

Shown in figure 15 are the mode shapes associated with three of the four modes of interest for Configuration 2 discussed previously. Recall that this configuration differs from the baseline in that the first fuselage bending mode frequency is reduced to approximately 9 radians per second. The baseline on the other hand had a first elastic mode of about 13 radians per second. It is evident in the figure that the "short period" mode actually includes a significant amount of elastic deformation. In contrast, the first aeroelastic mode also reflects the presence of rigid-body attitude in its mode shape. It is due to these modal characteristics that the rigid body response was degraded and the elastic mode's contribution was significant in the rigid-body pitch rate.

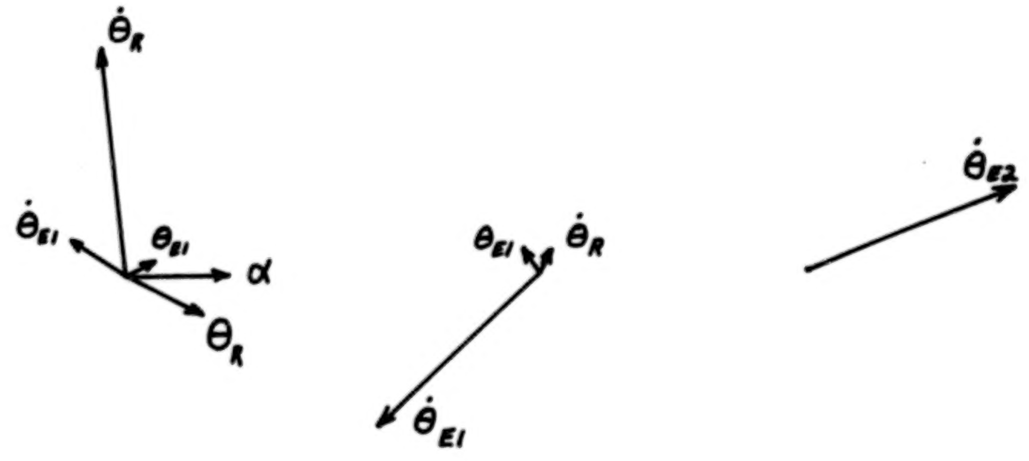

SHORT PERIOD ($\zeta = .52$, $\omega_n = 2.57$)

FIRST ELASTIC ($\zeta = .08$, $\omega_n = 8.8$)

SECOND ELASTIC ($\zeta = .02$, $\omega_n = 21.4$)

Figure 15

ORIGINAL PAGE IS
OF POOR QUALITY

UNAUGMENTED VEHICLE STEP RESPONSE

Shown in figure 16 is the rigid-body pitch rate step response for Configuration 2. The contribution of the first aeroelastic mode in this time response is clearly evident. The eigenspace assignment goal used for augmenting these dynamics included increasing the short period frequency slightly and increasing the damping of the first elastic mode from 0.08 to 0.20. In addition, the eigenvectors associated with these two modes were modified. The short-period eigenvector was to represent pure rigid-body response, while the first elastic eigenvector was selected for purely elastic deformation.

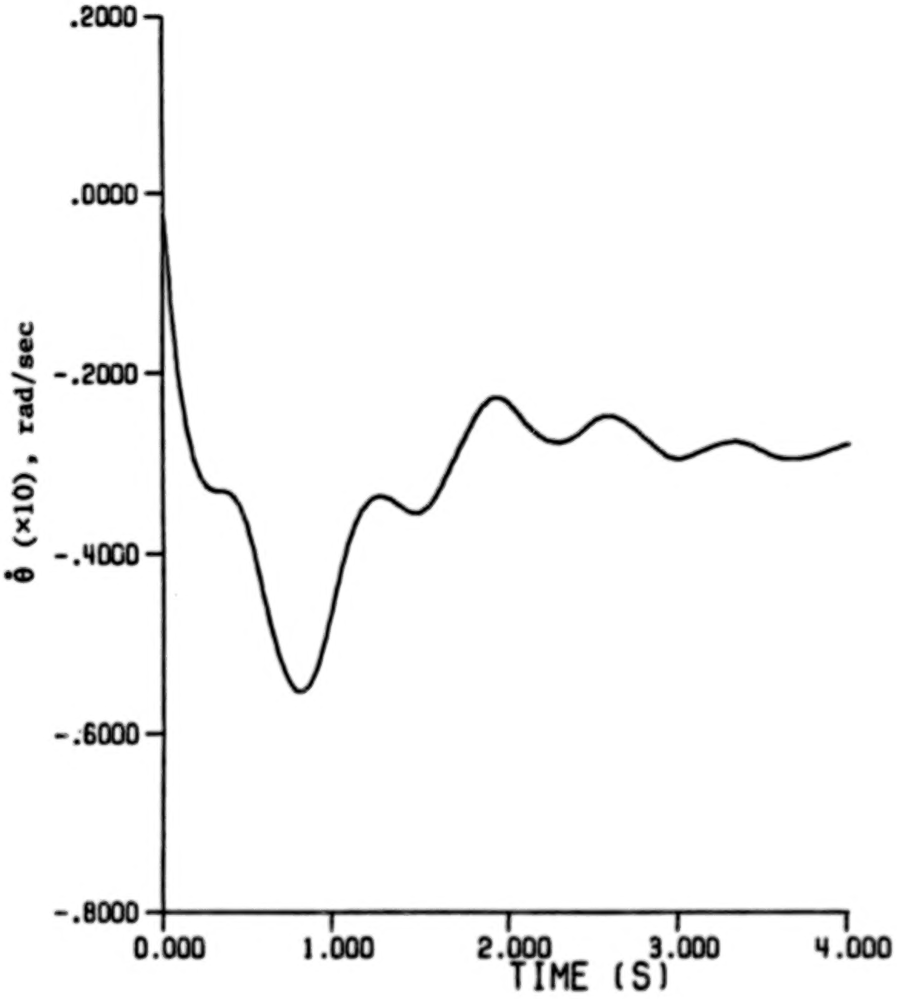

Figure 16

AUGMENTED VEHICLE MODE SHAPES

Shown in figure 17 are the eigenvectors of the augmented vehicle modified through modal control. Clearly, the short period mode approaches that of a "rigid" vehicle, while the first elastic mode is purified as well. In this example, only 4 measurements were selected for feedback (i.e., two accelerometers, appropriately positioned in the fuselage, along with pitch rate and pitch attitude gyros). Consequently, only 4 eigenvalues (or two modes) were specified The phugoid mode and the second aeroelastic mode were not placed in this case but could be if more measurements are made available. In addition, a control law with limited bandwidth should be selected such that the second elastic mode would be attenuated.

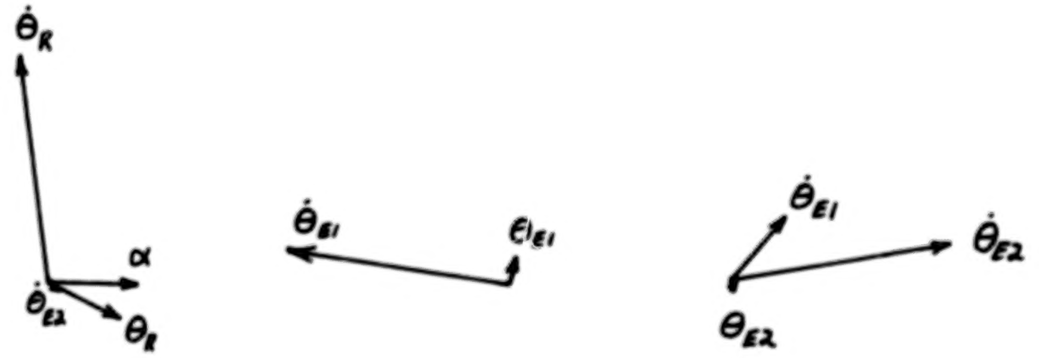

SHORT PERIOD (ζ = .53, ω_n = 2.8)

FIRST ELASTIC (ζ = .20, ω_n = 8.8)

SECOND ELASTIC (ζ = .02, ω_n = 20.8)

Figure 17

AUGMENTED VEHICLE STEP RESPONSE

Shown in figure 18 is the step response of the augmented vehicle. When compared to that in Configuration 2 the reduction of the contribution of the elastic mode to this rigid-body pitch rate response is evident. The long period divergence of this response is due to the phugoid mode instability. This demonstrates one of the shortcomings of implementing modal control through measurement feedback alone as cited previously. Additional measurements or equalization are required to stabilize the phugoid mode.

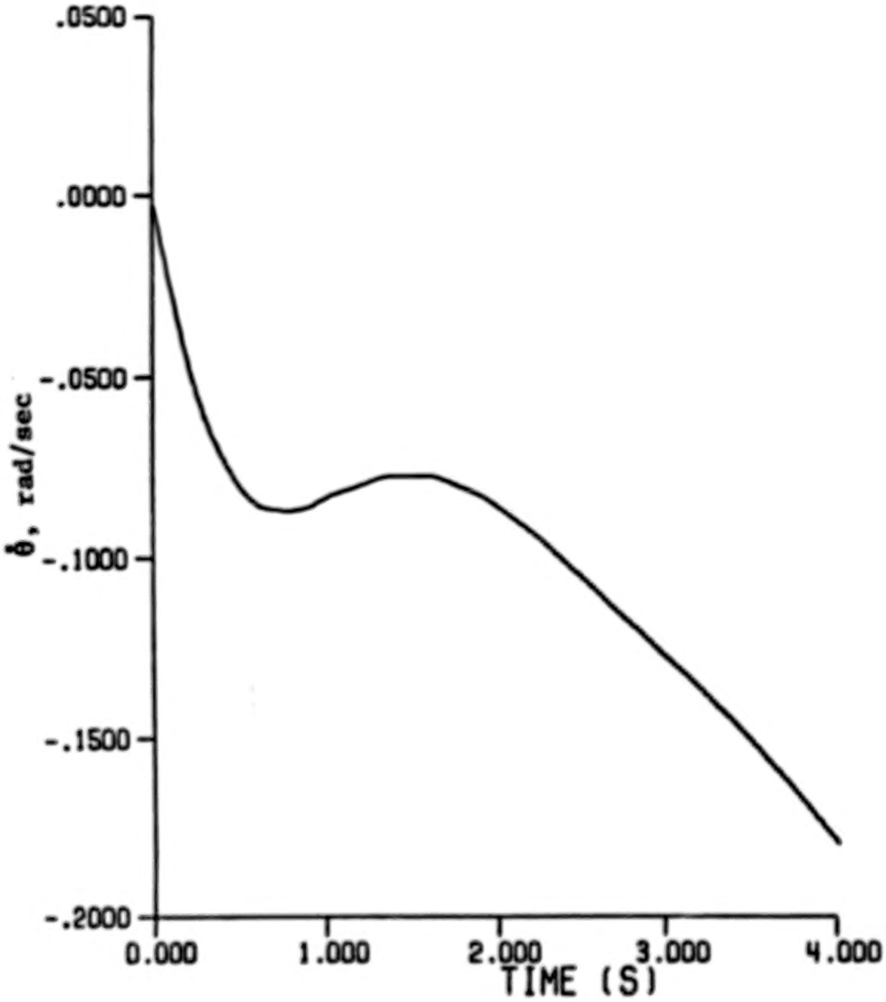

Figure 18

EFFECT OF AUGMENTATION ON RESIDUES

Shown in figure 19, finally, is the effect of the augmentation on residues for the pitch rate impulse response. These residues are comparable with those shown previously for the seven configurations. Compared to the unaugmented vehicle (Configuration 2), the results for the augmented vehicle clearly indicate the dominance of the short-period mode in this response.

In conclusion then, we see that handling characteristics, as measured by tracking performance and subjective rating in the tracking task, were significantly degraded due to the presence of dynamic aeroelastic effects. The rigid-body attitude angle was shown to be fundamental in the vehicle's response in this task. Furthermore, this response may be dominated by "aeroelastic" modes in severe cases. Clearly, from these results, a rigid-body mathematical model of the vehicle is inappropriate. Finally, the ability to modify the modal characteristics of the vehicle through modal control or eigenspace assignment appears to have merit in this application. Multiple control surfaces and an appropriate sensor complement will be required to implement practical modal controllers. Appropriate design criteria for flexible vehicles might be expressed in terms of allowable residue magnitudes of the higher order mode.

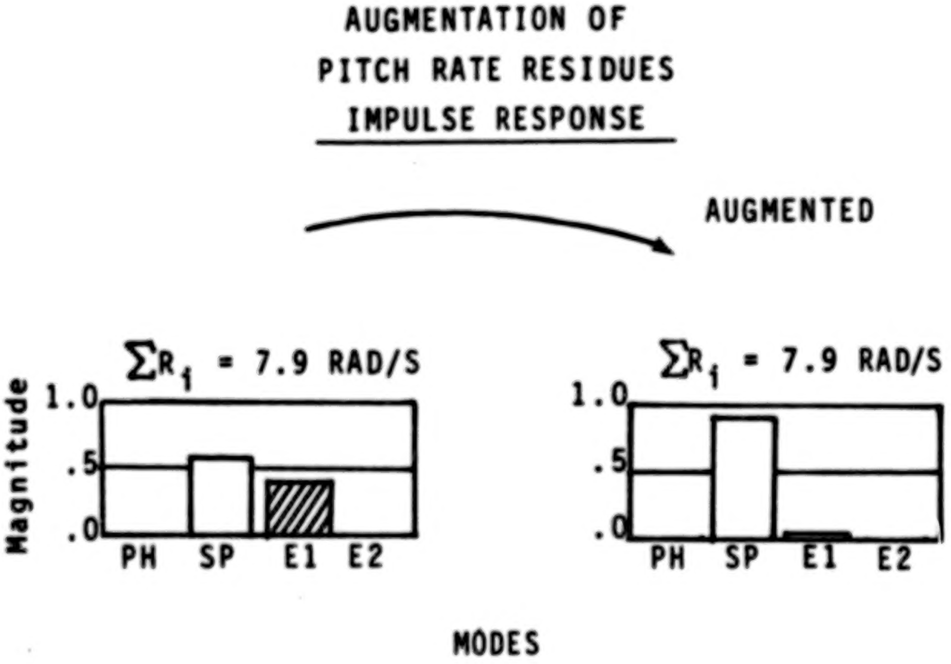

Figure 19

REFERENCES

1. Schmidt, K.K., "Pilot Modeling and Closed-Loop Analysis of Flexible Aircraft In the Pitch Tracking Task", AIAA Paper No. 83-2231, Guid. and Control Conference, August 1983.

2. Schmidt, D.K., "A Modal Analysis of Flexible Aircraft Dynamics With Handling Qualities Implications," AIAA Paper No. 83-2074, Atm. Flight Mech. Conference, August 1983.

3. Porter, B., and Crossby, T.R., Modal Control Theory and Applications, Barnes and Noble, New York, 1972.

4. Moore, B.C., "On the Flexibility Offered by State Feedback In Multivariable Systems Beyond Closed Loop Eigenvalue Assignment," IEEE Trans. Auto. Control, Vol. AC-21, No. 5, October 1976, pp. 689-691.

5. Harvey, C.A., Stein, G., and Doyle, J.C., "Optimal Linear Control (Characterization of Multi-Input Systems)," Office of Naval Research CR 215-238-2, March 1977.

N84
20585

UNCLAS

N84 20585 D18

NONLINEAR SYSTEMS APPROACH TO CONTROL SYSTEM DESIGN

George Meyer
NASA Ames Research Center
Moffett Field, CA

First Annual NASA Aircraft Controls Workshop
NASA Langley Research Center
Hampton, Virginia
October 25-27, 1983

PRECEDING PAGE BLANK NOT FILMED

PAGE 328 INTENTIONALLY BLANK

NONLINEAR CONTROL SYSTEM DESIGN METHODS

Consider some of the control system design methods for plants with nonlinear dynamics. If the nonlinearity is weak relative to the size of the operating region, then the linear methods apply directly. Fixed-gain design may be feasible even for significant nonlinearities. It may be possible to find a single gain which provides adequate control of the linear models at several perturbation points. If the nonlinearity is restricted to a sector, that fact may be used to obtain a fixed-gain controller. Otherwise, a gain may have to be associated with each perturbation point p_i. A gain schedule $K(p(v))$ is obtained by connecting the perturbation points by a function, say $p(v)$, of the scheduling parameter v (i.e., speed). When the scheduling parameter must be multidimensional, this approach is difficult; the objective of our research is to develop an easier procedure.

$$\dot{x} = f(x, u, z)$$

1. **SMALL OPERATING REGION – LINEAR METHODS**

   $$p = (x_o, u_o),\ \delta\dot{x} = \left(\frac{\partial f}{\partial x}\right)_p \delta x + \left(\frac{\partial f}{\partial u}\right)_p \delta u,\ \delta u = K(p)\,\delta x$$

2. **FIXED-GAIN DESIGN**
   - a. **ONE GAIN FOR ALL $\{p_i\}$**
   - b. **ONE GAIN FOR SECTOR NONLINEARITIES**
3. **GAIN SCHEDULING**

   $p_i = p(v_i)$, $K(p(v))$, v = **SCHEDULING PARAMETER**

4. **NONLINEAR TRANSFORMATION OF STATE AND CONTROL**

SIMPLIFICATION THROUGH COORDINATE CHANGE

We attempt to simplify the design problem by simplifying the representation of the plant. Here is an example. The state equation is nonsingular, but a fixed-gain design is impossible. The nonsingular matrix E represents rotation in the plane of x through the angle ψ. The change of control coordinates from u to v results in a globally constant, linear system. Even an approximate cancellation of E could be quite helpful, since the resulting system may be nearly constant and the fixed-gain design may be applicable.

$x \in R^2$, $u \in R^2$, $EE^T = I$

$\dot{x} = E\,(\psi(t))\,u$

$\psi = 0 \longrightarrow \dot{x} = u,\ \dot{x} = K_0 x$, STABLE

$\psi = \pi \longrightarrow \dot{x} = -u,\ \dot{x} = -K_0 x$, UNSTABLE

NEW CONTROL COORDINATES:

$v = E(\psi(t))\,u \longrightarrow \dot{x} = v$, GLOBALLY

APPROXIMATE TRANSFORMATION:

$v = E\,(\psi)\,u \longrightarrow \dot{x} = E\,(\delta\psi(t))\,v$ FIXED GAIN MAY WORK

BRUNOVSKY CANONICAL FORM

The first step in the design approach is to try to transform the given system into something more simple, i.e., ideally, a set of decoupled strings of integrators. This set is called the Brunovsky canonical form for controllable, constant, linear systems. The number of strings is given by the number of control axes m, and the number of integrators (dots in the figure) is given by a Kronecker index K_i. In general, $\Sigma K_i = n$. Two examples are shown for the case of $n = 12$ and $m = 4$. According to linear theory, the set of Kronecker indexes is invariant under nonsingular transformations and feedback.

GIVEN $\dot{x} = Ax + Bu$, $x \epsilon R^n$, $u \epsilon R^m$, (A, B) CONTROLLABLE

CAN BE TRANSFORMED WITH

$y = Tx$, $v = Rx + Wu$, (T, W) NONSINGULAR

INTO m DECOUPLED STRINGS OF INTEGRATORS, LENGTH = KRONECKER INDEX

EXAMPLE: $n = 12$, $m = 4$

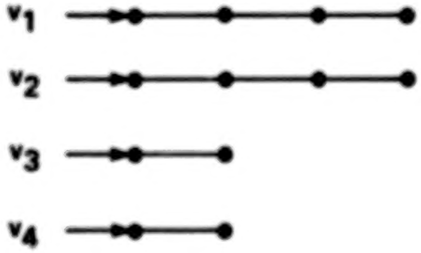

KI = (4,4,2,2)

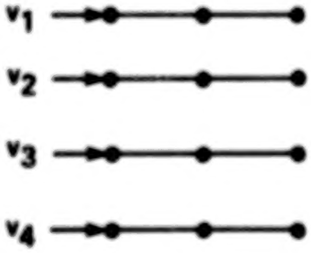

KI = (3,3,3,3)

OUTLINE OF DESIGN PROCEDURE

In principle, the design procedure is to transform the natural representation of the plant into the corresponding Brunovsky form, then design a control law $v = g(y)$ for the canonical system, and finally pull the law back into the natural coordinates in terms of which law must be implemented.

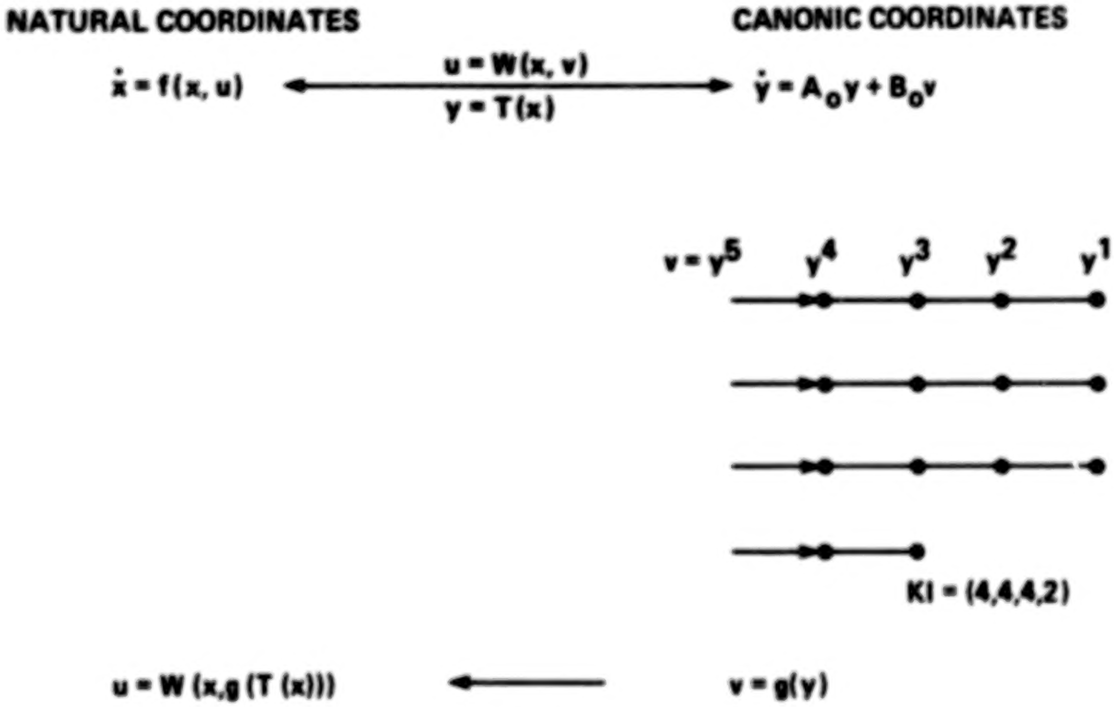
NATURAL COORDINATES
CANONIC COORDINATES
$\dot{x} = f(x, u)$
$u = W(x, v)$
$y = T(x)$
$\dot{y} = A_0 y + B_0 v$
$v = y^5$
y^4
y^3
y^2
y^1
KI = (4,4,4,2)
$u = W(x, g(T(x)))$
$v = g(y)$

DEVELOPMENT OF THE DESIGN APPROACH

Before this design approach becomes practical, several issues must be resolved.

(1) When can a given system be transformed into a linear model, how does one construct the required transformation, and how feasible is it to implement the resulting algorithm on flight computers?

(2) What is the structure of the complete control system that includes the linearization step?

(3) How robust is the resulting design?

(4) How can the constraints on control and state be enforced?

These issues have been explored both theoretically and experimentally. The results are summarized in the following figures.

1. **TRANSFORMATION**
    - a. **EXISTENCE**
    - b. **COMPUTATION**
    - c. **IMPLEMENTATION**

2. **STRUCTURE OF COMPLETE CONTROL SYSTEM**

3. **COMPLEXITY AND ACCURACY OF MODEL – ROBUSTNESS**
    - a. **EXACT STATE SPACE**
    - b. **TRUNCATED STATE SPACE**

4. **ENFORCEMENT OF DESIGN CONSTRAINTS**

5. **EXPERIMENTS**
    - a. **FORTRAN**
    - b. **REAL-TIME (FLIGHT COMPUTER, HYDRAULICS) SIMULATION**
    - c. **FLIGHT**

LIE BRACKETS

The key theoretical result from the existence of linearizing transformations is the result of work by Krener (ref. 1), Brockett (ref. 2), Jakubcyzk and Respondek (ref. 3), and Hunt and et al. (ref. 4). The necessary and sufficient conditions are best expressed in terms of lie brackets. A lie bracket (f, g) constructs a new vector field from the old ones f and g. A set is involutive if the brackets do not create new directions.

VECTOR FIELDS	$f, g: R^n \rightarrow R^n$
LIE BRACKETS	$[f, g] = \frac{\partial g}{\partial x} f - \frac{\partial f}{\partial x} g$
INVOLUTIVE SET	$\left\{h_1, \ldots, h_r\right\}$ IF $[h_i, h_j] \in \text{SPAN}\left\{h_1, \ldots, h_r\right\}$

CONDITIONS FOR LINEARIZABILITY

1. It is necessary to find control coordinates which appear linearly in the state equation. For aircraft this means angular acceleration instead of ailerons, elevator, and rudder.
2. The resulting system must have linear-like controllability.
3. The fields $\{f, g_1, g_2 \ldots, g_m\}$ must satisfy an involutivity condition. For example, let $n = 6$, $m = 2$, and the Kronecker index set $KI = (3, 3)$. Then, the six vector fields must span the state space and the first four must be involutive

1. $\dot{x} = f(x, u) \longrightarrow \dot{x} = f(x) + \Sigma\, g_i(x)\, u^*$
2. **LINEAR – CONTROLLABLE**
3. **INVOLUTIVE**

EXAMPLE: $\dot{x} = f(x) + g_1(x)u_1^* + g_2(x)u_2^*$

$KI = (3, 3)$

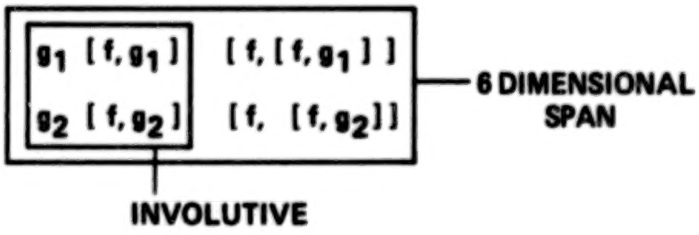

g_1 $[f, g_1]$ $[f, [f, g_1]]$

g_2 $[f, g_2]$ $[f, [f, g_2]]$

6 DIMENSIONAL SPAN

INVOLUTIVE

STRUCTURE OF THE COMPLETE CONTROL SYSTEM

The structure has the form of an exact model follower. The linearizing transformation is done in the WT-map. Through this map the plant is seen as a set of decoupled strings of integrators. The same set is employed as the dynamics (A_0, B_0) of the model servo, where the desired motion is defined by means of the input r^* and the, in general, nonlinear control law. The control of modeling inaccuracies and other disturbances is accomplished by the regulator which operates on the error e_y and outputs corrective control δv. It may be noted that the regulator works into the simple canonical dynamics and, in effect, the gain scheduling is done automatically by the WT-map.

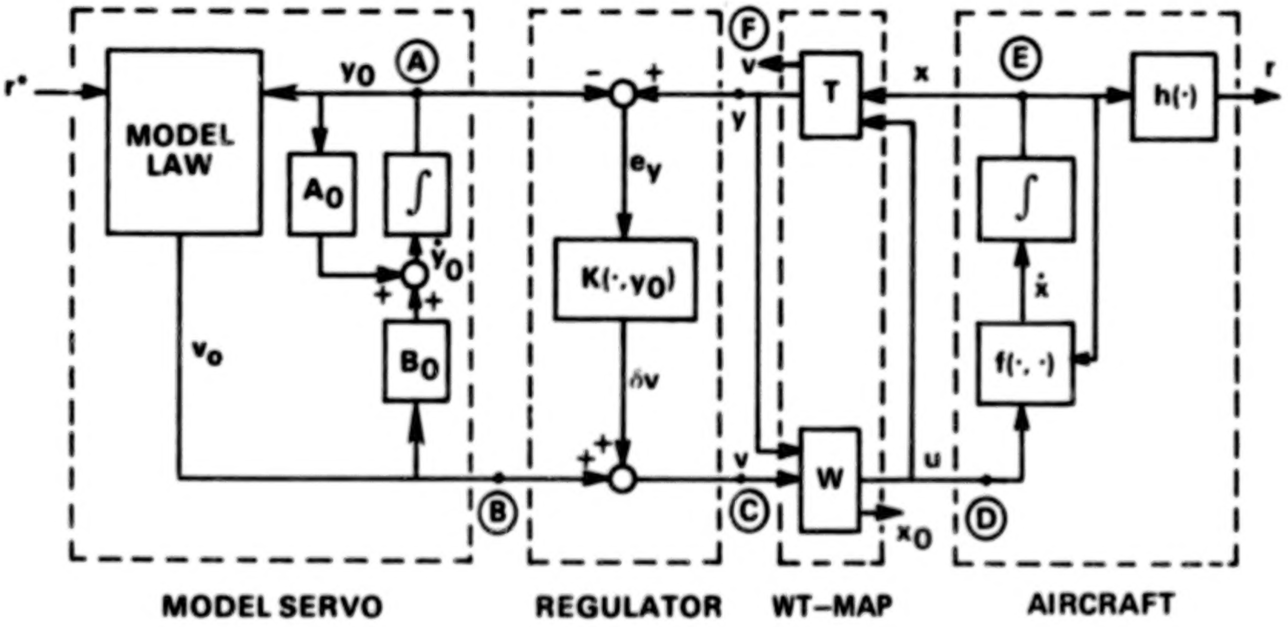
r*
MODEL LAW
y_0
Ⓐ
A_0
∫
$\dot{y}_0$
+
+
B_0
v_0
Ⓑ
-
+
e_y
$K(\cdot, y_0)$
δv
+
+
Ⓕ
v
y
v
Ⓒ
T
W
x_0
x
Ⓔ
u
Ⓓ
∫
$\dot{x}$
$f(\cdot,\cdot)$
$h(\cdot)$
r
MODEL SERVO
REGULATOR
WT–MAP
AIRCRAFT

HELICOPTER EXPERIMENT

The objective of this experiment is to investigate the effectiveness and realism of the design approach and to uncover potential problem areas. The current work is with the UH1H helicopter equipped with the VSTOLAND avionics system including the Sperry 1819B flight computer. The model used in the design is a rigid-body nonlinear force (f^F), and moment (f^M) generation process. Inertial coordinates (r, v) of position and velocity vectors, body attitude matrix C, and angular velocity ω form the state. The moment controls u^M are the roll and pitch cyclic and the pedals. The collective is the power control u^P.

STATE:

$$x = \begin{pmatrix} r \\ v \\ C \\ \omega \end{pmatrix} \in X \subset R^3 \times R^3 \times SO(3) \times R^3$$

CONTROL:

$$u = \begin{pmatrix} u^M \\ u^P \end{pmatrix} \in U \subset R^3 \times R$$

STATE EQUATION:

$$\begin{aligned} \dot{r} &= v \\ \dot{v} &= f^F(x, u) \\ \dot{C} &= S(\omega)\, C \\ \dot{\omega} &= f^M(x, u) \end{aligned}$$

A CANONICAL MODEL FOR THE HELICOPTER

The canonical model chosen is shown in the figure. There is a pair of strings, each four integrators long. This pair represents the two horizontal channels (r_x, r_y). In addition, there is a two-integrator string for altitude h. The fourth string is for the heading ψ. The canonical controls are the second derivatives of horizontal acceleration, vertical acceleration, and yaw acceleration. The transformation is computed by means of two Newton-Raphson trim routines. First, the controls are computed and yield the given accelerations ($\dot{w}_{bc}$, $\ddot{h}$) at the given state. Then the attitude C is computed for the given horizontal acceleration. The Jacobian matrices needed by Newton-Raphson are computed numerically.

CANONICAL MODEL

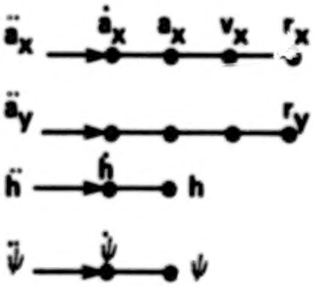

KI = (4,4,2,2)

TRANSFORMATION

a. **ON-LINE NEWTON-RAPHSON MOMENT TRIM**

$$\left.\begin{array}{l} f^M(r, v, C, w_b, u) = \dot{w}_{bc} \\ f_3^F(r, v, C, w_b, u) = \ddot{h}_c \end{array}\right\} \longrightarrow u_c = h^M(v, C, w_b, \ddot{h}_c, \dot{w}_{bc})$$

b. **ON-LINE N-R FORCE TRIM**

$$f_h^F(r, v, C, o, u_o) = a_h \longrightarrow (\phi, \theta) = h^F(r, v, \psi, a_h, o, o)$$

SUMMARY — UH1 EXPERIMENT

The experiment has progressed to the point that the following observations can be made.

(1) The implementation of the control scheme is practical. The complete code takes less than 22 msec on the Sperry 1819B flight computer

(2) Both FORTRAN and real-time simulations (real flight computer and hydraulics) are consistent with theory. The tracking accuracy along the trajectory including hover, climb, descent and high-speed flight indicates that the UH1 model routinely used for manned simulations is linearizable to a degree where a fixed-gain controller is possible. There is robustness with respect to weight, center of mass, moment of inertia, and force and moment models, but there is sensitivity to errors in wind estimates. The actuator dynamics (15 rad/sec) may be commuted with the TW-map for regulator bandwidth below 2 rad/sec

(3) Further research is needed to develop rigorous methods for including high-frequency dynamics and explicit enforcement of control and state constraints

1. IMPLEMENTATION IS PRACTICAL
   - SAMPLING TIME = 50 msec
   - NEW JACOBIANS FOR N - R TRIM EVERY 5TH SAMPLE
   - COMPLETE CODE = 22 msec ON SPERRY 1819B
2. FORTRAN AND MANNED SIMULATIONS ARE CONSISTENT WITH THEORY
   - TRACKING ACCURACY IMPLIES LINEARIZABILITY
   - ROBUSTNESS
   - ACTUATOR DYNAMICS
3. PROBLEM AREAS
   - METHOD FOR INCLUDING SERVO DYNAMICS
   - METHOD FOR EXPLICIT ENFORCEMENT OF CONSTRAINTS

REFERENCES

1. Krener, A. J.: On the Equivalence of Control Systems and the Linearization of Nonlinear Systems. Siam J. Control, vol. 11, no. 4, Nov. 1973, pp. 670-676.

2. Brockett, R. W.: Feedback Invariants for Nonlinear Systems. A Link Between Science and Applications of Automatic Control. Proceedings of the IFAC Congress (Helsinki, Finn.), vol. 2, 1978, pp. 1115-1120.

3. Jakubczyk, B.; and Respondek, W.: On Linearization of Control Systems. Bull. Acad. Polon. Sci., Ser. Sci. Math. Astronom. Phys., vol. 28, 1980, pp. 517-522.

4. Hunt, L. R.; Su, R.; and Meyer, G.: Global Transformations of Nonlinear Systems. IEEE Trans. on Automatic Control, vol. 28, no. 1, Jan. 1983, pp. 24-31.

N84
20586

UNCLAS

N84 20586 D19

ADAPTIVE CONTROL: MYTHS AND REALITIES

Michael Athans and Lena Valavani
Massachusetts Institute of Technology
Boston, Massachusetts

First Annual NASA Aircraft Controls Workshop
NASA Langley Research Center
Hampton, Virginia
October 25-27, 1983

PRECEDING PAGE BLANK NOT FILMED

PAGE 342 INTENTIONALLY BLANK

ADAPTIVE CONTROL: MYTHS AND REALITIES

In recent years, the area of adaptive control has received a great deal of attention by both theoreticians and practitioners. Considerable theoretical progress was made in the design of globally asymptotically stable adaptive algorithms and in unifying different design philosophies under the same mathematical framework. In this vein, it was found that all currently existing globally stable adaptive algorithms have three basic properties in common [1]: (1) positive realness of the error equation, (2) square-integrability of the parameter adjustment law and, (3) need for "sufficient excitation" for asymptotic parameter convergence. Of the three, the first property is of primary importance since it satisfies a sufficient condition for stability of the overall system, which is a baseline design objective. The second property has been instrumental in the proof of asymptotic error convergence to zero, while the third addresses the issue of parameter convergence.

Positive-real error dynamics can be generated only if the relative degree (excess of poles over zeroes) of the process to be controlled is known exactly; this, in turn, implies "perfect modeling." This and other assumptions, such as absence of nonminimum phase plant zeros on which the mathematical arguments are based, do not necessarily reflect properties of real systems. As a result, it is natural to inquire what happens to the designs under less than ideal assumptions. In particular, this paper will be concerned only with the issues arising from violation of the exact modeling assumption which is extremely restrictive in practice and impacts the most important system property, stability.

THEME

A variety of adaptive control algorithms which reflect different philosophical approaches to control system design have been suggested in the literature.

Such algorithms as a rule tend to improve control system performance due to enhanced information obtained while the system is in operation. In addition, in the late 1970's, certain classes of adaptive algorithms representing the majority of those available (among which the self-tuning regulators, model reference adaptive controllers, and the so-called dead-beat algorithms) were proven theoretically to be globally asymptotically stable. In practice, however, such algorithms would almost surely result in unstable physical control systems, as recent research has indicated.

- MYTH

  WE HAVE A VARIETY OF ADAPTIVE CONTROL ALGORITHMS THAT

  (1) IMPROVE CONTROL SYSTEMS PERFORMANCE

  (2) ARE PROVEN TO BE GLOBALLY STABLE

- REALITY

  ABOVE ADAPTIVE ALGORITHMS ALMOST SURELY WOULD RESULT IN UNSTABLE PHYSICAL CONTROL SYSTEMS

BASIC PROBLEM

The basic problem behind the apparent inconsistency between theory and practice can be attributed to the fact that existing adaptive control algorithms have been focused almost exclusively upon performance improvement, without due consideration for system robustness as required in the presence of unmodeled dynamics and/or other unstructured modeling errors. In fact, fundamental system concepts, such as operating system bandwidths, have been ignored in the design of adaptive algorithms that tend to invariably adjust the parameters in response to output errors, regardless of their origin. As a result, although at first sight performance seems to be greatly improved, the system bandwidth grows without bound, and eventually the hard constraints imposed by the presence of high-frequency unmodeled dynamics are violated. The final result is violent instability of the controlled system that makes apparent at the same time the nonlinear nature of the overall feedback adaptive loop.

- MODELS HAVE LIMITATIONS; STUPIDITY DOES NOT
- EXISTING ADAPTIVE CONTROL ALGORITHMS HAVE FOCUSED UPON PERFORMANCE IMPROVEMENT
- STABILITY/ROBUSTNESS ISSUE WAS NEGLECTED
    - HIGH-FREQUENCY UNMODELED DYNAMICS IMPOSE HARD LIMIT UPON CONTROL SYSTEM BANDWIDTH
- ADAPTIVE CONTROL SYSTEM BANDWIDTH CAN GROW WITHOUT BOUND
    - PERFORMANCE LOOKS GREAT
    - SYSTEM EVENTUALLY BREAKS INTO VIOLENT INSTABILITY.

ADAPTIVE ALGORITHMS CONSIDERED

The algorithms considered in the present study can be classified into one of the following three categories: (1) model reference adaptive control algorithms, otherwise known as direct adaptive control [2-7]; (2) self-tuning regulators, otherwise known as minimum variance controllers [8-10]; (3) dead-beat algorithms designed for discrete-time systems, otherwise referred to as projection or least-squares algorithms [11].

They all differ in the parameterization of the controller and, hence, the form of the resulting error equations, in the way they synthesize the control input and in the specific realization of the parameter adjustment laws. The common features of the above seemingly fundamentally different algorithms include the assumption of minimum phase plant zeros, the basic signal correlation of the learning mechanism, and the exact knowledge of the plant relative degree. The latter has proven crucial in obtaining global asymptotic stability proofs for all the above-mentioned algorithms.

- COMMON THEME: GLOBAL STABILITY PROOFS AVAILABLE

- MODEL REFERENCE ADAPTIVE CONTROL

  MONOPOLI ET AL, NARENDRA ET AL, MORSE ET AL, LANDAU ET AL

- SELF-TUNING CONTROLLERS

  ASTROM ET AL, EGARDT, LANDAU AND SILVIERA

- DEAD-BEAT ADAPTIVE CONTROL

  GOODWIN, RAMADGE, AND CAINES

STRUCTURE OF ADAPTIVE CONTROL

The general structure of an adaptive control system is shown in the first figure below. The term g(s) represents the nominal (low-frequency) plant transfer function, whose parameters are considered unknown. The term K(s) represents the compensator whose parameters are adjusted on-line on the basis of information generated by the adaptive logic block; its basic component is the "learning mechanism" that adjusts the compensator gains either directly or by identifying them first on the basis of the error e(t) and the signals r(t), u(t), and y(t), along with their associated auxiliary state variables. The term $\ell(s)$ represents a multiplicative high-frequency modeling error whose frequency profile is shown in the second figure below. The term $\ell(s)$ has been implicitly assumed to be identically zero at all frequencies in all the algorithms that have been proven to be globally asymptotically stable.

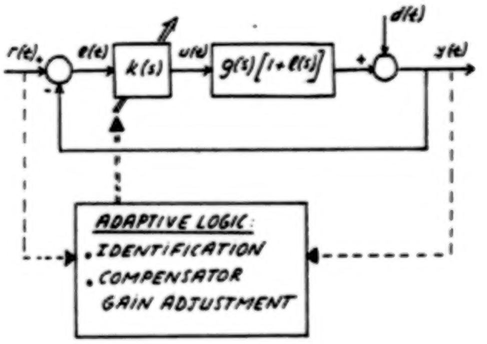

g(s): LOW-FREQUENCY MODEL OF PLANT
$\ell(s)$: HIGH-FREQUENCY MODELING ERROR
K(s): COMPENSATOR WITH ADJUSTABLE PARAMETERS

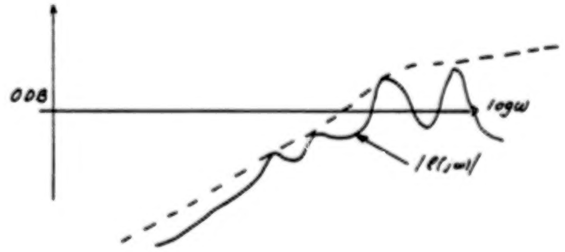

INSTABILITY MECHANISMS

When the ideal assumption of exact modeling is violated, at high frequencies, i.e., $\ell(s) \neq 0$, two mechanisms of instability were identified in the algorithms studied [12]. The first is the so-called "phase instability" that arises as a result of high-frequency inputs to the plant. For sufficiently high frequencies, the unmodeled dynamics contribute enough lag so that the total phase shift of the overall loop reaches 180°, at which point the feedback becomes positive and instability occurs. The second mechanism is referred to as "gain instability" and is due to persistent unmeasurable output disturbances and/or nonzero steady-state errors. In this case, the adaptive control system feedback gains keep drifting to increasingly larger values with a resulting increase in bandwidth; as a result, the high-frequency dynamics get excited, and the closed-loop system becomes unstable.

- INSTABILITY DUE TO HIGH-FREQUENCY INPUTS
  - HIGH-FREQUENCY DYNAMICS YIELD ±180° PHASE SHIFT
- INSTABILITY DUE TO PERSISTENT UNMEASURABLE OUTPUT DISTURBANCES
  - ADAPTIVE CONTROL SYSTEM FEEDBACK GAINS DRIFT AND GET LARGE
  - CONTROL SYSTEM BANDWIDTH INCREASES
  - HIGH-FREQUENCY DYNAMICS GET EXCITED
  - CLOSED-LOOP SYSTEM BECOMES UNSTABLE

ESSENCE OF PROOFS

The previously discussed error mechanisms can be better visualized in the figure below which is a generic representation of the error system complete with adjustment mechanism in the feedback path. Here $\underline{C}[y(t), u(t)]$ and $\underline{D}[y(t), u(t)]$ are linear operators that generate auxiliary state variables through stable filters, $\underline{F}(s)$ can represent a shaping filter, and $\underline{M}$ represents a matrix of constants.

The essence of global stability proofs is captured in the figure shown, with a positive-real transfer function in the forward path and a (passive) adaptation mechanism in the feedback [1]. All globally stable adaptive algorithms construct a positive-real function based upon the nominal plant model, which governs the error dynamics [1]. However, the positive-real condition is always violated in real applications due to unmodeled dynamics.

- REF: VALAVANI, PROC. JACC, 1980 (REF. 1)
- ALL GLOBAL STABILITY PROOFS AND ASSOCIATED ALGORITHMS CONSTRUCT A POSITIVE-REAL FUNCTION BASED UPON NOMINAL PLANT MODEL

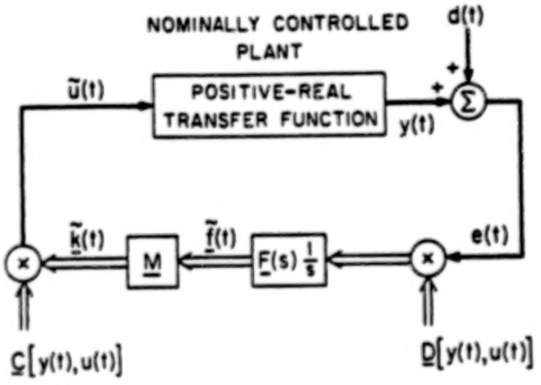

- PITFALL:

  POSITIVE-REAL CONDITION ALWAYS VIOLATED IN REAL APPLICATIONS

  - CAUSE: UNMODELED HIGH-FREQUENCY DYNAMICS

SIMPLEST MODEL REFERENCE ADAPTIVE CONTROL STRUCTURE

For the sake of example, the simplest model reference adaptive control structure is depicted below [3]. The model and plant transfer functions are given respectively by

$$\frac{g_M B_M(s)}{A_M(s)} \quad \text{and} \quad g_p \frac{B(s)}{A(s)}$$

Stable filters $\frac{1}{P(s)}$ generate from u(t) and g(t) auxiliary state variable vectors $\underline{w}_u(t)$ and $\underline{w}_y(t)$, which multiply feedback gain vectors $\underline{k}_u(t)$ and $\underline{k}_y(t)$, as shown. These gains, along with $k_r(t)$, are adjusted according to the equation in the square. The overall scheme looks indeed very simple for real-time implementation!

- STUDIED BY NARENDRA AND VALAVANI

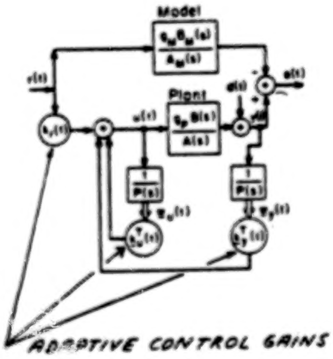
Model
$\frac{g_M B_M(s)}{A_M(s)}$
r(t)
Plant
$\frac{g_p B(s)}{A(s)}$
u(t)
d(t)
e(t)
$k_r(t)$
$\frac{1}{P(s)}$
$\frac{1}{P(s)}$
$w_u(t)$
$w_y(t)$
$k_u^T(t)$
$k_y^T(t)$
ADAPTIVE CONTROL GAINS

- ADAPTIVE CONTROL GAIN ADJUSTMENT

$$\boxed{\begin{gathered}\frac{d}{dt}\,\underline{k}(t) = \underline{\Gamma}\,\underline{w}(t)e(t)\\ \underline{\Gamma} = \underline{\Gamma}' \underline{>} 0\end{gathered}}$$

NUMERICAL EXAMPLE

The simple structure outlined on the previous page was employed for the adaptive control of a nominally first-order plant with a pair of complex poles. The reference model, the nominal plant complete with unmodeled dynamics, and the adjustment laws were as described below. The digital simulation results for a number of different reference input and disturbance combinations corroborate the foregoing discussion.

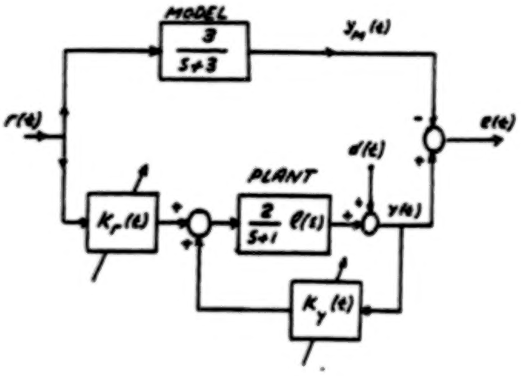

$$\dot{k}_r(t) = \gamma_1 r(t)e(t) \quad \dot{k}_y(t) = \gamma_2 y(t)e(t)$$

- UNMODELED DYNAMICS

  - $\ell(s) = \ell_1(s) = \dfrac{229}{s^2+30s+229}$

    POLES AT: $s=-15\pm j$

  - $\ell(s) = \ell_2(s) = \dfrac{100}{s^2+8s+100}$

    POLES AT: $s=-4\pm j8.33$

INSTABILITY DUE TO HIGH-FREQUENCY INPUT

The figures below show the plant output and adaptive gain evolution, respectively, when the reference input was chosen to have a d.c. and a sinusoidal component as shown below, in the absence of any output disturbance. The input frequency was precisely the frequency at which the "nominally controlled plant," with unmodeled dynamics $\ell_1(s)$, has 180° phase shift. The output displays an exponential-type oscillatory growth, while the parameters keep drifting and finally diverge.

- **DATA:** $\ell(s) = \ell_1(s)$

  $r(t)=0.3 + 1.85 \sin 16.1t; \; d(t)=0$

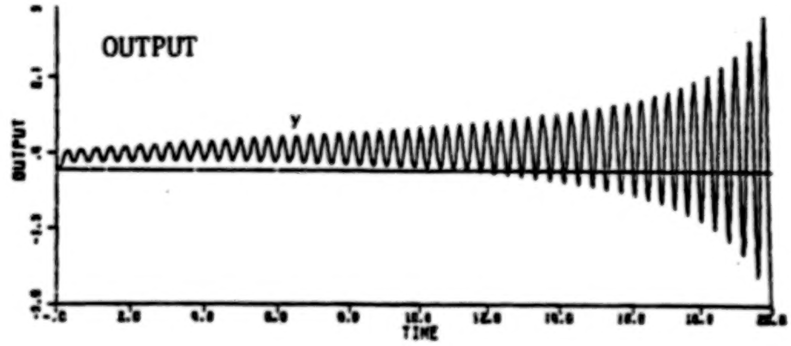

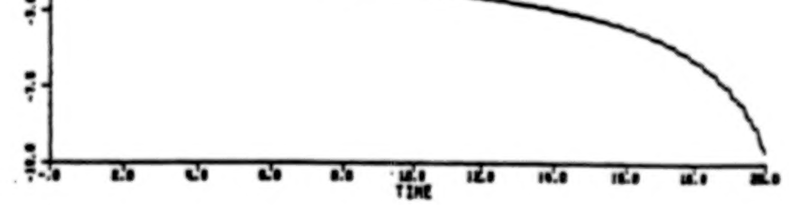

ORIGINAL PAGE IS
OF POOR QUALITY

INSTABILITY DUE TO SINUSOIDAL DISTURBANCE

With the same reference model, plant, and unmodeled dynamics, the reference input was now chosen to be a simple d.c. input of amplitude 2 (units); an output disturbance was added to the experiment. The frequency of the disturbance was lower than that which would cause a 180° phase lag. The figure below shows the plant output and parameter evolution, respectively. For a very extended period of time, it looks as if the plant output has converged to within a satisfactory deviation from the desired output; however, the parameters keep drifting. Finally, both plant and parameters break into abrupt instability. This is the gain instability mechanism that is indicative of the nonlinear nature of the overall adaptive loop.

- DATA: $\ell(s) = \ell_1(s)$

  $r(t)=2.0$ $d(t)=0.5 \sin 8t$

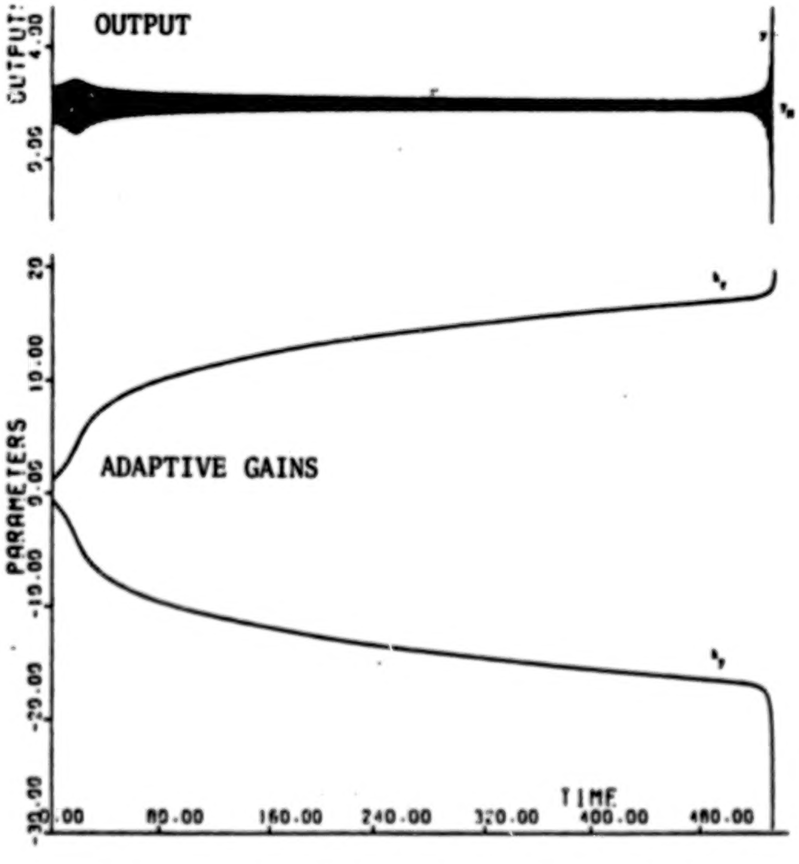

ORIGINAL PAGE IS
OF POOR QUALITY

INSTABILITY DUE TO SINUSOIDAL DISTURBANCE (CONCLUDED)

In the present experiment, the only difference from the preceding example is that the magnitude of the disturbance is smaller (by a factor of 5). Again, the same trends are observed, although now the plant output deviates much less from the reference model output and the parameter evolution is different in shape and magnitude. However, the final instability comes about in an almost identical manner.

- DATA: $\ell(s) = \ell_1(s)$
- $r(t)=2.0 \quad d(t)=0.1 \sin 8t$

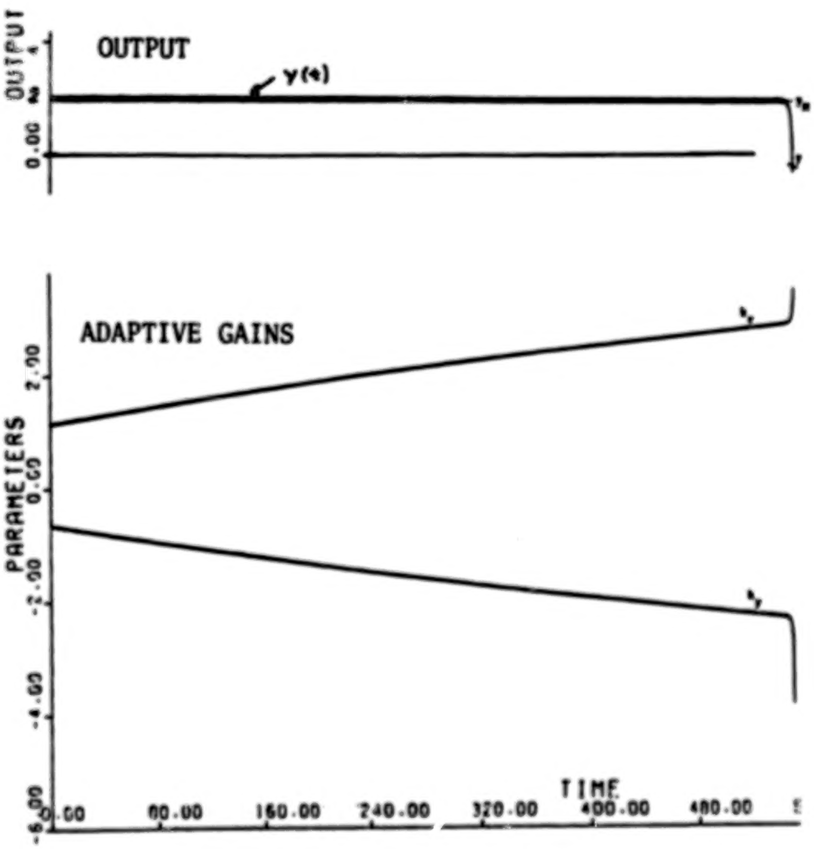

INSTABILITY DUE TO CONSTANT DISTURBANCE

This is a regulator-type experiment for the same setup as before. There is a zero reference input and a d.c. disturbance of amplitude 3 (units). Notice that the output behaves almost ideally for an infinitely long period of time compared to the system time constants. However, after about 1000 seconds some arrhythmia-type behavior is observed, after which point violent instability occurs in both plant output and parameter values. We remark that the parameters have continued to drift while the output was displaying a satisfactory behavior. The fact that the gain instability has taken such a long time to develop may have been a reason why the phenomenon was not discussed in the literature earlier. However, it was indeed observed in some applications to chemical processes [13].

- DATA: $\ell(s) = \ell_1(s)$

  $r(t)=0 \quad d(t)=3$

OUTPUT

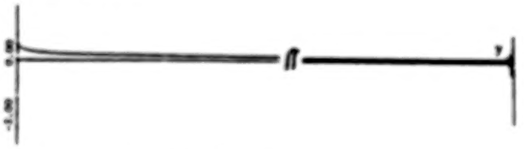

ADAPTIVE GAINS

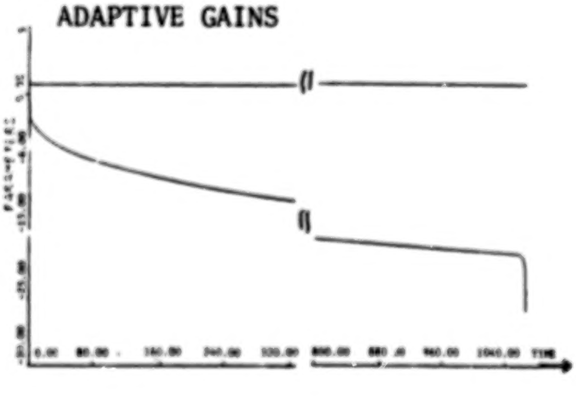

RULES OF THUMB

In general, although the time at which instability occurs may be large, the fact remains that it does occur. Factors that can prolong its onset are increased frequency separation between nominal plant model and unmodeled high-frequency dynamics and decreasing disturbance amplitudes. At present, there is no systematic way to prevent such a phenomenon from occurring. The reason is because the adaptive loop is highly nonlinear and, therefore, rigorous mathematical analysis is not easy. However, certain cures have been proposed, such as the use of dither signals in the reference inputs to stabilize the drifting process, exponential forgetting factors, and dead-zones to prevent the adaptation mechanisms from causing the parameters to drift [14-19]. None of the suggested methods, however, seems to hold general validity at the present time.

- TIME AT WHICH INSTABILITY SHOWS UP CAN BE LARGE
  - BUT SYSTEM IS UNSTABLE

- INSTABILITY TIME INCREASES
  - AS FREQUENCY SEPARATION OF LOW-FREQUENCY MODELED DYNAMICS AND HIGH-FREQUENCY UNMODELED DYNAMICS INCREASES
  - AS DISTURBANCE MAGNITUDE DECREASES

- CERTAIN CURES MAY WORK
  - DITHER SIGNALS
  - EXPONENTIAL FORGETTING
  - DEAD ZONE

  NOT CLEAR OF GENERAL VALIDITY

- ADAPTIVE LOOP HIGHLY NONLINEAR
  - ANALYSIS NOT EASY

FUTURE RESEARCH DIRECTIONS

Clearly, a lot more research is needed to understand the complex interplay between time-domain and frequency-domain quantities in an on-line adaptation mechanism. Key concepts such as finite-time identification need to be understood and developed further; input constraints and disturbance constraints have to be formulated and taken into consideration as part of the overall design along with a more precise mathematical representation of modeling uncertainty, perhaps in terms of a modeling error $\ell_M^T(\omega)$ as suggested below. To summarize, maximum allowable system bandwidth should be reflected in any design problem either explicitly or implicitly, and the mathematics of any adaptive algorithm should try not to violate the hard constraints imposed by it.

- EXAMINE FUNDAMENTAL ISSUES
    - INTEGRATED TIME-DOMAIN AND FREQUENCY-DOMAIN APPROACH

- FINITE-TIME IDENTIFICATION

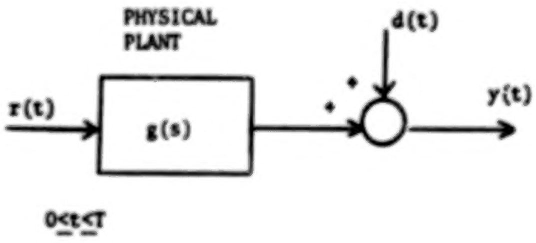

- INPUT CONSTRAINTS: $r(t) \in R$

- DISTURBANCE CONSTRAINTS: $d(t) \in D$

NOMINAL MODEL: $\hat{g}_T(s)$

MODEL ERROR BOUND:

$$\ell_M^T(\omega) > |g(j\omega) - \hat{g}_T(j\omega)|$$

NEED $\ell_M^T(\omega)$ TO LIMIT BANDWIDTH

MYTHS AND REALITIES

In conclusion, adaptive control algorithms as they now stand are deceptively simple and promising; they are proven theoretically stable and they improve performance by overcoming the conservativeness that nonadaptive designs typically have to contend with. Unfortunately, however, the advantages that these algorithms enjoy are based on mathematical assumptions that are always violated in practice. Moreover, the "ideal" properties that they seem to possess are very nonrobust to even subtle violations of the underlying assumptions. Consequently, they may result in unstable systems when applied in real engineering problems.

- MYTH:

  LET US RUSH TO IMPLEMENT ADAPTIVE CONTROLLERS: GOOD PERFORMANCE, PROVEN STABILITY

- REALITY:

  THE MATHEMATICAL ASSUMPTIONS THAT LEAD TO GLOBAL STABILITY PROOFS ALWAYS VIOLATED IN REAL LIFE.

  WATCH OUT: INSTABILITY MAY EVENTUALLY SET IN.

REFERENCES

1. Valavani, L., "Stability and Convergence of Adaptive Algorithms: A Survey and Some New Results," Proceedings of the Joint Automatic Control Conference, Vol. 1, pp. WA2-B, 1980.

2. Monopoli, R. V., "Model Reference Adaptive Control with Augmented Error Signal," IEEE Transactions on Automatic Control, Vol. AC-19, pp. 474-484, October 19 4.

3. Narendra, K. S. and Valavani, L. S., "Stable Adaptive Controller Design- Direct Control," IEEE Transactions on Automatic Control, Vol. AC-23, pp. 570-583, August 1978.

4. Feuer, A. and Morse, A. S., "Adaptive Control of Single-Input Single-Output Linear Systems," IEEE Transactions on Automatic Control, Vol. AC-23, pp. 557-570, August 1978.

5. Landau, I. D., "An Extension of a Stability Theorem Applicable to Adaptive Control," IEEE Transactions on Automatic Control, Vol. AC-25, pp. 814-817, August 1980.

6. Narendra K. S., Valavani, L. S. and Lin, Y. H., "Stable Adaptive Controller Design, Part II: Proof of Stability," IEEE Transactions on Automatic Control, Vol. AC-25, pp. 440-448, June 1980.

7. Landau, I. D. and Silveira, H. M., "A Stability Theorem with Applications to Adaptive Control," IEEE Transactions on Automatic Control, Vol. AC-24, pp. 305-312. April 1979.

8. Aström, K. J., Borisson, U., Ljung, L. and B. Wittenmark, "Theory and Applications of Self-Tuning Regulators," Automatica, Vol. 13, No. 5, pp. 457-476, September 1977.

9. Egardt, B., "Unification of Some Continuous-Time Adaptive Control Schemes," IEEE Transactions of Automatic Control, Vol. AC-24, pp. 588-592, August 1979.

10. Kreisselmeier, G., "On Adaptive State Regulation," IEEE Transactions on Automatic Control, Vol. AC-27, pp. 3-16, February 1982.

11. Goodwin, G. G., Ramadge, P. J. and Caines, P. E., "Discrete-Time Multivariable Adaptive Control," IEEE Transactions on Automatic Control, Vol AC-25, pp. 449-456, June 1980.

12. Rohrs, C. E., Adaptive Control in the Presence of Unmodeled Dynamics, Doctoral Dissertation, Dept. of Electrical Engineering and Computer Science, Massachusetts Institute of Technology, August 1982.

13. Dumont, G. and Belanger, P. R., "Successful Industrial Application of Advanced Control Theory to a Chemical Process," IEEE Control Systems Magazine, Vol. 1, No. 1, pp. 12-16, March 1980.

14. Krause, J., Adaptive Control in the Presence of High Frequency Modeling Errors, LIDS-TH-1314, M. S. Thesis, Dept. of Electrical Engineering and Computer Science, Massachusetts Institute of Technology, May 1983.

15. Ioannou, P. and Kokotovic, P., "Singular Perturbations and Robust Redesign of Adaptive Control," Paper presented at the IFAC Workshop on Singular Perturbations and Robustness of Control Systems, Lake Ohrid, Yugoslavia, July 1982.

16. Orlicki, D., Valavani, L. and Athans, M., "Comments on Bounded Error Adaptive Control," LIDS-P-1320, Massachusetts Institute of Technology, August 1983.

17. Peterson, B. and Narendra, K., "Bounded Error Adaptive Control," IEEE Transactions on Automatic Control, Vol. AC-27, No. 6, pp. 1161-1168, December 1982.

18. Anderson, B. D. O., "Exponential Stability of Linear Equations Arising in Adaptive Identification," IEEE Transactions on Automatic Control, Vol. AC-22, No. 1, pp. 83-88, February 1977.

19. Anderson, B. D. O. and Johnstone, R. M., "Adaptive Systems and Time-Varying Plants," International Journal of Control, Vol. 37, No. 2, pp. 367-377, February 1983.

SPECIAL REPORT

PRECEDING PAGE BLANK NOT FILMED

C-5

PAGE 362 INTENTIONALLY BLANK

N84
20587

UNCLAS

N84 20587 D20

FOREIGN TECHNOLOGY SUMMARY
OF
FLIGHT CRUCIAL FLIGHT CONTROL SYSTEMS

H. A. Rediess
H. R. Textron, Inc.
Irvine, California

First Annual NASA Aircraft Controls Workshop
NASA Langley Research Center
Hampton, Virginia
October 25-27, 1983

PRECEDING PAGE BLANK NOT FILMED

PAGE 364 INTENTIONALLY BLANK

INTRODUCTION

A survey of foreign technology in flight crucial flight controls is being conducted for NASA Langley Research Center as a data base for planning future research and technology programs. Only Free World countries were surveyed, and the primary emphasis was on Western Europe because that is where the most advanced technology resides. The survey includes major contemporary systems on operational aircraft, R&D flight programs, advanced aircraft developments, and major research and technology programs. The information was collected from open literature, personal communications, and a tour of several companies, government organizations, and research laboratories in the United Kingdom, France, and the Federal Republic of Germany. This paper provides a summary of the survey results to date.

Some of the figures are taken from a briefing to the NASA Administrator by Mr. Kenneth Szalai from Ames Research Center, Dryden Flight Research Facility, on the technology tour of Europe that Mr. Szalai and the author conducted in 1983. These figures are used with the permission of Mr. Szalai.

This survey was conducted under contract NAS1-17403, and the Technical Representative of the Contracting Officer was Mr. Cary Spitzer, NASA Langley Research Center. The material presented herein solely represents the findings and opinions of the author and is not to be construed as being endorsed by the U.S. Government or representatives of the National Aeronautics and Space Administration.

ORIGINAL PAGE IS
OF POOR QUALITY

FLIGHT CONTROL SYSTEMS EVOLUTION

Flight controls technology has undergone tremendous evolution over the past three decades. Figure 1 illustrates many of the key milestones in the evolution as represented by major R&D systems and operational systems. The term "nonflight critical fly-by-wire" refers to systems that are commanded by electric or optical signals, but loss of those signals is not likely to cause the aircraft to crash. Typically, there is also a mechanical/hydraulic path for primary control or as a backup system. Flight critical fly-by-wire means that loss of that system is likely to cause the aircraft to crash.

Although the chart emphasizes U.S. aircraft, several key developments in Europe are included, and those of current interest are discussed subsequently. The Concord had a very profound effect on European flight controls technology in two ways. It represented the first, and as yet only, high authority SAS/CAS in commercial transports and provided a very important experience base for the UK and France technologists and managers. That has helped influence an early commitment to fly-by-wire in the Airbus. Secondly, it accelerated the development of the technology in France because the French engineers gained valuable experience working directly with the Marconi engineers on the Concord system. There is now a solid base of DFBW technology in Europe and wide-spread commitment to DFBW for military aircraft and in some cases, commercial transports.

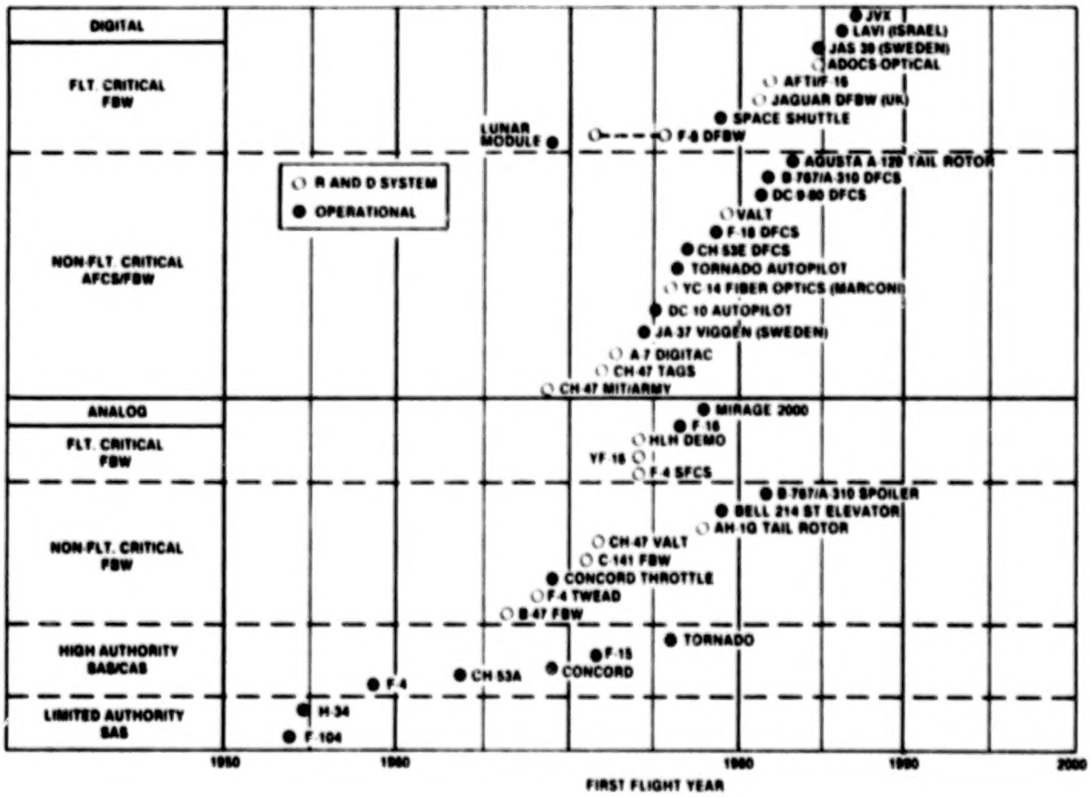

Figure 1

JA-37 AND AIRBUS A-310

The Swedish JA-37 Viggen fighter aircraft (Figure 2) developed by Saab-Scania underwent its first flight in 1974. The aircraft design features a single-channel high-authority digital automatic flight contro system (DAFCS) provided by Honeywell and mechanical primary FCS. Functions provided by the DAFCS include a control augmentation system, attitude hold (pitch, roll, heading, and control stick steering), altitude hold, and automatic airspeed control. The aircraft contains three primary control surfaces (right/left elevon and rudder) which are controlled by the pilot via the mechanical PFCS, by the DAFCS via secondary series servo, and via automatic or manual parallel and series trim actuators.

The Airbus A-310 transport, currently in production, was first flight tested in 1982, and features a mechanical primary flight control system, DFBW spoilers, and a digital automatic flight control system. The spoiler system is dual-channel fail safe with identical active and monitor channels and uses dissimilar hardware (processors) and software.

Operational Aircraft

JA-37

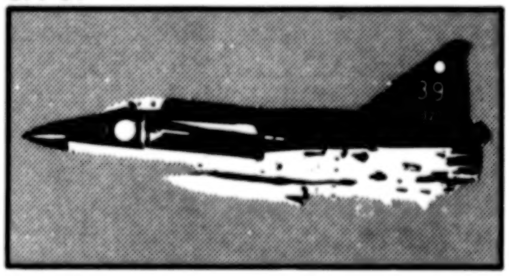

- **Swedish (SAAB-Scania)**
- **First flight 1974**
- **Single-channel full-authority digital automatic FCS, mechanical reversion**

Airbus A310

- **Multinational (Fr, FRG, Spain, UK)**
- **First flight 1982**
- **Mech primary controls, DFBW spoilers, digital autopilot**

Figure 2

ORIGINAL PAGE IS
OF POOR QUALITY

AIRBUS A-320

Airbus Industries (AI) is in the detailed design stage in the development of a 150-seat, short/medium range A-320 transport (Figure 3) featuring a quadruplex DFBW flight control system (FCS). Mechanical control rudder and mechanical backup pitch trim are retained to permit safe landing in the event of power loss. Tests in the Airbus A-300 flight test aircraft have verified that it is possible to land in this configuration. The system design includes dissimilar redundancy in both hardware and software of the same general type used in the A-310 spoilers. The A-320 will also incorporate relaxed static stability to at least the neutral point and possibly negative static stability.

A flight test program is underway using the A-300 test bed aircraft to evaluate the use of RSS and a side-stick controller on the A-320. The evaluations will determine the engineering operational and certification issues of such systems on civil aircraft. The engines will incorporate full-authority digital engine control integrated with the flight management system.

Operational Aircraft
Under Development

Airbus A320

- Multinational (Fr, FRG, Spain, UK)
- Detailed design in progress
- First flight 1986
- Quad DFBW — dissimilar redundancy hardware and software
- Mech backup on rudder and pitch trim
- ACT: relaxed static stability
- Side-stick controller

Figure 3

A-320 DFBW SYSTEM

A more detailed description of the A-320 DFBW system design features is shown in Figure 4. All primary flight control surfaces (elevators, horizontal stabilizer, ailerons, and roll spoilers) are quadraplex digital fly-by-wire using dissimilar redundancy in both hardware and software. The rudder control is mechanical, and the tail plane trim has a mechanical backup to provide emergency landing capability. The secondary controls (slats, trim, speed brakes, and lif dumpers) are commanded electrically.

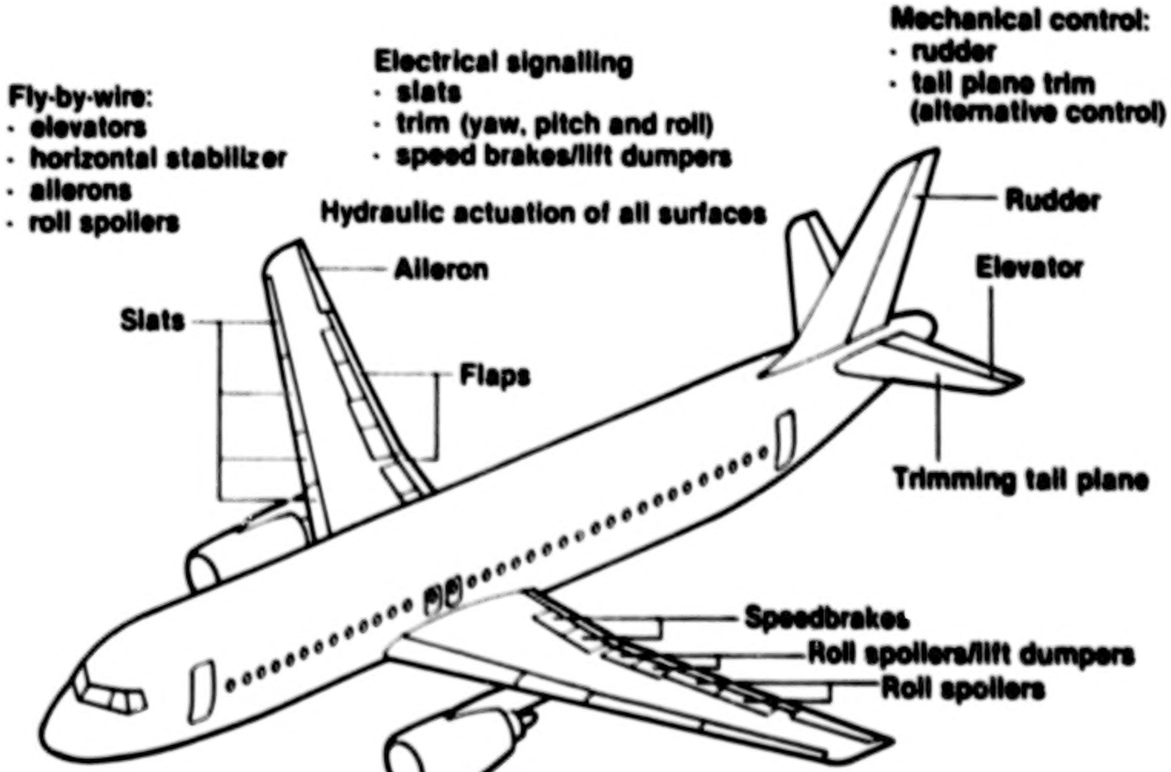
Fly-by-wire:
· elevators
· horizontal stabilizer
· ailerons
· roll spoilers
Electrical signalling
· slats
· trim (yaw, pitch and roll)
· speed brakes/lift dumpers
Hydraulic actuation of all surfaces
Mechanical control:
· rudder
· tail plane trim
(alternative control)
Rudder
Elevator
Aileron
Slats
Flaps
Trimming tail plane
Speedbrakes
Roll spoilers/lift dumpers
Roll spoilers

Figure 4

AIRBUS INDUSTRIES FLIGHT CONTROL SYSTEM EVOLUTION

Airbus Industries (AI) planned development of a transport family is illustrated in Figure 5. Based on a continued, vigorous research and development program, including full-scale experimental testing, advanced technologies are progressively introduced in aircraft designs providing practical, evolutionary changes rather than revolutionary. The next transport is the 150-seat A-320 described previously. A series of wide-body aircraft is in the preliminary design stage: a two-engine short/medium range TA-9; a four-engine long-range TA-11; and, a two-engine medium/long range TA-12. The first two of these, TA-9 and TA-11, are expected to incorporate full-authority digital fly-by-wire systems on all surfaces, extensive use of active controls, and reduced energy systems.

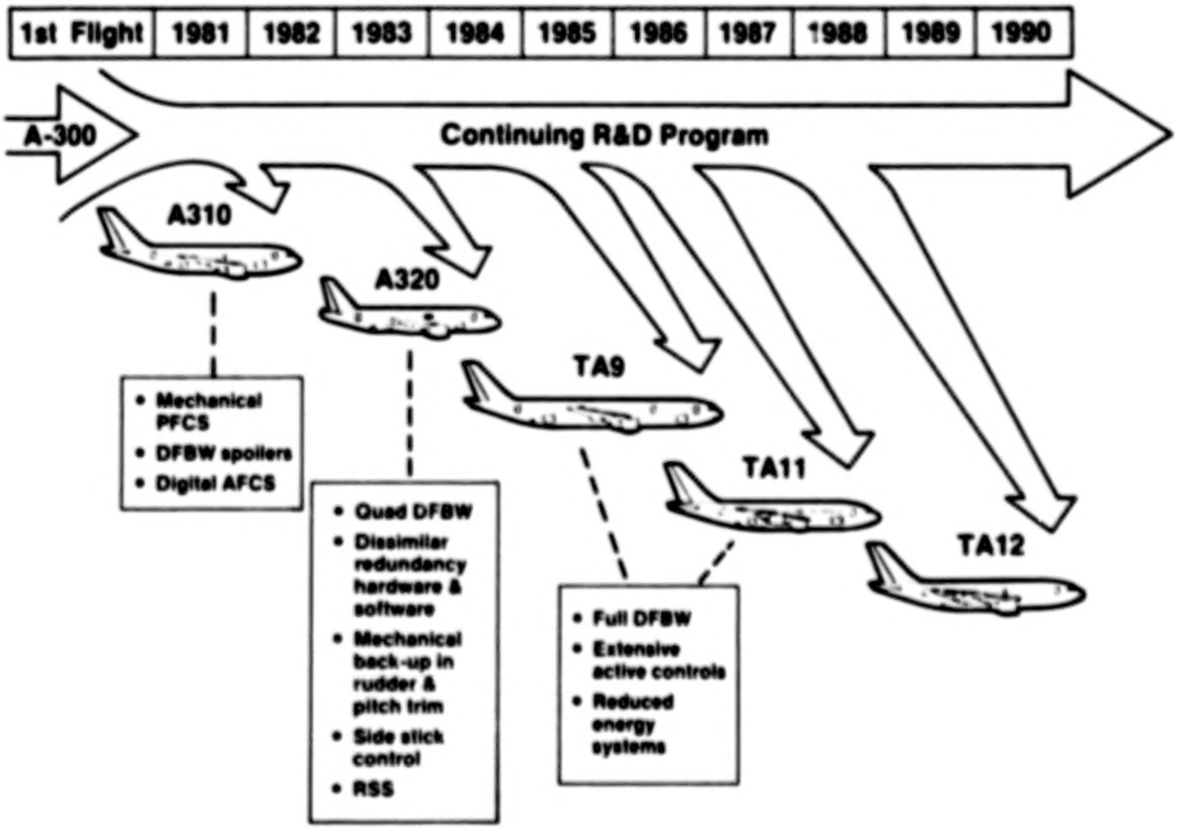
1st Flight
1981
1982
1983
1984
1985
1986
1987
1988
1989
1990
A-300
Continuing R&D Program
A310
A320
TA9
TA11
TA12
• Mechanical PFCS
• DFBW spoilers
• Digital AFCS
• Quad DFBW
• Dissimilar redundancy hardware & software
• Mechanical back-up in rudder & pitch trim
• Side stick control
• RSS
• Full DFBW
• Extensive active controls
• Reduced energy systems

Figure 5

TORNADO AND MIRAGE

Figure 6 illustrates basic characteristics of the multinational Tornado and French Mirage 2000/4000 aircraft currently in production.

The Tornado, a joint UK, FRG, and Italian project, underwent its first flight in 1976. The flight control system includes both analog and digital computing. The primary flight control function is performed by a command/stability augmentation system (CSAS) which is a triplex analog FBW maneuver demand system (Ref. 1). While no mechanical revision is provided for the rudder and spoilers, it is retained for the ailerons for safe return upon loss of CSAS computing. A dual digital autopilot/flight director (AFDS) integrated with the CSAS provides outer loop control. The AFDS uses cross-comparison techniques for failure detection and a signal consolidation scheme to provide triplex commands to the CSAS. It also provides a fail operational flight director capability to enable the pilot to monitor the autopilot performance and fly the aircraft manually if the autopilot malfunctions.

The first flights of the Dassault-Brequet Mirage 2000 and 4000 were conducted in 1978 and 1979, respectively. With no mechanical revision capability, both include a flight-critical analog FBW flight control system with digital autopilot. The 2000N version is nuclear hardened fitted with terrain-following radar. The Mirage 4000 features relaxed static stability and automatic variable camber to optimize performance.

Operational Aircraft

Tornado

- **Multinational (UK, FRG, Italy)**
- **First flight 1976**
- **Analog CSAS, dual digital autopilot, mechanical reversion**

Mirage 2000/4000

- **French (Dassault-Breguet)**
- **First flight 1978, 1979**
- **Analog FBW, digital autopilot, no mechanical reversion**
- **Relaxed static stability/auto variable camber (4000)**

Figure 6

JAS-39 AND LAVI

Flight critical DFBW flight control systems designs are under development for opertional fighter aircraft in both Sweden and Israel (Fig. 7). Saab-Scania of Sweden is developing the JAS-39 Gripen advanced strike fighter. Lear Siegler, Inc., will design, develop, and manufacture the flight control system. Under subcontracts, Moog Aerospace in cooperation with Saab Combitech will design the primary flight actuators, and Lucas Aerospace will supply the maneuvering-flap control actuation system. The JAS-39 will be a flight-critical triplex DFBW system and, thus, contains no mechanical backup capability. The fighter, scheduled for first flight in 1987, is being developed for specific mission needs of Sweden and may not favorably compete for an international market.

The Israeli Aircraft Industries is developing the LAVI tactical fighter to replace the A-4 and Kfir C2 aircraft with first flight scheduled for 1986. The flight controls, to be designed by Lear Siegler (Moog), will be a digital fly-by-wire system with relaxed static stability and include an analog but no mechanical backup system. Advanced digital avionics systems will be incorporated to operate with interactive multifunction displays/controls, fire control integrated with internal and external sensors, and enhanced active/passive self-defensive systems. As planned, much of the design and systems would be supplied by U.S. companies.

Operational Aircraft
Under Development

JAS-39

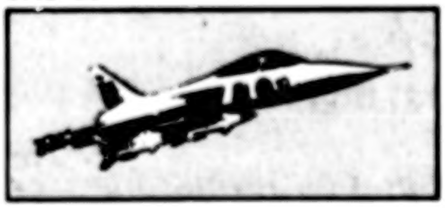

- Swedish (SAAB-Scania)
- First flight 1987
- Triplex DFBW (Lear Siegler), no mechanical backup

LAVI

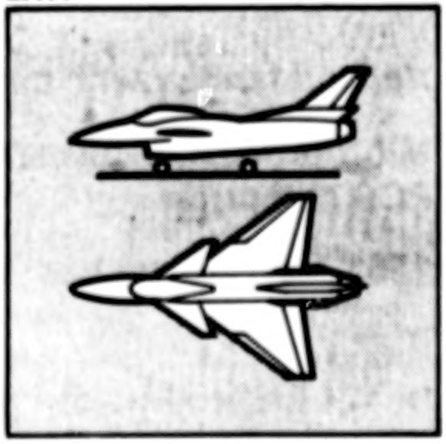

- Israel (IAI)
- First flight 1986
- Triplex DFBW (Lear Siegler), analog backup, no mechanical reversion
- ACT: relaxed static stability

Figure 7

ORIGINAL PAGE IS
OF POOR QUALITY

SKYSHIP 600

In the UK, Marconi Avionics, under contract to Airship Industries, is developing a digital fly-by-light (DFBL) flight control system for application to the Skyship 600 (see Figure 8). High inherent immunity to EM interference is achieved by a 1553 optical data bus between the FCC and the actuator drive system (ADS) and by providing dedicated electrical power at the ADS from a hydraulically driven electronic generator. The ADS includes a microprocessor to locally handle the failure detection and isolation. The actuators are duplex electric incorporating two samarium cobalt DC servomotors mounted on a common shaft, each fed by separate power. Torque is supplied by only one motor; the second is activated after failure of the first.

Operational Airship
Under Development

Skyship 600

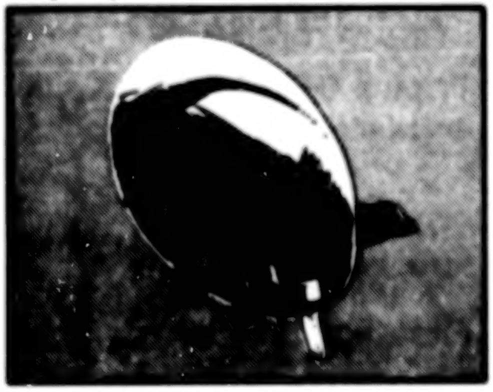

- UK (Airship Industries, Marconi)
- First flight 1983 (with DFBL)
- Digital fly-by-light (DFBL)
  - All four tail surfaces
  - Active/standby with pilot select
  - Microprocessor-based FCS computer
  - 1553 optical data bus

Figure 8

TIAWAN F-104

The Aeronautical Research Laboratories of the Aeronautical Industry Development Center (AIDC) of the Republic of China in Tiawan has initiated a program to develop a modern digital flight control system to upgrade 100 F-104 aircraft (Fig. 9). The system will be a half-authority dual digital command augmentation system (CAS) and stability augmentation system (SAS) for pitch, roll, and yaw. The existing mechanical system and a new direct electrical command system will provide emergency backup capability. The prototype development contract for five aircraft systems is now under competition, and the first flight is expected to be early in 1987.

Operational Aircraft
FCS Upgrade

F-104

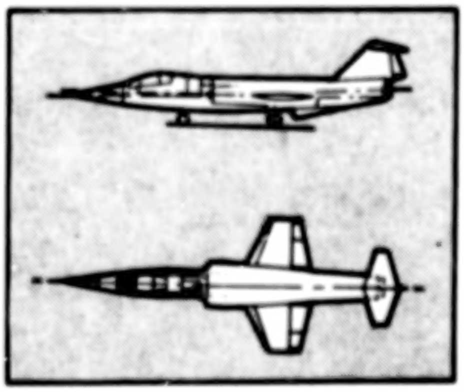

- **Republic of China-Taiwan (AIDC)**
- **FCS under competition**
- **First flight 1987**
- **Dual digital CAS/SAS, mechanical and direct electrical backups**

Figure 9

F-104 CCV AND JAGUAR DFBW

Among the European R&D flight programs are the German F-104CCV and the United Kindom's Jaguar DFBW aircraft shown in Figure 10. The purpose of the German demonstration program was to investigate stability and control characteristics of a supersonic aircraft (Ref. 2). A single-seat F104G was modified as a control-configured vehicle (CCV) with a newly developed full-authority quadruplex system while retaining the original system as a mechanical backup. After initial flights starting in December 1977 to evaluate the DFBW system, various degrees of destabilization were achieved by adding aft ballast and a canard. The highest instability reached in normal flight was up to 22% mean aerodynamic chord at an angle of attack of 11 degrees. The flight tests were highly successful in demonstrating aircraft controllability in a highly unstable configuration.

The Jaguar program was initiated to demonstrate a safe, practical, full-authority DFBW flight control system. This activity is of interest since it represents the first pure digital fly-by-wire system with no dissimilar backup. The program was initiated in 1977 under the technical sponsorship of the RAE and under contract to British Aerospace. Marconi Avionics furnished the flight control system. While more descriptions will follow, basically the FSC is a full-authority quadruplex DFBW system with optically coupled data transmission. The initial flight of aircraft was conducted in October 1981.

R & D Flight Programs

F-104 CCV

- German (MBB)
- First flight 1977
- Quad DFBW, full-authority, mechanical reversion
- Relaxed static stability

Jaguar

- UK (RAE/BAe, Marconi)
- First flight 1981
- Quad DFBW, no mechanical reversion
- Optical interchannel data links

Figure 10

ORIGINAL PAGE IS
OF POOR QUALITY

JAGUAR DFBW SYSTEM ARCHITECTURE

The overall system architecture is shown schematically in Figure 11 (Ref. 3). Quadruplex computers and primary sensors were used to satisfy specifications requiring survival of any two electrical failures in the system and reliance on majority voting rather than self monitoring within each redundant element. Sensors of lower redundancy were used for those functions not necessary for safety of flight. A sextuplex or duo-triplex first-stage actuation scheme was selected to conform with stringent redundancy specifications. The two additional actuator channels are driven by the actuator drive and monitor computers which were independently voted versions of the FCC's outputs. Comprehensive built-in-test features were included to measure the system functional characteristics. While designed to run synchronously, the system has been operated asynchronously for continued periods without observable degradation.

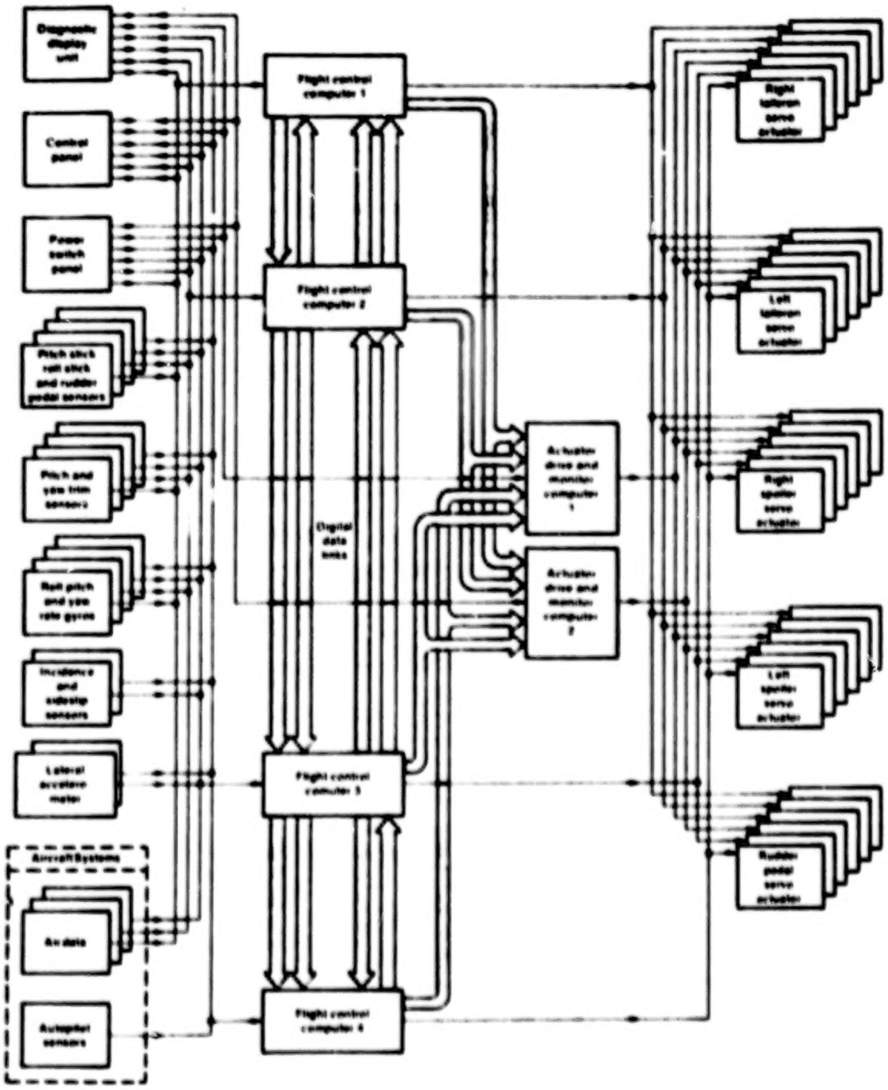
Diagnostic display unit
Control panel
Power switch panel
Pitch stick roll stick and rudder pedal sensors
Pitch and yaw trim sensors
Roll pitch and yaw rate gyros
Incidence and sideslip sensors
Lateral accelerometer
Aircraft Systems
Air data
Autopilot sensors
Flight control computer 1
Flight control computer 2
Digital data links
Flight control computer 3
Flight control computer 4
Actuator drive and monitor computer 1
Actuator drive and monitor computer 2
Right taileron servo actuator
Left taileron servo actuator
Right spoiler servo actuator
Left spoiler servo actuator
Rudder pedal servo actuator

Figure 11

ORIGINAL PAGE IS
OF POOR QUALITY

JAGUAR DFBW - COMPUTING AND MONITORING ARCHITECTURE

The basic system computing and monitoring architecture is presented in Figure 12 which illustrates a simplified primary control path (Ref. 4). Quadruplex primary sensors, those necessary for flight safety, are interfaced with four identical flight control computers (FCC) which process these as well as less critical sensor signals into commands for control of the actuators. Cross-channel data transmission is achieved by optically coupled serial data links. This scheme enables each computer to carry out bit for bit identical control law implementation. Voting and failure rejection logic contained in each computer satisfies the requirement for surviving two sequential failures of all critical sensors. The actuation architecture required six independent servo drive signals. To avoid the cost and complexity of a full six-channel system, the four FCC's were augmented by dual analog actuator drive and monitor computers (ADMC) which utilize independently voted versions of the FCC output signals to drive the additional two channels. Failed FCC channels are detected and latched out, and then the ADMC averages the remaining good FCC channels. These additional channels are mechanized to eliminate any interchannel failure propagation between the six parallel redundant output interfaces.

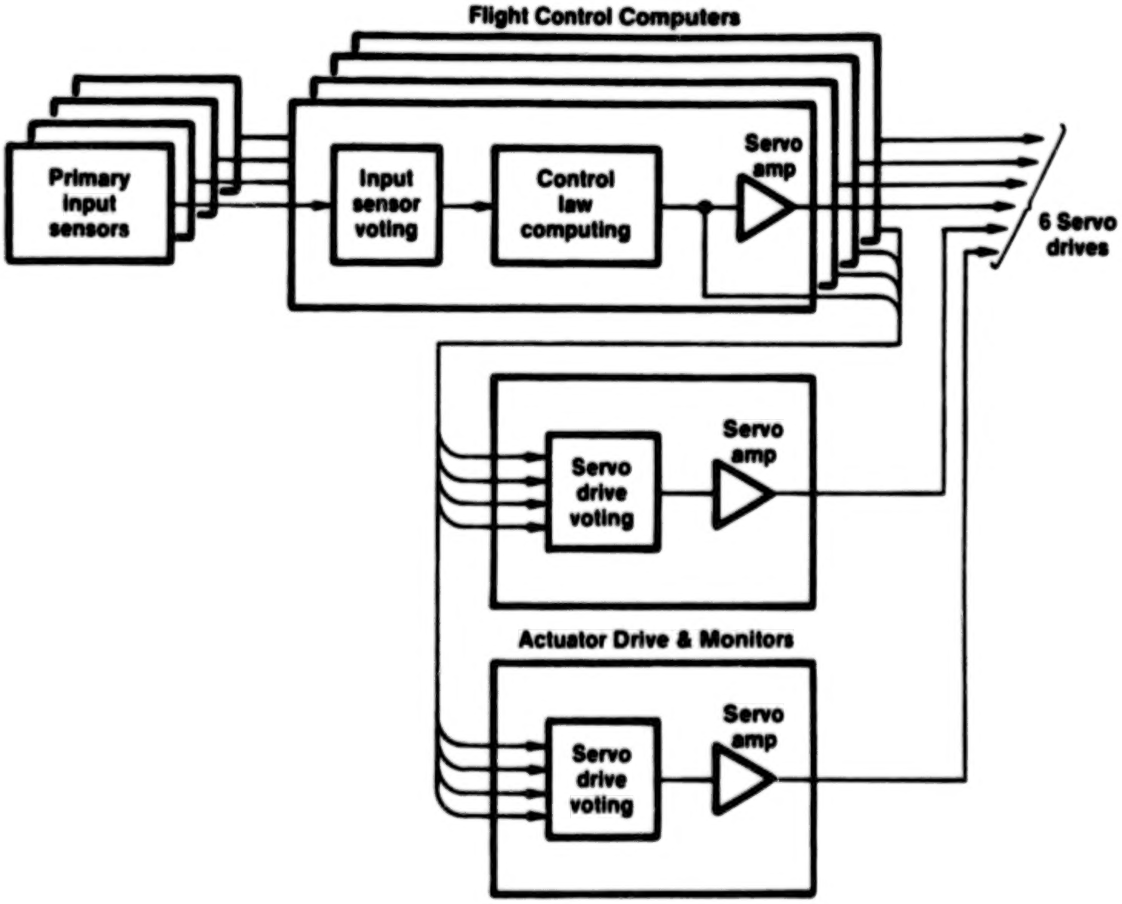
Flight Control Computers
Primary input sensors
Input sensor voting
Control law computing
Servo amp
6 Servo drives
Servo drive voting
Servo amp
Actuator Drive & Monitors
Servo drive voting
Servo amp

Figure 12

ORIGINAL PAGE IS
OF POOR QUALITY

JAGUAR DFBW-DUO-TRIPLEX ACTUATOR SCHEME

The basic specifications requiring that first-stage actuation has only two independent hydraulic supplies with no interconnect and that the system survives a hydraulic failure followed by an electrical system failure or the converse, led to the selection of duo-triplex first-stage actuation system design. While a quadruplex configuration would have offered an attractive one-to-one interface with the FCC's, designers were concerned with mechanizing some form of fast reaction actuator monitoring and channel isolation scheme to prevent uncontrolled surface movement in the event of an electrical followed by a hydraulic failure. Each of the five control surface actuation systems is similar, and Figure 13 illustrates the operation (Ref. 4). Each system contains six servovalves. An interactuator mechanical link assures that the spools move uniformly, which effectively sums the six servovalve outputs. Thus, failures in two channels are overridden by the other four. A separate hydraulic supply feeds each trio of servovalves and is also routed to the corresponding jack of the conventional tandem power control unit. A hydraulic supply failure is absorbed because the three associated servovalves are unable to oppose the correctly operating channels.

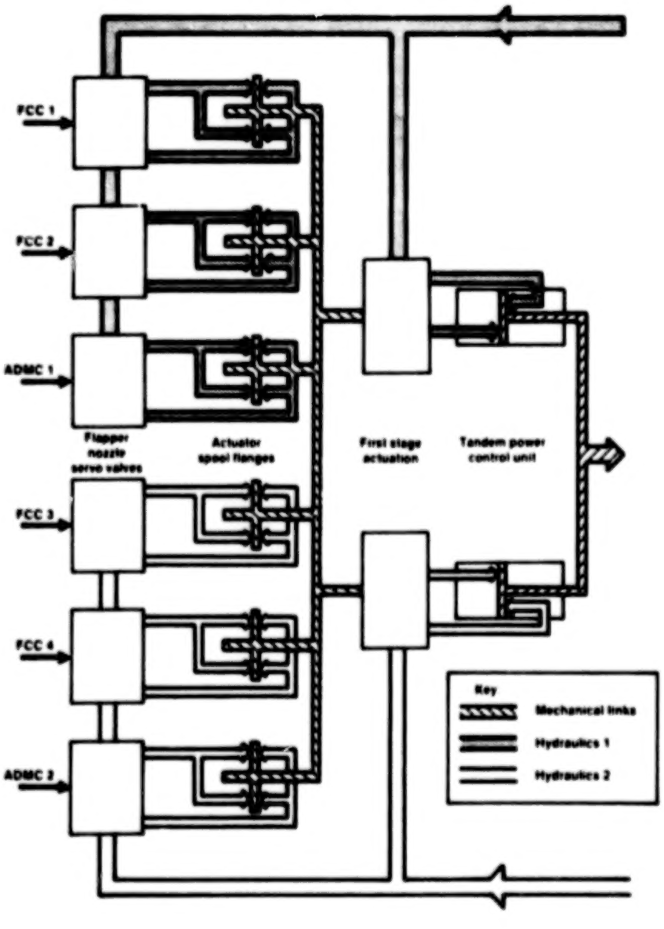
FCC 1
FCC 2
ADMC 1
Flapper nozzle servo valves
Actuator spool flanges
First stage actuation
Tandem power control unit
FCC 3
FCC 4
ADMC 2
Key
Mechanical links
Hydraulics 1
Hydraulics 2

Figure 13

ORIGINAL PAGE IS
OF POOR QUALITY

JAGUAR DFBW - SOFTWARE DEVELOPMENT PROCESS

The use of common software in the flight control system presented the potential of a generic error leading to a safety critical loss of control. Therefore it was necessary to provide maximum software visibility to facilitate thorough testing and functional auditing during the design phase, supplemented by clear requirements definition, detailed documentation, and stringent production and configuration control procedures (Ref. 5). The key documents controlling the software design are the System Requirements Document (SRD), which controls the design implementation, and the Software Structure Development (SSD). The SSD defines the running order of the modules within each program segment and is designed to assure strict sequential data flow.

The overall software development process is depicted in Figure 14. The SRD's are interpreted to produce software module design specifications which in turn are used for module coding. A module test specification is written by an independent programmer to minimize error carry-over. The module code is tested, and the results are documented. Senior programmers audit all module documentation to assure that the design requirements are satisfied, the design rules observed, and the test process followed. When the module coding is completed, the modules are assembled and loaded into the hardware for integration tests. All of the software documentation is subjected to strict configuration control with changes authorized only through a formal change request process.

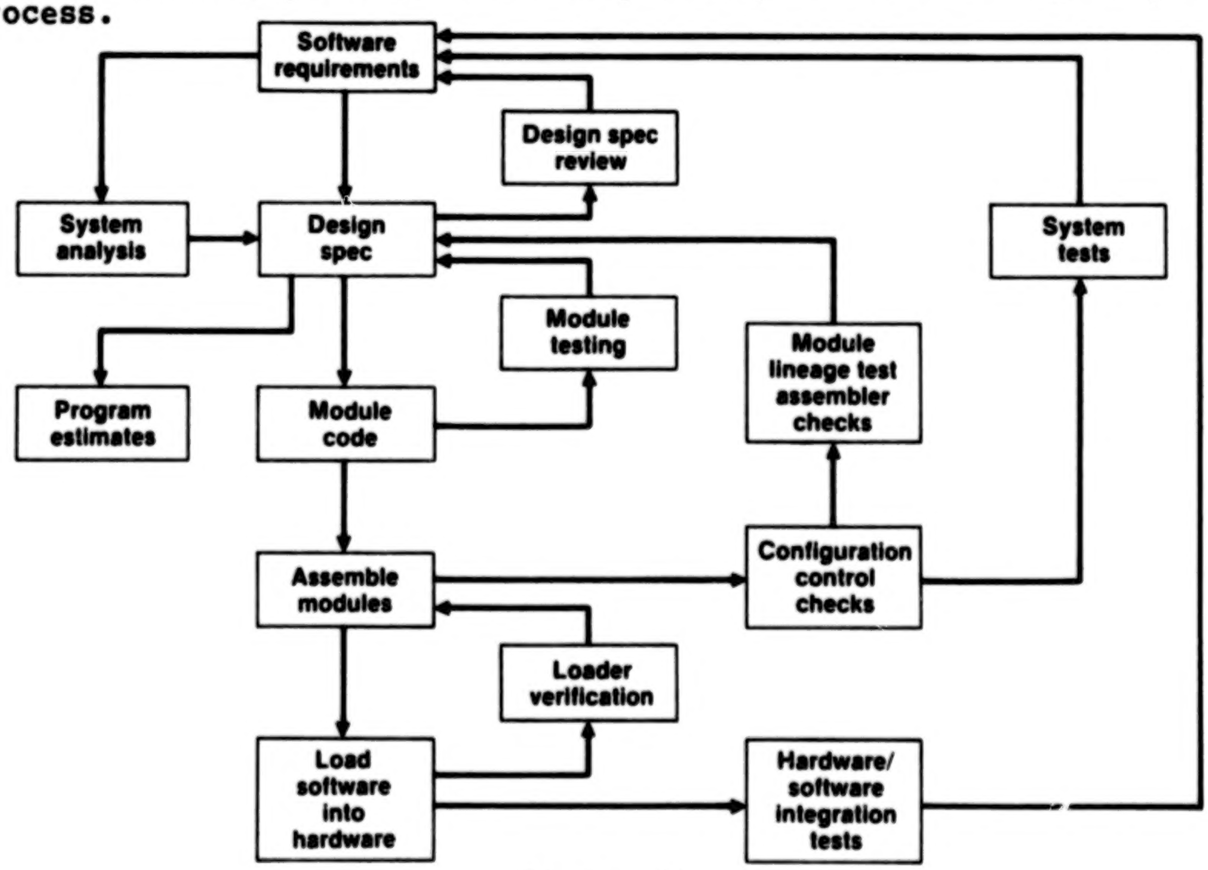
Software requirements
Design spec review
System analysis
Design spec
System tests
Module testing
Module lineage test assembler checks
Program estimates
Module code
Assemble modules
Configuration control checks
Loader verification
Load software into hardware
Hardware/ software integration tests

Figure 14

ORIGINAL PAGE IS
OF POOR QUALITY

JAGUAR DFBW - SYSTEM INTEGRITY APPRAISAL

The basic integrity of the system was achieved by the selection of the system architecture in conjunction with standard design practices, performance testing, and assessments of operational/safety considerations. For the Jaquar DFBW program, these procedures were extended to include an integrity appraisal or system audit as outlined in Figure 15. The main elements (Ref. 5) were:

- 100% coverage single-fault FMEA
- Multiple-fault FMEA for specific combinations
- Flight resident software integrity appraisal
- Appraisal of specific functions
- Configuration inspection
- Qualification program
- Burn-in program

These were supplemented by secondary analyses shown below the main elements in the figure. As part of the integrity appraisal, various functions and features of the system were subjected to technical evaluations as required from results of mainstream failure mode and effects analysis (FMEA) and/or engineering findings. While the appraisal was conducted by a team knowledgeable in the specific design, they reported to senior engineers.

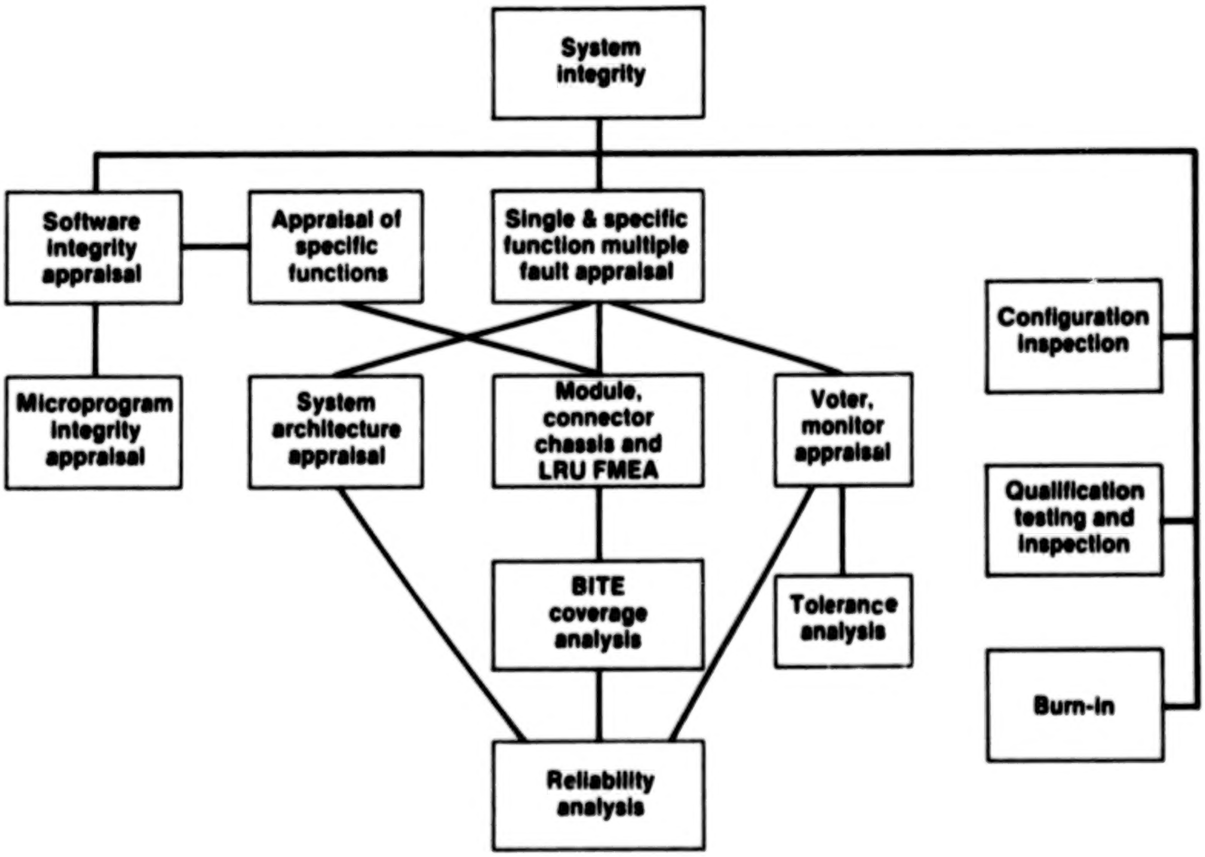
System integrity
Software integrity appraisal
Appraisal of specific functions
Single & specific function multiple fault appraisal
Configuration inspection
Microprogram integrity appraisal
System architecture appraisal
Module, connector chassis and LRU FMEA
Voter, monitor appraisal
Qualification testing and inspection
BITE coverage analysis
Tolerance analysis
Burn-in
Reliability analysis

Figure 15

JAGUAR DFBW - SYSTEM QUALIFICATION PROCESS

Once the design objectives had been specified as subsystem or elements, such as the FCS, it was necessary to integrate these elements into a functional system exhibiting the characteristics of the basic design requirement while assuring that no adverse intersystem reactions were present and verifying that the common software used contained no generic or other design defects. These tasks were conducted using a ground test rig, the aircraft, and an independent software audit, interrelated as shown in Figure 16 (Ref. 5).

The ground test rig was used to (1) verify the control laws by pilot assessment, (2) integrate the hardware, software, and ancillary equipment, (3) validate the final software before flight, and (4) gain overall system confidence. In addition, it served as a pilot training aid and as a preflight test bed.

The aircraft ground tests included complete checkout and test of the installed flight control system, electro-magnetic compatibility testing, aircraft systems testing, and simulated lightning tests.

It was considered essential that an independent software test by a disinterested group be used to supplement the rig and aircraft tests. The group was responsible for emulation of the flight control computer using a general purpose machine and for manual code analysis.

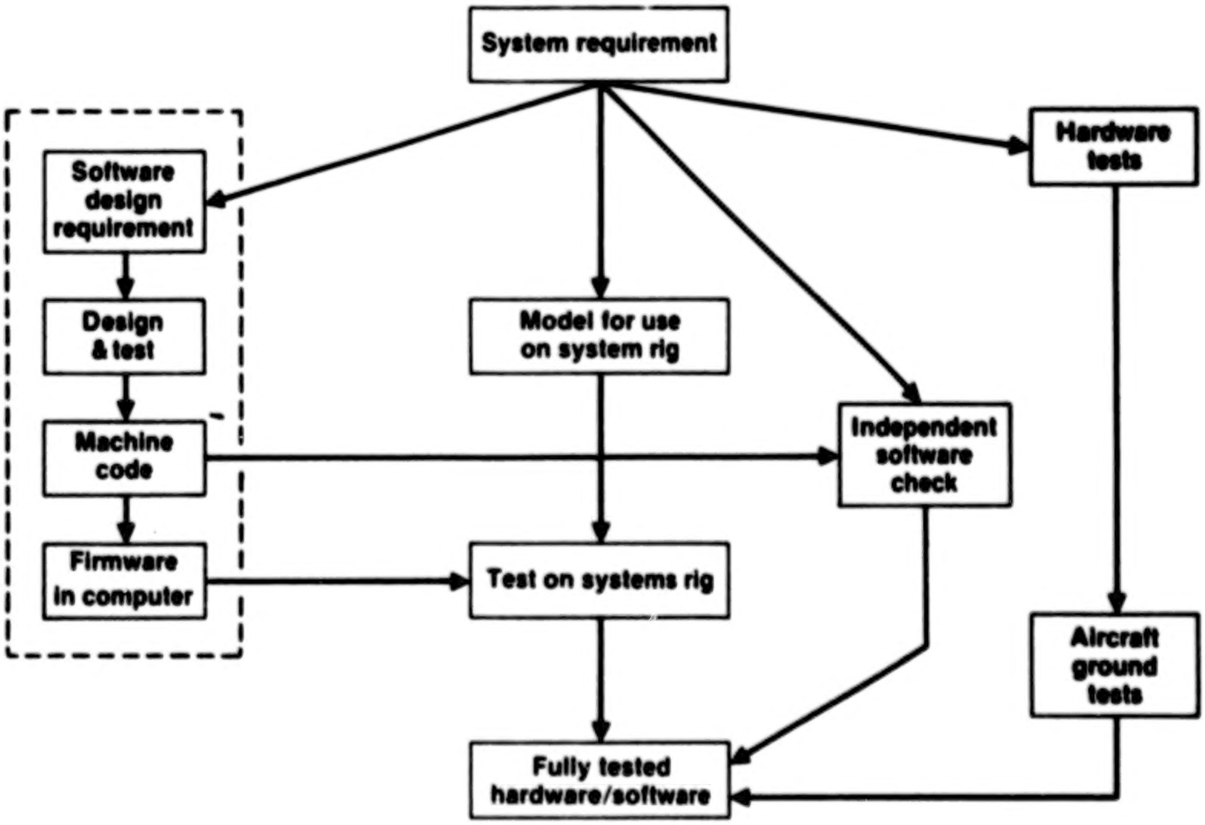
System requirement
Software design requirement
Design & test
Machine code
Firmware in computer
Model for use on system rig
Test on systems rig
Independent software check
Hardware tests
Aircraft ground tests
Fully tested hardware/software

Figure 16

AUGUSTA A-129 AND T-2 CCV

Flight test programs are being conducted by both Italy and Japan (Figure 17).

The Italian Augusta A-129 helicopter has been undergoing tests, and five prototype vehicles are to be manufactured in anticipation of production. The A-129 features a DFBW tail rotor (nonflight critical) but retains other mechanical controls. The design includes a digital autopilot and an integrated multiplexing system using microprocessors for aircraft/firing systems control.

Under contract to the Japanese Defense Agency, Mitsubishi has built a control-configured vehicle version of the T-2 advanced trainer for use as a research aircraft. The T-2 CCV has composite all-flying canards located on the inlets ahead of the wing leading edge and a composite ventral fin located on the fuselage center line. The flight control system is triplex digital with mechanical backup. The first flight was conducted in August 1983, and the aircraft is scheduled for a two-year experimental flight test program by the Japanese Air Self Defense Force.

R & D Flight Programs

Agusta A-129

- Italy
- First flight 1983
- DFBW tail rotor, digital autopilot, mechanical rotor controls
- Multiplex data bus/integrated avionics/ flight control

T2 CCV

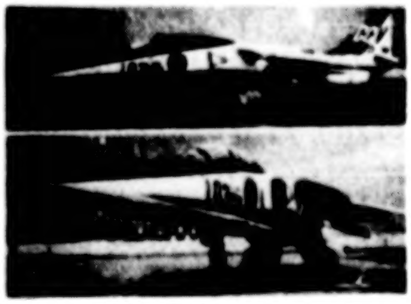

- Japan (Mitsubishi)
- First flight 1983
- Triplex DFBW, mechanical reversion
- All moving canard/RSS

Figure 17

ADVANCED AIRCRAFT DEVELOPMENT

Britain and France are currently competing for leadership of a new generation European combat aircraft advance development program which may lead to a joint development with Germany for 1990's fighter aircraft (Fig. 18).

Led by British Aerospace, a seven-member industrial consortium has an agreement with the British Ministry of Defense for government funding up to and including first flight for the development of an Agile Combat Aircraft (ACA) technology demonstrator called an experimental aircraft program (EAP). Both West German and Italian aerospace companies have contributed some funding, and while not committed, the West German and possibly the Italian governments may fund a second demonstrator aircraft. The ACA flight control system design by Marconi Avionics would be quadruplex digital fly-by-wire (DFBW) with no mechanical backup and no dissimilar redundancy. (Marconi considers that, while not required for military application, dissimilar redundancy is necessary in commercial aircraft for certification purposes.)

France has a comparable program since Dassault-Berguet (D-B) has begun manufacture of one technology demonstration aircraft, Avion de Combat Experimental (ACX). It will be a DFBW design with no mechanical backup and include electrical and fiber optics data busing, voice control system, holographic displays, and provision for antiturbulence ride control in the automtic computer-controlled flight control system.

The Federal Republic of Germany has need for a fast-reaction fighter, and their special requirements are prompting them to consider an entirely new fighter airframe called the TKF-90 which would employ existing avionics technologies to minimize costs. Two German companies, Messerschmett-Boelkow-Blohm (MBB) and Dornier, are pursuing test programs to satisfy the German Air Force needs but neither is committing to a flying demonstrator. MBB is using a modified Saab Viggen as a test bed to investigate various performance envelopes and is testing vectoring nozzle canards and other advanced control features. MBB has considerable experimental background in fire and flight control systems resulting from their F-104 CCV test bed.

Dornier in conjunction with Northrop has an ND-102 design and is using a modified Alpha jet to test a new transonic wing and to experiment with direct side force controls and maneuvering flaps/slats.

Thus, at the time of this writing, there are three fighter design plans among the UK, France, and FRG. Considering the economics involved, it is likely that more than one or possibly two will be fully developed. Both the UK and France seek partnership with the FRG, and it is likely that at least the TFK-90 will be a compromise between the ACA and ACX programs. MBB of West Germany is, in fact, a partner on the ACA and is being actively pursued as a partner in France's ACX program. MBB could become the catalyst for a European-wide project with British Aerospace and Dassault-Berquet and themselves as principals. While specific mission requirements would be compromised, such a triumvirate would create an attractive production market and serve as a formidable obstacle for U.S. competitors.

Italy (Aeritalia-Macchi) and Brazil (Embraer) are jointly developing the AMX fighter with first flight scheduled for 1984 and delivery in 1987. Initial production is expected to provide 185 aircraft for Italy and 80 for Brazil. The electronic flight control system designed by Marconi provides duplex analog fly-by-wire control of the tail plane, spoilers, and rudder together with mechanical elevators and ailerons. The design also incorporates automatic pitch, roll, and yaw stabilization. The equipment comprises two dual-redundant flight control computers based on 16-bit microprocessors organized for specially developed fail-safe software. To optimize hardware requirements, analog computing is used for the actuator control loops, pilot command path, and rate damping computations. Digital computing is used to handle gain schedules, electronics trim, and airbrake integrators. System performance is monitored by redundant processors in the flight control computers.

Advanced Aircraft Development

ACA, ACX

- **UK/FRG (BAe, MBB, Marconi)**
- **First flight 1986**
- **Quad DFBW, no mechanical reversion, no dissimilar redundancy**
- **Fr, FRG (Dassault-Breguet, MBB?)**
- **First flight 1986**
- **DFBW, no mechanical reversion, fiber optic data bus**
- **Ride control, voice command, holographic HUD**

AM-X

- **Italy, Brazil (Aeritalia/Marcchi, Embraer, Marconi)**
- **First flight 1984**
- **Duplex analog FBW, digital gain sched/monitoring (tailplane, spoilers, rudder)**

Figure 18

REFERENCES

1. Corney, J. M.: The Development of Multiple Redundant Flight Control Systems for High Integrity Applications. Aeronautical Journal, vol. 84, no. 837, Oct. 1980, pp. 327-338.

2. Korte, U.: Flight Test Experience with a Digital Integrated Guidance and Control System in a CCV Fighter Aircraft. AGARD CP-321, Lisbon, Portugal, October 1982, pp. 22-1 to 22-11.

3. Smith, T. D., et al.: Ground Flight Testing on the Fly-by-Wire Jaguar Equipped with a Full-Time Quadraplex Digital Integrated Flight Control System. AGARD-CP-321, Lisbon, Portugal, October 1982, pp. 23-1 to 23-20.

4. Marshall, R. E. W., et al.: Jaguar Fly-by-Wire Demonstrator Integrated Flight Control System. Paper presented at the 1981 Advanced Flight Control Symposium, Colorado Springs, CO, August 5-7, 1981.

5. Daley, E. and Smith R. B: Flight Clearance of the Jaguar Fly-by-Wire Aircraft. Proceedings of the Royal Aeronautical Society Symposium, Certification of Avionic Systems, April 27, 1982.

SESSION IV

RECENT EXPERIENCES IN IMPLEMENTATION OF ADVANCED CONTROL SYSTEMS

William E. Howell
Session Chairman

N84
20588

UNCLAS

D21

N84 20588

FUNCTIONAL INTEGRATION OF VERTICAL FLIGHT PATH AND SPEED CONTROL USING ENERGY PRINCIPLES

A. A. Lambregts
Boeing Commercial Airplane Company
Seattle, Washington

First Annual NASA Aircraft Controls Workshop
NASA Langley Research Center
Hampton, Virginia
October 25-27, 1983

PRECEDING PAGE BLANK NOT FILMED

PAGE 388 INTENTIONALLY BLANK

ABSTRACT

A generalized automatic flight control system has been developed which integrates all longitudinal flight path and speed control functions previously provided by a pitch autopilot and autothrottle. In this design, a net thrust command is computed based on total energy demand arising from both flight path and speed targets. The elevator command is computed based on the energy distribution error between flight path and speed. The engine control is configured to produce the commanded net thrust. The design incorporates control strategies and hierarchy to deal systematically and effectively with all aircraft operational requirements, control nonlinearities, and performance limits. Consistent decoupled maneuver control is achieved for all modes and flight conditions without outer loop gain schedules, control law submodes, or control function duplication.

STATE-OF-ART AUTOPILOT/AUTOTHROTTLE

Virtually every automatic flight control system (AFCS) in use today has been designed using a single-input, single-output control strategy. Although the elevator control loop may be closed on either speed or flight path, the autopilot path control modes have become the most widely used. Automatic speed control using the throttles was then developed as a natural complement to the autopilot path control modes.

Unfortunately, this historic system evolution has not resulted in optimum AFCS capabilities and performance. For certain flight conditions, the autopilot path control at constant thrust produces speed instabilities, while autothrottle speed control at constant elevator results in path instability. Together, they can provide stable flight path and speed control. However, the operation is far from coordinated teamwork. Generally, the autopilot is designed first and satisfactory path control using the powerful elevator is often obtained at the expense of speed control. This leaves the autothrottle in a no-win situation: poor speed control with acceptable throttle activity or acceptable speed control with objectionable throttle activity.

For large autopilot path change commands, the conventional control strategy breaks down because thrust will limit, causing loss of autothrottle speed control, with the ensuing risk of stalling or overspeeding the aircraft.

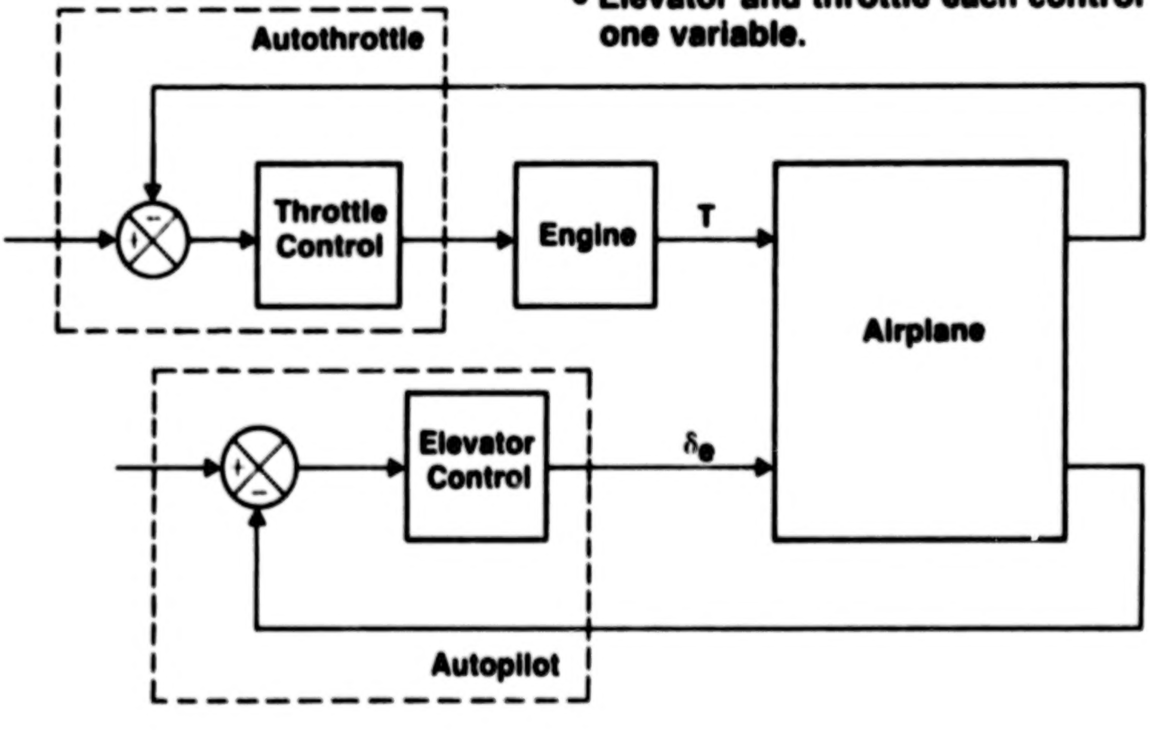

- Elevator and throttle each control one variable.

LIMITATIONS OF THE TRADITIONAL DESIGN APPROACH

The traditional single-input, single-output design approach has a number of other fundamental design limitations. Modes that have not specifically been designed to work together are generally incompatible. This has led to a proliferation of specialized control modes of limited use.

Still, pilots complain that the operation of the present generation automatic control systems is often contrary to the way the pilot uses the controls. The lack of short-term coordination of elevator and throttle commands results in undesirable and inefficient controller activity. This is especially true for the autothrottle system in energy-management-type situations.

Clearly, using the throttles to control speed is not an ideal control strategy. H. A. Soulé summed it all up in the title of his article (ref. 1), "The Throttles Control Speed, Right? Wrong!"

In the present designs, the thrust control loop is subject to extreme variations in loop gain and dynamics due to variations in aircraft weight and engine characteristics for different conditions. Poor system robustness causes wide performance variations.

The fragmented bottom-up design approach makes it difficult to efficiently implement general design requirements, such as limiting of speeds and maneuver rates, because provisions have to be made in many places.

Research Background

Traditional Single-Input – Single-Output Design Approach Has Inherent Deficiencies:

- Each mode combination is new problem
- Performance of one mode depends on other engaged mode
- Deficiency of one mode often basis for design of another
- Lack of control coordination leads to undesirable coupling
- Control coupling limits achievable damping
- Difficult to deal effectively with performance/safety limits
- Many difficult and iterative development programs have not resulted in fundamental design improvements

ORIGINAL PAGE IS
OF POOR QUALITY

FUNCTIONAL OVERLAP

The numerous efforts to overcome the limitations of the conventional autopilot and autothrottle designs have contributed much to the overall AFCS complexity, but little to the improvement in the fundamental design methodology. This is illustrated in this figure showing the functional overlap in the latest generation AFCS. Basic flight path and speed control capability now exists in all three computer systems! This results in operational ambiguities, unnecessary pilot workload, the need for numerous sensors, computers, interfaces, elaborate configuration control, and high cost of ownership. Obviously, the underlying system architecture is not ideal.

A top-down system synthesis capability, using an efficient control strategy providing maneuver decoupling and the correct control priorities, has been missing in the classical design methodology. Also, design tools using modern control theory remain inadequate for synthesis of multi-mode/multi-flight condition systems that can be implemented readily with today's hardware and software technology.

Typical Control Function Overlap, Conventional AFCS

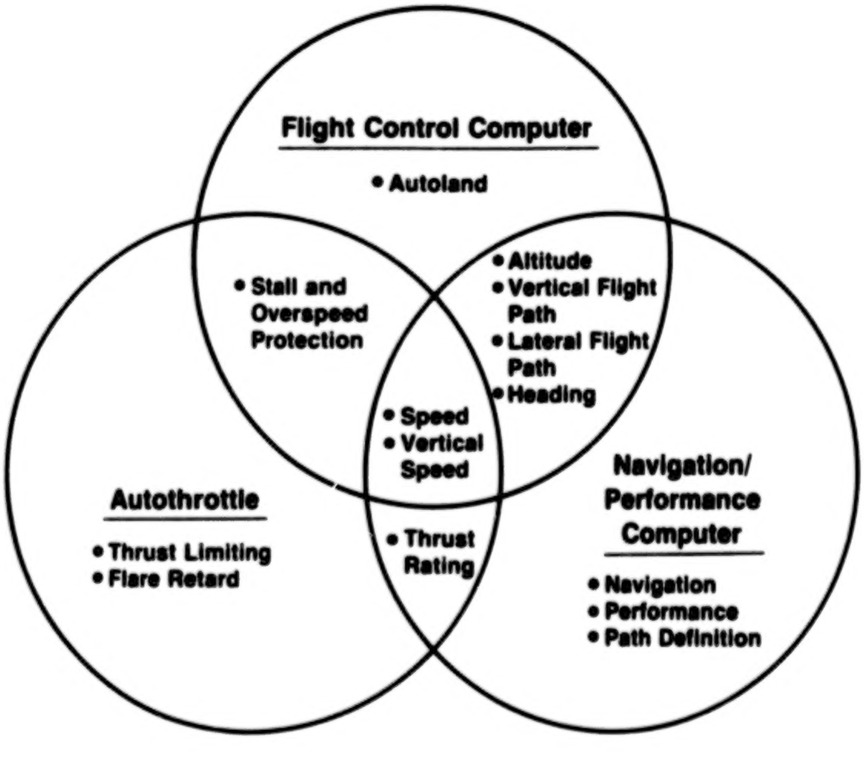
Flight Control Computer
• Autoland
• Stall and Overspeed Protection
• Altitude
• Vertical Flight Path
• Lateral Flight Path
• Heading
• Speed
• Vertical Speed
Autothrottle
• Thrust Limiting
• Flare Retard
• Thrust Rating
Navigation/ Performance Computer
• Navigation
• Performance
• Path Definition

DESIGN OBJECTIVES FOR THE INTEGRATED SYSTEM

The limitations of the traditional autopilot and autothrottle design have been encountered over and over. During the NASA Terminal Configured Vehicle Program guidance and control experiments using the NASA B-737 aircraft, which was equipped with an advanced autopilot and autothrottle, it was concluded that fundamental system improvements could only be obtained by a multi-input, multi-output design approach. As a result, NASA funded research work at Boeing during the 1979-1981 period to develop a fully integrated vertical flight path and speed control concept.

The primary objective was to devise a methodology for the design of a largely generic elevator and thrust command computation algorithm, providing decoupled flight path and speed maneuver control for any required control modes. A pilot-like control strategy, including energy management considerations, needed to be developed to achieve effective elevator and throttle coordination, along with an appropriate hierarchy of control modes to deal with thrust limiting and provide complete protection against stall and overspeed. A more robust system design was desired to reduce sensitivity to engine characteristics. Further design objectives are noted below.

Integrated Vertical Flight Path and Speed Control Design Objectives

- Improve operational capabilities and performance
  - Decoupled maneuver control
  - Complete stall and overspeed protection
  - Normal acceleration limiting
  - Simpler and more effective mode control
  - Consistent operation in all modes

- Reduce system complexity, weight, volume
  - Eliminate functional overlap
  - Integrate control laws, minimize software
  - Reduce hardware

- Reduce cost
  - Development and certification
  - Modifications and recertification
  - Maintenance

DESIGN APPROACH

The NASA-sponsored conceptual research work resulted in one very promising generalized design approach based largely on point mass energy control considerations. The basic longitudinal point mass airplane equation of motion, solved for thrust required (T_{REQ}) (shown below), indicates that the aircraft's energy rate is mainly controlled by thrust, while at constant thrust ($\dot{E}_S=0$), the elevator control results in equal and opposite responses of flight path angle and longitudinal acceleration (short-term D=constant). The elevator control is, in essence, energy conservative.

It follows then, that from an energy management point of view, the thrust should be used to control the total energy and the elevator to control the desired energy distribution between the flight path angle and acceleration, or altitude and speed.

Based on Energy Considerations

Equations:

$$T_{\text{required}} = \underbrace{\text{weight} \cdot \overbrace{(\text{SIN}\gamma + \dot{V}/g)}^{\text{Potential flight path angle } \gamma_p}}_{\text{Total energy rate}} + \underbrace{\text{drag}}_{T_{\text{level flight}}}$$

For T = constant: $\dfrac{\partial \gamma}{\partial \delta_e} = - \dfrac{\partial \dot{V}/g}{\partial \delta_e}$ **(short term)**

Therefore:
- Thrust used to control total energy
- Elevator used to control energy distribution

Result: Total Energy Control System (TECS)
- General control strategy for all modes
- Normalized, airplane independent control law
- Commonality with proven γ_p display
- Very simple, effective design

GENERIC TOTAL ENERGY AND ENERGY DISTRIBUTION CONTROL LAW

The previous considerations were used to synthesize a generic flight path angle and longitudinal acceleration control law. The total energy error of the aircraft is controlled by a thrust command proportional to the integral of the sum of flight path angle error γ_ε and normalized acceleration error $\dot{V}_\varepsilon/g$, relative to the targets γ_c and $\dot{V}_c/g$:

$$\Delta T_c = \frac{KTI}{S}(\dot{V}_\varepsilon/g+\gamma_\varepsilon)$$

Likewise, the energy distribution error is controlled by commanding a change in flight path angle and in turn an elevator change proportional to the integral of the difference of $\dot{V}_\varepsilon/g$ and γ_ε:

$$\Delta\delta_{e_c} = \frac{KIL.KEI}{S}(\dot{V}_\varepsilon/g-\gamma_\varepsilon)$$

In addition, proportional terms of $(\gamma+\dot{V}/g)$ and $(\dot{V}/g-\gamma)$ are used to achieve the desired control damping. The elevator command further includes pitch control damping terms that stabilize the short-period dynamics, while the specific net thrust command is scaled in proportion to aircraft weight to form the total net thrust command.

Natural decoupling of flight path and longitudinal acceleration maneuvers is achieved by feeding forward either command to both controllers and by selection of the proper relative gains.

Basic Total Energy Control System

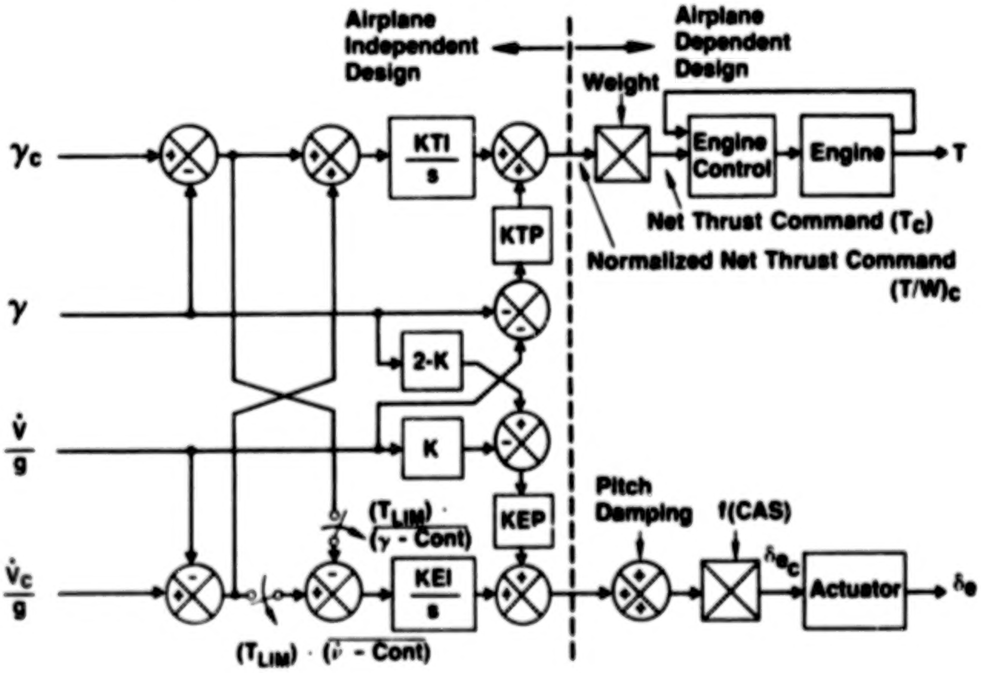
Airplane Independent Design
Airplane Dependent Design
Weight
γ_c
γ
$\dot{V}/g$
$\dot{V}_c/g$
KTI/s
KTP
2-K
K
KEP
KEI/s
Engine Control
Engine
T
Net Thrust Command (T_c)
Normalized Net Thrust Command $(T/W)_c$
$(T_{LIM})\cdot\overline{(\gamma - Cont)}$
$(T_{LIM})\cdot\overline{(\dot{V} - Cont)}$
Pitch Damping
f(CAS)
δ_{e_c}
Actuator
δ_e

ORIGINAL PAGE IS
OF POOR QUALITY

IMPLEMENTATION OF FLIGHT PATH AND SPEED MODES

Using this generalized design approach, all needed flight path and speed control modes of the AFCS can be provided without replication of functions and with the proper hierarchy. The resulting system is called "total energy control system" (TECS). For the outer loop flight path and speed control modes, the altitude and speed errors are simply normalized to form the γ_c and $\dot{V}_c$ signals.

The control law calls for an exponential reduction of the altitude and speed errors with a time constant τ inversely proportional to K_h, K_V. Thus, to preserve decoupling for simultaneous altitude and speed maneuvers and to maintain the correct relative energy relationship between altitude and speed errors, $K_h = K_V$ must be chosen.

All flight path modes ultimately produce a flight path angle command γ_c. All speed control modes produce a $\dot{V}_c/g$. The minimum and maximum speed limiting modes V_{MIN} and V_{MAX} enter downstream of all other speed modes and by autonomous engage logic provide stall and overspeed protection at all times. A more detailed system description is presented in reference 2.

TECS Architecture and Mode Hierarchy

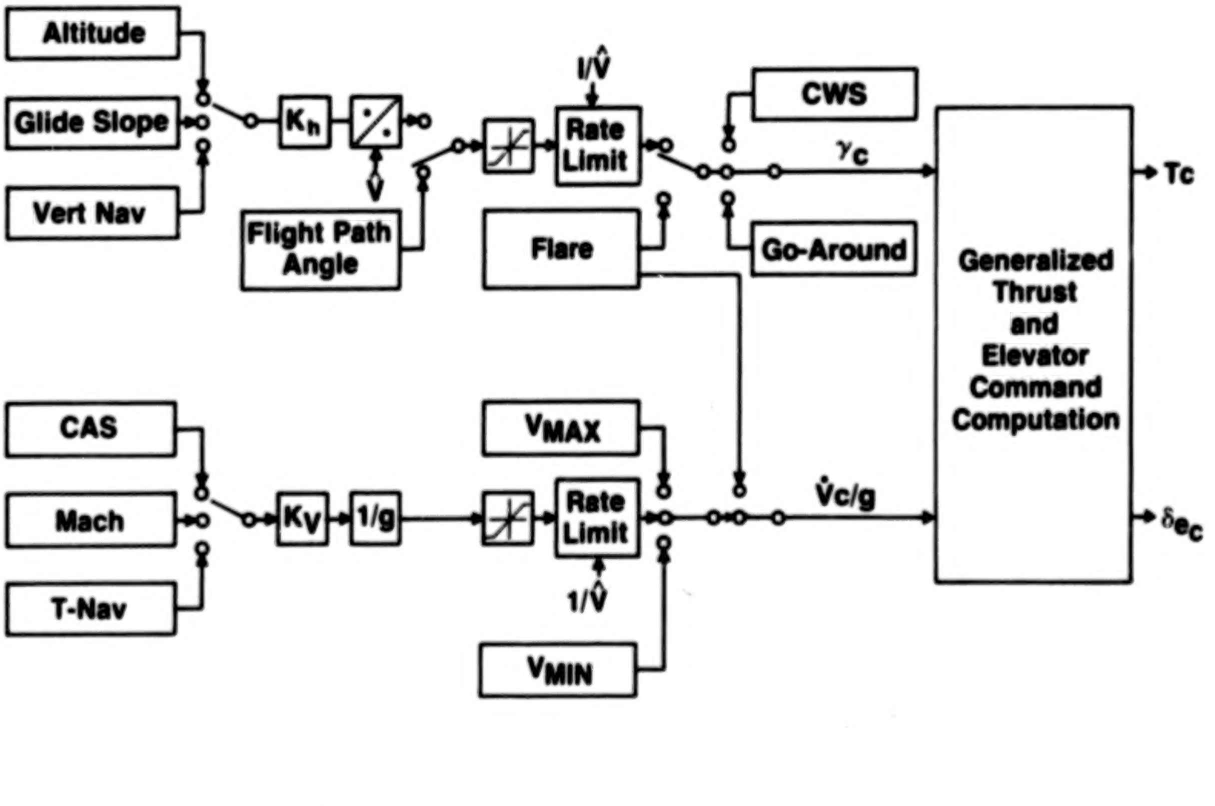
Altitude
Glide Slope
Vert Nav
K_h
Flight Path Angle
$1/\hat{V}$
Rate Limit
CWS
γ_c
Flare
Go-Around
Generalized Thrust and Elevator Command Computation
Tc
CAS
Mach
T-Nav
K_V
1/g
V_{MAX}
$\dot{V}c/g$
Rate Limit
$1/\hat{V}$
V_{MIN}
δ_{ec}

USE OF ENERGY COMMAND RATE LIMITS

The total energy control system meets all functional, operational, and performance requirements of the overall automatic flight control system. General system requirements are met by generic design solutions, implemented at strategic points in the signal processing, so they apply to all intended modes and do not have to be replicated.

Vertical Acceleration Limiting - Normal acceleration limiting has been implemented at one central point in the control law to cover all modes except GO-AROUND and FLARE, by simply rate limiting the γ_c, since $\ddot{h} = \dot{V}\gamma$.

This time history illustrates a case where the vertical acceleration is limited to 3.2 ft/sec^2 (0.1 g) during the executing of simultaneous commands in the ALTITUDE and CAS modes. Analogous to the rate limit in the γ_c path, an equivalent rate limit is provided in the $\dot{V}_c/g$ signal path.

This rate limit provides vertical acceleration limiting during speed control when thrust is limited, reduces controller activity induced by turbulence, and results in smooth thrust buildup for large speed maneuvers.

Energy Exchange Maneuvers - The equal (energy) rate limits on γ_c and $\dot{V}_c/g$ assure that for dual opposing commands, the system first exchanges energy to the maximum extent possible before commanding thrust to satisfy the required final total energy state. Thus, the system can handle any energy management problem efficiently and avoids unnecessary thrust applications, as the time response shows.

ALT/CAS Modes, Combined Descend/Acceleration

B-737 TECS

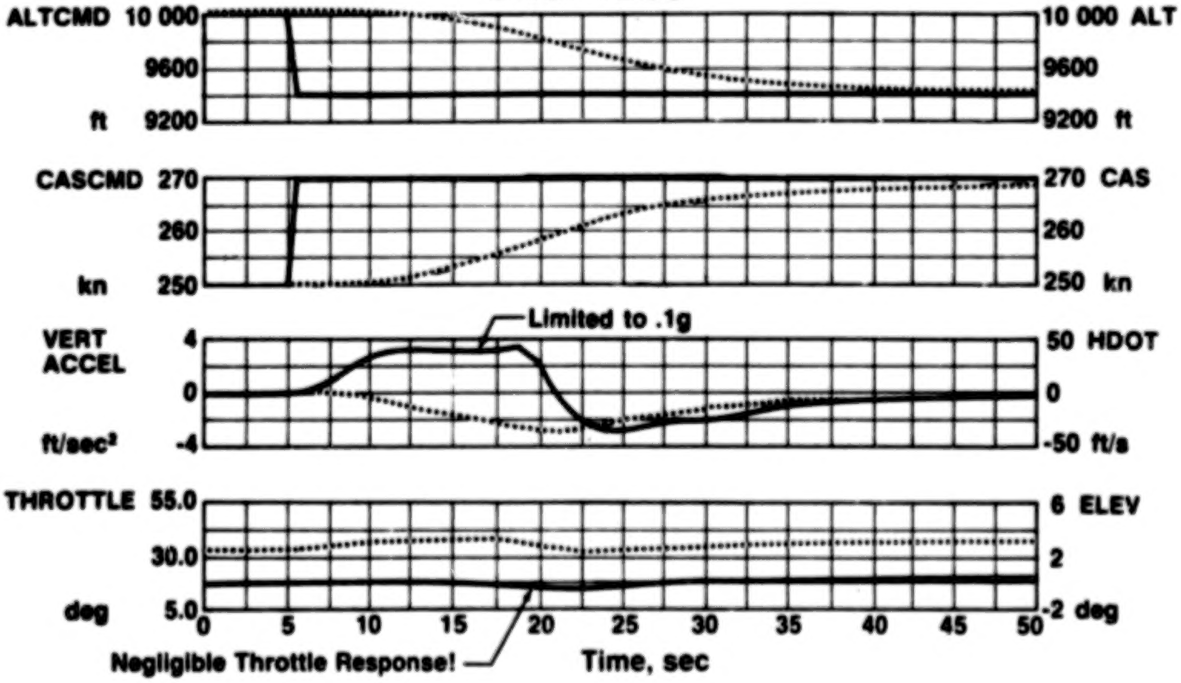

SPEED CONTROL PRIORITY

In the past, there have been numerous incidents where thrust limiting due to large autopilot path commands caused loss of speed control, resulting in airplane stall or overspeed. The TECS design solves this problem elegantly and without adding control laws or complex system reconfiguration.

The flight path angle error crossfeed to the elevator command computation is switched out, and the thrust command integrator is put in HOLD when the flight path command causes the thrust limit to be reached. In this configuration, the speed control is continued through the elevator, and the speed response dynamics remain the same as in the linear case because a change in flight path angle $\Delta\gamma = -\dot{V}_c/g$ is commanded that provides the same acceleration due to the gravity component along the flight path as the engine provides in the linear case. This figure shows the response to an altitude change command, causing the thrust to go to idle, while speed is being maintained through the elevator. Subsequently, the command to reduce speed is executed by temporarily changing the flight path angle, until the speed is captured. Finally, linear control is resumed when the altitude target is approached, and a thrust rate command is developed to drive the throttles out of the aft limit. During the speed change maneuver at idle thrust, the deceleration command was limited to the available total energy rate, represented by $\gamma+\dot{V}/g$, thereby preventing the flight path angle from going positive temporarily. Alternatively, the available total energy rate can be shared to provide simultaneous execution of flight path and speed commands at reduced rates.

ALT/CAS Modes, Descent With Subsequent Deceleration

B-737 TECS

(100% Deceleration Priority)

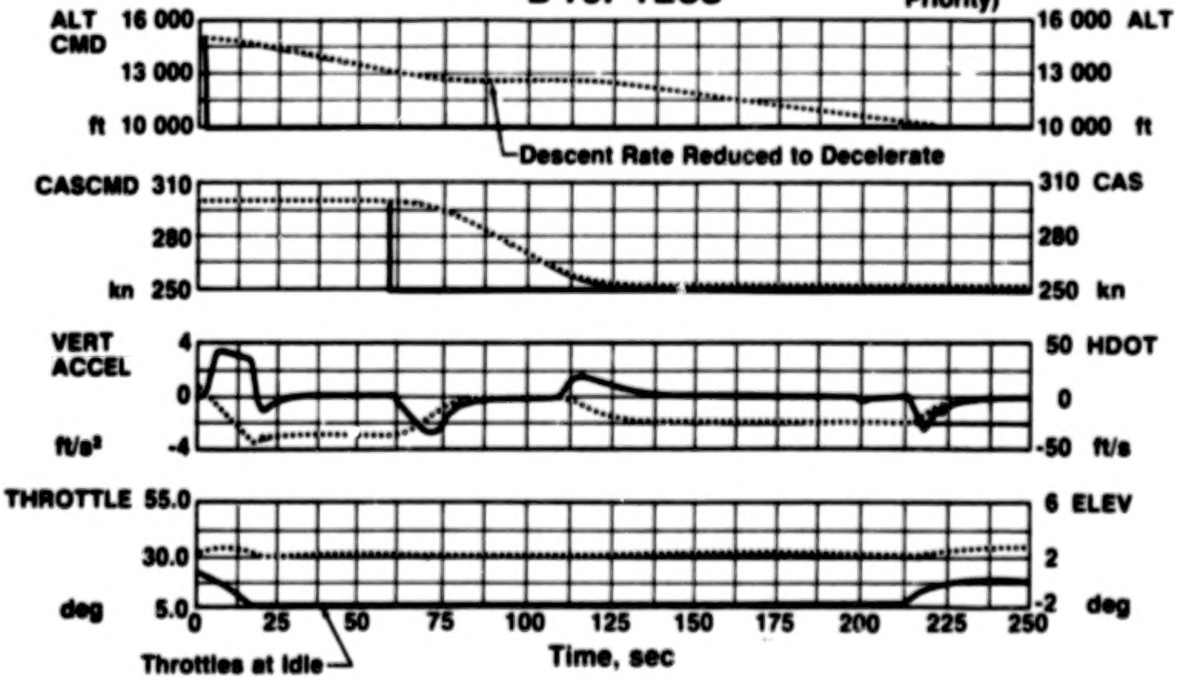

PATH CONTROL PRIORITY

Similar to the provisions to deal with thrust limiting due to large flight path commands, the TECS includes provisions to allow continued path control when the thrust limits due to large speed commands. This figure shows the system's capability to decelerate at idle thrust and capture the glide slope without overshoot while still at high speed. The flight-path-angle-based control provides inherent system adaptation to speed, resulting in consistent path captures and allowing error-free path tracking while changing speed.

In this case, the speed command was reduced to 100 kn before capture of the glide slope. However, the V_{MIN} mode limits the speed reduction to ~1.3 V_{STALL} at each flap setting. As the flaps are lowered beyond 15°, the throttles advance to arrest the deceleration rate, and they stabilize the airspeed when the final flap setting is reached.

High-Speed Glide Slope Capture With Flap Extension and V_{MIN} Control

737 TECS

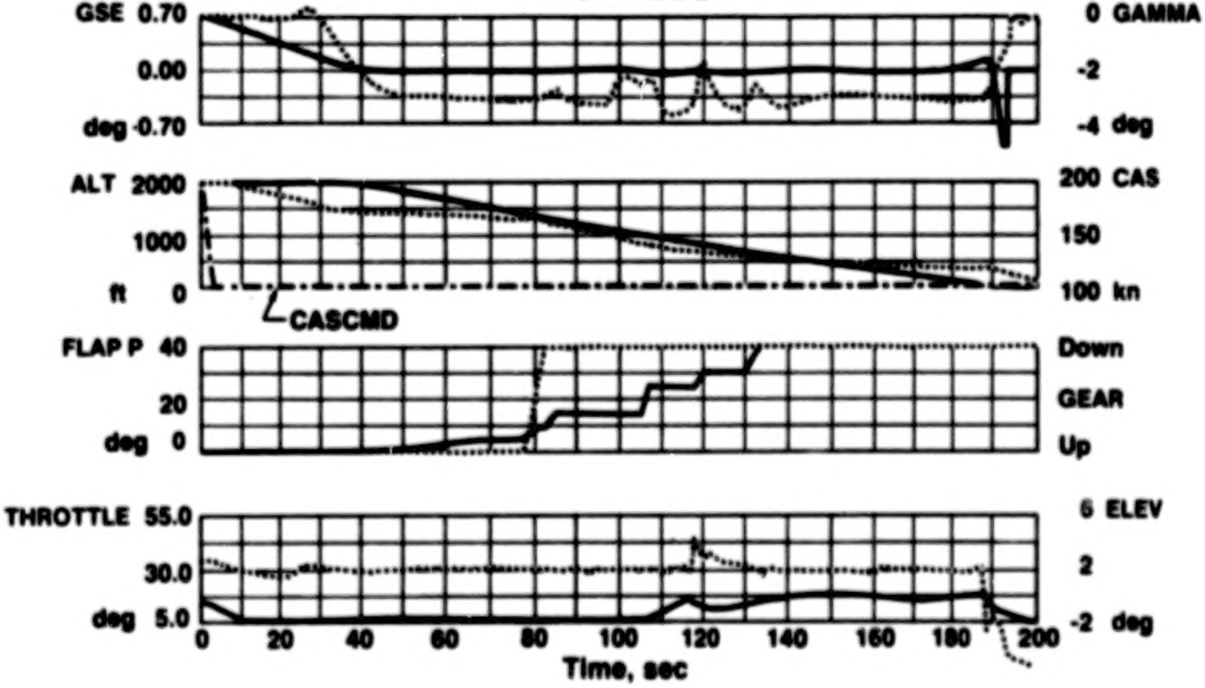

GO-AROUND PERFORMANCE

The GO-AROUND mode is implemented by simply switching to a fixed 10° flight path command (one line of software). Upon engagement of the mode, the commanded flight path angle causes a coordinated rapid throttle advancement and pitch-up. After the throttles reach the limit, the speed control reduces the pitch rate and normal acceleration to zero. The altitude loss after mode engagement is 31 ft for this condition. As shown, approximately a 0.5-g peak incremental load factor is achieved. This can easily be adjusted, as desired. Speed is maintained within ~1 kn, and the entire maneuver is very smooth. The attained steady-state climb rate and pitch attitude depend on the aircraft thrust and drag condition. For a heavyweight aircraft, or low available thrust, the 10° flight path angle cannot be achieved. In that case, a limit thrust climb with speed controlled through the elevator will result. For light weight, high available thrust, or low drag conditions, the $\gamma_c = 10°$ is achieved with only partial power. The partial power avoids excessive climb gradients and pitch attitudes.

The system is designed to safely handle engine failures and aircraft configuration changes. In case of flap retraction without a corresponding increase in the commanded speed, the V_{MIN} control takes over to maintain ~1.3 V_{STALL}.

Go-Around Mode — Engage at 100 ft; Weight, 560 000 lb; Flaps 30°; Altitude Loss 31 ft

B-747 TECS

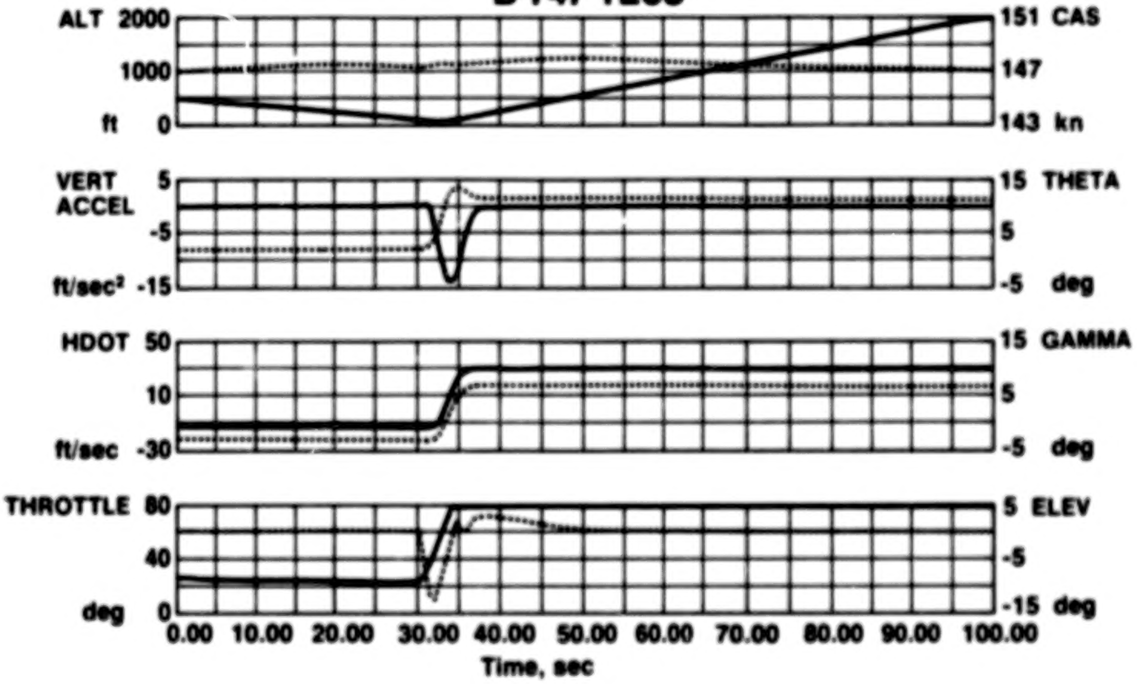

COMPUTER-AUGMENTED MANUAL CONTROL

The total energy control system is well suited for providing flight path angle based computer-augmented control because of the system's decoupled control characteristics. In this mode, also called Velocity Vector Control Wheel Steering (VCWS), a rate of change of flight path angle command (γ_c) proportional to the column force is developed. The column force signal is gain scheduled with 1/V to provide constant stickforce per "g", and integrated to develop the flight path angle command γ_c. An inertial flight path angle feedback $\gamma_I = \dot{h}/V_{GROUND}$ is used to develop the basic error signal γ_ε, and provide long-term control relative to an inertial reference. This γ_c signal is also fed forward to the thrust and elevator command to obtain the desired augmented response lag of γ relative to γ_c without causing speed perturbations.

The time history shows responses tailored to yield $\tau_\gamma = 2.5$ sec, the fastest response achievable with parallel servos while avoiding elevator overcontrol and stickforce reversal. It should be noted that this τ_γ is too long for closure of the primary pilot loop using γ display. To overcome this problem, the γ_c is displayed along with γ. The γ_c had been shown on the NASA B737 to be a satisfactory primary pilot display for the flight path angle CWS mode (ref. 3). This mode can be used on various transport aircraft to obtain virtually identical and optimized handling characteristics.

Velocity CWS Responses to 12-lb Column Pull/Push
B747 TECS

Flaps 30° Gear Down
±12 lb Pull/Push

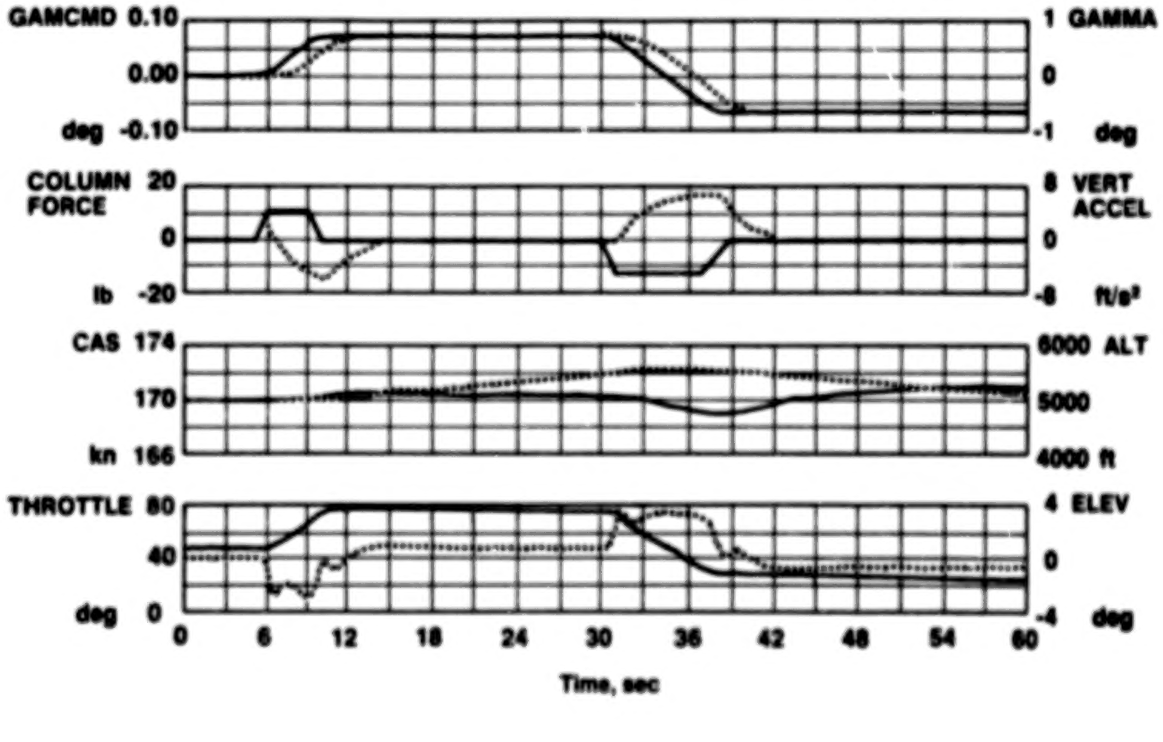

CONTROL IN WIND SHEAR AND TURBULENCE

To optimize the system's performance in wind shear and turbulence, numerous trade-offs and issues were analyzed, i.e., relative flight path and speed tracking, flight path and speed tracking performance versus control activity, and proper control reconfiguration when reaching performance limits.

A major advantage of the total energy and energy distribution control concept is that it takes maximum advantage of the control effectiveness of thrust and elevator by providing conflict-free decoupled control.

Where possible, the system uses airmass-referenced feedback signals, filtered to remove atmospheric noise in the frequency range where the controls cannot respond effectively.

The simulated time history shows how a severe wind shear of -5 kn/sec causes instant bleedoff of the airspeed and a slower departure from the commanded altitude of 5000 ft. This signifies a sharp loss of aircraft energy. The system responds by bringing the throttles forward quickly. Even when limit thrust is reached, the total energy rate remains negative, causing the V_{MIN} speed control mode to engage and the flight path control to be abandoned. The aircraft captures the minimum speed command (1.3 V_{stall} or α_{REF}) undershoot free and settles into a steady-state descent. In this case, the filtering of the airspeed related feedbacks was adjusted to yield quick response to wind shear.

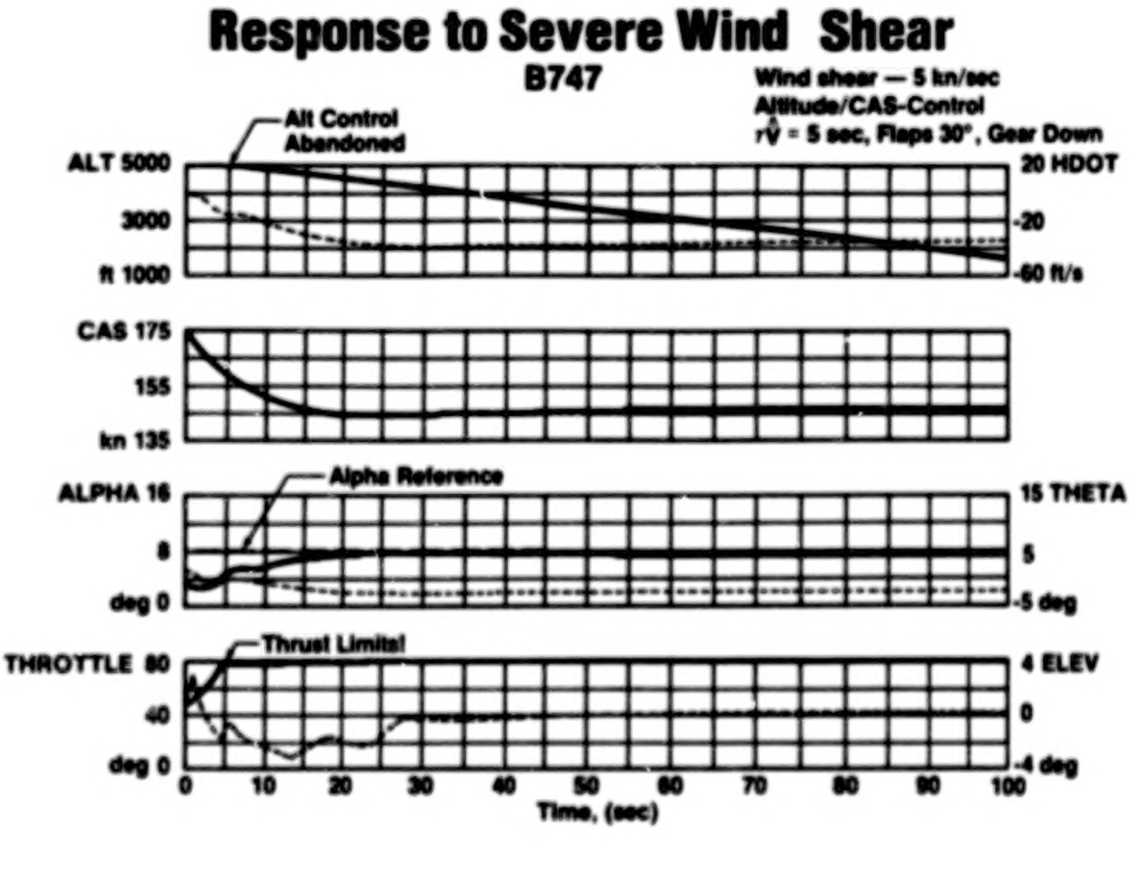

CONTROL IN WIND SHEAR AND TURBULENCE (CONT'D)

For the responses below, the same wind shear condition was run with the filtering of the airspeed control feedbacks adjusted to reduce controller activity in turbulence by ~50%. As a result, the throttles respond more slowly to the wind shear and more airspeed is lost. When the thrust limit is reached, the path control is abandoned and speed control is continued through the elevator. Since the total energy rate remains negative, causing the $\dot{V}_c$ of the V_{MIN} mode to be more positive than V_c of the selected speed mode, the V_{MIN} mode engages and the minimum speed is recaptured. In the process, the airplane comes very close to stall, but stays closer to the commanded altitude for a longer period of time, before settling into the steady descent.

In a similar situation on the glideslope, the system will stay at the V_{MIN} speed until the wind shear subsides to the point where the total energy rate once again becomes positive. At that time, the glideslope will be recaptured first before the pilot-selected speed will be reestablished.

As these time histories indicate, the best insurance in case of severe wind shear is to have excess airspeed energy, together with provisions that prevent the airplane from stalling.

Response to Severe Wind Shear

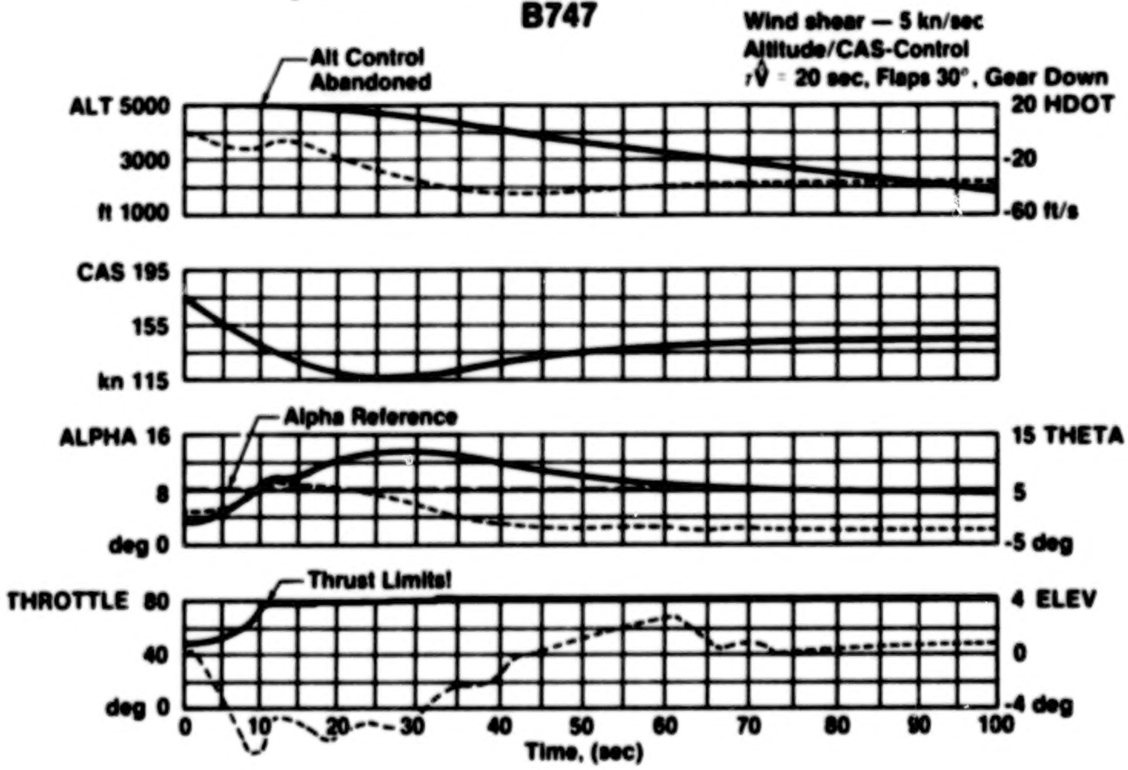

MODE CONTROL PANEL DESIGN

The integration of functions and enhanced operational capabilities of the TECS is reflected in the example mode control panel layout below.

The modes have been chosen to provide all necessary tactical and strategic capabilities. All modes are operable over the entire flight envelope. Any flight path mode is compatible with every speed mode. The panel provides the complete mode and control configuration status. For example, when either flight path or speed control is abandoned due to thrust limiting, the appropriate VARIABLE indication on the bottom of the panel is lit. At the same time, the THRUST LIMIT light on the left of the panel lights. The thrust rating mode selection has been integrated in this panel because the performance capability of the vertical flight path and speed control modes depends directly on the selected thrust rating mode.

The CAS and Mach modes can be preselected for automatic mode transition during climb-out and descent.

The T-NAV, V-NAV, and L-NAV modes allow the navigation/performance computer target speed, target vertical, and lateral paths to be input to the TECS for execution. Reference 2 discusses the operational aspects in more detail.

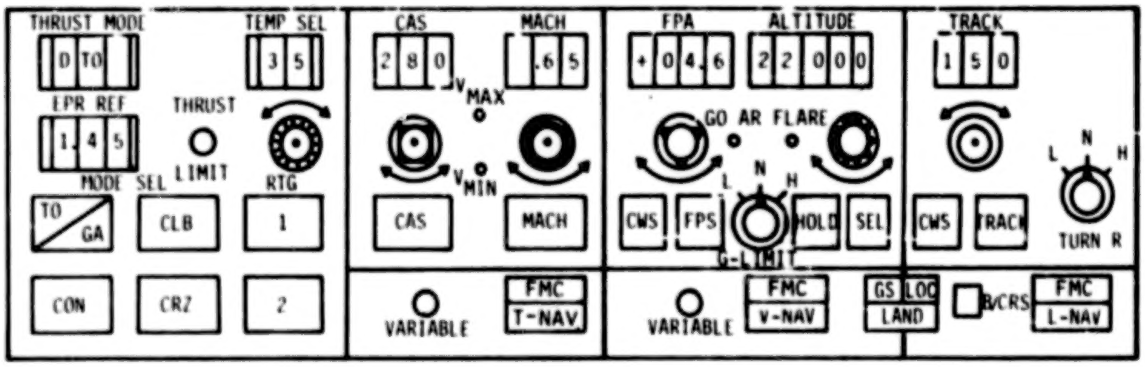
THRUST MODE
D TO
TEMP SEL
3 5
EPR REF
1.4 5
THRUST LIMIT
RTG
MODE SEL
TO GA
CLB
1
CON
CRZ
2
CAS
2 8 0
MACH
.6 5
V_{MAX}
V_{MIN}
CAS
MACH
VARIABLE
FMC
T-NAV
FPA
+0 4.6
ALTITUDE
2 2 0 0 0
GO AR FLARE
L N H
CWS
FPS
HOLD
SEL
G-LIMIT
VARIABLE
FMC
V-NAV
GS LOC
LAND
TRACK
1 5 0
L N H
CWS
TRACK
TURN R
B/CRS
FMC
L-NAV

- INTEGRATED THRUST RATING
- PERFORMANCE LIMIT INDICATION
- INTEGRATED ALT SEL/ALT CLEARANCE

TECS ENGINE CONTROL

The first major objective of the integrated flight and propulsion control system was the development of a more accurate net thrust command computation.

The second major objective of the design was the elimination of arbitrary engine thrust variation due to changes in environmental or flight conditions. Therefore, in the TECS design, all major engine environmental dependencies have been compensated to make the engine produce the desired net thrust on command.

The net thrust command is converted into an EPR command and used for closed-loop engine control. This involves dependencies on the pressure ratio $\delta = p/p_0$ and Mach number. Further, the EPR command is used to predict the steady-state throttle position command. To maintain constant loop gain, the total air temperature dependency has been compensated. The closed-loop EPR control law also serves to reduce the variation in the response dynamics of the engine and the effects of throttle actuation nonlinearities.

Feedback of throttle position and EPR in excess of selected limits to the thrust command computation serves to prevent engine overboost and ineffective throttle control in the low thrust region.

In the future, customization of the automatic flight control system to work with specific engines can largely be eliminated by designing the electronic engine controls to control to a net thrust command and to compensate for all major thrust environmental dependencies (ref. 4).

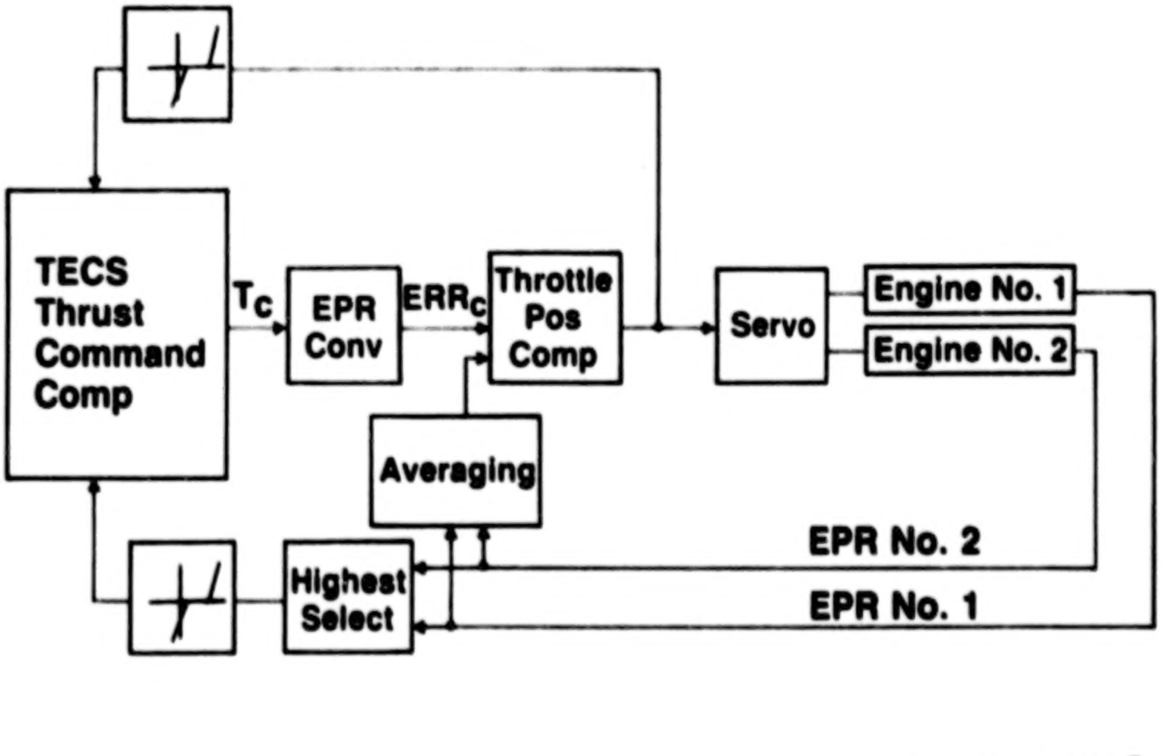

ORIGINAL PAGE IS
OF POOR QUALITY

AFCS FUNCTION DISTRIBUTION

The integration of all vertical flight path and speed control functions, together with future integration of lateral directional functions, allows a more efficient system architecture using fewer sensors, computers, interfaces, and a function distribution that is closer oriented toward airline needs.

As shown, all automatic control modes and safety-oriented functions are consolidated in the flight control computers, which will be designed with the necessary redundancy to provide the required integrity of the critical control functions.

The consolidation of all automatic control functions in the flight control computer (FCC) leaves the navigation/performance (flight management) computer with strictly airline-operations-oriented functions: navigation, performance, and path definition. The resulting flight control targets can be transmitted to the FCC for execution. No control loops would be closed in the navigation/performance computer. This design eliminates functional overlap and provides consistency of operation for all modes.

AFCS Function Distribution Using TECS Architecture

(NO FUNCTIONAL OVERLAP)

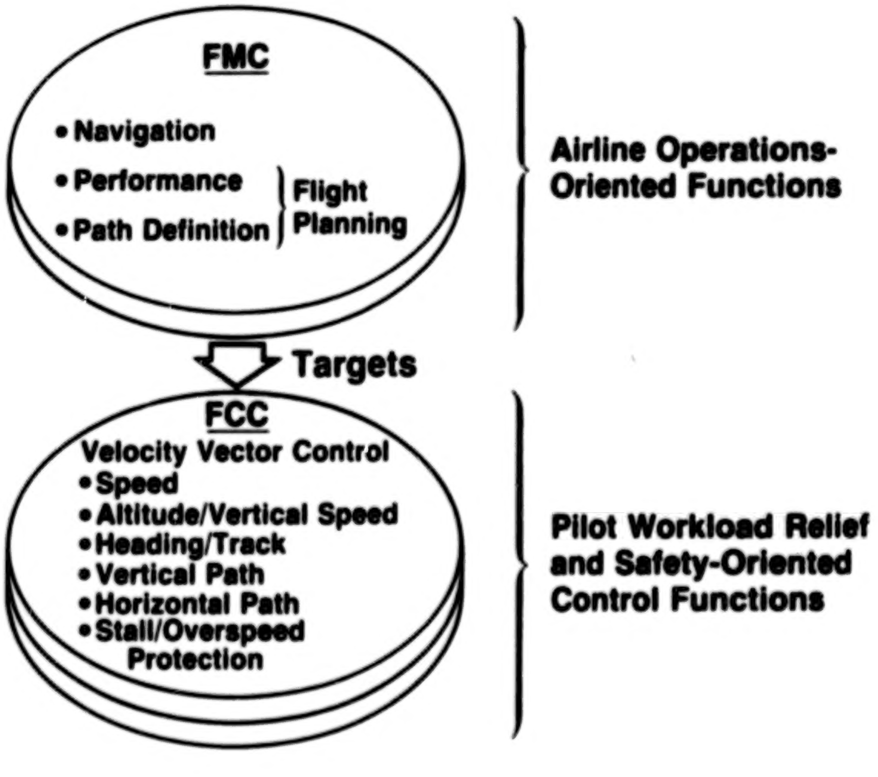

FMC

- Navigation
- Performance
- Path Definition

Flight Planning

Airline Operations-Oriented Functions

Targets

FCC

Velocity Vector Control
- Speed
- Altitude/Vertical Speed
- Heading/Track
- Vertical Path
- Horizontal Path
- Stall/Overspeed Protection

Pilot Workload Relief and Safety-Oriented Control Functions

TOTAL ENERGY CONTROL SYSTEM PAYOFF

The payoff of the total energy control system development is evident: the design provides proper integration of the flight path and speed control functions, resulting in optimum thrust and elevator control efficiency. The design eliminates the numerous limitations of the previous state-of-the-art autopilots and autothrottles. The system implementation is simple, without functional overlap or operational ambiguities, requiring less software and less hardware.

Safety has been enhanced by complete stall and overspeed protection in case of operational errors and severe wind shear.

The potential for cost reductions is substantial.

The design is largely generic. For example, transfer of the complete TECS design from the B737 to the B747 simulator, including adaptation and checkout of innerloops and V_{MIN}/V_{MAX} schedules, required only 6 engineering man months. No energy control concept related changes were needed. The total energy control system is scheduled to be evaluated in flight on the NASA B-737 aircraft under the Air Transport Operating System Program, in the summer of 1984. The Boeing Company will provide the system definition and under contract assist NASA with checkout of a complete TECS simulation, flight software specification, software test, and flight test.

- **Fully integrated, generally applicable design**
- **Improved performance for all modes**
  - **— Decoupled path and speed maneuvering**
  - **— Energy efficient thrust control**
  - **— Uniform stability bandwidth, transient responses**
- **Enhanced operational capabilities**
  - **— Complete safety and maneuver envelope limiting**
  - **— Configuration control when thrust limited**
  - **— Reduced pilot workload — (simpler mode control, VCWS)**
- **Control law software reduced ≈ 75%**
- **Fewer sensors, computers**
- **Large cost reductions**
  - **— Development, flight test, procurement, maintenance**

REFERENCES

1. H. A. Soulé, "The Throttles Control Speed, Right? Wrong!" AIAA Journal of Astronaut. & Aeronaut., vol. 7, no. 12, Dec. 1969, pp. 14-15 and 81.

2. A. A. Lambregts, "Operational Aspects of the Integrated Vertical Flight Path and Speed Control System," SAE Paper No. 831420, October 1983.

3. A. A. Lambregts and D. G. Cannon, "Development of a Control Wheel Steering Mode and Suitable Displays That Reduce Pilot Workload and Improve Efficiency and Safety of Operation in the Terminal Area and in Windshear," AIAA Paper No. 79-1887, August 1979.

4. A. A. Lambregts, "Integrated System Design for Flight and Propulsion Control Using Total Energy Principles," AIAA Paper No. 83-2561, October 1983.

N84
20589

UNCLAS

N84 20589 D22

FLIGHT TEST RESULTS FOR THE DIGITAL INTEGRATED AUTOMATIC LANDING SYSTEM (DIALS) - A MODERN CONTROL FULL-STATE FEEDBACK DESIGN

R. M. Hueschen
NASA Langley Research Center
Hampton, Virginia

First Annual NASA Aircraft Controls Workshop
NASA Langley Research Center
Hampton, Virginia
October 25-27, 1983

PRECEDING PAGE BLANK NOT FILMED

PAGE 410 INTENTIONALLY BLANK

DIALS INTRODUCTION

A goal of the Advanced Transport Operating Systems (ATOPS) Program at Langley Research Center is to increase airport capacity. One on-going effort contributing to this goal is the development of advanced autoland systems which can capture the localizer and glideslope with low overshoot and safely do so for short finals (1.5 to 2.0 nautical miles). Another capability being developed is the ability to fly selectable and steeper glideslopes with the potential for noise reduction and wake vortex avoidance. Systems with improved performance in turbulence and shear wind encounters are also desired. One autoland system designed to have these capabilities and flight tested within the ATOPS program is called the Digital Integrated Automatic Landing System (DIALS). The DIALS is a modern control theory design performing all the maneuver modes associated with current autoland systems: localizer capture and track, glideslope capture and track, decrab, and flare. The DIALS is an integrated full-state feedback system which was designed using direct-digital methods. The DIALS uses standard aircraft sensors and the digital Microwave Landing System (MLS) signals as measurements. It consists of separately designed longitudinal and lateral channels although some cross-coupling variables are fed between channels for improved state estimates and trajectory commands. The DIALS was implemented within the 16-bit fixed-point flight computers of the ATOPS research aircraft, a small twin jet commercial transport outfitted with a second research cockpit and a fly-by-wire system. The DIALS became the first modern control theory design to be successfully flight tested on a commercial-type aircraft. Flight tests were conducted in late 1981 using a wide coverage MLS on Runway 22 at Wallops Flight Center. All the modes were exercised including the capture and track of steep glidescopes up to 5 degrees.

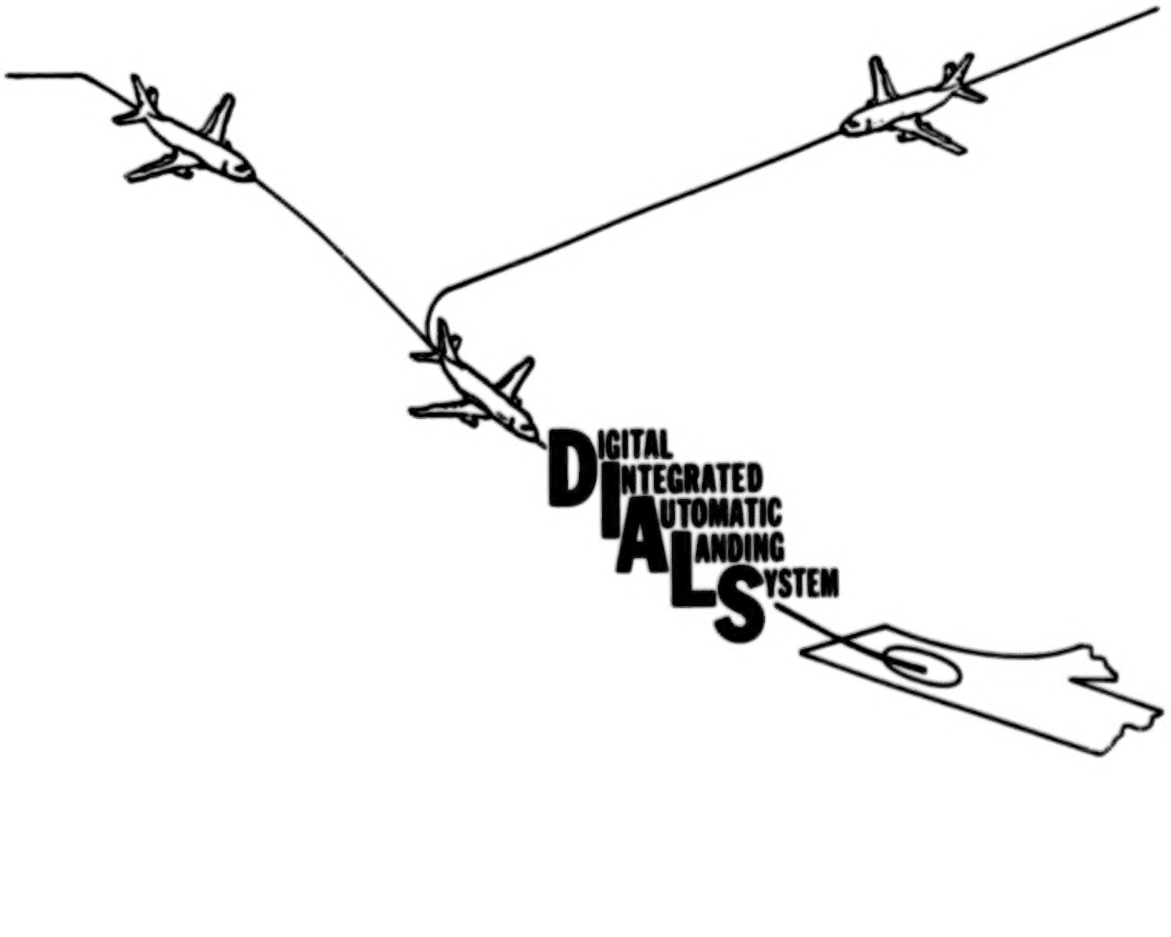

ATOPS TRANSPORTATION SYSTEM RESEARCH VEHICLE (TSRV)

The figure below shows a picture of the ATOPS research aircraft referred to as the TSRV which was used to flight test the DIALS. Flight test data of sensors and selected computer outputs were recorded on magnetic tape for postflight processing. In addition, on-line strip chart recorders provide real-time readouts of software selectable variables for in-flight system analysis and performance evaluation.

ADVANCED TRANSPORT OPERATING SYSTEMS (ATOPS)
TRANSPORTATION SYSTEMS RESEARCH VEHICLE (TSRV)

DIALS AUTOMATIC OPERATIONS

The pictorial illustrates the automatic operations performed by DIALS. Prior to beginning the DIALS operations, the pilot selects the desired glideslope and desired reference airspeed. Then the aircraft is flown towards the runway centerline at a desired heading or ground track angle up to ±60° from the runway heading. The DIALS will then automatically initiate the capture maneuver when the capture criteria, which **consider aircraft parameters, desired trajectory, and wind conditions, are** satisfied. Localizer and glideslope capture can occur independently, in any order, or simultaneously. Upon completing the capture mode, the localizer and glideslope track modes are engaged to maintain the aircraft along runway centerline and the selected glideslope. At an altitude of 250 feet, the decrab maneuver is engaged. The control law commands the aircraft into a sideslip maneuver, a maneuver that pilots often use, while maintaining the track along runway centerline. In an altitude range of 80 to 150 feet, the flare maneuver is engaged. The exact engagement altitude is a function of the glideslope angle, the vertical velocity, and other aircraft parameters. During the flare maneuver, the aircraft is commanded to follow a fixed trajectory in space to a prespecified touchdown point on the runway. The fixed trajectory was chosen as a means to enable precision or low dispersion touchdown. With a precision touchdown capability, an aircraft can reliably decelerate and exit the runway at its earliest convenience and reduce occupancy time.

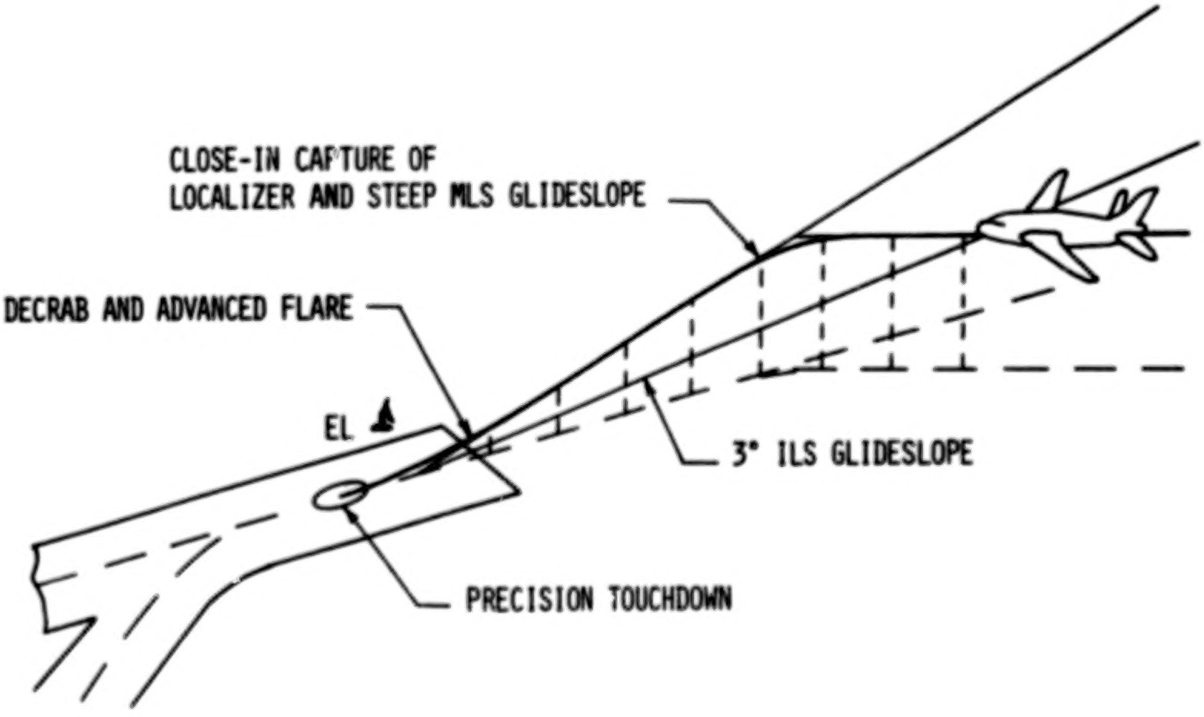

THE DIALS DESIGN AND SYSTEM DESCRIPTION

The DIALS was designed using stochastic modern control theory and direct-digital design methods. The system equations were linearized about a nominal glideslope, and a set of constant gains was determined according to a quadratic cost function. The gains were then used in one basic control law which accommodated all the autoland modes. The control law generates control commands at 10 Hz, which is one half that used in the digital baseline system on the research aircraft.

The sensors used for the DIALS flight tests were the digital MLS signals (azimuth, elevation, and range), pitch, roll, and yaw rate from standard rate gyros, body-mounted accelerometers, vertical velocity determined from MLS processing, calibrated airspeed, engine-pressure-ratio, throttle position, stabilizer position, barometric altitude, and radar altitude during flare. Pitch, roll, and yaw from an inertial platform were used although the design was intended to use standard vertical and directional gyros. However, these gyros were not available on the test vehicle.

DIALS has a full-state constant gain Kalman filter which estimates the states of the aircraft and steady, gust, and shear winds. The wind estimates are fed directly into the control law to provide improved performance to changing wind conditions.

The longitudinal and lateral control laws were each designed independently of one another. Each design was a multi-input multi-output problem resulting in integrated or coordinated controls. The controls coordinated in the longitudinal channel were throttle, elevator, and stabilizer while those coordinated in the lateral were the aileron and rudder.

☐ FULL-STATE DIRECT-DIGITAL DESIGN USING MODERN CONTROL THEORY

  - One Basic Control Law For All Modes
  - 10-Hz Sampling Rate

☐ SENSORS

  - Digital MLS Signals (Az, EL, R)
  - Attitudes & Attitude Rates
  - Body-Mounted Accelerometers
  - $\dot{h}_{MLS}$ & Calibrated Airspeed
  - EPR's, Throttle Position, & Stabilizer Position
  - Barometric Altitude & Radar Altimeter During Flare

☐ FULL-STATE KALMAN FILTER (CONSTANT GAINS) WITH WIND ESTIMATES THAT ARE USED DIRECTLY IN CONTROL LAW.

☐ LONGITUDINAL CONTROL LAW HAS INTEGRATED THROTTLE, ELEVATOR, & STABILIZER AND LATERAL LAW HAS INTEGRATED AILERON & RUDDER.

MODIFICATIONS TO DIALS NOMINAL DESIGN

One basic control law structure was used for the DIALS but some modifications were made to the nominal design as a result of evaluation in a nonlinear simulation to achieve desired performance for the various control modes.

For the glideslope capture mode, at the instant of engagement, the desired vertical velocity along the glideslope was commanded to the desired value through an easy-on rather than letting the command to the control law be a step command.

In the glideslope mode, the vertical position error is integrated and used in the control law when this mode is engaged. Also the gains on vertical position and vertical velocity are increased by means of an easy-on for tighter tracking.

Some similar changes were made for the localizer track mode. At track mode, engagement gains on the lateral position are increased through an easy-on, and the lateral position and roll errors each are integrated to eliminate position standoff and to drive roll attitude to wing level. The roll integrator insures that the control law will achieve the desired crab angle and zero sideslip in steady-state wind conditions.

During the decrab mode, the aircraft heading is commanded to align with the runway through trajectory commands. To insure a sideslip condition, the gain on the roll integrator used during localizer tracking was ramped to zero, and the heading error was integrated and fed back to the control commands.

To insure close tracking of the flare trajectory, the gains on altitude, altitude rate, and pitch rate were increased by means of an easy-on at the initiation of the flare mode.

- G/S CAPTURE MODE
  - COMMANDED VERTICAL VELOCITY AT ENGAGEMENT WITH EASY-ON
- G/S TRACK
  - ADD INTEGRATOR ON VERTICAL POSITION ERROR
  - INCREASE GAINS (WITH EASY-ON) ON VERTICAL POSITION & VELOCITY ERRORS)
- LOC TRACK
  - ADD INTEGRATORS FOR LATERAL POSITION & ROLL ERRORS
  - INCREASE GAIN (WITH EASY-ON) ON LATERAL POSITION ERROR
- DECRAB
  - ADD INTEGRATOR TO HEADING ERROR
  - REMOVE FEEDBACK OF ROLL INTEGRATOR WITH EASY-OFF
- FLARE
  - INCREASE GAINS (WITH EASY-ON) ON VERTICAL POS & VEL & PITCH RATE

ORIGINAL PAGE IS
OF POOR QUALITY

BLOCK DIAGRAM OF FEEDBACK LOOP

The block diagram shows the feedback loops associated with the DIALS longitudinal and lateral control laws. The Kalman filter processes the MLS and aircraft sensor data to determine estimates of the aircraft states and winds. There are 16 aircraft and wind states for the longitudinal channel and 13 for the lateral channel. The Kalman filter makes path predictions of the aircraft at the next iteration. These predictions are differenced with the flight path generator path, and the result is fed back to the controls to provide path lead information. The aircraft state estimates are differenced with desired trajectory from the flight path generator to form trajectory error signals. The desired trajectory signals are also fed back to the control law to provide the control law information about trajectory deviations from the nominal glideslope. Using the wind estimates and the above described signals, the control commands are generated ten times a second. The commands generated for the longitudinal controls are elevator position δ_e, throttle rate $\dot{\delta}_{th}$, and stabilizer rate $\dot{\delta}_s$. By choosing throttle rate as a command, it was possible to achieve satisfactory throttle rate activity by appropriate weighting of it in the quadratic cost function. Stabilizer rate was weighted in the cost so that this command acted primarily as a trimming function. By using rate commands, no penalty is incurred in the cost function for position deviations from the nominal values for the stabilizer and throttle. However, for the elevator, the desire is to keep it nominally near the neutral position so that maximum authority is always available. The commands from the lateral control law are aileron position δ_a and rudder rate $\dot{\delta}_r$. The three rate commands were integrated at a 20-Hz rate to provide smoother position commands to the aircraft servos. The stabilizer position is added to the elevator command. In the design, the stabilizer rate was intended to control the trim logic in such a manner as to turn the stabilizer trim motor on and off on the test vehicle; however, due to built-in restrictions on the direction of stabilizer movement as a function of elevator position, the stabilizer trimming was achieved by logic driven by the elevator deflection (logic that existed on the baseline test vehicle).

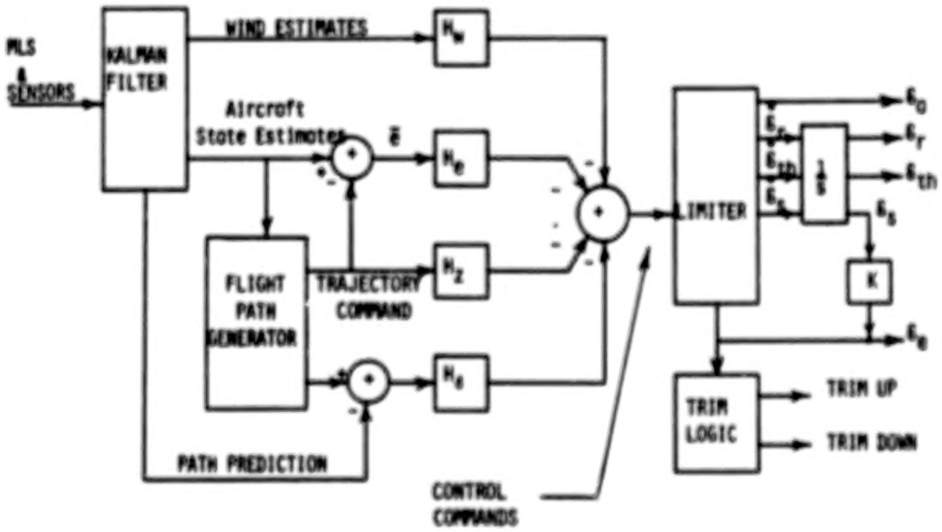
MLS
&
SENSORS
KALMAN
FILTER
WIND ESTIMATES
H_w
Aircraft
State Estimates
$\bar{e}$
H_e
FLIGHT
PATH
GENERATOR
TRAJECTORY
COMMAND
H_z
H_ϵ
PATH PREDICTION
CONTROL
COMMANDS
LIMITER
$\frac{1}{S}$
δ_a
$\dot{\delta}_r$
$\dot{\delta}_{th}$
$\dot{\delta}_s$
δ_r
δ_{th}
δ_s
K
δ_e
TRIM
LOGIC
TRIM UP
TRIM DOWN

DIALS LOCALIZER CAPTURE - FLT 361, RUN 7

The capture of the localizer using a 30-degree intercept angle is shown below. This flight was conducted in 12 knot crosswinds with 2 to 3 knot gust variations. The top graph is a plot of the deviation of the aircraft from the runway centerline, the middle plot is the aircraft roll attitude, and the bottom graph is the aircraft yaw or true heading with respect to runway centerline. The capture maneuver was initiated at 5 seconds on the plots. The aircraft captures the localizer with no overshoot and was settled on runway centerline by 35 seconds. The aircraft heading smoothly achieves the crab angle with no oscillation indicating that the estimate of crosswind used by the control law is accurate. At 97 seconds into the flight, a lateral wind shear of 8 knots/100 feet was encountered. Incidently, this magnitude of wind shear is that specified in the FAA Advisory Circular No. 20-57a for certification of autoland systems. The aircraft heading again smoothly changed to the runway heading as the wind diminished. The aircraft deviated approximately 25 feet from the runway centerline during the shear but corrected back to centerline within 10 seconds after the shear stopped.

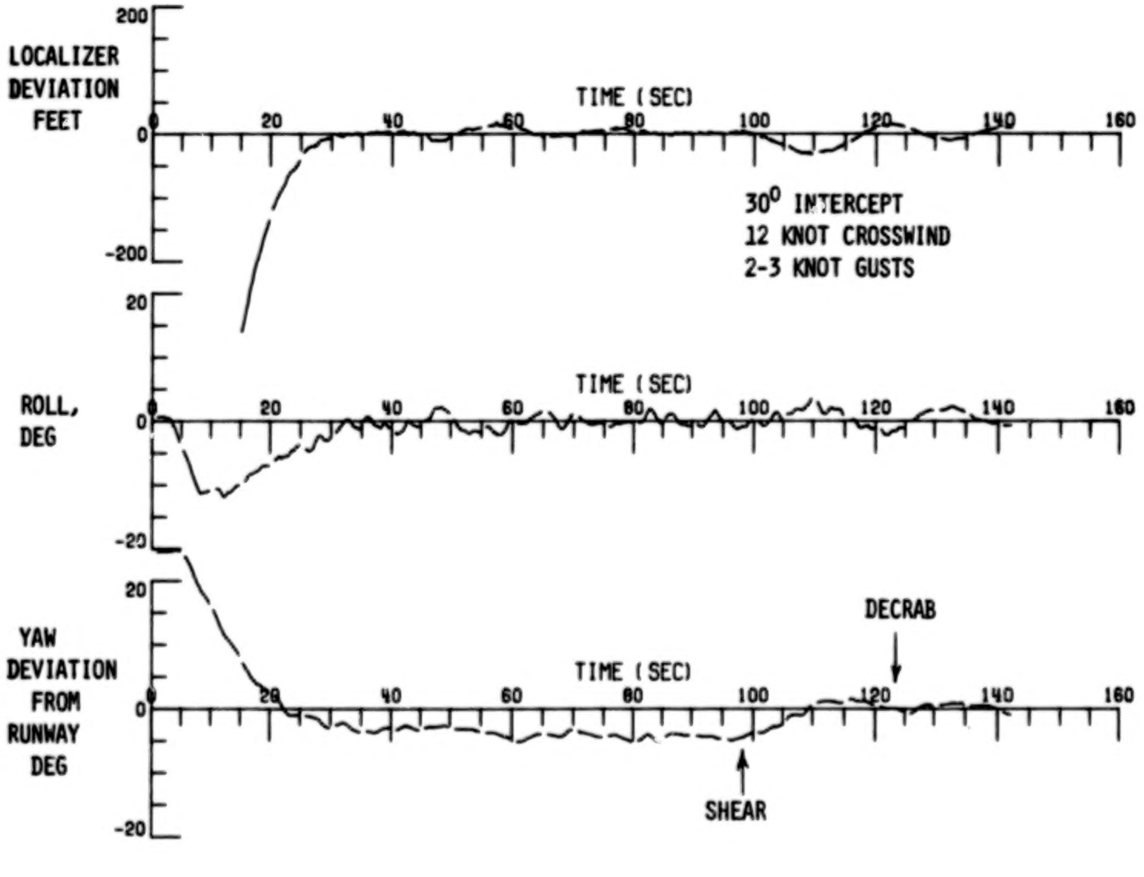

DIALS 3-DEGREE GLIDESLOPE CAPTURE AND TRACK - FLT 361, RUN 7

The graphs below show the capture of the 3-degree glideslope which begin at 24 seconds during the time the localizer capture was being completed. The top plot shows the aircraft deviation from the desired glideslope during the glideslope capture and track mode, and during the flare mode, it shows the deviation from the flare trajectory. The middle graph is a plot of the aircraft pitch attitude, and the bottom graph shows the vertical velocity from MLS processing. The glideslope is captured with no position overshoot although some overshoot does occur in the desired glideslope vertical velocity. This velocity overshoot is not present in the steeper glideslope captures and was not shown in the developmental simulation runs suggesting that an error was present in the glideslope capture criteria flight software. The shortness of time for the capture when compared to simulation times and the capture times for the steeper glideslope captures, to be discussed in subsequent figures, suggest that the capture maneuver was initiated too late or too close to the glideslope. The flare maneuver is initiated at 130 seconds into the flight. The pitch attitude reaches about 2 degrees for good nose wheel clearance, and the vertical velocity is smoothly reduced to an acceptable touchdown sink rate.

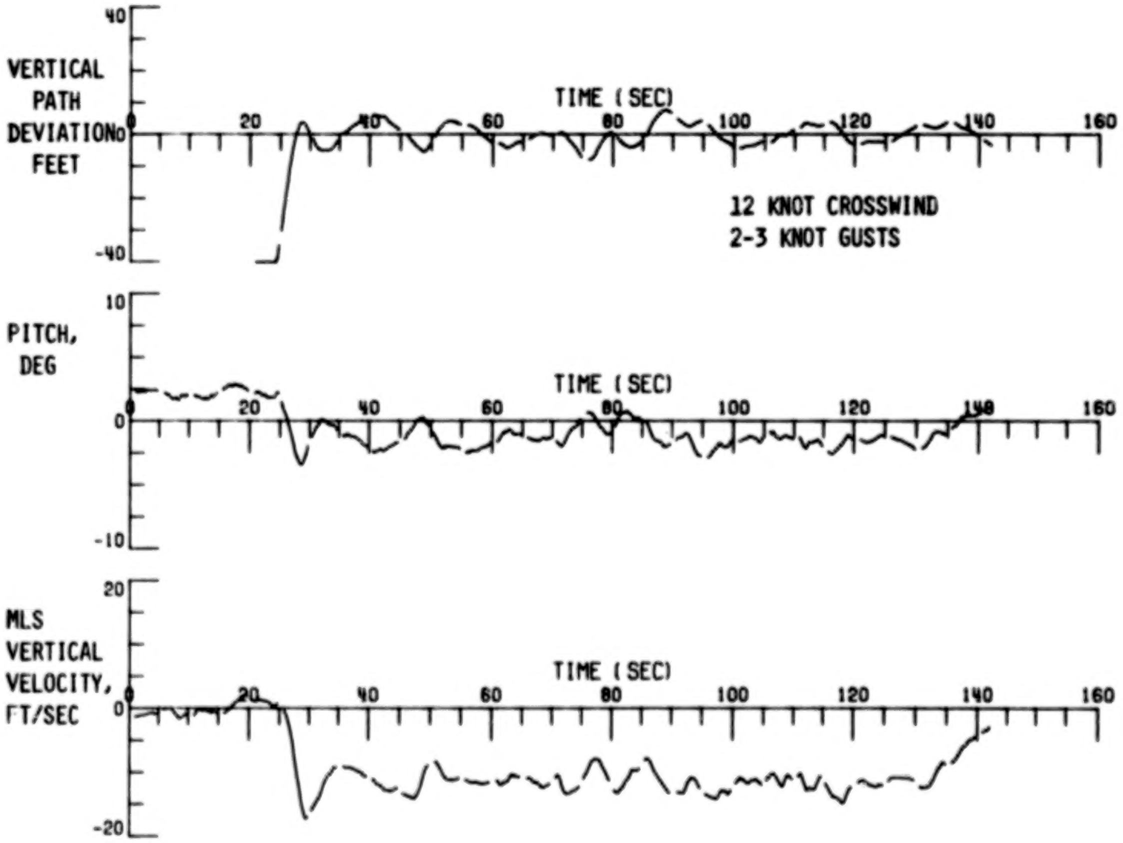

DIALS FLIGHT DATA - FLT 361, RUN 7

The flight data shown below are plots of calibrated airspeed (top graph), throttle position (middle graph), and total elevator position (bottom graph) which includes the mechanical downrigging of the elevator due to stabilizer trim position. This is companion data for the test run discussed in the previous two figures. The reference airspeed for this run was set to 130 knots. The data shows that the measured airspeed was somewhat higher than the selected reference by 5 to 8 knots. DIALS had a tendency to control the airspeed about 3 to 5 knots higher than the selected reference. The tendency may be related to the way the desired airspeed is achieved by DIALS. The current airspeed is estimated in DIALS by adding its estimate of ground speed and wind along the longitudinal axis. If this estimate is low, the DIALS will advance the throttle to increase inertial speed and thus airspeed. The slightly higher airspeed may be due to a bias in the measurement or a low estimate of airspeed. Coordination of the throttle and elevator is shown in the plots. At glideslope capture (24 seconds), the elevator goes positive (trailing edge down) to pitch the aircraft down while the throttle is immediately reduced towards glideslope thrust. Although the glideslope pitch is achieved at 30 seconds, the elevator continues to adjust to counteract the pitching moment due to thrust changes. During flare, the elevator moves to pitch the aircraft up while the throttle decreases to satisfy a commanded reduction in airspeed. Note that the throttle is not driven to idle but to a position to achieve the commanded airspeed.

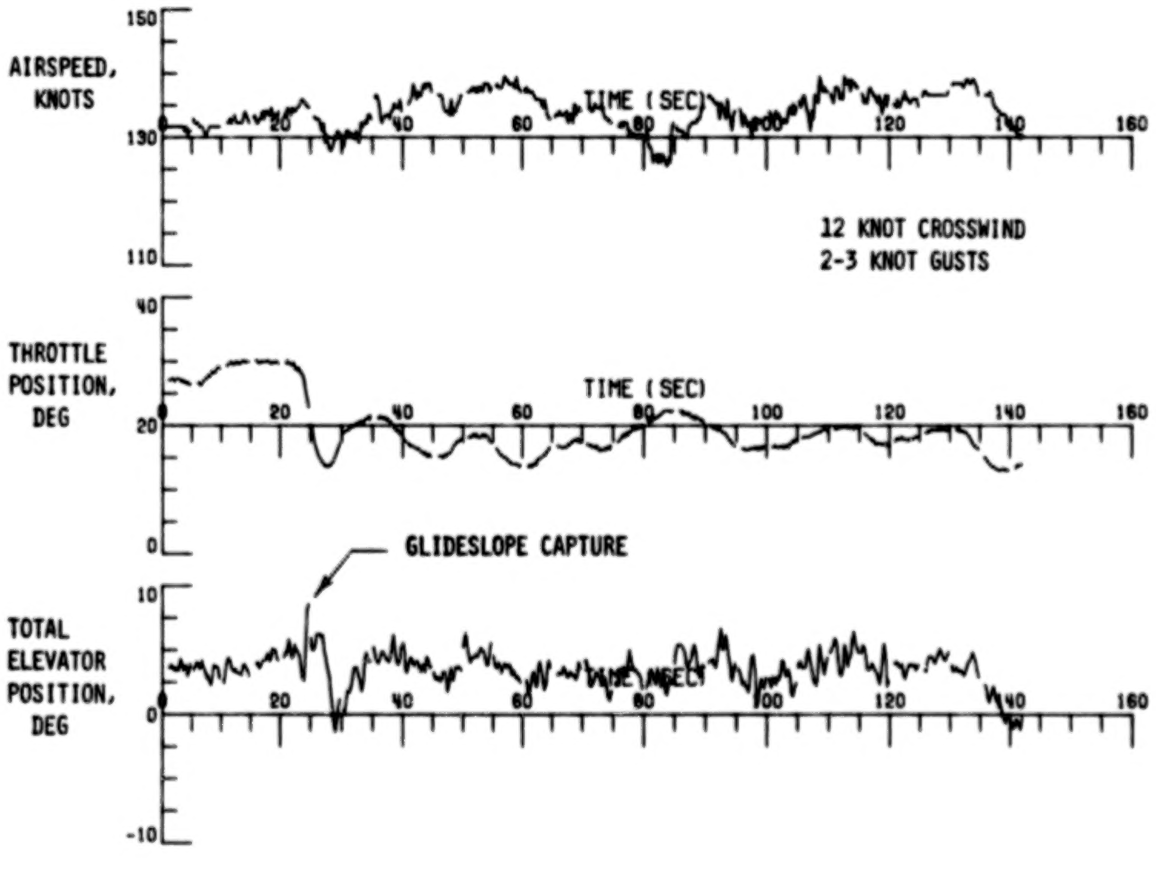

DIALS 4.5-DEGREE GLIDESLOPE CAPTURE AND TRACK - FLT 361, RUN 8

The variables plotted below are the same as those plotted two figures earlier. These plots show the glideslope capture and track and flare for a 4.5-degree glideslope. This flight test encountered 15 knot crosswinds and 2 to 3 knot gusts. The 40- to 80-second time period, which included portions of the localizer capture and track, has been omitted. The glideslope capture begins at 113 seconds and is completed at 126 seconds with no overshoot in position or vertical velocity. The flare maneuver begins at 177 seconds and touchdown occurs at 192 seconds for a 15-second flare duration. The flare maneuver was initiated at 134 feet above the touchdown point. The flare is automatically initiated at higher altitudes for the steeper glideslopes to reduce the sink rate to reasonable levels before the lower altitudes are reached for safety purposes. The pitch attitude at touchdown was 2.5 degrees, and the touchdown sink rate was 2 feet/second.

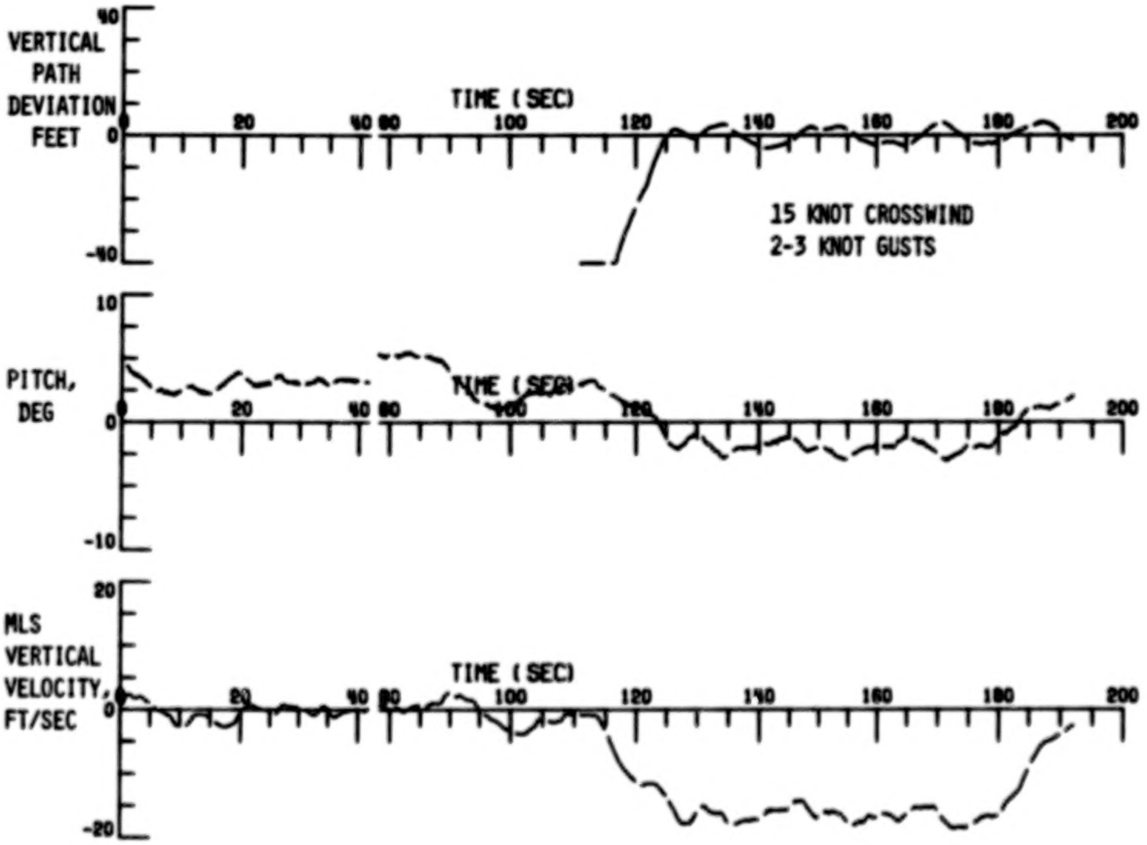

DIALS FLIGHT DATA - FLT 361, RUN 8

The graphs below are plots of additional variables for the same run discussed in the previous figure. The reference airspeed selected for this flight was 126 knots. The control of the baseline autothrottle on the test vehicle can be seen prior to glideslope capture which occurred at 113 seconds. The DIALS again controls the airspeed above the selected reference similar in magnitude to that discussed for the previous Run 7 of Flight 361. However, the variations in airspeed are much smaller than variations of the baseline control. A small positive elevator pulse is seen at 113 seconds along with a throttle reduction to initiate the glideslope capture. However, DIALS "sees" an airspeed error and immediately advances the throttle. The estimated thrust is fed back to the elevator control, and it moves positive to counteract the thrust increase and to push the nose of the aircraft down. At flare, the elevator goes negative to pitch the nose of the aircraft up while very little change is seen in throttle. The thrust must be maintained to add energy to the system to achieve the reduction in sink rate. The airspeed is being reduced to the commanded value without throttle change by the pitch-up maneuver.

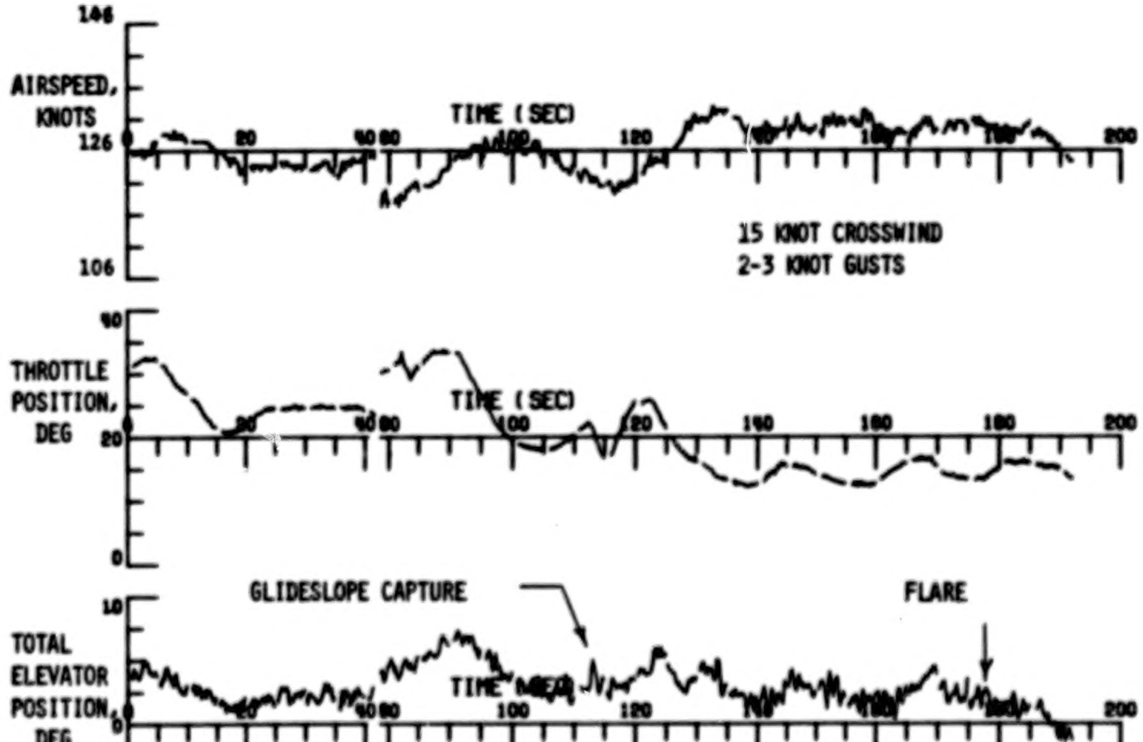

DIALS 5-DEGREE GLIDESLOPE CAPTURE AND TRACK - FLT 364, RUN 7

The graphs below show flight data for the steepest glideslope capture and track flight tested with **DIALS, a 5-degree glideslope. This run was flown in strong wind** conditions. The crosswind component was 20 knots and the headwind component was 10 knots with gust variations of 8 to 10 knots. The variables plotted are the same as those plotted in earlier figures. The glideslope capture occurs at 57 seconds and is completed by 70 seconds. The capture was achieved with essentially no overshoot in the glideslope or desired vertical velocity. The flare maneuver was initiated at 124 **seconds, and a positive pitch attitude of 3 degrees was obtained. However, the touch**down was not completed due to lateral position drift during decrab. The drift was caused by rudder limiting built into the servos for safety purposes during these flight tests. The rudder limit was encountered due to the 20-knot crosswinds.

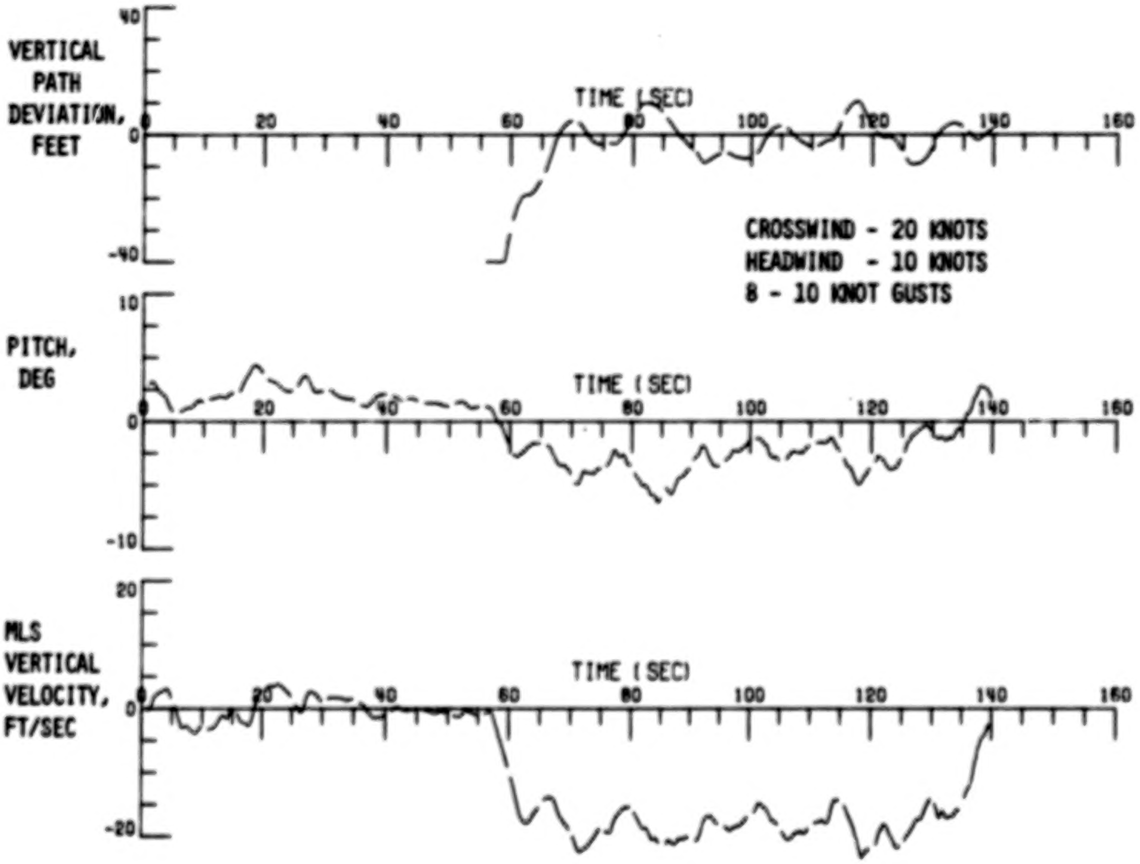

DIALS FLIGHT TEST DATA - FLT 364, RUN 7

The variables plotted below are additional data for the flight just discussed in the prior figure, and the variables are the same as those plotted in earlier figures. The reference airspeed for this flight was selected at 129 knots. Again, airspeed errors are biased to the positive side although the errors are closer to the selected airspeed than in runs discussed earlier. The throttle position plot shows that throttle limiting occurred at 10 degrees during the periods of 82 to 95 seconds, 104 to 106 seconds, and 121 to 125 seconds. The lower throttle limit is set to 10 degrees when the system is not in the flare mode to keep the engine spooled up. In flare, the throttle is allowed to go to idle, zero degrees. In spite of this limiting, the integrated control maintains stability and track of the glideslope. At flare (124 seconds), the throttle increases rather than decreases as was the case for the 3-degree glideslope because more energy must be added to the system to reduce the high sink rate that occurs along the 5-degree glideslope. Even at the point of near touchdown, the throttle is increasing while airspeed was decreasing.

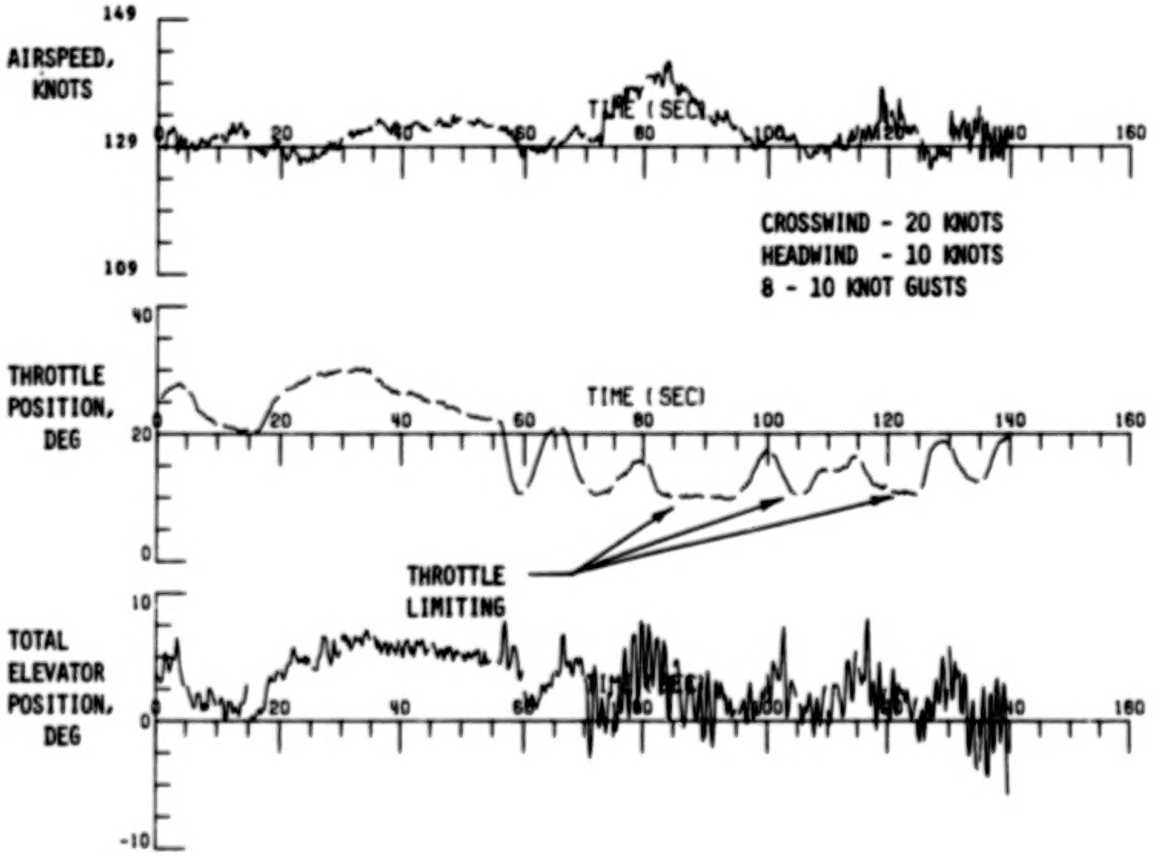

DIALS FLIGHT TEST PERFORMANCE - LOCALIZER AND GLIDESLOPE

Below is a pictorial to illustrate the performance improvement of DIALS compared to conventional ILS systems. The improved performance was attributable both to the use of the MLS (the MLS signals have more accuracy and expanded coverage over ILS) and the advanced control law design. It shows that overshoot performance is better by an order of magnitude. DIALS achieved the improved glideslope overshoot with the additional capability to fly selected and steep glideslopes. The time required from localizer capture initiation to engagement of the track mode was a factor of 3 less than the conventional system time. The time to capture the glideslope (for the 3-degree glideslopes since conventional autolands for steeper glidescopes do not exist) was a factor of 4 less for DIALS. The reduced time to capture the localizer and glideslope provides the capability to fly shorter final approach paths and, in general, more path flexibility. The low overshoot during localizer capture will allow closer spacing of parallel runways. The capability to fly steeper glideslopes reduces the noise level on the ground and also provides a means for trailing aircraft to avoid wake vortices by selecting a glideslope steeper than that of the aircraft in front of it. The use of parallel runways spaced closer and the capability to fly short approach paths should result in greater terminal area capacity.

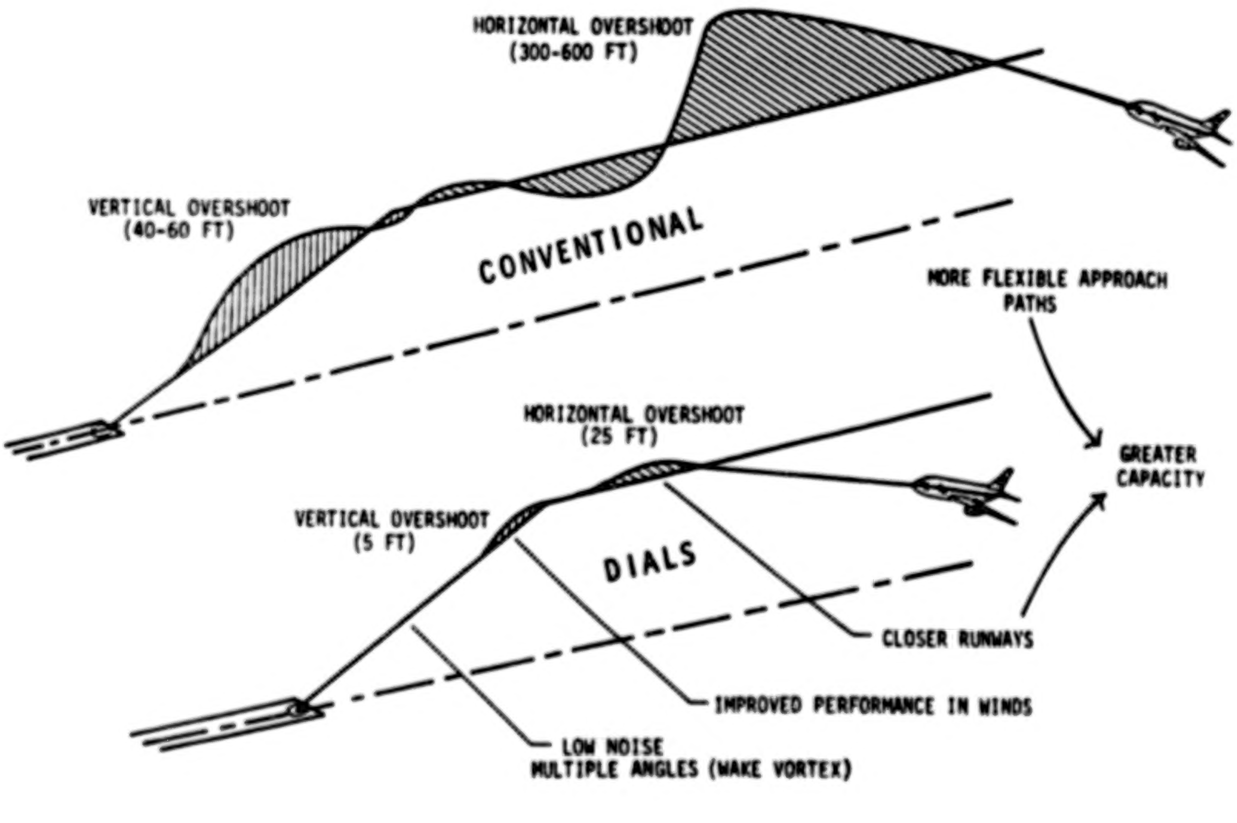
HORIZONTAL OVERSHOOT
(300-600 FT)
VERTICAL OVERSHOOT
(40-60 FT)
CONVENTIONAL
MORE FLEXIBLE APPROACH PATHS
HORIZONTAL OVERSHOOT
(25 FT)
VERTICAL OVERSHOOT
(5 FT)
DIALS
GREATER CAPACITY
CLOSER RUNWAYS
IMPROVED PERFORMANCE IN WINDS
LOW NOISE
MULTIPLE ANGLES (WAKE VORTEX)

DIALS FLIGHT TEST RESULTS

The figure below summarizes the number and types of captures and automatic landings that were achieved during the DIALS flight tests. Three-, four-and-one-half-, and five-degree glideslopes were successfully captured. For 21 captures, the mean overshoot of the glideslopes was 4.6 feet with a standard deviation of 2.3 feet. The numbers in parentheses at the right represent a conventional system. The localizer captures were initiated from ground track angles of 20, 30, 40, and 50 degrees. The statistics of 41 captures resulted in a mean overshoot of 24.2 feet with a standard deviation of 25.7 feet. Typical overshoot distances for a conventional system are shown in parentheses at the right. The decrab maneuver was successfully performed in crosswinds up to 12 knots. Successful decrabs in higher crosswinds were prevented due to rudder limiting in the experimental system of the test vehicle. Ten completely automatic (hands-off) landings were achieved from both the 3- and 4.5-degree glideslopes. In addition, seven additional landings were made in which the pilots had only a slight column input and did not disengage the automatics. The statistics for the ten hands-off landings were a mean touchdown vertical velocity of -2.4 feet/second with a standard deviation of 0.7 feet/second. The numbers to the right are, respectively, the mean and standard deviation for an advanced flare designed by classical methods and previously flight tested on the same aircraft using MLS signals.

- **HAVE SUCCESSFULLY CAPTURED AND TRACKED 3, 4.5, AND 5° GLIDESLOPES**

$$\left.\begin{array}{r}\text{MEAN OVERSHOOT} = 4.6\ \text{FT}\\ \sigma = 2.3\ \text{FT}\end{array}\right\}\ \text{21 CAPTURES}\qquad (40\text{-}60)$$

- **HAVE SUCCESSFULLY CAPTURED RUNWAY CENTERLINE (LOCALIZED) AT 20°, 30°, 40° AND 50° INTERCEPT ANGLES**

$$\left.\begin{array}{r}\text{MEAN OVERSHOOT} = 24.2\ \text{FT}\\ \sigma = 25.7\ \text{FT}\end{array}\right\}\ \text{41 CAPTURES}\qquad (300\text{-}1000)$$

- **HAVE PERFORMED SUCCESSFULLY DECRAB MANEUVERS IN CROSSWINDS UP TO 12 KNOTS**

- **PERFORMED TEN COMPLETELY AUTOMATIC (HANDS-OFF) LANDINGS FROM BOTH 3° AND 4.5° GLIDESLOPES, PLUS SEVEN ADDITIONAL WITH SLIGHT COLUMN INPUT**

$$\left.\begin{array}{r}\text{MEAN}\ \dot{h}_{td} = -2.4\ \text{FT/SEC}\\ \sigma = .7\ \text{FT/SEC}\end{array}\right\}\ \begin{array}{c}(-2.34)\\ \text{10 LANDINGS}\\ (1.41)\end{array}$$

DIALS PLANS

A goal of the advanced control law research has been to develop methods and techniques whereby modern control theory can be applied readily to practical applications. While excellent experimental results were obtained from the DIALS flight test, the full-state design with its accompanying Kalman filter can be rather cumbersome resulting in large software memory requirements. Also certain practical considerations, such as the dynamics of existing sensor filters and stability augmentation systems, are difficult to incorporate in full-state designs. These practical considerations tend to make full-state designs less practical for direct commercial applications. Thus, the plans are to use the DIALS results as a bench mark and to continue development of modern control theory methods for more direct solutions to practical problems. With the recent development of a digital computer algorithm that efficiently and reliably solves the output feedback problem, the design of control systems with modern control theory becomes more practical. Successful 3-D guidance and control designs were recently achieved using this algorithm. Thus, the design and the development of an autoland system using output feedback techniques have begun. For this design, a third-order complementary filter along with MLS processing is being used to provide estimates of velocity and position rather than a Kalman filter. The existing SAS (yaw damper) on the test vehicle will be used rather than providing this damping in the design as was done with DIALS. The output feedback design allows inclusion of SAS dynamics and filter dynamics in the model without having to feed back these states as is necessary in full-state design. This system will be designed as a Type 1 system whereas DIALS was designed as a Type 0 system with integrators added to the various modes during development to achieve Type 1 properties. The new design will use the integrated control surfaces like DIALS as listed in the figure below. In addition, more attention will be given to methods to account for computational delays than was done in DIALS. Full nonlinear simulation development is planned along with flight tests in late 1984 or early 1985.

☐ NEW MORE PRACTICAL DESIGN USING LSF TECHNIQUES

- Direct Digital Design
- Use Third-Order Complementary Filter (Developed for ICAO MLS Processing) Rather Than Steady-State Kalman Filter
- Use Existing SAS (Yaw Damper)
- Design as Type 1 System (Path Integrators)
- Integrated/Coordinated Controls For Elevator, Throttle And Stabilizer For Long. Axis And Aileron And Rudder For Lateral Axis
- Design To Account For Transport Delays (Computational)

☐ DEVELOP BY MEANS OF FULL NONLINEAR SIMULATION INCLUDING SENSORS NOISES AND WINDS.

☐ PREPARE S/W REQUIREMENTS FOR FLIGHT TESTS IN CY 84.

BIBLIOGRAPHY

(1) Halyo, N., "Development of an Optimal Automatic Control Law and Filter Algorithm for Steep Glideslope Capture and Glideslope Tracking," NASA CR-2720, Aug. 1976.

(2) Halyo, N., "Development of a Digital Automatic Control Law for Steep Glideslope Capture and Flare," NASA CR-2834, June 1977.

(3) Halyo, N., "Development of a Digital Guidance and Control Law for Steep Approach Automatic Landings Using Modern Control Theory Techniques," NASA CR-3074, Feb. 1979.

(4) Halyo, N., "Terminal Area Automatic Navigation, Guidance and Control Research Using the Microwave Landing System (MLS): Part 5 - Design and Developmemt of a Digital Integrated Automatic Landing System (DIALS) for Steep Final Approach Using Modern Control Techniques," NASA CR-3681, April 1983.

(5) FAA Dept. of Transportation, "Automatic Landing Systems," FAA Advisory Circular 20-57a, 12 Jan. 1971, p. 2.

N84
20590

UNCLAS

N84 20590 D23

APPLICATION OF ADVANCED CONTROL TECHNIQUES TO AIRCRAFT PROPULSION SYSTEMS

Bruce Lehtinen
NASA Lewis Research Center
Cleveland, Ohio

First Annual NASA Aircraft Controls Workshop
NASA Langley Research Center
Hampton, Virginia
October 24-26, 1983

CONTROLS FOR ADVANCED TURBINE ENGINES

The trend in advanced aircraft turbine engine design is toward more sophisticated cycles and mechanical complexity. This is done primarily to achieve improved thrust-to-weight ratios and improved specific fuel consumption. Control system complexity has also increased due to the increase in the number of engine variables which must be scheduled or controlled. Hydromechanical controls are rapidly being replaced by full-authority digital electronic controls in order to handle the added computational burden. The digital computer, however, does allow more sophisticated control algorithms to be used. In this paper, two Lewis Research Center sponsored programs will be described which involve the application of advanced control techniques to the design of engine control algorithms. Multivariable control theory has been used in the F100 MVCS (multivariable control synthesis) program to design controls which coordinate the control inputs for improved engine performance, and it presents a systematic method for handling a complex control design task (fig. 1). Methods of analytical redundancy are aimed at increasing the control system's reliability. The F100 DIA (detection, isolation, and accommodation) program will be described, which investigates the uses of software to replace or augment hardware redundancy for certain critical engine sensors.

GOALS OF -

IMPROVED PERFORMANCE AND EFFICIENCY

LEAD TO -

INCREASED COMPLEXITY AND DECREASED RELIABILITY

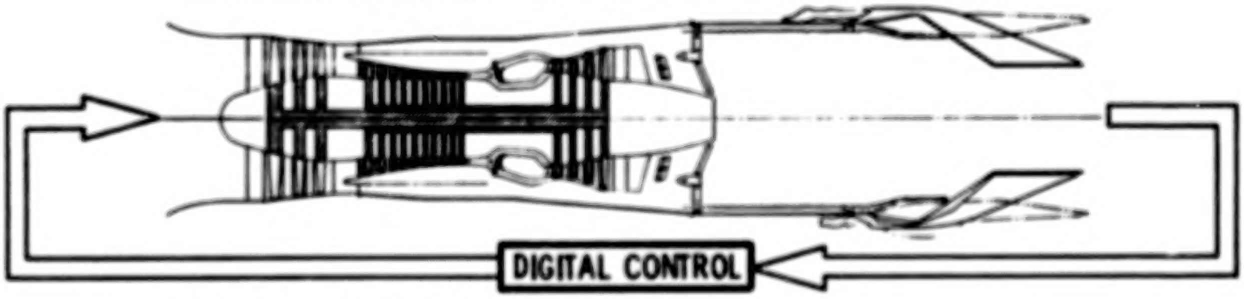

ADVANCED CONTROL TECHNIQUES

- MULTIVARIABLE CONTROL THEORY
  - COORDINATE CONTROL VARIABLES FOR IMPROVED PERFORMANCE
  - SYSTEMATIC APPROACH TO COMPLEXITY
- ANALYTICAL REDUNDANCY
  - SOFTWARE REPLACES HARDWARE REDUNDANCY
  - IMPROVE RELIABILITY WITH RESPECT TO SENSOR FAILURES

Figure 1

The interrelationship of the two programs is depicted in figure 2. Activity in applying multivariable control methods to engine controls began in the mid 1970's (refs. 1 and 2). Motivated by these early results, a comprehensive program (F100 MVCS) was begun to demonstrate the benefits of using control theory to design a full envelope control for an F100 engine and to verify the design with both simulated and actual engine testing. Figure 2 shows the NASA LeRC facilities which were used in performing the evaluations of the MVC logic. The facilities consist of 1) a research-type control computer on which the control algorithms are programmed, 2) a real-time (hybrid) simulation of the F100 engine, and 3) an altitude test cell in which a full-size engine can be run. The F100 DIA program, which is now beginning the evaluation phase, built upon early theoretical work (ref. 3) in analytical redundancy as applied to flight control systems. The F100 MVCS control forms the basis for the control logic used in the DIA program, with sensor failure DIA logic being incorporated with it to produce the overall control. As in the MVCS program, the DIA logic will utilize the LeRC facilities for overall performance evaluation.

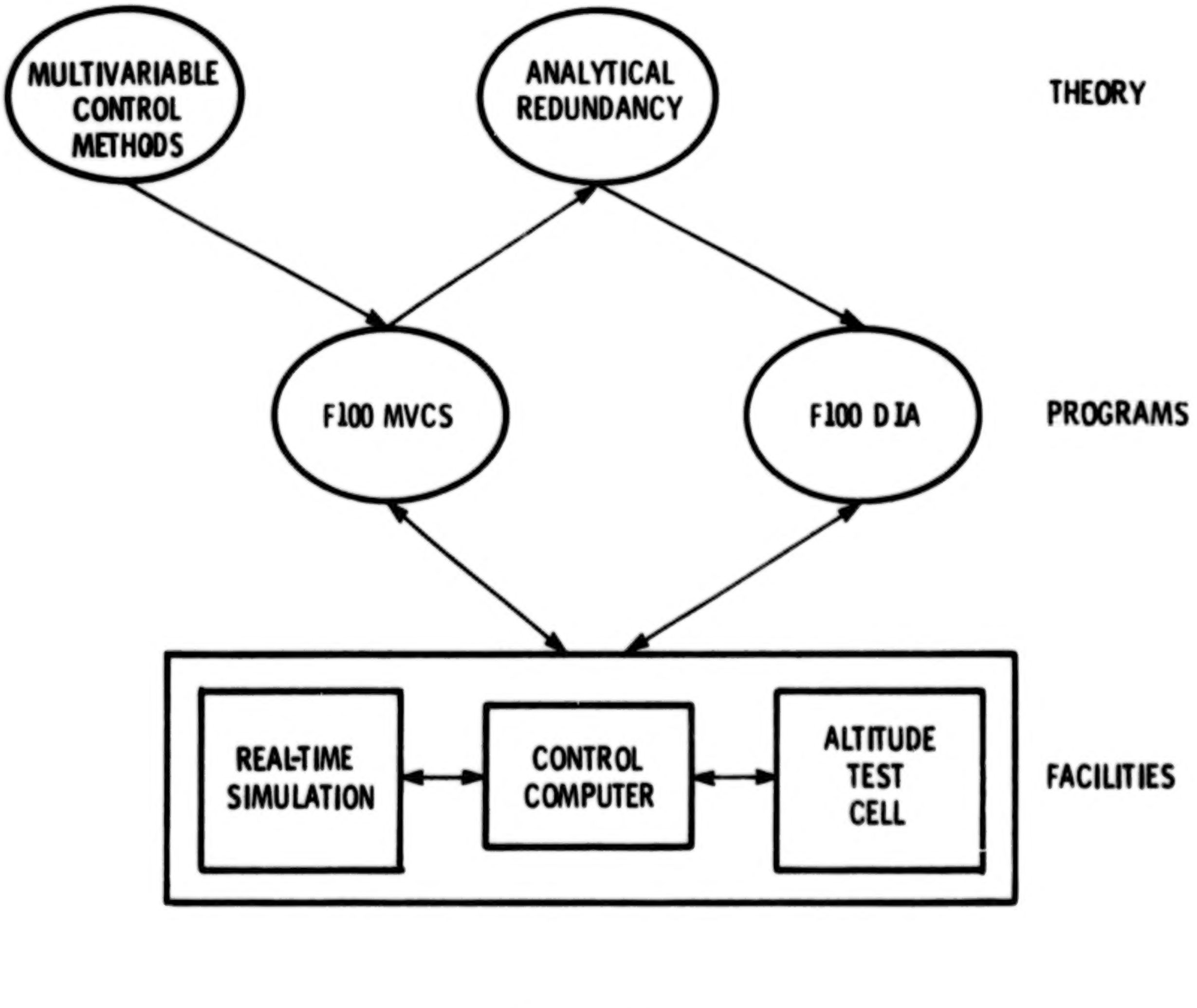
MULTIVARIABLE CONTROL METHODS
ANALYTICAL REDUNDANCY
THEORY
F100 MVCS
F100 DIA
PROGRAMS
REAL-TIME SIMULATION
CONTROL COMPUTER
ALTITUDE TEST CELL
FACILITIES

Figure 2

F100 MVCS PROGRAM PARTICIPANTS

Figure 3 shows the organizations involved in the F100 MVCS program and outlines the activities involved in the various phases of the program. The contracted portions, funded and monitored jointly by NASA LeRC and the Air Force Wright Aeronautical Laboratories, were carried out by Pratt and Whitney Aircraft (P&WA) and Systems Control, Inc. (SCI). The overall program objective was to demonstrate the benefits of using linear quadratic regulator (LQR) synthesis procedures in designing a practical multivariable control system that could operate a turbofan engine through its operating envelope. P&WA provided a digital simulation of the F100, a set of linear design models, and performance criteria on which the design was based. SCI conducted the overall multivariable control design, which was then evaluated by P&WA on the digital engine simulation. NASA LeRC programmed the control logic on a research control computer and evaluated it using its real-time hybrid F100 engine simulation. Upon successful evaluation with the simulation, NASA conducted full-scale altitude tests to verify proper operation throughout the engine's flight envelope. References 4 to 7 document in detail the complete program

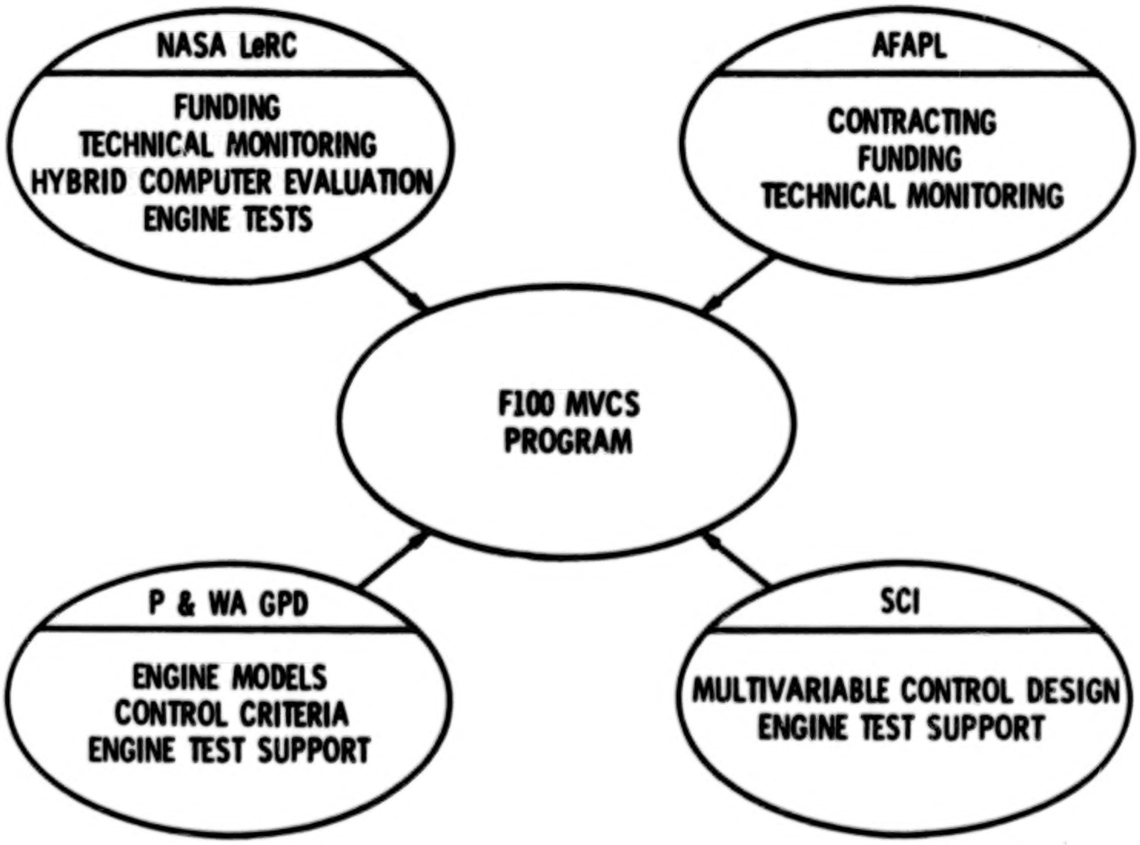
NASA LeRC
FUNDING
TECHNICAL MONITORING
HYBRID COMPUTER EVALUATION
ENGINE TESTS
AFAPL
CONTRACTING
FUNDING
TECHNICAL MONITORING
F100 MVCS
PROGRAM
P & WA GPD
ENGINE MODELS
CONTROL CRITERIA
ENGINE TEST SUPPORT
SCI
MULTIVARIABLE CONTROL DESIGN
ENGINE TEST SUPPORT

Figure 3

STRUCTURE OF F100 MULTIVARIABLE CONTROL

The LQR-based control logic was designed to meet the following criteria. Primarily, the logic must protect the engine against surge and maintain speeds, pressures, and temperatures below maximum limits. Airframe-engine inlet compatibility requires adhering to minimum burner pressure limits and maximum and minimum airflow limits at certain flight conditions. The control must keep thrust and specific fuel consumption within tolerance for specified engine degradations. The engine must accelerate and decelerate rapidly and repeatably and must remain stable in the presence of external disturbances. The basic structure of the F100 multivariable control logic is shown in figure 4. The five manipulated engine inputs are fuel flow, exhaust nozzle area, inlet guide vanes, compressor variable geometry, and compressor exit bleed airflow. Primary sensed engine outputs are fan speed, compressor speed, main burner pressure, afterburner pressure, and fan turbine inlet temperature. Basic components of the control are: 1) reference point schedules and transition control logic, which produce desired state and output and approximate control vectors, 2) gain schedules, which produce feedback matrix elements as functions of flight conditions, 3) proportional and integral control loops which produce acceptable steady-state and transient engine behavior without operating limit exceedance, and 4) engine protect logic that places absolute limits on engine inputs to assure safe operation in the test cell despite sensor or logic failures.

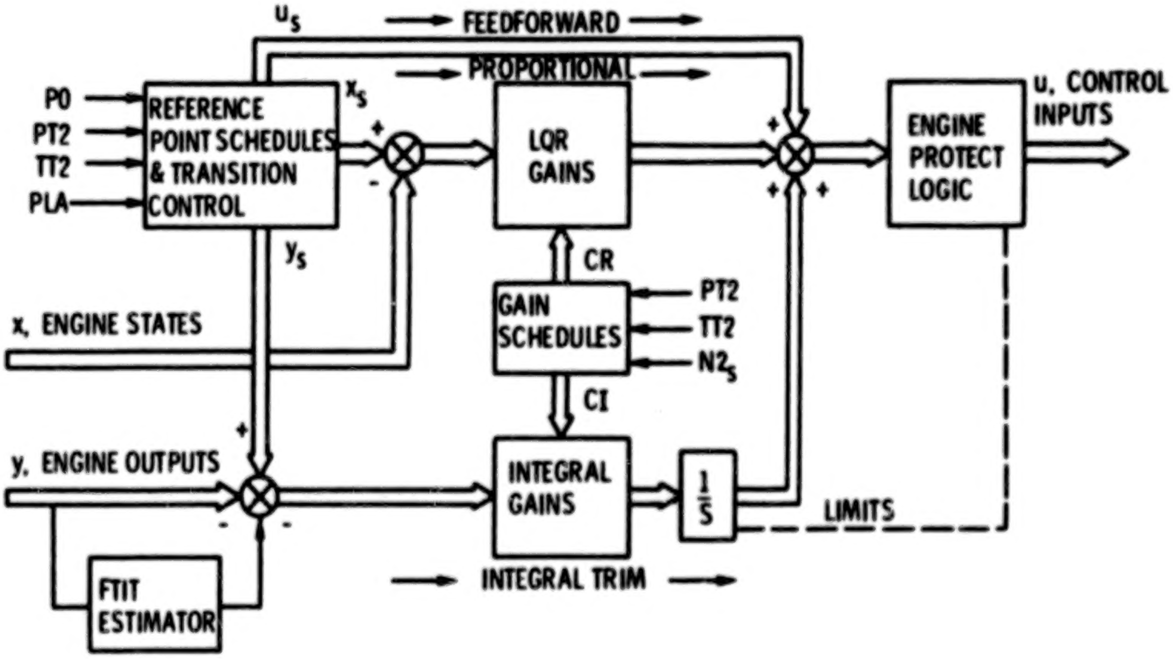
u_s
FEEDFORWARD
PROPORTIONAL
x_s
PO
PT2
TT2
PLA
REFERENCE POINT SCHEDULES & TRANSITION CONTROL
+
-
LQR GAINS
+
+
+
ENGINE PROTECT LOGIC
u, CONTROL INPUTS
y_s
CR
GAIN SCHEDULES
PT2
TT2
$N2_s$
CI
x, ENGINE STATES
y, ENGINE OUTPUTS
+
-
-
INTEGRAL GAINS
$\frac{1}{S}$
LIMITS
FTIT ESTIMATOR
INTEGRAL TRIM

Figure 4

CONTROL SYSTEM SCHEMATIC FOR ALTITUDE TESTS

The MVC logic shown in figure 4 was programmed in fixed-point ASSEMBLY language on a 16-bit minicomputer and debugged while controlling the LeRC real-time hybrid engine simulation. The simulation was a nonlinear, component-level representation of the engine and included lumped-volume and rotor dynamics. It accurately represents the engine's operation across the entire flight envelope. After completion of the hybrid evaluation, the same logic was used to conduct the altitude test evaluation, as shown in figure 5. Bill of material (BOM) hydromechanical engine actuators were modified to allow input of electrical commands from the minicomputer, and suitable research sensors were provided for feedback signals. Portions of the BOM control system were retained to serve as backup control and for engine start-up. A complete steady-state and transient evaluation was performed over the entire flight envelope. The LQR-based control logic performed well at all conditions. In addition, the real-time simulation was used periodically during the altitude tests for rapidly solving any logic problems encountered. The modular interface system between the computer and simulation or engine greatly facilitated this mode of operation.

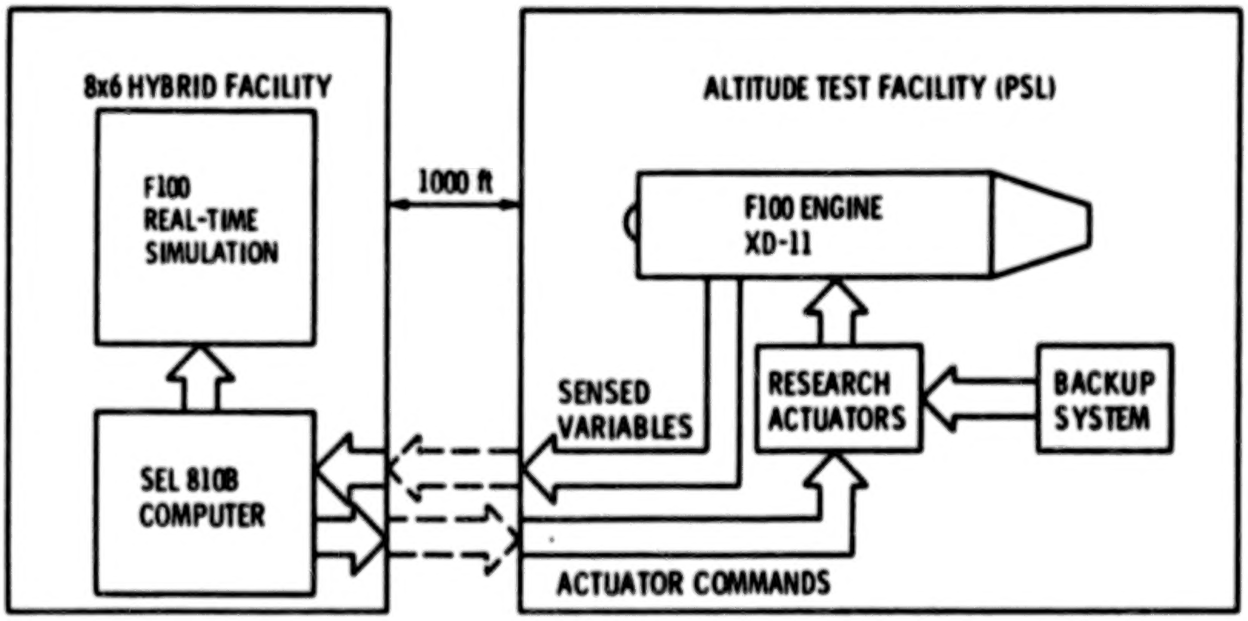
8x6 HYBRID FACILITY
F100
REAL-TIME
SIMULATION
SEL 810B
COMPUTER
1000 ft
ALTITUDE TEST FACILITY (PSL)
F100 ENGINE
XD-11
SENSED
VARIABLES
RESEARCH
ACTUATORS
BACKUP
SYSTEM
ACTUATOR COMMANDS

Figure 5

TYPICAL F100 MULTIVARIABLE CONTROL PERFORMANCE IN LARGE PLA TRANSIENT

Figure 6 shows an F100 engine transient response test performed during the altitude tests at a simulated altitude of 10,000 feet and Mach number of 0.6. The input is a power lever angle step (snap) from 50° to 83° (maximum, non-afterburning). This transient caused a number of MVC logic functions to be exercised: transfer from fan speed integral control to fan turbine inlet temperature (FTIT) limit control, regulator and integral control gains being varied as functions of compressor speed, use of the FTIT estimator output, and control of the exhaust nozzle area to control fan discharge ΔP/P, a fan air flow parameter. Initially, the control maintains the desired engine operating point by keeping fan speed and fan discharge ΔP/P on desired schedules. During the transient, engine outputs generally follow their desired trajectories. Fuel flow is modulated to keep FTIT at or near its allowed limit during the initial portion of the transient. At steady state, the logic has closed down the nozzle area and trimmed fuel flow so that both fan speed and fan discharge ΔP/P are on schedule. This transient was one of over ninety performed using the multivariable control, with inputs being a wide variety of PLA trajectories, afterburner ignitions, and flight condition excursions. The MVCS program demonstrated that digital engine controls can be successfully designed using techniques based on LQR theory. As demands for engine performance lead to engine designs which have larger numbers of control variables, LQR methods will be increasingly useful for algorithm design.

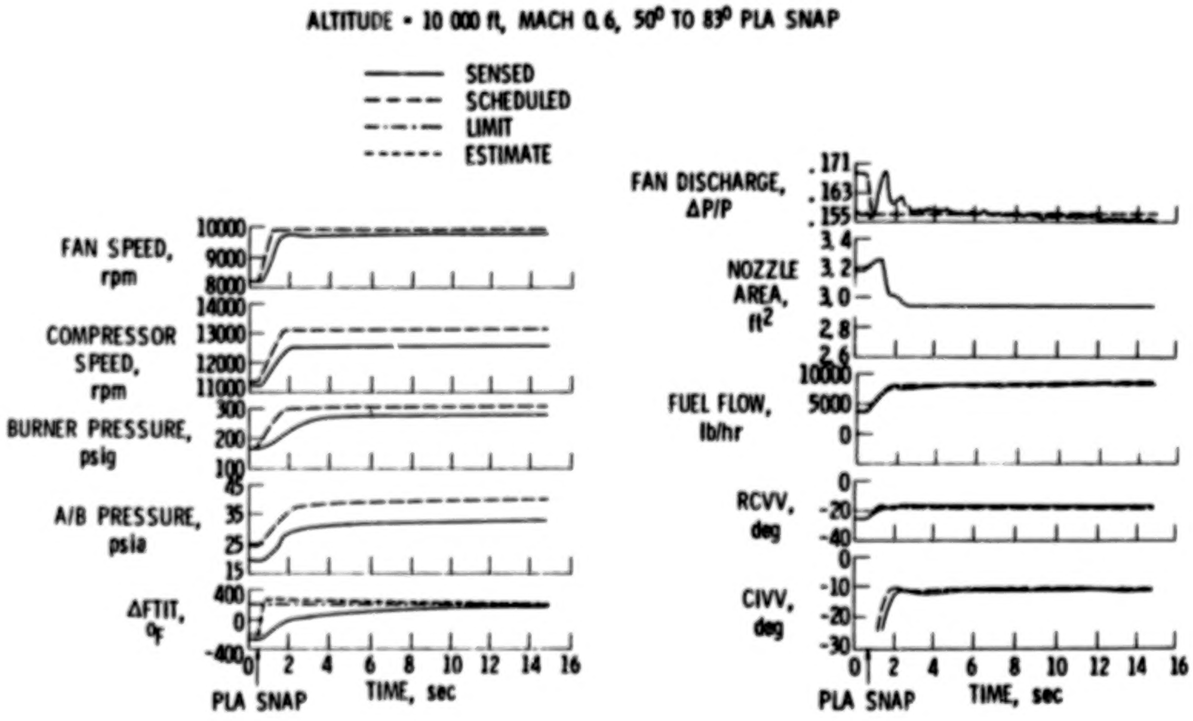

Figure 6

ORIGINAL PAGE IS
OF POOR QUALITY

ORIGINAL PAGE IS
OF POOR QUALITY

AESOP - INTERACTIVE COMPUTER-AIDED CONTROL SYSTEM DESIGN

A tool that was developed at Lewis and used during the F100 MVCS program to verify and update the contractor's multivariable control designs was the AESOP computer program (Algorithms for EStimator and OPtimal regulator design). An interactive program which solves the LQR and Kalman filter design problems for time invariant systems, it is an outgrowth of an earlier batch program LSOCE (ref. 8). As shown in figure 7, the user typically accesses AESOP by using a light pen to select desired AESOP functions from a menu displayed on a terminal screen. Available functions fall into the categories shown: open-loop system analysis (controllability, observability, eigenvalues, etc.), LQR and Kalman filter design, system response to noise inputs (both open- and closed-loop system covariance matrices), system transient responses (open and closed loop, for step and initial condition inputs), and transfer functions and frequency responses (system poles, zeroes, and generation of open- and closed-loop Bode plots). Graphic output can be produced either at the terminal screen or plotted off-line. AESOP also aids the user by checking the validity of requested function sequences. A user's manual has been prepared (ref. 9).

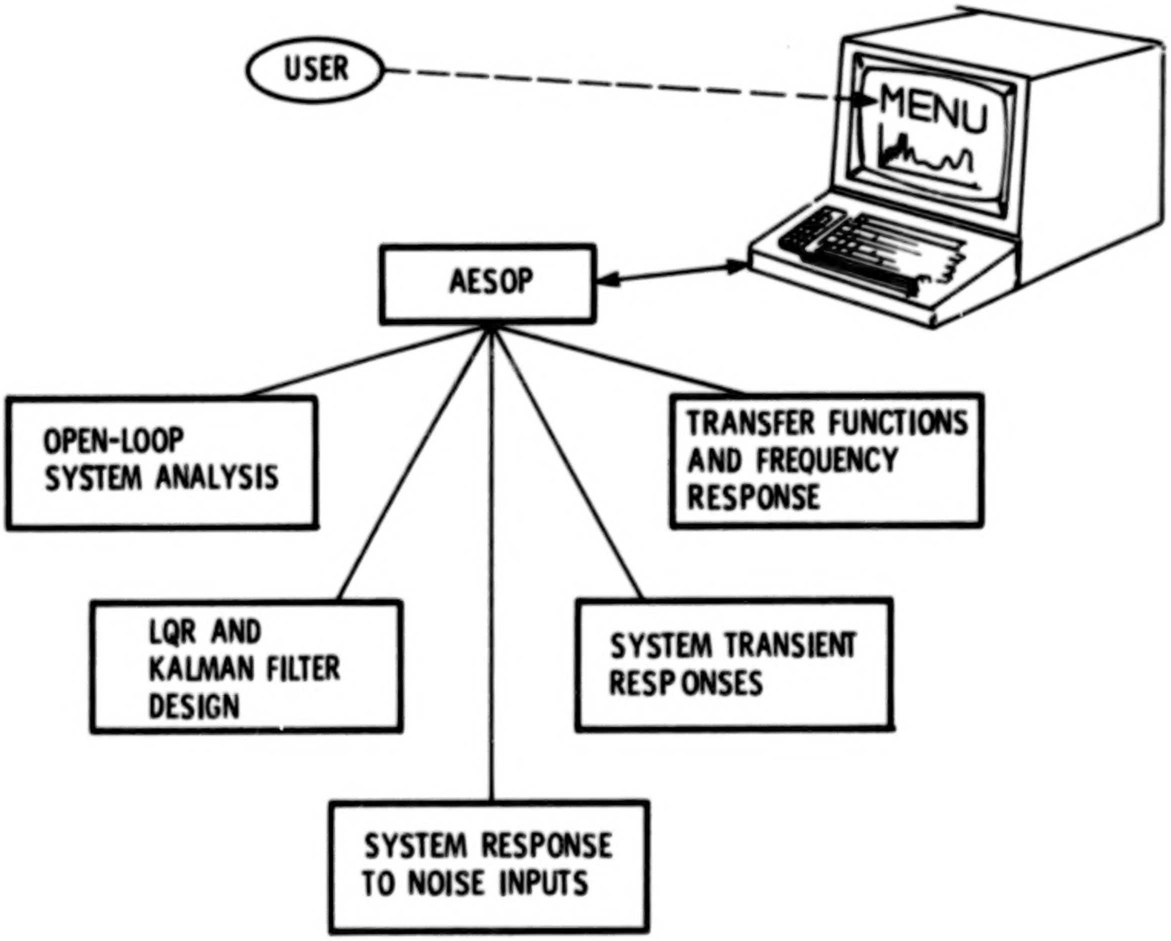
USER
MENU
AESOP
OPEN-LOOP SYSTEM ANALYSIS
TRANSFER FUNCTIONS AND FREQUENCY RESPONSE
LQR AND KALMAN FILTER DESIGN
SYSTEM TRANSIENT RESPONSES
SYSTEM RESPONSE TO NOISE INPUTS

Figure 7

SENSOR FAILURE DETECTION AND ACCOMMODATION

The relative immaturity of digital electronics compared to hydromechanical controls has raised concerns with respect to control system reliability. Past studies have shown that the least reliable parts of a digital electronic engine control system are the sensors. For this reason, as a follow-on to the F100 MVCS program, the F100 DIA program (sensor failure detection, isolation, and accommodation) was initiated to develop algorithms for enhancing digital control system reliability by using analytical redundancy. The general concept of analytical redundancy in the context of an engine control system is illustrated in figure 8. Assume that the reliability of turbine inlet temperature sensor T_4 is insufficient to meet mission-reliability goals. The normal procedure (hardware redundancy) would be to add two additional temperature sensors and voting logic to determine if and when a sensor has failed. The analytical redundancy approach is to incorporate a model of the engine which relates T_4 with other sensed engine variables (for example, P_4 and N). The model is then used to generate an estimate of T_4 which can be used with a statistical testing procedure to detect and isolate a T_4 sensor failure. Once a failure has been detected, the estimate can be used to replace the failed sensor and allow acceptable but possibly degraded control performance. In the F100 DIA program, contractors P&WA and Systems Control Technology (SCT) have: 1) quantified sensor failure types and frequency of occurrence, 2) determined the relative criticality of various failures, and 3) developed a sensor failure DIA algorithm for the F100 engine (ref. 10).

PRINCIPLE- REPLACE HARDWARE REDUNDANCY WITH ANALYTICAL REDUNDANCY

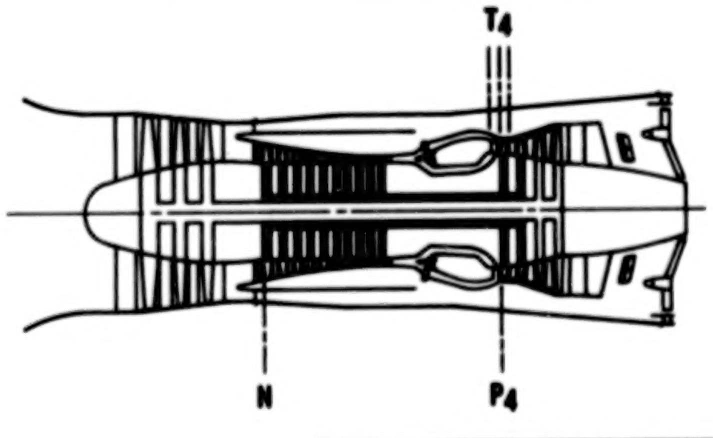

HARDWARE REDUNDANCY

- 3 SENSORS ⟶ T_4
- MAJORITY VOTE DETECTS FAILURE

ANALYTICAL REDUNDANCY

- 1 SENSOR ⟶ T_4
- REFERENCE MODEL DETECTS FAILURE
- REDUNDANT INFORMATION (P_4, N) GENERATES $T_{4, EST}$

Figure 8

SENSOR FAILURE DETECTION, ISOLATION, AND ACCOMMODATION CONCEPT

The structure of the F100 DIA logic and the manner in which it interfaces with the MVC logic are shown in figure 9. The two portions of the DIA logic are an on-line state estimator and detection and isolation logic. The estimator incorporates an accurate, full envelope model of the engine which is updated in real time. Estimator residuals are continuously monitored by the detection logic, and if a failure is detected, isolation and accommodation algorithms are initiated. During normal unfailed conditions, an estimate of state x is fed to the LQR gain portion of the multivariable control and the integrally controlled engine output variables y are sent directly to the integral control portion. This insures that any possible bias in the estimate of y will not cause a shift in the desired engine operating point. Once a failure has been detected and isolated, the on-line estimator is reconfigured to exclude the bad sensor, and an estimate of the failed sensor signal is sent to the integral control. Due to the modular design of the MVC logic, the only change required after addition of the DIA logic was to eliminate the FTIT estimator, a task now taken over by the DIA logic.

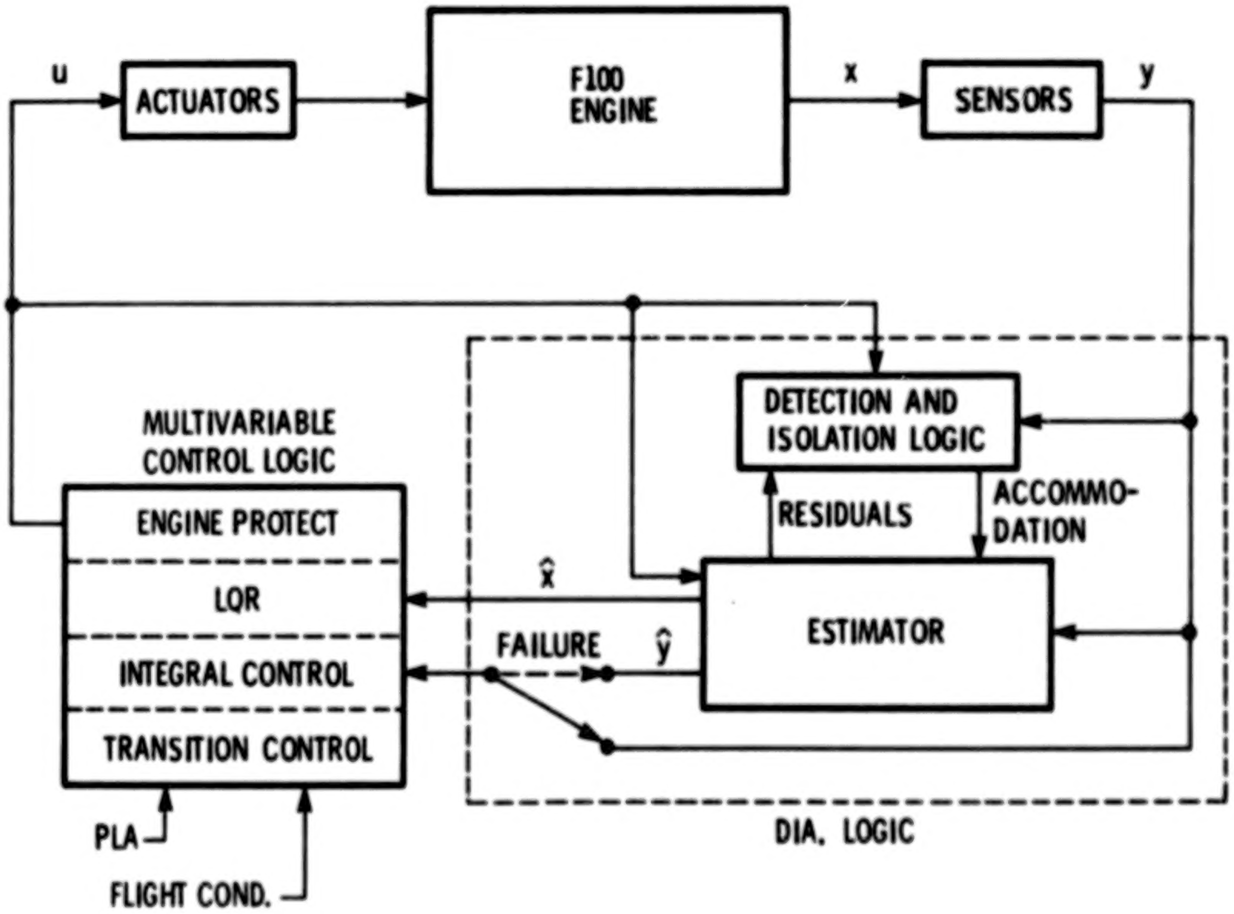

u
ACTUATORS
F100 ENGINE
x
SENSORS
y
MULTIVARIABLE CONTROL LOGIC
ENGINE PROTECT
LQR
INTEGRAL CONTROL
TRANSITION CONTROL
PLA
FLIGHT COND.
DETECTION AND ISOLATION LOGIC
RESIDUALS
ACCOMMODATION
$\hat{x}$
FAILURE
$\hat{y}$
ESTIMATOR
DIA. LOGIC

Figure 9

ORIGINAL PAGE IS
OF POOR QUALITY

DIA LOGIC SEQUENCE

The specific algorithm used by the F100 DIA logic begins with the generation of residuals for each of five engine measurements using an estimator which is designed to work with all sensors present (fig. 10). Detection and isolation algorithms are different, depending on whether a hard (out-of-range), sudden within-range shift) or soft (slow drift, slowly increasing noise intensity) failure is being detected. A hard failure is detected (and isolated) by simply comparing the sensor residual against a threshold. A soft failure is detected by computing the weighted-sum-squared of all residuals for N past observations and comparing that value against a threshold. To isolate a soft failure, a generalized likelihood ratio hypothesis test is performed, using residuals computed by a bank of five "off-line" estimators, to compute which sensor is most likely to have failed. Each of the five off-line estimates has one sensor input left out. The accommodation procedure consists of reconfiguring the on-line estimator by changing the gain matrix and omitting the bad sensor signal from its input plus resetting of the estimator's initial conditions. The F100 DIA logic has been successfully evaluated on a detailed non-real-time engine simulation while coupled to the MVC logic. The logic has been coded for a Lewis-developed microprocessor-based computer control facility and will subsequently be evaluated while controlling a real-time hybrid simulation.

(1) GENERATE RESIDUALS WITH ON-LINE ESTIMATOR

(2) DETECT FAILURE

- HARD : RESIDUAL > THRESHOLD
- SOFT : WEIGHTED SUM-SQUARED RESIDUALS (WSSR) > THRESHOLD

(3) ISOLATE FAILURE WITH GENERALIZED LIKELIHOOD RATIO TESTS

- HARD : ON-LINE RESIDUAL TEST
- SOFT : OFF-LINE USING BANK (5) OF ESTIMATORS

(4) ACCOMMODATE FAILURE

- RECONFIGURE ON-LINE ESTIMATOR TO EXCLUDE BAD SENSOR
- REINITIALIZE ESTIMATOR

Figure 10

SENSOR FAILURE DIA LOGIC IMPLEMENTATION

The Lewis computer control facility being used in conjunction with the F100 DIA program is based on an Intel 8086 16-bit microprocessor and replaces the minicomputer facility used during the F100 MVCS program. It includes both an interface unit which allows information interchange between a simulation or an engine and a monitoring unit which displays and records information during a test. Figure 11 shows the basic configuration of the facility for implementing the DIA logic. Rapid control update requirements led to the use of two microprocessors, one for the control logic and one for the DIA logic, which communicate through interrupts and transmit data over a multibus. Specialized D/A and A/D allow communication with the engine, also through the bus. The timing diagram in figure 11 shows the subtasks performed by each processor and the inter-processor interrupt timing. The MVC processor processes the sensed inputs and sends an interrupt to begin the DIA processors's detection algorithm. Both processors then operate in parallel until the Kalman filter (estimator) has updated the state estimates, at which time an interrupt from the DIA processor allows the estimates to be used by the MVC processor in the multivariable control calculations. The DIA processor then searches for a possible soft failure, and only if detected, begins the isolation calculation, requiring the updating of five additional Kalman filters and the use of the GLR algorithm. Languages used in programming the logic were both ASSEMBLY language and FORTRAN with special machine language procedures developed for certain time-critical tasks.

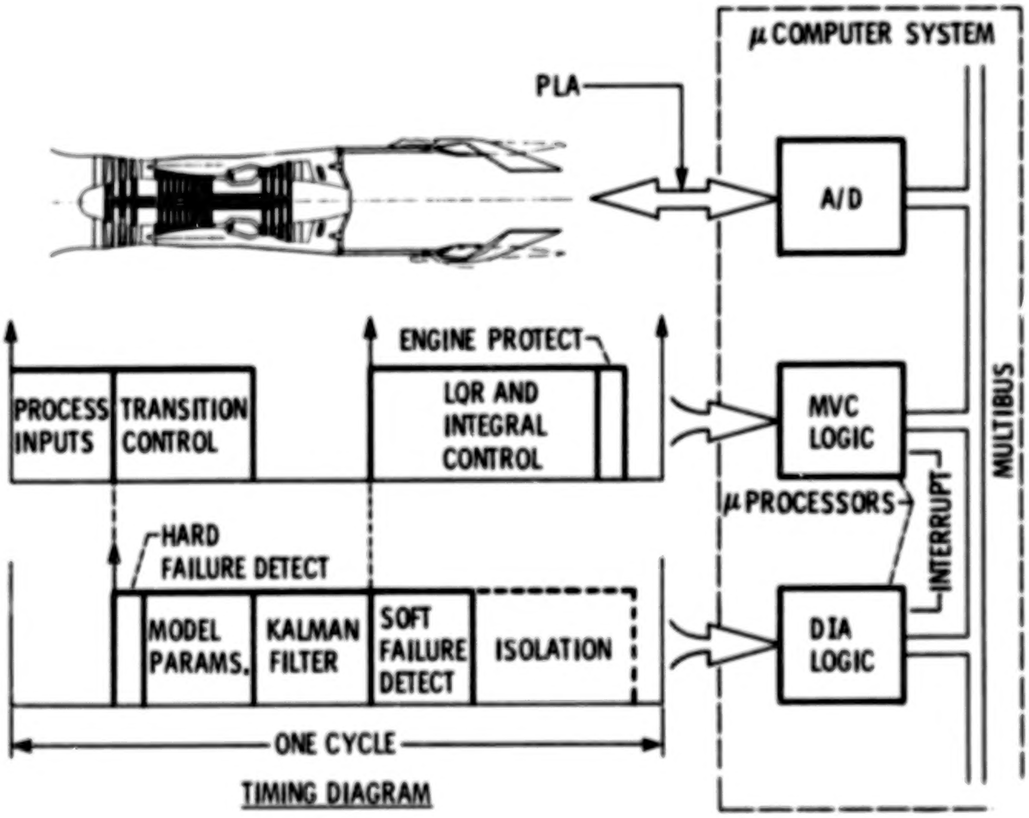
μ COMPUTER SYSTEM
PLA
A/D
ENGINE PROTECT
PROCESS INPUTS
TRANSITION CONTROL
LQR AND INTEGRAL CONTROL
MVC LOGIC
μ PROCESSORS
INTERRUPT
MULTIBUS
HARD FAILURE DETECT
MODEL PARAMS.
KALMAN FILTER
SOFT FAILURE DETECT
ISOLATION
DIA LOGIC
ONE CYCLE
TIMING DIAGRAM

Figure 11

FUTURE EFFORTS IN ADVANCED PROPULSION CONTROL

Advanced control related activities which are or will soon be underway at LeRC are outlined in figure 12. The F100 DIA logic will be evaluated on a real-time engine simulation throughout the flight envelope and will then be tested in the LeRC altitude facility. An operating-point control design will be performed for the F100 engine using an alternate frequency-domain method (the multivariable Nyquist array) and compared to the existing MVC design. Also, the use of modern robust control methodology to design engine controls will be investigated with an eye toward decreased sensitivity to modeling errors and simplified control algorithms. Contracts have just been awarded to investigate how best to incorporate robustness into the initial design of sensor failure DIA algorithms. Finally, in-house computer-aided control design capability (such as the AESOP program) will be enhanced so as to be better able to interactively design and analyze multivariable control and failure detection algorithms for future propulsion systems.

FUTURE EFFORTS IN ADVANCED PROPULSION CONTROL

- EXPERIMENTAL EVALUATION OF DIA LOGIC
- MNA - LQR DESIGN METHOD COMPARISON
- ROBUST CONTROL DESIGN APPLICATION
- ROBUST SENSOR DIA LOGIC
- ENHANCED INTERACTIVE CAD FOR PROPULSION CONTROL SYSTEMS

Figure 12

REFERENCES

1. Michael, G.J.; and Farrar, F.A.: Development of Optimal Control Modes for Advanced Technology Propulsion Systems. United Aircraft Corp., East Hartford, CT, UARL-N911620-2, May 1974.

2. Weinberg, M.S.: Multivariable Control for the F100 Engine Operating at Sea Level Static. Aeronautical Systems Division, Wright-Patterson Air Force Base, OH, ASD-TR-75-28, Nov. 1975.

3. Montgomery, R.C.; and Price, D.B.: Failure Accommodation in Digital Flight Control Systems Accounting for Nonlinear Aircraft Dynamics. Journal of Aircraft, vol. 13, no. 2, Feb. 1876, pp. 76-82.

4. DeHoff, R.L.; Hall, W.E., Jr.; Adams, R.J.; and Gupta, N.K.: F100 Multivariable Control Synthesis Program - Vol. 1. Development of F100 Control Systems. Systems Control, Inc. (VT), Palo Alto, CA, AFAPL-TR-77-35-Vol.-1, June 1977.

5. Szuch, J.R.; Soeder, J.F.; Seldner, K.; and Cwynar, D.S.: F100 Multivariable Control Synthesis Program - Evaluation of a Multivariable Control Using a Real-Time Engine Simulation. NASA TP-1056, 1977.

6. Lehtinen, B.; Costakis, W.M.; Soeder, J.F.; and Seldner, K.: F100 Multivariable Control Synthesis Program - Results of Engine Altitude Tests. NASA TMS-83367, July 1983.

7. Soeder, J.F.; F100 Multivariable Control Synthesis Program - Computer Implementation of the F100 Multivariable Control Algorithm. NASA TP-2231, 1983.

8. Geyser, L.C.; and Lehtinen, B.: Digital Program for Solving the Linear Stochastic Optimal Control and Estimation Problem. NASA TN D-7820, March 1975.

9. Lehtinen, B.; and Geyser, L.C.: AESOP: An Interactive Computer Program for the Design of Linear Quadratic Regulators and Kalman Filters, NASA TP-2221, 1983.

10. Beattie, E.C.; LaPrad, R.F.; Akhter, M.M.; and Rock, S.M.: Sensor Failure Detection for Jet Engines Final Report. NASA CR-168190, May 1983.

N84
20591

UNCLAS

D24

N84 20591

L-1011 TESTING WITH RELAXED STATIC STABILITY

J. J. Rising and K. R. Henke
Lockheed California Company
Burbank, California

First Annual NASA Aircraft Controls Workshop
NASA Langley Research Center
Hampton, Virginia
October 25-27, 1983

Wind tunnel and flight tests indicate that fuel savings of 2 percent can be achieved by c.g. management for an L-1011 with the current wing configuration. The normal c.g. location is at 25 percent MAC as shown in figure 1. The maximum fuel saving occurs for a c.g. location of 35 percent MAC. However, flight at 35 percent requires that the c.g. range be extended aft of the 35-percent point. Flight at c.g. locations aft of 35 percent requires a pitch active control system (PACS) so that handling qualities are not significantly degraded. Figure 1 shows that the near-term PACS was flight tested with the c.g. at 39 percent MAC.

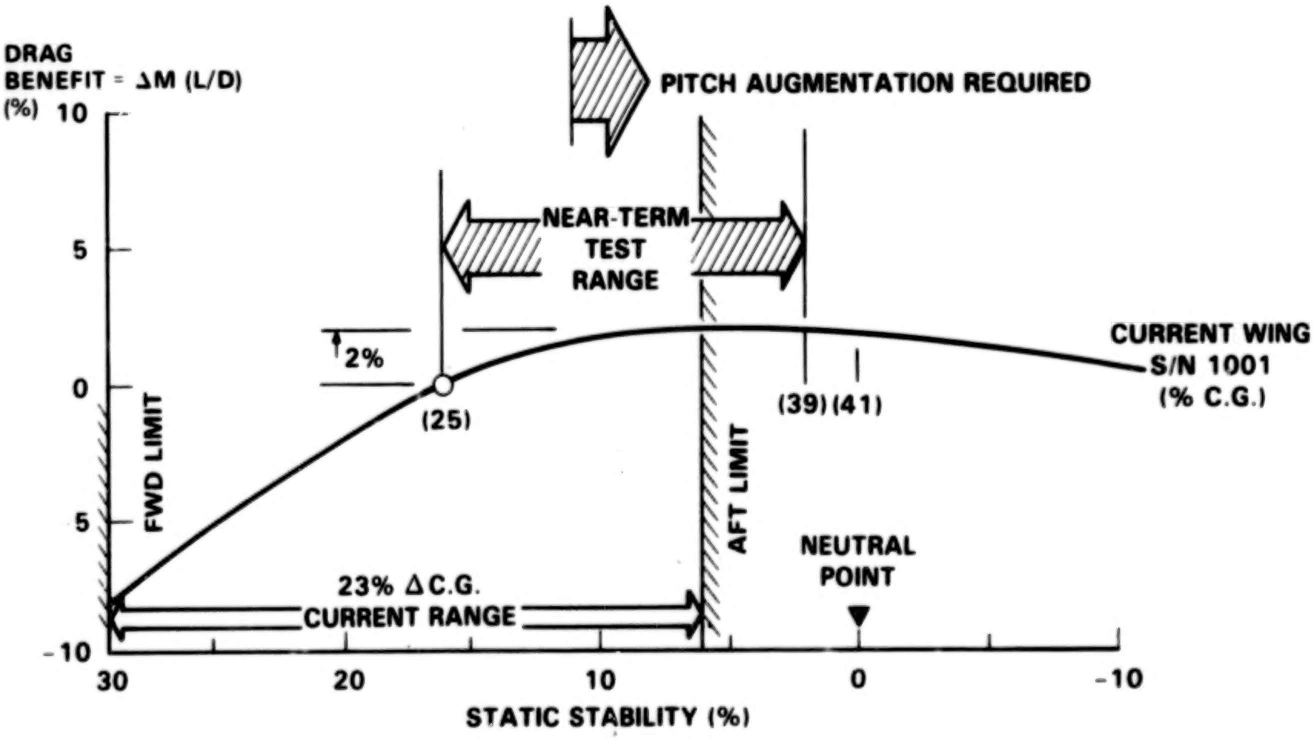

Figure 1

The near-term pitch stability augmentation system consists of a lagged pitch rate damper with washed-out column feed-forward loop. The damper serves to provide the necessary short-period frequency and damping characteristics while also suppressing turbulence effects, and the feed forward was designed to "quicken" the pitch rate response and reduce stick force gradients without affecting system stability. A block diagram of the system is shown in figure 2.

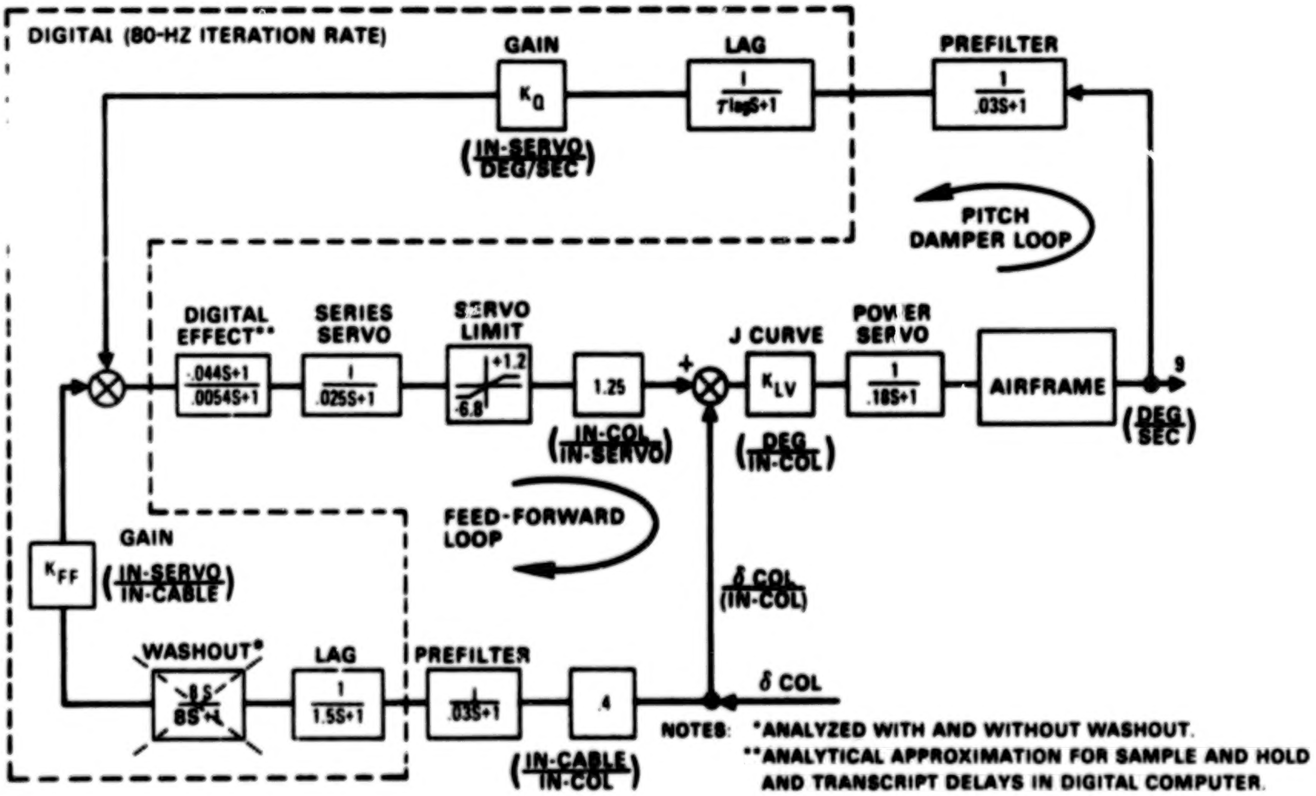
DIGITAL (80-HZ ITERATION RATE)
GAIN
K_Q
$\left(\frac{\text{IN-SERVO}}{\text{DEG/SEC}}\right)$
LAG
$\frac{1}{\tau_{lag}S+1}$
PREFILTER
$\frac{1}{.03S+1}$
PITCH DAMPER LOOP
DIGITAL EFFECT**
$\frac{.044S+1}{.0054S+1}$
SERIES SERVO
$\frac{1}{.025S+1}$
SERVO LIMIT
+1.2
-6.8
1.25
$\left(\frac{\text{IN-COL}}{\text{IN-SERVO}}\right)$
+
J CURVE
K_{LV}
$\left(\frac{\text{DEG}}{\text{IN-COL}}\right)$
POWER SERVO
$\frac{1}{.18S+1}$
AIRFRAME
q
$\left(\frac{\text{DEG}}{\text{SEC}}\right)$
FEED-FORWARD LOOP
K_{FF}
GAIN
$\left(\frac{\text{IN-SERVO}}{\text{IN-CABLE}}\right)$
$\frac{\delta\text{ COL}}{(\text{IN-COL})}$
WASHOUT*
$\frac{8S}{8S+1}$
LAG
$\frac{1}{1.5S+1}$
PREFILTER
$\frac{1}{.03S+1}$
.4
$\left(\frac{\text{IN-CABLE}}{\text{IN-COL}}\right)$
δ COL

NOTES: *ANALYZED WITH AND WITHOUT WASHOUT.
**ANALYTICAL APPROXIMATION FOR SAMPLE AND HOLD AND TRANSCRIPT DELAYS IN DIGITAL COMPUTER.

Figure 2

The schedules of pitch rate feedback gain and lag time constant were chosen so that the augmented stability L-1011 has good short-period frequency and damping characteristics for the complete center-of-gravity range (25 to 39 percent $\bar{c}$) investigated in flight test. The gain and lag schedules are defined as a function of calibrated airspeed. Characteristics with and without augmentation are shown in figure 3.

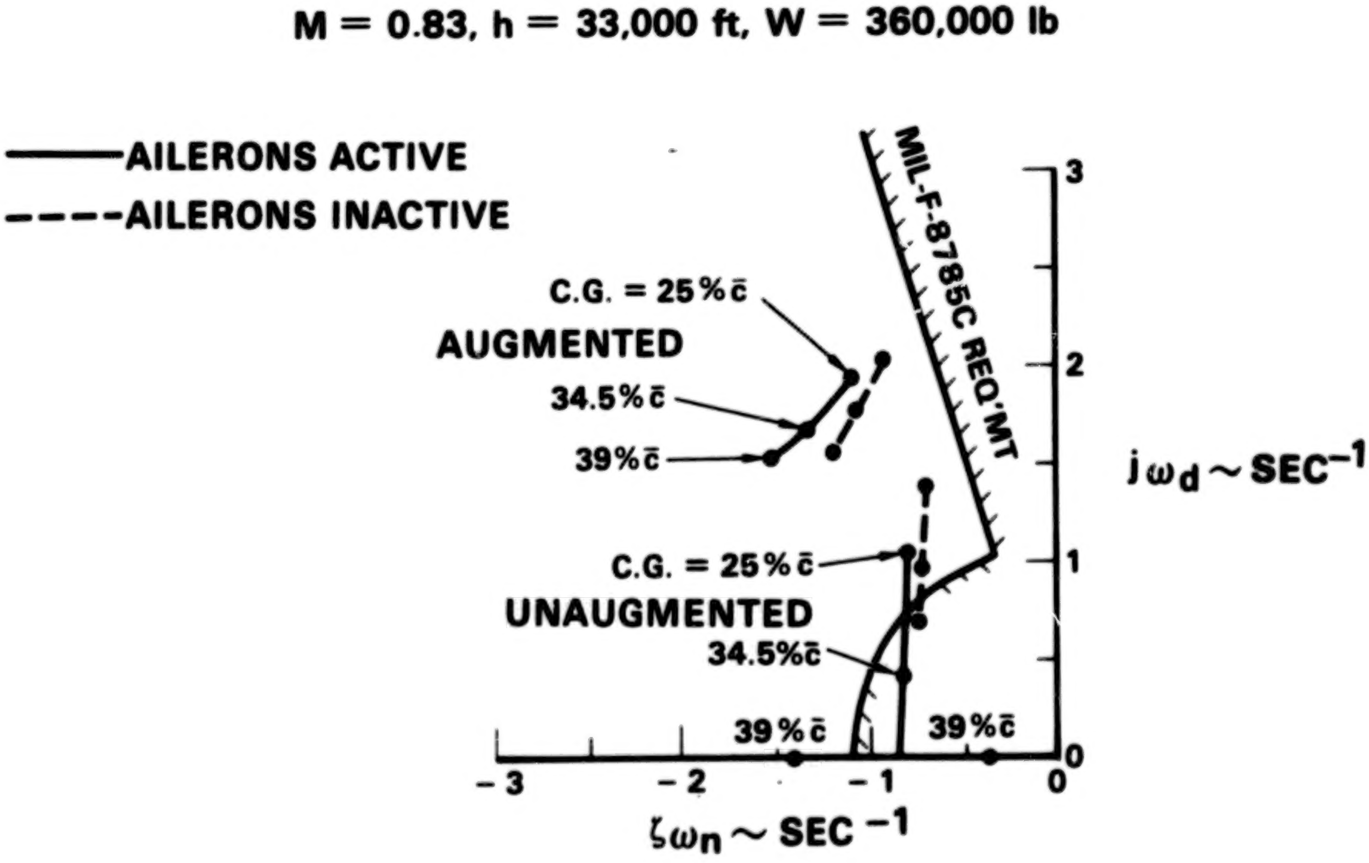

Figure 3

ORIGINAL PAGE IS
OF POOR QUALITY

In cruise, the near-term augmentation system without feed-forward compensation provides slightly higher maneuver stability column force gradients at the relaxed static stability aft limit than the basic airplane has at mid c.g. without augmentation. The effect of feed-forward compensation is to reduce the column force gradients to levels comparable to the basic unaugmented airplane at typical c.g. locations. The initial force gradients comply with MIL-F-8785C (ref. 1) requirements; however, there is a deviation from linearity which results in a short-term negative gradient in the 1.6- to 2.0-g range which is unacceptable in terms of MIL-F-8785C requirements. These characteristics are shown in figure 4. While these negative gradient characteristics may not be desirable, they are not uncommon to Class III transport configurations which cruise at Mach numbers above 0.8. It is suggested that some narrow region of negative gradient may be acceptable as long as a substantial force level is maintained and there is adequate buffet onset or other warning prior to limit load factor.

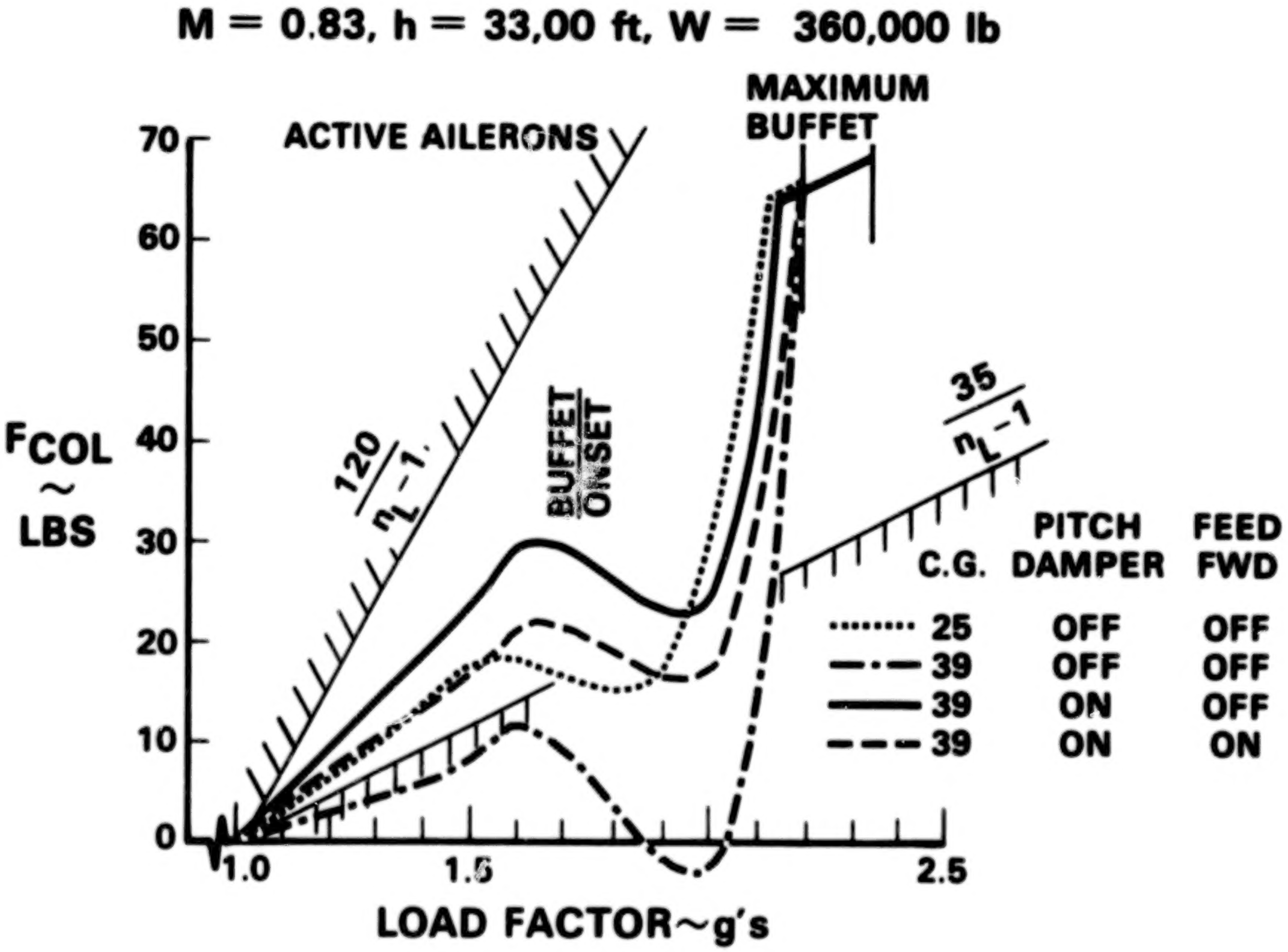
M = 0.83, h = 33,00 ft, W = 360,000 lb

Figure 4

The near-term pitch active control system was ultimately evaluated in an actual flight test program utilizing the Lockheed in-house research airplane, L-1011 S/N 1001.

The near-term PACS flight test aircraft is fully instrumented for performance of flight test programs. This aircraft has been equipped with extended wing tips and an aileron active control system. The increase in wing aspect ratio increases the aerodynamic efficiency of the aircraft, and the aileron active control system provides wing load alleviation which results in lower structure weight. This increased aerodynamic efficiency and lower structural weight provide approximately a 3-percent fuel savings. A unique feature of the basic L-1011 longitudinal control system is the flying stabilizer with a geared elevator. Modifications made to the L-1011 for the near-term PACS program are shown in figure 5.

Three pilots participated in the evaluation, which concentrated on two cruise altitude conditions and an overspeed condition (V_{MO}) at high dynamic pressure. The test program covered 47 hours of flying, 14 for flutter clearance, and 33 for flying qualities evaluation. Flying qualities were evaluated at c.g.'s from 25 to 39 percent $\bar{c}$, where the airplane with active ailerons is close to being neutrally stable (1 to 2 percent static margin) at high-altitude trim conditions.

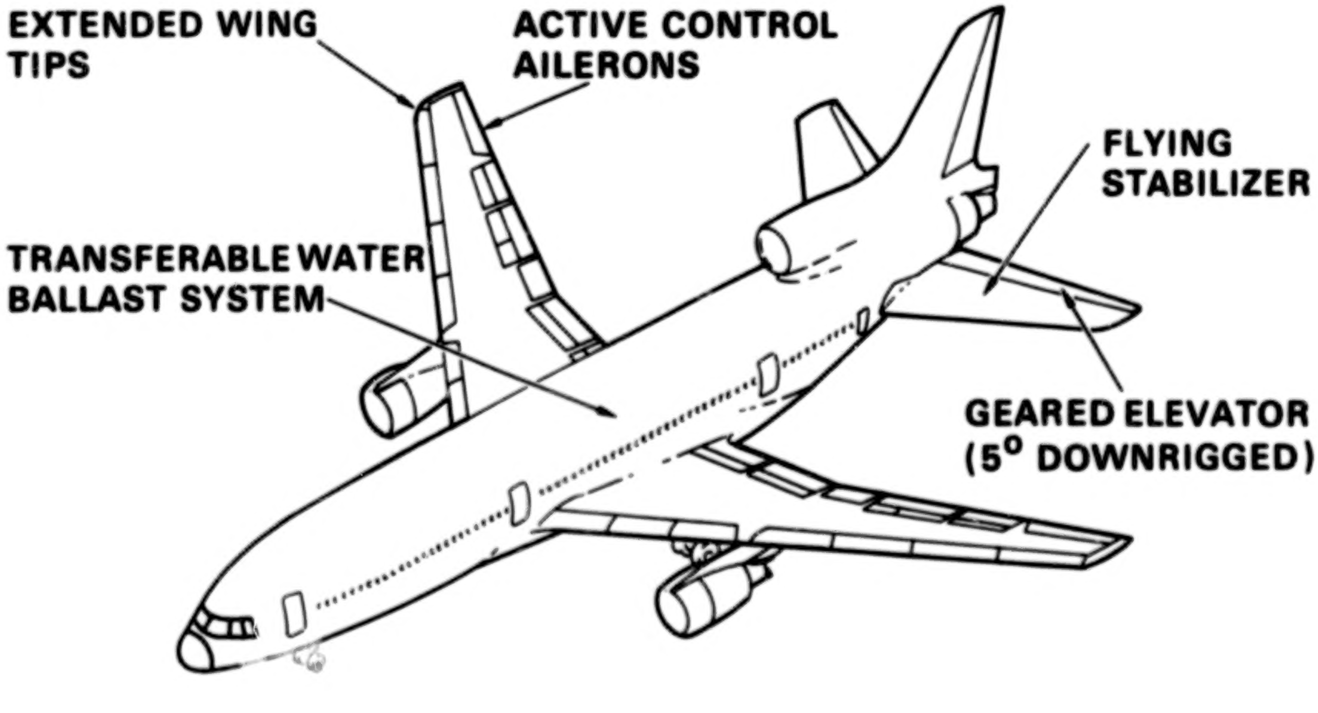
EXTENDED WING TIPS
ACTIVE CONTROL AILERONS
FLYING STABILIZER
TRANSFERABLE WATER BALLAST SYSTEM
GEARED ELEVATOR (5° DOWNRIGGED)

Figure 5

The pitch active control system utilizes a series servo which connects to the pitch control system in such a manner that the PACS commands are fed into the stabilizer power actuators without reflecting these commands into the pilot input control column. This is shown in figure 6.

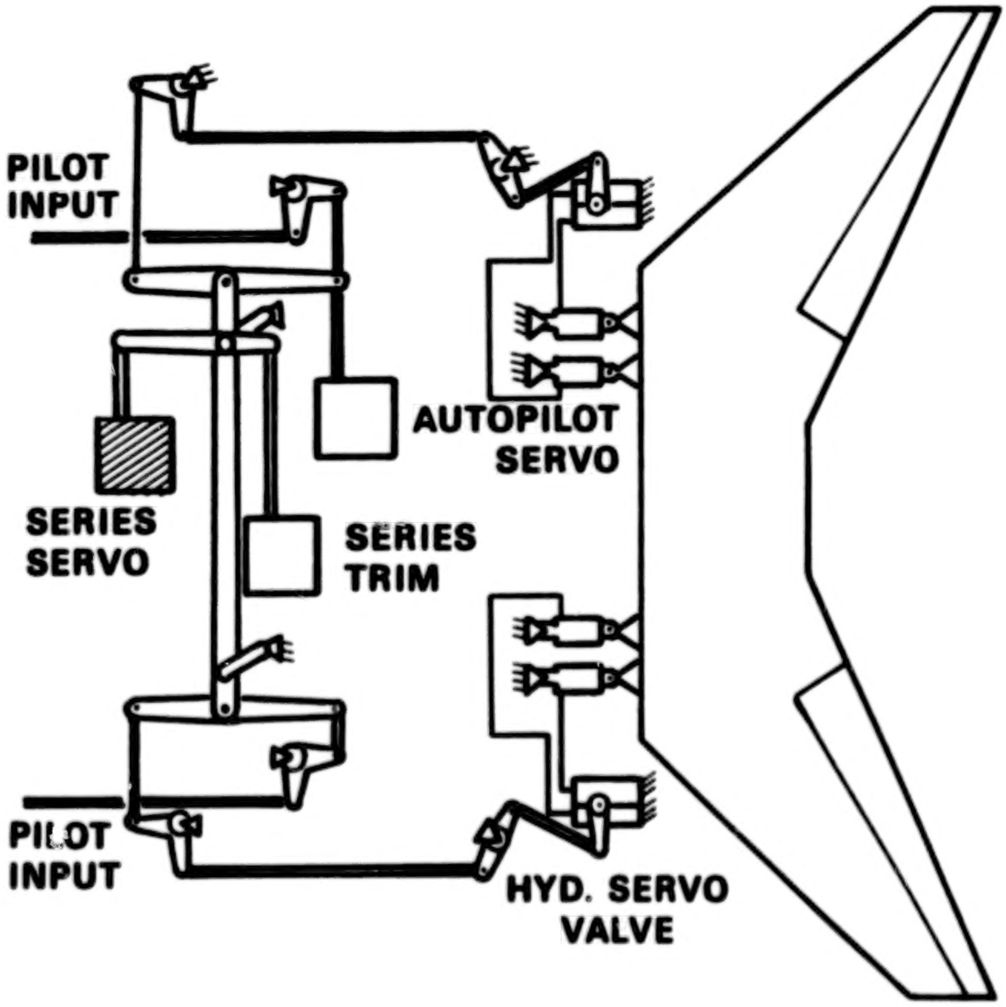
PILOT
INPUT
AUTOPILOT
SERVO
SERIES
SERVO
SERIES
TRIM
PILOT
INPUT
HYD. SERVO
VALVE

Figure 6

Flight test evaluation of the L-1011 with the near-term PACS operative shows a significant improvement in pilot ratings resulting in acceptable ratings to the flight test limit of 39 percent MAC which was 1 percent from the neutral stability point. The variations of pilot ratings with center-of-gravity locations with and without augmentation are shown in figure 7.

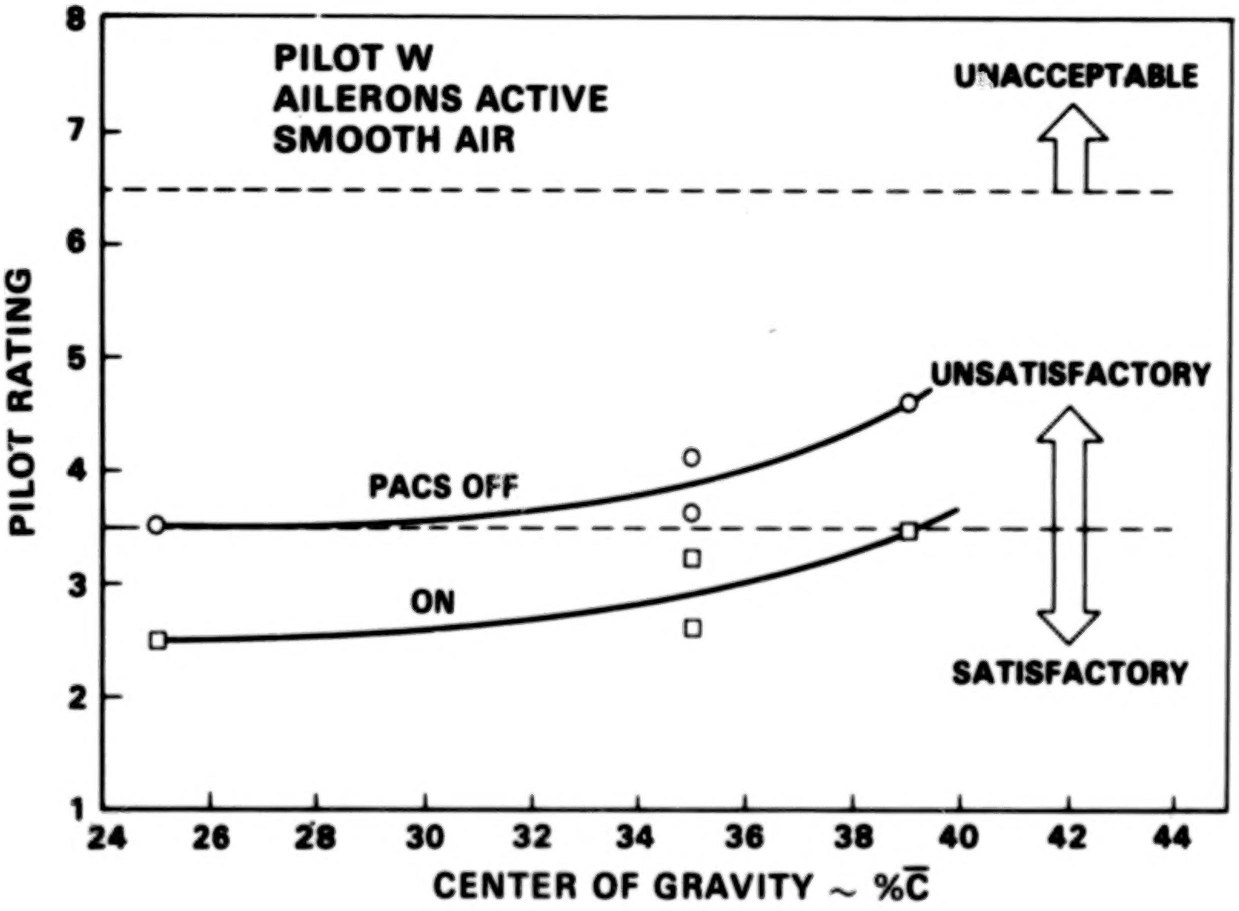

Figure 7

ORIGINAL PAGE IS
OF POOR QUALITY

The fuel saving benefits to be gained by c.g. management are highly dependent on the aircraft wing configuration. Figure 8 shows that for advanced wing concepts aft movement of the c.g. location may result in fuel savings up to 4 percent. This 4 percent is based on increased aerodynamic efficiency determined by analyses and wind tunnel tests. The maximum benefits occur when the c.g. location is at approximately a -10-percent static stability margin. An advanced PACS that has a reliability of 10^{-9} is required for flight at this negative stability margin.

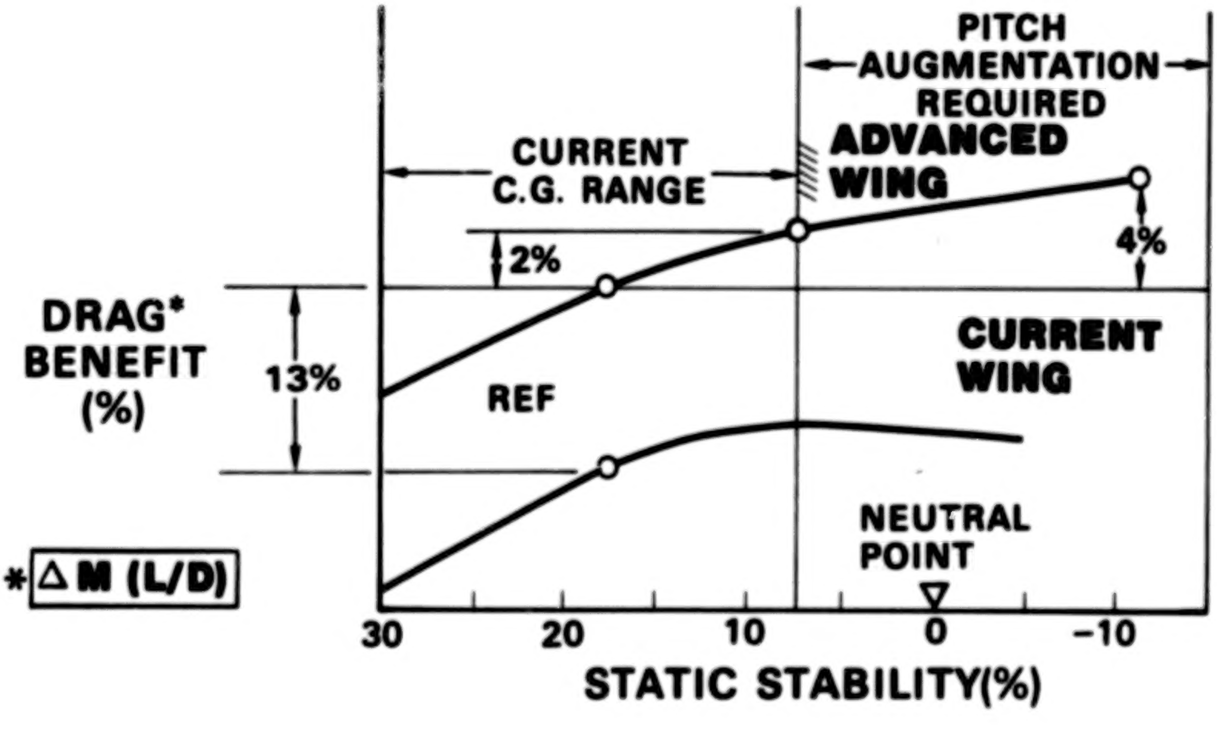

Figure 8

Figure 9 shows the control model used in an eigenstructure placement control law synthesis technique.

With the feedback matrix $[F]$ closed, the state-space equation becomes

$$\{\dot{x}\} = [\ A + BFC\ ]\ \{x\} + \{Z\}$$

In the synthesis process, $[F]$ is computed such that the eigenvalues and eigenvectors of $[A + BFC]$ at any c.g. condition are nearly the same as those for $[A]$ with the c.g. at 25 percent $\bar{c}$.

$$[F] = [K_\theta\ K_u\ K_{NZ}\ K_{\dot{\theta}}\ ]$$

This set of gains operates on the four feedback signals: incremental pitch attitude, incremental speed, normal acceleration, and pitch rate.

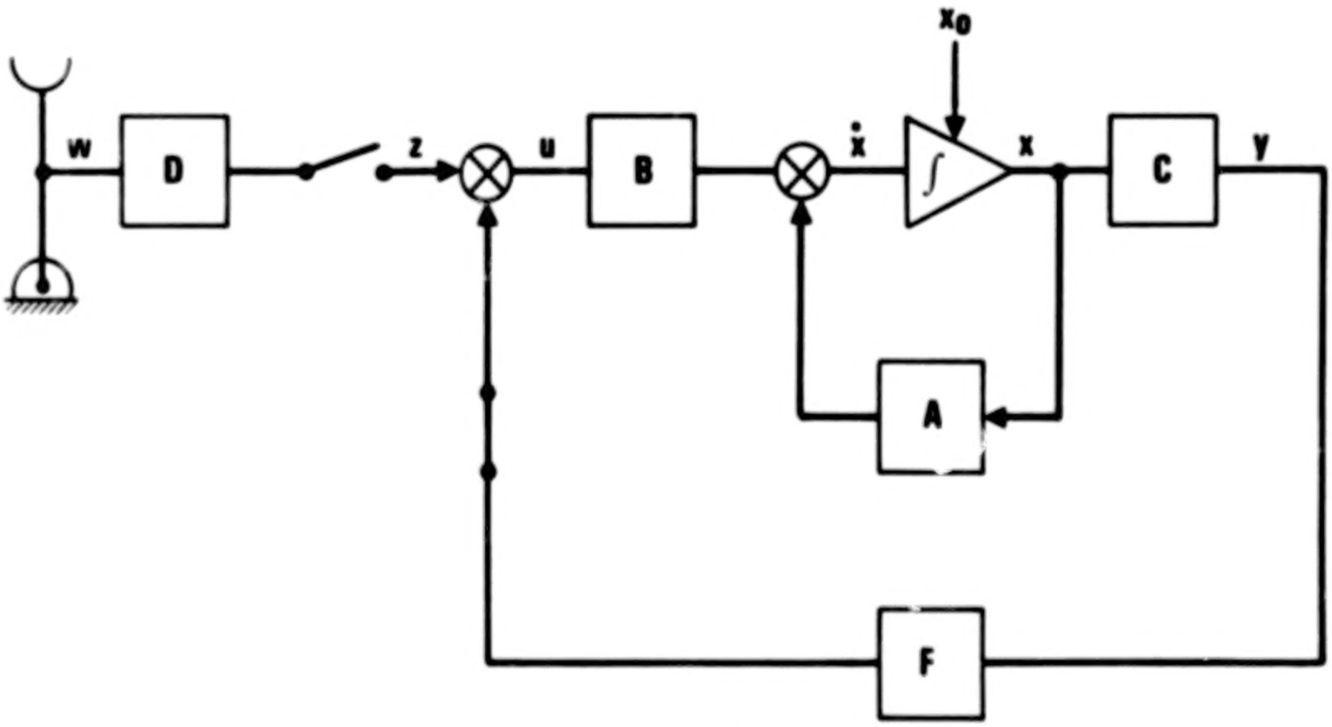

$$\{\dot{x}\} = [A + BFC]\ \{x\} + \{z\}$$

Figure 9

Plots of the feedback gains indicated that gain scheduling could be expressed as polynomial functions of dynamic pressure q and of horizontal stabilizer trim position δ_{HT}. Comparisons of least-mean-square (LMS) values determined the order of polynomials to be used for each set of curves. The second-order polynomial format

$$K = a + bq + cq^2 + d\delta_{HT} + e\delta_{HT}^2$$

was found to provide satisfactory curve fits for all gains. Pseudo-inverse matrix operations efficiently determined the coefficients to yield the least-squares fit for each set of gain values. Scheduled feedback curves of the pitch rate input are shown in figure 10.

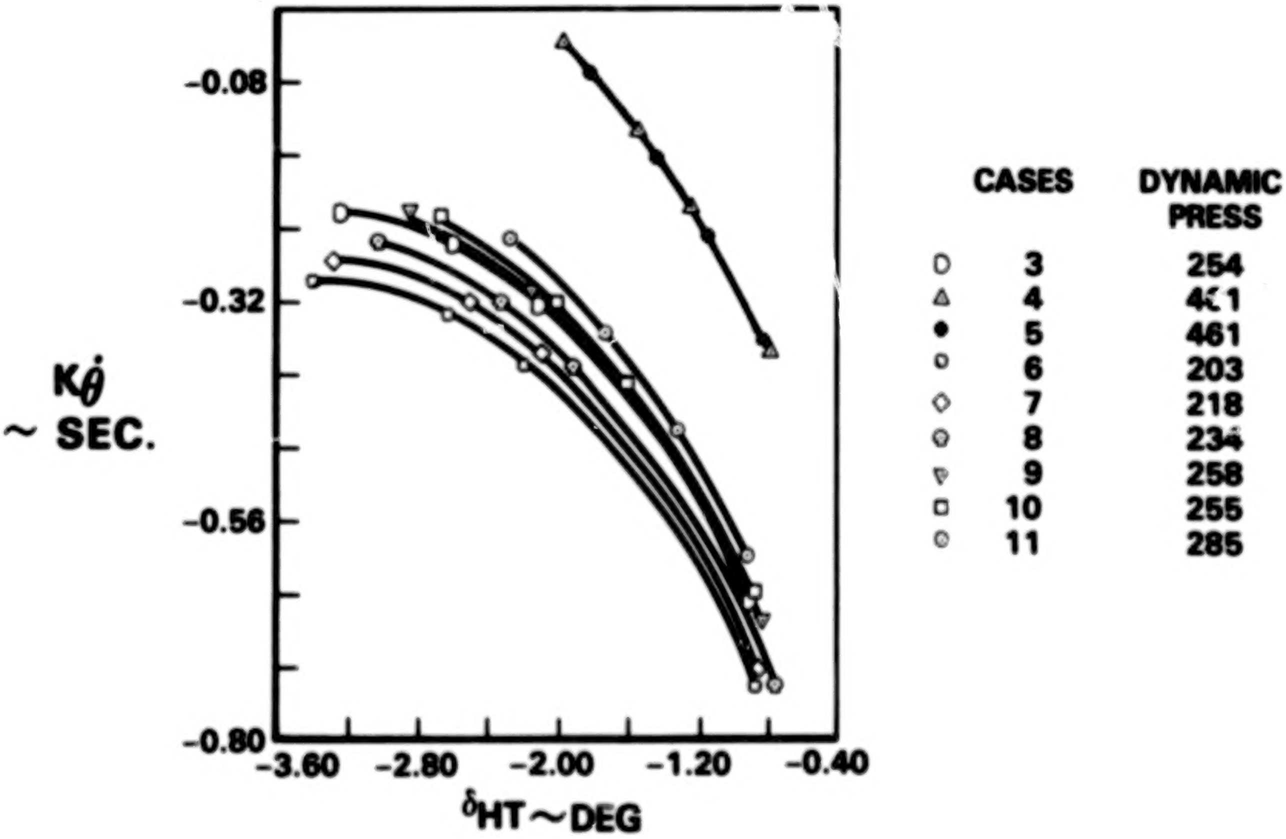

Figure 10

Figure 11 shows conglomerate short-period poles on the S-plane for all flaps-up flight conditions. Nearly all closed-loop poles fall within the objective boundaries:

- Short Period Mode
  $\omega_o \leq \omega_n \leq 2\omega_o$
  $0.5 \leq \zeta \leq 0.8$

where ω_o is the short-period frequency of the corresponding open-loop configuration at 25 percent $\bar{c}$. A few of the short-period damping ratios are higher than 0.8 but are considered to be acceptable.

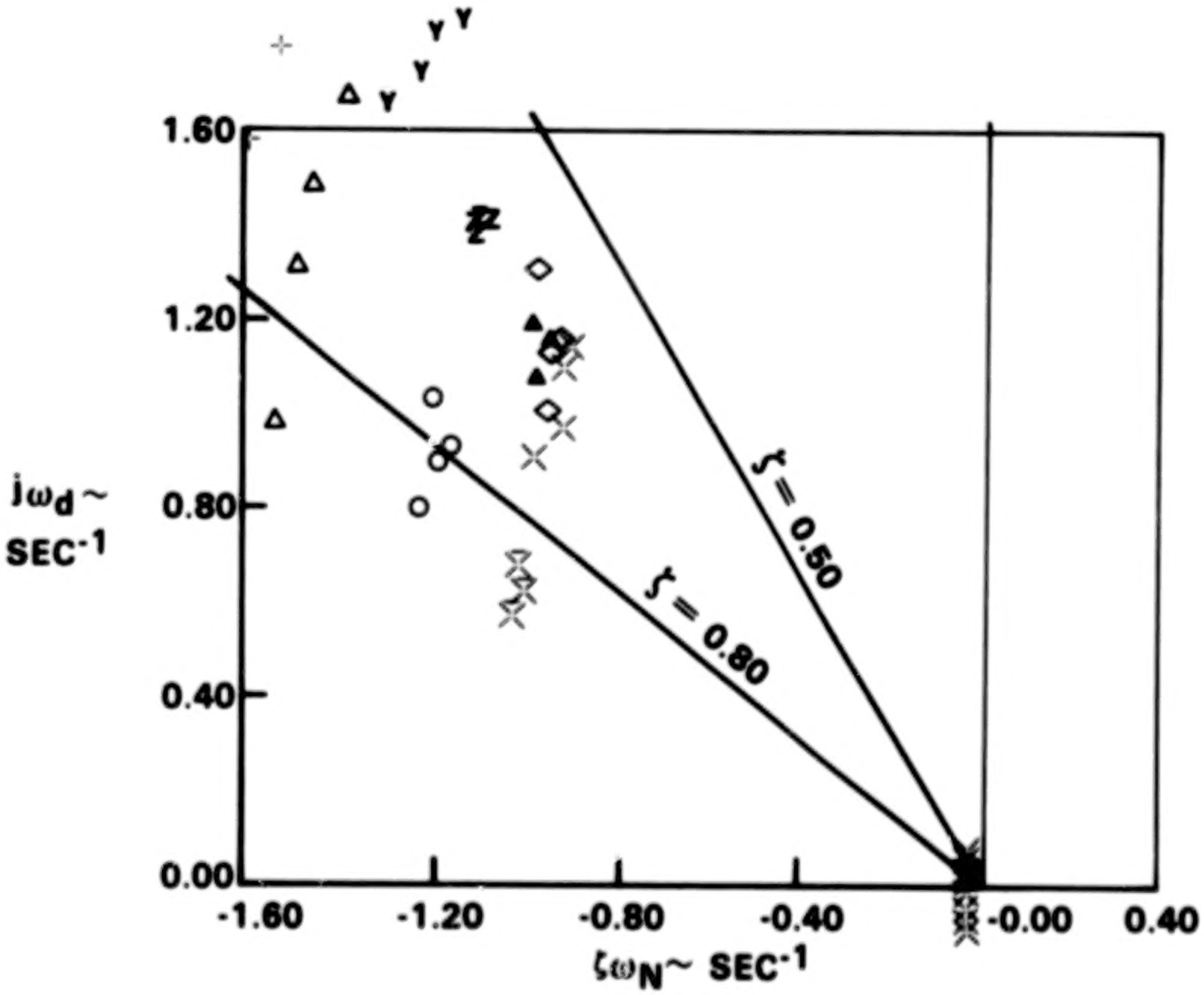

Figure 11

Control of the phugoid mode requires a velocity component, K_u u, in the feedback signal. Because of frequent velocity changes associated with changing trim conditions, however, use of a velocity sensor is undesirable. Knowledge of the transfer functions implicit in the equation

$$\{x\} = [IS-A]^{-1} [B] \{u\}$$

provides the transfer function relating u and θ, as shown in the figure. The composite signal β can be closely approximated by passing θ through a lag-lead network as shown in figure 12 resulting in the following:

$$\frac{\beta}{\theta} = \frac{K_3(\tau_1 s+1)}{(\tau_2 s+1)}$$

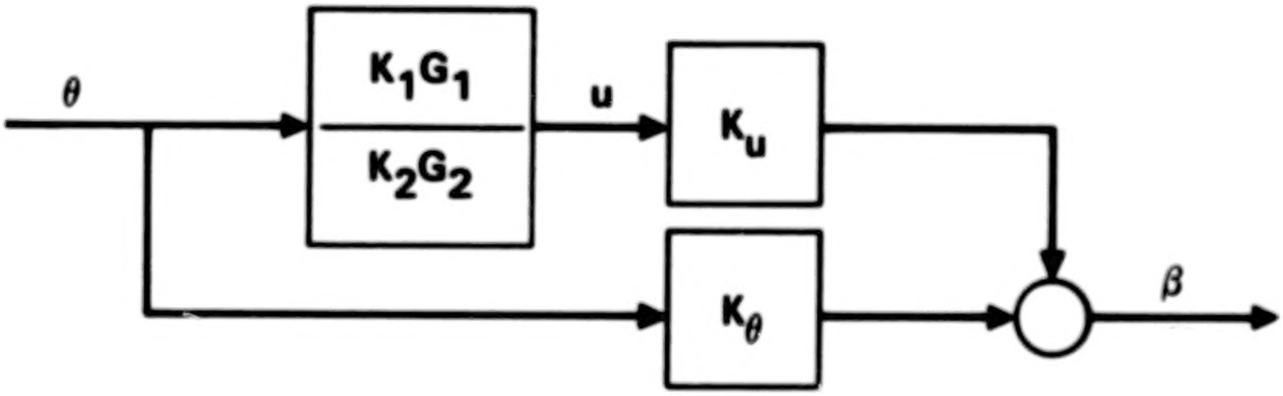

Figure 12

Figure 13 shows conglomerate phugoid poles on the S-plane for all flaps-up flight conditions. Nearly all closed-loop poles fall within the objective boundaries:

- Phugoid Mode
  $\omega_n \leq 0.16$ (40-second period)
  $0.1 \leq \zeta \leq 0.5$

ORIGINAL PAGE IS
OF POOR QUALITY

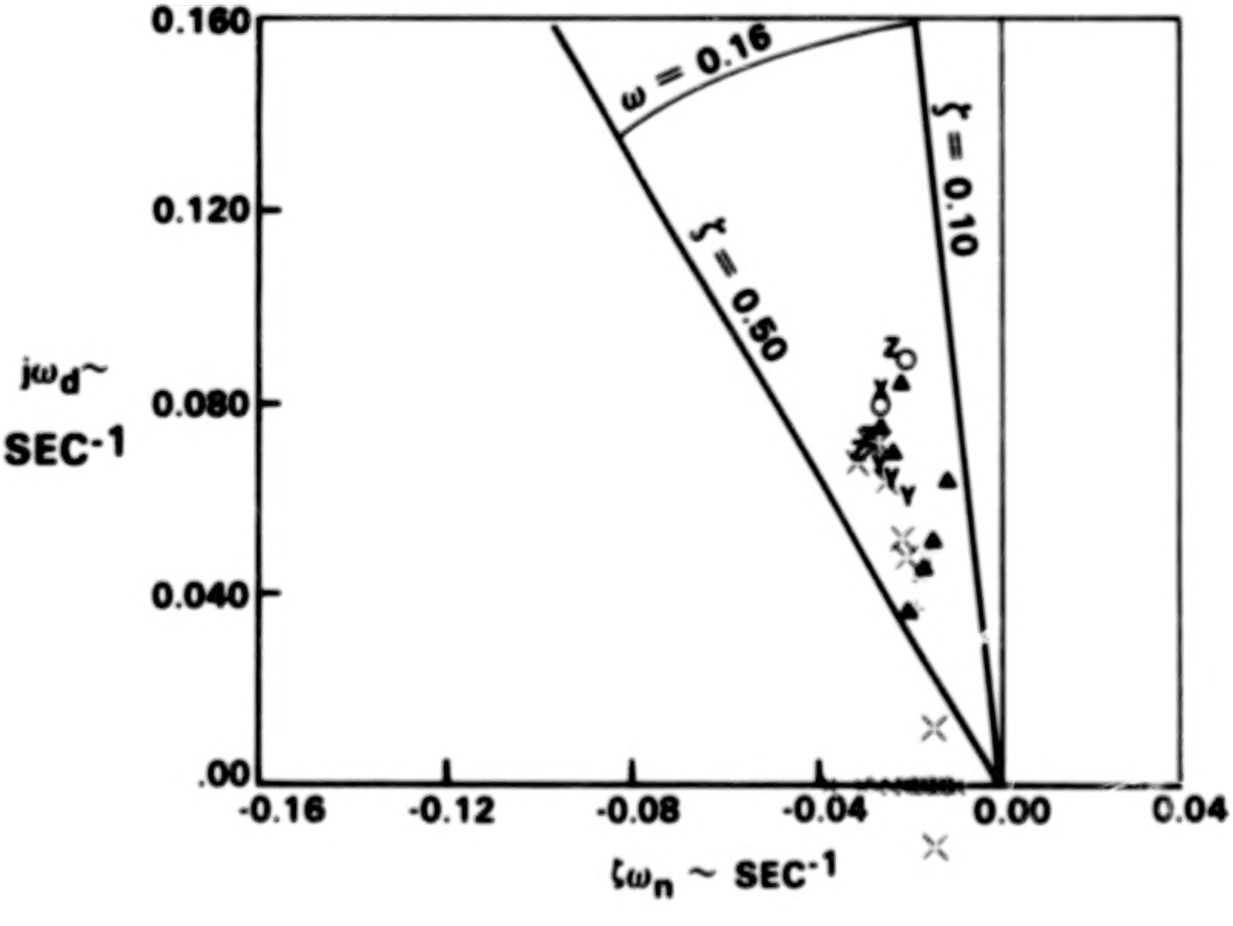

Figure 13

With the feedback and feed-forward loops closed, the system equation is

$$\{\dot{x}\} = [A + BFC]\,\{\chi\} + D\{w\}$$

where {w} is the input vector comprising column displacement. Figure 14 shows the PACS control model with feed-forward loop closed.

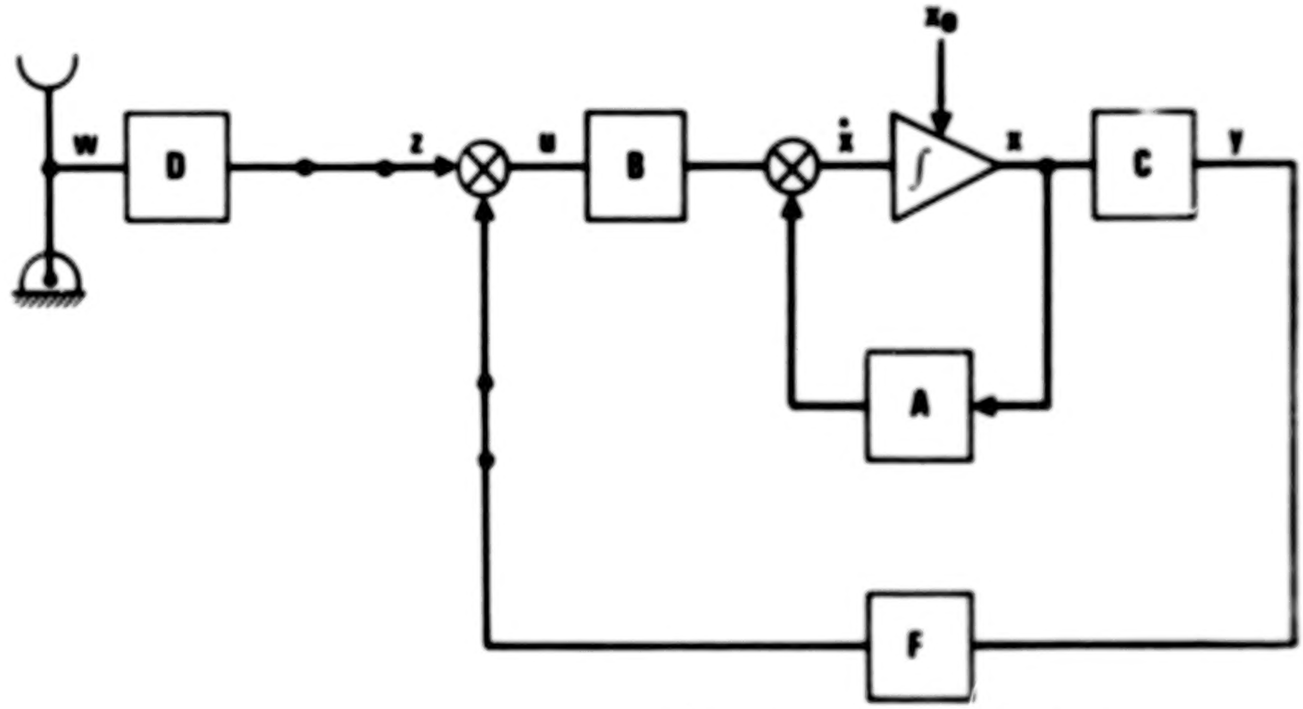

$$\{\dot{x}\} = [A + BFC]\{x\} + [D]\{w\}$$

Figure 14

The feedback transfer function $K_{FB}G_{FB}(S)$ is a composite of all four feedback signals, as shown in the figure. It should be noted that the total transfer function from the input δ_H is the same regardless of which signal is designated to be fed back. This transfer function is

$$\frac{K_{NZ}N_{NZ}(S) + K_uN_u(S) + F_\theta N_\theta(S) + K_{\dot\theta}N_{\dot\theta}(S)}{D(S)}$$

The frequency variant part of this transfer function can be simplified for the purpose of computing $G_{FF}(S)$, because the PACS is not sensitive to this function. Simplifying assumptions permitted the approximation:

$$G_{FF} = 1/(S/\omega_{SP} + 1)$$

A block diagram of this logic is shown in figure 15.

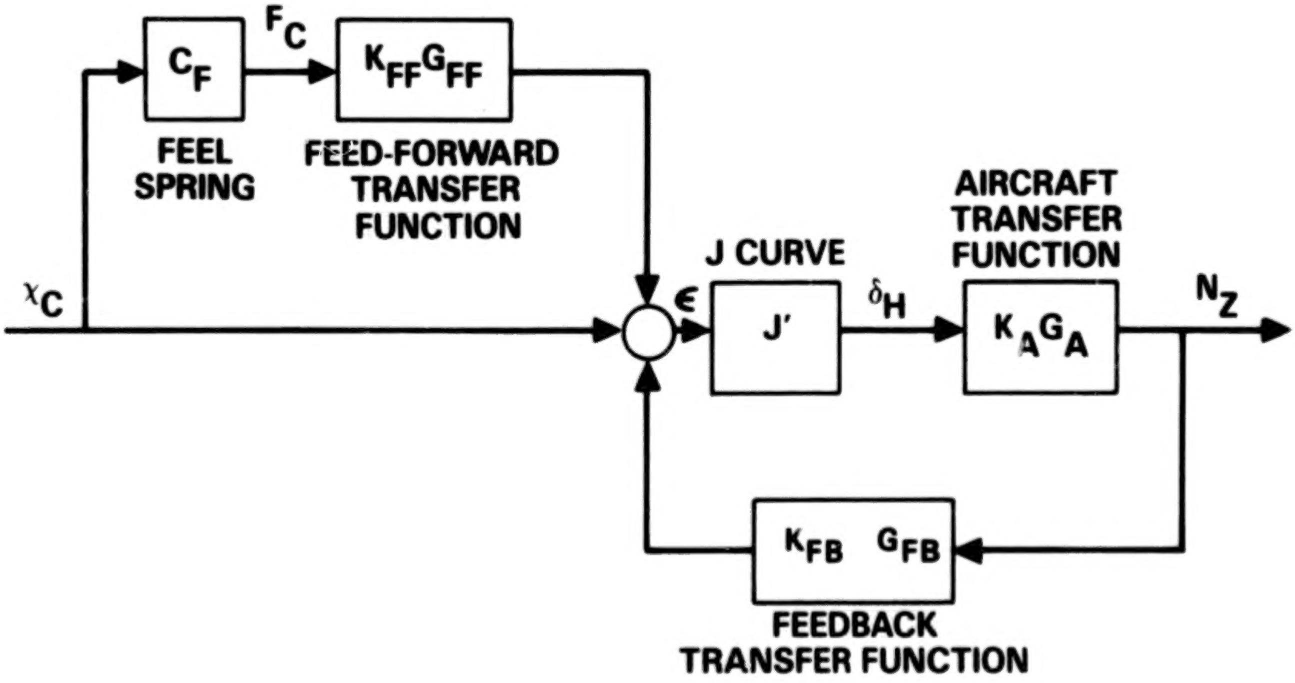
C_F
F_C
$K_{FF}G_{FF}$
FEEL SPRING
FEED-FORWARD TRANSFER FUNCTION
AIRCRAFT TRANSFER FUNCTION
J CURVE
X_C
ϵ
J'
δ_H
K_AG_A
N_Z
K_{FB} G_{FB}
FEEDBACK TRANSFER FUNCTION

Figure 15

The secondary gain scheduling is used to compensate for:

- Pitch-up at high-mach/high-g flight conditions
- Outboard aileron symmetric effects when the aileron active control system (AACS) is activated.

The secondary gain scheduling causes the system "to think" it has an additional c.g. aft increment by adding an increment to the stabilizer gain-scheduling signal, $\delta_{HT}*$. This occurs when the pitch-up phenomena or the AACS mode is sensed in accordance with the block diagram of the secondary-gain controller. The increment produced by the bank angle ($C_\theta \delta_{HT}^2 (1 - \cos\theta)$) is designed to "straighten" the force gradients during high-g turns. The secondary gain controller block diagram logic is shown in figure 16.

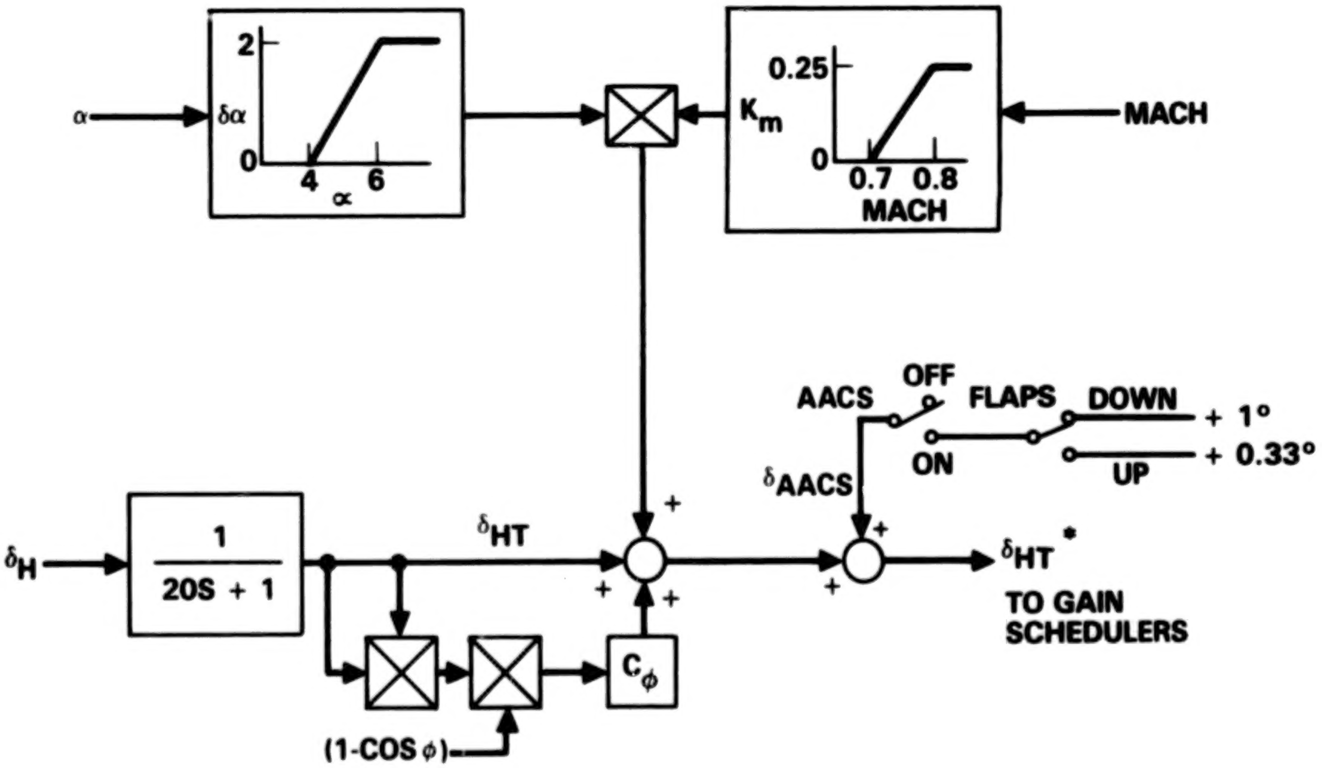
α
2
δα
0
4
6
α
0.25
K_m
0
0.7
0.8
MACH
MACH
AACS
OFF
FLAPS
DOWN
+ 1°
ON
UP
+ 0.33°
δAACS
δH
1
20S + 1
δHT
+
+
+
+
+
δHT *
TO GAIN SCHEDULERS
Cφ
(1-COS φ)

Figure 16

Figure 17 shows that the advanced pitch active control system with pitch excursion compensator completely removes the unstable dip in column dip force gradient characteristics. The data show that column maneuver force gradient characteristics are satisfactory for all c.g. locations. The initial force gradients are essentially the same for all c.g. locations, and they also fall in the middle of MIL-F-8785C specified design limits (ref. 1).

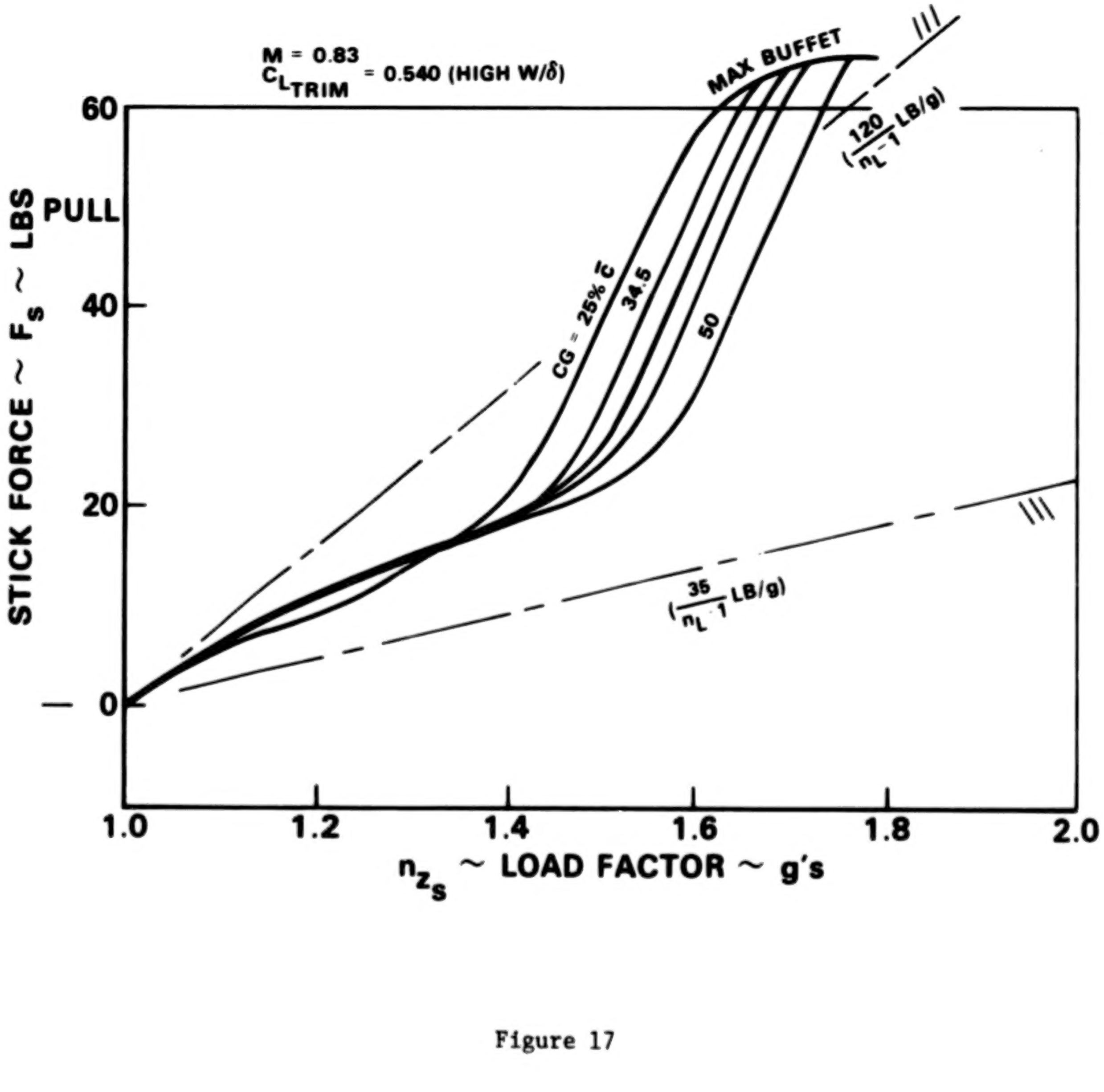

Figure 17

With the advanced pitch active control system engaged, the response of the airplane to a severe vertical gust (heavy thunderstorm magnitude of 54 fps) is shown in figure 18 to be essentially the same for all c.g.'s from 25 percent $\bar{c}$ (15 percent stable) to 50 percent $\bar{c}$ (10 percent unstable).

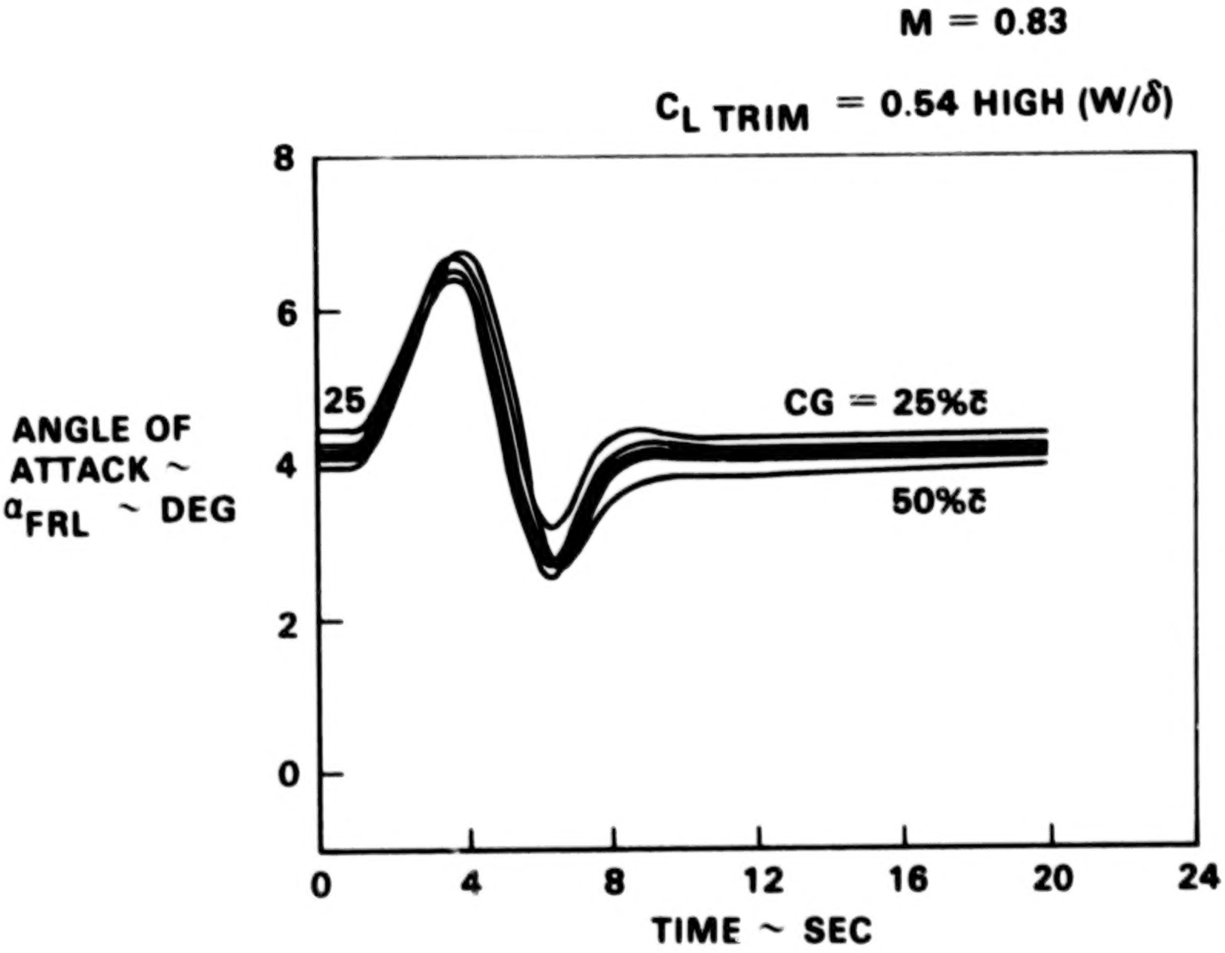

Figure 18

The advanced PACS signals can be grouped into four categories.

- Feedback signals to provide desired stability
- The feed-forward signal to provide the desired column-force gradient
- Primary gain scheduling signals to compensate for flight condition changes
- Secondary gain scheduling to provide additional stability compensation and force-gradient compensation during special flight conditions

Figure 19 shows these signals as used in the advanced PACS.

SYMBOL	SIGNAL	TYPE	USE
F_C	COLUMN FORCE	FEED-FORWARD	COLUMN FORCE GRADIENT
N_Z $\dot{\theta}$ θ	NORMAL ACCELERATION PITCH RATE PITCH ATTITUDE	FEEDBACK	SHORT PERIOD MODE PHUGOID MODE
q δ^*_{HT} S_F	DYNAMIC PRESSURE HORIZONTAL STABILIZER TRIM FLAP SWITCH	PRIMARY GAIN SCHEDULING	COMPENSATION FOR FLIGHT CONDITION CHANGES
α ϕ M	ANGLE OF ATTACK BANK ANGLE MACH NUMBER	SECONDARY GAIN SCHEDULING	COMPENSATION FOR PITCH-UP AND AACS OUTBOARD AILERON OPERATIONS

Figure 19

The advanced PACS is shown by the solid lines in figure 20. Inputs to the controller are:

Feedback

N_z = Normal acceleration

θ = Pitch attitude

$\dot{\theta}$ = Pitch rate

Feed forward

F_c = Column force

Primary gain scheduling

q = Dynamic pressure

δ_{HT} = Stabilizer trim angle

Secondary gain scheduling

α = Angle of attack

ϕ = Bank angle

m = Mach number

The controller output is provided in this planned flight test mechanization to two series servos which have position-summed outputs that limit hardover stabilizer deflections to ±3/4 degree if one series servo fails. The total PACS authority is ±1.5 degrees of stabilizer authority.

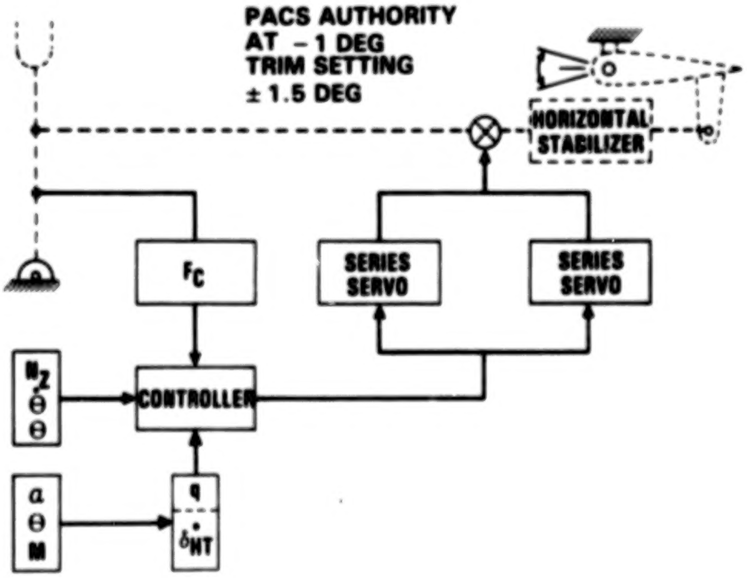
PACS AUTHORITY
AT − 1 DEG
TRIM SETTING
± 1.5 DEG
HORIZONTAL STABILIZER
F_C
SERIES SERVO
SERIES SERVO
N_Z
$\dot{\theta}$
θ
CONTROLLER
α
θ
M
q
$\dot{\delta}_{HT}$

Figure 20

The purpose of the pitch-attitude synchronizer is to remove bias offsets from the pitch-attitude signal, and thus to avoid saturating the series servos. The integrator provides a reference level which tends to command the airplane as if it were in an attitude-hold mode. It has two modes of operation which are pilot optional: (1) fixed reference, or (2) controlled reference, selected by the switch S_2, as shown in the circuit below. With $S_2 = \overline{C}$, the system is in the fixed reference mode and provides a reference attitude θ_R equal to the aircraft trim attitude θ_T. A block diagram of the pitch synchronizer function is shown in figure 21.

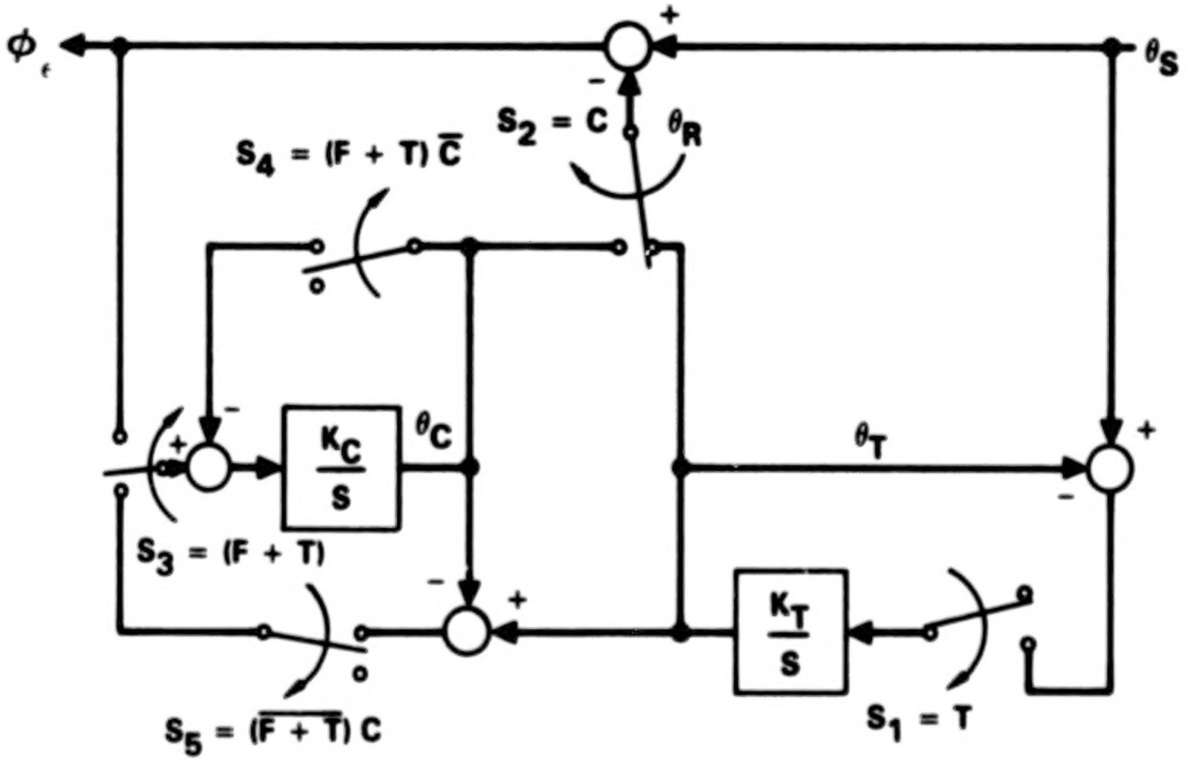
ϕ_ϵ
θ_S
+
−
$S_2 = C$
θ_R
$S_4 = (F + T)\,\overline{C}$
θ_C
$\frac{K_C}{S}$
θ_T
$S_3 = (F + T)$
$\frac{K_T}{S}$
$S_5 = \overline{(F + T)}\,C$
$S_1 = T$

Figure 21

The advanced pitch active control system was evaluated on the Langley visual motion system (VMS) simulator pictured in figure 22. This is a general purpose simulator consisting of a two-man cockpit mounted on a six-degree-of-freedom synergistic motion base. Motion cues are provided by the relative extension or retraction of the six hydraulic cylinders of the motion base. Washout techniques are used to return the motion base to the neutral point once the onset motion cues have been commanded.

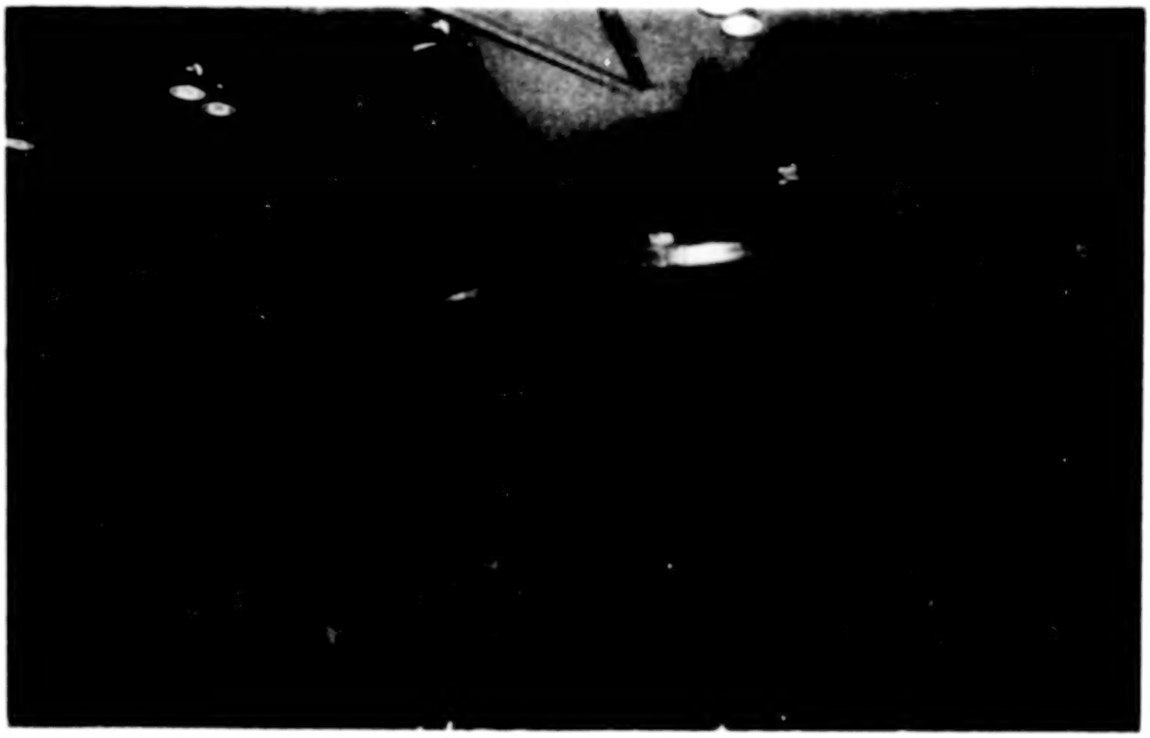

Figure 22

The handling qualities evaluation at each flight condition covered the c.g. range from 25 to 50 percent c̄, for which the control law was designed; this represents a stability range in cruise of 15 percent positive static margin to 10 percent unstable.

Results of the simulation in figure 23 show that the advanced flight control system completely fulfills the function for which it was designed. Pilot ratings indicate that handling qualities of the augmented airplane with c.g. at 25 percent c̄ (10 percent statically unstable) are as good as the basic unaugmented airplane with c.g. at 25 percent c̄ (15 percent statically stable). The results are most impressive at high-speed conditions where handling qualities of the unaugmented airplane quickly degrade to unacceptable levels for c.g.'s aft of 40 percent c̄.

Flight condition 10 is an intermediate altitude cruise condition. At this condition, maneuvering stability about trim is essentially linear.

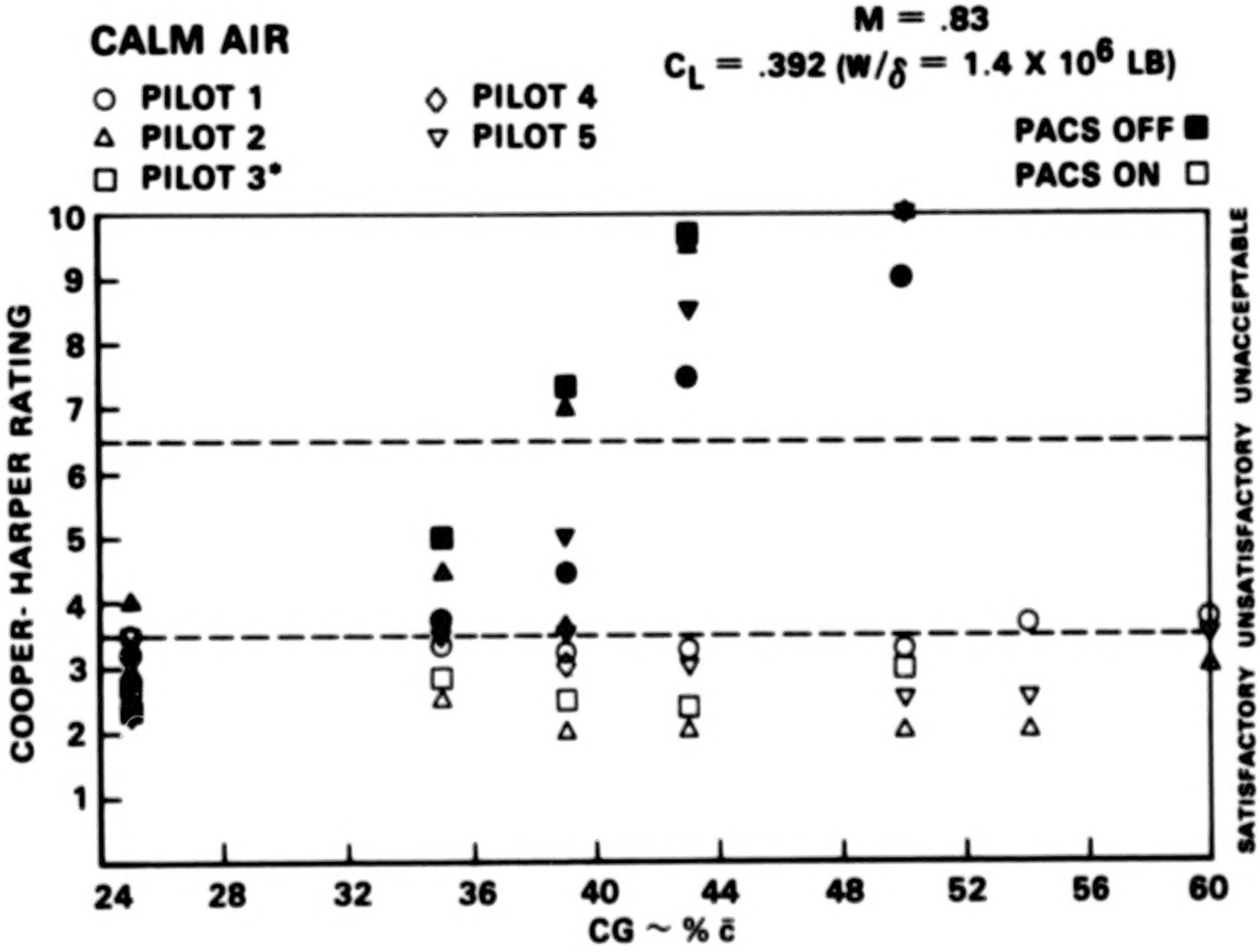

Figure 23

REFERENCE

1. Military Specification, Flying Qualities of Piloted Airplanes, MIL-F-8785C, November 1980.

N84
20592

UNCLAS

N84 20592 D25

AFTI/F-16 DIGITAL FLIGHT CONTROL SYSTEM EXPERIENCE

Dale A. Mackall
NASA Ames Research Center
Dryden Flight Research Facility
Edwards, California

First Annual NASA Aircraft Controls Workshop
NASA Langley Research Center
Hampton, Virginia
October 25-27, 1983

PRECEDING PAGE BLANK NOT FILMED

PAGE 468 INTENTIONALLY BLANK

ABSTRACT

The Advanced Fighter Technology Integration (AFTI) F-16 program is investigating the integration of emerging technologies into an advanced fighter aircraft. The three major technologies involved are the (1) triplex digital flight control system; (2) decoupled aircraft flight control; and (3) integration of avionics, pilot displays, and flight control. In addition to investigating improvements in fighter performance, the AFTI/F-16 program provides a look at generic problems facing highly integrated, flight-crucial digital controls. An overview of the AFTI/F-16 systems is followed by a summary of flight test experience and recommendations.

AFTI/F-16

The Advanced Fighter Technology Integration, AFTI/F-16, is a joint Air Force, NASA, and Navy program. The Air Force's objective is the integration of emerging technologies into a single test bed fighter aircraft. The technologies include a triplex, dual fail/operate digital flight control system; decoupled flight control; and integration of the cockpit functions, avionics, and flight control system. NASA's primary goals for the program were to assure safety of flight of the vehicle and provide an independent assessment of these advanced technologies. The primary contractor is General Dynamics, Fort Worth, Texas.

The AFTI/F-16 is a modified full-scale-development (FSD) F-16. Most of the changes were made to the on-board electronic systems, flight control, and avionics. However, two external modifications were made. Vertical canards were installed below the engine inlet to support decoupled aircraft control. A dorsal fairing was added to house additional avionics and instrumentation.

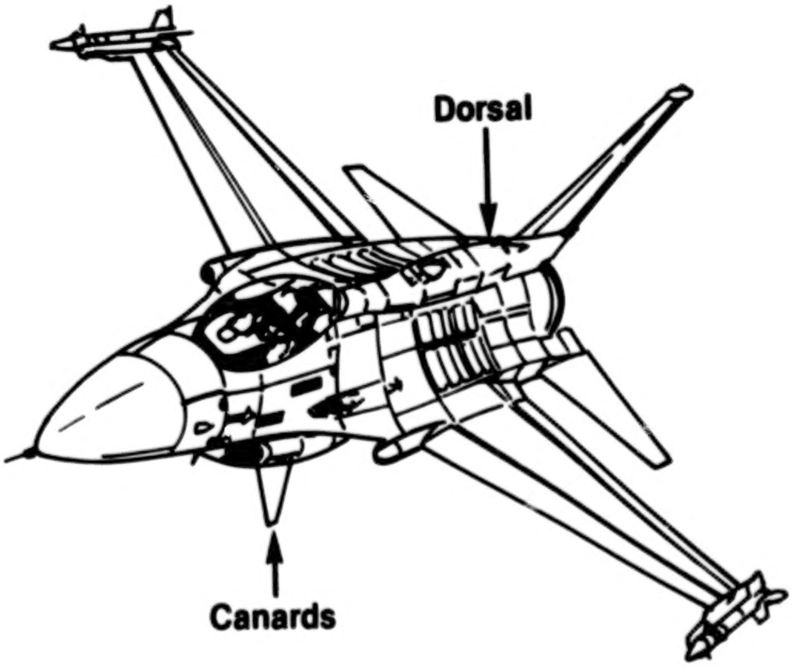

AFTI'S INTEGRATED TECHNOLOGIES

The digital flight control system is the heart of the technologies integrated into the AFTI. In the area of fault tolerance, the dual fail/operate system provides dual fail/operate capability 95% of the time for computer CPU faults. Dual fail/operate was a goal in addressing dual failures of sensors and discrete inputs for the AFTI program. The control law design includes mission-specific and decoupled-control modes. The primary goal is to improve aircraft survivability in an attack.

Another goal to reduce pilot workload is approached by integrating avionics and flight control functions with cockpit displays. One selection of a mission phase switch configures avionics, weapons, and flight control to a specific mode. The multipurpose displays allow for a centralized information display for all systems.

These main technologies resulted in two spinoff technology goals for the flight control system, asynchronous computer operation, and a software-intensive design. Asynchronous operation is a major design characteristic which affects the dual fail/operate capability, decoupled control law design, and the pilot's display of flight control status. The primary purpose of software-intensive design is to avoid additional unique hardware in accomplishing the dual fail/operate requirement.

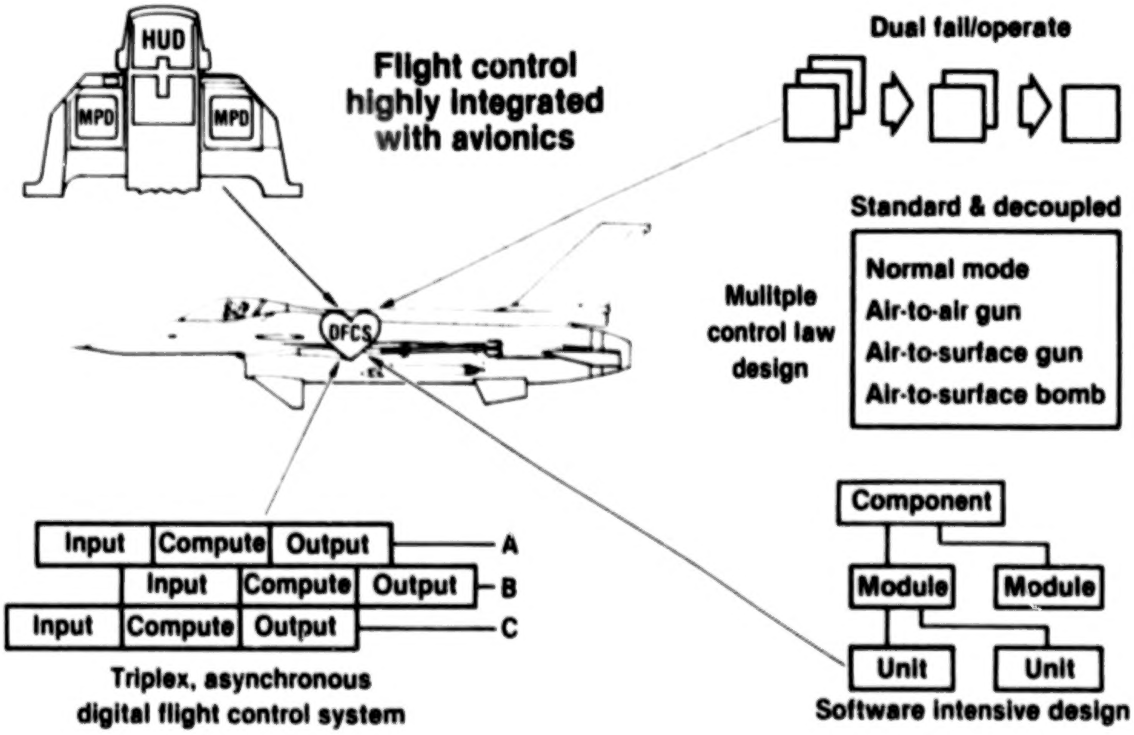
HUD
MPD
MPD
Flight control highly integrated with avionics
Dual fail/operate
Standard & decoupled
Mulitple control law design
Normal mode
Air-to-air gun
Air-to-surface gun
Air-to-surface bomb
DFCS
Input
Compute
Output
A
Input
Compute
Output
B
Input
Compute
Output
C
Triplex, asynchronous digital flight control system
Component
Module
Module
Unit
Unit
Software intensive design

RELIABILITY AND FAULT TOLERANCE

Experience with the AFTI F-16 digital flight control system has highlighted the relationship of fault tolerance and reliability. The software-intensive design of AFTI for aircraft control and fault detection emphasizes the role software plays in overall system reliability. Hardware reliability, based on the replication of hardware components, has been the only contributor to system reliability numbers and loss of control probabilities. The reliability of the software and the functions, such as fault detection algorithms, designed in software must be considered in overall system reliability.

Software reliability continues to be difficult to determine. Software reliability for AFTI was accomplished through test and configuration control. Adequate software reliability was determined indirectly after confidence in system operation was achieved by successful completion of verification and validation testing.

The relationship of fault tolerance to reliability comes through the software. The proper detection of hardware component failures by the software is essential to support the reliability figures for the hardware. If a single failure which caused loss of control went undetected, the reliability for the system would be greatly reduced. Reliability is a function of the fault detection software. Here again, reliability is assured through the testing process.

Total system reliability must consider the basic hardware architecture, the software testing process, and the fault detection algorithms which reside in the software. It is these last two considerations which will determine the validity of loss of control probabilities such as 1×10^{-7}/hr.

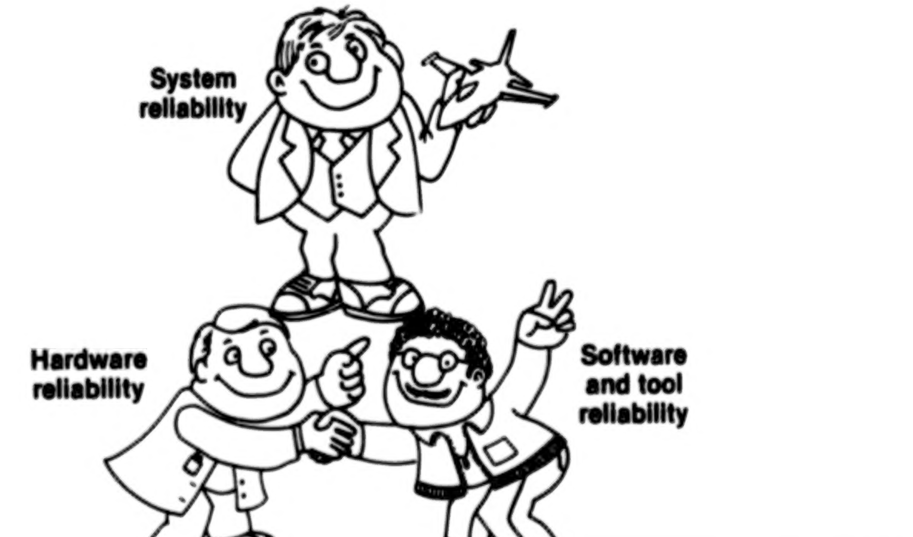
System reliability
Hardware reliability
Software and tool reliability
• Architectural design (replication)
• Environmental test
• EMI compatibility
• MIL standard parts
• Software design (BIT, IFFD, self-test)
• Verification (software)
• Validation (system)
• Configuration control

FAULT-TOLERANT DESIGN

The AFTI F-16 fault-tolerant design consists of two separate sets of checks to increase fault tolerance and provide the dual fail/operate capability. The first set of checks consists of selection and fault detection on input signals. The second set of checks selects values and provides fault detection on the computers and actuators.

The purpose of the input signal selection and fault detection is to increase the system's ability to tolerate failures through cross-channel monitoring of the redundant hardware. Unique characteristics of the AFTI design include: signal selection based on the failure status of higher level devices, such as the inverter; an averaging selection routine; a 15% failure threshold allowance; and reconfiguration of control laws for unresolved dual-sensor failure.

Computer and actuator fault detection work together to provide the highest probability for valid aircraft command in the face of single and multiple failures. The primary aspect is to accomplish the dual fail/operate capability centered on self-test computer coverage. The self-test feature is responsible for identifying the last good computing channel when only two channels remain and their commands are not tracking. A unique characteristic of the output selector and fault detection design is the choosing of one computer's command, with a 15% failure threshold allowance, to control the actuators. This design choice resulted from asynchronous computer operation and interfacing constraints with the actuators.

In-flight Fault Detection

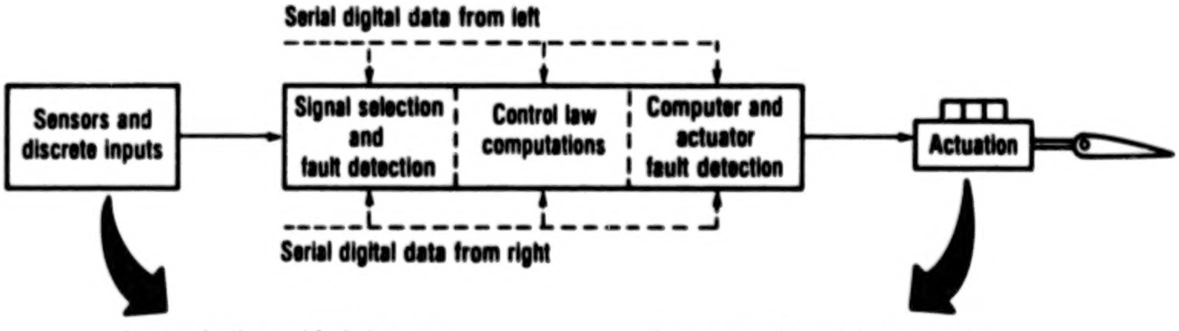
Serial digital data from left
Sensors and discrete inputs
Signal selection and fault detection
Control law computations
Computer and actuator fault detection
Actuation
Serial digital data from right

Input selection and fault detection

Selection: Good signal average

Fault detection: Good signal comparison; tracking to 15% of full-scale failure threshold

Reconfiguration: Loss of a sensor's data causes reconfiguration of control laws or default to safe value

Output selection and fault detection

Selection: Use one channel's value. Channel used is function of computer and hydraulic system failures

Fault detection: Good signal comparison; tracking to 15% failure threshold

Reconfiguration: Computer self-test run for dual failures.

ASYNCHRONOUS COMPUTER OPERATION

Although not intended to be a primary objective of the AFTI program, the investigation of the asynchronous computer operation became a major activity. The asynchronous architectural concept started with the intent to increase EMI immunity and overall system fault tolerance. It was believed that concerns about asynchronous operation (testability, data congruency, and nondeterministic operation) would be alleviated as the design matured. Considerable engineering effort went into designing and qualifying the DFCS with much being learned about asynchronous computer operation. Despite considerable effort and improvements in the qualification process, concerns for testability remained because anomalies related to asynchronous operation occurred in flight testing. Asynchronous operation, coupled with the complexities of decoupled control and dual fail/operate capability, resulted in an increased design task, extended qualification period, and marginal testability. After envelope expansion, flight test evaluation of the DFCS for mission performance did not identify any new anomalies related to asynchronous operation.

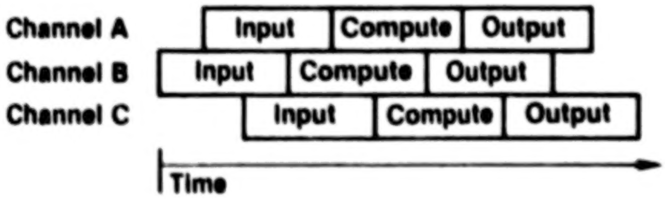

Concept

- Increase immunity to EMI/lightning
- Increase computer channel independence
- Increase fault tolerance over synchronized system

Results

- Design task complicated by asynchronism
- Qualification time extended, repeatability poor
- Complex interactions due to sampling skews
- Flight test operations affected due to marginal testability

Concerns

- Random computer relationship, nondeterministic
- Incongruent data sets due to sampling skew
- Testability; assuring reliable operation for all conditions

FLIGHT CONTROL MODE STRUCTURE

The AFTI digital flight control system consists of eight flight control modes, four standard and four decoupled options. The four mission-specific categories include normal, air-to-air gunnery, air-to-surface gunnery, and air-to-surface bomb modes. Mission-specific mode selection is accomplished through a mode panel or through hands-on selectors on the throttle. Mode selection configures both flight control and avionics. Decoupled mode options are selected through a CCV lever on the right-hand side stick controller. Decoupled options include pointing, translation, and direct force in both pitch and yaw axes. The decoupled options also include enhanced maneuvering modes utilizing the pitch stick. The decoupled air-to-air gun mode provides an adaptive mode for the pitch stick, changing control structure based on pitch rate errors. This allows for control optimization of gross acquisition and fine tracking in the air-to-air mission.

In addition to the advanced decoupled modes, reconfiguration modes are included to provide dual fail/operate capability for sensor failure; however, there is a loss of decoupled and mission-specific modes. A reconfiguration mode is derived from the standard normal mode for dual failures of all primary feedback sensors, both longitudinal and lateral-directional. Reconfiguration modes use either synthesized sensor information or zero values as required. The digital system is backed up with an independent analog reversion mode. This provides protection for common mode errors which could cause loss of the digital system.

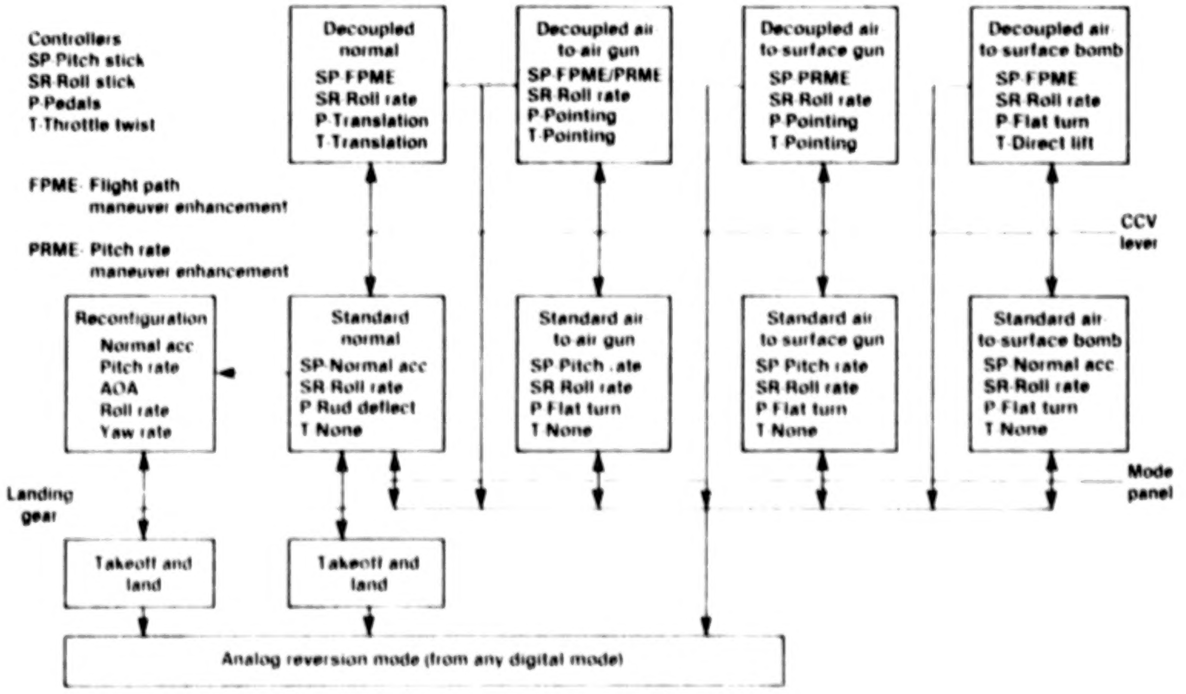
Controllers
SP Pitch stick
SR Roll stick
P Pedals
T Throttle twist
FPME Flight path maneuver enhancement
PRME Pitch rate maneuver enhancement
Decoupled normal
SP FPME
SR Roll rate
P Translation
T Translation
Decoupled air to air gun
SP FPME/PRME
SR Roll rate
P Pointing
T Pointing
Decoupled air to surface gun
SP PRME
SR Roll rate
P Pointing
T Pointing
Decoupled air to surface bomb
SP FPME
SR Roll rate
P Flat turn
T Direct lift
CCV lever
Reconfiguration
Normal acc
Pitch rate
AOA
Roll rate
Yaw rate
Standard normal
SP Normal acc
SR Roll rate
P Rud deflect
T None
Standard air to air gun
SP Pitch rate
SR Roll rate
P Flat turn
T None
Standard air to surface gun
SP Pitch rate
SR Roll rate
P Flat turn
T None
Standard air to surface bomb
SP Normal acc
SR Roll rate
P Flat turn
T None
Mode panel
Landing gear
Takeoff and land
Takeoff and land
Analog reversion mode (from any digital mode)

DECOUPLED CONTROL OPTIONS

Decoupled control options consist of pointing, translation, and direct force for both pitch and yaw axes. Pitch axis modes use elevator and flap commands, and yaw axis modes use canards, rudder, differential elevator, and aileron commands. Pointing allows for changing aircraft attitude without affecting flight path. Pointing angles are equivalent to changes in angle of attack and sideslip for each axis. Translation commands a constant velocity without affecting aircraft attitude. Angle of attack and sideslip vary with the command. The direct-force modes command accelerations, affecting flight path, while keeping angle of attack and sideslip constant. The evaluation of decoupled options centered around weapon effectiveness while increasing aircraft survivability.

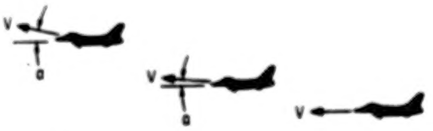

Vertical translation

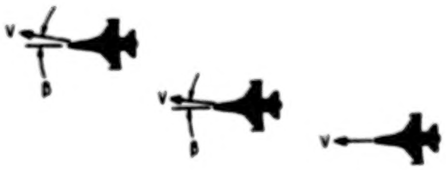

Lateral translation

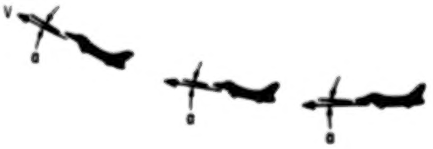

Direct lift

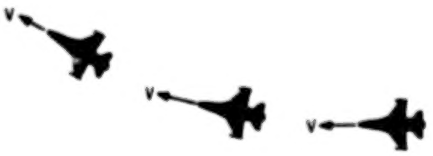

Direct sideforce

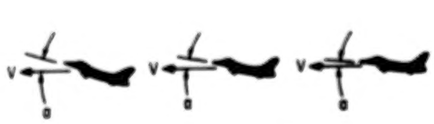

Pitch pointing

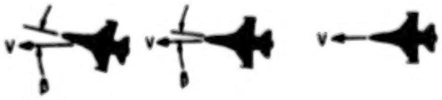

Yaw pointing

SYSTEM INTERACTIONS

An example of the interactions which occurred between the redundancy management functions and control law is illustrated below. Triple analog input sensors are sampled asynchronously and compared within each computer. If the inputs are within an established trip level, the control laws in each computer use an average value for the triplex inputs. Because the system is asynchronous, the average value used by the control laws is slightly different in each computer. The complex control law structure, with its high gains, amplifies the difference in generating an output command. The output command is monitored by each computer to assure that the differences between output commands are within a given difference (that is, trip level). The amplified differences generated by the high-gain control law function cause nuisance failures in the output command monitor. If three output surface commands fail within one computer, a channel is failed. This was particularly evident in the advanced and decoupled modes during ground qualification. The control gains were reduced to prevent nuisance failures as a consequence of the redundancy management/control law interactions.

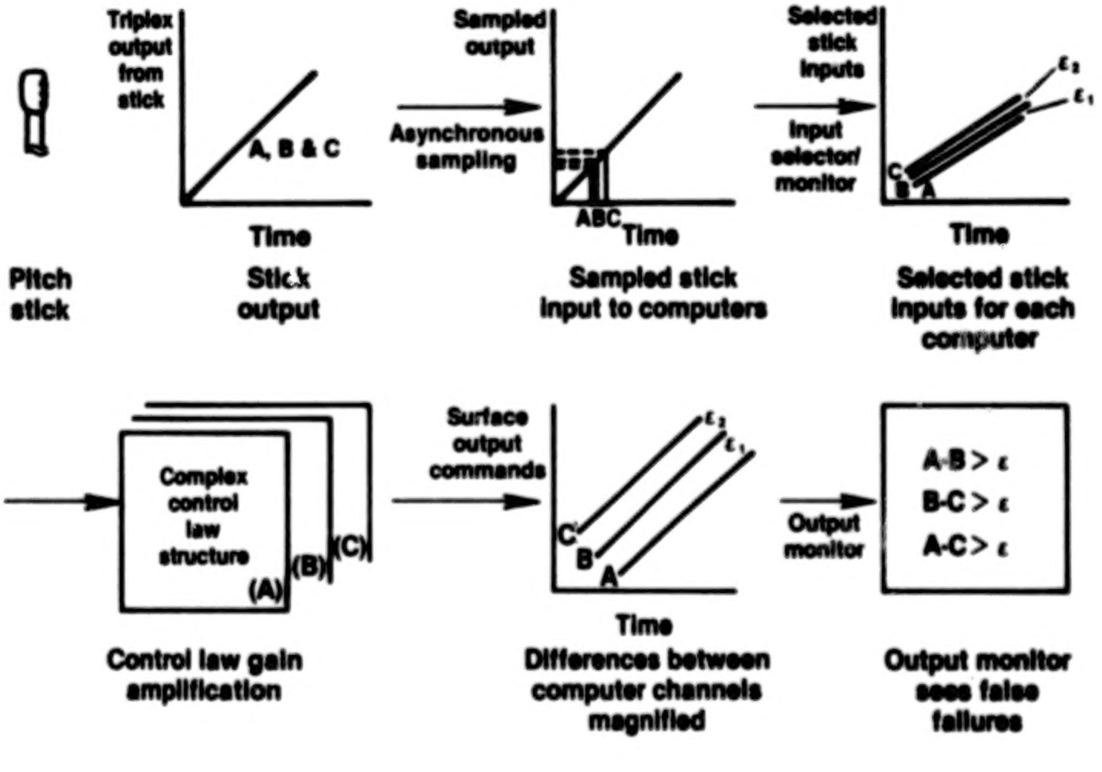
Triplex output from stick
A, B & C
Time
Pitch stick
Stick output
Sampled output
Asynchronous sampling
ABC
Time
Sampled stick input to computers
Selected stick inputs
Input selector/ monitor
ε₂
ε₁
C
B
A
Time
Selected stick inputs for each computer
Complex control law structure
(A)
(B)
(C)
Control law gain amplification
Surface output commands
ε₂
ε₁
C
B
A
Time
Differences between computer channels magnified
Output monitor
A-B > ε
B-C > ε
A-C > ε
Output monitor sees false failures

SOFTWARE DESIGN AND TEST APPROACH

The digital flight control software design and test activities are summarized as a top-down design with bottom-up testing. The design, test, and redesign cycle is accomplished through a configuration control/ discrepancy reporting process. Top-down design began with a function breakdown based on the design specification. The functional breakdown was carried directly into a structured software design. The lowest breakdown of the software is termed a unit and is required to have one exit and entry point and be less than 100 lines of code. Strict documentation, commenting, and software design reviews were essential to the software design process.

Software testing took a bottom-up approach, beginning with unit testing. The module and the component testing were accomplished as the necessary units were integrated. Testing to this level is done by the software design team, with a final integrated software package going to an independent test group. The independent test group performed verification (proper software implementation of the functions) and validation (proper system level operation testing of the flight control system). Detailed specification and design documents were used by the test team to assure proper testing of all flight control functions. Details of the qualification can be found in references 1, 2, and 3.

The configuration control process provided the means to document discrepancies found in test and to correct the discrepancies in the software or hardware as needed. The key to the process is a systems-wide approach covering control laws, fault tolerances, avionics, hardware, and software. Interdisciplinary knowledge and resolution of problems are essential in such heavily integrated systems.

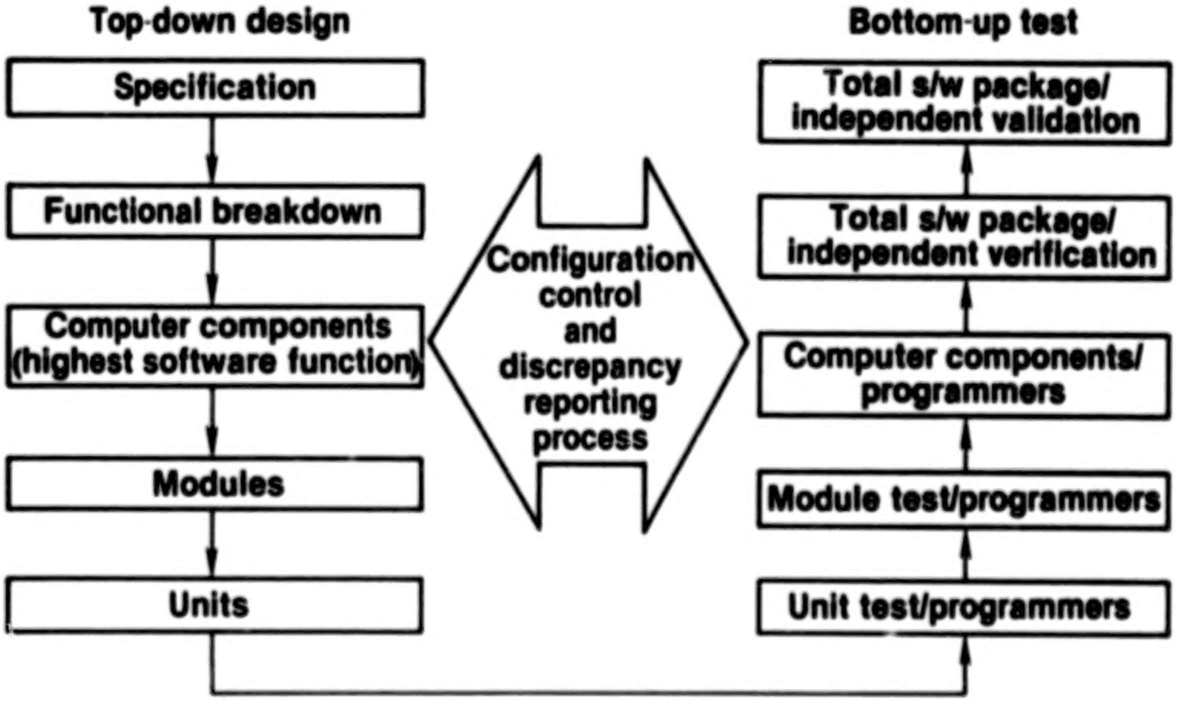
Top-down design
Specification
Functional breakdown
Computer components (highest software function)
Modules
Units
Configuration control and discrepancy reporting process
Bottom-up test
Total s/w package/ independent validation
Total s/w package/ independent verification
Computer components/ programmers
Module test/programmers
Unit test/programmers

FLIGHT TEST RESULTS: GENERAL

Flight testing of the AFTI F-16 was successfully accomplished over a 13-month period in 1982 and 1983. A total of 118 flights were flown by pilots from four organizations: Air Force, NASA, Navy, and General Dynamics. All major objectives were completed, including envelope expansion for high angles of attack and Mach numbers up to 1.2, combat mission evaluations of decoupled control, and structural load clearance for the decoupled motions. Low flight rates early in the program were due to anomalies of the basic aircraft as well as to the AFTI unique systems.

Thirteen software releases were made during flight test to the digital flight control system. Software changes were made to correct discrepancies and provide improvements in flying qualities, fault-tolerant operation, and structural-load-limit items. An efficient software change process is required to provide safe, timely changes needed to accomplish flight test objectives.

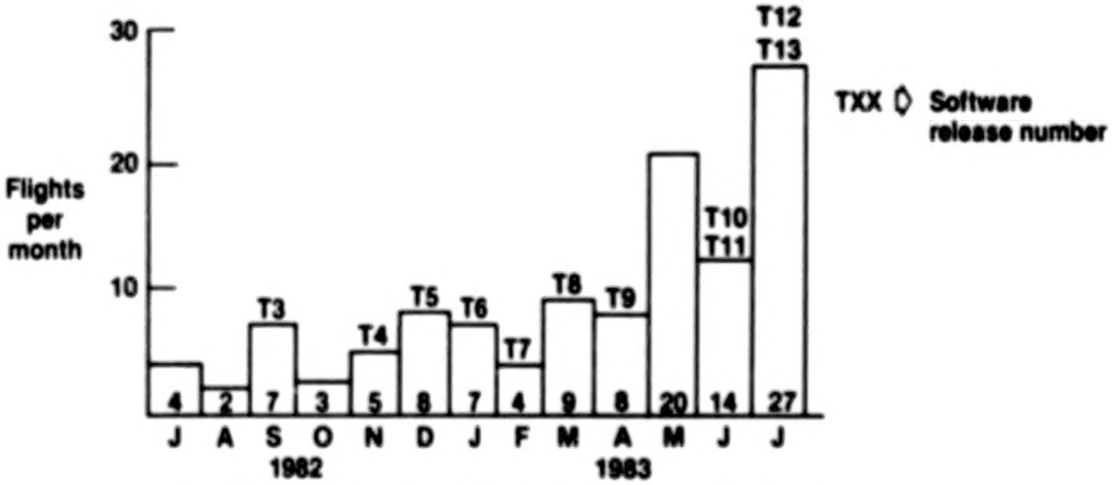

- 118 total flights by Air Force, NASA, Navy, and General Dynamics pilots
- Thirteen releases of flight control software
- Full envelope expansion of three separate flight control modes
- Air-to-air and air-to-ground mission evaluations of decoupled control options

FAULT TOLERANCE

Built-in test (BIT) is a highly automated test sequence that assures the digital flight control system (DFCS) is free of hardware failures prior to takeoff. BIT is run prior to each flight and takes approximately 2.5 min. Two failures of the hardware were detected by BIT during flight testing. The first was a failure of the flap actuator, the second involved memory chips which didn't meet timing specifications at cooler temperatures. Nuisance failures of BIT occurred a number of times. The cause is believed to be EMI.

In-flight fault detection is accomplished by comparing the three values for tracking among the different channels. The only real failure was an input signal which was traced to a pushed-back pin in the aircraft wiring. The 15 false failures were due to design deficiencies rather than actual hardware failures. The design deficiencies, which resulted in both temporary (resettable) and permanent loss of flight control redundancy, were corrected in subsequent software releases.

The asynchronous computer architecture affected a wide range of developmental activities including design, software/system qualification, and flight test operations. Initially DFCS qualification was not full proof because of the dependence of failure modes on computer skew. Testing at predetermined "worst case" computer skew improved testing results; however, some deficiencies still escaped detection. Ground operations during aircraft preflight were impacted by the asynchronous computer architecture. The most common problem resulted in DFCS failures, requiring reset by pilot or cycling of aircraft electrical power.

The false failures, not hardware induced, were the result of the design deficiencies associated with asynchronous computer operation. The design deficiencies resulted from the coupling of unique computer skews with characteristics of the flight environment, such as sensor noise. Undetected during qualification, these in-flight failures resulted in envelope and flight control mode limitations until they were corrected by software changes.

The software configuration control process details the procedures equivalent to the maintenance procedures for hardware, but in the software environment. Maintaining safe, operational software requires specification, design, test, and documentation for every change. Software change, specification, and time line for incorporation directly involved flight test planning. Testing and documentation provide details for operating characteristics and/or restrictions.

The 13 flight test software releases, in which design, coding, and test of the changes were performed at General Dynamics, Fort Worth, supported the needed changes for flight test. The first four releases provided full envelope capability for the AFTI vehicle in all flight control modes. The remaining nine releases modified the control system's control laws to improve flying qualities and the fault-detection function to improve reliability.

Software errors are software design or coding errors which escaped detection by the software verification and system validation testing. Two of the errors resulted from a loosening of the detailed established procedures. The third error was caused by a coding error involved in the correction of a previous false in-flight failure condition. The error was found when the in-flight failure condition recurred. It was found that the configuration control process provided excellent software operation in the face of constant change. The testing and documentation process, when strictly followed, will detect software design and coding errors.

Flight Test Results: Fault-Tolerant Design And Software Maintainability

Fault tolerance

- Built-in test
  - Comprehensive, automated 2-min preflight check
  - Some nuisance failures due to EMI
- In-flight fault detection
  - Fifteen false failures detected
  - Three failures, cause not known
  - One real failure detected
- Asynchronous computer operation, problems
  - Adversely affected DFCS qualification
  - Accomplice to in-flight failures

Software maintenance

- Software configuration control process
  - Details configuration/operating restrictions
  - Provides specification, design, test and documentation process
  - Interfaces to flight test planning
- Software changes, always
  - 129 total changes in 13 separate releases
  - Changes to both fault-tolerant/control-law designs
- Software errors occurred
  - Three errors found in flight releases
  - Process keeps serious errors from affecting flight operations

FLIGHT TEST RESULTS: CONTROL LAWS

A primary objective of the AFTI F-16 program was the evaluation of a multimode digital flight control system with decoupled aircraft control. The six different decoupled options and right-hand control options were evaluated with the decoupled feature best suited for a given task identified.

The adaptive control law, which uses pitch rate error to optimize performance in gross acquisition and fine tracking, was shown to be the best option for the air-to-air combat task. The adaptive gain control law was implemented using the right-hand controller; decoupled pointing with the pedals and twist grip showed no significant improvement for the air-to-air task.

The best feature for the air-to-ground task was again through the pitch stick with improved flight path stability and ride smoothness in turbulence. Direct side force or flat turn which is commanded through the rudder pedals improved the task by reducing pilot workload for obtaining lateral axis solutions. Problems with roll ratcheting affected all the advanced combat modes. Prefilter tuning was not sufficient to completely resolve the problem.

The standard normal mode, configured for gear-down, provided a greatly improved mode for power approach. Using more of a pitch-rate command system versus the normal acceleration command system on the F-16's, improvements in flight path and angle-of-attack stability were made.

The need for and design of the analog reversion mode to protect against common mode failures proved most interesting. Although the analog reversion mode (ARM) was never engaged because of digital system failure, flight test experience indicates ARMs are needed. Complexity of the ARM becomes a primary issue; a simple ARM cannot provide protection at envelope extremes which are possible with the digital systems. Furthermore, the relaxed static characteristic requires a certain level of augmentation. The simplified reversion mode used on AFTI provided get-home capability and level 2 flying qualities for landing as specified. However, simulation and flight test indicated a more capable ARM is needed to cover transitions from the envelope extremes possible with the digital control system (ref. 4).

Flight Test Results: Control Laws

- Air-to-air combat task
  - Longitudinal axis pitch stick control excellent based on adaptive, pitch rate error, gain system
  - Decoupled pointing showed no significant improvements for task completion
- Air-to-ground task
  - Longitudinal axis pitch stick control improved, better flight path stability/ride quality
  - Flat turn, direct side force useful, simplified task, reduced pilot workload
  - Roll ratcheting problem in all combat modes
- Power-approach task
  - Longitudinal axis control improvement over F-16, better flight path/angle-of-attack stability, precise attitude control
- Analog reversion mode
  - No automatic engagement of mode
  - Design of mode too simplified, reduced failure envelope, compromised flying qualities

FLIGHT TEST RESULTS: SUMMARY

Successful flight test accomplishments included envelope expansion for the primary flight control modes for stability and control and for structural loads. Envelope expansion included testing for low-speed, high-angle-of-attack, and high-speed-to-Mach-1.2 conditions. Evaluation of the advanced control modes, the final goal, was accomplished in the last 15 flights.

Advanced control options were evaluated in a variety of air-to-air and air-to-surface combat tasks. Advanced flight control modes for the right-hand controller gave the best performance of the decoupled control options; flat turn showed significant improvements over conventional control methods.

The asynchronous computer architecture proved to be one of the most interesting aspects of AFTI/F-16 because of its wide-ranging effects. The fact that a given architectural design feature can affect design, qualification, and flight test is noteworthy. Flight test was culminated with no fault-tolerant-type anomalies affecting flight test operations.

Representing a state-of-the-art, flight-crucial, highly integrated control system, AFTI provided the opportunity to find weaknesses in the developmental process resulting from the new technologies. Design and testing tools to support the development of increasing complex systems need to be developed. The goal is to develop tools which can support a generic set of digital control applications. Tools that assist in the design and testing of the fault-tolerant and software aspects of new highly integrated systems would prove beneficial.

- **Successful accomplishment of flight test goals**
- **Advanced control options improve aircraft performance**
- **Asynchronous computer architecture gave difficulties, costly**
- **Flight-crucial controls/integrated systems stress developmental process**

FUTURE CONSIDERATIONS

The AFTI F-16 program provided the engineering community another look at the development of a highly integrated flight-crucial system. Considerable knowledge was gained in the development and flight test of decoupled aircraft control, asynchronous computer operation, and flight-crucial software. As the dust settles and the results are reviewed, several areas for further consideration surface.

The time for a fault-tolerant system design tool has come. As any new technology begins to succeed and grow, design tools are needed to increase engineering productivity and provide better, safer product designs. Information exists to develop a design tool which documents fault-tolerant designs and allows for systematic test approaches that can increase operational reliability. The tool would allow for early integration of the fault-tolerant design with the control law functions to avoid costly downstream changes. The design tool would essentially be an expert system which would help guide the engineer in the specification, design, and qualification of a fault-tolerant design.

The development and the use of software and system-level testing tools also need to be applied to the development of flight-crucial controls. By increasing test coverage, automating the testing process, and providing integral configuration control, operational reliability and development time could both be improved.

Further consideration is also being given to the primary AFTI technologies. The use of AFTI flight control laws in an automated-flight fire control system is one example. Increasing weapon delivery accuracy while increasing aircraft survivability will be a primary emphasis of AFTI's second phase, Automated Maneuvering Attack System (AMAS).

- **Fault-tolerant design tool**
  - **– Design documentation**
  - **– Systematic testing capability**
  - **– Integration of control functions**
  - **– Architectural studies**
  - **– Expert system**
- **Software/system testing tools**
  - **– Increase/measure test coverage**
  - **– Automate testing process**
  - **– Provide configuration control**
- **Decoupled control in automated attack**
  - **Increase survivability**
  - **Weapon accuracy**

REFERENCES

1. Mackall, D.; Ishmael, S.; and Regenie, V.: Qualification of Flight Critical AFTI/F-16 Digital Flight Control System, AIAA Paper No. 83-0060, Jan. 1983.

2. Mackall, D.; Regenie, V.; and Gordoa, M.: Qualification of the AFTI/F-16 Digital Flight Control System, Paper presented at the IEEE National Aerospace and Electronics Conference NAECON, 1983, Dayton, Ohio, May 17-19, 1983.

3. Griswold, M. R.; Gordoa, M.; and Toles, R.: AFTI/F-16 DFCS Development Summary - A Report To Industry, Verification and Validation Testing. Proceedings of the IEEE 1983 National Aerospace and Electronics Conference NAECON 1983, vol. 2, 1983, pp. 1236-1240.

4. Ishmael, S.; Regenie, V.; and Mackall, D.: Design Implications From AFTI F-16 Flight Test, IEEE/AIAA 5th Digital Avionics Systems Conference, Seattle, WA, Oct. 31 - Nov. 3, 1983.

N84
20593

UNCLAS

N84 20593 D26

EXPERIENCES WITH THE DESIGN AND IMPLEMENTATION OF FLUTTER SUPPRESSION SYSTEMS

Jerry R. Newsom and Irving Abel
NASA Langley Research Center
Hampton, Virginia

First Annual NASA Aircraft Controls Workshop
NASA Langley Research Center
Hampton, Virginia
October 25-27, 1983

PRECEDING PAGE BLANK NOT FILMED

PAGE 2/88 INTENTIONALLY BLANK

ABSTRACT

A considerable amount of research has been conducted on the application of active controls to increase aircraft performance. Because of its impact on safety of flight, flutter suppression is probably the active controls concept furthest from practical implementation and, therefore, requires significant attention. This attention spans both analytical and experimental studies. Research efforts at NASA have been directed towards the development of analysis and design methodology and the correlation of experimental results with analytical predictions. The purpose of this paper is to discuss some experiences with the design and testing of several flutter suppression systems. Emphasis will be on the experimental activities.

ACTIVE CONTROLS TECHNOLOGY

The application of active controls technology (ACT) to reduce aeroelastic response of aircraft structures offers a potential for significant payoff in terms of aerodynamic efficiency and weight savings. To reduce the technical risk associated with this new technology, research was begun in the early 1970's to advance this concept. The technical program encompasses three areas: control law synthesis, aeroservoelastic analysis, and experiments aimed at verifying both the analysis and synthesis methodology. In the area of control law synthesis, classical methods are being applied where applicable. The latest "state-of-the-art" optimal methods are being refined and applied to the aeroservoelastic case. Innovative approaches are being developed to take highly theoretical synthesis methods which result in complex (high-order) control systems and modify these methods in the design of simpler (low-order) control systems. Strategies are being developed to investigate the sensitivity of the resulting control systems to uncertainty and to incorporate this knowledge into the design cycle. Analysis methods include a comprehensive program (DYLOFLEX) (ref. 1) for calculating the loads on an aeroelastic vehicle equipped with active controls. The evaluation of vehicle static and dynamic stability is being accomplished using programs and methods developed in-house at LaRC. The experimental program is aimed at validating the analysis and synthesis methods by comparison with wind tunnel tests and flight results using a remotely piloted drone. The flight test program, called DAST (Drones for Aerodynamic and Structural Testing) (ref. 2), has become the focal point of the experimental validation.

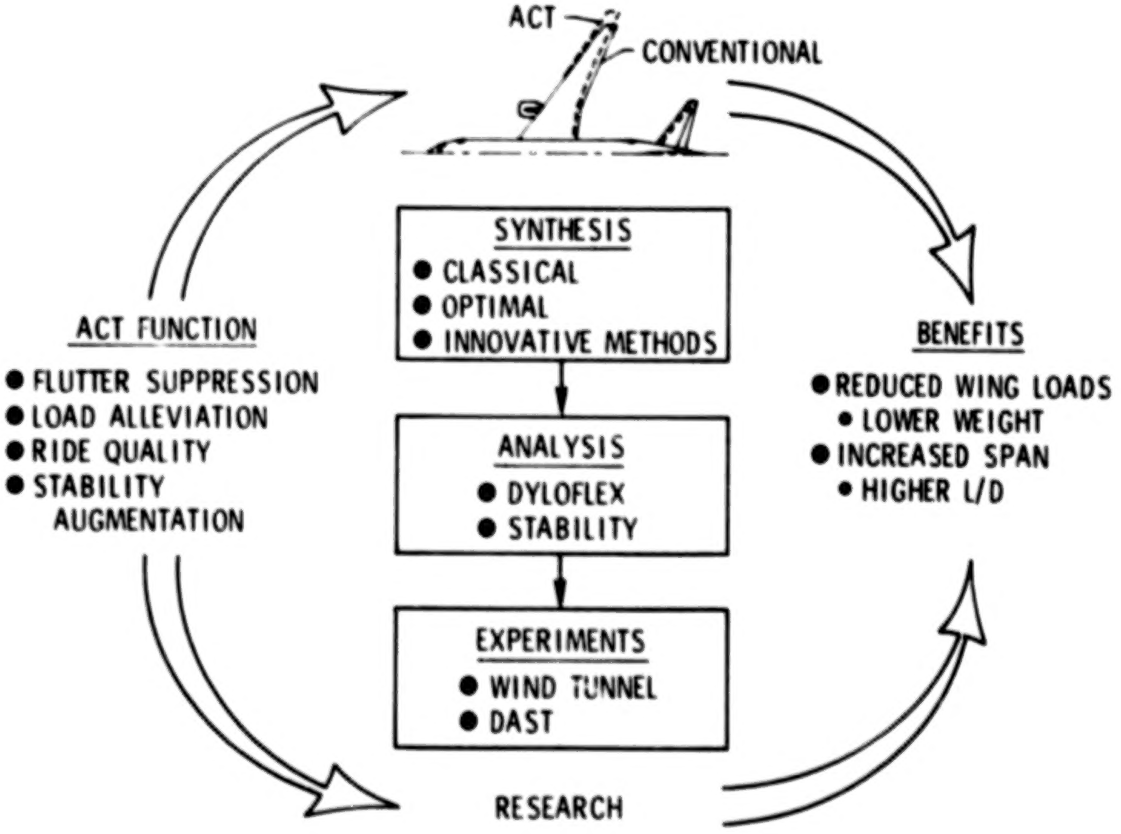
ACT
CONVENTIONAL
SYNTHESIS
● CLASSICAL
● OPTIMAL
● INNOVATIVE METHODS
ACT FUNCTION
● FLUTTER SUPPRESSION
● LOAD ALLEVIATION
● RIDE QUALITY
● STABILITY AUGMENTATION
BENEFITS
● REDUCED WING LOADS
• LOWER WEIGHT
● INCREASED SPAN
• HIGHER L/D
ANALYSIS
● DYLOFLEX
● STABILITY
EXPERIMENTS
● WIND TUNNEL
● DAST
RESEARCH

ACTIVE FLUTTER SUPPRESSION

Active flutter suppression is a concept to increase the flutter speed of a vehicle through the use of active feedback control. The active control system consists of (1) control surfaces, (2) sensors, and (3) control laws. Through proper selection of the control surfaces and sensors and design of the control laws, the damping of the aeroelastic system can be augmented and thereby increase the flutter speed. The benefit to be derived from flutter suppression is usually reduced structural weight.

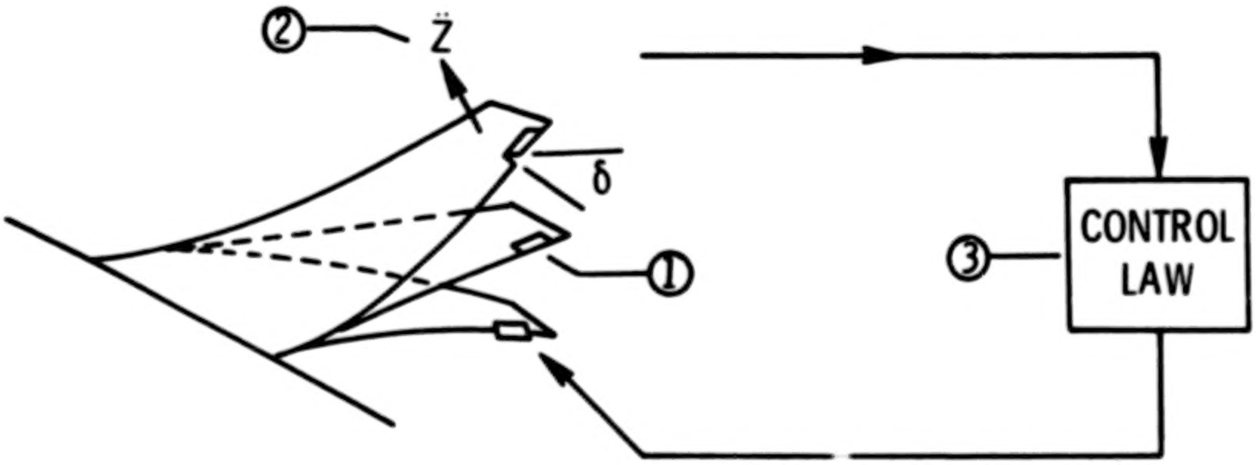

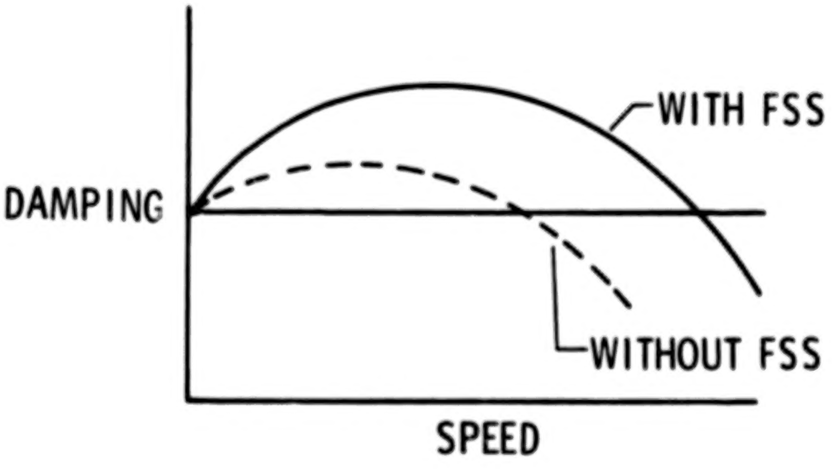

CONTROL LAW DESIGN PROCESS

The development of methodology to design flutter suppression systems has been an integral part of this research program. This development ranges from analytical synthesis techniques to the overall control law design process. A flowchart of the approach to the overall control law design process is shown below. The first element of the process is the selection of design objectives (i.e., gain margin, phase margin, etc.). The second element is the selection of a design point (i.e., Mach number and altitude). Control law synthesis is then performed at the design point. The next element, analysis, provides information on the performance of the control law at off-design flight conditions. If the design objectives at the off-design flight conditions are not met, then a gain scheduler which may be a function of Mach number and/or dynamic pressure is evaluated. If a gain scheduler will not meet the design objectives, then a path back to control law synthesis is selected.

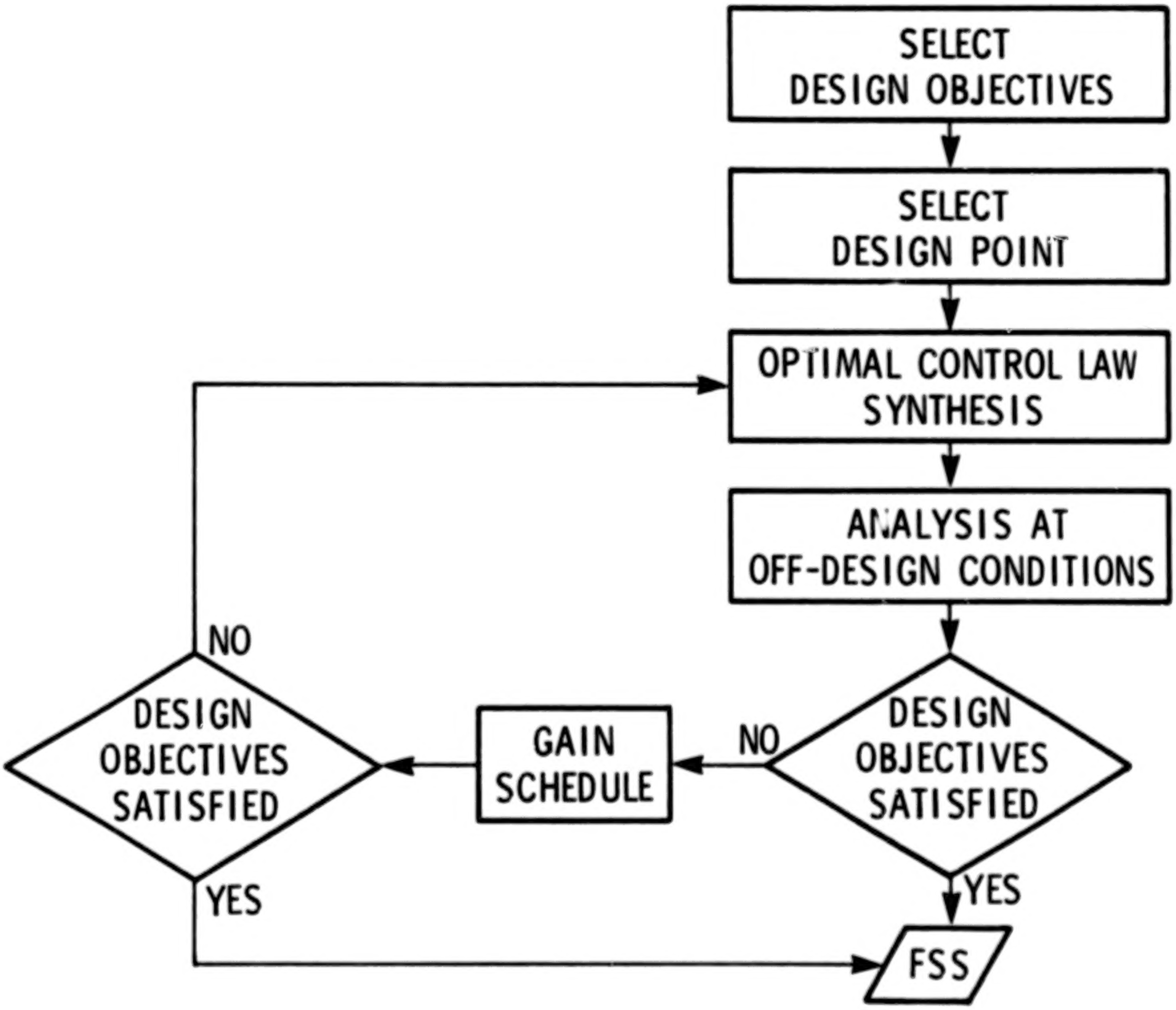
SELECT DESIGN OBJECTIVES
SELECT DESIGN POINT
OPTIMAL CONTROL LAW SYNTHESIS
ANALYSIS AT OFF-DESIGN CONDITIONS
DESIGN OBJECTIVES SATISFIED
NO
YES
GAIN SCHEDULE
DESIGN OBJECTIVES SATISFIED
NO
YES
FSS

CONTROL LAW SYNTHESIS

The major emphasis in the development of design methodology has been in the area of control law synthesis. To accomplish the objectives of control law synthesis, as stated below, the practical problems in control law implementation must be recognized. The historical development of control law synthesis methodology has proceeded from classical techniques to optimal control theory to optimization techniques (refs. 3-8). Both unconstrained and constrained optimization techniques have been evaluated. Beginning recently, emphasis is being given to the use of constrained optimization techniques since several design objectives can then be satisfied simultaneously.

- OBJECTIVE:
    - DESIGN A LOW-ORDER CONTROL LAW FOR A HIGH-ORDER SYSTEM TO MEET SEVERAL DESIGN OBJECTIVES
    - LOW ORDER → SIMPLE IMPLEMENTATION
HIGH ORDER → CHARACTERISTIC OF AEROELASTIC SYSTEMS
- METHODOLOGY DEVELOPMENT
    - CLASSICAL TECHNIQUES
    - OPTIMAL CONTROL THEORY/ORDER REDUCTION
    - OPTIMIZATION TECHNIQUES
        - UNCONSTRAINED OPTIMIZATION
        - CONSTRAINED OPTIMIZATION

WIND TUNNEL STUDIES

Wind tunnel studies of aeroelastic models have been a cornerstone of the NASA research program. Presented in this chart are a number of models that have been used to demonstrate active control concepts on a variety of configurations. The Delta-wing model was an early experimental demonstration of flutter suppression (ref. 9). The B-52 model was tested in support of a USAF/Boeing flight study on active controls (ref. 10). Wing load alleviation was studied in support of a USAF/Lockheed program using a C-5A model (ref. 11). The DAST ARW-1 model was used for a variety of flutter suppression studies including an evaluation of a control system that would ultimately be tested on a remotely piloted research flight vehicle. Control laws were synthesized and tested on the model using classical, aerodynamic energy, and optimal methods (ref. 12). The F-16 and YF-17 model tests have shown active flutter suppression to be a promising method for preventing wing/external store flutter (refs. 13 and 14). Use of active controls is especially attractive for fighters because of the multitude of possible store configurations. These studies are part of an Air Force Flight Dynamics Laboratory/General Dynamics/Northrop/NASA cooperative effort. A cooperative effort was also conducted with the McDonnell Douglas Corporation on a DC-10 derivative wing. Increases in flutter speeds in excess of 26 percent were demonstrated. This study is reported in reference 15.

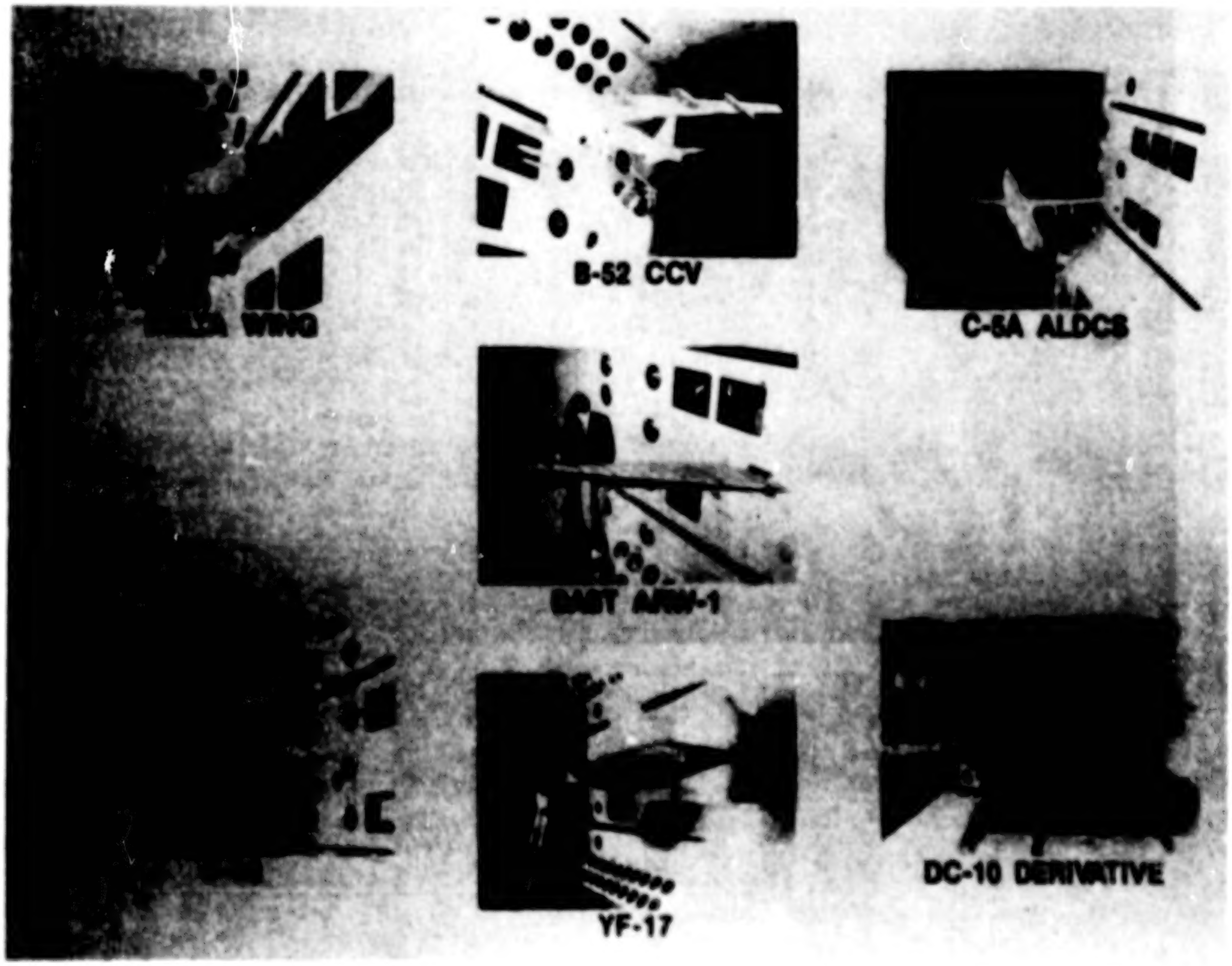

DELTA-WING MODEL

Experimental studies have made a major contribution to the active control technology program developed at NASA. The Delta-wing model (whose photograph is in this chart) was the first experimental demonstration of flutter suppression in this country (ref. 9). At a Mach number of 0.9, increases in the flutter dynamic pressure ranging from 12.5 percent to 30 percent were demonstrated with active controls. One of the major contributions of this wind tunnel program was the development of miniature hydraulic actuators. These actuators paved the way for future wind tunnel tests of aeroelastically scaled models. To evaluate the performance of an active flutter suppression (AFS) system, subcritical response techniques must be employed. Three different methods were used to determine subcritical response of the Delta-wing model, and the results are described in reference 9. Analytical methods were used to predict both open-loop and closed-loop stability, and the results agreed reasonably well with the experiment. However, for the closed-loop case, it was necessary to use a control surface aerodynamic correction factor that was derived using measured hinge moment data.

DAST MODEL

The aeroelastic model used for this study was originally built to support the DAST flight program (ref. 2). The objective of the wind tunnel study was to demonstrate a 44-percent increase in flutter dynamic pressure. Two control laws were designed (ref. 12). One control law was based on the aerodynamic energy method, and the other was based on the results of optimal control theory. At Mach 0.95, a 44-percent increase in flutter dynamic pressure was achieved with both control laws, thereby validating the two synthesis methodologies. Experimental results indicated, however, that the performance of the systems was not as good as that predicted by analysis. The results also indicated that wind tunnel turbulence is an important factor in both control law synthesis and experimental demonstration.

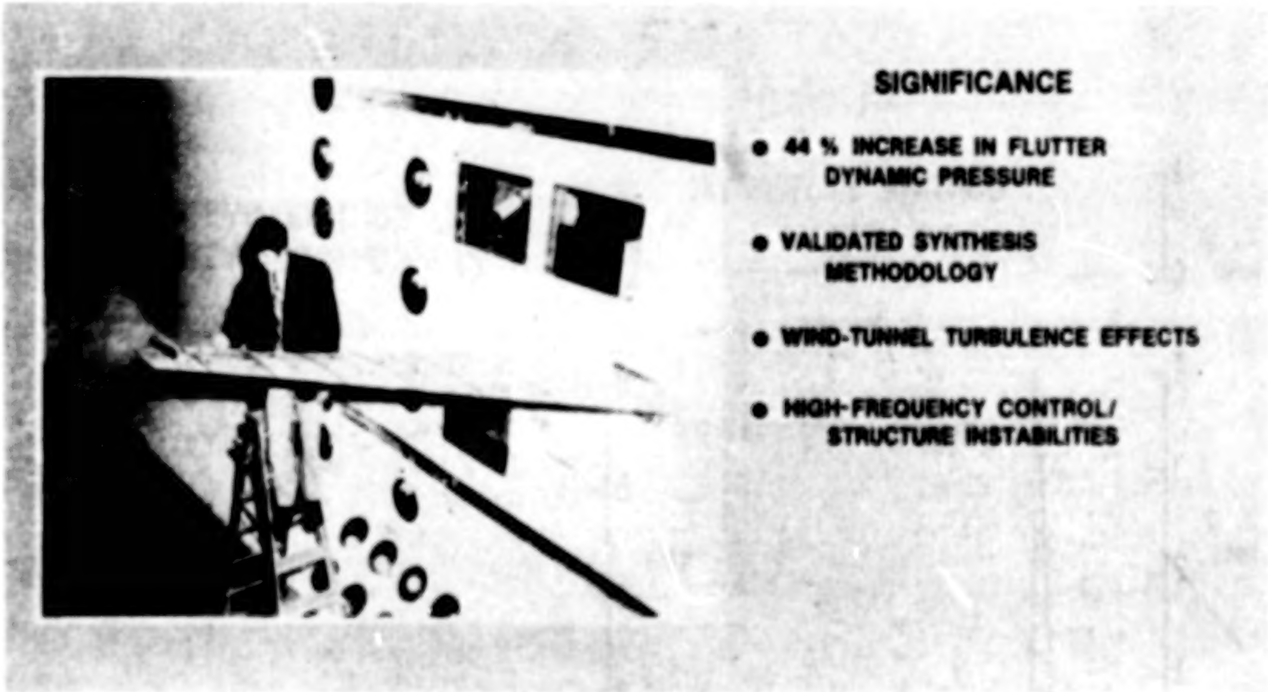

SIGNIFICANCE

- 44 % INCREASE IN FLUTTER DYNAMIC PRESSURE
- VALIDATED SYNTHESIS METHODOLOGY
- WIND-TUNNEL TURBULENCE EFFECTS
- HIGH-FREQUENCY CONTROL/ STRUCTURE INSTABILITIES

CONTROL LAW PERFORMANCE

An illustration of flutter suppression performance for the DAST model is shown below. On the left, the spectrum of outboard peak accelerations for the wing with system off is compared to that for the system on. The model was being excited by tunnel turbulence. The data were measured at a dynamic pressure just below the system-off flutter boundary at M = 0.90. The decrease in amplitude and shift in the maximum response frequency resulting from the control law is evident. Also presented is a plot of flutter dynamic pressure as a function of Mach number. Data for both system off and system on are shown. The flutter suppression system is most effective (i.e., provides the largest increase in flutter dynamic pressure) at the higher Mach numbers. The effectiveness is significantly reduced at lower Mach numbers. A discussion of these results is given in reference 12.

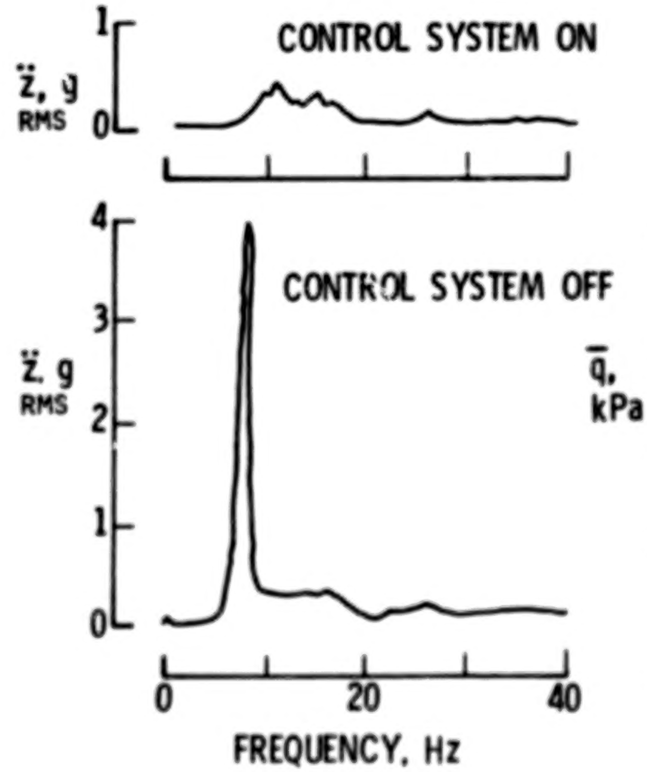

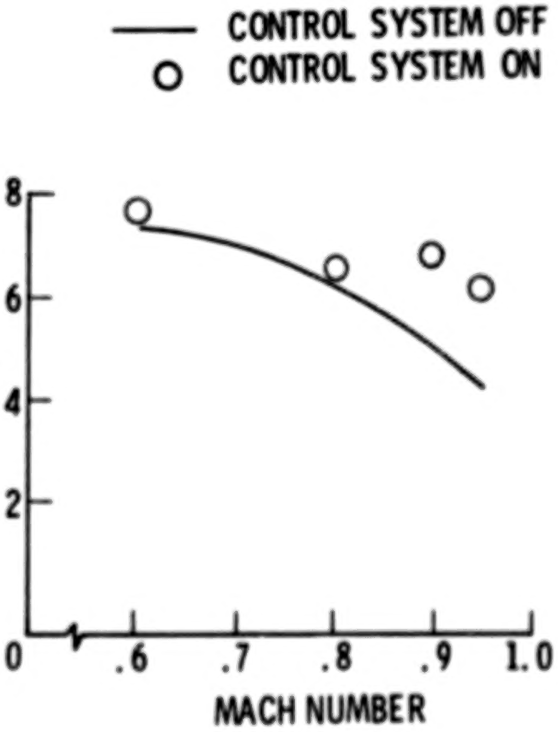

DC-10 MODEL

A cooperative study was conducted with the Douglas Aircraft Company to apply control law design methods developed by NASA to a realistic transport configuration and to provide a rapid transfer of research technology to industry. These studies were an extension of previous wind tunnel tests performed by Douglas (ref. 16). The aeroelastic model (shown in the photograph on this chart) is representative of a wing which has a 4.27-m-span increase over the standard DC-10 wing.

Two control laws were designed at NASA Langley using different design methods (ref. 15). Both control laws resulted in a 59-percent increase in flutter dynamic pressure. The performance of the control laws as a function of gain and phase was also evaluated. Calculations performed prior to wind tunnel testing predicted all experimental trends. During the wind tunnel tests, both structural damping and phase characteristics of the actuator were identified as very important factors related to the effectiveness of the control laws. In addition, a correction factor was used to account for control surface effectiveness and did improve the correlation between measured and predicted characteristics.

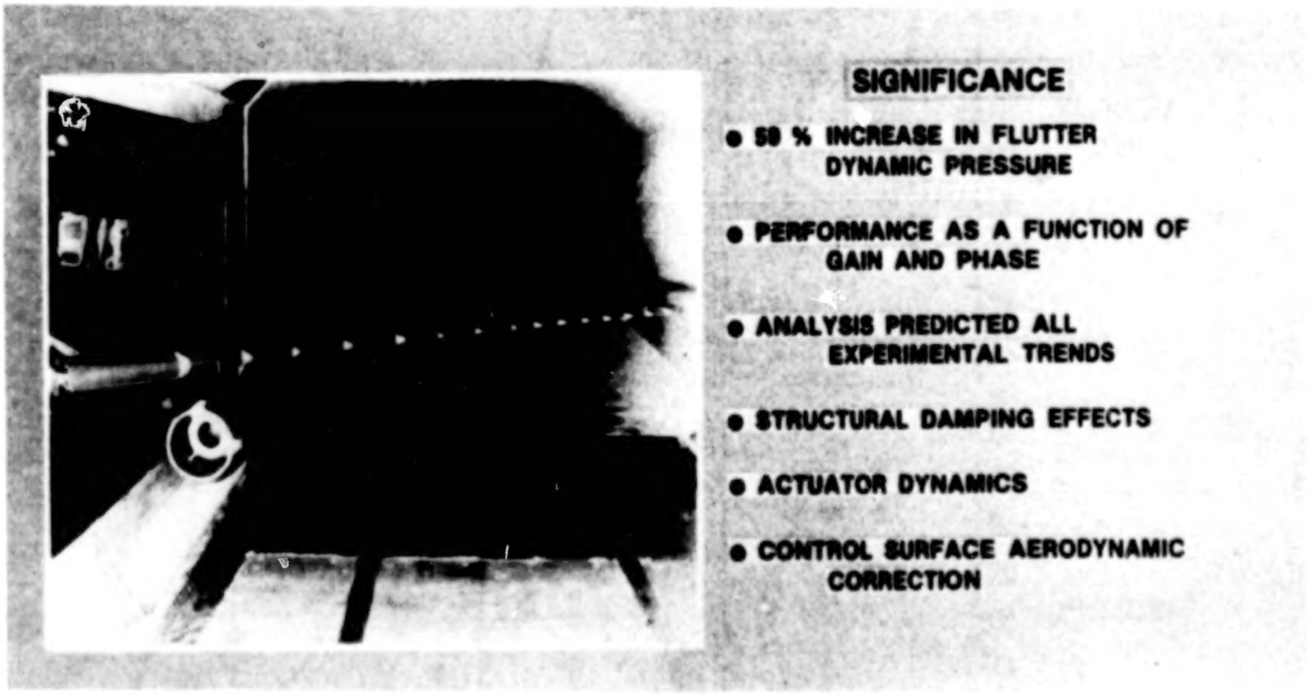

SIGNIFICANCE

- 59 % INCREASE IN FLUTTER DYNAMIC PRESSURE
- PERFORMANCE AS A FUNCTION OF GAIN AND PHASE
- ANALYSIS PREDICTED ALL EXPERIMENTAL TRENDS
- STRUCTURAL DAMPING EFFECTS
- ACTUATOR DYNAMICS
- CONTROL SURFACE AERODYNAMIC CORRECTION

MEASURED AND PREDICTED STABILITY BOUNDARIES AS A FUNCTION OF SYSTEM GAIN AND PHASE FOR DC-10 WIND TUNNEL MODEL

Measured and predicted stability boundaries in terms of flutter velocity versus system gain and phase are presented below. Three or four distinct flutter modes are exhibited, depending on phase angle. For all phase angles analyzed, a decrease in flutter velocity is shown for mode 3 at low values of gain. At negative phase angles, the reduction in flutter velocity is more pronounced. The velocity at which mode 8 goes unstable is nearly independent of system gain and phase. The mode 4 instability is aggravated by negative phase angles and stays relatively fixed for positive phase angles. At phase angles of +20° and above, a new flutter mode resulting from a coupling between the feedback filter mode and the first wing bending mode becomes critical. A detailed discussion of these results can be found in reference 15.

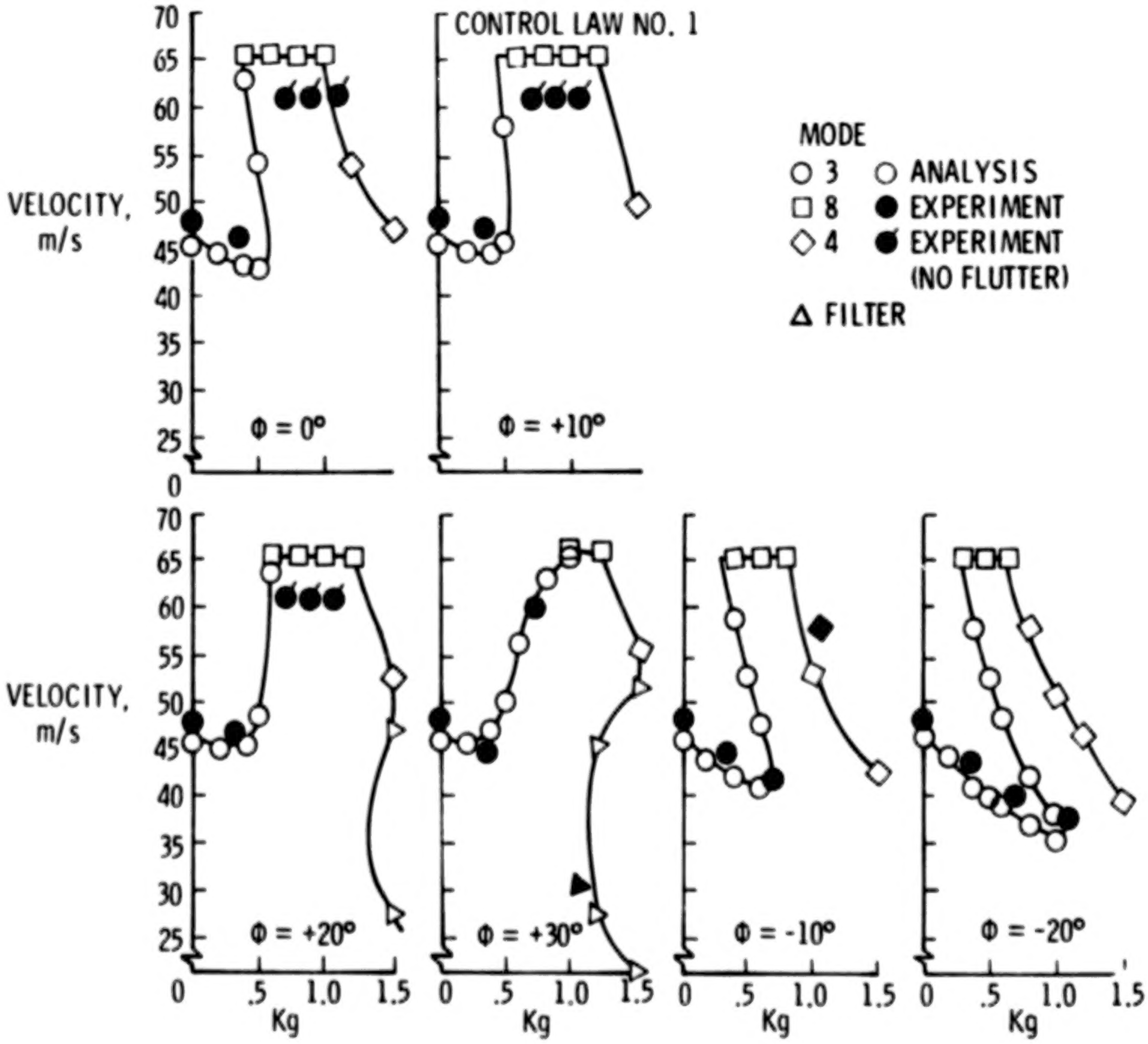

DAST: WHAT IS IT?

The concept of the DAST program (ref. 2) is to provide a focus for evaluation and improvement of synthesis and analysis procedures for aerodynamic loads prediction and design of active control systems on wings with significant aeroelastic effects. Major challenges include applications to wings with supercritical airfoil and tests emphasizing the transonic speed range. The program requires complete solutions to real-world problems since research wings are fabricated and flight tested. Because of the risky nature of the flight testing, especially with regard to flutter, target drone aircraft are modified for use as test bed aircraft.

PRINCIPAL RESEARCH AREAS

- ACTIVE CONTROL SYSTEMS EVALUATIONS
- AERODYNAMIC LOADS MEASUREMENT
- STRUCTURAL INVESTIGATIONS
- STABILITY AND PERFORMANCE STUDIES

EMPHASIS

- TRANSONIC REGION
- AEROELASTIC EFFECTS

ORIGINAL PAGE IS
OF POOR QUALITY

DAST: HOW DO WE DO IT?

DAST uses an Air Force version of the Firebee II target drone as the basic test bed. The standard Firebee wing is removed and replaced with the research wing of interest. The operational sequence, as depicted in this chart, involves an air launch from beneath the wing of a carrier aircraft; a free-flight test phase of between 20 and 40 minutes (depending on Mach number and altitude); followed by a mid-air retrieval by helicopter via a parachute recovery system. During the free-flight phase, a test pilot controls the vehicle from a ground cockpit. An F-104 aircraft is used as chase, and the copilot of this aircraft serves as a backup flight controller for the drone in case of a malfunction with the uplink system. Data from the experiments are provided in real time to the ground by means of a pulse-code-modulated telemetry system. Experimenters provide real-time assessments of the status of the research wing and its associated active control systems. This assessment is based on the response of the wing to control surface sweeps and pulses. Flight tests are performed at the NASA Dryden Flight Research Facility located at Edwards Air Force Base, California.

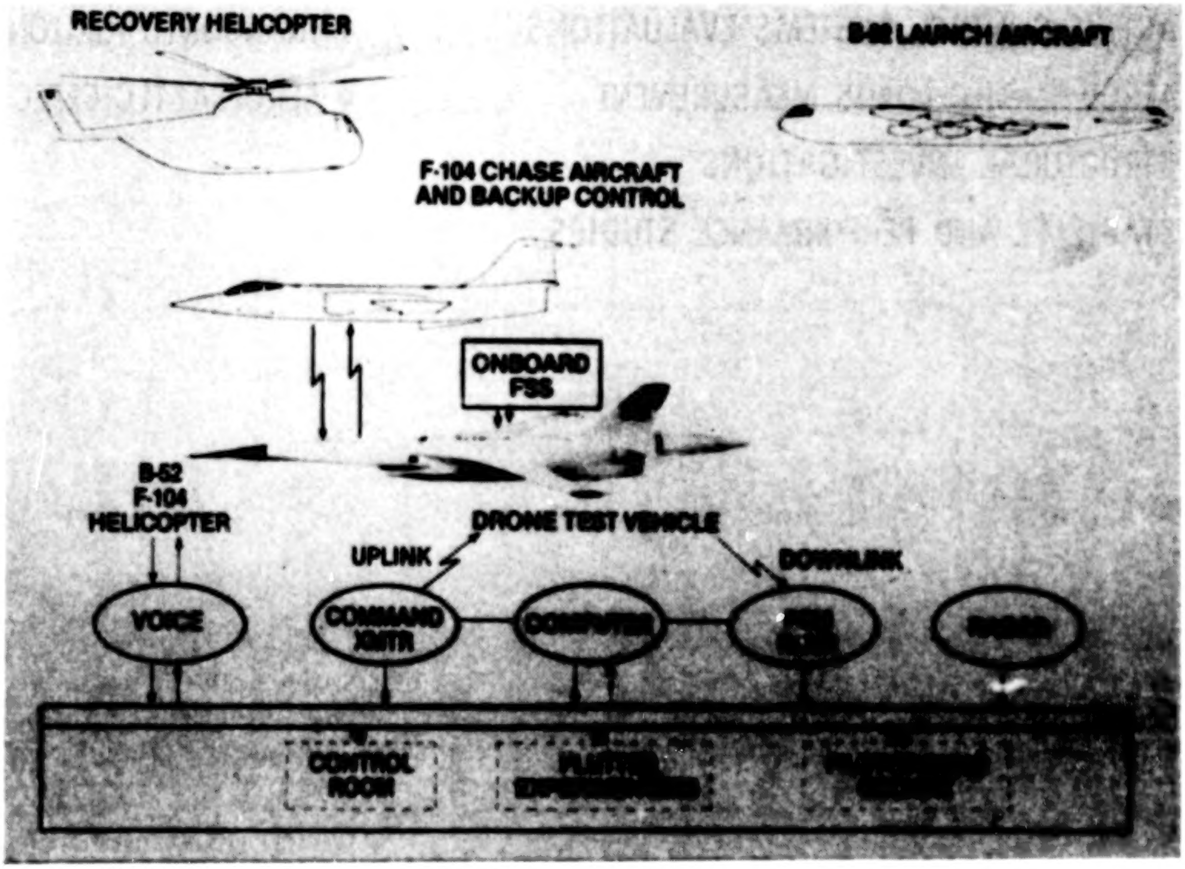
RECOVERY HELICOPTER
B-52 LAUNCH AIRCRAFT
F-104 CHASE AIRCRAFT
AND BACKUP CONTROL
ONBOARD
FSS
B-52
F-104
HELICOPTER
DRONE TEST VEHICLE
UPLINK
DOWNLINK
VOICE
COMMAND
XMTR
COMPUTER
RADAR
CONTROL
ROOM
FLUTTER
EXPERIMENTERS

DAST: WHAT ARE WE DOING IT WITH?

Two transport-type research wings have been built for flight testing. The first wing, Aeroelastic Research Wing No. 1 (ARW-1), was designed for M = 0.98 cruise and was purposely designed to flutter within the flight envelope. Tests of the first research wing configuration have been terminated due to loss of the aircraft resulting from vehicle systems problems. However, valuable flutter data and test technique experience were acquired. References 17-20 provide a description of these results.

The wing fabrication and test planning for the second research wing (ARW-2) have been sponsored by the NASA Aircraft Energy Efficiency program. This design involved what is believed to be the first exercise of an iterative procedure integrating aerodynamics, structures, and controls technologies in a design loop resulting in flight hardware. Evaluation of multiple active controls systems operating simultaneously, the operation of which is necessary to preserve structural integrity for various flight conditions, is the primary objective of the flight tests on this fuel-conservative-type research wing.

DAST RESEARCH WINGS

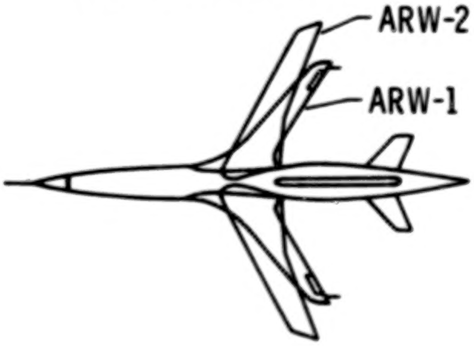

ARW-1

- FLUTTER WITHIN FLIGHT ENVELOPE
- ACTIVE FLUTTER SUPPRESSION SYSTEM
- SUPERCRITICAL AIRFOIL

ARW-2

- FUEL CONSERVATIVE WING DESIGN
  - HIGH ASPECT RATIO (AR = 10.3)
  - LOW SWEEP ($\Lambda = 25°$)
  - ADVANCED SUPERCRITICAL AIRFOIL
- MULTIPLE ACTIVE CONTROLS CRITICAL TO FLIGHT OPERATION
  - FSS
  - MLA
  - GLA
  - RSS

CORRELATION OF MEASURED AND PREDICTED DAMPING AND FREQUENCY VARIATIONS (ARW-1)

The frequency and damping of the dominant mode for the symmetric case are shown below. The analysis and flight test data are for a test altitude of 4.56 kilometers. The change in frequency with Mach number is predicted well for both the FSS-off and FSS-on cases. However, analysis overpredicts the damping for both the FSS-off and FSS-on cases. The experimental flutter speed is extrapolated to be approximately M = 0.80 for the FSS-off case. An actual flutter point was encountered for the FSS-on case at M = 0.82. Other data comparisons can be found in reference 17.

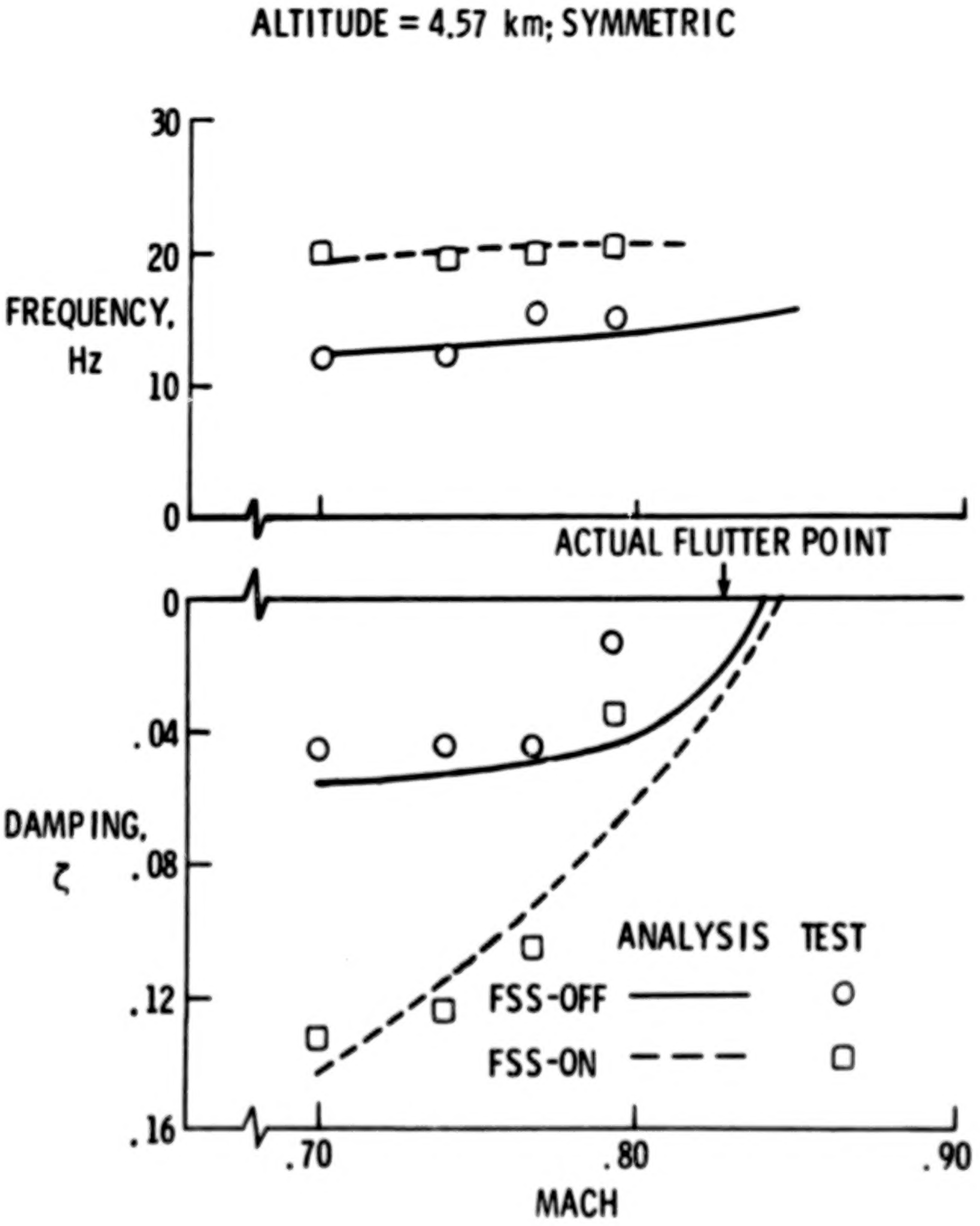

ORIGINAL PAGE IS
OF POOR QUALITY

ARW-2 RIGHT SEMISPAN IN LAB PRIOR TO WIND TUNNEL TESTING

The ARW-2 wing panels have been fabricated and are being used to support two ground tests. The left semispan has been used to conduct a hardware-in-the-loop test of the active control system electronics. The right semispan shown in the photograph below has been tested in the Langley Transonic Dynamics Tunnel to obtain unsteady pressure distributions. This is believed to be the first measurement of unsteady pressures on a flexible supercritical wing. The pressure measurements from the wind tunnel will be compared against those measured during the flight tests. A secondary objective of the wind tunnel test is to investigate possible angle-of-attack effects on the flutter boundary at high transonic speeds.

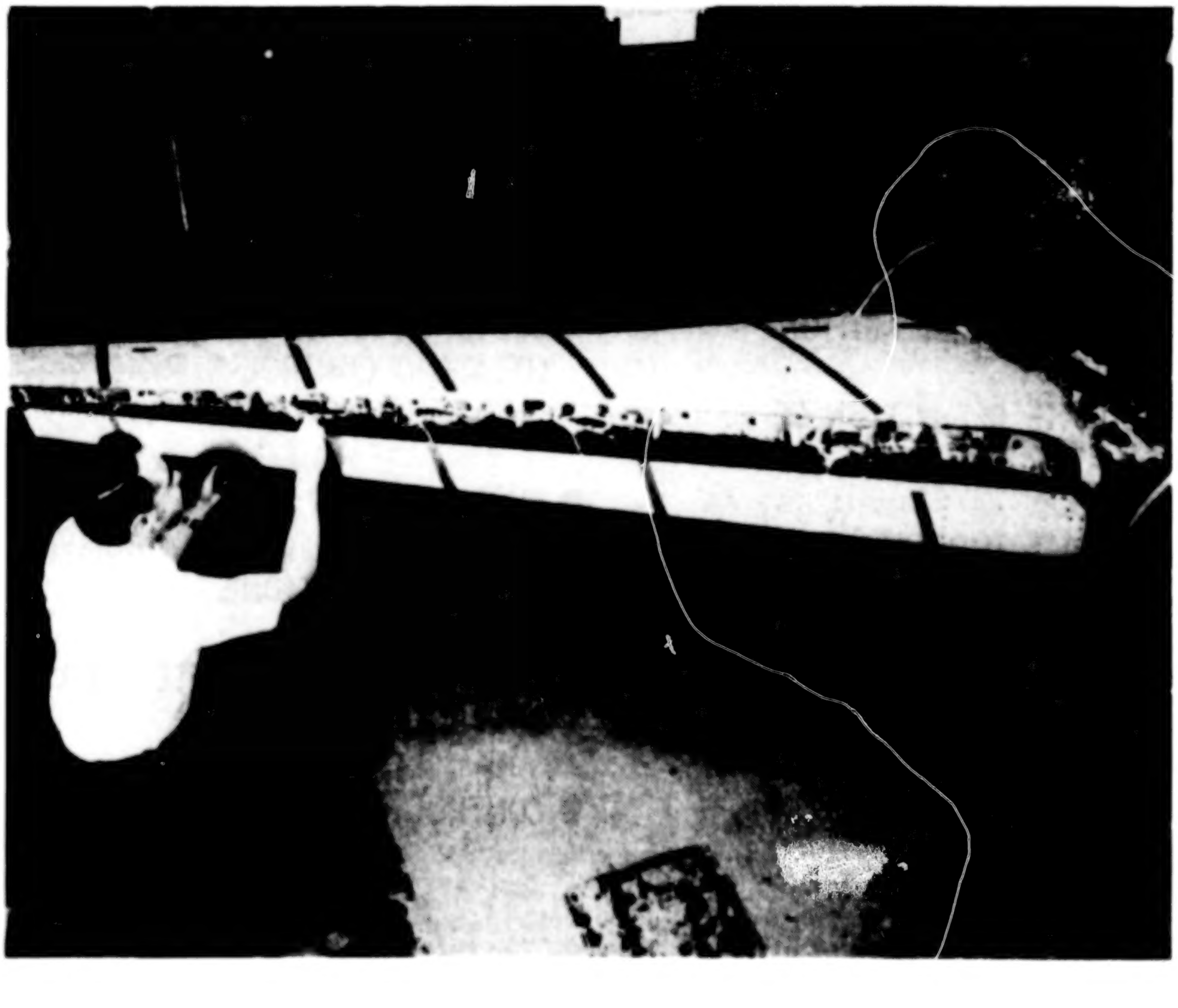

CONCLUSIONS

A large amount of expertise has been acquired through the analytical and experimental studies conducted to date. Many lessons have been learned that help guide the future research directions. A few of these lessons are shown below. The first three lessons are technical in nature and have been or are presently receiving attention. However, even though the last lesson is nontechnical in nature, it certainly needs to receive more attention. Several of the future thrusts listed below are being researched at the present. These include the use of transonic time plane unsteady aerodynamics, applying flutter suppression methodology to other active control functions, and synthesis of multiple active control systems. The other thrusts are not presently being emphasized but are still on the list of future work.

LESSONS LEARNED

- UNSTEADY AERO THEORY NEEDS
  - CONTROL SURFACE
  - ARBITRARY MOTION
- ACCURATE DEFINITION OF ACTUATOR DYNAMICS
- ACCURATE TURBULENCE MODEL
- CLOSER COOPERATION BETWEEN AEROELASTICIAN AND CONTROLS ANALYST

FUTURE THRUSTS

- TRANSONIC TIME PLANE UNSTEADY AERO
- SYSTEMATIC METHODS FOR LOCATING CONTROL SURFACES AND SENSORS
- APPLY FLUTTER SUPPRESSION METHODOLOGY TO OTHER ACTIVE CONTROL FUNCTIONS
- SYNTHESIS OF MULTIPLE ACTIVE CONTROL SYSTEMS
- CONTROL CONFIGURED VEHICLES

REFERENCES

1. Perry, B. III; Kroll, R. I., Miller, R. D.; and Goetz, R. C.: DYLOFLEX: A Computer Program for Flexible Aircraft Flight Dynamic Loads Analyses With Active Controls. J. Aircraft, Vol. 17, No. 4, April 1980, pp. 275-282.

2. Murrow, H. N.; and Eckstrom, C. V.: Drones for Aerodynamic and Structural Testing (DAST)--A Status Report. J. Aircraft, Vol. 16, No. 8, August 1979, pp. 521-526.

3. Newsom, J. R.: A Method for Obtaining Practical Flutter Suppression Control Laws Using Results of Optimal Control Theory. NASA TP 1471, Aug. 1979.

4. Gangsaas, Dagfinn; and Ly, Vy-Loi: Application of a Modified Linear Quadratic Gaussian Design to Active Control of a Transport Airplane. AIAA Paper No. 79-1746, August 1979.

5. Mahesh, J. K.; Stone, C. R.; Garrard, W. L.; and Hausman, P. D.: Active Flutter Control for Flexible Vehicles. NASA CR-159160, Nov. 1979.

6. Nissim, E.; and Abel, I.: Development and Application of an Optimization Procedure for Flutter Suppression Using the Aerodynamic Energy Concept. NASA TP 1137, Feb. 1978.

7. Mukhopadhyay, V.; Newsom, J. R.; and Abel, I.: A Method for Obtaining Reduced Order Control Laws for High Order Systems Using Optimization Techniques. NASA TP 1876, 1981.

8. Newsom, J. R.; and Mukhopadhyay, V.: Application of Constrained Optimization to Active Control of Aeroelastic Response. NASA TM 83150, June 1981.

9. Sandford, M. C.; Abel, I.; and Gray, D. L.: Development and Demonstration of a Flutter Suppression System Using Active Controls. NASA TR 450, December 1975.

10. Redd, L. T.; Gilman, J., Jr.; Cooley, D. E.; and Sevart, F. D.: A Wind Tunnel Study of B-52 Model Flutter Suppression. AIAA Paper No. 74-401, April 1974.

11. Doggett, R. V., Jr.; Abel, I.; and Ruhlin, C. L.: Some Experiences Using Wind Tunnel Models in Active Control Studies. NASA TM X-3409, August 1976, pp. 831-892.

12. Newsom, J. R.; Abel, I.; and Dunn, H. J.: Application of Two Design Methods for Active Flutter Suppression and Wind Tunnel Test Results. NASA TP 1653, May 1980.

13. Peloubet, R. P., Jr.; Haller, R. L.; and Bolding, R. M.: F-16 Flutter Suppression System Investigation. AIAA Paper No. 80-0768, May 1980.

14. Hwang, C.; Johnson, E. H.; and Pi, W. S.: Recent Developments of the YF-17 Active Flutter Suppression System. AIAA Paper No. 80-0769, May 1980.

15. Abel, I.; and Newsom, J. R.: Wind Tunnel Evaluation of NASA-Developed Control Laws for Flutter Suppression on a DC-10 Derivative Wing. AIAA Paper No. 81-0639, April 1981.

16. Winther, B. A.; Shirley, W. A.,; and Heimbough, R. M.: Wind Tunnel Investigation of Active Controls Technology Applied to a DC-10 Derivative. AIAA Paper No. 80-0771, May 1980.

17. Newsom, Jerry R.; and Pototzky, Anthony S.: Comparison of Analysis and Flight Test Data for a Drone Aircraft with Active Flutter Suppression. AIAA Paper No. 81-0640, April 1981.

18. Edwards, J. W.: Flight Test Results of an Active Flutter Suppression System Installed on a Remotely-Piloted Research Vehicle. AIAA Paper No. 81-0655, April 1981.

19. Bennett, R. M.; and Abel, I.: Application of a Flight Test and Data Anaysis Technique to Flutter of a Drone Aircraft. AIAA Paper No. 81-0652, April 1981.

20. Newsom, Jerry R.; Pototzky, Anthony S.; and Abel, Irving: Design of the Flutter Suppression System for DAST ARW-1R - A Status Report. NASA TM 84642, March 1983.

SESSION V

RESEARCH OPPORTUNITIES FOR THE FUTURE

Duncan E. McIver
Moderator

N84
20594

UNCLAS

N84 20594 D27

RESEARCH OPPORTUNITIES FOR FUTURE COMMERCIAL TRANSPORTS

J. F. Longshore
Douglas Aircraft Company
Long Beach, California

First Annual NASA Aircraft Controls Workshop
NASA Langley Research Center
Hampton, Virginia
October 25-27, 1983

PRECEDING PAGE BLANK NOT FILMED

PAGE 510 INTENTIONALLY BLANK

ORIGINAL PAGE IS
OF POOR QUALITY

MD-100 COCKPIT

This photo of one of the MD-100 flight deck configurations being discussed with the airlines illustrates the flexibility in display formats afforded by today's CRT technology. All of the formats shown can be extensively tailored to phase of flight and aircraft configuration and can be configured to provide unique data to the flight crews for special situations.

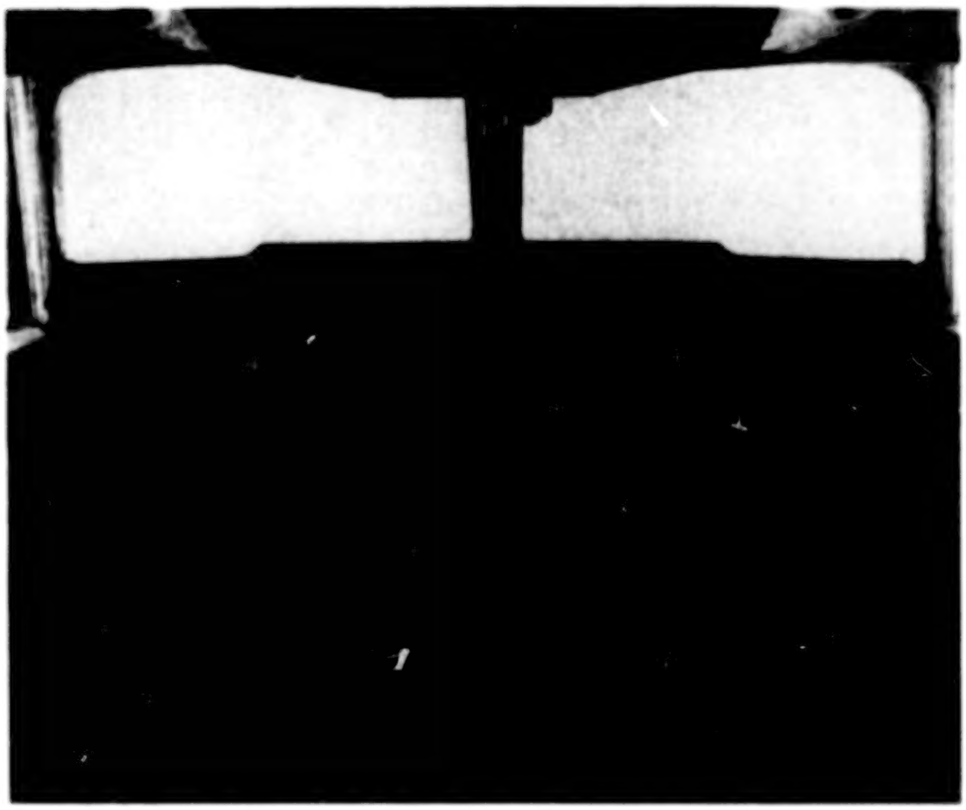

MD-100 PRIMARY FLIGHT DISPLAY

This photo illustrates the typical primary flight display format. Note that this display includes all air data, flight control system mode annunciation, radio altitude and decision height, as well as the traditional attitude director functions. The navigation display on an adjacent CRT is typical of those found in recently certified flight management systems.

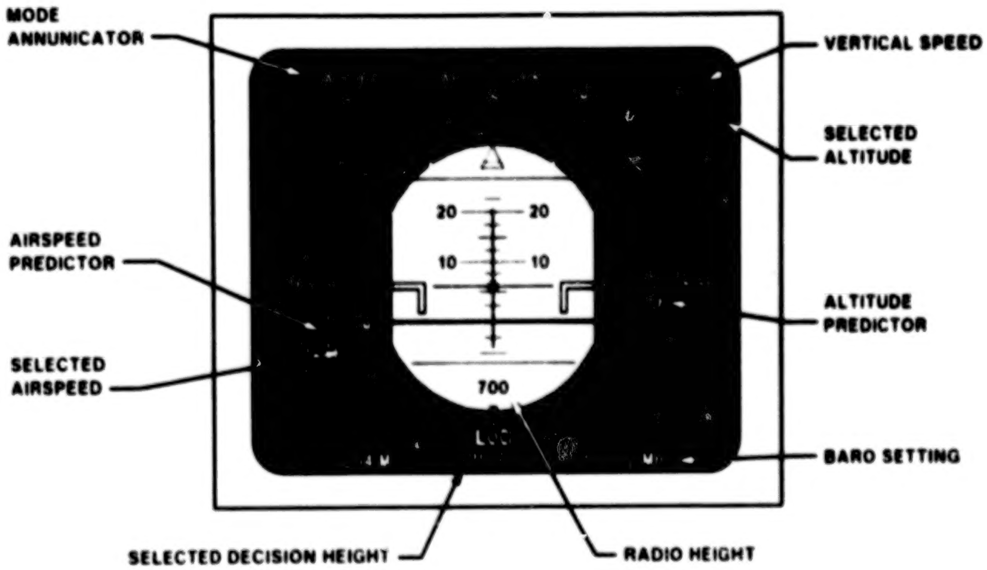
MODE ANNUNICATOR
VERTICAL SPEED
SELECTED ALTITUDE
AIRSPEED PREDICTOR
20
20
10
10
ALTITUDE PREDICTOR
SELECTED AIRSPEED
700
LOC
BARO SETTING
SELECTED DECISION HEIGHT
RADIO HEIGHT

ORIGINAL PAGE IS
OF POOR QUALITY

MD-100 MULTIFUNCTION DISPLAYS

These display formats are typical of the MD-100 subsystem displays. A synoptic system display is used for the fuel, pneumatic, electrical, and hydraulic systems. These can be called up by the crew. Color and symbology changes are used in the synoptics to identify system configuration and annunciate system failures.

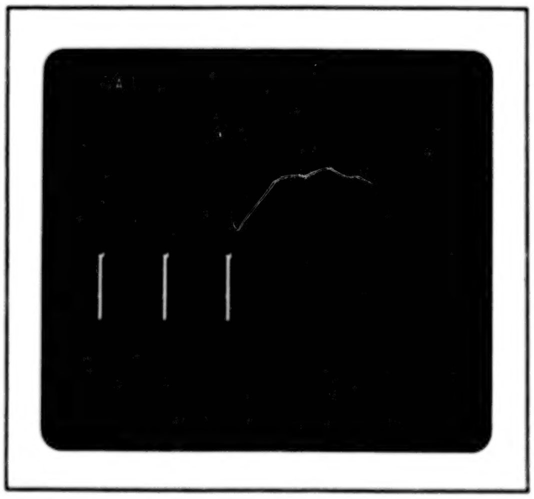

ENGINE PARAMETERS IN MFD 1

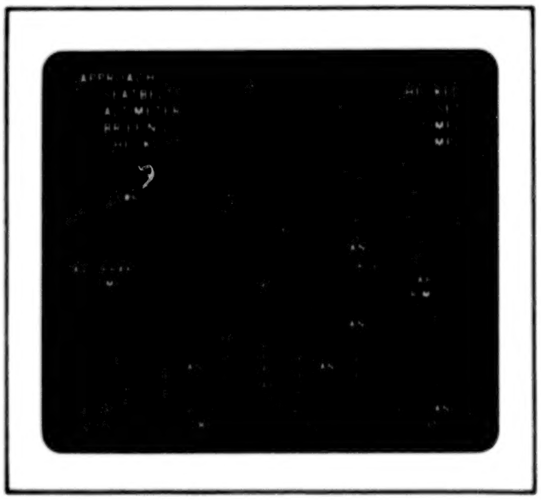

PHASE-OF-FLIGHT DISPLAY IN MFD 2

FLIGHT DECK/FLIGHT CONTROL SYSTEM CONCEPTS

- The objective of the ongoing NASA fault-tolerant architectural studies is to identify architectural concepts that have sufficient reliability for full-time fly-by-wire applications. Additional effort will be required to develop the methodology and criteria to be used in certifying such systems. NASA would function as the facilitating agency working with the air transport community and the FAA to define these methods and criteria.

- The impact of failures and the appropriate corrective action in future highly integrated fault-tolerant aircraft systems will be difficult to determine. Artificial intelligence (expert systems) concepts may be applicable to the aircraft system management computers required to manage such systems. Expert systems require extensive data bases to be effective. NASA research would focus on building failure mode and effects and degraded mode data bases and on defining and validating expert system concepts for aircraft system management.

FAULT-TOLERANT CONTROL SYSTEM
CERTIFICATION CRITERIA AND METHODOLOGY

ARTIFICIAL INTELLIGENCE/EXPERT SYSTEM
CONCEPTS FOR AIRCRAFT SYSTEM
CONTROL AND DISPLAY SYSTEMS

AIRCRAFT/NATIONAL AIR SPACE SYSTEM COMPATIBILITY

- The air transport industry has invested considerable effort in the design and development of fuel-saving flight management systems. To be effective, these systems must be allowed to control the climb, cruise, and descent flight profiles without undue air traffic control interference. The FAA is in the beginning phases of defining a national air space system aimed at increasing air space and airport capacity through the use of increased automation. This system could potentially increase air traffic control constraints to the detriment of efficient aircraft operation. NASA research would be directed at achieving maximum synergy between the desires of air transport operators to minimize costs and the desires of the FAA to increase air space and airport capacity.
- The FAA national air space system plan makes increased use of automation and assumes increased aircraft densities in airport approach and departure areas. NASA research would be directed at investigating approach and departure route saturation sensitivities to abnormal conditions such as weather, in-flight emergencies, etc.

AIRCRAFT TRAFFIC CONTROL FLIGHT PROFILE AND PROCEDURE CONSTRAINTS

AIRPORT/AIR TRAFFIC CONTROL APPROACH AND DEPARTURE SATURATION SENSITIVITIES

DISPLAY RESEARCH

- The objective of the generic non-airframe peculiar display research activities would be to develop standard display formats that would be accepted and used by the air transport community.
- The objective of the display format human factors studies would be to develop standards pertaining to the use of colors, synoptics, etc., for communicating aircraft status and situation to the flight crew.

GENERIC NON-AIRFRAME PECULIAR DISPLAY FORMATS

- **PRIMARY FLIGHT INSTRUMENTS**
- **APPROACH,ROLLOUT,TAXI,TAKEOFF,AND DEPARTURE AIDS**
- **AIR TRAFFIC CONTROL RELATED DISPLAYS**

HUMAN FACTOR DISPLAY FORMAT STUDIES

- **FORMAT INFORMATION TRANSFER EFFICIENCY**
- **WORK LOAD ANALYSIS**
- **DATA REQUIREMENTS**
- **COLOR STANDARDS**

N84
20595

UNCLAS

N84 20595 D28

A BRIEF REVIEW OF AIRCRAFT CONTROLS RESEARCH OPPORTUNITIES IN THE GENERAL AVIATION FIELD

Eric R. Kendall
Gates Learjet Corporation
Wichita, Kansas

First Annual NASA Aircraft Controls Workshop
NASA Langley Research Center
Hampton, Virginia
October 25-27, 1983

PRECEDING PAGE BLANK NOT FILMED

PAGE 518 INTENTIONALLY BLANK

CONTROLS TECHNOLOGY REVIEW

The review process itself is part of a feedback control system (Figure 1). The work already accomplished by NASA on flight test programs (Block A) and on trade studies (Block B) must be reviewed to determine the potential controls technology benefits available to the general aviation industry (Block C). General aviation industry constraints (Block D) must be defined and applied to determine the currently useable controls technology (Block E). Any shortfall between the required technology (Block F) and the useable technology shows up as a technology deficiency (Block G) and identifies the future research opportunities (Block H). Additional future research by NASA (Block J) can increase the controls technology benefits and ultimately nullify the technology deficiency.

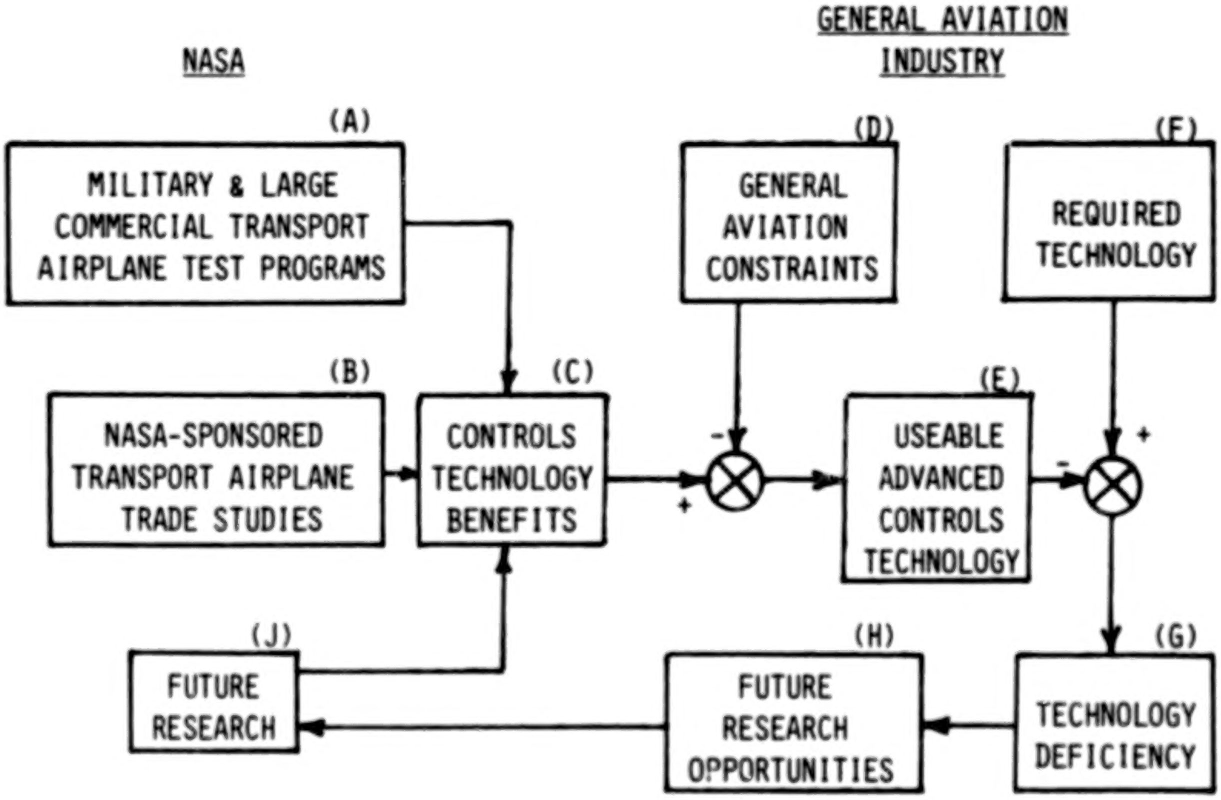
NASA
GENERAL AVIATION INDUSTRY
(A)
MILITARY & LARGE COMMERCIAL TRANSPORT AIRPLANE TEST PROGRAMS
(B)
NASA-SPONSORED TRANSPORT AIRPLANE TRADE STUDIES
(C)
CONTROLS TECHNOLOGY BENEFITS
(D)
GENERAL AVIATION CONSTRAINTS
(E)
USEABLE ADVANCED CONTROLS TECHNOLOGY
(F)
REQUIRED TECHNOLOGY
(G)
TECHNOLOGY DEFICIENCY
(H)
FUTURE RESEARCH OPPORTUNITIES
(J)
FUTURE RESEARCH
+
-
+
-

Figure 1

MILITARY AND COMMERCIAL TEST PROGRAMS

A significant number of flight test programs related to ACT have been conducted during the last 25 years. Some of these are shown in Figure 2. Most are related to very large airplanes with flexible structures. The technology is 'acronym saturated'. Richard Holloway defines the more commonly used acronyms and explains system functions in Ref. (1). Those used here are:

CCV.......Control Configured Vehicle
FMS.......Flutter Mode Suppression
GASDSAS...Gust Alleviation & Structural Dynamic Stability Augmentation System
ALDCS.....Active Load Distribution Control System
AS........Augmented Stability
WLA.......Wing Load Alleviation

- B-52..........................CCV, FMS
- XB-70.........................GASDSAS
- YF16..........................AS
- C-5A..........................ALDCS
- L-1011........................WLA

Figure 2

NASA-SPONSORED TRADE STUDIES

A few of the many trade studies sponsored by NASA are shown in Figure 3. These all relate to commercial transports or commuter airplanes. The STAT program, which started in 1978, was reported by Louis Williams of NASA Langley at the 1982 SAE Commuter Aircraft and Airline Operations Meeting in Savannah, GA (Ref. 4). The report contains much material relevant to the application of advanced technologies in the general aviation industry. ACT benefits were explored on two candidate airplane designs. Controls technology benefits need to be separately identified.

1970 - LOW WING LOADING STOL STUDY(2)....................NASA/BOEING WICHITA

1972 - APPLICATION OF ADVANCED TECHNOLOGIES
TO LONG-RANGE TRANSPORT AIRCRAFT(3)...............NASA/BOEING SEATTLE

1978 - SMALL TRANSPORT AIRCRAFT TECHNOLOGY
(STAT) PROGRAM(4).................................NASA/INDUSTRY

1982 - INTEGRATED APPLICATION OF ACTIVE
CONTROLS TECHNOLOGY TO AN ADVANCED
SUBSONIC TRANSPORT(5).............................NASA/BOEING SEATTLE

Figure 3

CONTROLS TECHNOLOGY BENEFITS (TEST RESULTS)

Some of the benefits which have been obtained as a result of the flight test programs are listed in Figure 4. Active control systems on the B-52 and on the C-5A are incorporated as retrofits to production airplanes. The L-1011 systems permit increased wing span which leads to improved cruise performance.

- ECP 1195 ON B-52 REDUCES FATIGUE & ALLEVIATES GUST LOADS
- ALDCS ON C-5A IMPROVES FATIGUE LIFE BY GUST AND MANEUVER LOAD REDUCTIONS
- L-1011 SYSTEMS REDUCE LATERAL GUST DESIGN LOADS AND PERMIT WING TIP EXTENSION WITH NO BEEF-UP

Figure 4

CONTROLS TECHNOLOGY BENEFITS (TRADE STUDIES)

NASA-sponsored trade studies have shown significant synergistic design benefits for a wide range of commercial airplane types. Some results from these studies are shown in Figure 5 for STOL, commuter, and subsonic commercial transport airplanes.

GLA.....Gust Load Alleviation
PAS.....Pitch Augmentation System
AAL.....Angle-of-Attack Limiting

- REF.(2) STOL STUDY SHOWS 10% TO 30% GROSS WEIGHT REDUCTION WITH MECHANICAL FLAP 'GLA' (F.L. <2500 FT.)
- REF.(3) MACH 0.98 AIRPLANE GROSS WEIGHT REDUCED BY 11% THROUGH USE OF 'AS'
- REF.(4) 'ACT' BENEFITS CONVAIR & LOCKHEED COMMUTER AIRPLANE DESIGNS
- REF.(5) 10% IMPROVED FUEL EFFICIENCY ON SUBSONIC TRANSPORT THRU USE OF PAS, AAL & WLA

Figure 5

GENERAL AVIATION 'ACT' CONSTRAINTS

The constraints listed in Figure 6 are typical of some which might be specified by the general aviation industry. Coordination within the industry is required before these can be considered as an official industry input. However, judging from the complexity levels of systems in use today, constraints such as these will produce significant future research opportunities. The need to be compatible with manual (unpowered) primary flight control systems was addressed by Dr. Jan Roskam and others in Ref. (6). This considered the use of a separate surface stability augmentation system for general aviation aircraft. Design philosophies and hardware implementation schemes were defined and evaluated in Ref. (7).

- MUST BE SIMPLE
- MUST BE EASY TO MAINTAIN
- MUST NOT BE SAFETY CRITICAL
- MUST BE COMPATIBLE WITH MANUAL (UNPOWERED) PRIMARY FLIGHT CONTROL SYSTEMS
- MUST IMPROVE AIRPLANE SALES POTENTIAL

Figure 6

GENERAL AVIATION FLIGHT TESTS

General aviation constraints such as those just mentioned have been recognized for some time. As a result, several NASA 'ACT' programs have been directed specifically towards the general aviation type of airplane. A recent review has been presented in Ref. (8) by Dr. David Downing and others of KU. A few of the programs are listed in Figure 7.

VRS	Vertical Ride Smoothing
GPAS	General Purpose Airborne Simulator
RSS	Relaxed Static Stability
SSSAS	Separate Surface Stability Augmentation System

C-45	VRS
C-140	GPAS/RSS
BEECH 99	SSSAS

Figure 7

10^{-3} BUMP SIZE

The potential need for ride quality control on some commuter airplanes can be seen by comparing the estimated ride quality of various types of unaugmented airplanes. Figure 8 shows the estimated 10^{-3} bump size for three types normalized to that of a commercial transport flying at an altitude of 35,000 feet. It is apparent that the commuter with its relatively high response to vertical gusts flying in the more gust-prone lower altitude bands will present a rougher ride in turbulent conditions. Technology trends in many of the emerging new commuters are towards simplicity, and it may be some time before ride quality systems are generally accepted. Research should continue to take advantage of the rapid developments in electronics and controls to make these systems more attractive for future high-technology commuter airplanes.

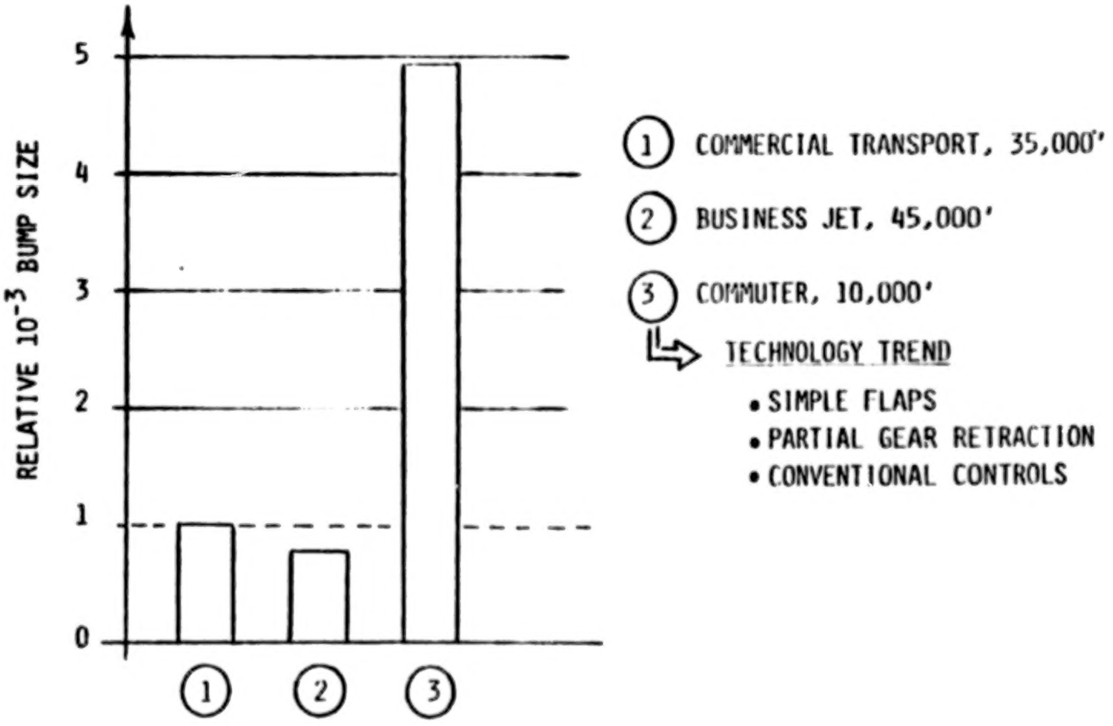

Figure 8

TECHNOLOGY CHOICES

General aviation airplane designers tend to use simpler control technologies than those employed on military and large commercial transport airplanes. As a result, a larger reserve of well-proven controls technology is available as an alternative to the adoption of advanced state-of-the-art controls technology. This is depicted in Figure 9.

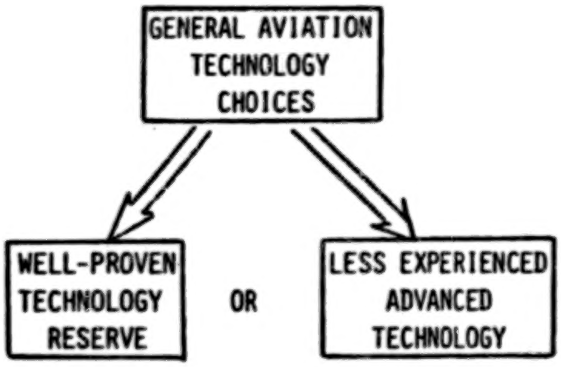
GENERAL AVIATION TECHNOLOGY CHOICES
WELL-PROVEN TECHNOLOGY RESERVE
OR
LESS EXPERIENCED ADVANCED TECHNOLOGY

Figure 9

SOME GENERAL AVIATION PREFERENCES

A brief list of some general aviation airplane design preferences is presented in Figure 10. This is included to emphasize a point that in many instances a simple technology is chosen over a more complex and more effective one. The tendency to use simple flap systems and low wing loadings is an example of the 'trade towards simplicity' approach. Quite often there is a tendency to reject any beneficial external features if they are considered detrimental to styling, and the preference is to eliminate avionic systems rather than to add them. Clearly much research will be required to produce ACT benefits which are marketable in the general aviation sector.

- SIMPLE FLAPS & LOW WING LOADINGS
- CONFIGURATION FEATURES WHICH ARE BOTH BENEFICIAL & STYLISH (E.G., WINGLETS)
- MINIMAL DEPENDENCE ON AVIONIC SYSTEMS (E.G. YAW DAMPERS, STALL PREVENTION)

Figure 10

ORIGINAL PAGE IS
OF POOR QUALITY

SIMPLE FLAPS AND LOW WING LOADINGS

The 'trade-towards-simplicity' tendency just noted is seen from the data presented in Figure 11. This compares the stall speeds and wing loadings of some general aviation airplanes with those for commercial transports and advanced high-lift airplanes. In general, the landing $C_{L_{MAX}}$ for the general aviation types is around 1.8, which is achievable by simple single-slotted partial span flaps. The commercial transports have a landing $C_{L_{MAX}}$ close to 2.8, which requires more complex flap arrangements. The general aviation landing stall speeds are kept to an acceptable level by using lower wing loadings than are commonly used by the commercial transports. Clearly there is some tradeability towards more complex flaps to obtain the cruise benefits of a higher wing loading. This is an example of an available technology not being fully exploited due to the preference for simplicity. Similar trends were noted by Dr. Jan Roskam, Ref. (9), who proposed new airfoils, higher wing loadings, and a new look at general aviation airplane design.

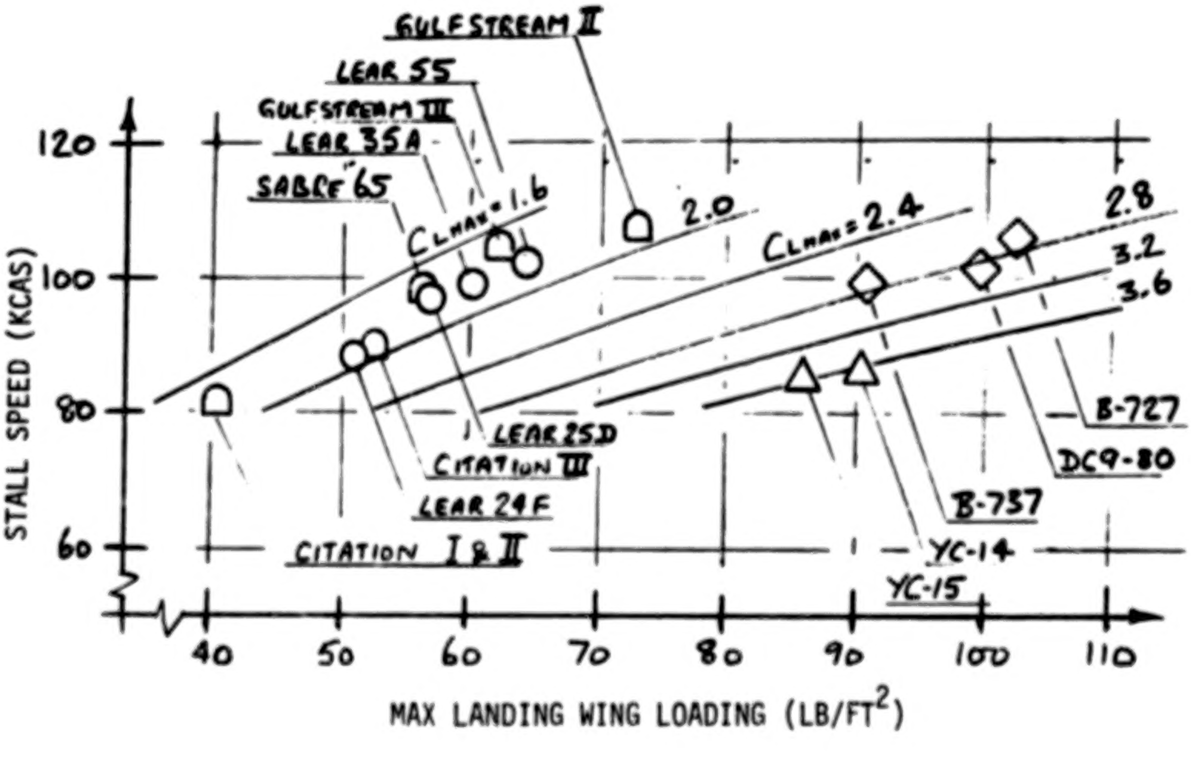

Figure 11

THE MAGNITUDE OF AIRPLANE PERFORMANCE BENEFITS

Quite often the magnitude of airplane cruise performance benefits available from ACT is small (e.g., 2 or 3 percent). While such improvements cannot be ignored, the cost effectiveness of systems needed to obtain them must be carefully considered. A basic requirement must be that the improvement will be sustained throughout the life of the airplane and that the benefits definitely will be felt by the airplane owner.

To give some indication of performance improvement 'detectability', data on airplane fleet performance variability are presented in Figure 12. This is a histogram of incremental percentage fuel flow gathered from forty-one new production airplanes all of the same model designation and all flown on the same route by production flight test crews. Data were corrected for observed ambient conditions. About half the measurements are contained within ±2% of the nominal value.

Even though a cruise performance 'improver' ACT system might make a small but statistically significant improvement to the fleet picture, it may not be of any practical significance to a particular one-airplane operator.

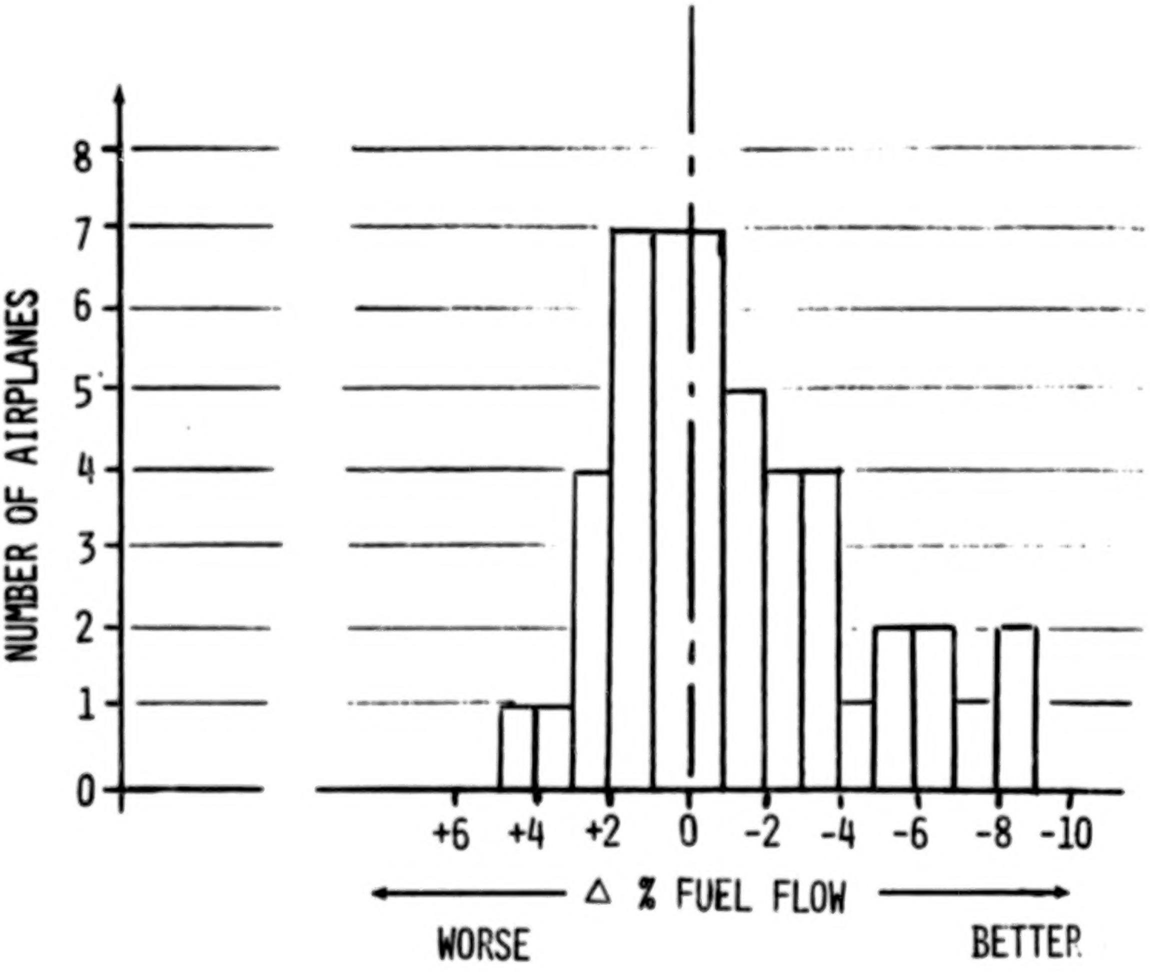

Figure 12

ACT USED IN TOUGH COMPETITIVE SITUATIONS

Williams (Ref. 4) wrote that "...competitive pressures will accelerate the use of technological advances...". The data in Figure 13 confirm this statement and show how ACT was introduced in a tough competitive situation between two general aviation business airplanes. The cruise performance of each airplane is comparable with airplane A's passenger miles per pound of fuel used being better than B's on the short range. The higher wing loading and winglet used on airplane 'A' more than offsets the low wing loading and supercritical section of airplane 'B'. Then, airplane A's balanced field length was made comparable with B's by introducing automatic performance reserve (APR) and automatic spoilers. These change engine thrust and spoiler setting without a direct command from the pilot and therefore can be classified as active control systems.

AIRPLANE	W/S	AR	Λ.25	SECTION	WINGLET	PERFORMANCE			
						PARAMETER/RANGE	300 NM	600 NM	1500 NM
A	79.4	6.72 (7.92)*	13°	NACA 64 (MODIFIED)	YES	PM/LB	1.13	1.35	1.48
						FLT. TIME	0 + 45	1 + 26	3 + 35
						BFL(1)	3,150	3,400	4,400
B	64.1	8.94	25°	SUPER CRITICAL	NO	PM/LB	0.93	1.22	1.48
						FLT. TIME	0 + 44	1 + 30	3 + 43
						BFL	3,200	3,420	4,200

*WINGLET EFFECT INCLUDED.

(1) BFL IMPROVED WITH APR & AUTOSPOILERS.

Figure 13

GENERAL AVIATION ACT SUGGESTIONS

Based on the very brief discussion of some general aviation design trends and preferences (still to be coordinated within the industry sector), Figure 14 presents a summary of suggestions for ACT activities. It seems that avionic cruise performance improvers will not sell easily unless the advantages are large. Since many general aviation airplanes have low wing loadings and fly at relatively low altitudes, the emphasis should probably be on ride quality improvement and gust alleviation systems. Retrofittable systems could be attractive since few airplanes are likely to be designed with optimal structures and no growth capability.

- 'CRUISE IMPROVERS' SHOULD:
  - A) COMPLY WITH CONSTRAINTS
  - B) COMPETE WITH FLAP/WING-LOADING TRADE-OFF.
  - C) PRODUCE SIGNIFICANT REDUCTION IN CRUISE FUEL-FLOW.
- RIDE CONTROL & GUST ALLEVIATION SYSTEMS MAY BE MOST LIKELY 'ACT' FUNCTIONS TO FIND APPLICATON
- RETROFITTABLE LOAD ALLEVIATORS MIGHT BE ATTRACTIVE FOR PROVIDING AIRPLANE GROWTH CAPABILITY WITH MINIMUM STRUCTURAL BEEF-UP.

Figure 14

GENERAL AVIATION CCV

Information and discussion presented so far might give the impression that the general aviation industry is ultra-conservative and not likely to adopt any significantly new controls concept in the forseeable future. However, even though there may be a natural reluctance to adopt a complicated avionics ACT system, the field of 'non-electronic' CCV technology might be regarded differently. The new designs introduced by Beech and by the Gates-Piaggio team at this year's National Business Aircraft Association (NBAA) show in Dallas show once again that "...competitive pressures will accelerate the use of technological advances..." (Ref. 4). Figure 15 shows the competitive 'canard' and 'three-surface' designs relative to a conventional configuration. NASA research has been strongly supportive of these unconventional designs. Much is left to be done.

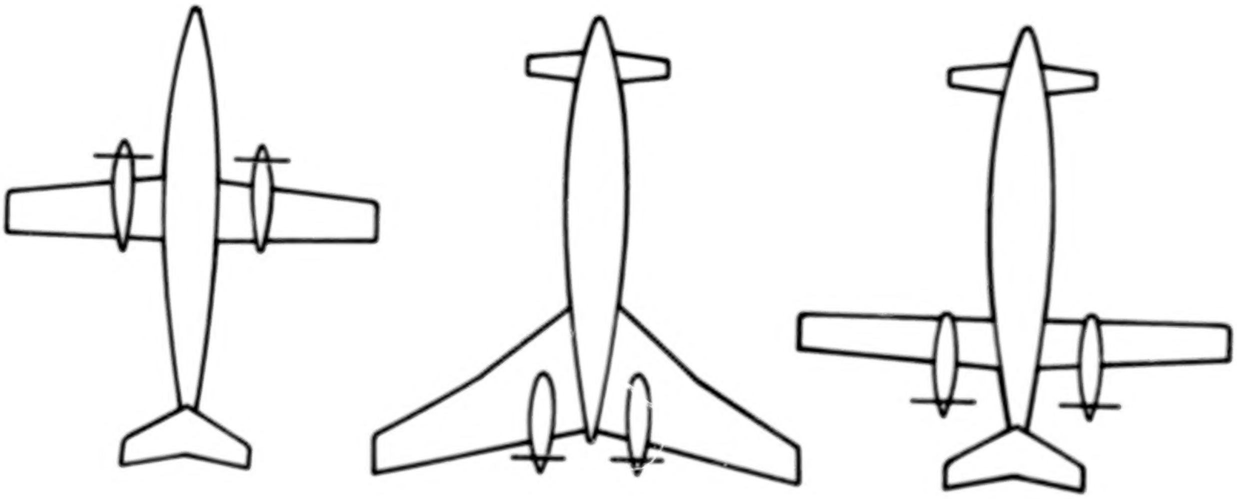

CONVENTIONAL CANARD THREE-SURFACE

Figure 15

GENERAL AVIATION RESEARCH OPPORTUNITIES IN THE FLIGHT CONTROLS TECHNOLOGY

The research opportunities in the fields of ACT and CCV for general aviation are enormous. This review has attempted to forsee some of these opportunities by assessing general aviation needs and trends relative to the currently available technology. A few ideas are listed in Figure 16. Coordination within the general aviation industry and between industry and NASA should be intensified in the near term to try to provide NASA with a more complete and representative feedback.

A) OVERALL

- CONTINUE STAT FOR SMALLER G.A. AIRPLANES (<10 PAX.)
- DETERMINE POTENTIAL 'ACT' CONTRIBUTION
- CATALOG ALL ACT BENEFITS.

B) AVIONIC SYSTEMS

- EXPLORE FEASIBILITY OF RETROFITTABLE LOAD ALLEVIATORS & RIDE QUALITY IMPROVERS.
- RUN SIMULATOR STUDIES & FLIGHT TESTS.
- DEVELOP ANALYTICAL METHODS AFFORDABLE TO GENERAL AVIATION USERS

C) AIRPLANE CONFIGURATIONS

- INCLUDE CANARDS & THREE-SURFACE AIRPLANES IN A) & B) ABOVE.
- CONTINUE WIND TUNNEL TESTS TO DETERMINE THE STABILITY AND CONTROL CHARACTERISTICS OF UNCONVENTIONAL AIRFRAME/PROPULSION ARRANGEMENTS

Figure 16

REFERENCES

1. Holloway, Richard B., "Introduction of CCV Technology Into Airplane Design," AGARD-CP-147, vol. 1, June 1974, pp. 23-1 to 23-16.

2. Holloway, R. B., Thompson, G. O., and Rohling, W. J., "Prospects for Low-Wing-Loading STOL Transports With Ride Smoothing," Journal of Aircraft, volume 9, no. 8, August 1972, pp. 525-530.

3. Boeing Co., "Study of the Application of Advanced Technologies to Long Range Transport Aircraft," NASA CR-112093, May 1972.

4. Williams, Louis J., "Advanced Technology for Future Regional Transport Aircraft," SAE 1982 Transactions, vol. 91, section 3, 1982, pp. 2481-2497.

5. Boeing Co., "Integrated Application of Active Controls (IAAC) Technology to an Advanced Subsonic Transport Project," NASA CR-165963, December 1982.

6. Roskam, J., et al., "An Investigation of Separate Surface Stability Augmentation Systems for General Aviation Aircraft," University of Kansas, Center for Research, Inc., August 1972.

7. Roskam, J., "Design Philosophy & Hardware Implementation of Separate Surface Automatic Flight Control Systems," University of Kansas, Center for Research, Inc., May 1974.

8. Downing, D., Hammond, T., and Amin, S., "Ride Quality Systems for Commuter Aircraft," NASA CR-166118, May 1983.

9. Roskam, J., "New Airfoils and Higher Wing Loadings: A New Look at General Aviation Airplane Design," University of Kansas, Center for Research, Inc., May 20, 1974.

N84
20596

UNCLAS

N84 20596 D29

RESEARCH OPPORTUNITIES FOR ROTORCRAFT

Bruce Blake
Boeing-Vertol Company
Philadelphia, Pennsylvania

First Annual NASA Aircraft Controls Workshop
NASA Langley Research Center
Hampton, Virginia
October 25-27, 1983

HELICOPTER ROTOR VIBRATORY LOADS

Helicopter vibration reduces crew performance, comfort, component life, and reliability. It originates primarily in unsteady aerodynamic loads on the rotor blades. Both lift and drag vary periodically because blade angle of attack and local velocity change as the blades rotate relative to the direction of flight and travel above and through the vortex wake, as depicted in this figure. Some harmonic components of the periodic blade loads are transmitted to the fuselage, where they produce airframe vibration. The absorbers and isolation systems currently used to reduce this vibration have undesirable weight penalties and often do not achieve vibration levels that are fully satisfactory.

A concept known as higher harmonic control is capable of suppressing vibration through active control of blade pitch at frequencies above the normal once-per-revolution pitch changes.

Successful results have been obtained in wind tunnel tests conducted at Boeing Vertol and by other researchers as well as in flight tests at Hughes Helicopter.

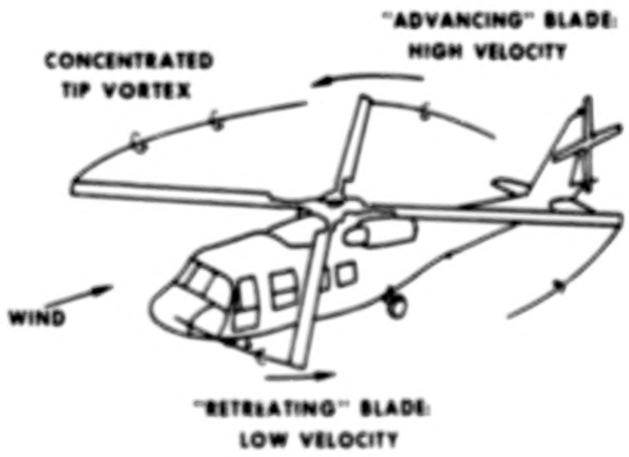

PRIMARY SOURCES	SECONDARY SOURCES
ROTOR BLADE SPEED DIFFERENTIAL	ARTICULATED BLADE MOTIONS
VELOCITIES INDUCED BY VORTEX WAKE	ELASTIC BLADE DEFLECTIONS

ACTIVE CONTROL

To achieve near-term results, most current R&D efforts have chosen to obtain the required pitch harmonics using the conventional swashplate control configuration rather than individual blade actuators in the rotating system. The swashplate is already used by both the pilot and the automatic flight control system to provide thrust control by setting the average blade pitch, called collective, and to provide trim and flight path control by creating a one-per-rev variation in blade pitch, called cyclic. The new control will superimpose higher frequency oscillations on the standard swashplate motions to control blade pitch and aerodynamic loads at the vibration harmonics and the adjacent harmonic frequencies. The harmonic hub loads are not to be eliminated completely, but reduced and rephased until their effects in the airframe cancel the effects of other vibration sources, particularly the unsteady aerodynamic loads on the fuselage itself. Higher harmonic control requires an automatic controller because the harmonic blade pitch which achieves optimal results varies greatly with flight condition. The automatic system must analyze vibration measurements in real time to determine the optimum harmonic control, in terms of amplitude and phase of several frequencies.

OPPORTUNITIES

- FUSELAGE VIBRATION REDUCTION ← CURRENT R&D EMPHASIS
- POWER REDUCTION
- FLIGHT ENVELOPE EXPANSION (RETREATING BLADE STALL ALLEVIATION)
- FATIGUE LOAD REDUCTION BLADES CONTROL SYSTEM
    - BLADES
    - CONTROL SYSTEM
- IMPROVED HANDLING QUALITIES BY REDUCING APPARENT CONTROL LAG

THE EXTENT OF THE BENEFITS ATTAINABLE DEPENDS ON ROTOR AND FUSELAGE DYNAMICS AND WILL VARY AMONG HELICOPTER DESIGNS

VIBRATION REDUCTION - WIND TUNNEL DEMONSTRATION

The benefits of active control in vibration treatment are shown in this figure. An experimental investigation involving a 10-foot diameter hingeless rotor was conducted at the Boeing Vertol V/STOL wind tunnel. This chart shows that the simultaneous application of three harmonic control inputs resulted in a dramatic reduction in the three vibratory hub loads presented here.

These results were achieved through closed-loop control using hub strain gage balance loads as feedback parameters. The demonstrated response time was 0.075 sec. Typically, higher harmonic control requires a frequency response that is 10 to 20 times greater than primary flight control to provide suppression of higher harmonic loads, particularly during maneuvers and in turbulence. Continued operation at these high frequencies requires improved bearing and seal designs to avoid rapid wear. Furthermore, precise control of the pitch actuation system at higher harmonic frequencies is required for effective vibration reduction.

WIND TUNNEL DEMONSTRATION

- 10-FOOT DIAMETER HINGELESS ROTOR
- THREE HARMONICS APPLIED SIMULTANEOUSLY
- INPUTS SELECTED BY ACTIVE (CLOSED-LOOP) CONTROLLER WITH 0.075 SEC. RESPONSE TIME

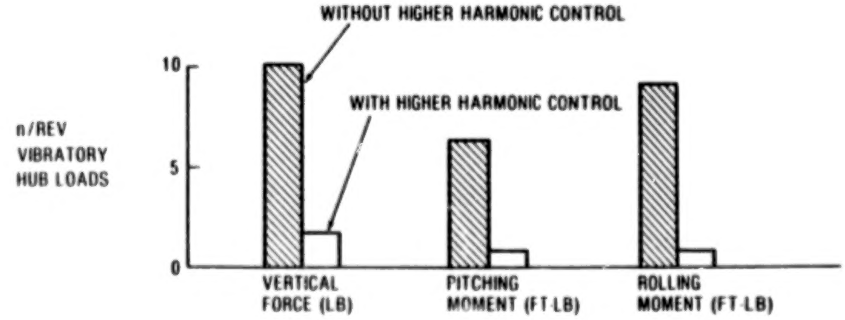

REFS. 1 AND 2

CONTROL ACTUATOR RESPONSE

Flight control power actuators used in all current helicopters have a response bandwidth sufficient for good handling qualities and automatic flight control system performance. Since rotor dynamics dictate a sharp cutoff at rotor rotational speed, there is no need for high system response. Vibration control through higher harmonic pitch demands that control system output be predictable and well defined in both gain and phase at frequencies up to 30 to 40 Hz for small aircraft.

Accurate control at 90 Hz has been experimentally demonstrated in the wind tunnel although at actuator amplitudes and service lives considerably below flight vehicle requirements.

FREQUENCY RANGE OF VIBRATION CONTROL

MUCH HIGHER THAN CURRENT FLIGHT CONTROL PRACTICE

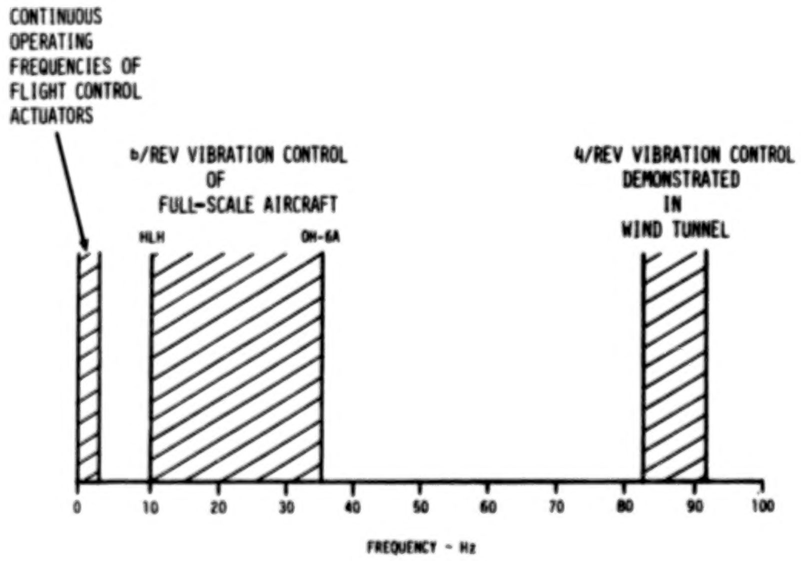

REQUIRED IMPROVEMENTS

Required improvements include:

- Feedback measurements, algorithm design, and closed-loop response to keep pace with the rapidly changing blade pitch requirements needed during maneuvers. Large transient vibration levels are very objectionable to the pilot. It is necessary to understand the effect on aircraft performance and component loads.
- Substantially upgraded control system performance.
- Service life characteristics suitable for production aircraft.

- REAL-TIME COMPUTATION OF HIGHER HARMONIC INPUTS TO KEEP UP WITH RAPID CHANGE OF FLIGHT CONDITIONS
- LARGE INCREASE IN PITCH ACTUATION POWER AND RATE CAPABILITIES
- DESIGN FOR GOOD RELIABILITY AND MAINTAINABILITY
- PRECISE CONTROL OF PITCH ACTUATION SYSTEM AT HIGHER HARMONIC FREQUENCIES

SYSTEM BENEFITS

Since vibration has always been a generic problem with helicopters, all research efforts to date have concentrated on reducing aircraft vibration. Unlike other vibration control devices such as isolators and absorbers which add weight and therefore reduce payload, higher harmonic control offers the unique opportunity of more than paying its own way. Redistribution of blade section lift and drag over the rotor disc can significantly reduce power required and increase the usable flight envelope.

It may also be possible to reduce fatigue loads and improve handling qualities. It may not be possible to achieve all these simultaneously. However, the potential benefits to helicopter users are so large that this additional tool now available to helicopter designers must be explored to its fullest.

ACTIVE CONTROL USES ROTOR BLADE PITCH TO CONTROL THE UNSTEADY AERODYNAMIC LOADS

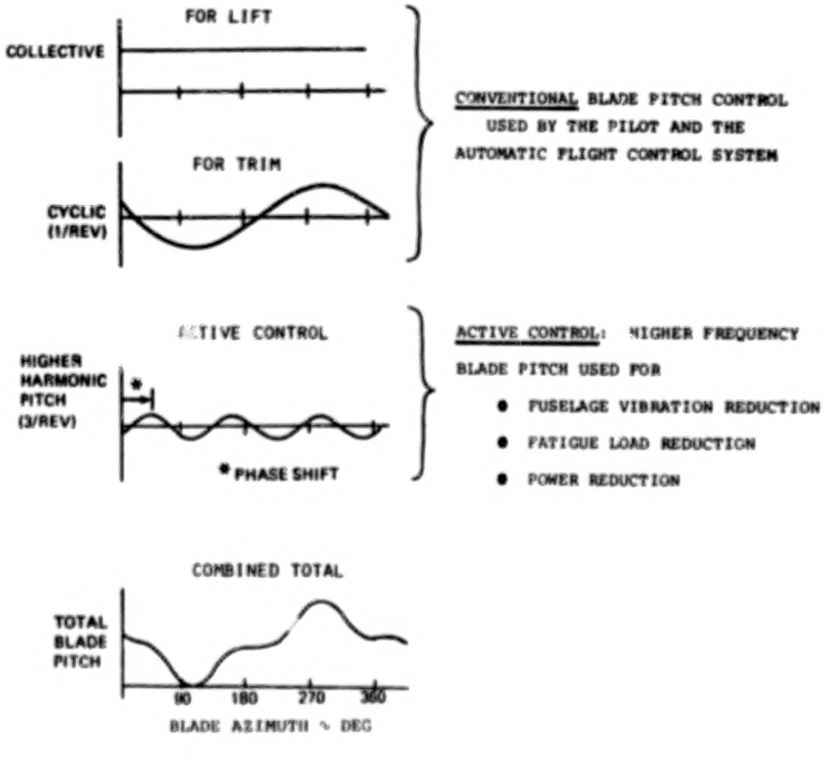
FOR LIFT
COLLECTIVE
CONVENTIONAL BLADE PITCH CONTROL
USED BY THE PILOT AND THE
AUTOMATIC FLIGHT CONTROL SYSTEM
FOR TRIM
CYCLIC
(1/REV)
ACTIVE CONTROL
ACTIVE CONTROL: HIGHER FREQUENCY
BLADE PITCH USED FOR
● FUSELAGE VIBRATION REDUCTION
● FATIGUE LOAD REDUCTION
● POWER REDUCTION
HIGHER
HARMONIC
PITCH
(3/REV)
*
* PHASE SHIFT
COMBINED TOTAL
TOTAL
BLADE
PITCH
90
180
270
360
BLADE AZIMUTH ~ DEG

ENGINE/FLIGHT CONTROL INTEGRATION

For advanced rotorcraft applications, especially those with more than one mode of operation, improved integration between systems results from including thrust/power management in the AFCS. Generally, functions related to blade pitch control are performed within the aircraft system. By uniting thrust and power management, simpler, more flexible mode transition and selection are possible. The engine control may then act solely as a power control with required limitations, resulting in a more adaptable engine.

- CONTROL CONFIGURATION FOR ADVANCED APPLICATIONS
    - ADVANCED HELICOPTER
    - TILT ROTOR
    - X-WING
    - CONVERTIBLE ENGINE APPLICATIONS

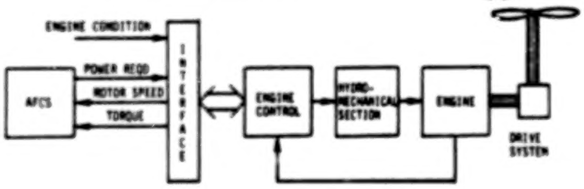
ROTOR
ENGINE CONDITION
POWER REQD
ROTOR SPEED
TORQUE
AFCS
INTERFACE
ENGINE CONTROL
HYDRO-MECHANICAL SECTION
ENGINE
DRIVE SYSTEM

- POWER MANAGEMENT ACCOMPLISHED IN AFCS
    - RESPONSIBILITY FOR ROTOR CONTROL (SPEED & PITCH) IS ENTIRELY WITHIN AFCS - NOT SPLIT AS WITH CONVENTIONAL SYSTEM
    - MULTI-MODE INTERACTIONS AND INCREASED INTEGRATION REQUIREMENTS ARE BEST HANDLED WITHIN AFCS
- ENGINE CONTROL PROVIDES GAS GENERATOR GOVERNING & LIMITING
    - SIMPLER ENGINE CONTROL FUNCTIONING AS POWER CONTROLLER
    - EACH APPLICATION DOES NOT NEED A TAILORED ENGINE CONTROL
- FEWER ENGINE AIRFRAME INTERCONNECTIONS
- PROVIDES HIGH LEVEL OF REDUNDANCY

OVERALL INTEGRATION GOALS

Primary goals for integrating engines and flight controls are to improve handling qualities and system performance. Aircraft control response characteristics may be enhanced through selective inputs to the engine control. Reducing pilot workload by providing simpler engine cockpit controls and eliminating manual backup are important considerations. Automatically optimizing engine performance and establishing diagnostic requirements aimed at improving mission reliability and safety are also engine-related goals of an integration program.

- **IMPROVED HANDLING QUALITIES**
    - **IMPROVE AIRCRAFT CONTROL RESPONSE CAPABILITY**
    - **SIMPLIFY PILOT CONTROL**
        - **ELIMINATE MANUAL BACKUP**
- **OPTIMIZE SYSTEM PERFORMANCE**
    - **OPTIMIZE ENGINE PERFORMANCE**
    - **IMPROVE MISSION RELIABILITY/SAFETY**
    - **DEVELOP DIAGNOSTIC REQUIREMENTS**

INTEGRATION OBJECTIVES

Program objectives should be to optimize response of the integrated system and to upgrade overall engine performance. Specifically, the program should be aimed at improving torsional stability of the engine-rotor/drive when considering multi-mode configurations and engine-out conditions; emphasis should be placed on increasing rotor thrust response to decrease rotor speed droop during rapid maneuvers, gust rejection, and precision hover conditions. Engine and control diagnostics and trend monitoring represent important considerations toward improving engine/aircraft availability. Methods for displaying power margin in conjunction with power assurance and techniques for continuously optimizing system performance should be addressed. An additional objective of a program should be engine failure recognition and indication with subsequent corrective action by the flight guidance system.

OPPORTUNITIES

- OPTIMIZE RESPONSE

  INCREASED TORSIONAL STABILITY
  OF ROTOR/DRIVE SYSTEM

  IMPROVED ROTOR THRUST RESPONSE TO CONTROL
    - RAPID MANEUVERS
    - GUST REJECTION
    - PRECISION HOVER

- UPGRADE ENGINE PERFORMANCE

  ENGINE AND CONTROL DIAGNOSTICS

  TREND MONITORING

  POWER MARGIN/POWER ASSURANCE

  PERFORMANCE OPTIMIZATION

  FAILURE RECOGNITION

ADDITIONAL RESEARCH TOPICS

- DEVELOP LOW-ALTITUDE ATMOSPHERIC TURBULENCE MODEL

  AERODYNAMIC ENVIRONMENT BELOW 100 ft. NEAR OBSTRUCTIONS IS NOT WELL QUANTIFIED

- HUMAN FACTORS

  FLIGHT SIMULATION VISUAL AND MOTION CUE REQUIREMENTS

  METHOD(S) FOR MEASURING PILOT WORKLOAD

- SENSOR TECHNOLOGY

  APPROACHES TO USE OF MULTISPECTRAL IMAGING

  ANALYTICAL REDUNDANCY

  WIRE FINDERS

- PARAMETER IDENTIFICATION

  COMPLEXITY OF REQUIRED MODELS HAS RETARDED PROGRESS RELATIVE TO FIXED-WING AIRCRAFT

REFERENCES

1. Shaw, John and Albion, Nicholas: Active Control of Rotor Blade Pitch for Vibration Reduction: A Wind Tunnel Demonstration. Vertica, vol. 4, no. 1, 1980, pp. 3-11.

2. Shaw, John and Albion, Nicholas: Active Control of the Helicopter Rotor for Vibration Reduction. J. Amer. Helicopter Society, vol. 26, no. 3, July 1981, pp. 32-39.

N84
20597

UNCLAS

N84 20597 D30

FIGHTER AIRCRAFT FLIGHT CONTROL TECHNOLOGY DESIGN REQUIREMENTS

W. E. Nelson, Jr.
Northrop Corporation, Aircraft Division
Hawthorne, California

First Annual NASA Aircraft Controls Workshop
NASA Langley Research Center
Hampton, Virginia
October 25-27, 1983

ORIGINAL PAGE IS
OF POOR QUALITY

This figure represents the evolution of control technology. As we compare the current day fighters with the Wright brothers' airplane, we notice that they had achieved control technology and mastered their applications without electronics. But the future demands further emphasis of pursuing the aspects of control with the extension of research going into exotic concepts such as vortex management.

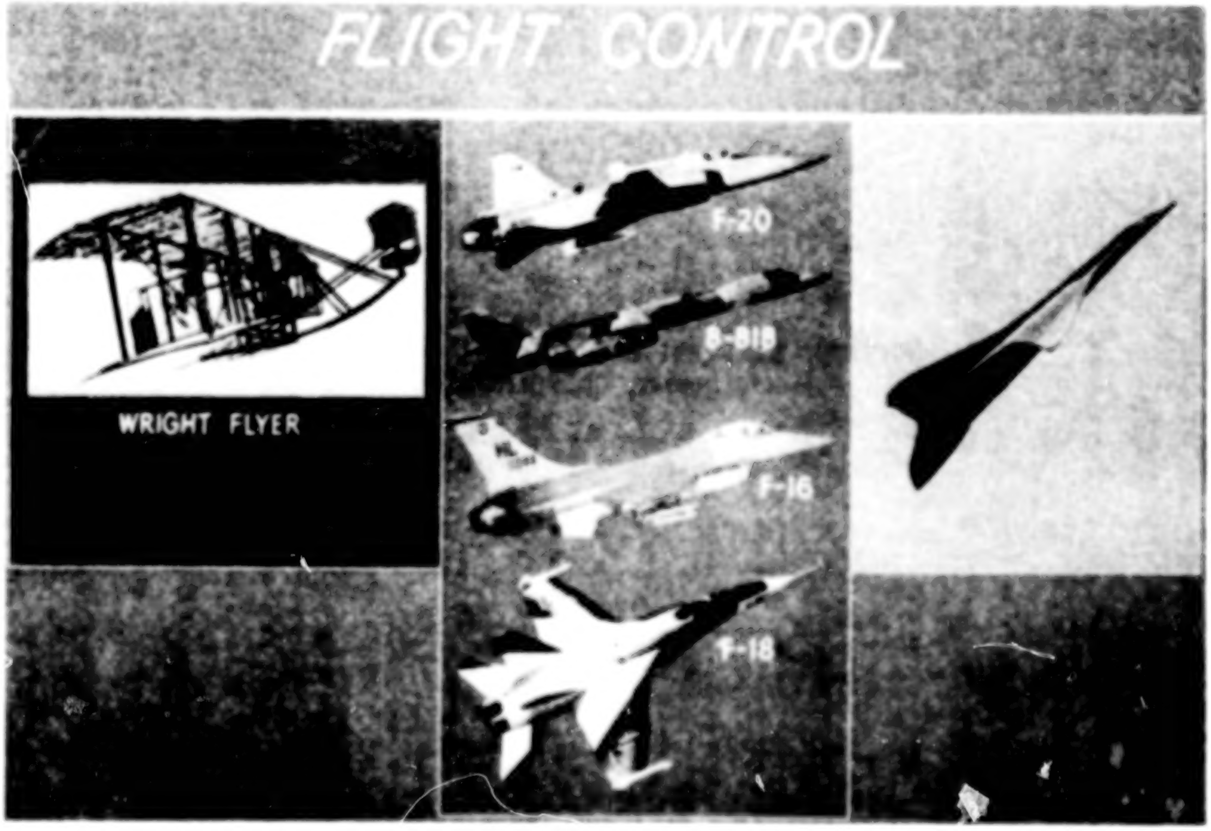
FLIGHT CONTROL

**ORIGINAL PAGE IS
OF POOR QUALITY**

Truly, the day of the pilot controlling the aircraft will diminish. As weapon system integration and flight path and navigational integration become more heavily automated, the pilot will become a manager. His primary task will be selecting the right functional requirements; his secondary task will be as backup. He will act in the fashion he presently performs, that of a pilot.

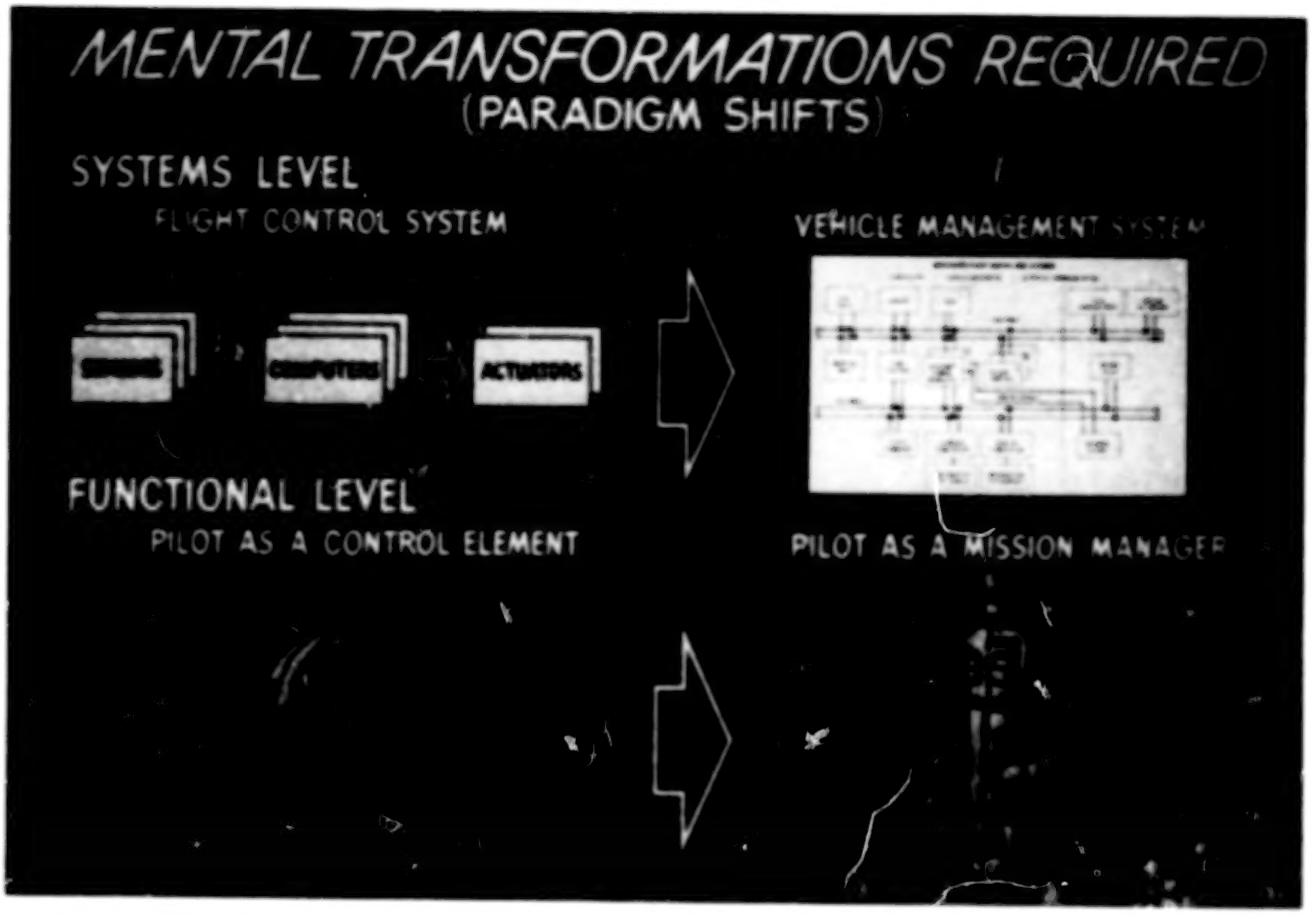

MENTAL TRANSFORMATIONS REQUIRED
(PARADIGM SHIFTS)

SYSTEMS LEVEL

FLIGHT CONTROL SYSTEM

VEHICLE MANAGEMENT SYSTEM

FUNCTIONAL LEVEL

PILOT AS A CONTROL ELEMENT

PILOT AS A MISSION MANAGER

SENSORS
COMPUTERS
ACTUATORS

This figure humorously depicts the challenge the future pilot will have. However, it is not unattainable, as work on the AFTI and the present F-18 has demonstrated. The research needed is to establish standards that the designer can utilize to evaluate his concepts.

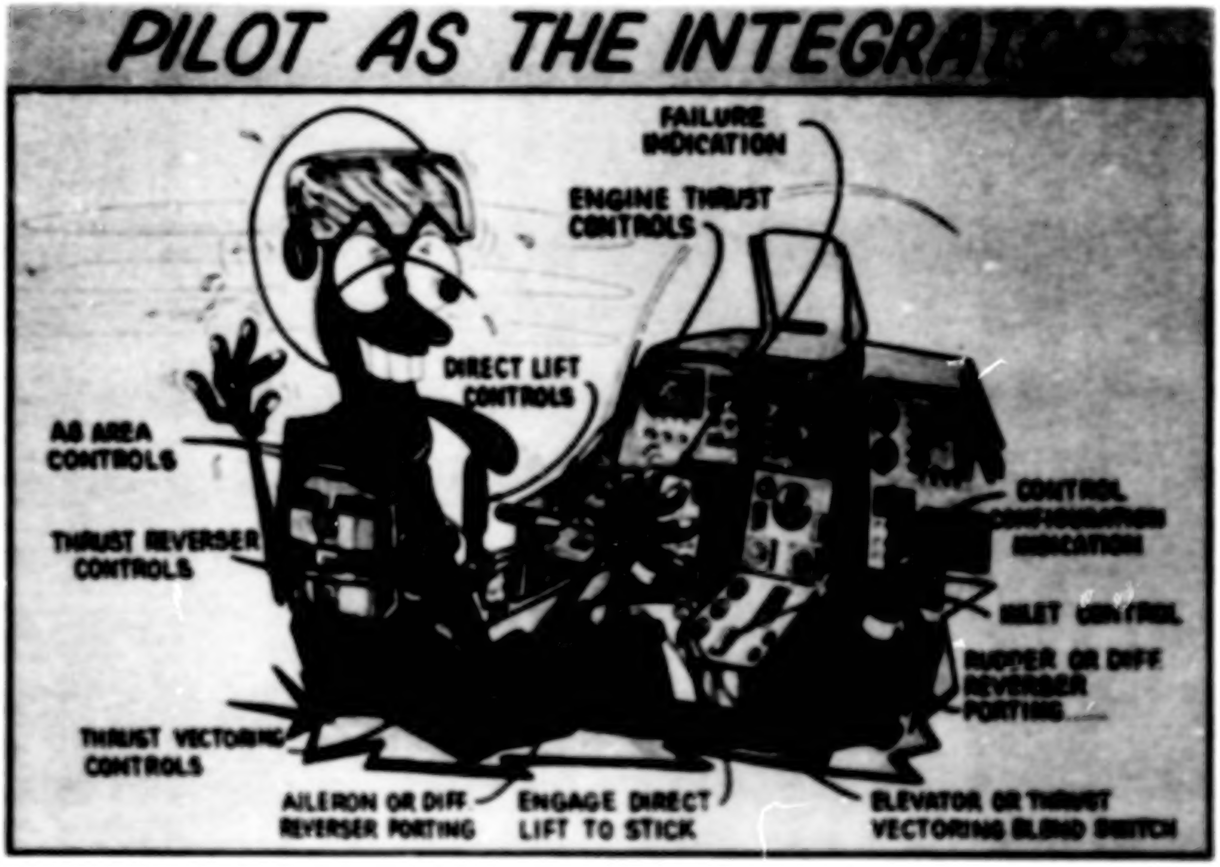
PILOT AS THE INTEGRATOR
FAILURE INDICATION
ENGINE THRUST CONTROLS
DIRECT LIFT CONTROLS
AB AREA CONTROLS
THRUST REVERSER CONTROLS
CONTROL CONFIGURATION INDICATION
INLET CONTROL
RUDDER OR DIFF REVERSER PORTING
THRUST VECTORING CONTROLS
AILERON OR DIFF REVERSER PORTING
ENGAGE DIRECT LIFT TO STICK
ELEVATOR OR THRUST VECTORING BLEND SWITCH

Active control elements in flight control technology encompass many technical disciplines. Electronic chip development will result in achieving potential architectures of control laws operating in real time during flight. The high densities and improved computation times will allow greater design flexibility for fault-tolerant applications. Data communications, actuation technology, and electrical power concept, when combined with the elements of the computer, will lead to the indicated technology objectives.

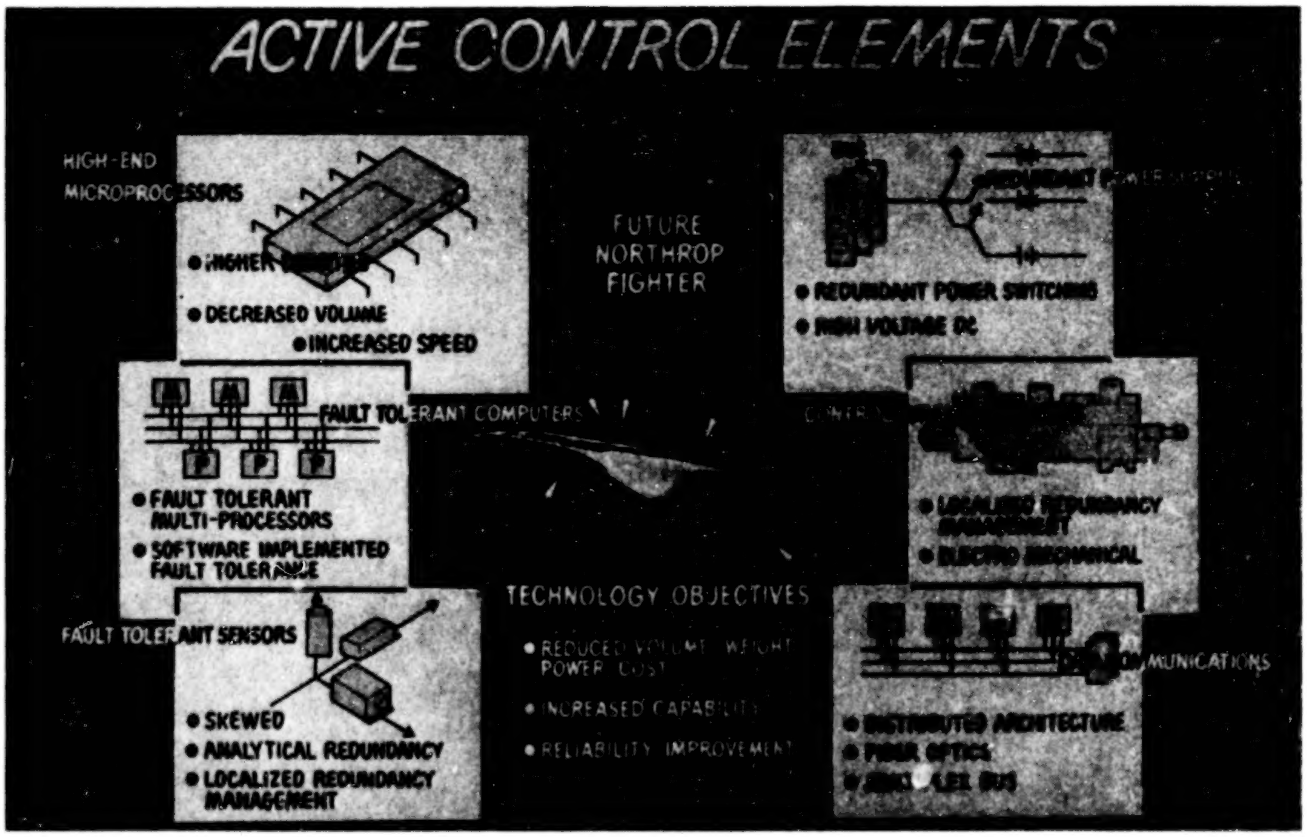

ACTIVE CONTROL ELEMENTS

HIGH-END MICROPROCESSORS
- HIGHER DENSITIES
- DECREASED VOLUME
- INCREASED SPEED

FAULT TOLERANT COMPUTERS
- FAULT TOLERANT MULTI-PROCESSORS
- SOFTWARE IMPLEMENTED FAULT TOLERANCE

FAULT TOLERANT SENSORS
- SKEWED
- ANALYTICAL REDUNDANCY
- LOCALIZED REDUNDANCY MANAGEMENT

FUTURE NORTHROP FIGHTER

TECHNOLOGY OBJECTIVES
- REDUCED VOLUME, WEIGHT, POWER, COST
- INCREASED CAPABILITY
- RELIABILITY IMPROVEMENT

REDUNDANT POWER SUPPLIES
- REDUNDANT POWER SWITCHING
- HIGH VOLTAGE DC

CONTROL [illegible]
- LOCALIZED REDUNDANCY MANAGEMENT
- ELECTRO MECHANICAL

DATA COMMUNICATIONS
- DISTRIBUTED ARCHITECTURE
- FIBER OPTICS
- MULTIPLEX BUS

C-7

Flight control technology has evolved to a total systems engineering discipline as depicted in this figure. The mission requirements set the needs. The available electronic technology provides the capability. The interface with all avionic and other aircraft subsystems increases the flexibility of the control capability. But hidden inside the effort is an item that can deter the design performance, the validation testing. Thus, a need exists for design standards to relate the desired methods and procedures to be used in the design effort of future vehicles.

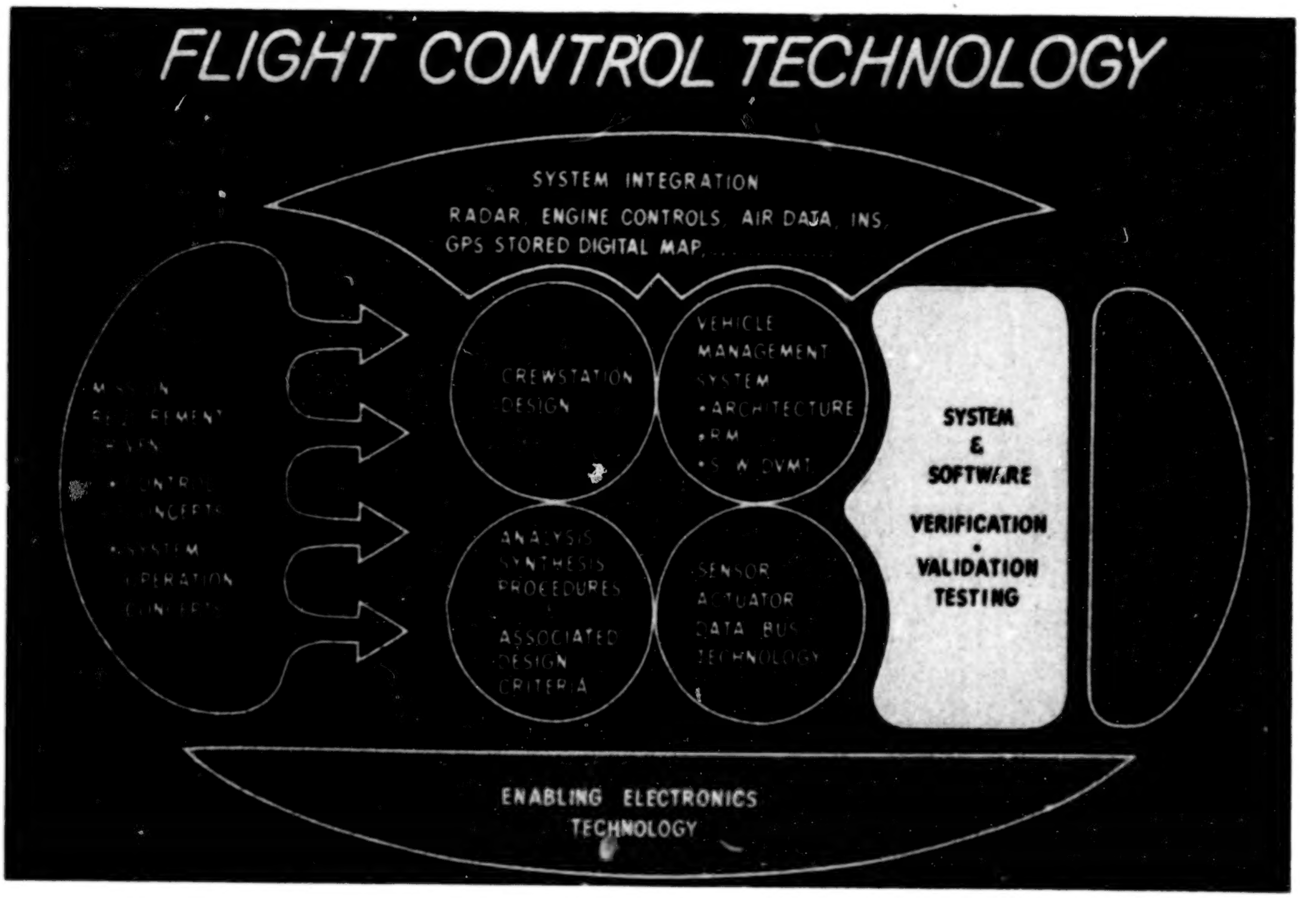

FLIGHT CONTROL TECHNOLOGY

SYSTEM INTEGRATION
RADAR, ENGINE CONTROLS, AIR DATA, INS,
GPS STORED DIGITAL MAP, ...

MISSION
REQUIREMENT
DRIVEN
• CONTROL
CONCEPTS
• SYSTEM
OPERATION
CONCEPTS

CREWSTATION
DESIGN

VEHICLE
MANAGEMENT
SYSTEM
• ARCHITECTURE
• R/M
• S/W DVMT

ANALYSIS
SYNTHESIS
PROCEDURES
&
ASSOCIATED
DESIGN
CRITERIA

SENSOR
ACTUATOR
DATA BUS
TECHNOLOGY

SYSTEM
&
SOFTWARE
VERIFICATION
•
VALIDATION
TESTING

ENABLING ELECTRONICS
TECHNOLOGY

Here is a specific example of a control application that is in its infancy. The payoff on potential aircraft can be related into reduced structural weight. However, further research is needed to explore various concepts and to demonstrate them in both wind tunnel and flight tests.

BATTLE DAMAGE CONSIDERATIONS FOR ADAPTIVE FLUTTER SUPPRESSION

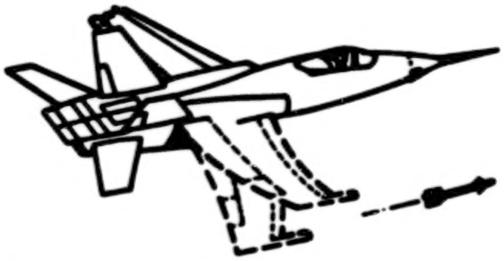

OBJECTIVE

- SUSTAIN FLUTTER FREE OPERATION FOLLOWING AN ARRAY OF BATTLE DAMAGE STATES
- ENHANCE THE EXISTING ADAPTIVE ALGORITHM BY SELF-REPAIRING CONCEPTS

PAYOFF

- IMPROVED COMBAT EFFECTIVENESS
- RAPID BATTLE DAMAGE REPAIR
- REDUCED PEACE TIME COST

- INCREASED SOFTWARE COMPLEXITY
- COMPUTATIONAL (FRAME TIME) PENALTY

APPROACH

- DEVELOP ALGORITHMS FOR BATTLE DAMAGE
  - DETECTION – VOTING SCHEME
  - ISOLATION – VARIANCE COMPARISON
  - CONTROL RECONFIGURATION – REDUNDANT CONTROL SURFACE OPERATION
- EMPHASIS ON YF-17 WIND TUNNEL TEST MODEL
- CREW INTERFACE ISSUES

The role of "in-flight simulation" needs to be revived. This area is valuable to relate new design features of control law, systems operation, and interaction with the pilot in a near real-life environment and to reflect the needed design changes into the new vehicle before a large change impact of cost and schedule is imposed on the project. A new airframe platform is needed to replace the antiquated T-33.

FUTURE FLIGHT CONTROL SYSTEM NEEDS - IMPROVED IN-FLIGHT SIMULATION

- VARIETY OF HANDLING QUALITIES ISSUES NEED FURTHER STUDY - LATERAL SENSITIVITY, CONTROL HARMONY, PILOT MODES, CRITERIA
- AVIONICS/PROPULSION INTEGRATION REQUIRE FLIGHT INVESTIGATION
- HIGH "G" CAPABILITY REQUIRED
- SOFTWARE INTENSE SYSTEMS REQUIRED

"Artificial intelligence" (AI) is now the term used to mean what we once referred to as computer capability. However, much effort needs to be applied in this area to determine the best approaches and resulting payoffs in using the AI concept during real-time computer operation. The figure indicates examples of applications.

APPLICATION OF AI METHODS TO FCS AND AIRCRAFT TECHNOLOGIES
(NEAR AND LONG TERM)

- PVI, PILOT DECISION AIDING, PILOT AS SYSTEM MANAGER
- FAULT-TOLERANT COMPUTING (REAL TIME)
- ANALYSIS/SYNTHESIS PROGRAM (NON-REAL TIME)
- INTEGRATED PROPULSION/CONTROL SYSTEMS
- ADAPTIVE CONTROLLERS
- OPTIMIZATION WITH REGARD TO HANDLING QUALITIES, TERRAIN FOLLOWING AND AVOIDANCE, TURBULENCE, FLUTTER SUPPRESSION AND LOAD ALLEVIATION, ETC.
- "SUPER-MANEUVERABLE" AIRCRAFT
- AVIONICS
- ROBOTICS
- MANUFACTURING
- QUALITY ASSURANCE AND CONTROL
- INDUSTRIAL CONTROL
- FACTORY OF THE FUTURE

N84
20598

UNCLAS

N84 20598 D31

MILITARY AIRCRAFT RESEARCH OPPORTUNITIES FOR THE FUTURE

Robert C. Schwanz
Air Force Wright Aeronautical Laboratories
Wright-Patterson Air Force Base, Ohio

First Annual NASA Aircraft Controls Workshop
NASA Langley Research Center
Hampton, Virginia
October 25-27, 1983

PRECEDING PAGE BLANK NOT FILMED

PAGE 558 INTENTIONALLY BLANK

DESIGN OF DECENTRALIZED CONTROL SYSTEMS: "INTEGRATED CONTROL"

The objective is to develop a methodology for the design of control systems for interacting dynamical systems which employ only local measurements and control devices.

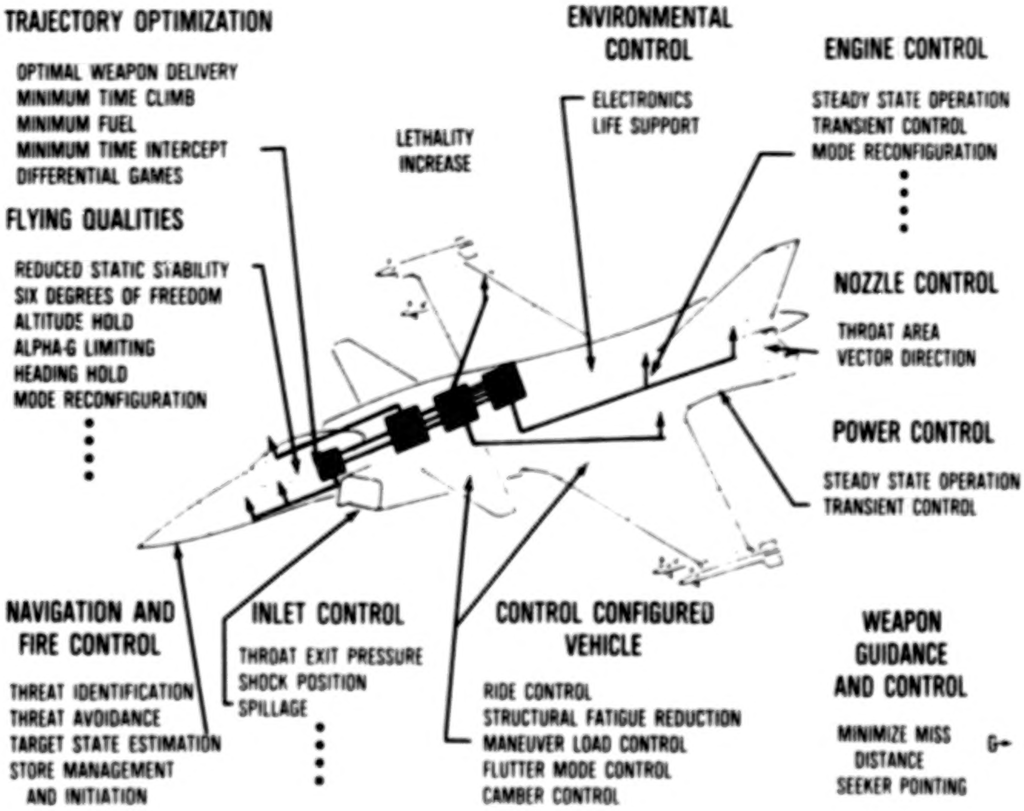
TRAJECTORY OPTIMIZATION
OPTIMAL WEAPON DELIVERY
MINIMUM TIME CLIMB
MINIMUM FUEL
MINIMUM TIME INTERCEPT
DIFFERENTIAL GAMES
FLYING QUALITIES
REDUCED STATIC STABILITY
SIX DEGREES OF FREEDOM
ALTITUDE HOLD
ALPHA-G LIMITING
HEADING HOLD
MODE RECONFIGURATION
LETHALITY INCREASE
ENVIRONMENTAL CONTROL
ELECTRONICS
LIFE SUPPORT
ENGINE CONTROL
STEADY STATE OPERATION
TRANSIENT CONTROL
MODE RECONFIGURATION
NOZZLE CONTROL
THROAT AREA
VECTOR DIRECTION
POWER CONTROL
STEADY STATE OPERATION
TRANSIENT CONTROL
NAVIGATION AND FIRE CONTROL
THREAT IDENTIFICATION
THREAT AVOIDANCE
TARGET STATE ESTIMATION
STORE MANAGEMENT AND INITIATION
INLET CONTROL
THROAT EXIT PRESSURE
SHOCK POSITION
SPILLAGE
CONTROL CONFIGURED VEHICLE
RIDE CONTROL
STRUCTURAL FATIGUE REDUCTION
MANEUVER LOAD CONTROL
FLUTTER MODE CONTROL
CAMBER CONTROL
WEAPON GUIDANCE AND CONTROL
MINIMIZE MISS DISTANCE
SEEKER POINTING

HISTORICAL PERSPECTIVE

Relative to the design of decentralized control systems, recent publications by the IEEE (e.g., ref. 1) and results of military development programs indicate that serious engineering problems prevent reliable control of interacting dynamical systems.

"LARGE-SCALE SYSTEMS AND DECENTRALIZED CONTROL"

- (SPECIAL ISSUE, IEEE TRANS. AUTO. CONTROL, APRIL 1978)

- INEFFICIENT OPERATION OF LARGE SCALE INTERCONNECTED SYSTEMS
    - LACK OF FUNDAMENTAL UNDERSTANDING OF PHYSICS MODELS
    - LACK OF COORDINATED CONTROL STRATEGIES
    - USE OF DETERMINISTIC STATIC STRATEGIES ON STOCHASTIC DYNAMIC SYSTEMS
- EXISTING TOOLS FOR CENTRALIZED CONTROL ARE INAPPROPRIATE
    - SERVOMECHANISM THEORY
    - RECENT THEORY
        - MAXIMUM PRINCIPLE
        - LYAPUNOV STABILITY
        - ESTIMATION
        - DYNAMIC PROGRAMMING
- IMPLEMENTATION REQUIREMENTS UNKNOWN
    - NEED FOR AND COST OF COMMUNICATION CHANNELS
    - FIDELITY AND RELIABILITY OF INFORMATION
    - ALLOWABLE TIME DELAYS IN INFORMATION

ORIGINAL PAGE IS
OF POOR QUALITY

AVAILABLE DECENTRALIZED CONTROL DESIGN METHODS

The current practice is to employ both hierarchical and heterarchical design procedures. They are evolutions of the centralized control theory design methods of the last 30 years. Current development applications depend heavily upon insight gained from centralized design of large-scale systems. Research activity seeks to understand relationships among the decentralized control theories.

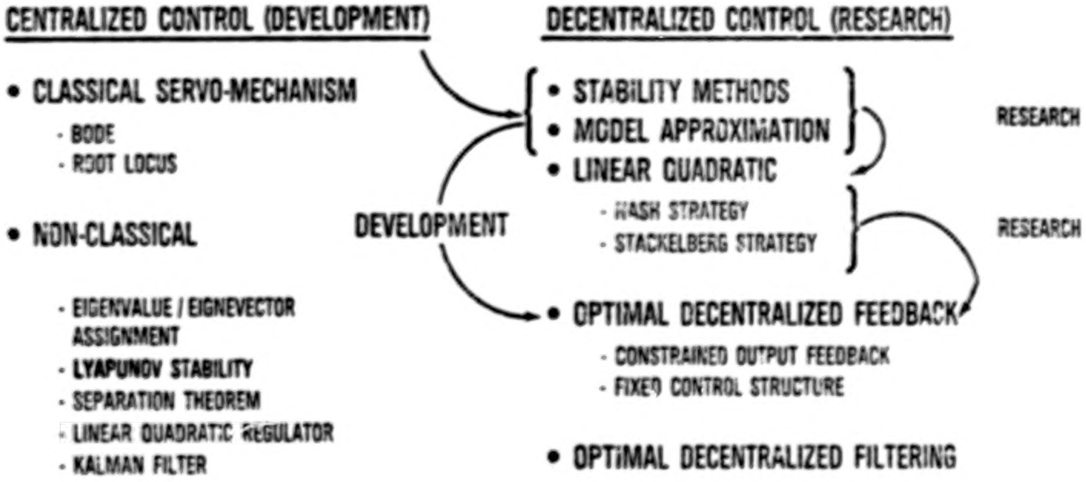
CENTRALIZED CONTROL (DEVELOPMENT)
• CLASSICAL SERVO-MECHANISM
- BODE
- ROOT LOCUS
• NON-CLASSICAL
- EIGENVALUE / EIGNEVECTOR ASSIGNMENT
- LYAPUNOV STABILITY
- SEPARATION THEOREM
- LINEAR QUADRATIC REGULATOR
- KALMAN FILTER
DEVELOPMENT
DECENTRALIZED CONTROL (RESEARCH)
• STABILITY METHODS
• MODEL APPROXIMATION
• LINEAR QUADRATIC
- NASH STRATEGY
- STACKELBERG STRATEGY
• OPTIMAL DECENTRALIZED FEEDBACK
- CONSTRAINED OUTPUT FEEDBACK
- FIXED CONTROL STRUCTURE
• OPTIMAL DECENTRALIZED FILTERING
RESEARCH
RESEARCH

RESEARCH AND DEVELOPMENT NEEDS IN DESIGN OF DECENTRALIZED CONTROL SYSTEMS

Research needs include the development of (1) clearer mathematical relationships among the various existing methods and (2) the practical significance of the Witsenhauser nonlinear counter-example for linear Gaussian design. Development needs include the definition of (1) suitable dynamics problems of varying complexity for testing of new methods and (2) an efficient computerized methodology that minimizes mathematical complexity and presents the physics essentials of both problem and solution. This method should store user experience in a data base.

FLYING QUALITIES OF ADVANCED VEHICLES

The objective is to manually employ the decentralized control of many on-board systems to achieve full dynamics control in highly maneuverable vehicles.

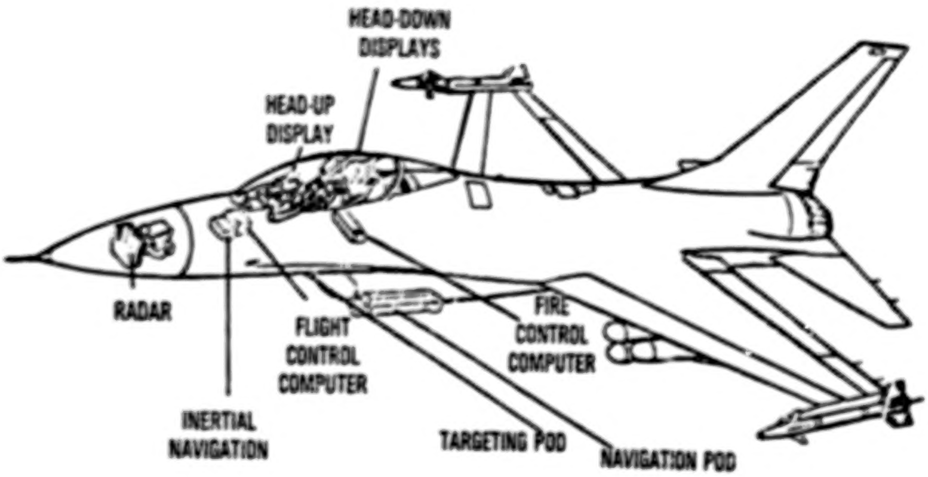
HEAD-DOWN DISPLAYS
HEAD-UP DISPLAY
RADAR
FLIGHT CONTROL COMPUTER
FIRE CONTROL COMPUTER
INERTIAL NAVIGATION
TARGETING POD
NAVIGATION POD

SYSTEM INTEGRATION EMPHASIZES CONTROL USING LARGER MEASUREMENT SETS

HISTORICAL PERSPECTIVE;
FLYING QUALITIES/CONTROL SYSTEM DYNAMICS

Recent development programs have experienced manual control problems as the flight control system increases in complexity. If increasing complexity occurs in many control systems, can the manual control problem become easier?

AIRCRAFT	PROBLEM AREA	PROBLEM SOURCE	PROBLEM SOLUTION
①	TAKE OFF AND LANDING	BLENDED AOA / LOAD FACTOR COMMAND SYSTEM, AOA SIGNAL FADE OUT TIME = .01 SEC	INSTALL PITCH RATE COMMAND SYSTEM, INCREASE SIGNAL FADE OUT TIME TO 1.1 SEC
	ROLL RACHETING	TOO SENSITIVE TO SMALL INPUTS	CAS MODIFICATION
②	PIO PRONE AT TOUCHDOWN	TIME DELAY IN PITCH	FCS PITCH TIME DELAY ADJUSTED
③	PITCH PROBLEMS AT TOUCHDOWN	EXCESSIVE INITIAL RESPONSE DELAY	?
④	PIO PITCH PROBLEMS AT TOUCHDOWN	?	?
⑤	MANUAL TERRAIN FOLLOWING	LARGE AMPLITUDE PITCH DAMPING	RESIDUAL OSCILLATION FROM PILOT INPUTS ELIMINATED
	LANDING APPROACH PIO	?	?

HISTORICAL PERSPECTIVE;
FLYING QUALITIES/DISPLAY DYNAMICS

Recent development programs have also been characterized by displays designed with inattention to display/computer dynamics. Displaying additional information from many decentralized systems may decrease manual flight safety.

FLYING QUALITIES - LEVEL 1 .. PILOT INPUT TO AIRPLANE RESPONSE $\leq$ 100 MS

- TYPICAL PILOT TRACKING TIME DELAY, $\zeta \approx 300$ MS
    - EFFECT OF 0.25 CM QUANTIZATION OF ERROR DISPLAY → $\Delta\zeta \approx 34\% \approx 100$ MS
- TYPICAL DISPLAY TIME DELAYS

AIRCRAFT	DISPLAY
①	FLIGHT PATH MARKER, 30 MS; AOA INDICATOR, 50 MS
②	TARGET PREDICTOR, 70 MS
③	PITCH LADDER, 50 MS CALCULATION, 20 MS REFRESH NAV MAP CHANGE, 1 SEC
④	DATE UPDATE, 40 MS; REFRESH, 1 SEC

HISTORICAL PERSPECTIVE:
FLYING QUALITIES/VEHICLE DYNAMICS

Much of the nonlinear dynamics information in the MIL SPEC/MIL STD 8785C (ref. 2) must be made more quantitative to manually control many dynamical processes in highly maneuverable tasks. What does a pilot require to utilize nonlinear dynamic phenomena? What is too much of a good thing? What does he want if some system failure occurs?

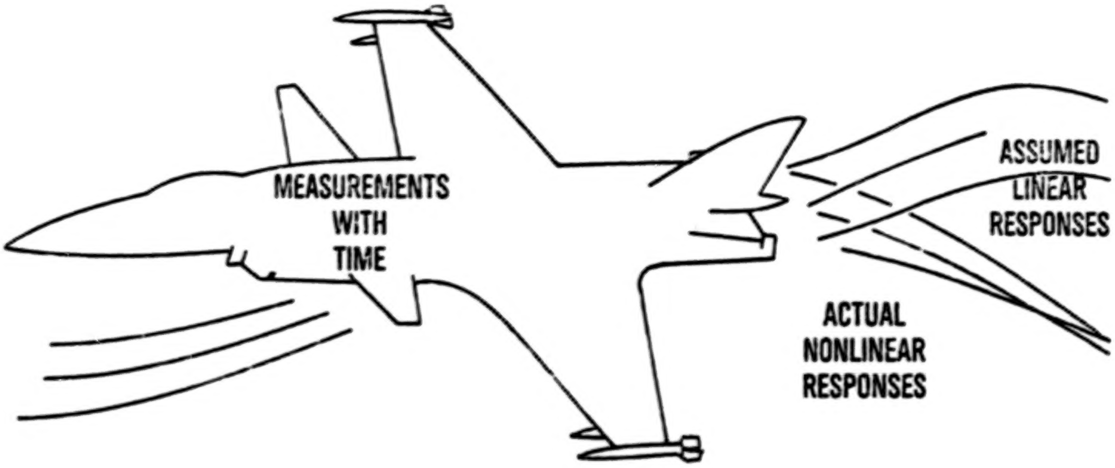

$$\left\{\begin{array}{c}\text{RESPONSES}\\ \hdashline \text{MEASUREMENTS}\end{array}\right\} = \left[\overset{\text{LINEAR}}{\left[\begin{array}{c:c}\dot{\theta}/F_s & \\ \hdashline & \end{array}\right]} + \overset{\text{NONLINEAR}}{\left[\begin{array}{c:c}\dot{\theta}^2/F_s & \\ \hdashline & \end{array}\right]}\right]\left\{\begin{array}{c}\text{CONTROLLERS}\\ \hdashline \text{COMMANDS}\end{array}\right\}$$

ORIGINAL PAGE IS
OF POOR QUALITY

HISTORICAL PERSPECTIVE:
FLYING QUALITIES/VEHICLE DYNAMICS (CONCLUDED)

The MIL SPEC/MIL STD 8785C (ref. 2) describes many design objectives as eigenvalue/eigenvector relationships. Typical of these are the n/α versus ω_n charts describing manual control requirements at "moderate frequencies."

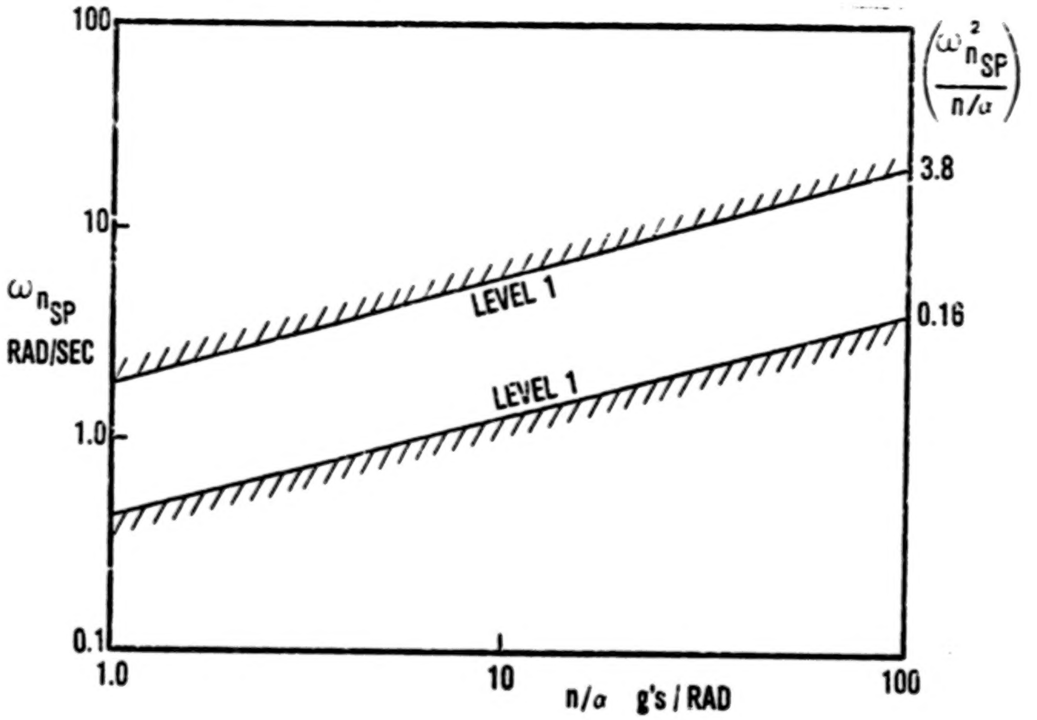

RESEARCH AND DEVELOPMENT NEEDS IN FLYING QUALITIES OF ADVANCED VEHICLES

Research needs include the parametric characterization of nonlinear systems:

Volterra series
Least-squares errors projection
Least-squares error/orthonormal projection
Energy concepts

Development needs include the evaluation of experimental procedures and data used to characterize flying qualities boundaries for centralized/decentralized control; the definition of metrics to identify manual/automatic system interface boundaries; and the creation of a generic, nonlinear dynamics, manned flight simulator.

REFERENCES

1. Athans, M.: Guest Editorial on Large-Scale Systems and Decentralized Control, IEEE Transactions on Automatic Control, vol. AC-23, no. 2, April 1978, pp. 105-106.

2. Military Specifications, Flying Qualities of Piloted Airplanes, MIL-F-8785C, 5 November 1980.

N84
20599

UNCLAS

N84 20599 D32

OPPORTUNITIES FOR AIRCRAFT CONTROLS RESEARCH

Thomas B. Cunningham
Honeywell, Inc.
Systems and Research Center
Minneapolis, MN

First Annual NASA Aircraft Controls Workshop
NASA Langley Research Center
Hampton, Virginia
October 25-27, 1983

PRECEDING PAGE BLANK NOT FILMED

PAGE 570 INTENTIONALLY BLANK

AIRCRAFT PROBLEMS THAT DRIVE CONTROL TECHNOLOGY

In the course of this discussion, I'd like to deal with what I consider to be four categories of aircraft problems which drive our technology. First are highly unstable vehicles that are emerging. Second, control technology is being driven by the current thrust and ultimate benefits that can be achieved by expanding the flutter boundary of combat aircraft. Third, we are witnessing, both in the fixed-wing and the rotary-wing world, a new emphasis on low-level penetration. This, as I'll discuss, will have some direct impacts on control technology. Fourth, in general, we along with other members of the avionics community have suffered some setbacks in our attempts to demonstrate "ilities" in the past. NASA and DoD have made great strides in this area; however, improved "ilities", if I can use the word as such, will continue to drive our control research technology.

- **HIGHLY UNSTABLE VEHICLES**
- **FLUTTER SPEED BOUNDARY EXPANSION**
- **LOW LEVEL AUTOMATED FLIGHT**
- **IMPROVED "ILITIES"**

CONTROL RESEARCH AREAS

Breaking down our discussions into technology research areas, I'd like to deal with control from a system theoretic standpoint, particularly multivariable control theory and adaptive control. Many of the aircraft technology drivers I discussed earlier are going to affect what we do in the future of physical device research, particularly actuators, but also sensors, computers, and data transmissions. Some overall system concepts are going to be impacted by these directions, such as fault-tolerant architectures and some continued work required in the analytical fault-tolerant areas. This latter category is technology that we have pretty well in hand in our controls area, but other avionics system people really need the benefit of our experiences. Two other areas I'll just touch on basically are what control technology will have as an impact for future flight research and some comments on higher order language software.

SYSTEM THEORETIC
- MULTIVARIABLE CONTROL THEORY
- ADAPTIVE CONTROL

PHYSICAL/DEVICE RESEARCH
- ACTUATION
- SENSORS
- COMPUTERS
- DATA TRANSMISSION

SYSTEM CONCEPTS
- FAULT-TOLERANT ARCHITECTURES
- ANALYTICAL FAULT TOLERANCE

OTHERS
- FLIGHT RESEARCH
- HOL SOFTWARE

BANDWIDTH INCREASES DUE TO RELAYED STATIC STABILITY

Beginning with highly unstable aircraft, we may be witnessing a significant increase in bandwidth requirements for fighter aircraft, in particular due to the desire to achieve the benefits of low drag and maneuverability at supersonic speeds.

This chart shows a simple single-input/single-output Bode relationship. For instance, we can think of instability being measured by the magnitude of the root that is farthest to the right in the right half plane. If we denote that by the letter "a" in a frequency response plot, we'd like to be 6 dB in gain above this position as a rule of thumb. Another rule of thumb for control design engineers is that we'd like to be in the area of 20 dB per decade roll-off in the region of crossover. This simple relationship would then put the crossover frequency at 2 a. Likewise, for stability and robustness, we'd like to be at least 6 dB below zero gain at a frequency of 4 a.

Two examples of the loop requirements to stabilize the vehicle are the X-29 and the F-16. The only one that is in production is the F-16 fighter. Its worst flight condition in terms of stability contains a root at +2, which means our crossover frequency is at 4 radians per second, and we must be rolled off to the tune of 6 dB at 8 radians per second. However, if we look at the X-29 Forward Swept Wing fighter, we see that at its most unstable flight condition, it has a root at +7, which is approximately 3 1/2 times what the F-16 represents. This impacts our control bandwidth because we need a crossover at 14 radians per second, and we must be rolled off 6 dB at 28 radians per second.

Historically, flight control designers have had 6 dB to model systems that have the highest accuracy near crossover, i.e., 2 a and ± a half of decade either side. In the case of the X-29 and potentially the emerging ATF class of fighters, this could easily mean that we need to know in greater detail the dynamics of the vehicle about 3 1/2 times higher in frequency than we've ever dealt with before. This would logically include more detailed knowledge of the bending/aeroelastic characteristics of the vehicle.

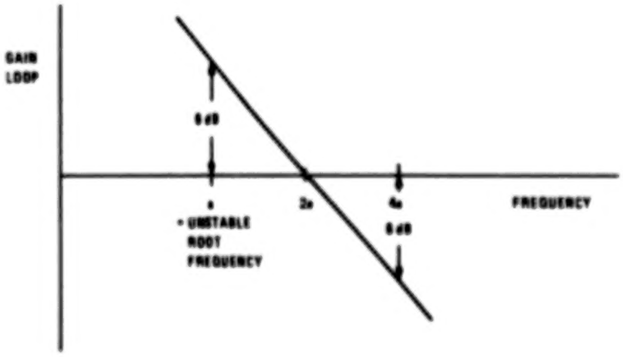

EXAMPLES:

F-16 FIGHTER

a = 2 rad/sec
⇒ CROSSOVER (2a) = 4 rad/sec
⇒ 6 dB DOWN (4a) = 8 rad/sec

X-29 FORWARD SWEPT WING

a = 7 rad/sec
⇒ CROSSOVER (2a) = 14 rad/sec
⇒ 6 dB DOWN (4a) = 28 rad/sec

FLIGHT RESEARCH

One of the initial impacts that high bandwidth control poses is in the area of flight research, and the goal as stated earlier is to achieve model uncertainty reduction in the vicinity of control bandpass. In the case of highly unstable vehicles, this means that we have to deal with higher and higher frequencies, and one of the ways we achieve model uncertainty reduction is through a series of flight examinations and parameter identification. The payoff, obviously, is to achieve an ultimate lowering of the eventual actuator rate excitations for high bandwidth control.

GOAL → MODEL UNCERTAINTY REDUCTION IN CONTROL PASSBAND

CHALLENGE → PARAMETER ID AT HIGHER FREQUENCIES

PAYOFF → LOWER ACTUATOR RATE EXCITATIONS FOR HIGH BANDWIDTH CONTROLS

SENSORS

Let us look at how this nature of highly unstable vehicles impacts various hardware components. Historically, flight control sensors have had ample bandwidth. We at Honeywell feel that if more bandwidth is needed, then expansion is already feasible within the state of the art. Another issue that is cropping up here more and more is the notion of shared flight control/navigation/weapon delivery sensors. The placement issue is the one that we have to deal with in the flight control community, and the real goal here is to achieve a robust multivariable control for sensor fault tolerance and high bandwidth performance in the face of ill-placed and dispersed sensors. This technology development should continue.

- **FLIGHT CONTROL SENSORS – BANDWIDTH EXPANSION FEASIBLE**
- **SHARED FLIGHT CONTROL/NAVIGATION/WEAPON DELIVERY SENSORS**
  - **PLACEMENT ISSUES: ROBUST MVC FOR SENSOR FAULT TOLERANCE HIGH BANDWIDTH PERFORMANCE**

ACTUATION TECHNOLOGY

The next technology area relating to controls is in the area of actuators. We have three issues that we must deal with here.

The first issue is fault tolerance. There is an emerging class of technical developments dealing with digital servo electronics which will indeed make the actuators more fault tolerant. This is required, because if one looks at the reliability analysis of a current flight control system, we see that from a research standpoint we have been dealing effectively with computers and somewhat effectively with sensors, but the real reliability bottleneck in aircraft flight control is the actuator system.

The next issue is this bandwidth expansion that we've been discussing. Although I'm not an expert in actuator technology, I'll pose a couple of issues and concerns that I have. One concern is whether we have the hydraulic technology available to achieve the high authority and rate/bandwidth we need for unstable vehicles. I'll also note that electromechanical actuators are emerging, which might give us high authority and expanded rate and bandwidth. This technology development should be pursued.

Third, there is the rate expansion itself for highly unstable vehicles. One possible solution, within the system theoretic framework, is the capability to formalize an optimal blending, if you will, of multivariable control solutions which allows us to share the rate requirement among a number of different surfaces.

- **FAULT TOLERANCE**
  - **DIGITAL SERVO ELECTRONICS**

- **BANDWIDTH EXPANSION**
  - **HYDRAULIC → COMPRESSIBILITY LIMITS**
  - **ELECTRO-MECHANICAL → EMERGING**

- **RATE EXPANSION**
  - **MVC SOLUTIONS FOR OPTIMUM BLENDING**

COMPUTERS

Another important element in our control loop is the onboard digital flight computer. Computer technology is being driven by a number of different applications, flight control being one. For instance, throughput is really being driven by signal processing requirements on various aircraft and spacecraft applications. The word length related to the accuracy of the computations is being driven more by other avionics functions, such as navigation. Memory, likewise, is being driven by other functions also. Some of the storage requirements for digital landmass data, etc., come to mind.

One area that is currently being driven by flight control is fault tolerance. In the emerging set of research issues from a hardware standpoint, one needs to look at integrated-functions architectures such as integrated flight/navigation and integrated flight/propulsions.

Software on the other hand is being driven to higher order languages such as Ada. We have to be careful in the controls community not to accept massive, unreliable compilers that aren't necessary to do control work. One possible solution that is being explored by the software community is to allow defined subsets of higher order languages to be used by highly flight crucial functions like flight control.

In summary, control problems in general do not drive computer technology. Certainly the first three issues I've listed here are being driven by other requirements. Fault tolerance is currently being driven by flight control, but as we'll see when we get into the impact of low-level penetration, we will find that other avionics systems indeed need the same kind of fault tolerance that flight control currently does.

- **THROUGHPUT → DRIVEN BY SIGNAL PROCESSING**
- **WORD LENGTH → DRIVEN BY NAVIGATION**
- **MEMORY → DRIVEN BY OTHER FUNCTIONS**
- **FAULT TOLERANCE**
  - **HARDWARE: INTEGRATED FUNCTIONS ARCHITECTURES**
  - **SOFTWARE: HOL COMPILER SUBSETS**

BOTTOM LINE → CONTROL PROBLEMS DO NOT DRIVE COMPUTER TECHNOLOGY

MULTIVARIABLE CONTROL THEORY

I would like to comment on aircraft research problems that drive the control theoretical developments. Two areas I'll talk about are the actual basic mathematical theory itself and additionally how we might look at a research area for applying these techniques. First, in my discussion of unstable vehicles, I've alluded to uncertainty reductions and new regions in frequency that have yet to be dealt with. Likewise, in our development of mathematical theory, we have to formalize ways of dealing with uncertainties. For instance, if we can generate a mathematical description of uncertainty in a given frequency range, we should seek to formalize our control design problem to deal directly with that level of uncertainty. There is a body of research being conducted at Honeywell and other places actually dealing with what we call structured uncertainties.

The other side of the structured uncertainty issue is the design itself. One design technique we're looking at is direct frequency domain optimization that attempts to deal with a formalized approach to achieve performance goals in the face of uncertainty constraints.

Uncertainty representations for practical aircraft control design problems have not been developed beyond simple examples. Therefore, formalized uncertainty boundaries for practical examples should be examined.

The next item concerns the state of the art in analysis and design itself for the whole hierarchy of preliminary design to flight control development, to actual production of flight control systems. We in the control theoretic community have been remiss for decades in not providing the end-user, i.e., the guy who's actually going to design a flight control system, with the proper CAD tools to do his job. And even though we've taken a useful step back towards the frequency domain, the ultimate flight control designer will never use the tools if all he has is a published paper out of the Transactions on Automatic Control.

Third, more directly to the flight control problem itself, I alluded earlier to some sharing of surfaces to achieve some overall higher bandwidth goals. Coupling this idea with the proliferation of control effectors on board modern aircraft, one should look at ways to formalize the control law design. Once again, a driving goal is to achieve higher bandwidth control for highly unstable vehicles. In addition, emerging classes of work include the areas of integrated flight and propulsion control and also some rather higher risk areas dealing with robust reconfiguration of control surfaces in combat situations, which could have high payoffs.

- **DEVELOPMENT:**
  - **– STRUCTURED UNCERTAINTIES**
  - **– DIRECT FREQUENCY DOMAIN OPTIMIZATION**

- **APPLIED:**
  - **– FORMALIZED UNCERTAINTY BOUNDARIES**
  - **– ANALYSIS AND DESIGN TOOLS – CAD**
  - **– MULTIPLE EFFECTOR BLENDING FOR COMMON GOALS**
    - **HIGHLY UNSTABLE VEHICLES**
    - **INTEGRATED FLIGHT/PROPULSION**
    - **ROBUST RECONFIGURATION**

ADAPTIVE CONTROL RESULTS

There have been some discussions about the usefulness of the adaptive control theory that has been developed over the last couple of decades. I'd like to go on record as saying that despite these emerging reservations, we at Honeywell are pretty proud of the adaptive control work that we've performed in the past, particularly under NASA sponsorship. This chart shows some of the more recent efforts at the Honeywell Systems and Research Center. This figure shows some successful adaptive work that we've done with NASA and also a very effective technology spinoff. Without going into detail, we essentially used the techniques we developed for the F-8 aircraft and the CH47 helicopter (which were demonstrated at Dryden in 1977) to design an off-shore drilling ship positioning concept that is now in production.

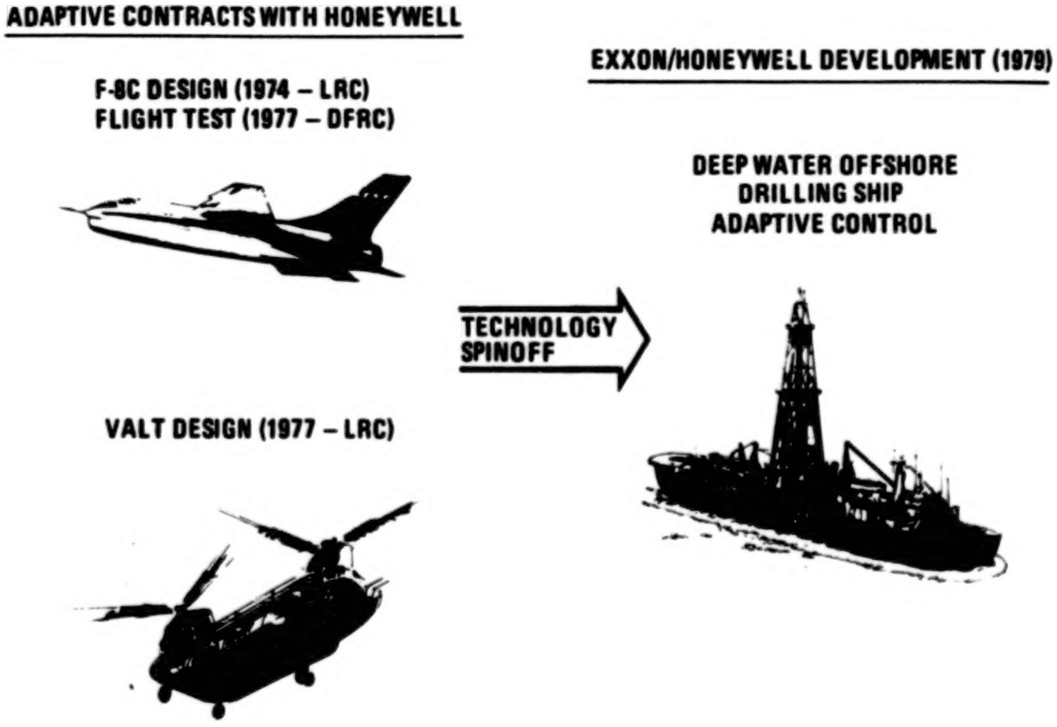

ADAPTIVE CONTRACTS WITH HONEYWELL

F-8C DESIGN (1974 – LRC)
FLIGHT TEST (1977 – DFRC)

VALT DESIGN (1977 – LRC)

TECHNOLOGY SPINOFF

EXXON/HONEYWELL DEVELOPMENT (1979)

DEEP WATER OFFSHORE
DRILLING SHIP
ADAPTIVE CONTROL

ACTIVE FLUTTER CONTROL

Active flutter control has some obvious payoffs that have been recognized for a number of years. The technology necessary to perform this is not mature and also the notion of active flutter mode control, particularly the frequencies we're dealing with, is a risky business. It is one problem to stabilize an airfoil flutter condition on a wing with known characteristics, however, from a practical standpoint, future fighter aircraft flutter mode control needs to deal with wings that have numerous dynamic configurations due to the different kinds and placements of stores.

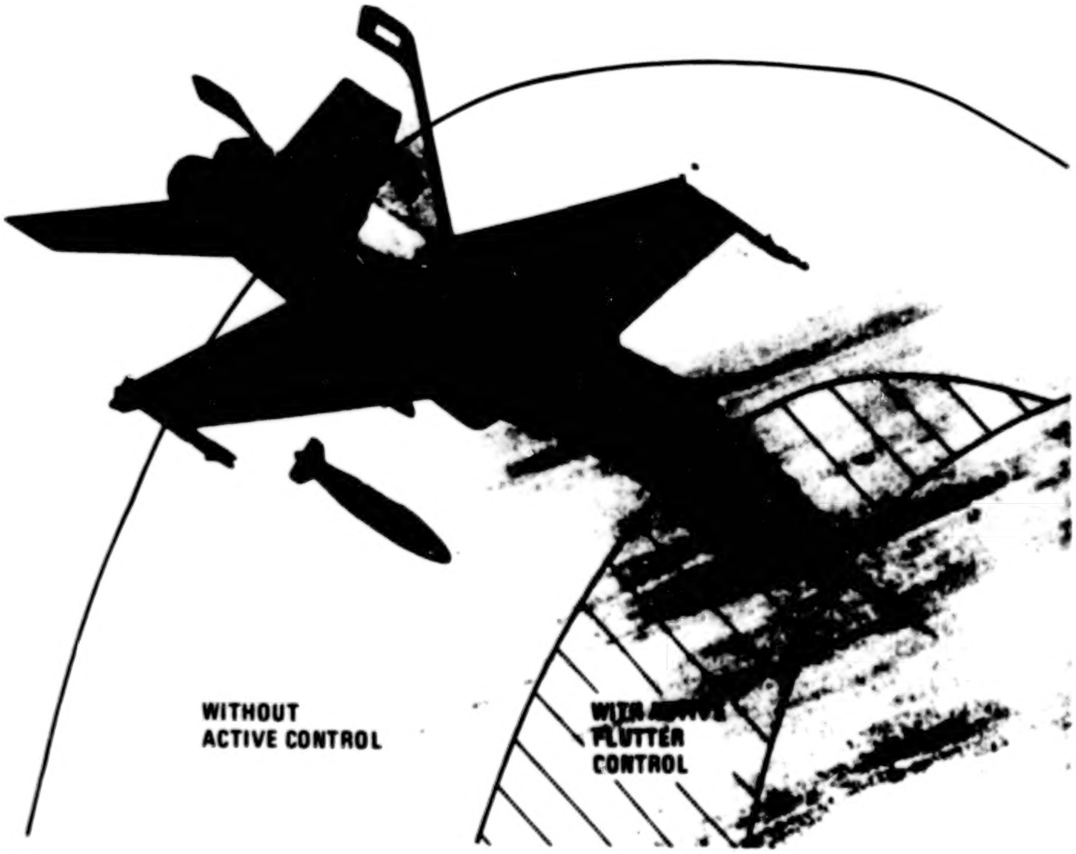

ADAPTIVE CONTROL

This leads us to a body of work that exists in adaptive control which has some demonstrated potential in dealing with this. The issue is to identify very rapidly the onset of a dynamic change in a configuration and to modify the control structure accordingly. A concept, based upon maximum likelihood estimation, has been demonstrated in wind tunnel tests of active flutter control with wing store changes.

Another payoff area for adaptive control deals with the prospect of doing onboard real-time reconfigurations due to battle damages for future military aircraft.

RAPID PARAMETER IDENTIFICATION:

- **ACTIVE FLUTTER CONTROL WITH CHANGING CONDITIONS**
- **BATTLE DAMAGE RECONFIGURATION**

ADVANCED AUTOMATIC TERRAIN FOLLOWING/TERRAIN AVOIDANCE

The final two areas are combined treatment of low-level penetration and improved "ilities." This figure points out one area of great interest within DoD; this is the notion of combined terrain following/terrain avoidance and threat avoidance. As shown schematically, this involves flying very low altitudes automatically while incorporating high g maneuvers, appropriate pilot interface, and a high level of flight safety. All of the avionics subsystems which interface to attack this problem become flight safety crucial. This would certainly include the guidance portion of the flight control area, navigation, and portions of the mission management.

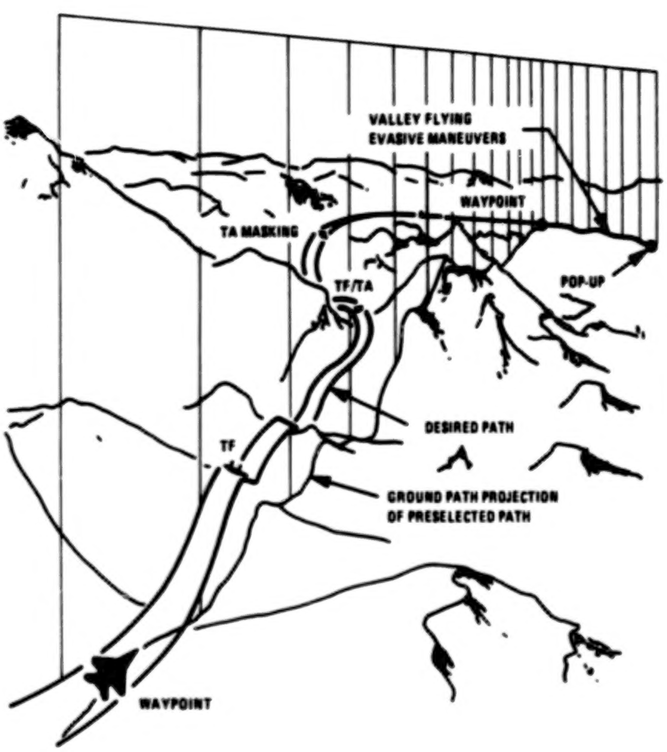
VALLEY FLYING
EVASIVE MANEUVERS
WAYPOINT
TA MASKING
TF/TA
POP-UP
DESIRED PATH
TF
GROUND PATH PROJECTION
OF PRESELECTED PATH
WAYPOINT

- ALGORITHMS FOR AUTOMATIC, SIMULTANEOUS TERRAIN FOLLOWING/TERRAIN AVOIDANCE
    - – LOW ALTITUDES
    - – HIGH g MANEUVERING
- PILOT INTERFACE
- FLIGHT SAFETY
- SENSITIVITY ANALYSIS
- COMPUTATIONAL REQUIREMENTS

LOW-LEVEL PENETRATION

In addition to the fixed-wing terrain following/terrain avoidance and threat avoidance, there is an emerging set of concepts that the Army would like to develop for a single-seat light helicopter for nap-of-the-Earth flight. The challenge that I believe exists is to somehow integrate flight, navigation, propulsion, weapons, etc., in a fault-tolerant system to allow us to do nap-of-the-Earth flight with high performance and a high degree of safety.

One research area is sensor blending. I think our estimation technology applies here. We also need more creative failure management solutions. Again, I think estimation technology applies, such as expanding upon things like analytic redundancy, plus development of emerging AI concepts based on expert systems and advanced planning. Also there is this critical need to automate verification and validation of systems, both the hardware and the software, for future flight management systems. And finally in the area of flight path management, we need to somehow go down the road and actually install trajectory optimization capabilities that operate in real time for onboard applications. In addition to that, there are some front- end decision making functions that perhaps could be handled by AI planning concepts.

EXAMPLES

- AUTOMATIC TF/TA/DA
- SINGLE-SEAT LIGHT HELICOPTER – NOE

CHALLENGE

- FAULT-TOLERANT INTEGRATED FLIGHT/NAV/PROPULSION/WEAPONS

RESEARCH AREAS

- SENSOR BLENDING – ESTIMATION
- CREATIVE FAILURE MANAGEMENT – ESTIMATION, AI
- AUTOMATED VERIFICATION AND VALIDATION
- FLIGHT PATH MANAGEMENT – TRAJECTORY OPTIMIZATION, AI

N84
20600

UNCLAS

N84 20600

D33

PROPULSION CONTROL TECHNOLOGY

Edward C. Beattie
United Technologies Corp., Pratt & Whitney Group
East Hartford, Connecticut

First Annual NASA Aircraft Controls Workshop
NASA Langley Research Center
Hampton, Virginia
October 25-27, 1983

Turbine Engine Control Evolution

Control systems for both commercial and military gas turbine engines are being transitioned in an orderly fashion from pure hydromechanical to full-authority digital electronic control in order to obtain the associated operational and performance benefits. Additional benefits will be available with further advancements in electronic control system technology and through increased integration with aircraft systems. At Pratt & Whitney, supervisory digital electronic control systems are in current operational service, and full-authority digital electronic control systems will be in service on upcoming models of commercial and military engines.

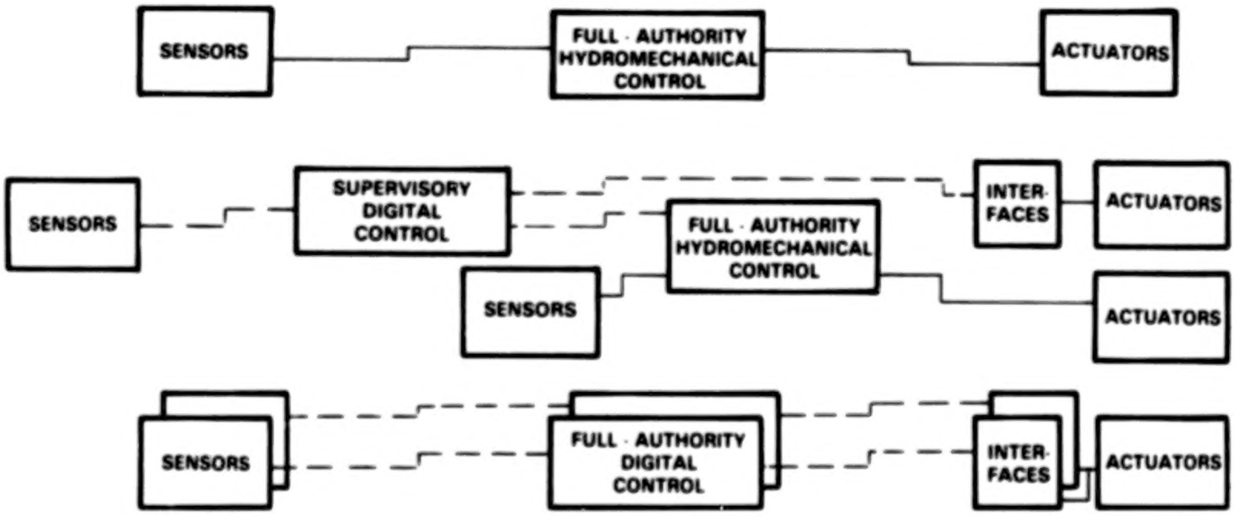
SENSORS
FULL - AUTHORITY HYDROMECHANICAL CONTROL
ACTUATORS
SENSORS
SUPERVISORY DIGITAL CONTROL
INTER-FACES
ACTUATORS
FULL - AUTHORITY HYDROMECHANICAL CONTROL
SENSORS
ACTUATORS
SENSORS
FULL - AUTHORITY DIGITAL CONTROL
INTER-FACES
ACTUATORS

Digital Electronic Control Systems Are Incorporated
in Pratt and Whitney Military and Commercial Engines

Supervisory digital electronic control systems are in current operational service on the F100 engine in F15 and F16 aircraft and on the JT9D-7R4 engine in Boeing 767 and Airbus A310 aircraft. Full-authority digital electronic control systems have been developed for the F100 engine, available for future F15 and F16 aircraft and for the PW2037 engine in the Boeing 757. The PW2037 engine and control system will be certified by the end of 1983. Pratt & Whitney is also developing a full-authority digital electronic control system for its new PW4000 engine which will be available for future versions of all wide-bodied aircraft.

Supervisory

- F100 — F15, F16
- JT9D-7R4 — B-767, A310, A300-600

Full Authority

- PW2037 — B-757
- F100 DEEC — F15, F16
- PW4000 — B-767, B-747, A310, A300, MD100

Electronic Control System Has Substantial Experience

Pratt & Whitney's digital electronic control systems have substantial operational and test experience. The current supervisory control system for the F100 engine has over 1.5 million hours of in-service operating time. The JT9D-7R4 engine's supervisory control system, recently introduced into service on Boeing 767 and Airbus A310 aircraft, has over 130,000 hours of operating time in revenue service. Pratt & Whitney has also conducted or participated in, with NASA and the Air Force, a number of electronic control system technology development and demonstration programs dating from the early 1970's. These programs have played a key role in developing digital electronic control system technology to a state of readiness for incorporation in production engines. With the advent of the full-authority electronic control system, continuing technology programs are required to obtain the benefits of control system technology advancements.

F100 supervisory — 1,500,000+ flight hours, F15 and F16 engines
JT9D-7R4 supervisory — 767 airline service; 130,000+ engine hours
JT8D EEC reliability evaluation — 300,000+ hours on 727 aircraft
JT8D EPCS, 1975 — Boeing demonstration at Boardman, Oregon
TF30 IPCS, 1975 — F111 flight test at Edwards AFB
F100 DEEC, 1978 — F100 altitude test at Tullahoma
F401 FADEC, 1979 — F401 altitude test at NASA Lewis
JT9D EPCS, 1980 — 747 flight test at Boeing
F100 DEEC, 1980 — F15 flight test
F100 DEEC, 1983 — F15 flight test
F100 DEEC, 1983 — F16 flight test
PW2037 full authority, 1983 — Ground, altitude and flight test

ORIGINAL PAGE IS
OF POOR QUALITY

JT9D Supervisory Electronic Control System

The JT9D-7R4 Supervisory Electronic Control System incorporates a conventional hydromechanical control system coupled with a digital electronic control which trims the hydromechanical control to provide accurate control of the desired engine power setting. Digital communication links with the cockpit provide simplified cockpit power setting procedures. The electronic control for the JT9D engine is mounted on the engine's fan case and is air cooled. Design of the electronic control was completed in the late 1970's, and the engine was introduced into service in 1982 on Boeing's 767 aircraft and in 1983 on Airbus' A310 aircraft. Operation of the JT9D-7R4 control system is similar to that of the F100 supervisory control system.

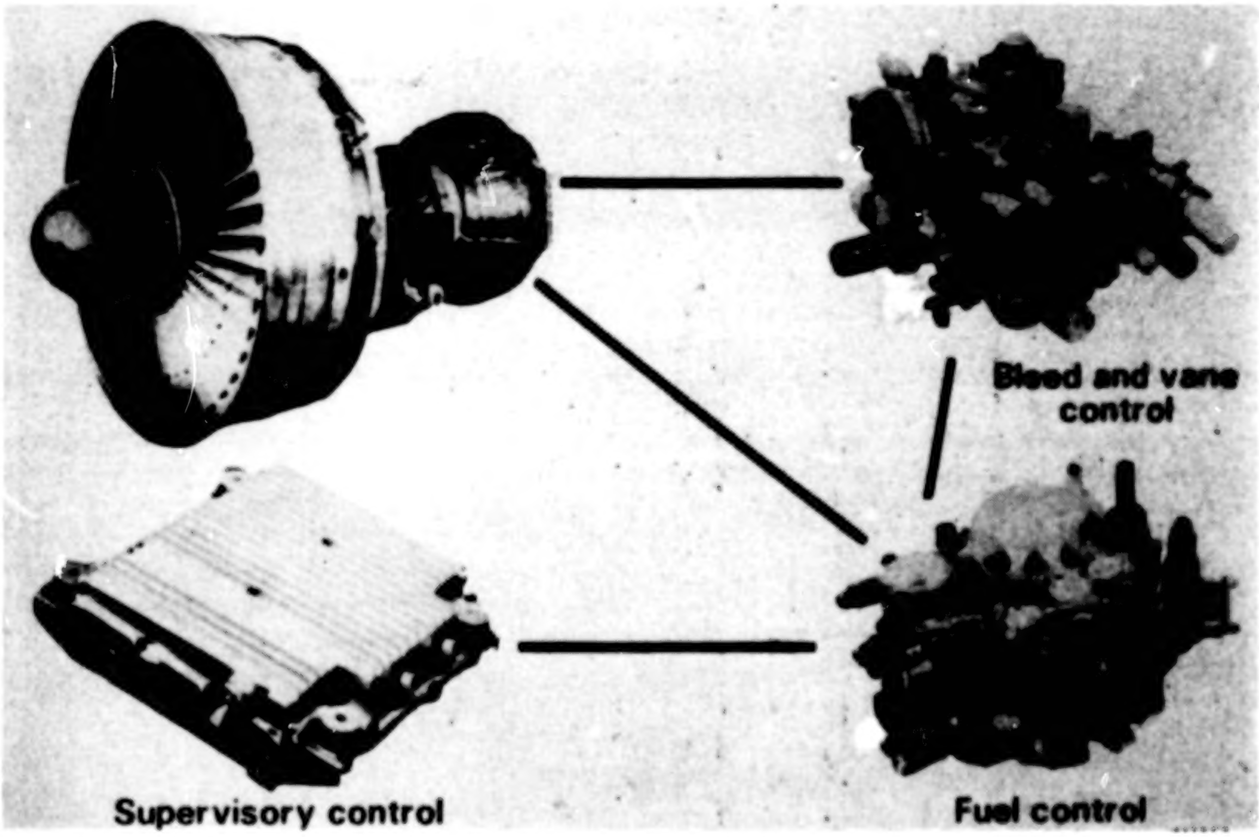

PW2037 Control System

The PW2037 Control System incorporates a dual-channel, full-authority digital electronic control and utilizes full redundancy of all inputs and outputs. As with the JT9D-7R4 supervisory control system, digital communication links with the cockpit provide for optimum aircraft/engine control communication and simplified power setting procedures. The electronic control design was completed in 1981 and incorporates advancements in circuit integration which provide for a substantial increase in functional capacity, compared to the supervisory control, with a significantly less than proportional increase in parts count. Engine and control system certification will be completed in December, 1983, and introduction into service on Boeing's 737 aircraft is scheduled for November 1984.

PW2037 CONTROL SYSTEM

Electronic Engine Control

[redacted]

- **Dual-channel Full-Authority Digital Electronic Control (FADEC)**
- **Dual redundancy of all inputs and outputs**

ORIGINAL PAGE IS
OF POOR QUALITY

F100 Digital Electronic Engine Control (DEEC) System

A full-authority digital electronic control system has been developed for the F100 engine. This control system incorporates a single-channel electronic control and provides hydromechanical backup capability to meet mission reliability requirements for single-engine applications. The electronic control design incorporates the same electronic component technology as the PW2037 control. DEEC control systems have successfully completed sea level and altitude engine testing and flight testing on NASA's F15 and Air Force F16 aircraft.

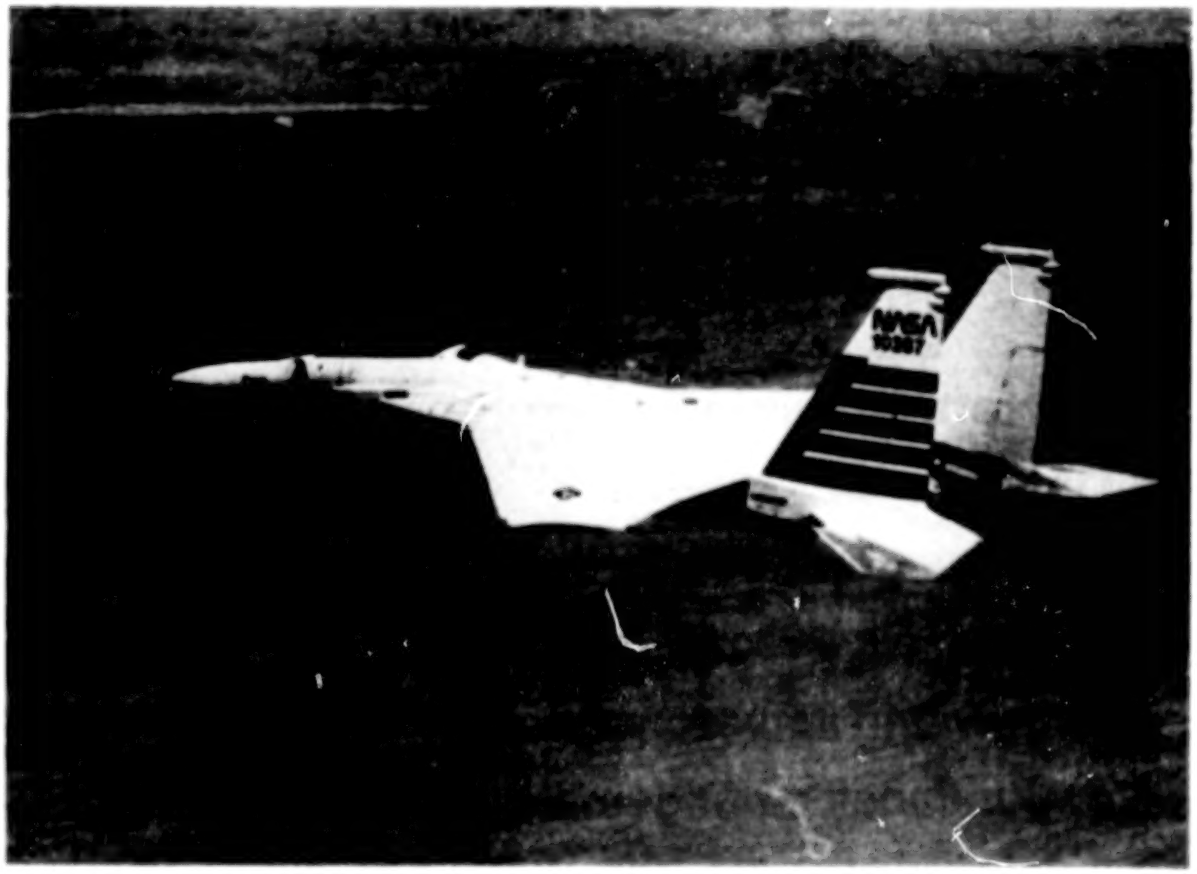

Propulsion Control: Research Needs and Opportunities

Significant advances in propulsion control system technology have led to the near-term incorporation of full-authority digital electronic controls in production engines. Substantial propulsion system benefits can be obtained through continuing advancements in control system technology. Integration of aircraft and engine control systems and functions can provide optimized hardware configurations and control modes. Development and application of optical interfaces, high-temperature electronics, and continuing advancements in large-scale circuit integration are likely candidates for electronic control design improvements to provide size, weight, and reliability benefits. Continuing development of advanced sensor and actuator concepts is required to evaluate potential benefits of optical interfacing and design concepts for increased reliability. NASA has sponsored a number of programs concerned with the development of advanced concepts for detection, isolation, and accommodation of sensor faults. Continuing work is required in this area to develop optimum redundancy management concepts. Adaptive control modes can contribute to more predictable system operation and may show significant benefits for integrated aircraft/engine control modes. Improvements in propulsion system modelling techniques become increasingly important as advanced propulsion system design concepts are developed for performance and operability improvements. Finally, software tools and documentation/testing concepts need to be developed for a high-level-language-based software development methodology which can meet regulatory agency certification requirements.

- **Aircraft/propulsion control system integration**
- **Optics**
- **High-temperature electronics**
- **Large-scale integration**
- **Sensor and actuator concepts**
- **Redundancy management**
- **Adaptive control modes**
- **Propulsion system modelling**
- **High-level-language-based software methodology**

END

DATE

FILMED

MAY 30 1984